Nitrile Triggered Access of *N*-Heterocycles under Thermal and Photochemical Processes

A dissertation submitted in partial fulfillment for the degree of

Doctor of Philosophy

Submitted By

Amitava Rakshit

Roll No. 166122029

Under the supervision of

Prof. Bhisma Kumar Patel

Department of Chemistry

Indian Institute of Technology Guwahati

Guwahati-781039, Assam, India

June, 2022

Nitrile Triggered Access of *N*-Heterocycles under Thermal and Photochemical Processes

A dissertation submitted in partial fulfillment for the degree of

Doctor of Philosophy

Submitted By

Amitava Rakshit

Roll No. 166122029

Under the supervision of

Prof. Bhisma Kumar Patel

Department of Chemistry

Indian Institute of Technology Guwahati

Guwahati-781039, Assam, India

June, 2022

भारतीय प्रौद्योगिकी संस्थान गुवाहाटी
Indian Institute of Technology Guwahati

DEDICATED TO

MY PARENTS & FAMILY

MY SUPERVISOR

PROF. BHISMA K. PATEL

MY BEST FRIENDS

SANDIP MONDAL

RIYA MALLIK

भारतीय प्रौद्योगिकी संस्थान गुवाहाटी
Indian Institute of Technology Guwahati

INDIAN INSTITUTE OF TECHNOLOGY GUWAHATI

Department of Chemistry

STATEMENT

I do hereby declare that the matter embodied in this thesis is the result of investigations carried out by me in the Department of Chemistry, Indian Institute of Technology Guwahati, India, under the guidance of *Prof. Bhisma K. Patel*.

In keeping with the general practice of reporting scientific observations, due acknowledgements have been made wherever the work described is based on the findings of other investigators.

June, 2022
IIT Guwahati

Amitava Rakshit

Amitava Rakshit

INDIAN INSTITUTE OF TECHNOLOGY GUWAHATI

Department of Chemistry

CERTIFICATE

This is to certify that *Amitava Rakshit* has been working under my supervision since July 2016 as a regular registered Ph.D. student. His thesis entitled "***Nitrile Triggered Access of N-Heterocycles under Thermal and Photochemical Processes***" is an authentic record of the results obtained from the research work in the Department of Chemistry, Indian Institute of Technology Guwahati, Assam, India. I am forwarding his thesis to submit for the Ph.D. (Science) degree from this institute. I certify that he has fulfilled all the requirements according to the rules of this institute regarding the investigations embodied in his thesis and this work has not been submitted elsewhere for a degree.

June, 2022
IIT Guwahati

Prof. Bhisma K. Patel
(Thesis Supervisor)
Department of Chemistry

ACKNOWLEDGEMENT

I would like to express my sincere gratitude to all the people around me who have helped, supported, and encouraged me during my Ph.D. studies.

First and foremost, I want to express my deepest respect and profound gratitude to my supervisor Prof. Bhisma K. Patel for providing me the opportunity to work under his guidance. His continuous support, and inspiration through creative and unique scientific ideas helped me to explore the domain of my work assembled in this thesis.

I would also like to extend my heartiest thanks to the doctoral committee members, Prof. Bhubaneswar Mandal, Prof. Subhas Chandra Pan, and Prof. Shyam Prosad Biswas for their timely evaluation of my Ph.D. work, encouragement, and precious suggestions.

My honest regards to all the faculty and staff members of the Department of Chemistry, IIT Guwahati for their cooperative nature. I would like to thank Babulal da for single-crystal XRD, Imdadul da for NMR, Aniruddha da for HRMS, Diganta da, Basab da, and John for various official work and support in the Department of Chemistry.

I wish to express sincere gratitude to MHRD for financial support and IIT Guwahati for all the facilities that were made available to me for learning several analytical instruments required during my research work. I would also like to especially thank to the Department of Chemistry, IIT Guwahati for providing me the opportunity to become an operator of the HRMS instrument. I am grateful to the central Instruments Facility (CIF) for the 600 MHz NMR and single-crystal XRD facilities, MHRD for the 400 MHz NMR facility under the COE-FAST program, DST for the 500 MHz NMR facility under the DST-FIST program, NECBH, IIT Guwahati, and DBT, Govt. of India for the 400 MHz NMR and single-crystal XRD facilities.

I would like to express my gratitude and a big thanks to all the operators inside or outside IIT Guwahati for successfully carried out all the instrumental experiments required during my research work. Further I am extremely thankful to all the co-authors, editors, associate editors and reviwers for their valuable comments and suggestion.

I would like to express my deepest gratitude to my Ph.D. senior Prasenit da for his guidance and encouragement during my earlier stage in the lab. I would like to thank wonderful lab seniors Sourav da, Wajid da, Anju di, Ahalya di, Suresh da, Prakash da, and Bilal da for their help, precious suggestions, and encouragement. I would like to thank postdoctoral lab seniors Joy da, Suman da, Ritush da, Gaurav da, Pakiza di, Binoy da, Bhaskar da, Gongutri di, and Kamal sir for their support.

I would like to express my heartiest thanks to my co-lab members cum friends Anjali, Subhendu, lab-juniors cum friends Tipu, Ashish, Nikita, Tamanna, Hiru, Bubul, Pritashree, Raju for their help, support, and creating a friendly environment in the lab.

I would like to thanks to my junior Ph.D. student Hiru and M.Sc. project students Kunika and Prashant for their assistance, support, and giving me the opportunity to guide during their projects and sharing the basic ideas, techniques and knowledge of Chemistry.

I would like to express millions of gratitude from the bottom of my heart to my best friends Sandip, Riya, Anjali and Subhasish (Master) for their help, support, and staying by my side to make good times even better, and the hard times a whole lot easier. Thank you for motivating me at this stage of my life.

I would also like to thank my Ph.D. friends, seniors and juniors here in IITG, Rabi (bandhu), Kanu, Govinda, Tukhar, Subhajit, Suhaib, Dipanjan, Tanumay, Asesh, Mihir, Chiranjib, Debasish, Rabi, Sayanta, Altab, Sukesh, Avishek, Gourab da, Sumit da, Karuna, Shantiram, Santanu, Arin, Jyoti di, Srijita di, Sujan di, Tapasi di, Anisha di, Archana, Eileen, Madhusmita, Shilpa for making the journey a lot better, easier and entertaining.

I would like to express a big thanks to my village friends and seniors Milan da, Kanta da, Krishna da, Dipak da, Ranjit da, Fuchu da, Gouranga da, Babin da, Rana da, Ganesh da, Mithu da, Jagu da, Habu master, Sadhan Master, Bappa, Papu, Sanu, Bura, Gede, Chhoton, Badal, Benu, Anup and all others members of Murgaboni A to Z Club for giving various kind of support and entertaining during this period of journey.

Finally, my Ph. D. endeavour could not have been completed without the endless love, unending support, tolerance and blessings from my family. I am very much grateful to my Didi, Jamaibabu, Dada, and Boudi for their unconditional support, affection and deep concern for my career. I would like to express my deepest gratitude to my parents whose unconditional love in every stage of my life motivated me to overcome all the challenges and I owe my entire life to them.

Last but not the least; I am thankful to Almighty for continuous blessing during my research carrier to accomplish this remarkable journey.

Amitava Rakshit

SYNOPSIS

The contents embodied in this thesis are divided into five chapters including one introductory chapter based on experimental results obtained during the research period. The introductory chapter represents an overview of nitrile-triggered access of *N*-heterocycles *under* thermal and photochemical processes. This includes a brief discussion about transition-metal-catalyzed C–H/N and C–H/N–H oxidative alkyne annulations, insertion of an alkyne into the nitrile (C≡N), thermal and visible-light mediated cascade addition/cyclization to the nitrile leading to the formation of C–C and C–N bonds.

Chapter II demonstrates a one-pot sequential synthesis of fused isoquinolines *via* intramolecular-cyclization/annulation and their photophysical investigations.

Chapter III illustrates a Pd(II)-catalyzed synthesis of furo[2,3-*b*]pyridines from β-ketodinitriles and alkynes *via* cyclization and N–H/C annulation.

Chapter IV describes Cu(II)-promoted cascade synthesis of fused imidazo-pyridine-carbonitriles.

Chapter V defines visible-light-accelerated Pd-catalyzed cascade addition/cyclization of arylboronic acids to γ- and β-Ketodinitriles for the construction of 3-cyanopyridines and 3-cyanopyrrole analogues.

CHAPTER I. An Overview of Nitrile Triggered Access of *N*-Heterocycles *under* Thermal and Photochemical Processes

The development of efficient methods for nitrogenous heterocycles synthesis is the most important objective in organic synthesis. This is owing to the omnipresence of *N*-heterocycles in various organic substances which are not only found in naturally occurring bioactive compounds, and medicinally related drug molecules but also widely used in material sciences. In particular, the highly substituted π-conjugated fused polycyclic *N*-heterocycles are versatile building blocks of many natural products and found to be very useful in functional materials such as luminescent materials, organic semiconductors, liquid crystal displays (LCDs), organic light-emitting diodes (OLEDs), and several others multifaceted applications. Therefore, in the light of its importance over the decades, numerous numbers of effective methods have been developed for their synthesis. Among varieties of methods, the transition metal-catalyzed addition to a nitrile functionality and subsequent cyclization serves as one of the elegant

methodologies for the synthesis of *N*-heterocycles. The nitrile assists as a flexible precursor for various other functional groups like amine, amide, aldehydes, ketone, and carboxylic acid which can undergo further intramolecular cyclization with suitable functional groups present in the proximity (Figure I.1). In this regard, the thermal and visible-light mediated addition of suitable nucleophiles/radicals to the nitrile followed by cyclization, or intermolecular [3 + 2] and [2 + 2 + 2] cycloadditions are well explored. Therefore the presence of nitrile functionality act as a prominent precursor for constructing nitrogenous heterocycles when suitably functionalized or activated in an organic molecule.

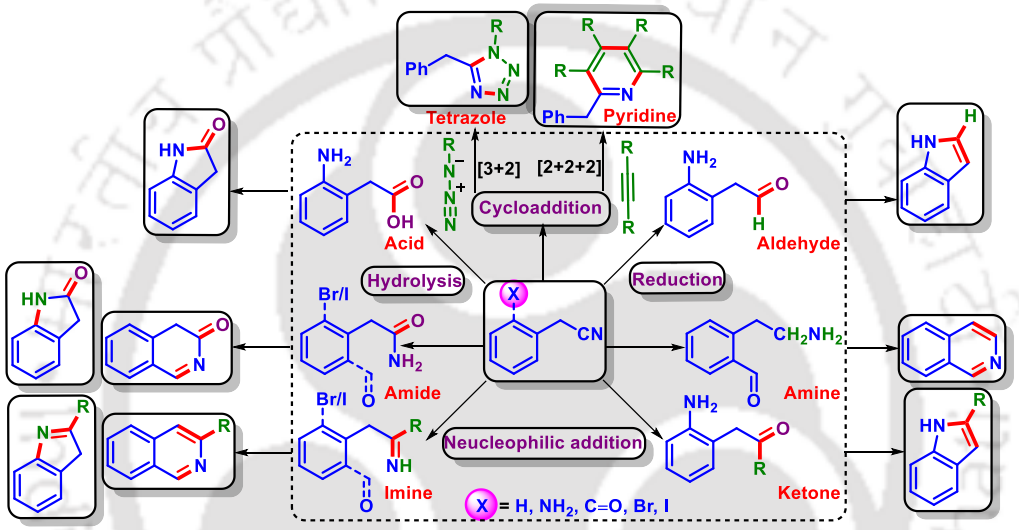

Figure I.1. *Conversion of nitrile to other functional groups and N-heterocycles.*

One of the cheapest and environmentally benign ways to introduce such nitrile functionality is the use of malononitrile to design synthetic precursors like 2-(2-oxo-2-phenylethyl)malononitrile (β-ketodinitrile) and 2-(3-oxo-1,3-diphenylpropyl)malononitrile (γ-ketodinitriles) (Figure I.2). These precursors contain nitrile functionality having proximity to the keto group and therefore could be very much useful as synthetic precursors for the synthesis of *N*-heterocycles. However, these synthetic precursors remain less explored in literature either thermally or photochemically.

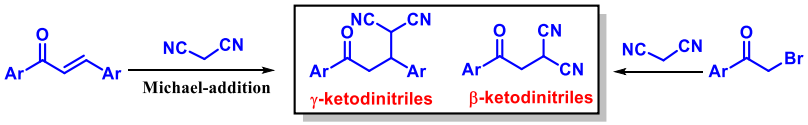

Figure I.2. *Synthesis of nitrile precursors.*

This synopsis contains newer methodologies to synthesize the privileged *N*-heterocycles from β-ketodinitriles and γ-ketodinitriles *via* nitrile-triggered thermal and visible-light mediated reactions *via* the construction of C–C and C–N bonds concerning the followings:

I.1. Synthesis of *N*-heterocycles *via* transition-metal-catalyzed C–H/N and C–H/N–H oxidative alkyne annulations.

I.2. Synthesis of cyclic compounds *via* alkyne insertion into the nitriles.

I.3. Synthesis of *N*-heterocycles *via* thermal and photochemical cascade addition/cyclization of nitriles.

I.1. Synthesis of *N*-Heterocycles *via* Transition-Metal-Catalyzed C–H/N and C–H/N–H Oxidative Alkyne Annulations:

In the chelation-assisted transition-metal-catalyzed C–H bond activation, nitrogen-directing groups have been used for the synthesis of *N*-heterocycles through the formation of C–C and C–N bonds. Based on the nature of the nitrogenous directing group the annulation process can be divided into the following two categories.

I.1.1. C–H/N Alkyne Annulation:

In this annulation process, the lone pair on the nitrogen atom directs the active metal species to get inserted into the *ortho*-C–H bond, thereby forming a cyclic metal complex. The cyclic metal complex on subsequent alkyne insertion followed by the reductive elimination leaves the nitrogen atom as part of the final product (Scheme I.1.1.1).

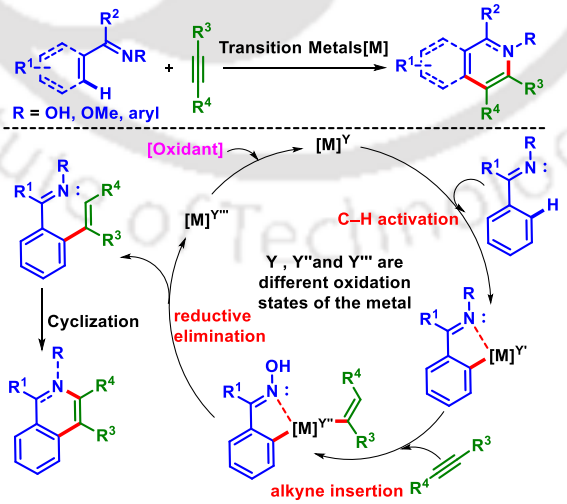

Scheme I.1.1.1. *Synthesis of N-heterocycles via C–H/N alkyne annulation.*

I.1.2. C–H/N–H Alkyne Annulation:

When the nitrogen atom of the directing group has acidic hydrogen then concurrent activation of both C–H and N–H bonds occurs. In this case, at first, the active metal catalyst forms a cyclic metal complex *via* a concerted deprotonative metalation generally through N–H/C–H dual activation. A subsequent alkyne insertion and reductive elimination of the metal affords *N*-heterocycles *via* C–C and C–N bond formation (Scheme I.1.2.1).

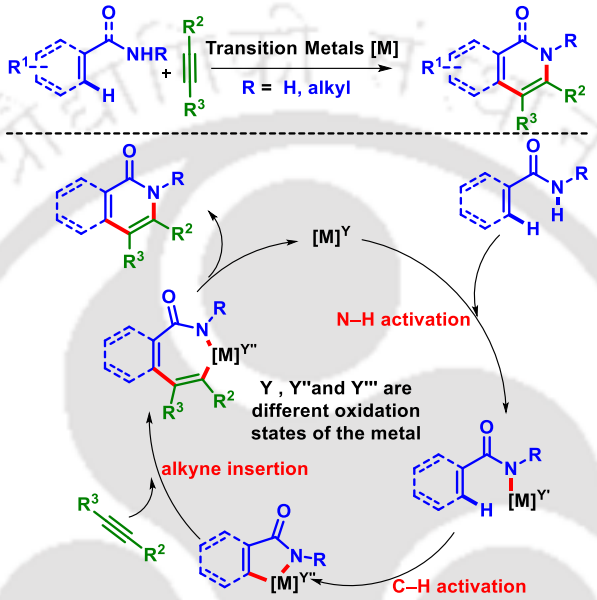

Scheme I.1.2.1. *Synthesis of N-heterocycles via C–H/N–H alkyne annulation.*

I.2. Synthesis of Cyclic Compound *via* Alkyne Insertion into the Nitrile:

The transition-metal-catalyzed oxidative alkyne annulation has been verified as a powerful and prevalent synthetic tool for the construction of diverse *N*-heterocycles *via* the formation of C–C and C–N bonds efficiently and economically. In this endeavor development of newer unprecedented annulation methodologies involving nitrile, remains an important quest in organic synthesis.

I.2.1. Alkyne Insertion *via* Carbopalladation of Nitrile:

The nitrile functionality has long been considered inactive in organometallic reagents. Hence the nitriles such as acetonitrile, benzonitrile, etc have been widely employed as a solvent in most transition-metal mediated reactions. However, after the finding of Pd-catalyzed alkyne insertion into nitrile by Larock *et al*. this area becomes exciting and explored rapidly. They developed the synthesis of 2,3-diarylindenones or 3,4-disubstituted 2-aminonaphthalenes from 2-

iodobenzonitrile or 2-iodophenylacetonitrile and internal alkyne *via* intramolecular carbopalladation of the cyano group (Scheme I.2.1.1). A plausible reaction mechanism for these transformations is shown. The reactions were initiated *via* the oxidative addition of Pd(0) into the C–I bond thereby giving an aryl-Pd(II) species. Next insertion of the alkyne between *in situ* generated aryl–palladium bond produces alkenylpalladium(II) which is followed by nucleophilic addition to the proximal nitrile and finally, hydrolysis or aromatization provides a wide variety of 2,3-diarylindenones or 3,4-disubstituted 2-aminonaphthalenes.

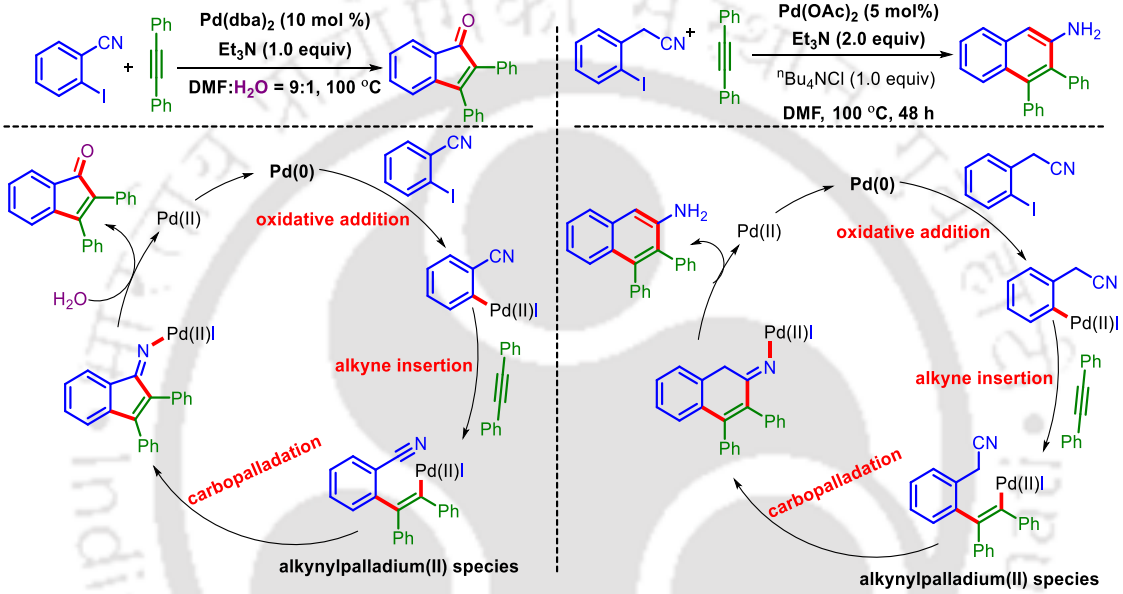

Scheme I.2.1.1. *Alkyne insertion into the nitrile via carbopalladation.*

I.2.2. Alkyne Insertion *via* [2 + 2 + 2] Cycloaddition of Nitrile:

Extensive and well-organized advancements have been made in the area of transition-metal-catalyzed alkynes insertion into the nitrile partners to construct specific nitrogenous heteroarenes. The transition-metal-catalyzed [2 + 2 + 2] cycloaddition reaction between alkyne and nitrile proved to be a dominant and atom economical practice for the synthesis of multi-substituted pyridine. A general mechanistic pathway for this cycloaddition between alkynes and nitrile is shown in Scheme I.2.2.1. Initially, the metal [M] coordinated with two alkyne partners giving a metallacyclopentadiene *via* oxidative coupling. Next, the nitrile partner can coordinate through two possible pathways. (i) insertion into the [M]–C bond to give cycloheptametallacycle or (ii) intramolecular [4 + 2] cycloaddition to form a bicyclic complex. Finally, reductive

elimination or isomerization of the cycloheptametallacycle or bicyclic complex affords the pyridine skeleton and the metal catalyst is released.

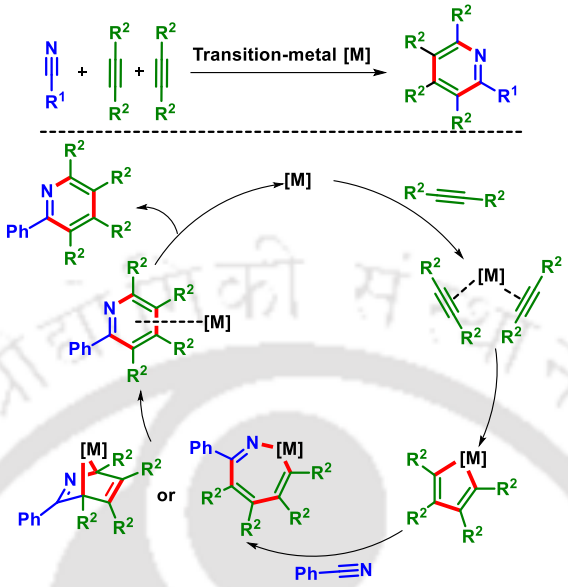

Scheme I.2.2.1. *Alkyne insertion via [2 + 2 + 2] cycloaddition of nitriles.*

I.2.3. Alkyne Insertion *via* Hydrolysis of Nitrile:

The oxidative alkyne insertion into the nitrile *via* hydrolysis into an amide provides the synthesis of multi-substituted isoquinolines. In this regard, Ru(II)/Cu(II)-catalyzed cyclization between aromatic or heteroaromatic nitriles and internal alkynes in an acetic acid medium afforded isoquinolones in good to excellent yields (Scheme I.2.3.1). The reaction proceeds through the hydrolysis of the nitrile into an amide ($CONH_2$) in the presence of $Cu(OAc)_2{\cdot}H_2O$ in acetic acid. Further amide-directed C–H/N–H oxidative annulation with internal alkyne provided substituted isoquinolones.

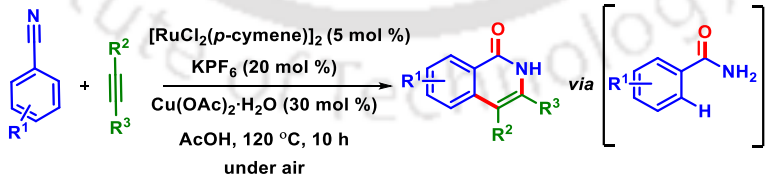

Scheme I.2.3.1. *Alkyne insertion via hydrolysis of nitriles.*

I.2.4. Intramolecular Alkyne insertion into the Nitrile:

The development of nitrile-triggered access to nitrogen heterocycles proceeds when both the nitrile and alkyne are an integral part of the same precursors such as *o*-alkynylarylnitriles (Figure I.2.4.1). Here, the alkynes implanted at the ortho position upgraded the reactivity of the

precursor leading to the synthesis of diverse *N*-heteroarenes through nucleophilic addition to the nitrile followed by intramolecular insertion with the alkyne. Another possible way of accessing nitrogenous heterocycles is the nucleophilic attack of an *N*-nucleophile to the nitrile followed by annulation with the alkyne triggered through an external nucleophile. However, in the latter case alkyne is not inserted into the nitrile rather it triggered the process allowing the nucleophile to be a part of the heteroarenes.

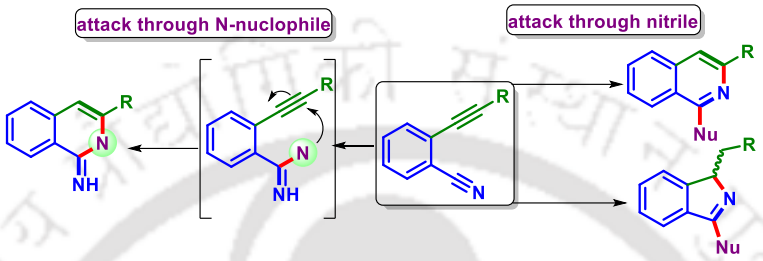

Scheme I.2.4.1. *Synthesis of N-heterocycles from o-alkynylarylnitriles.*

I.3. Synthesis of *N*-Heterocycles *via* Thermal and Photochemical Cascade Addition/Cyclization of Nitriles:

In the past few decades, cascade addition/cyclization has been established as one of the most attractive approaches for the construction of diverse *N*-heterocycles. In this regards nitrile functionality has appeared as the most prevalent synthetic precursor achieving diverse nitrogen-containing heterocycles through cascade addition/cyclization sequences either thermally or photochemically.

I.3.1. Transition Metal-Catalysed Cascade Addition/Cyclizations of Nitrile:

The transition metal-catalyzed cascade addition/cyclizations of nitriles (CN) have provided a novel convenient, superior, and straightforward route to create a wide range of *N*-heteroarenes through efficient construction of C–C and C–N bonds. Transition metals such as manganese (Mn), nickel (Ni), copper (Cu), palladium (Pd), and Silver (Ag), have been used frequently in this nitrile-triggered transformation in recent years. These reactions can proceed either with nucleophilic/electrophilic mechanism or free radical mechanism. In the process, the transition metal converts the nitrile into an iminyl group (C=N) through the addition by (i) using the σ-coordination of nitrogen to the metal as a Lewis acid, (ii) 1,2-insertion, or (iii) *in situ* generations of a radical and undergoes further cyclization. (Scheme I.3.1.1).

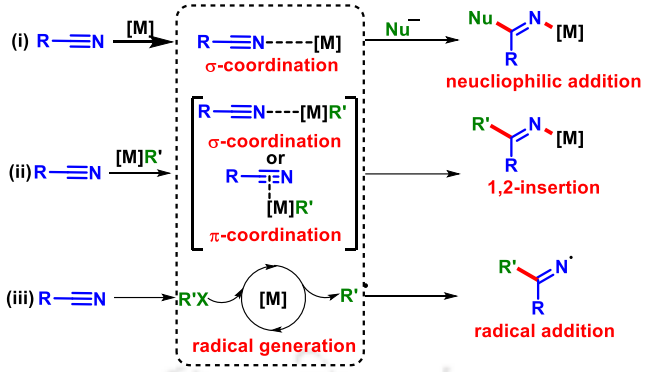

Scheme I.3.1.1. *Transition-metal-catalyzed addition of nitrile.*

I.3.1.1. Transition-Metal-Catalyzed Nucleophilic/Electrophilic cascades:

In this transition-metal-catalyzed cascades reaction, the nitrile precursors react with different coupling partners such as amine, Grignard reagent, arylboronic acids, aryl iodides, indoles, arylhydrazines, and aryl carboxylic acid to afford various *N*-heterocycles. During the process, the nitrile group acts as an electrophile and undergoes addition with aryl nucleophile generated from the coupling partners.

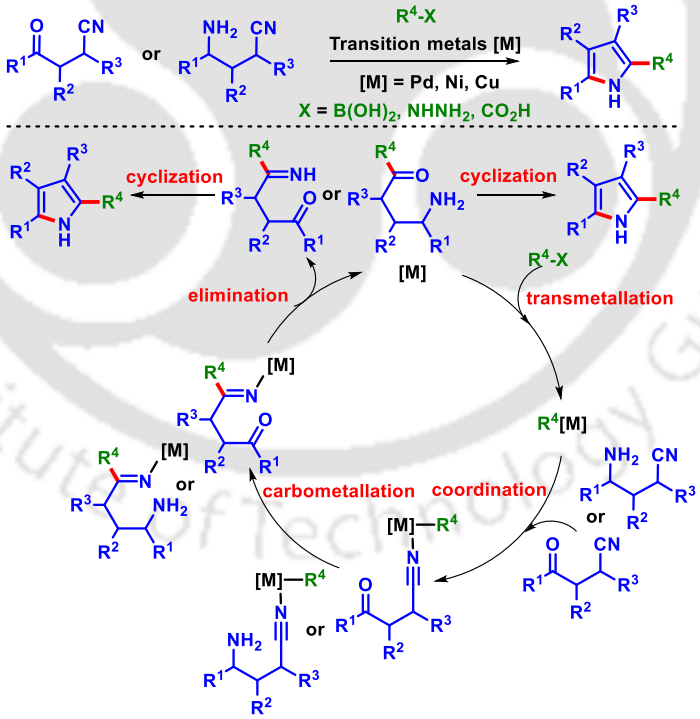

Scheme I.3.1.1.1. *Carbometallation of nitriles to synthesize N-heterocycles.*

After Larock's pioneering work in the field of catalytic carbopalladation of nitrile, this concept has been explored for the synthesis of various *N*-heterocycles. In these transformations,

the nitrile *N*-atom undergoes cyclization with a proximal carbonyl (C=O) group or hydrolyzed into a ketone and cyclized with proximal amine (NH_2) to provide various *N*-heterocycles. A general mechanism for this carbometallation of nitrile is shown in Scheme I.3.1.1.1, where the coupling partner undergoes transmetallation with the metal catalyst to provide an aryl-metal species. Next coordination with the cyano group followed by the addition of the aryl group through carbometallation of nitrile provides an immine or ketone and the metal catalyst is regenerated through elimination. Finally, cyclization of the imine or ketone with the proximal keto or amine group of the starting nitrile precursor gives a cyclic product.

I.3.1.2. Transition-Metal-Catalyzed Radical cascades:

The transition-metal-catalyzed radical cascade process involving the nitrile functionality provides a convenient route for the construction of various important *N*-heterocycles. The application of the cyano group as a radical acceptor is shown below (Scheme I.3.1.2.1). An iminyl radical is formed when an *in situ* generated radical adds to the nitrile group of a precursor (Path A). An iminyl radical can also be generated through the radical addition to the nitrile *via* an appropriately placed C=C bond or another unsaturated group (Path B). Finally, nitrile insertion onto the aryl ring through the iminyl radical produces the corresponding *N*-heterocycle.

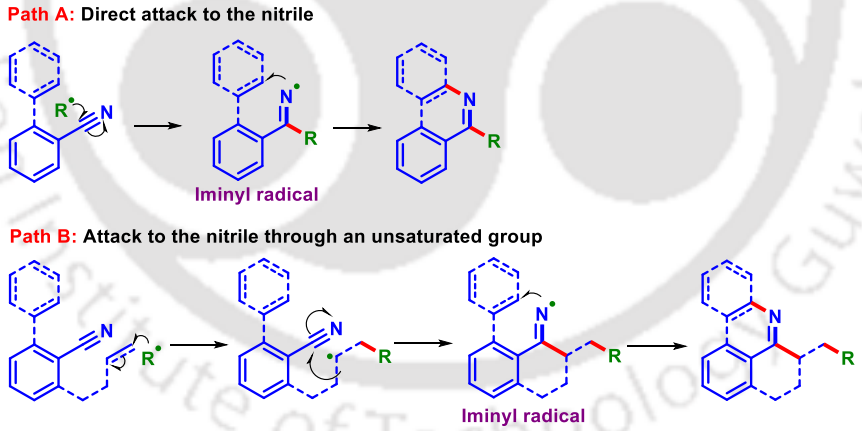

Scheme I.3.1.2.1. *Nitrile as a radical acceptor for synthesis of N-heterocycle.*

I.3.2. Visible-Light mediated Radical Cascade Addition/Cyclizations with Nitrile:

The Visible-light-induced radical cascade addition/cyclization processes have been successfully used for the construction of *N*-heterocycles because of their simplicity, efficiency, and unique activation.[112] In this context construction of C–C and C–N bonds using photoredox catalysis has grabbed significant attention giving prominence to the nitrile functionality. In

contrast to that of transition-metal-catalyzed radical reactions herein the radical is generated through the photocatalysts (PC) in its excited state (PC*) *via* single electron transfer (SET) by the influence of visible-light (Figure I.3.2.1). The generated radical adds to the cyano group to obtain an iminyl radical which subsequently underwent intramolecular cyclization to access *N*-heterocycles through a radical or a cationic species. The photocatalyst is regenerated to its ground state either *via* oxidative quenching or reductive quenching cycle (Scheme I.3.2).

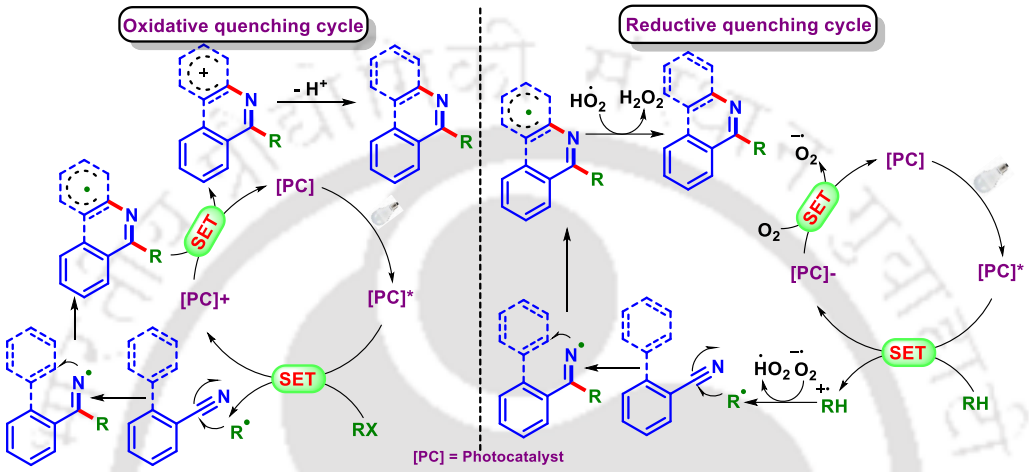

Scheme I.3.2.1. *Visible-light mediated radical addition to nitrile.*

CHAPTER II. One-pot Sequential Synthesis of Fused Isoquinolines *via* Intramolecular-Cyclization/Annulation and their Photophysical Investigations

This chapter describes the synthesis of fused isoquinolones, 4-oxo-2,6,7-triaryl-4*H*-pyrido[2,1-*a*]isoquinoline-3-carbonitriles from γ-ketomalononitriles and internal alkynes in the presence of Cu(II) and Ru(II) catalysts. This one-pot process consisting of Cu(II)-catalyzed selective hydrolysis of a cyano group to an amide, dehydrative cyclization of the amide to a cyclic amide, aromatization of the cyclic amide to a 1,2-dihydropyridone and finally, the Ru(II)-catalyzed C–H/N–H annulation with an internal alkyne. This overall process is associated with the formation of one C–C, two C–N, two C=C, and a C=O bonds leading to highly fluorescence active fused isoquinolone having emission in the green region (502–560) nm and absorption (λ_{max}) in the range of (454–490) nm. The $\Delta E_{(LUMO-HOMO)}$ of the synthesized compounds is in the range of 2.88 to 3.45 eV which is calculated based on DFT

The transition-metal-catalyzed C–H bond activation has gained great attention for the synthesis of nitrogen-containing fused heterocycles, especially, isoquinolines and isoquinolones. In this context Rh(III), Pd(II), Ni(II), and Ru(II) catalysts are most common and have been used extensively to obtain isoquinolones *via* the oxidative coupling between an internal alkyne and an amide. Inspired by this transition-metal-catalyzed direct annulation of C–H bonds we envisaged the synthesis of fused isoquinolines from γ-ketomalononitriles. Our initial investigation started using 2-(3-oxo-1,3-diphenylpropyl)malononitrile (**1**) (0.2 mmol), diphenylacetylene (**a**) (1 equiv), $Cu(OAc)_2 \cdot H_2O$ (1 equiv), and $[Ru(p\text{-cymene})Cl_2]_2$ (2 mol %) in glacial AcOH at 110 °C [Scheme II.1, (i)]. Interestingly, the reaction resulted in the formation of a new yellow fluorescent spot (viewed under 365 nm UV lamp) as observed by TLC. Unfortunately, the compound could not be separated for characterization as it was associated with several other side products. However, a decent amount (18%) of expected cyclic 1,2-dihydropyridone intermediate *viz.* 2-oxo-4,6-diphenyl-1,2-dihydropyridine-3-carbonitrile (**1´**) could be isolated.

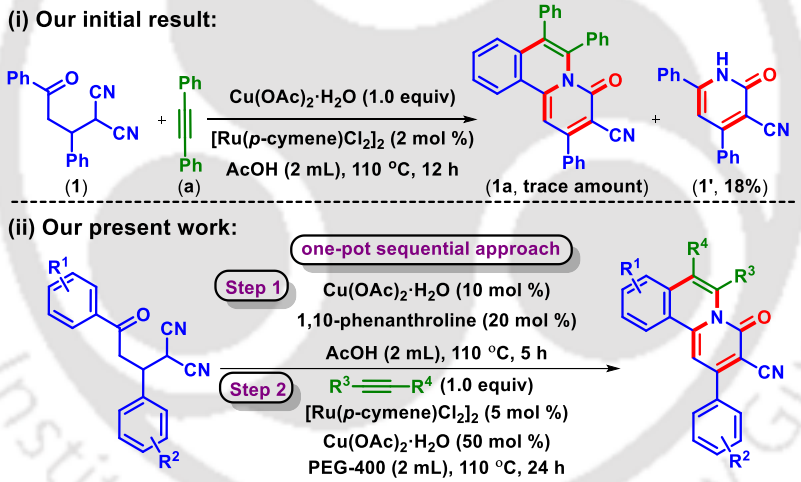

Scheme II.1. *One-pot synthesis of fused isoquinolones.*

Encourage by the success of our anticipated strategy we adopted a two-step protocol. In the first step the 2-(3-oxo-1,3-diphenylpropyl)malononitrile (0.2 mmol) (**1**) was treated with $Cu(OAc)_2 \cdot H_2O$ (1 equiv) in AcOH (2 mL) at 110 °C and the reaction was continued for 5 h, during this period all the starting materials got consumed giving 1,2-dihydropyridone intermediate (**1´**) which has potential C–H/N–H sites for annulation with an alkyne. To this crude reaction mixture, diphenylacetylene (**a**) (1 equiv) and $[Ru(p\text{-cymene})Cl_2]_2$ (5 mol %) were added and the reaction was allowed to proceed for 12 h. The reaction was found to be much

cleaner and the product (**1a**) was isolated in 30% yield. The product was separated and characterized by spectroscopic analysis (IR, ^{1}HNMR, ^{13}CNMR, and HRMS) and the structure was found to be 4-oxo-2,6,7-triphenyl-4*H*-pyrido[2,1-*a*]isoquinoline-3-carbonitrile (**1a**).

Next, further optimizations were carried out by varying various reaction parameters. The optimized condition for this transformation in the first step is found to be the use of γ-ketomalononitriles (0.2 mmol), $Cu(OAc)_2 \cdot H_2O$ (10 mol %), and 1,10-phenanthroline (20 mol %), at 110 °C in AcOH (2 mL). The optimized condition for this annulation step is the use of diphenylacetylenes (0.2 mmol), $[Ru(p\text{-cymene})Cl_2]_2$ (5 mol %). $Cu(OAc)_2 \cdot H_2O$ (50 mol %), at 110 °C in PEG-400 (2 mL) for 24 h [Scheme II.1, (ii)].

Next, this one-pot two-step synthesis was then explored with various other γ-keto-malononitriles and internal alkynes under the optimized reaction conditions. To understand the mechanism and nature of the C–H bond activation, and whether the C–H metalation step is reversible or irreversible a deuterium-scrambling experiment and kinetic isotope effect experiments were performed (Scheme II.2). These experiments conclude that the irreversible C–Ru bond formation is the rate-limiting step.

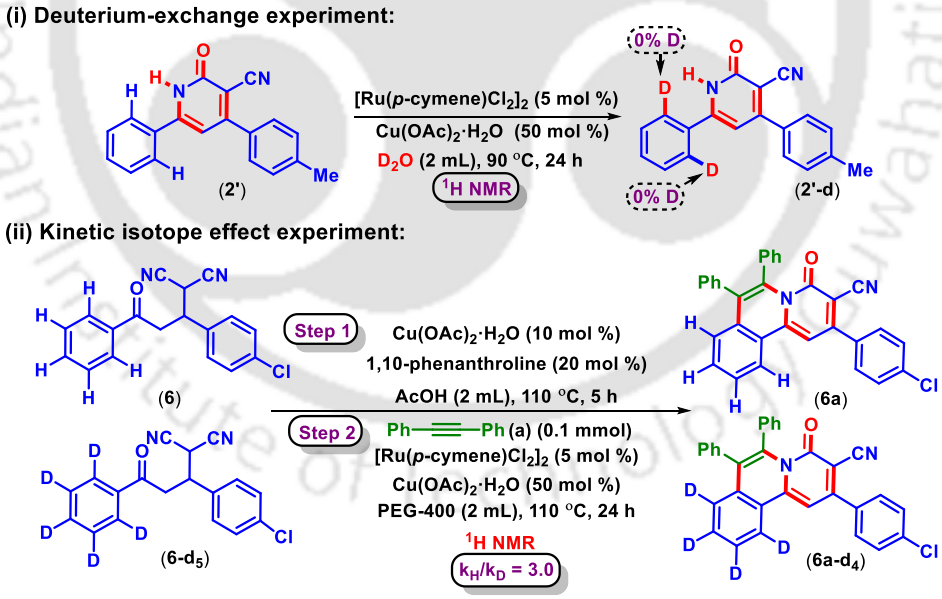

Scheme II.2. *Experiments with isotopically labeled compound.*

Based on this a plausible mechanism is depicted in Scheme II.3. In the first step, one of the nitrile (–CN) groups of the substrate (**1**) is hydrolyzed selectively to a mono amidic intermediate (**I**). The NH_2 of the amide then attacks the carbonyl group and undergoes a

dehydrative cyclization to produce a six-membered cyclic intermediate (**II**). The intermediate (**II**) is oxidized/aromatized under the reaction conditions to an aromatic pyridone intermediate (**III**). The formation of intermediate (**I**), (**II**), and (**III**) has been detected by the HRMS analysis of the reaction aliquots at various time intervals. In the second step, the catalyst $[RuCl_2(p\text{-cymene})]_2$ undergoes ligand exchange with $Cu(OAc)_2{\cdot}H_2O$ to generate the active catalytic species, which coordinates with the nitrogen atom of the intermediate (**III**) *via* N–H deprotonation. This is then followed by ortho C–H bond activation through the elimination of AcOH, forming a five-membered ruthenacycle (**V**). Further coordination of the alkyne (**a**), followed by an alkyne insertion and reductive elimination afforded the final product (**1a**) *via* the intermediate (**VI**). The active catalyst species is then regenerated by the oxidant $Cu(OAc)_2{\cdot}H_2O$ and air for the next catalytic cycle.

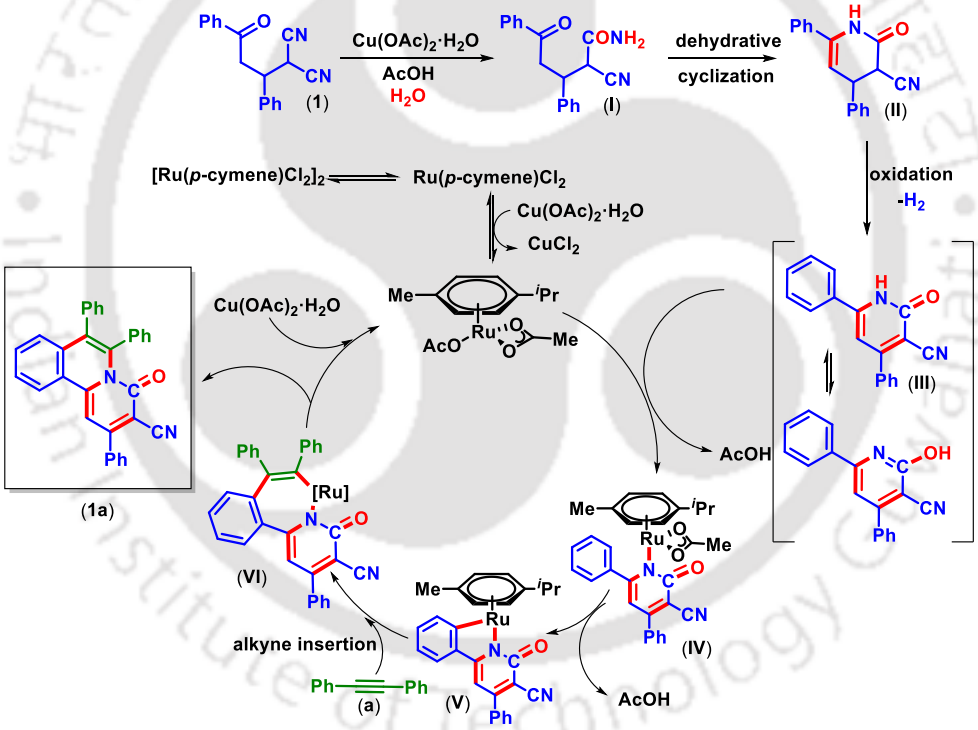

Scheme II.3. *Proposed mechanistic pathway.*

To further ascertain the geometry and electronic structure of the annulated fused isoquinoline, density functional theory (DFT) calculations were performed with a B3LYP/6-31G (d, p) basis set level in acetonitrile solvent modelled by the PCM approach (the Gaussian 09 programme). The density functional theory (DFT) calculation of (**1a**) reveals that the electron density in the highest occupied molecular orbital (HOMO) is localized at the central core

extending to the nitrile and minor contributions from the two phenyl rings originating from the diphenylacetylene. Whereas the lowest unoccupied molecular orbital (LUMO) is again localized at the central core and extended up to the phenyl ring originating from the α to malononitrile (Figure II.1). In a donor-acceptor (D-π-A) type system, the $\Delta E_{(LUMO-HOMO)}$ energy can be directly correlated with the presence of either electron-donating or electron-withdrawing groups on the donor (HOMO) or the acceptor (LUMO) part of the molecule. Here, since both the HOMO and LUMO are localized on the central molecular core with very insignificant contributions from the three phenyl rings, no proper correlation between the HOMO-LUMO energy gap could be found due to the presence of EDG or EWG groups.

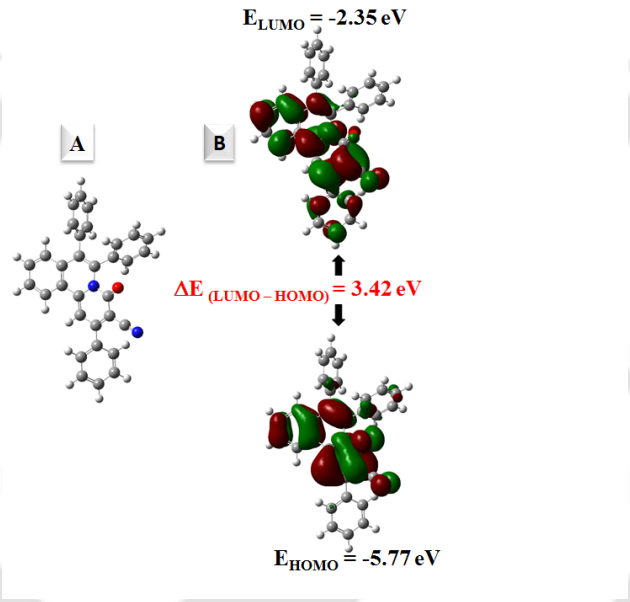

Figure II.1. *(A) Optimized structure of* ***1a****. (B) Molecular Orbitals amplitude plots of HOMO and LUMO of* ***1a*** *using density functional theory calculation at the B3LYP/6-31G (d, p) basis set level in acetonitrile solvent modelled by the PCM approach.*

As stated earlier that the newly synthesized compounds having highly conjugated fused isoquinoline core display yellow fluorescent therefore, their photophysical properties such as UV visible and photoluminescence were investigated. The absorption spectra (λ_{abs}) and emission spectra (λ_{em}) were measured for a few selected compounds in CH_2Cl_2. The UV-Vis and photoluminescence spectra of selected compounds are shown in Figure II.2. All these synthesized compounds showed strong absorptions, with the positions of maximum ranging from 454–490 nm. The compounds exhibit three distinct absorption maxima, a band in the

region of 313–321 nm, a band in the region of 428–467 nm, and another in the region of 454–490 nm. All exhibit strong fluorescence emission in the range of 502–560 nm which belongs to the green region of the visible light spectrum.

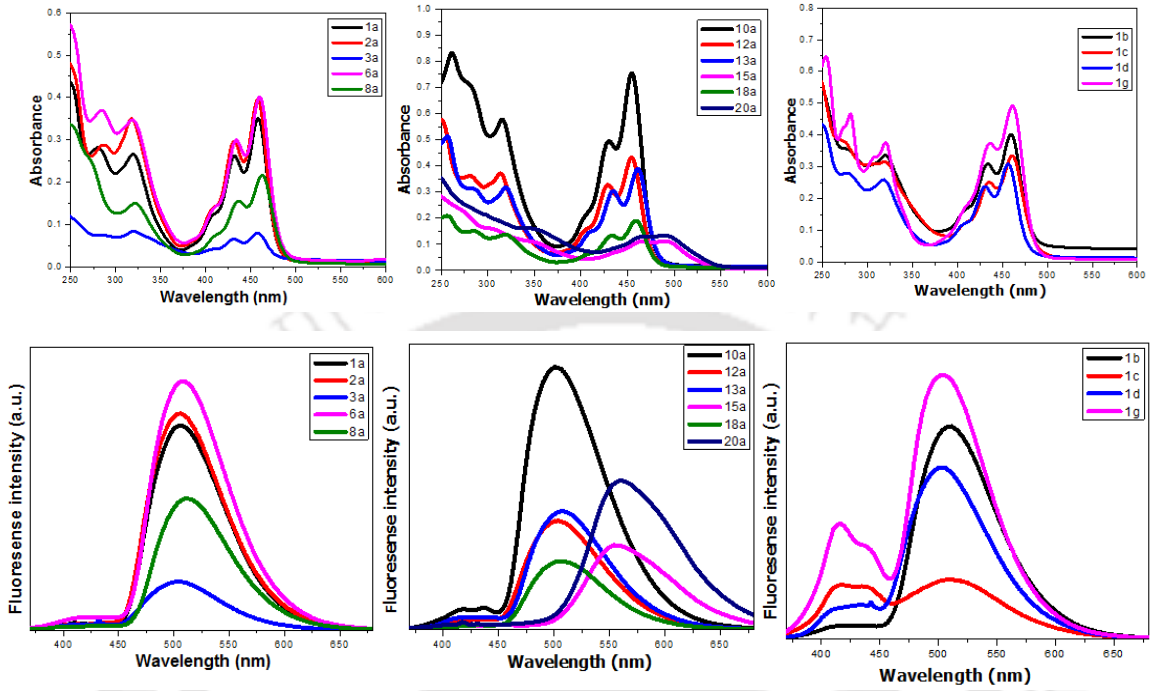

Figure II.2. *(a) UV-vis and (b) Photoluminescence spectra in CH_2Cl_2 (1 x 10^{-5} M).*

CHAPTER III. Pd(II)-Catalyzed Synthesis of Furo[2,3-*b*]pyridine from β-Ketodinitriles and Alkynes *via* Cyclization and N–H/C Annulation

This chapter describes a Pd(II)-catalyzed synthesis of furopyridines from β-ketodinitriles and internal alkynes *via* an unusual N–H/C annulation. The participation of both the nitrile groups along with the concurrent construction of furan and pyridine rings through the formation of C–C, C=C, C–O, C–N, and C=N bonds are the important features. The synthetic applicability was further demonstrated through a series of post-synthetic alterations.

The past decade has witnessed an upsurge in the transition-metal-catalyzed alkyne insertion into the C–H/N–H bonds for the synthesis of various fused heterocycles. In this rapidly developing realm of oxidative annulation with internal alkynes, the Pd(II)-catalyzed annulation is gaining prominence to deliver diverse carbocycles, heterocycles, and spirocycles in minimal

steps. Owing to the inertness of the cyano group towards organopalladium reagents this was an underdeveloped area of research. However, after the discovery of Pd-catalyzed annulation by the Larock group involving nitrile functionality this area is becoming exciting and rapidly expanding. In the recent past Pd(II)-catalyzed reactions are rapidly developing extending the concept of catalytic carbopalladation of nitriles. Taking advantage of this, subsequently, our group developed the synthesis of pyridines and pyrroles using γ-ketodinitriles and β-ketodinitriles respectively in the presence of Pd(II) under visible-light excitation. With our increasing interest in the Pd-catalyzed alkyne insertion into the nitrile, herein we report the synthesis of furo[2,3-*b*]pyridine employing β-ketodinitrile and internal alkyne (Scheme III.1). Gratifyingly, in this protocol both the cyano groups participate and the reaction is initiated through the keto oxygen leading to the simultaneous construction of furan and pyridine rings through the formation of C–C, C=C, C–O, C–N, and C=N bonds in one pot.

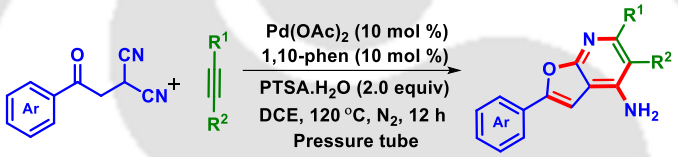

Scheme III.1. *Pd(II)-catalyzed alkyne insertion into the nitrile.*

We began this Pd(II)-catalyzed coupling of β-ketodinitrile (**1**) (0.25 mmol) and diphenylacetylene (**a**) (0.25 mmol, 1 equiv) in the presence of $Pd(OAc)_2$ (5 mol %), 2,2′-bipyridine (5 mol %) and *p*-toluenesulfonic acid ($PTSA{\cdot}H_2O$, 2 equiv) in 1,2-dichloroethane (DCE) (2 mL) at 120 °C in a pressure tube under N_2 atmosphere for 12 h. A new blue fluorescent spot was observed from TLC and the product isolated after column chromatography was found to be furo[2,3-*b*]pyridine (**1a**) obtained in 37% yield. From the spectroscopic evidence, the structure was assigned to be 2,5,6-triphenylfuro[2,3-*b*]pyridin-4-amine (**1a**) which was reconfirmed by a single-crystal X-ray diffraction study (**1a**). To establish the optimal reaction conditions further screening process was carried out and the best-optimized condition was found to be the use of β-ketodinitrile (**1**) (0.25 mmol), diphenylacetylene (**a**) (0.375 mmol, 1.5 equiv), $Pd(OAc)_2$ (10 mol %), 1,10-phenanthroline (10 mol %) and $PTSA{\cdot}H_2O$ (2 equiv) in 1,2-dichloroethane (DCE) (2 mL) at 120 °C in a pressure tube under N_2 atmosphere for 12 h.

Having established the best-optimized conditions, the effect of substituents on β-ketomalononitriles and internal alkynes were studied. Next, to illuminate a plausible reaction mechanism few control experiments were performed. Based on control experiments and literature reports, a tentative reaction mechanism is demonstrated (Scheme III.2). Initially, the β-ketodinitrile (**1**) undergoes an acid-catalyzed enol formation in the presence of PTSA·H_2O to obtain an intermediate (**I**). The intermediate (**I**) then undergoes another acid-catalyzed intramolecular cyclization to afford a five-membered cyclic intermediate (**1′**). In the presence of 1,10-phenanthroline (L) a ligand-coordinated Pd(II) complex (**A**) is generated *in situ*, which undergoes a deprotonative coordination with the amino group of intermediate (**1′**) to form another intermediate (**II**) eliminating AcOH. Next, the diphenylacytelelene (**a**) is inserted intermolecularly into the *N* atom giving an alkynyl Pd(II) species (**III**). This intermediate (**III**) undergoes intramolecular insertion of the alkyne to another nitrile through a carbopalladation giving a six-membered pyridine ring (I**V**) and the Pd(II) is coordinated with the other nitrile *N*-atom. Protonolysis of (I**V**) with PTSA·H_2O gives an imine intermediate (**V**) and the OTs ligated Pd(II) complex (**B**), which on acetate ligand exchange regenerates the initial Pd(II) complex (**A**). Finally, the aromatization of intermediate **V** produces the corresponding furopyridine (**1a**).

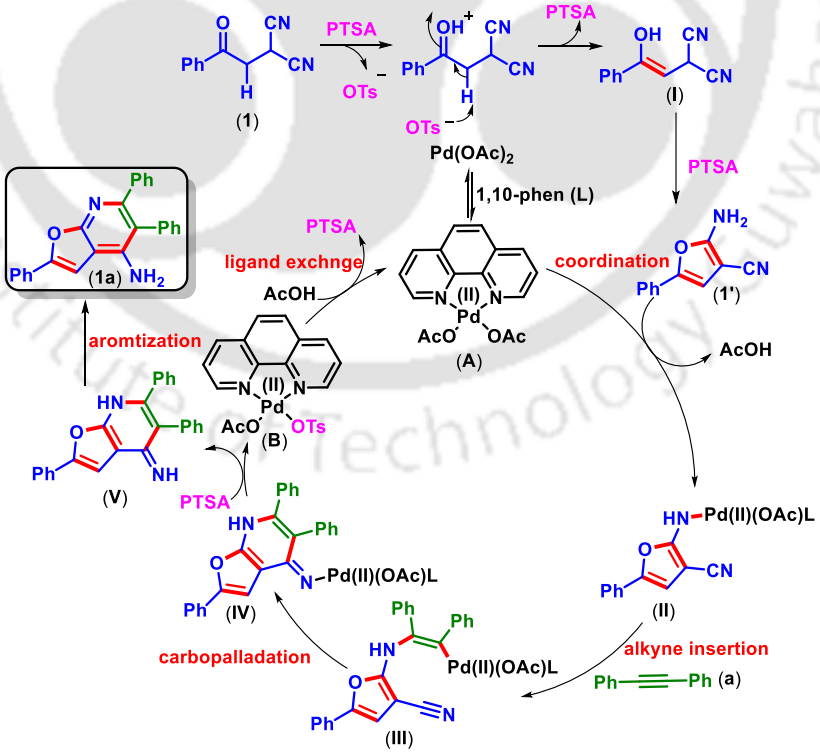

Scheme III.2. *Proposed reaction path.*

To explore the synthetic utility and to expand the substrate scope, a few late-stage functionalizations were successfully carried out as shown in Scheme III.3. The 2-phenyl pyridine of **1a** involves Ru(II)-catalyzed annulation reaction with diphenylacetylene (**a**) and C–H functionalization with *n*-propylmalimide (**r**) giving the corresponding functionalized product (**1aa**, 80%) and (**1aw**, 72%) respectively [Scheme III.3 (i) and (ii)]. Further *p*-Br substituted furopyridine (**7a**) undergoes Pd(II)-catalyzed Suzuki coupling with phenylboronic acid (**x**) [Scheme III.3 (iii)], Sonogashira coupling with 4-ethynyltoluene (**y**) [Scheme III.3 (iv)] and Heck coupling with *p*-tolylstyrine (**z**) [Scheme III.3 (v)] giving corresponding cross-coupled products (**7ax**, 68%), (**7ay**, 75%) and (**7az**, 70%) respectively.

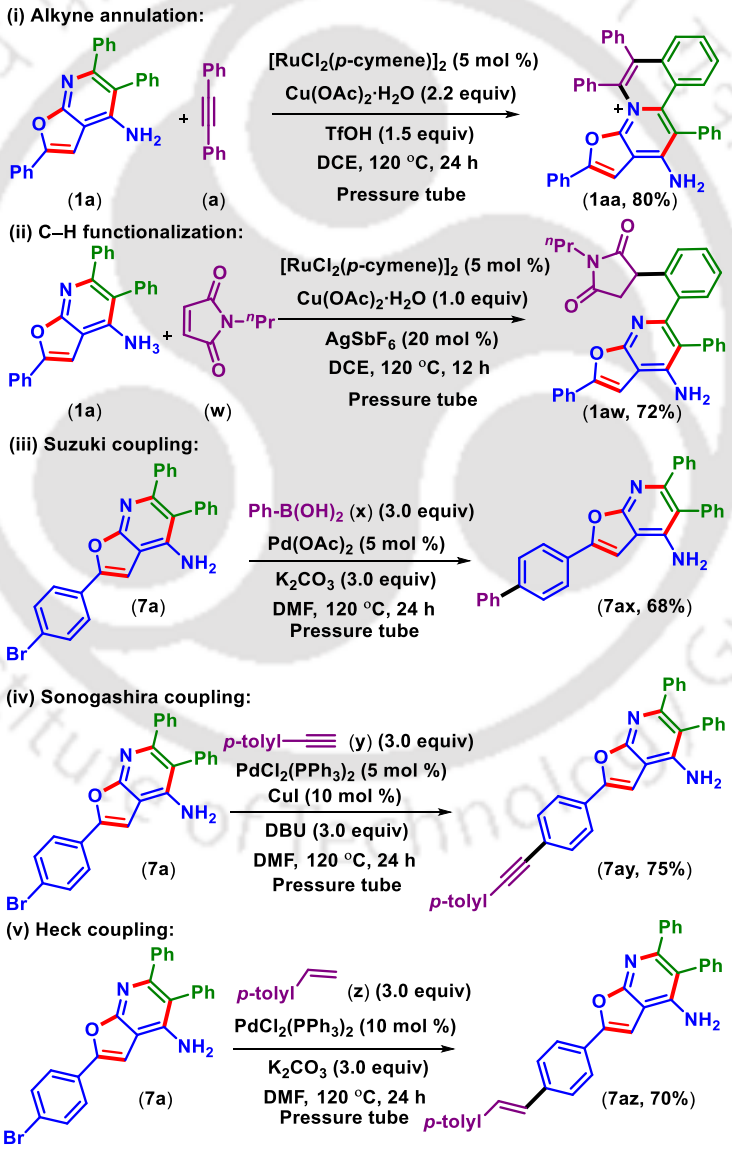

Scheme III.3. *Post-synthetic functionalizations.*

CHAPTER IV. Cu(II) Promoted Cascade Synthesis of Fused Imidazo-Pyridine-Carbonitriles

This chapter describes the synthesis of aza-fused *N*-heterocycle having a benz-imidazopyridine scaffold *via* an addition-cyclization followed by an Ullmann-type C–N coupling between *o*-iodoanilines and γ-ketodinitriles. The synthesized fused imidazo-pyridines show excellent photoluminescence properties having emission maxima in the range of 502–533 nm and HOMO-LUMO energy gap of 3.49–3.57 eV. A few post-synthetic modifications were also demonstrated to enhance the synthetic utility.

The transition-metal-catalyzed synthesis of nitrogen-heterocycles *via* C–N cross-coupling mainly involves Pd or Cu catalysts. But, the latter is preferred due to its low cost and high environmental acceptability. *o*-Iodoanilines have been used as valuable precursors in transition-metal catalysis especially, copper-catalyzed couplings *via* the addition/cyclization cascade process. The nucleophilic amino group promotes the intermolecular addition with the unsaturated electrophilic center, while the *o*-iodo group takes part in an intramolecular cyclization *via* a metal-mediated C–C or C–heteroatom bond formation. Further, substrates bearing functionalized or activated cyano group has drawn substantial attention owing to their well-recognized potential to transform into a variety of nitrogen-containing heterocycles. Based on our interest in nitrile triggered process to access *N*-heterocycles and taking cues from the copper-catalyzed cascade addition/cyclization of *o*-iodoaniline herein, we report a Cu(II)-promoted strategy for the construction of benzo[4,5]imidazo[1,2-*a*] pyridine-4-carbonitriles (Scheme IV.1).

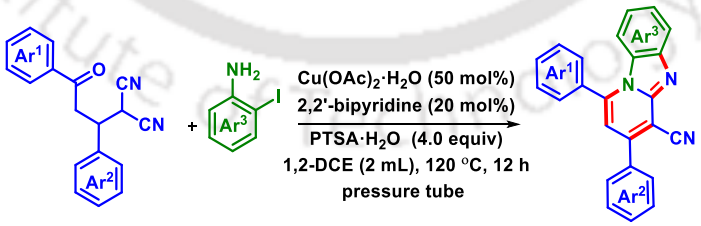

Scheme IV.1. *Synthesis of benzo[4,5]imidazo[1,2-a]pyridine-4-carbonitriles.*

The initial assays were carried out by taking γ-ketodinitrile (**1**) (0.25 mmol) and 2-iodoaniline (**a**) (0.50 mmol, 2 equiv) as the reacting partners in the presence of $Cu(OAc)_2 \cdot H_2O$ (10 mol %) as the catalyst, 2,2′-bipyridine (20 mol %) as ligand and *p*-toluenesulfonic acid

(PTSA·H_2O, 2 equiv) as an additive in 1,2-dichloroethane (DCE) (2 mL) at 120 ^oC in a pressure tube for 12 h. The reaction furnished a yellow fluorescent spot (viewed under 365 nm UV lamp) as observed by TLC, and the product (**1a**) was isolated in 15% yield. Further, increasing the loading of $Cu(OAc)_2·H_2O$ (50 mol %) produces (**1a**) an improved yield of 58%. From the spectroscopic analysis, the structure of the isolated product was found to be 1,3-diphenylbenzo[4,5]imidazo[1,2-*a*]pyridine-4-carbonitrile (**1a**) and was further confirmed by a single-crystal X-ray diffraction study of one of its derivative. To find the optimal reaction conditions further screening process was initiated and after the screening of various reaction parameters, the optimized condition for this transformation was found to be the use of (**1**) (0.25 mmol), (**a**) (0.50 mmol, 2 equiv), $Cu(OAc)_2·H_2O$ (50 mol %), 2,2′-bipyridine (20 mol %), and PTSA·H_2O (4 equiv) in DCE (2 mL) at 120 ^oC in a pressure tube for 12 h.

With the best-optimized conditions in hand, the effect of substituents on γ-keto-malononitriles and *o*-iodoanilines were tested. Next, several control experiments were carried out to elucidate a plausible reaction mechanism for this Cu(II)-promoted transformation. Based on the control experiments, literature reports, and intermediate detected by HRMS analysis, a plausible reaction mechanism was proposed (Scheme IV.2). Initially, the γ-ketodinitrile (**1**) undergoes an acid-catalyzed imine formation with 2-iodoaniline (**a**) to form an intermediate (**I**). In the presence of 2,2′-bipyridine (L) and PTSA, the *in situ* generated ligand-bound Cu(II) complex (**A**) undergo coordination with one of the nitrile groups of intermediate (**I**) to form intermediate (**II**). The intramolecular cyclization of (**II**) produces a six-membered cyclic intermediate (**III**) in which the Cu(II) is coordinated with the nitrile *N* atom with the elimination of PTSA. Protonolysis of (**III**) gives intermediate (**IV**) and regenerates the Cu(II) complex (**A**). In the presence of $Cu(OAc)_2·H_2O$/bpy, the intermediate (**IV**) aromatizes to a cyclic imine (**V**) which coordinates with complex (**A**) to give an intermediate (**VI**) *via* elimination of AcOH. The Cu(II) bound intermediate (**VI**) undergo disproportionation in the presence of *in situ* generated Cu(I)OAc to generate a Cu(I) coordinated species (**VII**). A subsequent intramolecular oxidative addition with the iodoaryl generates a Cu(III) intermediate (**VIII**). Next, the exchange of acetate ligand produces an intermediate (**IX**) with the elimination of HI. Finally, the reductive elimination gives the product (**1a**) with the formation of [Cu(I)(OAc)(bpy)] complex which coordinates with PTSA to regenerate the active catalyst (**A**).

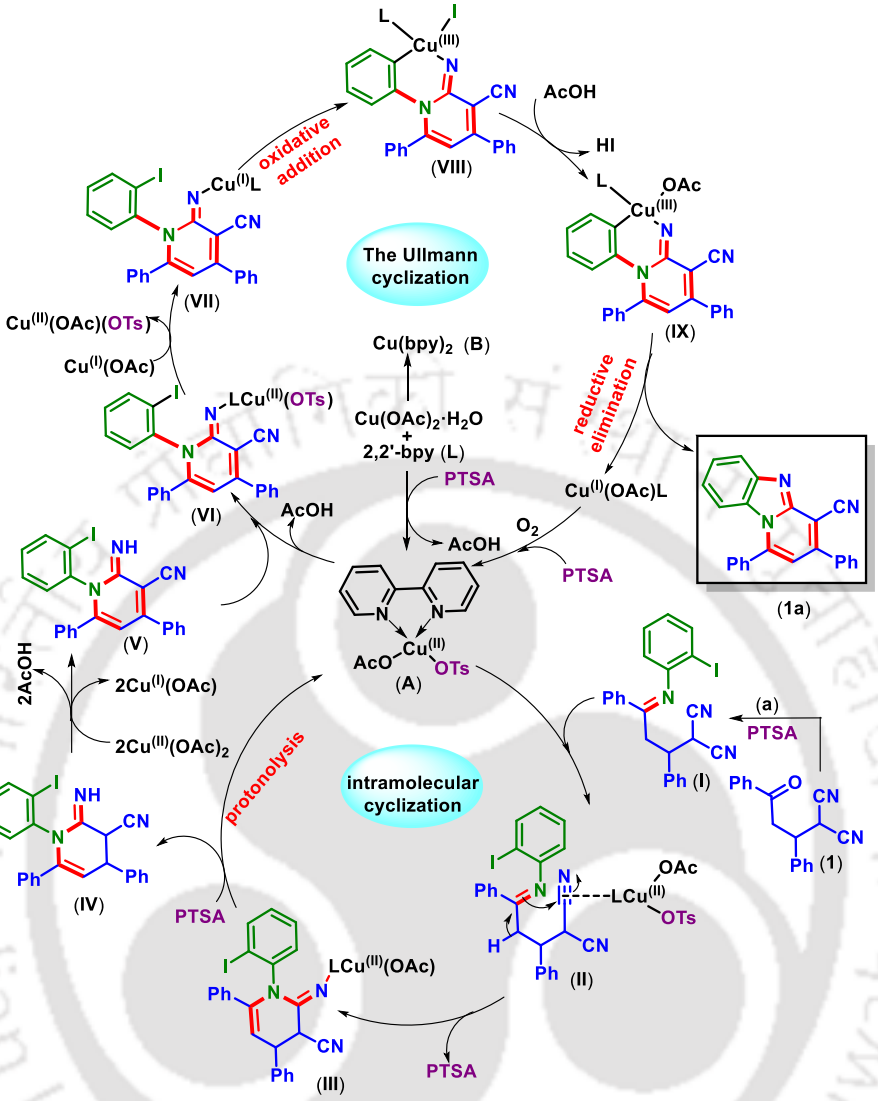

Scheme IV.2. *Proposed reaction path.*

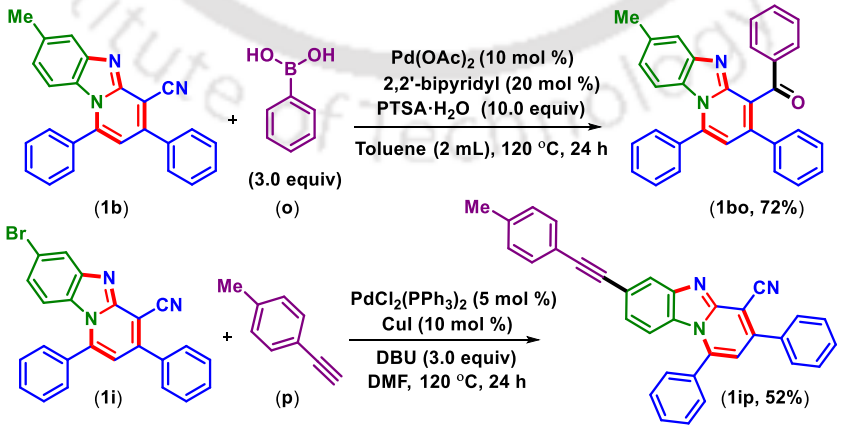

Scheme IV.3. *Post-synthetic applications.*

To further explore the synthetic utility, a few late-stage functionalizations were successfully carried out as shown in Scheme IV.3. As expected the nitrile moiety of **1b** convert into a keto group via Pd(II)-catalyzed addition with phenylboronic acid (**o**) to obtain **1b0** with 72% yield. Further Pd(II)-catalyzed Sonogashira coupling was performed between **1i** and 4-ethyniletoluene (**p**) to produce an alkyne functionalized benz-imidazopyridine (**1ip**) with 52% yield

Usually, π-conjugated nitrogen-containing flat, planner heterocycles display luminogenic behavior under UV light. Thus, the photophysical behavior of some of the synthesized compounds was inspected. The UV-Visible absorption and photoluminescence spectra of **1a**, **3a**, **6a**, **7a**, **8a** [Figure IV.1, (a) and (b)] exhibit two absorption maxima, one in the region of 270–280 nm and the other 338–350 nm and fluorescence emission between 502–533 nm (green region. Therefore, they could be developed as good organic fluorophores having important applications in materials sciences.

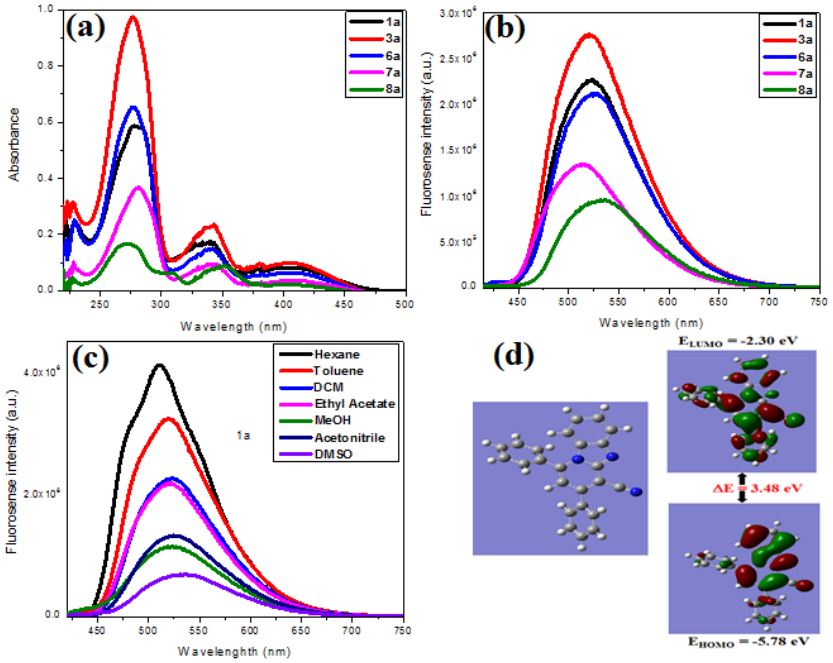

Figure IV.1. *(a) UV-Vis and (b) Photoluminescence spectra of **1a**, **3a**, **6a**, **7a**, **8a** in CH_2Cl_2 (c) Photoluminescence spectra of **1a** in different solvents [concentrations: 1 x 10^{-5} M, excitation wavelength 380 nm] (d) DFT optimized structure and Molecular Orbitals amplitude plots of HOMO and LUMO of **1a** using density functional theory calculation at the B3LYP/6-31G (d, p) basis set level in dichloromethane solvent modelled by the PCM approach.*

The effect of solvent polarity was also examined by measuring the fluorescence emissions of compounds **1a** [Figure IV.1, (c)] in hexane, toluene, DCM, ethyl acetate, MeOH, acetonitrile, and DMSO. The emission wavelengths of compound **1a** in both polar and non-polar solvents were unaffected, suggesting a negligible solvent effect. From the DFT calculation using Gaussian 09 program at the B3LYP/6-31G (d, p) basis set level in dichloromethane solvent modelled by the PCM approach it was found that the LUMO's of compound **1a** is distributed over the entire molecule, while the HOMO is primarily on the benzo[4,5]imidazo[1,2-*a*]pyridine skeleton excluding the two aryl rings at 1 and 3 positions having an energy gap in the range of 3.46–3.57 eV [Figure IV.1, (d)].

CHAPTER V. Visible-Light-Accelerated Pd-Catalyzed Cascade Addition/Cyclization of Arylboronic Acids to γ- and β-Ketodinitriles for the Construction of 3-Cyanopyridines and 3-Cyanopyrrole Analogues

This chapter describes the synthesis of 2,4,6-triarylnicotinonitriles and 2,5-diaryl-1*H*-pyrrole-3-carbonitriles *via* a Pd(II)-catalyzed coupling of arylboronic acid with γ-ketodinitriles and β-ketodinitriles respectively under mild reaction conditions followed by intramolecular cyclization of an intermediate formed after the regeneration of catalyst under acidic reaction conditions. The cascade reactions proceed in 1,2-dichloroethane solvent under visible-light irradiation, and the active catalyst is generated *in situ* in the presence of catalytic amounts of $Pd(OAc)_2$ and 2,2′-bipyridine. The active Pd-catalyst undergoes photoexcitation by the virtue of MLCT, and subsequent redox trans-metalation occurs with arylboronic acid, thus obviating the necessity of any exogenous photosensitizer. The targeted products, composed of a new C–C, a C–N, a C=N, and two new C=C bonds, were isolated in good yields.

In the last couple of decades, visible-light mediated organic syntheses have gained immense popularity due to the advantages associated with this regime. Several organic, as well as transition metal-based photocatalysts, have been developed to harness the energy of abundant visible light and transform it into chemical energy, thereby enabling the generation of carbon-centered radicals under mild catalytic conditions, and hence tapping the novel reactivity of these intermediates. Unprecedented Pd-catalyzed transformations have been achieved under visible-

light irradiation, although an exogenous photo-catalyst may or may not be required. In the case of the latter, the Pd-catalyst plays a dual role in several elegant reactions, for instance, the C_{sp3}-C_{sp2} Heck coupling reaction, carbonylative cross-coupling reactions, and others. The successful underpinnings of these strategies can be attributed to the fact that irradiation of Pd(0) catalyst induces a facile single electron transfer (SET) oxidative addition of unactivated alkyl halide, and the subsequent photoexcitation of Pd(II)-alkyl complex restrains the undesired β-hydride elimination process, which otherwise plagues the traditional reactions.

Previously, our group developed a cascade [4 + 2] Ru(II)-catalyzed annulation strategy for accessing fused isoquinolines, wherein, we noticed that one of the cyano groups, associated with malononitrile moiety, was selectively hydrolyzed. We envisioned that the five-carbon core of the γ-ketomalononitrile may act as a harbinger of pyridine nucleus, if cross-coupled with a suitable partner *via* a cascade [5 + 1] annulation strategy. A thorough literature survey revealed that recently several protocols have been developed for the synthesis of 5- and 6-membered nitrogen heterocycles. These studies are an extension of the catalytic carbopalladation/carbonickelation of eclectic nitrile substrates with suitable coupling partners such as arylboronic acids and arylhydrazines to obtain ketones and imines followed by intramolecular cyclization to afford diverse *N*-heterocycles. A commonality that can be discerned from the mechanisms is that the initial step engages arylboronic acids in a traditional two-electron trans-metalation with electron-deficient Pd(II)-catalysts. The high activation energy barrier associated with this step predisposes the necessity of elevated temperatures. Keeping in mind the natural propensity of Pd-catalyzed reactions to follow a facile SET mechanistic pathway under visible-light irradiation, and arylboronic acids as readily available radical progenitors, we envisaged the synthesis of 2,4,6-triaryl-3-cyanopyridines and 2,5-diaryl-3-cyanopyrrole derivatives (Scheme V.1).

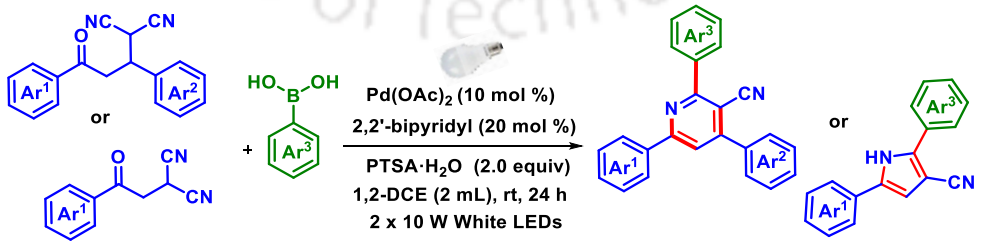

Scheme V.I. *Pd(II)-catalyzed photochemical synthesis of pyridines and pyrroles.*

We embarked on our experimentation by selecting 2-(3-oxo-1,3-diphenylpropyl)malononitrile (0.25 mmol) and phenylboronic acid (1 equiv), $Pd(OAc)_2$ (5 mol %), 2,2′-bipyridine (10 mol %), and $PTSA{\cdot}H_2O$ (1 equiv) in Toluene (2 mL) under 20 W (2 x 10 W) white LEDs at room temperature. The new compound was isolated, and characterized by standard spectroscopic techniques (IR, ^1H NMR, ^{13}C NMR, and HRMS). Delightfully, the analysis confirmed that the isolated compound was 2,4,6-triphenylnicotinonitrile and the yield was estimated to be 33%. Subsequently, single-crystal X-ray diffraction studies were performed on one of the derivatives which further validated the structure of the product**.** After successfully characterizing the desired product, a further screening process was carried out to find the optimal reaction condition. After screening of various reaction parameters, the optimized standard conditions for this transformation were established to be the use of 2-(3-oxo-1,3-diphenylpropyl)malononitrile (**1)** (0.25 mmol), phenylboronic acid (**a)** (3 equiv), $Pd(OAc)_2$ (10 mol %), 2,2′-bipyridine (20 mol %) and $PTSA{\cdot}H_2O$ (2 equiv) in 1,2-DCE (2 mL) as the solvent under irradiation by 20 W (2 x 10 W) white LEDs at room temperature.

With the optimized reaction conditions in hand, this photoreaction was subjected to further studies for the elucidation of substrate scope. Firstly, various γ-ketomalononitriles and arylboronic acids bearing electron-donating and electron-withdrawing groups were taken in a series of different reactions to generate the corresponding triarylsubstituted cyanopyridines. The synthetic utility of this photoreaction was further extended by investigating the addition/cyclization of phenylboronic acids to a few β-ketomalononitriles under the optimized reaction conditions to yield the substituted pyrroles.

Next, to understand the mechanistic underpinnings of the photoreaction, a few control experiments and HRMS analyses of the reaction mixtures at different time intervals were performed. Based on these facts, the likelihood of a conventional SET mechanism involving organic radicals due to visible-light irradiation is not obvious in our case, and a plausible reaction mechanism is outlined (Scheme V.2). Initially, $Pd(OAc)_2$ combines with 2,2′-bipyridyl ligand (**L**) to form a complex $Pd(II)(bpy)(OAc)_2$. The protocol requires 3 equivalents of arylboronic acid with respect to the reacting substrate. The requirement of excess boronic acid can be rationalized by the *in situ* generations of Pd(0) by the reduction of $Pd(II)(bpy)(OAc)_2$, which is also accelerated under visible-light irradiation. Another 2,2′-bipyridine ligand (**L**) combines with the *in situ* generated Pd(0) species, which subsequently undergoes

photoexcitation *via* MLCT to form an excited palladium complex, [L_2Pd(0)*]. Although the next step, that is, transmetalation is not fully understood, we speculate that a redox reaction may be occurring, wherein the excited palladium complex, [L_2Pd(0)*] reduces the phenylboronic acid (**a**). Concomitantly, transfer of aryl group (of boronic acid), and elimination of 2,2′-bipyridine ligand (**L**) occur to give the intermediate (**I**). The redox step may involve the M→Z σ-interaction between the palladium centre and the boron centre of boronic acid. The Pd(II) centre of intermediate (**I**) then coordinates with the γ-ketomalononitrile substrate (**1**) to give the intermediate (**II**). Next, intramolecular carbopalladation of nitrile occurs *via* the insertion of the phenyl group to the nitrile moiety followed by the insertion of an acetate anion to the palladium centre which results in the corresponding ketimine complex (**III**). Later, PTSA·H_2O protonates this intermediate to release 2-(imino(phenyl)methyl)-5-oxo-3,5-diphenylpentanenitrile (**IV**) and coordination of PTSA to the Pd(II) centre forms the intermediate (**VIII**). The intial Pd(II) species is regenerated via the intermidecy of (**IX**) and continues the catalytic cycle. Finally, PTSA·H_2O triggers the intramolecular cyclization of **IV**, which is followed by dehydration to form the intermediate **VII**. Finally, aromatization of the intermediate **VII** affords the desired product, 3-cyano-2,4,6-triphenylpyridine (**1a**).

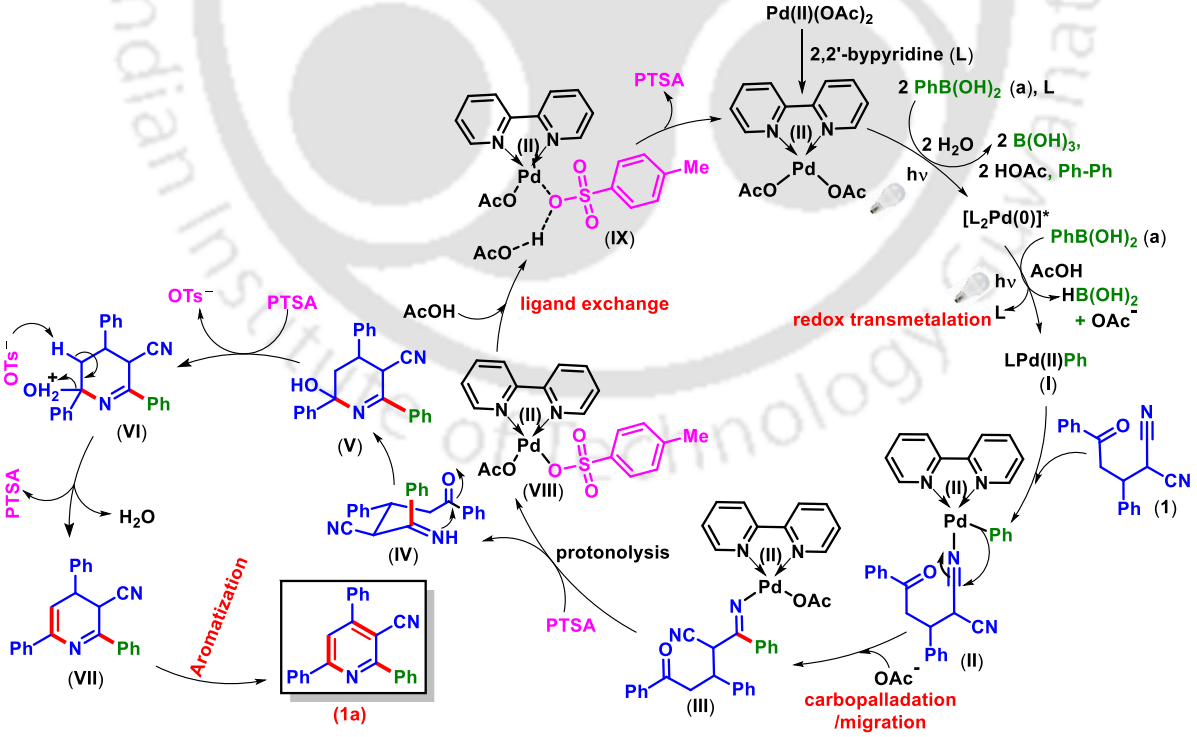

***Scheme V.2**. Proposed mechanistic pathway.*

CONTENTS

Chapter I. An Overview of Nitrile Triggered Access of *N*-Heterocycles under Thermal and Photochemical Processes

Chapter V. Visible-Light-Accelerated Pd-Catalyzed Cascade Addition/Cyclization of Arylboronic Acids to γ- and β-Ketodinitriles for the Construction of 3-Cyanopyridines and 3-Cyanopyrrole Analogues

CHAPTER I

An Overview of Nitrile Triggered Access of N-Heterocycles under Thermal and Photochemical Processes

भारतीय प्रौद्योगिकी संस्थान गुवाहाटी
Indian Institute of Technology Guwahati

CHAPTER I

An Overview of Nitrile Triggered Access of *N*-Heterocycles under Thermal and Photochemical Processes

I.1. Introduction:

The development of effective synthetic methodologies to construct valuable nitrogenous heterocycles is one of the most indispensable targets in organic synthesis. *N*-heterocycles such as pyrroles,[1] pyridone/pyridines,[2] indoles,[3] isoquinolines/isoquinolones,[4] imidazopyridines,[5] furopyridines[6] and other fused rings *N*-containing compounds[7] (Figure I.1.1) have grabbed extensive attention in synthetic organic chemistry. These *N*-heteroarenes are appreciated as key building blocks in many bioactive compounds, constitute the core skeleton of many drug molecules, found as a ubiquitous unit in various natural products, playing important roles in the pharmaceuticals especially, as antitumor, antibacterial, antiviral, antifungal, anticancer, anti-inflammatory agents, treatment of specified contagious diseases, and used as key intermediates and ligands in many organic transformations.

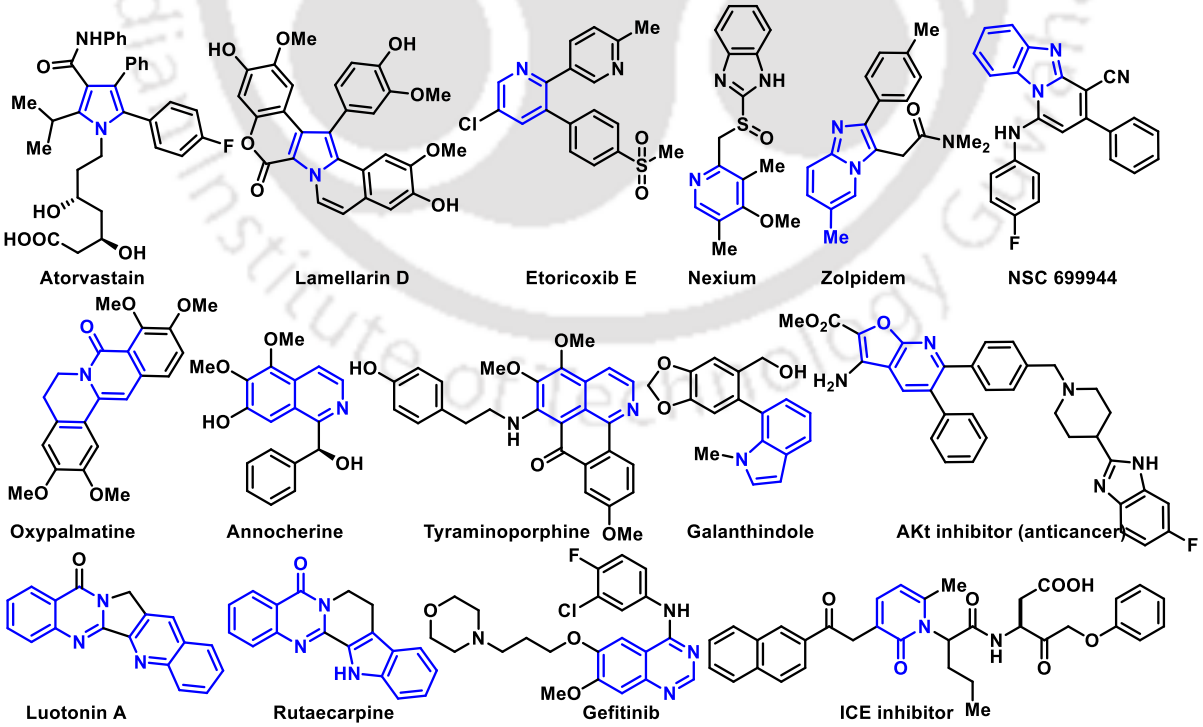

Figure I.1.1. *Representative active N-heterocycles as core fragments.*

Additionally, due to conspicuous photo and electrochemical properties, they have broadly been used in the arena of materials chemistry and other fields of research.[8] In particular, highly substituted π-conjugated polycyclic *N*-heteroarenes were found to be very useful in functional materials. They have been comprehensively used as organic semiconductors, luminescent materials, organic light-emitting diodes (OLEDs), liquid crystal displays (LCDs), cell imaging, and several other multifaceted applications (Figure I.1.2).[9] Therefore, given the importance there is continuous interest in the improvement of convenient, efficient, environmentally benign synthetic methods and successful implementation for the construction of these essential *N*-heterocycles.

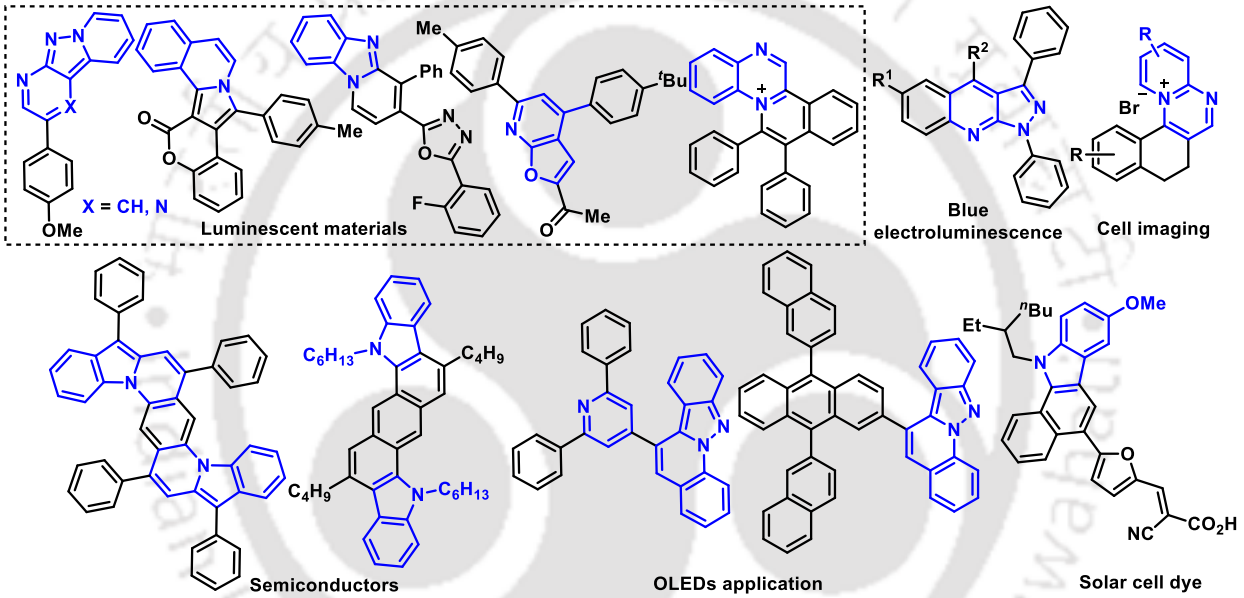

Figure I.1.2. *Representative N-heterocycles as functional materials.*

Amidst the varieties of methods established, the synthesis of *N*-heterocycles involving cyano or nitrile functionality is of significant interest and an exciting concept either *via* thermal or photochemical processes. Generally, the nitrile group (–C≡N) is playing a pivotal role in the field of organic synthesis as a predominant precursor of various other functional groups or intermediates such as imine, ketone, amide, acid, amine, aldehyde, as a versatile directing group in C–H bond functionalization reactions and as a radical acceptor in radical cascade reactions.[10] The conversion of nitrile into other functional groups mainly proceeds *via* nucleophilic addition, hydrolysis, or reduction under transition metal or metal-free conditions. Typically, (i) the nucleophilic reactivity of lone electron pairs on the *N*-atom, (ii) the π-coordination reactivity of

the C–N triple bond, and (iii) the electrophilic reactivity of the carbon center of the cyano group contribute towards its numerous transformations. Due to the presence of this polar unsaturated C–N triple bond, mostly the reactions of nitriles concentrated on their transformations into carbonyl (C=O), amine/imine (NH_2, =NH), amide/acid ($CONH_2$, CO_2H). Further, cyclization with suitable functional groups, especially with the amine /keto group present in the proximity or transition-metal-catalyzed intramolecular amination with bromo (Br) or iodo (I) group or C–H amination gives diverse *N*-heterocycles (Figure I.1.3).[11] On the contrary the intermolecular [3 + 2] or [2 + 2 + 2] cycloadditions of nitriles with azides or alkynes provide tetrazoles or pyridines without functional group interconversion and the nitrile nitrogen atom becomes an intrinsic part of these heteroarenes (Figure I.1.3).[12] Consequently the presence of nitrile functionality offers a fascinating and emerging opportunity for the construction of *N*-heterocyclic skeletons when it is suitably functionalized or activated in an organic molecule.

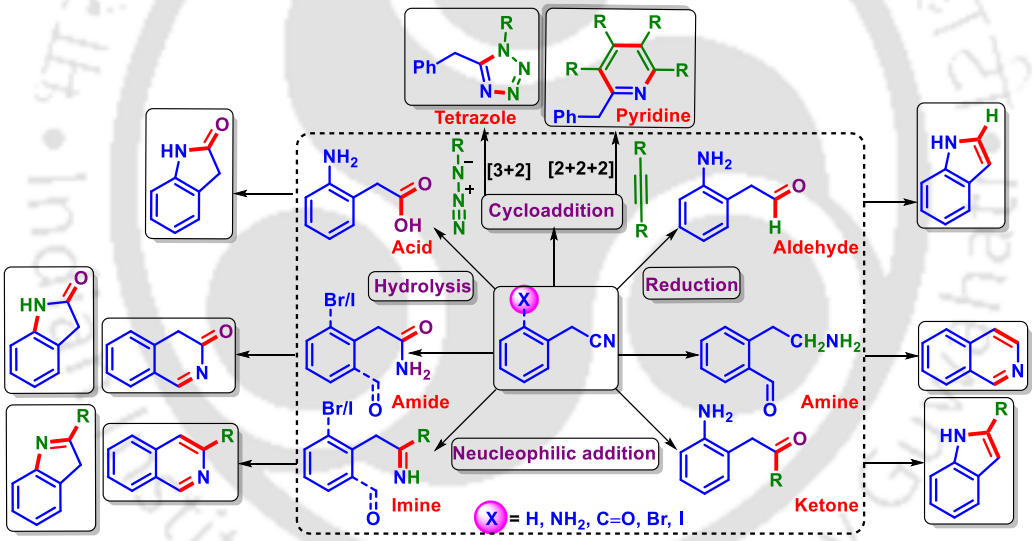

Figure I.1.3. *Conversion of nitrile to other functional groups and N-heterocycles.*

One of the cheapest and environmentally benign ways to introduce such nitrile functionality into an organic molecule is the use of malononitrile for the synthesis of a wide range of *N*-heterocycles.[13] Malononitrile is used to design synthetic precursors *viz.* 2-(2-oxo-2-arylethyl)malononitrile (β-ketodinitrile), and 2-(3-oxo-1,3-diarylpropyl)malononitrile (γ-ketodinitriles) *via* the nucleophilic substitution of α-bromoacetophenone and Michael addition with chalcone (Figure I.1.4).[14] These precursors contain nitrile functionality that is close to the keto group and thus very much expedient as synthetic precursors for diverse *N*-heteroarenes.

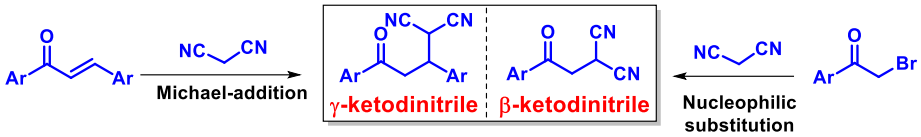

Figure I.1.4. *Synthesis of nitrile precursors.*

However, these synthetic precursors remain less explored in literature either thermally or photochemically. There are few reports available utilizing both these β- and γ-ketodinitriles for the synthesis of nitrogen and oxygen heterocycles as well as carbocycles.[15] For example, in 2017, Wang *et. al*. developed an efficient synthesis of enantioenriched 3,4-dihydro-2*H*-pyran-carbonitriles from racemic γ-ketodinitriles *via* dynamic kinetic resolution (DKR)–asymmetric transfer hydrogenation (ATH) followed by a cascade cyclization process (Scheme I.1.1).[15a] This powerful DKR–ATH–cyclization cascade process delivers the targeted enantioenriched 3,4-dihydro-2*H*-pyran-carbonitriles with high enantio- and diastereoselectivities.

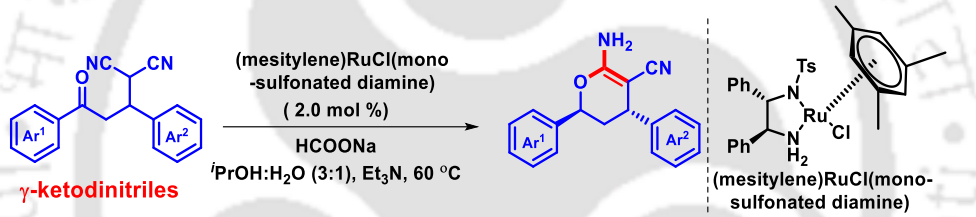

Scheme I.1.1. *Synthesis of o-heterocycles from γ-ketodinitriles.*

In 2018, Han and co-workers used the β-ketodinitriles for a one-step, effective synthesis of highly functionalized cyclopentenes *via* cascade cycloaddition with electron-deficient olefins (Scheme I.1.2).[15b] Herein tetrabutylammonium fluoride (TBAF) works as an effective organocatalyst allowing the construction of multi-functionalized cyclopentenes having an allylic quaternary carbon center bearing both cyano and carboxamide groups with high diastereoselectivity.

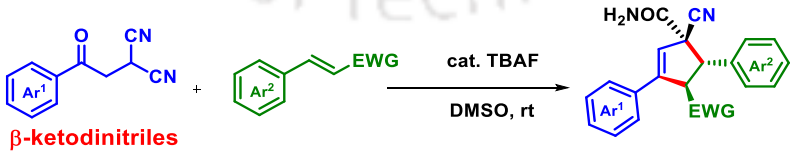

Scheme I.1.2. *Synthesis of functionalized cyclopentenes from β-ketodinitriles.*

In the same year, Wei-Ke Su and Zhen-Hua Li group utilize both the β- and γ-ketodinitriles for a one-pot cascade strategy to achieve 2,4-dichloro-substituted

pyrano[2,3-*d*]pyrimidines and furo[2,3-*d*]pyrimidines respectively (Scheme I.1.3).[15c] The reaction is mediated by triphosgene and triphenylphosphine oxide to afford synthetically useful products in moderate to good yields.

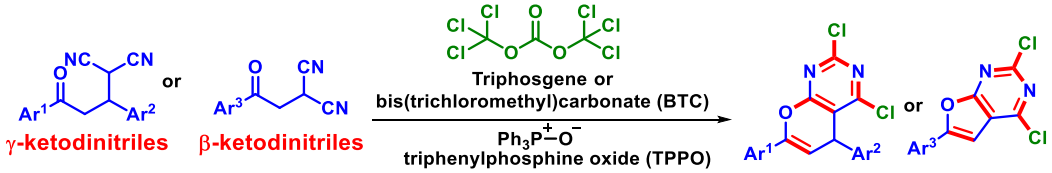

Scheme I.1.3. *Synthesis of N-heterocycles from β- and γ-ketodinitriles.*

In 2019, Ban and co-workers disclosed the enantioselective synthesis of functionalized cyclopentenes containing a quaternary chiral center (Scheme I.1.4).[15d] The reaction proceeded through a thiosquaramide-catalyzed cascade Michael−Henry reaction between nitroolefins and β-ketodinitriles giving the product up to 98% enantioselectivity.

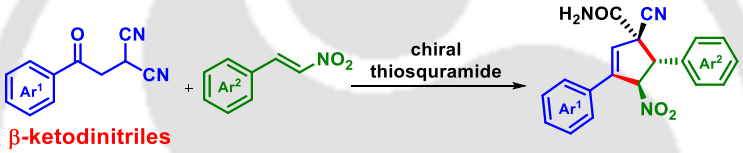

Scheme I.1.4. *Synthesis of functionalized cyclopentenes from β-ketodinitriles.*

In 2019, Sun *et al.* developed *a* synthesis of diverse 4,5-substituted-1*H*-pyrrole-3-carbonitriles in excellent yields using commercially available HZSM-5 and Pd/C as recyclable heterogeneous catalysts (Scheme I.1.5).[15e]

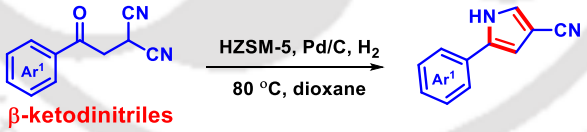

Scheme I.1.5. *Synthesis of NH-pyrroles from β-ketodinitriles.*

In 2020, a similar synthesis of substituted 1*H*-pyrrole-3-carbonitriles was developed by the Yu group *via a* palladium(II)-catalyzed C_{sp}–C_{sp2} coupling of arylboronic acids with β-ketodinitriles through the intramolecular formation of C–N bonds (Scheme I.1.6).[15f]

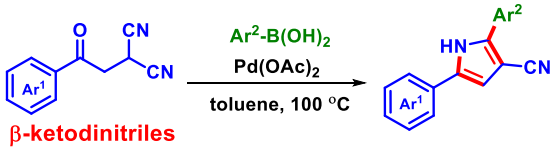

Scheme I.1.6. *Pd(II)-catalyzed synthesis of N-H-pyrroles from β-ketodinitriles.*

A substrate-controlled tributylphosphine-catalyzed [3 + 2] annulation of β-ketodinitriles with allenoates was demonstrated by Kishor Mohanan (Scheme I.1.7).[15g] This procedure enables the synthesis of multi-functionalized cyclopentene carboxamides and cyclopentenols *via* Michael/aldol/nucleophilic cyclization sequence. The allenic esters bearing a substituent at the c-position provided an unprecedented formation of cyclopentene carboxamide while unsubstituted allenoates produced cyclopentenols.

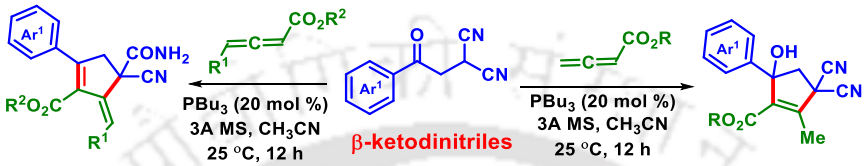

Scheme I.1.7. *Substrate-controlled synthesis of carbocycles from β-ketodinitriles.*

In 2022, our group reported the synthesis of thio-functionalized pyrroles using β-ketodinitriles and thiophenols in the presence of Eosin Y as a photocatalyst under green light irradiation (Scheme I.1.8).[15h] The mechanistic investigation reveals a photo-induced selective thiyl radical addition to one of the nitrile groups of β-ketodinitriles followed by a nucleophilic attack and aromatization process.

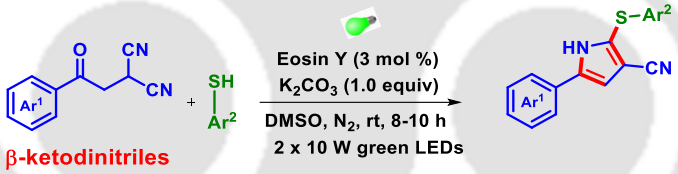

Scheme I.1.8. *Photochemical synthesis of thio-functionalized pyrroles from β-ketodinitriles.*

This thesis report comprises newer methodologies demonstrating the synthesis of privileged *N*-heterocycles from β- and γ-ketodinitrile precursors under thermal and photochemical conditions through the construction of C–C and C–N bonds concerning the followings:

I.2. Synthesis of *N*-heterocycles *via* transition-metal-catalyzed C–H/N and C–H/N–H oxidative alkyne annulations.

I.3. Synthesis of cyclic compounds *via* alkyne insertion into the nitriles.

I.4. Synthesis of *N*-heterocycles *via* thermal and photochemical cascade addition/cyclization of nitriles.

I.2. Synthesis of *N*-Heterocycles *via* Transition-Metal-Catalyzed C–H/N and C–H/N–H Oxidative Alkyne Annulations:

I.2.1. Directing Group-Assisted C–H Bond Activation:

The transition-metal-catalyzed C–H bond activation is prevalent in organic synthesis for the construction of the C–C bond.[16] In general, the directing group (DG) assisted C–H bond activation by the use of a coordinative functional group has offered important advantages.[17] This activation strategy uses the proximate effect *via* the coordination of functional group-containing heteroatoms such as nitrogen (N), oxygen (O), and sulfur (S) which can chelate with the metal center of the catalyst that brings about regioselective C–H bond activation. In the course of C−H bond activation, a metal (M) is inserted in between the C−H bond thereby forming a C−M species. This is followed by the formation of either a five or a six-member chelated metallacycle which is the key intermediate in coupling reactions (Scheme I.2.1.1).[18] The commonly used transition metals in the C−H bond activation process are generally cobalt (Co), rhodium (Rh), iridium (Ir), ruthenium (Ru), palladium (Pd), and nickel (Ni).

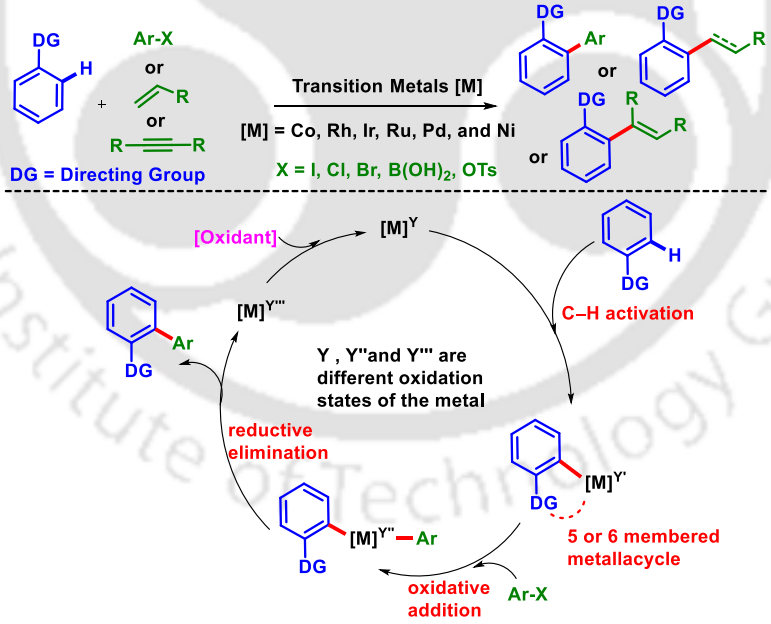

Scheme I.2.1.1. *Transition metal-catalyzed C–H bond activation.*

I.2.2. Directing Group-Assisted Oxidative Alkyne Annulation:

The directing group (DG) assisted transition-metal-catalyzed incorporation of alkynes leading to cyclic product is known as oxidative alkyne annulation. An alkyne can be inserted

into the *ortho*-C_{Sp2}–H bond, either *via* an intramolecular cyclization with the directing heteroatom or *via* simultaneous insertion between the C_{Sp2}–H/heteroatom(X)–H bonds. These oxidative alkyne annulations are environmentally friendly and are useful for the synthesis of a variety of heterocyclic compounds *via* the formation of C–C and C–heteroatom(X) bonds in a step economical fashion (Scheme I.2.2.1).[19] The directing group assisted alkyne annulation has several advantages, such as (i) DGs participate in subsequent organometallic transformation as nucleophiles or electrophiles, (ii) DGs remain an intrinsic part of the desired cyclic product, and (iii) it avoids extra steps.

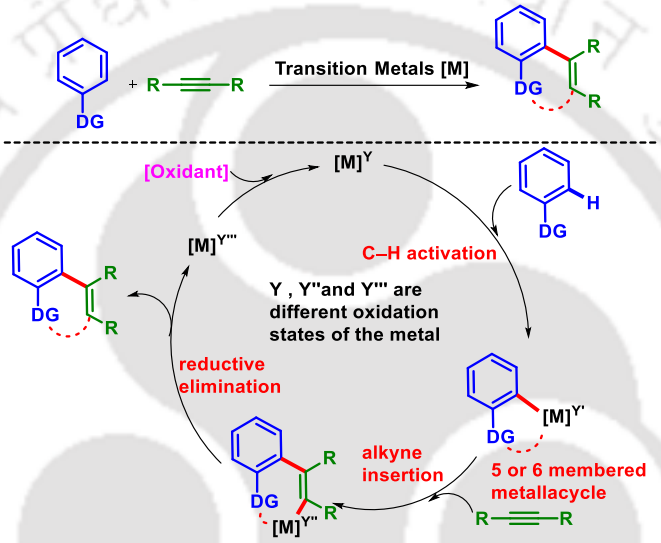

Scheme I.2.2.1. *Directing group-assisted oxidative alkyne annulation.*

I.2.3. Nitrogen Directing Group for the Synthesis of *N*-Heterocycles *via* Oxidative Alkyne Annulation:

In the chelation-assisted transition-metal-catalyzed C–H bond activation, nitrogen directing groups have been used for the synthesis of *N*-heterocycles through the formation of C–C and C–N bonds. Based on the nature of the nitrogenous directing group the annulation process can be divided into the following two categories.

I.2.3.1. C–H/N Alkyne Annulation:

In this annulation process, the lone pair on the nitrogen atom directs the active metal species to get inserted into the *ortho*-C–H bond, thereby forming a cyclic metal complex. The cyclic metal complex on subsequent alkyne insertion followed by the reductive elimination leaves the nitrogen atom as part of the final product (Scheme I.2.3.1.1).

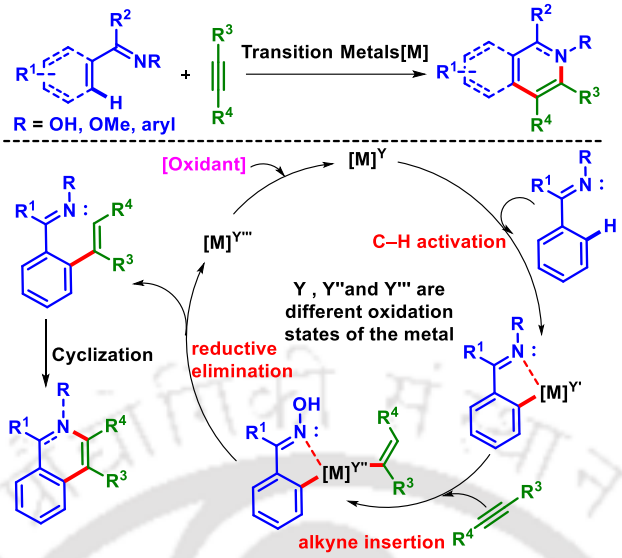

Scheme I.2.3.1.1. *C–H/N oxidative alkyne annulation.*

I.2.3.2. C–H/N–H Alkyne Annulation:

When the nitrogen atom of the directing group has acidic hydrogen then concurrent activation of both C–H and N–H bonds occurs. In this case, at first, the active metal catalyst forms a cyclic metal complex *via* a concerted deprotonative metalation generally through N–H/C–H dual activation. A subsequent alkyne insertion and reductive elimination of the metal affords *N*-heterocycles *via* C–C and C–N bond formation (Scheme I.2.3.2.1).

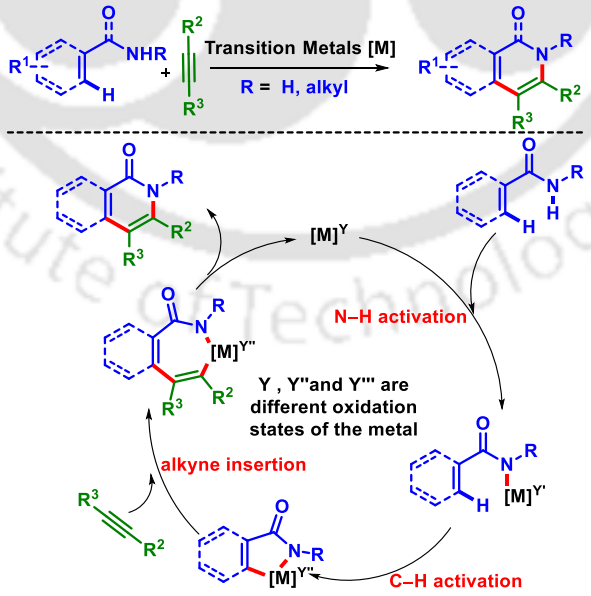

Scheme I.2.3.2.1. *C–H/N–H oxidative alkyne annulation.*

These sequential C–H/N or C–H/N–H oxidative alkyne annulations are exploited for the assembly of valuable *N*-heterocycles particularly (i) pyrroles, (ii) pyridines/pyridones, (iii) indoles, (iv) isoquinolines/isoquinolones, and (v) various other π-conjugated polycyclic *N*-heteroaromatics.

I.2.3.3. Synthesis of Pyrrols:

The five-membered heterocycle, pyrrole is synthesized *via* transition metal-catalyzed C–H/N–H alkyne annulation. In 2010, Glorius *et al.* described a Rh(III)-catalyzed pyrrole synthesis *via* the allylic C(sp^3)–H bond activation of enamines followed by an intermolecular coupling with unactivated alkynes under oxidative conditions (Scheme I.2.3.3.1).[20]

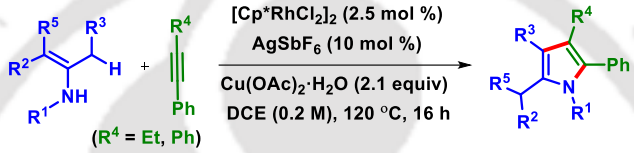

Scheme I.2.3.3.1. *Synthesis of pyrrole via allylic C(sp^3)–H/N–H alkyne annulation.*

In 2013, the Ackermann group reported a Ru(II)-catalyzed synthesis of diversely decorated pyrrole through C–H/N–H oxidative alkyne annulation strategy using electron-rich enamines (Scheme I.2.3.3.2).[21] This expedient pyrrole synthesis was accomplished aerobically with air as the ideal terminal oxidant.

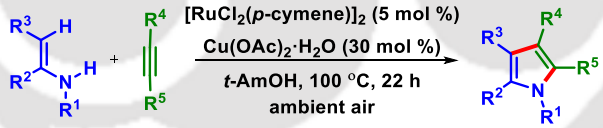

Scheme I.2.3.3.2. *Ru(II)-catalyzed pyrrole synthesis by C–H/N–H alkyne annulation.*

In the same year, Baiquan Wang and co-workers reported a Ru(II)-catalyzed pyrrole synthesis *via* oxidative annulation of enamides and alkynes (Scheme I.2.3.3.3).[22] The reaction provides both *N*-acyl substituted or NH pyrroles by slightly modifying the reaction conditions.

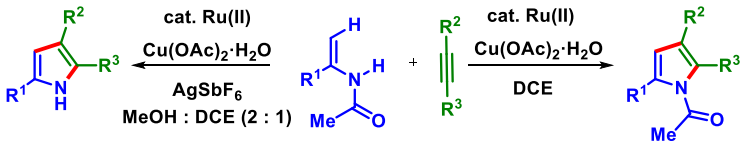

Scheme I.2.3.3.3. *Ru(II)-catalyzed pyrrole synthesis.*

In 2013, Liu *et al*. developed a competent synthesis of *N*-acetylpyrroles *via* cationic Ru(II)-catalyzed oxidative alkyne annulation of enamides in dimethoxyethane (DME) (Scheme I.2.3.3.4).[23] The reaction can also be carried out in an aqueous medium providing 95% yield when diphenylacetylene was used but with substituted diphenylacetylenes, the yield decreased significantly in the aqueous medium.

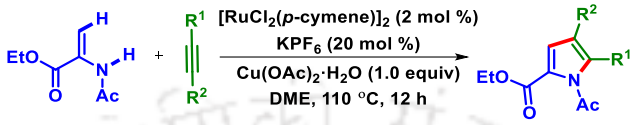

Scheme I.2.3.3.4. *Cationic Ru(II)-catalyzed synthesis of N-acetylpyrroles.*

In 2014, Guan *et al.* established an efficient Pd(II)-catalyzed alkenyl C–H activation and oxidative alkyne annulation of enamides for the synthesis of substituted *N*-acetylpyrroles (Scheme I.2.3.3.5).[24] This Pd(II)-catalyzed oxidative annulation tolerates a wide range of functional groups and is a reliable procedure for rapid elaboration of readily available aryl enamides into a variety of valuable triaryl substituted pyrroles in high yields.

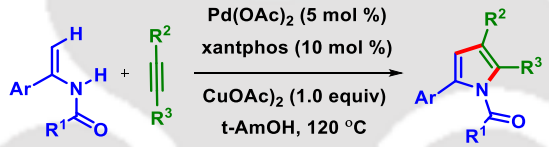

Scheme I.2.3.3.5. *Pd(II)-catalyzed synthesis of N-acetylpyrroles.*

In the same year, Loh and co-workers demonstrated another Pd(II)-catalyzed cyclization between enamides and alkynes using oxygen as the sole oxidant. The simple reaction conditions permit this methodology to be used as a general tool for the preparation of multi-substituted pyrroles (Scheme I.2.3.3.6).[25]

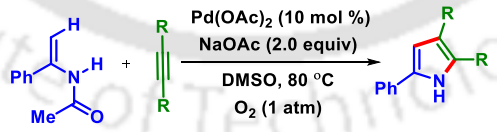

Scheme I.2.3.3.6. *Pd(II)-catalyzed synthesis of multi-substituted pyrroles.*

In 2016, Pawar *et al.* described a Co(III)-catalyzed oxidative alkyne annulation with enamides for the synthesis of *N*-acetylpyrroles at room temperature in excellent yields (Scheme I.2.3.3.7).[26] The reaction works well with various internal alkynes with broad substates scope and functional group tolerance. Synthetically useful *NH* pyrroles can also be obtained through this protocol at elevated temperatures.

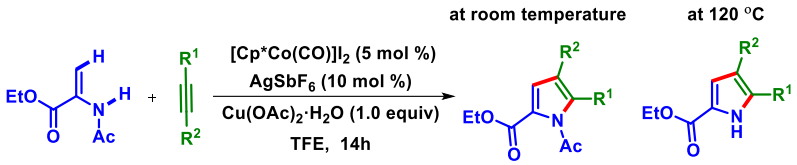

Scheme I.2.3.3.7. *Co(III)-catalyzed synthesis of substituted pyrroles.*

I.2.3.4. Synthesis of Pyridines and 2-Pyridones:

The six-membered nitrogen-containing heterocycles pyridines and 2-pyridones can be synthesized *via* transition metal-catalyzed alkyne annulation. For example, in 2008, the Cheng group reported a synthesis of pentasubstituted pyridines through a Rh(I)-catalyzed insertion of alkynes into the alkenyl C–H bond of α,β-unsaturated ketoximes followed by an intramolecular 6π-electrocyclization (Scheme I.2.3.4.1).[27]

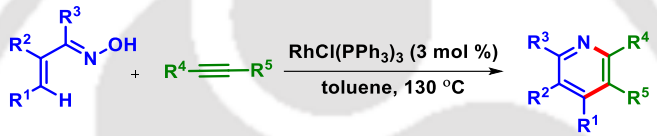

Scheme I.2.3.4.1. *Rh(I)-catalyzed synthesis of substituted pyridines.*

In 2010, Li *et al*. demonstrated the synthesis of 2-pyridones *via* a Rh(III)-catalyzed oxidative C–H/N–H alkyne annulation with acrylamides in the presence of $Cu(OAc)_2$ as an oxidant (Scheme I.2.3.4.2).[28]

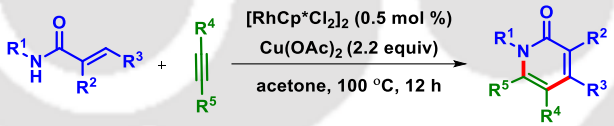

Scheme I.2.3.4.2. *Rh(III)-catalyzed synthesis of 2-pyridones.*

In 2011, a similar synthesis of substituted 2-pyridones was developed by Ackermann and co-workers executing a Ru(II)-catalyzed C–H/N–H oxidative alkyne annulation through C–C and C–N bond formation (Scheme I.2.3.4.3).[29] They used various electron-rich and electron-deficient *N*-substituted acrylamides as well as diaryl- and dialkyl-substituted internal alkynes which shows a broad and improved range of substrates scope.

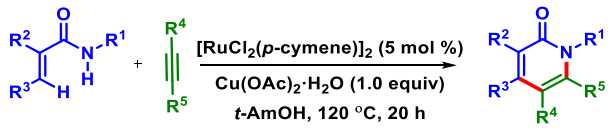

Scheme I.2.3.4.3. *Ru(II)-catalyzed synthesis of 2-pyridones.*

I.2.3.5. Synthesis of Indoles:

Indoles are well-known nitrogen-containing heterocycles having fused six and five-membered rings and can be synthesized through transition metal-catalyzed C–H/N–H alkyne annulation. In 2008, Fagnou and co-workers reported a synthesis of indoles *via* a Rh(III)-catalyzed oxidative coupling between *N*-acetyl anilines and internal alkynes (Scheme I.2.3.5.1).[30]

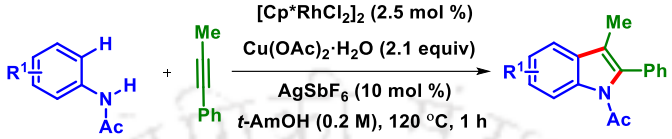

Scheme I.2.3.5.1. *Indole synthesis via Rh(III)-catalyzed C–H/N–H alkyne annulation.*

In 2012, Ackermann and co-workers demonstrated a cationic Ru(II)-catalyzed oxidative C–H/N–H alkyne annulation with 2-pyrimidyl substituted anilines to synthesize substituted indole derivatives (Scheme I.2.3.5.2).[31] Herein, the oxidative alkyne annulation occurs through the construction of C–C and C–N bonds using water as the solvent. Mechanistic studies indicate that the reaction proceeds through the reversible formation of a six-membered ruthenacycle as the key intermediate.

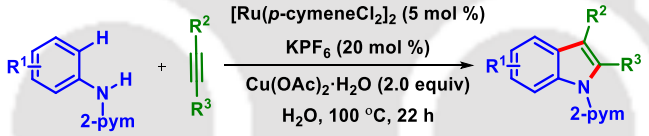

Scheme I.2.3.5.2. *Ru(II)-catalyzed synthesis of indoles.*

In 2013, Ackermann disclosed a Ni(0)-catalyzed step-economical synthesis of indoles through alkyne annulations with anilines bearing removable directing groups. The C–H/N–H activation strategy efficiently occurred in the absence of any metal oxidants with excellent selectivities (Scheme I.2.3.5.3).[32]

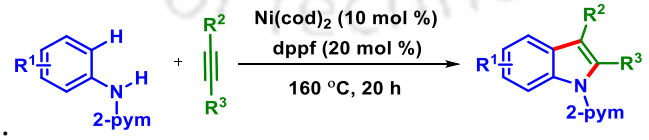

Scheme I.2.3.5.3. *Ni(0)-catalyzed solvent-free synthesis of indoles.*

In 2014, Huang *et al.* developed a synthesis of *N*-substituted indoles *via* N–N bond cleavage of pyrazolidin-3-one followed by a Ru(II)-catalyzed redox-neutral C–H activation

(Scheme I.2.3.5.4).[33] The reaction proceeds *via* a Ru(II)-catalyzed C–H/N–H bond activation, alkyne insertion, internal oxidation of Ru(II) to Ru(IV), and reductive elimination pathways.

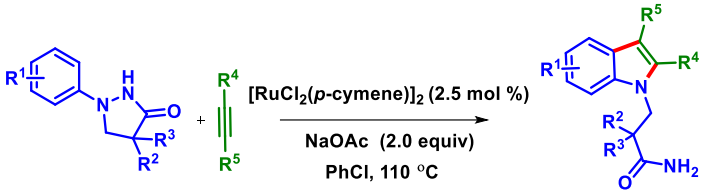

Scheme I.2.3.5.4. *Ru(II)-catalyzed synthesis of indoles via N–N bond cleavage.*

In 2018, Xu *et al*. established a Ru(II)-catalyzed C–H/N–H oxidative annulation for the efficient synthesis of indoles (Scheme I.2.3.5.5).[34] The reaction occurs electrochemically in a simple undivided cell in an aqueous solution using *N*-2-pyrimidyl-substituted anilines and internal alkynes as coupling partners. In this electrolysis reaction, the electric current is used to regenerate the active ruthenium catalyst instead of any external oxidant.

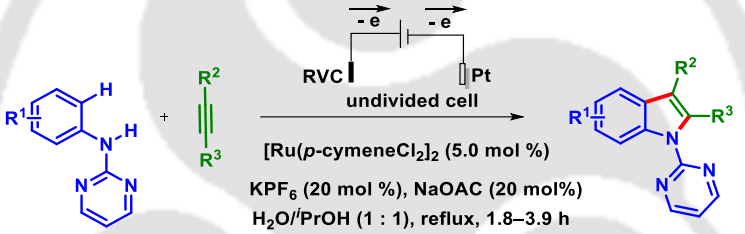

Scheme I.2.3.5.5. *Ru(II)-catalyzed electrochemical synthesis of indoles.*

I.2.3.6. Synthesis of Isoquinolines/Isoquinolones:

Among fused ring nitrogen-containing heterocycles, isoquinolines/isoquinolones are well-known for having two fused six-membered rings. Over the years a tremendous number of publications have appeared on their synthesis *via* transition metal-catalyzed alkyne annulation. In 2009, Miura and co-workers reported a Rh(III)-catalyzed oxidative coupling between aromatic imines with internal alkynes for the synthesis of isoquinolines through *a* regioselective C–H bond cleavage (Scheme I.2.3.6.1).[35]

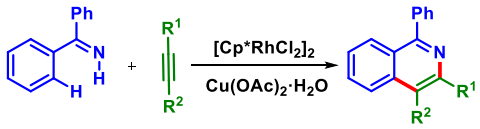

Scheme I.2.3.6.1. *Rh(III)-catalyzed synthesis of isoquinolines.*

In 2011, Ackermann *et al*. reported a Ru(II)-catalyzed annulations between *N*-substituted benzamides and internal alkynes for the chemo- and site-selective synthesis of isoquinolones

(Scheme I.2.3.6.2).[36] Herein, functionalization of both C–H and N–H bonds occurs during the reaction and mechanistic studies in deuterated ^{t}AmOH suggest an irreversible C–H bond ruthenation. Further, the kinetic isotope effect (KIE) study provided strong evidence for a carboxylate assistance rate-limiting C–H bond ruthenation.

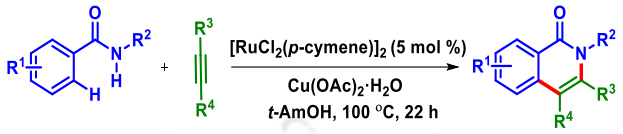

Scheme I.2.3.6.2. *Ruthenium-catalyzed synthesis of isoquinolones.*

In the same year, the Ackermann group established a synthesis of isoquinolones *via* an external oxidant-free carboxylate assisted Ru(II)-catalyzed C–H/N–H annulation from *N*-methoxybenzamides and *N*-hydroxybenzamides in an aqueous medium (Scheme I.2.3.6.3).[37] In this annulation process, the N–O bond of *N*-methoxybenzamides served as the internal oxidant, and free hydroxamic acids were also found to be good substrates due to the chemoselectivity of the ruthenium(II) carboxylate catalyst.

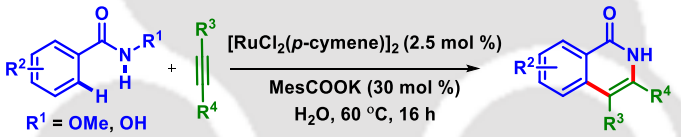

Scheme I.2.3.6.3. *Ru(II)-catalyzed synthesis of isoquinolines in an aqueous medium.*

In 2012, the Huang group reported a Pd(II)-catalyzed atom economical synthesis of isoquinolones *via* C–H/N–H oxidative annulation between *N*-substituted benzamides and internal alkynes (Scheme I.2.3.6.4).[38] Further, the unsymmetrical alkynes provided excellent yields and good regioselectivity in this Pd(II)-catalyzed alkyne annulation.

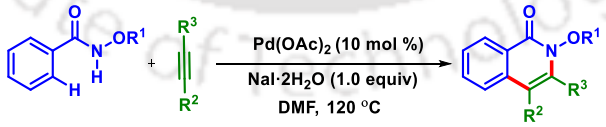

Scheme I.2.3.6.4. *Pd(II)-catalyzed synthesis of isoquinolones.*

In 2012, Jaganmohan and co-workers reported a synthesis of substituted isoquinolines *via* a Ru(II)-catalyzed C–H/N annulation between aromatic/heteroaromatic ketoximes and internal alkynes as well as terminal alkynes in good to excellent yields with high regioselectivity (Scheme I.2.3.6.5).[39]

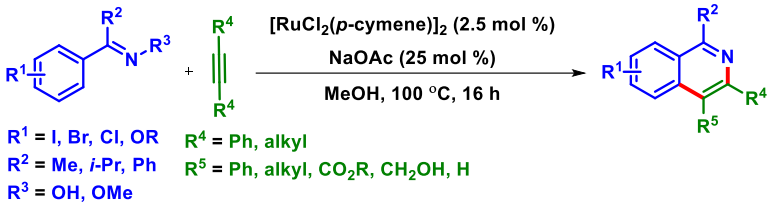

Scheme I.2.3.6.5. *Ru(II)-catalyzed regioselective synthesis of isoquinolines.*

In 2012, Ackermann *et al.* also reported a redox-neutral alkyne annulation between ketoximes and internal alkynes for the expedient synthesis of isoquinolines (Scheme I.2.3.6.6).[40] The reaction proceeds through carboxylate-free cationic ruthenium(II)-catalyzed C–H bond activation with reversible cycloruthenation.

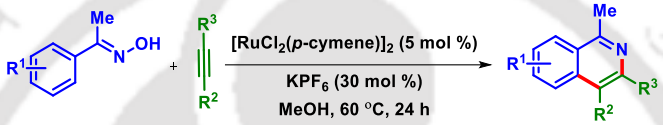

Scheme I.2.3.6.6. *Cationic Ru(II)-catalyzed synthesis of isoquinolines.*

In 2013, Urriolabeitia and co-workers developed a Ru(II)-catalyzed oxidative C–H/N–H annulation between unprotected primary amines (benzylamines) and internal alkynes for the synthesis of isoquinolines (Scheme I.2.3.6.7).[41]

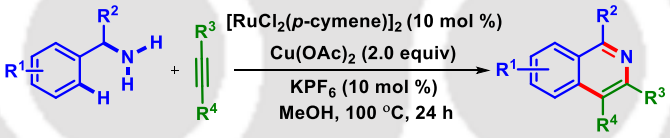

Scheme I.2.3.6.7. *Ru(II)-catalyzed synthesis of isoquinolines from benzylamines.*

In 2014, the Li group reported a Rh(III)-catalyzed synthesis of isoquinolines from benzylidenehydrazones and internal alkynes *via* C–H/N annulation (Scheme I.2.3.6.8).[42] This process is understood *via* cleavage of the N–N bond followed by sequential C–H activation and cyclization with internal alkynes.

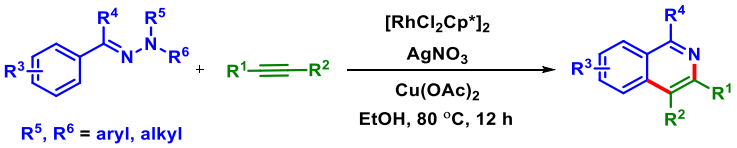

Scheme I.2.3.6.8. *Rh(III)-catalyzed synthesis of isoquinolines from benzylidenehydrazones.*

In 2014, Daugulis *et al.* reported a Co(II)-catalyzed synthesis of isoquinolones *via* aminoquinoline-directed C(sp^2)–H bond activation (Scheme I.2.3.6.9).[43] This method provides excellent functional-group tolerance and both internal and terminal alkynes are also compatible in this coupling process.

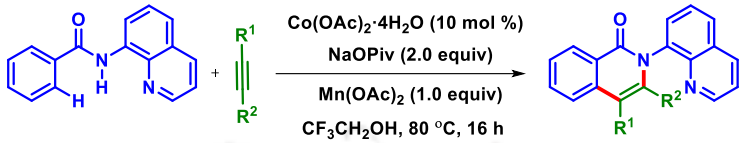

Scheme I.2.3.6.9. *Co(II)-catalyzed synthesis of isoquinolones.*

In 2014, Ackermann reported an external oxidant-free dehydrative alkyne annulation *via* an *in situ* generated Ru(II) biscarboxylate catalyst. This reaction proceeds through a C–H/N–H oxidative alkyne annulation followed by N–OH cleavage to give isoquinolones in an aqueous medium (Scheme I.2.3.6.10).[44] The ruthenium(II) catalyst derived from the electron-deficient carboxylic acid *m*-$(F_3C)C_6H_4CO_2H$ displayed highly regio- and site-selective C–H functionalizations with a broad substrate scope. Further, detailed mechanistic studies suggest a kinetically relevant C–H metalation by carboxylate assistance along with subsequent migratory alkyne insertion, reductive elimination, and intramolecular oxidative addition.

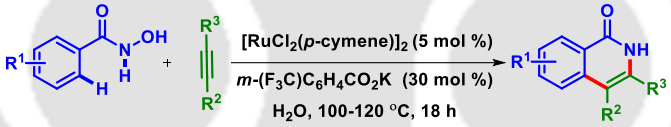

Scheme I.2.3.6.10. *Ru(II)-catalyzed external oxidant free synthesis of isoquinolones.*

In the same year, the Ackermann group demonstrated the synthesis of 1-aminoisoquinolines *via* C–H/N–H oxidative alkyne annulation of aryl and heteroaryl amidines (Scheme I.2.3.6.11).[45] In this reaction a cationic Ru(II) complex is generated *in situ* from KPF_6 or AgOAc and displayed a reversible C–H bond activation followed by C–H/N–H alkyne annulation with the high site-, regio- and, chemoselectivity.

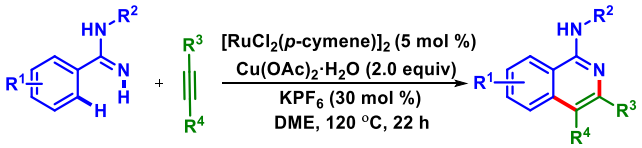

Scheme I.2.3.6.11. *Ru(II)-catalyzed synthesis of 1-aminoisoquinolines.*

In the year 2014, Swamy and co-workers used 8-aminoquinoline as an auxiliary bidentate directing group for a Ru(II)-catalyzed oxidative annulation of *N*-quinolin-8-yl-benzamides with alkynes to achieve isoquinolones with high regioselectivity, broad substrates scope and broad functional group tolerance (Scheme I.2.3.6.12).[46] The reaction occurs in the presence of $[RuCl_2(p\text{-cymene})]_2$ as the catalyst and $Cu(OAc)_2{\cdot}H_2O$ as an oxidant with the involvement of a monoacetate complex [RuCl(OAc)(*p*-cymene)] instead of the bis-acetate complex $[Ru(OAc)_2(p\text{-cymene})]$. The mechanistic studies reveal the involvement of a ruthenium *N*-quinolin-8-yl-benzamide complex (i.e. *N*, *N*-bidentate chelate complex).

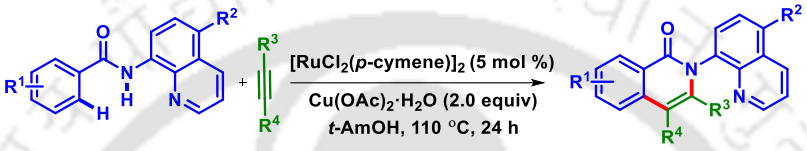

Scheme I.2.3.6.12. *Ru(II)-catalyzed synthesis of isoquinolones.*

In 2015, Sundararaju *et al.* described an efficient Co(III)-catalyzed external oxidant free redox-neutral C–H/N oxidative alkyne annulation between aromatic ketoximes and internal alkynes (Scheme I.2.3.6.13).[47] The reaction offers multi-substituted isoquinolines with decent yields and excellent functional group tolerance including heterocycles.

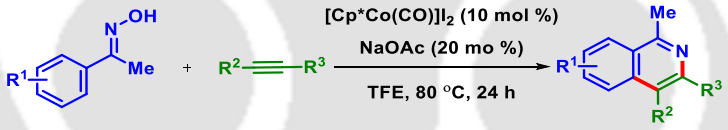

Scheme I.2.3.6.13. *Co(III)-catalyzed synthesis of isoquinolines.*

In 2017, Gogoi *et al.* reported a Ru(II)-catalyzed C–H/N–H oxidative annulation of benzamidines and internal alkynes for the facile synthesis of 1-aminoisoquinolines with excellent regioselectivity (Scheme I.2.3.6.14).[48]

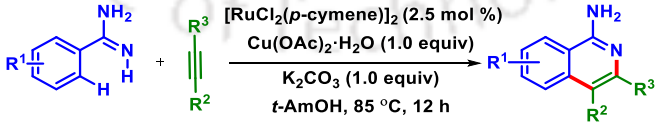

Scheme I.2.3.6.14. *Ru(II)-catalyzed synthesis of isoquinolines.*

In 2017, Urriolabeitia *et al.* described a carboxylate-assisted Ru(II)-catalyzed synthesis of isoquinoline-1-carboxylate derivatives through C–H/N–H oxidative alkyne annulation between *N*-unprotected methyl esters of phenyl glycine and internal alkynes (Scheme I.2.3.6.15).[49] The *N*-

fluoro-2,4,6-trimethylpyridinium triflate works as the terminal oxidant and the process shows a remarkable tolerance to the presence of diverse electron-releasing and electron-donating functional groups at the phenyl ring of the amino acid.

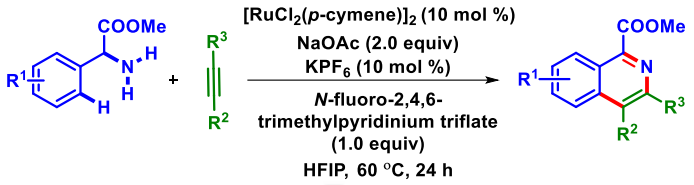

Scheme I.2.3.6.15. *Ru(II)-catalyzed synthesis of isoquinoline-1-carboxylate.*

I.2.3.7. Synthesis of π-Conjugated Polycyclic *N*-Heteroarenes:

The transition-metal-catalyzed C–H/N–H oxidative alkyne annulation is an excellent method for the construction of various π-conjugated polycyclic *N*-heteroaromatics. For example, in 2010, the Li group reported a Rh(III)-catalyzed oxidative C–H/N–H annulation between primary benzamides and internal alkynes to synthesize 5,6,13-triaryl-8*H*-isoquinolino[3,2-*a*]isoquinolin-8-ones (Scheme I.2.3.7.1).[50]

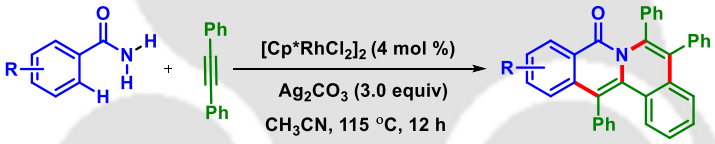

Scheme I.2.3.7.1. *Rh(III)-catalyzed synthesis of polycyclic N-heteroarenes.*

In 2012, Ackermann *et al.* reported a Ru(II)-catalyzed synthesis of fused polycyclic indolo[2,1-*a*]isoquinolines and pyrrolo[2,1-*a*]isoquinolines *via* an aerobic oxidative coupling of internal alkynes with 2-arylindoles and 2-aryl pyrroles respectively (Scheme I.2.3.7.2).[51] The reaction occurs in the presence of the catalytic amount of $Cu(OAc)_2 \cdot H_2O$ and air as the oxidant.

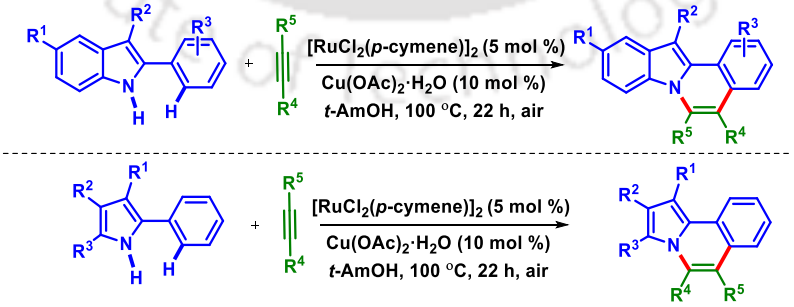

Scheme I.2.3.7.2. *Ru(II)-catalyzed synthesis fused polycyclic N-heteroarenes.*

In the same year, the Ackermann group developed a cationic Ru(II)-catalyzed effective C–H/N–H oxidative annulations strategy to provide conjugated pyrazolo[5,1-*a*]isoquinolines with both aryl- and alkyl-substituted alkynes (Scheme I.2.3.7.3).[52]

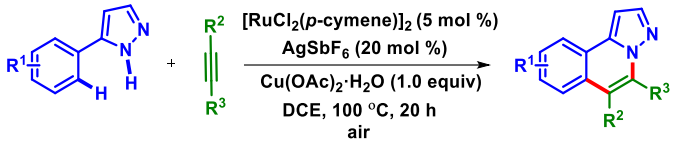

Scheme I.2.3.7.3. *Cationic Ru (II)-catalyzed synthesis of pyrazolo[5,1-a]isoquinolines.*

In 2014, Wang and co-workers reported a Ru(II)-catalyzed oxidative C–H/N–H alkyne annulation of 2-phenyl imidazoles to access imidazo[2,1-*a*]isoquinolines in the presence of para-benzoquinone as the oxidant (Scheme I.2.3.7.4).[53] A wide range of electron-deficient alkynes are converted into fused isoquinolines with high chemo- and regioselectivity.

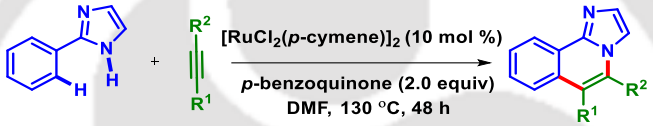

Scheme I.2.3.7.4. *Ru (II)-catalyzed synthesis of imidazo[2,1-a]isoquinolines.*

In 2014, Chien-Hong Cheng reported a one-pot synthesis of naphthyridine-based polyheteroaromatic compounds *via* a Rh(III)-catalyzed multiple C–H/N–H alkyne annulation between *N*-hydroxybenzamidines and alkynes in excellent yields (Scheme I.2.3.7.5).[54]

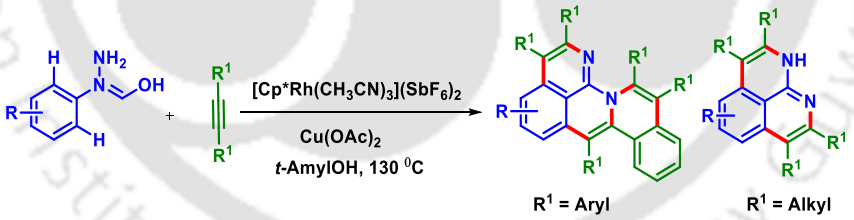

Scheme I.2.3.7.5. *Rh(III)-catalyzed synthesis of naphthyridine-based poly-N-heterocycles.*

In the same year, the Peng group demonstrated a C–H/N–H annulation of quinazolones with internal alkynes for the facile construction of fused tetracyclic heteroarenes in the presence of $[RuCl_2(p\text{-cymene})]_2$ and $Cu(OAc)_2{\cdot}H_2O$ under mild reaction conditions (Scheme I.2.3.7.6).[55]

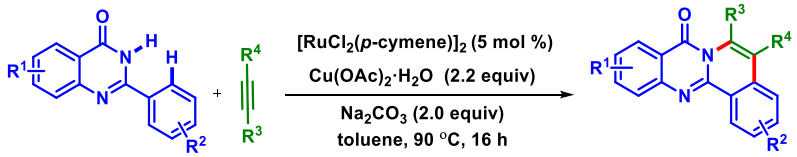

Scheme I.2.3.7.6. *Ru(II)-catalyzed synthesis of tetracyclic heteroarenes.*

In 2015, one-pot synthesis of fused polycyclic nitrogen-heteroarenes, 5,6-aryl-8*H*-isoquinolino[1,2-*b*]quinazolin-8-ones was reported by Nanubolu *et al. via* a Ru(II)-catalyzed oxidative C–H/N–H annulation between heteroaryl dihydroquinazolinones and internal alkynes followed by dehydrogenation (Scheme I.2.3.7.7).[56] This method does not require copper salt as the external oxidant, rather oxidation occurs by molecular oxygen.

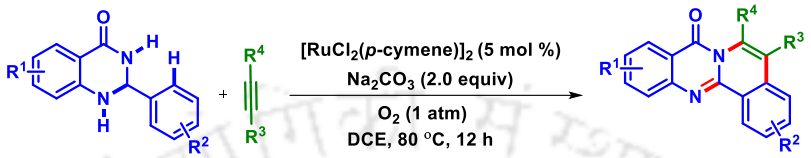

Scheme I.2.3.7.7. *Ru (II)-catalyzed external oxidant free synthesis of N-heteroarenes*

In 2017, Swamy and co-workers achieved an *N*-aryl substituted amide group-directed, Ru(II)-catalyzed regioselective C–H/N–H oxidative annulation between 2*H*-chromene-3-carboxamides with internal alkynes (Scheme I.2.3.7.8).[57] The method provides easy access to benzopyran-fused 2-pyridones. In addition, using an excess of the alkyne a double C–H bond activation occurred in the same pot, which most likely involves a Ru–N covalent bond and a Ru–O coordinative bond.

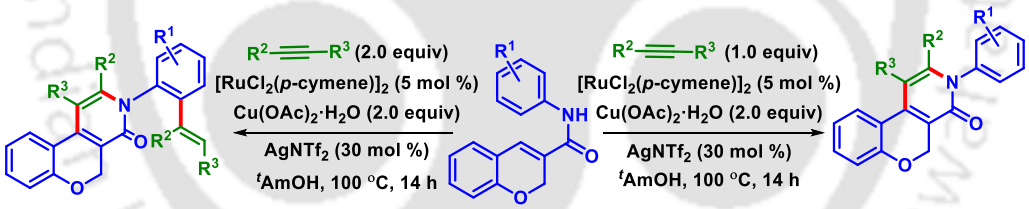

Scheme I.2.3.7.8. *Ru(II)-catalyzed synthesis of benzopyran-fused 2-pyridones.*

In 2019, Tang and co-workers reported an electrochemically enabled Ru(II)-catalyzed dehydrogenative C–H/N–H alkyne annulation of primary benzamides (Scheme I.2.3.7.9).[58] The method provides the synthesis of 5,6,13-triaryl-8*H*-isoquinolino[3,2-*a*]isoquinolin-8-ones through a double C−H/N–H bond activation process.

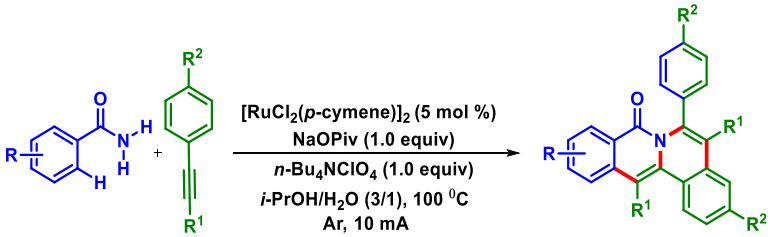

Scheme I.2.3.7.9. *Ru(II)-catalyzed electrochemical synthesis of polycyclic isoquinolinones.*

I.3. Synthesis of Cyclic Compounds *via* Alkyne Insertion into the Nitriles (–C≡N):

The transition-metal-catalyzed oxidative alkyne annulation has been verified as a powerful and prevalent synthetic tool for the construction of diverse *N*-heterocycles *via* the formation of C–C and C–N bonds efficiently and economically. In this endeavor development of newer unprecedented annulation methodologies involving the nitrile or cyano, functionality remains an important quest in organic synthesis. Despite the flexibility to transform into various other functional groups, nitrile functionality has long been considered inactive in organometallic reagents. Hence the nitriles such as acetonitrile, benzonitrile, etc are widely employed as a solvent in most transition metal-mediated reactions. Further, the nitrile group remains as a ligand in a few metal catalysts like palladium chloride bisacetonitrile or palladium chloride bisbenzonitrile.[59] Therefore, owing to the inherent inertness of the cyano group towards organometallic reagents the transition-metal-catalyzed oxidative alkyne annulations strategies involving nitrile functionality offers a challenging but exciting opportunity to the synthetic organic chemist for creating cyclic compounds.

I.3.1. Synthesis of Carbocycles *via* Alkyne insertion into the Nitriles:

The alkyne insertion methodology has been developed as a convenient route to various carbocycles involving intramolecular cyclization with the nitrile group. In this regard long back ago in 2002, Larock developed the synthesis of 2,3-diarylindenones from 2-iodobenzonitrile and internal alkyne *via* an intramolecular carbopalladation of the nitrile (Scheme I.3.1.1).[60] This reaction is the first example of the addition of an organopalladium species across the carbon-nitrogen triple bond and is familiarly known as Larock's annulation.

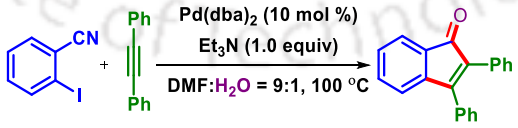

Scheme I.3.1.1. *Pd(0)-catalyzed synthesis of indenones.*

A plausible reaction mechanism for this transformation is shown below (Scheme I.3.1.2). The reaction is initiated *via* the oxidative addition of Pd(0) into the C–I bond thereby giving an aryl-Pd(II) species. Next the alkyne insertion between *in situ* generated aryl–palladium bond

produces alkenylpalladium(II) which is followed by nucleophilic addition to the proximal nitrile and finally hydrolysis provides a wide variety of 2,3-diarylindenones.

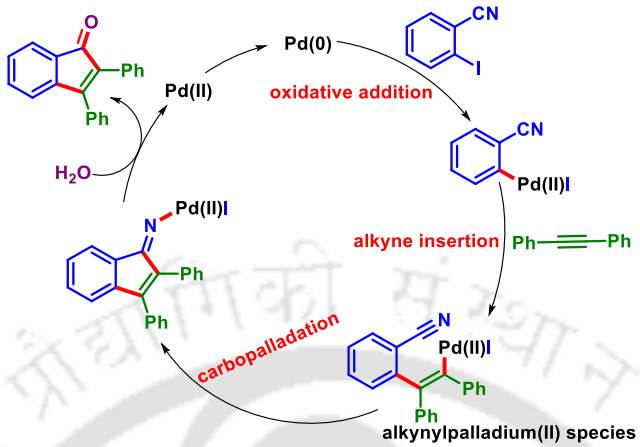

Scheme I.3.1.2. *The mechanism for the Pd(0)-catalyzed synthesis of indenones.*

Following the same intramolecular carbopalladation of the cyano group, in 2003, they developed a Pd(II)-catalyzed synthesis of 3,4-disubstituted 2-aminonaphthalenes from 2-iodophenylacetonitriles and internal alkynes with good yields and regioselectivity (Scheme I.3.1.3).[61] Herin the reaction is initiated *via* the *in situ* generations of Pd(0) from Pd(II), oxidative addition with C–I bond, alkyne insertion between aryl–palladium bond, nucleophilic addition of alkenylpalladium(II) to the proximal nitrile and finally aromatization.

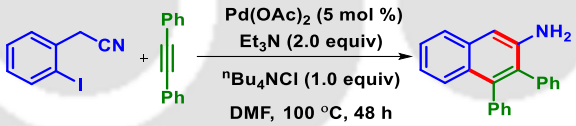

Scheme I.3.1.3. *Pd(II)-catalyzed synthesis of 2-aminonaphthalenes.*

In 2005, Murakami and co-workers reported a Rh(I)-catalyzed [3 + 2] annulation strategy between 2-cyanophenylboronic acids and internal alkynes leading to the formation of 2,3-indenones (Scheme I.3.1.4).[62] The reaction is conducted *via* an intramolecular nucleophilic addition of an *in situ* generated organo-rhodium(I) species to the cyano group.

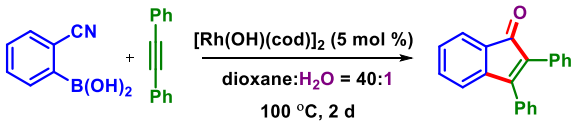

Scheme I.3.1.4. *Rh(I)-catalyzed synthesis of indenones.*

Later in 2016, Tsukamoto *et al.* improved this annulation with internal alkynes by taking 2-(cyanomethyl)phenylboronates as the nitrile precursors leading to the formation of 3,4-disubstituted 2-naphthalenamines (Scheme I.3.1.5).[63] The reaction is catalyzed by a (dppe)-ligated palladium(II) complex in methanol under relatively mild reaction conditions. The reaction proceeds *via* initial transmetalation of the palladium(II) complexes with the boronates, then alkyne insertion to generate an alkenylpalladium(II) species, followed by an intramolecular nucleophilic addition to the cyano group.

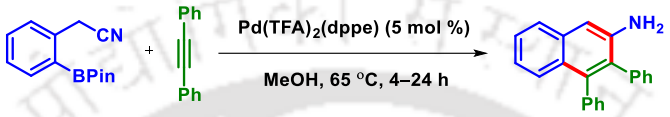

Scheme I.3.1.5. *Pd(II)-catalyzed synthesis of 2-aminonaphthalenes.*

I.3.2. Synthesis of *N*-heterocycles *via* Alkyne Insertion into the Nitriles:

Extensive and well-organized advancement has been made in the field of transition metal-catalyzed alkyne insertion into the nitrile for the construction of specific nitrogenous heteroarenes. In this context, the transition metal-catalyzed [2 + 2 + 2] cycloaddition of alkynes with nitriles provides multi-substituted pyridines, and the oxidative alkyne annulation of nitriles *via* hydrolysis into amides gives isoquinolines.

I.3.2.1. Alkyne Insertion *via* [2 + 2 + 2] cycloaddition with Nitrile:

The [2 + 2 + 2] cycloaddition of a nitrile with alkyne-alkyne or alkyne-nitrile with an alkyne provided substituted pyridine. For example. in 2005, Louie and co-workers reported a mild and efficient method for the synthesis of a wide range of cyclopentane-fused pyridines from methyl terminated tethered alkynes and benzonitriles *via* a combination of a Ni(0) catalyst and an imidazolylidene (Scheme I.3.2.1.1).[64a] The reaction is also subjected to an untethered alkyne namely 3-hexyne to obtain pentasubstituted pyridine. Later in 2013, a detailed mechanistic investigation was conducted for a $Ni(IPr)_2$-catalyzed [2 + 2 + 2] cycloaddition of diynes and nitriles through kinetic analysis of these reactions which give the evidence for the formation of a Key η1-$Ni(IPr)_2(RCN)$ intermediate.[64b]

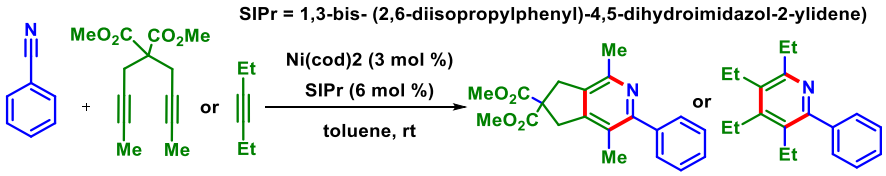

Scheme I.3.2.1.1. *Ni(0)-catalyzed synthesis of pyridines from benzonitrile.*

In 2012, Takeuchi *et al.* developed a similar cycloaddition of α,ω-diynes accommodating a wide range of nitriles catalyzed by $[Ir(cod)Cl]_2$/DPPF or BINAP (Scheme I.3.2.1.2).[65] In this protocol both aliphatic and aromatic nitriles smoothly reacted with α,ω-diynes to give pyridines. The high regioselectivity is obtained with unsymmetrical diyne bearing two different internal alkyne moieties.

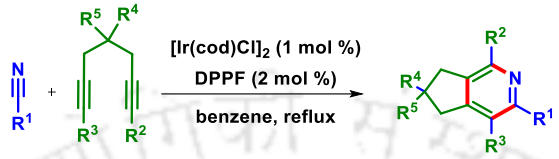

Scheme I.3.2.1.2. *Ir(I)-catalyzed synthesis of pyridines from nitriles.*

In 2020, the Wang group demonstrated an iron(II)–cobalt(II) co-catalysis for the cycloaddition of untethered internal as well as terminal alkynes to nitriles under mild reaction conditions leading to the synthesis of polysubstituted pyridines in a single step. (Scheme I.3.2.1.3).[66] This reaction facilitates the preparation of 2,3,4,5,6-pentafuntionalized pyridines which are valuable luminescent materials.

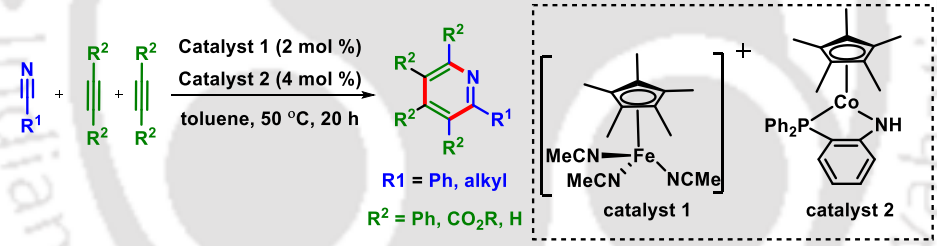

Scheme I.3.2.1.3. *Fe(II)/Co(II)-catalyzed synthesis of pyridines from nitriles.*

Recently in 2021, an inexpensive Co(II)-catalyzed fully intermolecular [2 + 2+ 2] cycloaddition using unactivated nitriles and internal alkynes leading to pentasubstituted pyridines is reported (Scheme I.3.2.1.4).[67] The reaction is well-tolerated with a broad range of substrates scope covering aryl, heteroaryl, and alkyl substituents in all of the reacting partners. The reaction proceeds through the oxidative coupling of two alkynes, insertion of the nitrile into a cobaltacyclopentadiene, and finally, C–N reductive elimination is supported by DFT.

Scheme I.3.2.1.4. *Co(II)-catalyzed synthesis of pyridines from nitriles.*

A general mechanistic pathway for this metal-catalyzed cycloaddition between alkynes and nitrile for the synthesis of pyridine is shown below (Scheme I.3.2.1.5). Initially, the metal [M] coordinated with two alkyne partners giving a metallacyclopentadiene *via* subsequent oxidative coupling. Next, the nitrile partner coordinates through two possible pathways. (i) insertion into the [M]–C bond to give cycloheptametallacycle or (ii) intramolecular [4 + 2] cycloaddition to form a bicyclic complex. Finally, after reductive elimination or isomerization of the cycloheptametallacycle or bicyclic complex respectively affords the pyridine and the metal is decoordinated.

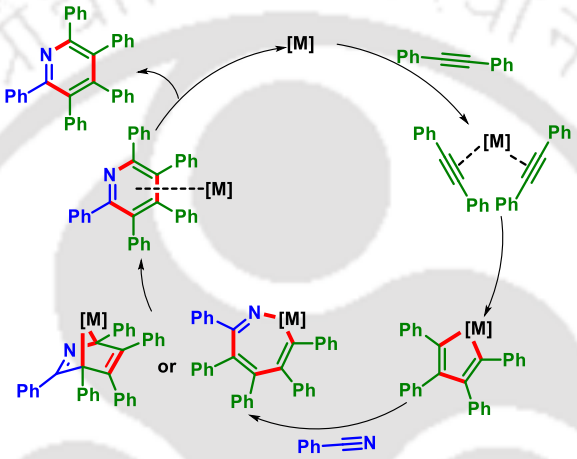

Scheme I.3.2.1.5. *Mechanistic pathway for the [2 + 2 + 2] cycloaddition of nitriles.*

In 2016, Liu and co-workers developed an efficient Ni(0)-catalyzed synthesis of multi-substituted fused-pyridines in the presence of a Lewis acid *via* a [2 + 2 + 2] cycloaddition of alkyne-nitriles with alkynes (Scheme I.3.2.1.6).[68] Mechanistic studies reveal the formation of a five-membered azanickelacycle intermediate through intramolecular hetero coupling between alkyne and nitrile followed by intermolecular insertion of an alkyne.

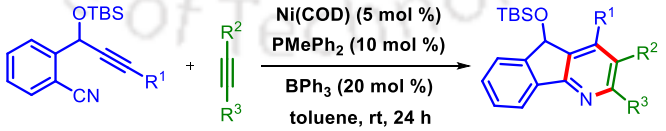

Scheme I.3.2.1.6. *[2 + 2 + 2] cycloaddition of benzene-tethered alkyne-nitriles with alkynes.*

I.3.2.2. Alkyne Insertion *via* hydrolysis of Nitrile:

In 2013, Jaganmohan *et al*. described a Ru(II)/Cu(II)-catalyzed cyclization of aromatic and heteroaromatic nitriles *via* oxidative annulation with internal alkynes in the acetic acid

medium under air to afford substituted isoquinolones in good to excellent yields (Scheme I.3.2.2.1).[69] The reaction is initiated through the hydrolysis of the nitrile into a primary amide ($CONH_2$) in the presence of $Cu(OAc)_2{\cdot}H_2O$ in acetic acid. Further, an amide-directed Ru(II)-catalyzed C–H/N–H oxidative annulation with internal alkyne provided substituted isoquinolone.

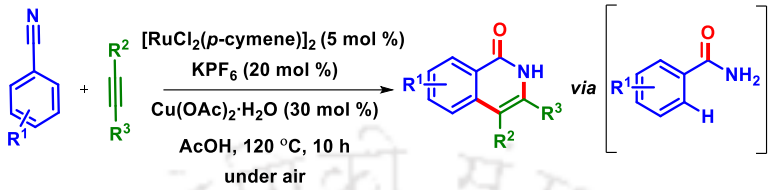

Scheme I.3.2.2.1. *Synthesis of isoquinolones via hydrolysis of nitriles.*

I.3.3. Synthesis of *N*-Heterocycles *via* Intramolecular Alkyne Insertion into the Nitriles:

The development of nitrile-triggered access of *N*-heterocycles further proceeds when both the nitrile and alkyne remain as an integral part of the same precursors such as *o*-alkynylarylnitriles (Figure I.3.3.1).[70] Herein, the alkynes attached at the *ortho* position trigger the reactivity of the precursor leading to the synthesis of diverse *N*-heteroarenes through nucleophilic addition to the nitrile followed by intramolecular insertion with the alkyne. Another possible way of accessing nitrogenous compounds from this precursor is the nucleophilic attack of an *N*-nucleophile onto the nitrile followed by annulation with the alkyne. However, in the latter case alkyne is not inserted into the nitrile rather it triggered the process allowing the nucleophile to be a part of the heteroarenes.

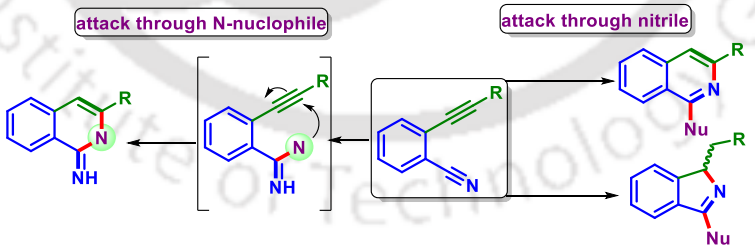

Figure I.3.3.1. *Synthesis of N-heterocycles from o-alkynylarylnitrile.*

In 2010, a Pt(II)-catalyzed facile synthesis of 1-alkoxyisoquinolines *via* intramolecular 6-endo-dig cyclization of ortho-alkynylbenzonitriles was reported by Li in an alcoholic medium (Scheme I.3.3.1).[70a]. The reaction is initiated by the Pt(II)-induced nucleophilic addition of an

alkoxide to the nitrile, and then the addition of the alkyne occurs to form the C–Pt bond. Protonation of the C–Pt bond provides the isoquinoline and regenerates the Pt catalyst.

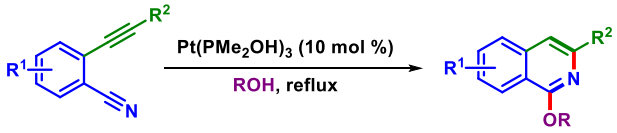

Scheme I.3.3.1. *Pt(II)-catalyzed synthesis of isoquinolines from o-alkynylbenzonitriles.*

In the same year, Xei and co-workers developed titanium catalyzed stereospecific synthesis of aminoisoindole from the reaction between *o*-alkynylarynitrile and amine with various functional groups tolerance (Scheme I.3.3.2).[70b]. The reaction is initiated *via* a nucleophilic attack on the nitrile by amine followed by a 5-exo-dig cyclization to deliver the aminoisoindoles.

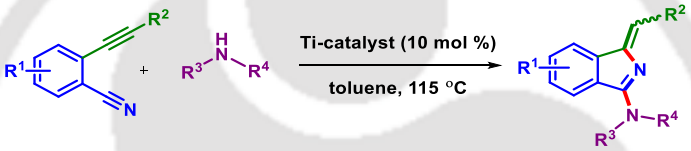

Scheme I.3.3.2. *Ti-catalyzed synthesis of isoindolines from o-alkynylbenzonitriles.*

In 2017, Kumar *et. al.* explored the transformation of o-alkynylarylnitrile to sulfur and nitrogen substituted benzo naphthyridine *via* Pd(II)-catalyzed 6-endo-dig protocol using secondary amine and thio nucleophiles (Scheme I.3.3.3).[70c]

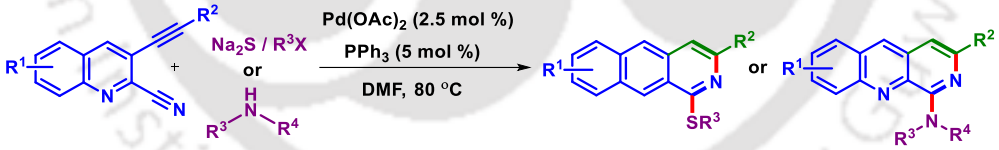

Scheme I.3.3.3. *Pd(II)-catalyzed synthesis of benzo naphthyridine from o-alkynylbenzonitriles.*

In 2018, Liang groups reported an efficient Cu(II)-catalyzed heteroannulation reaction for the synthesis of benzo [4,5]imidazo[2,1-*a*]isoquinoline derivatives captivating *o*-alkynylbenzonitriles and 2-iodoanilines (Scheme I.3.3.4).[70d] The efficiency of this protocol relies on the nitrogen of the aniline to undergo both nucleophilic attacks on nitrile and alkyne.

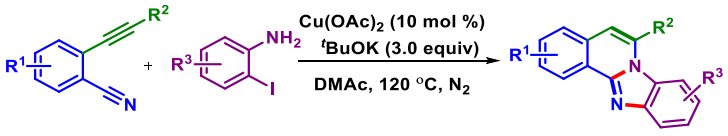

Scheme I.3.3.4. *Cu(II)-catalyzed coupling between 2-iodoaniline and o-alkynylbenzonitriles.*

I.4. Synthesis of *N*-Heterocycles *via* Thermal and Photochemical Cascade Addition/Cyclization of Nitriles:

A cascade strategy, also recognized as a domino or tandem reaction, is a chemical process that includes at least two successive reactions such that each subsequent reaction takes place only in virtue of the chemical functionality formed in the previous step (Figure I.4.1).[71] In general, the cascade strategies allow several bond formations in one sequence, thus isolation of each intermediate is not required at all, no additional reagent or catalyst is required, and no change in the reaction condition as each reaction composing the sequences occurs spontaneously.

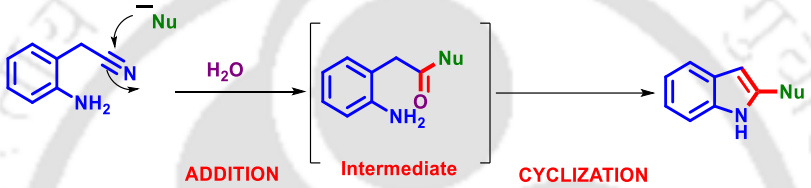

Figure I.4.1. *Cascade addition/cyclization with nitrile precursor*

Advantages of Cascade Strategies:

- ✓ Complex molecule synthesis in one pot.
- ✓ The reaction is fast and clean.
- ✓ Displays high atom economy.
- ✓ Step economy.
- ✓ Reduce the production time and amount of waste generated.

Classification of Cascade Strategies:

The classifications of cascade reactions are very difficult due to the involvement of miscellaneous reaction sequences either thermally or photochemically. Therefore considering the various nature of reaction mechanisms or steps and the catalysts involved the cascade strategy can be arbitrarily distinguished into the following categories:

1. Nucleophilic or electrophilic cascades.
2. The radical cascades.
3. Pericyclic cascades.
4. Transition-metal-catalyzed cascades.
5. Enzyme-catalyzed cascades.

The use of these cascade strategies has flourished not only in the area of total synthesis[72] but also the development of each cascade-driven organic methodologies has been also growing tremendously. In the past few decades, cascade addition/cyclization has been established as one of the most attractive approaches, for the construction of diverse *N*-heterocycles.[73] In this consequence the nitrile (–CN) functionality has appeared as the most prevalent synthetic precursor to achieving diverse nitrogen-containing heterocycles through cascade addition cyclization sequences either thermally or photochemically. Among the various cascade processes, herein we are going to discuss the construction of various *N*-heterocyclic compounds introducing various nitrile precursors under the following two categories:

I.4.1. Transition-metal-catalyzed cascade addition/cyclization (going through nucleophilic/electrophilic mechanism or radical mechanism)

I.4.2. Visible-light mediated radical cascade addition/cyclization (going through radical mechanism)

I.4.1. Transition Metal-Catalysed Cascade Addition/Cyclizations:

The transition metal-catalyzed cascade addition/cyclizations of nitriles (–CN) have provided a novel convenient, superior, and straightforward route to create a wide range of *N*-heteroarenes through efficient construction of C–C and C–N bonds. Transition metals such as manganese (Mn), nickel (Ni), copper (Cu), palladium (Pd), and Silver (Ag), have been used frequently in this nitrile-triggered transformation in recent years. These reactions can proceed either with nucleophilic/electrophilic mechanism or free radical mechanism. In the process, the transition metal converts the nitrile into an iminyl group (C=N) through the addition by (i) using the σ-coordination of nitrogen to the metal as a Lewis acid, (ii) 1,2-insertion, or (iii) *in situ* generations of a radical (Figure I.4.1.1) and undergoes further cyclization.

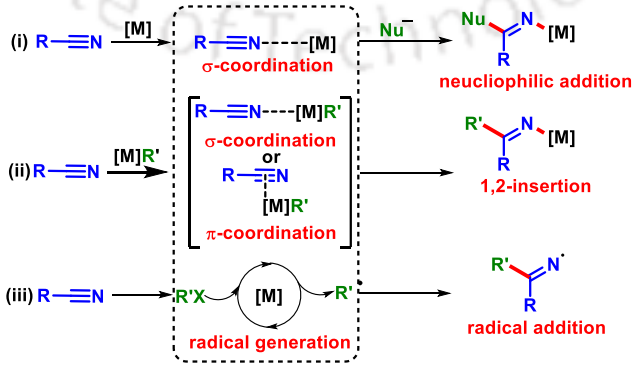

Figure I.4.1.1*. Transition-metal-catalyzed addition of nitrile.*

After Larock's pioneering work in the field of catalytic carbopalladation of nitrile, this concept has been explored for the synthesis of various *N*-heterocycles. In these transformations, the nitrile *N*-atom undergoes cyclization with a proximal carbonyl (C=O) group or hydrolyzed into a ketone and cyclized with proximal amine (NH_2) to provide various *N*-heterocycles. A general mechanism for this carbometallation of nitrile is shown in Figure I.4.1.2, where the coupling partner undergoes transmetallation with the metal catalyst to provide an aryl-metal species. Next coordination with the cyano group followed by the addition of the aryl group through carbometallation of nitrile provides an immine or ketone and the metal catalyst is regenerated through elimination. Finally, cyclization of the imine or ketone with the proximal keto or amine group of the starting nitrile precursor gives a cyclic product.

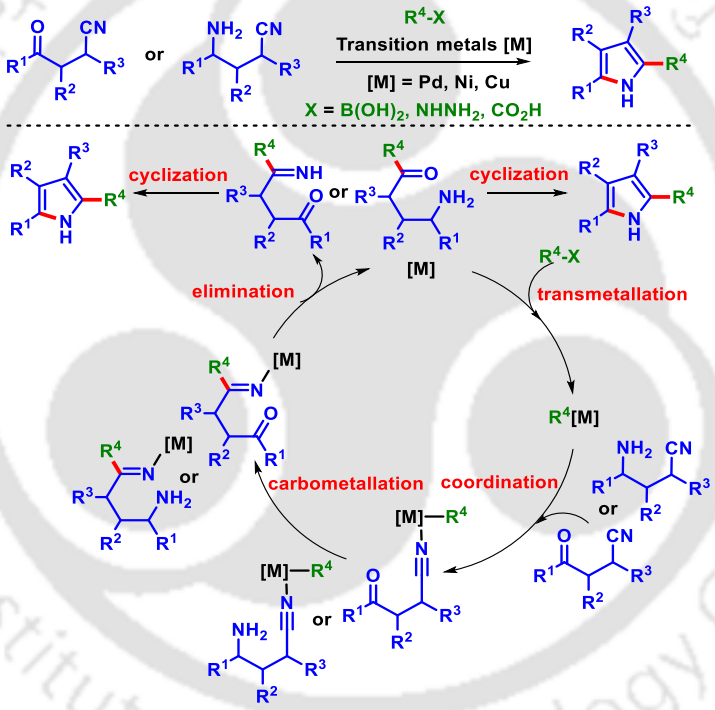

Figure I.4.1.2. *Carbometallation of nitriles to synthesize N-heterocycles.*

I.4.1.1. Transition-Metal-Catalyzed Nucleophilic/Electrophilic Cascades:

In this transition-metal-catalyzed cascade reaction, the nitrile precursors react with different coupling partners such as amine, Grignard reagent, arylboronic acids, aryl iodides, indoles, arylhydrazines, and aryl carboxylic acid to afford various *N*-heterocycles. During the process, the nitrile group acts as an electrophile and undergoes addition with aryl nucleophile generated from the coupling partners.

In 2009, Nagasawa reported a Cu(I)-catalyzed facile synthesis of 1,2,4-triazoles through tandem addition of 2-aminopyridines to the nitriles followed by oxidative cyclization. (Scheme I.4.1.1.1).[74] The reaction proceeds *via* nucleophilic attack by the amine on the nitrile and subsequent cyclization gives triazoles through the formation of C–N and N–N bonds.

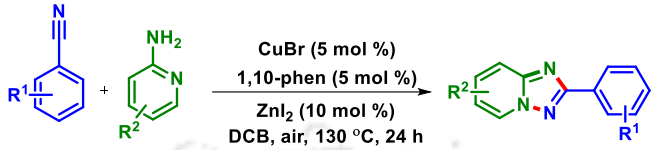

Scheme I.4.1.1.1. *Cu(I)-catalyzed synthesis of 1,2,4-triazoles from nitriles.*

In 2014, the Jen-Chieh Hsieh group developed a copper(I)-catalyzed addition of Grignard reagent to the nitriles followed by intramolecular cyclization to afford various polysubstituted phenanthridines through the formation of C–N bond (Scheme I.4.1.1.2).[75] The mechanistic investigations demonstrated that the reaction proceeded more likely through a Cu(I)/Cu(III) catalytic cycle.

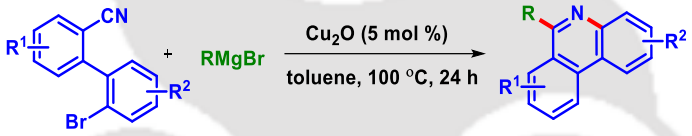

Scheme I.4.1.1.2. *Cascade addition/cyclization of Grignard reagent to nitrile.*

Liu and Li disclosed a copper(II)-catalyzed synthesis of quinazolines through cascade addition/cyclization between aromatic nitriles and 2-aminobenzylamines followed by aerobic oxidation using molecular oxygen as the sole oxidant (Scheme I.4.1.1.3).[76] Interestingly, herein, none of the nitrogen present in the quinozaline comes from the nitrile source because the method proceeds *via* the addition of the nitrile followed by the elimination of ammonia and Cu(II).

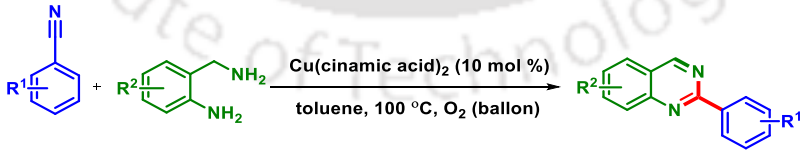

Scheme I.4.1.1.3. *Cu(II)-catalyzed synthesis of quinozalines from nitriles.*

In 2017, Wu and Chen's group established a Pd(II)-catalyzed tandem addition and cyclization of arylboronic acids with functionalized nitriles for the construction of 2-substituted indoles (Scheme I.4.1.1.4).[77] This transformation has excellent substrate tolerance with remarkable chemoselectivity.

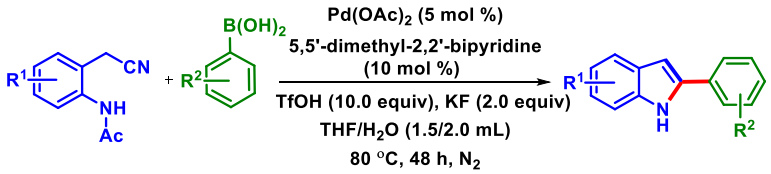

Scheme I.4.1.1.4. *Pd(II)-catalyzed synthesis of indoles from nitriles.*

In the same year, Adhikari *et al*. reported a Pd(II)-catalyzed addition of arylboronic acids to substituted aliphatic nitriles in an aqueous acetic acid medium to achieve 3-carboxy-nitrile 2-aryl pyrroles (Scheme I.4.1.1.5).[78] The reaction has excellent functional group tolerance with good yields for both electron-donating as well as electron-withdrawing substituents.

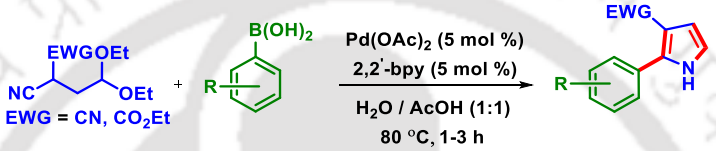

Scheme I.4.1.1.5. *Pd(II)-catalyzed synthesis of pyrroles from aliphatic nitriles.*

Yang and Shao groups developed a Pd(II)-catalyzed synthesis of multi-substituted imidazoles *via* the addition of arylboronic acids to aminoacetonitriles through the formation of C–C and C–N bonds (Scheme I.4.1.1.6).[79]

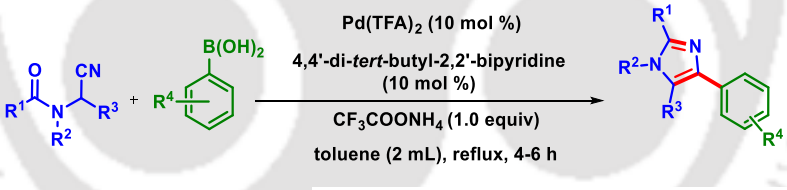

Scheme I.4.1.1.6. *Pd(II)-catalyzed synthesis of substituted imidazoles from nitriles.*

Chen and Wu groups reported a Pd(II)-catalyzed synthesis of isoquinolines *via* a similar sequential nucleophilic addition cyclization of arylboronic acid to functionalized γ-ketonitriles (Scheme I.4.1.1.7).[80]

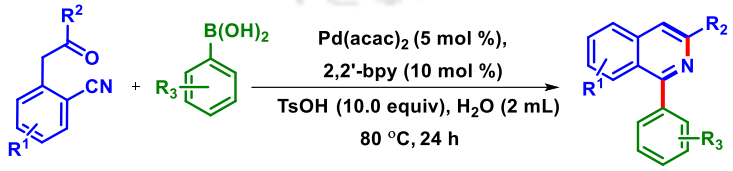

Scheme I.4.1.1.7. *Pd(II)-catalyzed access of isoquinolines from nitriles.*

Chen and co-workers developed another alternative pathway to access symmetrical and unsymmetrical isoquinolines through a Pd(II)-catalyzed tandem reaction of 2-

(cyanomethyl)benzonitriles or 2-(carbonylphenyl)acetonitriles with arylboronic acids in an aqueous medium (Scheme I.4.1.1.8).[81]

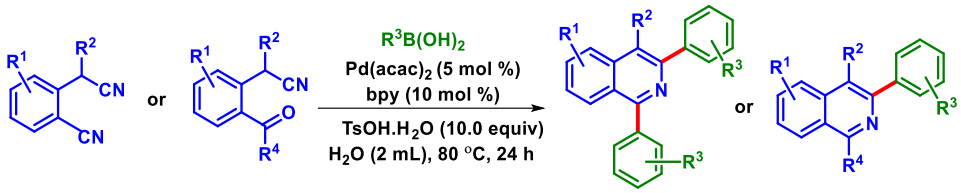

Scheme I.4.1.1.8. *Synthesis of symmetrical or unsymmetrical isoquinolines from nitriles.*

In 2018, the Bao group introduced a convenient Cu(II)-catalyzed cascade process between *o*-halobenzamides and nitriles to synthesize quinazolinones (Scheme I.4.1.1.9).[82] The methodology proceeds through a Cu(II)-assisted nucleophilic addition of 2-halobenzamides to the nitriles followed by an intramolecular Cu(II)-catalyzed *N*-arylation in the presence of a base to give quinozalinone derivatives. The reaction proceeds smoothly with aryl, alkyl, or heteroaromatic nitriles.

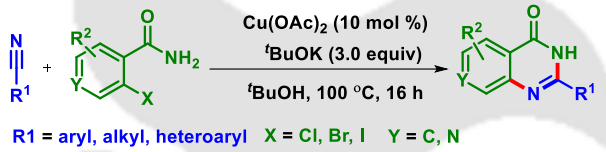

Scheme I.4.1.1.9. *Cu(II)-catalyzed synthesis of quinozalinones from nitriles.*

Kumar *et al.* introduced a Pd(II)-catalyzed intermolecular cyclization process for the regioselective synthesis of polysubstituted phenanthridines using aryl iodides and alkyl/aryl nitriles (Scheme I.4.1.1.10).[83] The reaction is initiated *via* the nucleophilic insertion of aryl iodides into nitriles followed by *in situ* generated imine-directed sequential two-fold C–H activation through the cascade formation of C–C and C–N bonds.

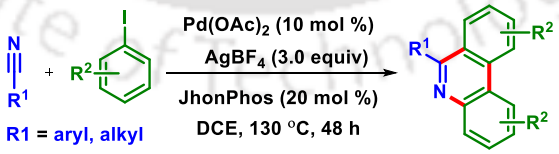

Scheme I.4.1.1.10. *Pd(II)-catalyzed synthesis of phenanthridines from nitriles.*

Liao *et al.* explored a Pd(II)-catalyzed redox-free C–H addition of indoles to nitriles for the synthesis of functionalized β-carbolines and γ-carbolines in good to excellent yields *via* addition/cyclization sequences with broad substrates scope (Scheme I.4.1.1.11).[84]

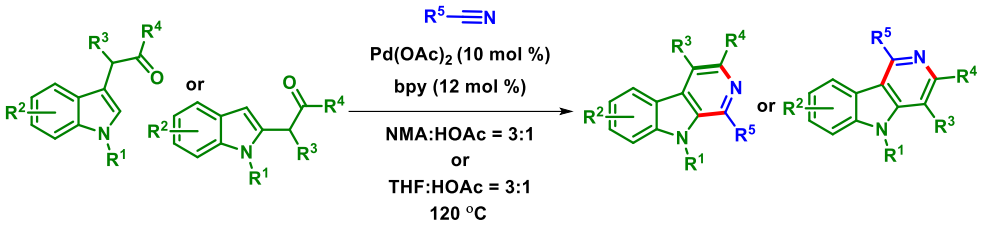

Scheme I.4.1.1.11. *Pd(II)-catalyzed addition of indoles to nitriles.*

Chen and co-workers further demonstrated the synthesis of 2,4-disubstituted quinazolines *via* a Pd(II)-catalyzed tandem reaction of arylboronic acids with *N*-(2-cyanoaryl)benzamides (Scheme I.4.1.1.12).[85] The reaction is compatible with both these substrates and various functional groups are well-tolerated.

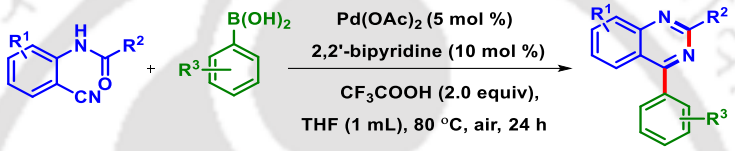

Scheme I.4.1.1.12. *Pd(II)-catalyzed synthesis of quinozalines from nitriles.*

Chen group proposed a Pd(II)-catalyzed sequential nucleophilic addition followed by intramolecular cyclization of a quinazoline-based nitrile, 2-(quinazoline-3(4*H*)-yl)benzonitriles with arylboronic acids to synthesize 2-(a-arylquinazoline-2-yl)anilines containing a free amino group (Scheme I.4.1.1.13).[86] The free amino group in the final product is favorable to further synthetic elaborations to expand its diversity in both synthetics as well as in medicinal chemistry. Both substrates with strongly electron-donating and electron-withdrawing groups are compatible with this reaction.

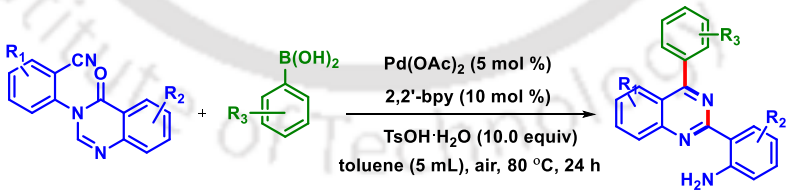

Scheme I.4.1.1.13. *Pd(II)-catalyzed tandem reaction of quinazolinone-based nitriles.*

Shao and Yang's group developed a novel and regioselective construction of 3-aryl-1-aminoisoquinolines *via* a Ni(I)-catalyzed C–C and C–N coupling reactions of 2-(cyanomethyl)benzonitriles and arylboronic acids (Scheme I.4.1.1.14).[87] The reaction is atom-

economic and has a broad substrate scope with a wide range of both aryl or heteroaryl boronic acids as well as 2-(cyanomethyl)benzonitriles.

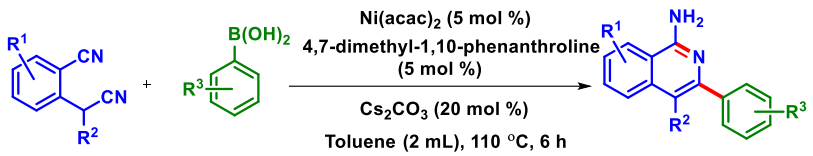

Scheme I.4.1.1.14. *Ni(I)-catalyzed access of aminoisoquinolines from nitriles.*

In 2019, Chen and co-workers developed a Pd(II)-catalyzed cascade reaction of 2′-acetyl-[1,1′-biphenyl]-2-carbonitriles with arylboronic acids for the construction of a seven-membered ring compound 5-arylidene-7-aryl-5*H*-dibenzo[*c*,*e*]azepines (Scheme I.4.1.1.15).[88] This methodology proceeds through sequential nucleophilic addition, intramolecular cyclization, and oxidative Heck coupling.

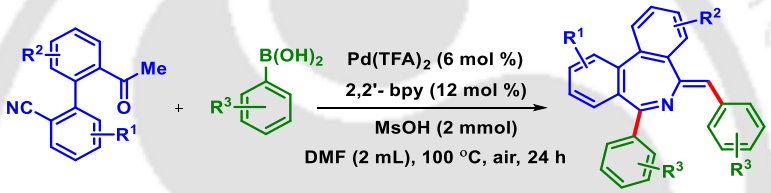

Scheme I.4.1.1.15. *Pd(II)-catalyzed cascade reaction of o-cyanobiaryls*

Chen's group further developed another Pd(II)-catalyzed tandem addition and cyclization of 2′-formyl-[1,1′-biaryl]-2-carbonitriles with arylboronic acids with excellent selectivity for the efficient synthesis of dibenzo[*c*,*e*]azepin-5-ols (Scheme I.4.1.1.16).[89]

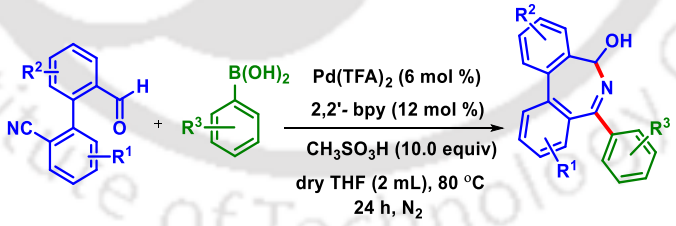

Scheme I.4.1.1.16. *Palladium(II)-catalyzed synthesis of dibenzo[c,e]azepin-5-ols.*

Shao and Li's group accomplished a convenient method for the synthesis of 2,4-disubstituted imidazoles *via* a Ni(II)-catalyzed C–C coupling of aryl boronic acids with N-(cyanomethyl)benzamides followed by intramolecular C–N bond formation (Scheme I.4.1.1.17).[90] The method is compatible with a variety of aryl or aliphatic substituents, halogen, and *N*-containing heterocyclic groups demonstrating further synthetic explorations.

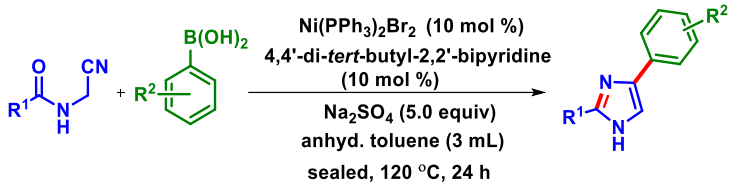

Scheme I.4.1.1.17. *Ni(II)-catalyzed synthesis of 2,4-disubstituted imidazoles.*

Shao and Chen's group developed the synthesis of 2-arylquinolines *via* a Pd(II)-catalyzed tandem reaction of 2-aminostyryl nitriles with arylboronic acids having good substrates and functional groups tolerance (Scheme I.4.1.1.18).[91]

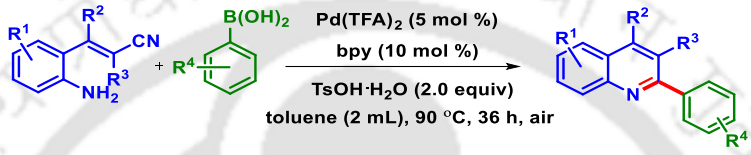

Scheme I.4.1.1.18. *Pd(II)-catalyzed synthesis of 2-arylquinolines.*

Neuville's group described a Cu(II)-catalyzed synthesis of benzimidazo[1,2-*c*]quinazolines *via* three-components gathering of cyanamides, 2-cyanoarylboronic acids, and amines (Scheme I.4.1.1.19).[92] The reaction is initiated *via* a copper-catalyzed nucleophilic addition between arylcyanamide and amine to obtain a guanidine unite which adds to the 2-cyanoarylboronic acid *via* Chan-Evans-Lam type coupling followed by intramolecular cyclization with the *o*-cyano group to provide quinazolin-4(*H*)-imines. Finally a Cu(II)-catalyzed intramolecular C–H amination provides benzimidazo[1,2-*c*]quinazolines.

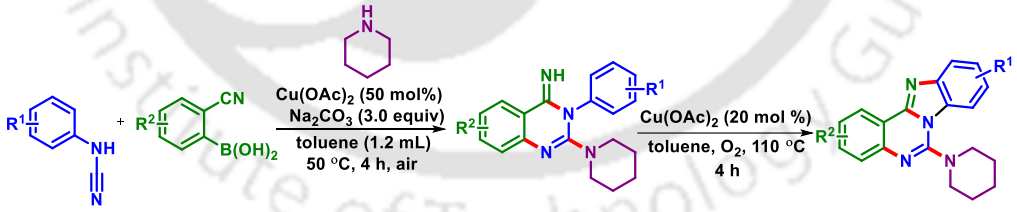

Scheme I.4.1.1.19. *Cu-(II)-promoted synthesis of benzimidazo[1,2-c]quinazolines.*

Chen and Shao's group reported the construction of 2,4-diarylquinazolines *via* a Pd(II)-catalyzed tandem addition/cyclization of 2-(benzylidenamino)benzonitriles with arylboronic acids (Scheme I.4.1.1.20).[93] The reaction has broad substrate scopes with different functional groups tolerability concerning both the substrates.

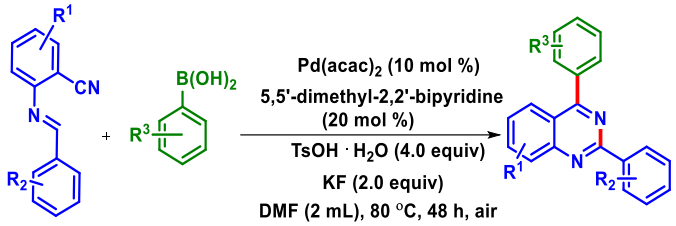

Scheme I.4.1.1.20. *Access of 2,4-diarylquinazolines from nitriles.*

In 2020, Chen's group reported a Ni(II)-catalyzed tandem addition/cyclization of 2-(cyanomethyl)benzonitriles and methyl 2-(cyanomethyl)benzoates with arylboronic acids in a 2-Me-THF solvent, providing a new strategy for the construction of diverse aminoisoquinolines and isoquinolones under mild conditions (Scheme I.4.1.1.21).[94]

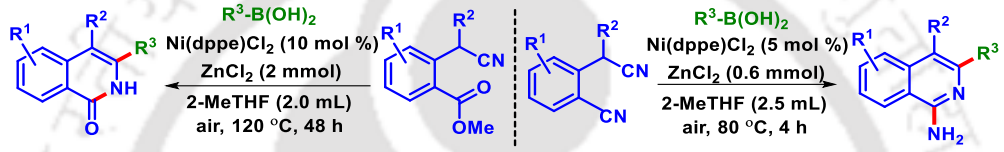

Scheme I.4.1.1.21. *Ni(II)-catalyzed synthesis of aminoisoquinolines and isoquinolones.*

Chen, Shao, and Li's group reported a selective synthesis of benzofuro[2,3-*c*]pyridines *via* a Pd(II)-catalyzed cascade reaction of 2-(cyanomethoxy)chalcones with arylboronic acids (Scheme I.4.1.1.22).[95] The mechanistic studies of this transformation informed that the reaction proceeds *via* a sequential carbopalladation of nitrile, an intramolecular Micheal addition, cyclization, and aromatization leading to the formation of C–C and C–N bonds.

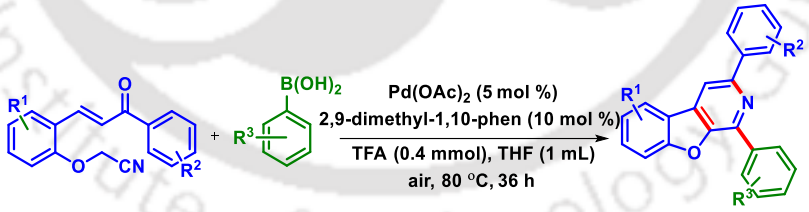

Scheme I.4.1.1.22. *Synthesis of benzofuro[2,3-c]pyridines.*

Shao and Chen's group developed a Pd(II)-catalyzed tandem reaction of 2-(arylamino)benzonitriles with arylboronic acids in an aqueous medium for the synthesis of 9-arylacridines (Scheme I.4.1.1.23).[96] Mechanistic studies showed that the reaction involves a nucleophilic addition of aryl palladium intermediate to the nitrile group to form an aryl ketone followed by an intramolecular Friedel-Craft acylation and dehydration.

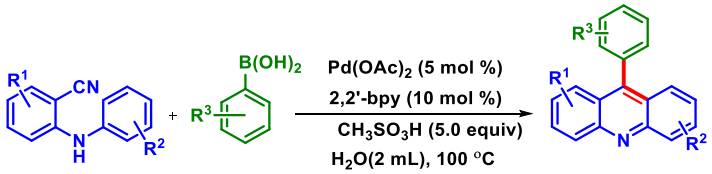

Scheme I.4.1.1.23. *Pd(II)-Catalyzed synthesis of 9-arylacridines.*

Chen, Hu, and Li group reported the construction of 2,6-disubstituted pyridines *via* a Pd(II)-catalyzed C–C, C–N coupling using δ-ketonitriles and arylboronic acids (Scheme I.4.1.1.24).[97] This method has the advantage of its atom economical, mild reaction condition, excellent functional group tolerance, and broad substrate scope.

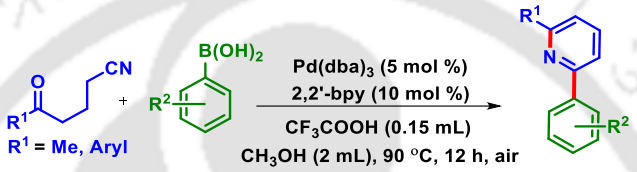

Scheme I.4.1.1.24. *Pd(II)-catalyzed cascade reactions of γ-ketonitriles.*

In 2020 Chen group demonstrated a Pd(II)-catalyzed denitrogenative addition of arylhydrazines with *o*-aminocinnamonitriles followed by cyclization to achieve quinolines in moderate to good yields (Scheme I.4.1.1.25).[98]

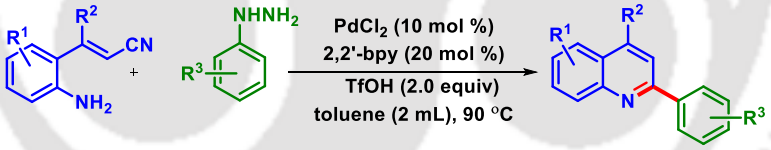

Scheme I.4.1.1.25. *Pd(II)-catalyzed cascade reactions with phenylhydrazine.*

Chen and Shao developed a Pd(II)-catalyzed C–C activation-initiated reaction of 2-(3-phenyloxiran-2-yl)-benzonitriles with arylboronic acids to synthesize benzo-fused dipyrromethene derivatives (Scheme I.4.1.1.26).[99]

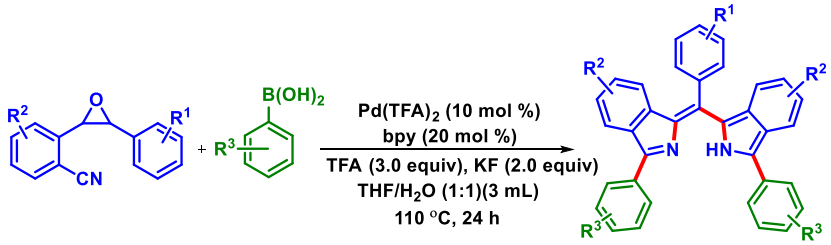

Scheme I.4.1.1.26. *Pd(II)-catalyzed synthesis of benzo dipyrromethenes.*

Chen and Li *et al.* developed an effective Ni(II)-catalyzed C–C and C–N coupling of ketonitriles with arylboronic acids to access biologically active 3-carboxylate-2,5-diaryl-pyrroles and 2,6-diarylpyridines (Scheme I.4.1.1.27).[100] This transformation is highly versatile, atom-economical has broad substrate scope, and has excellent functional group tolerance.

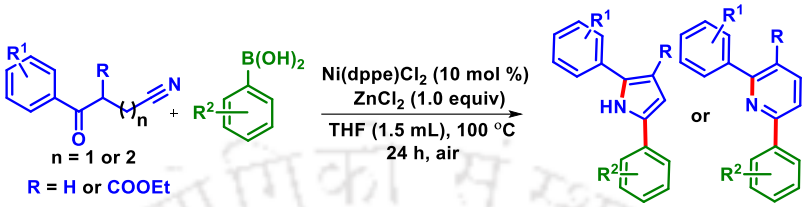

Scheme I.4.1.1.27. *Ni(II)-catalyzed synthesis of substituted pyrroles and pyridines.*

In 2021, Yu and Zhang's group developed a novel and efficient strategy for the construction of functionalized pyrrolo[1,2-*a*]pyrazine derivatives through a Pd(II)-catalyzed C_{sp}–C_{sp2} bond formation and an intramolecular cyclization (Scheme I.4.1.1.28).[101]

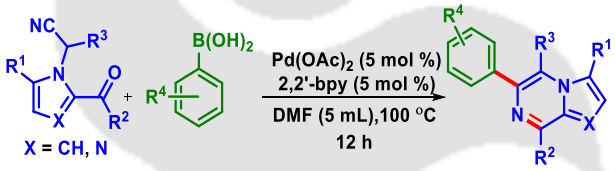

Scheme I.4.1.1.28. *Pd(II)-catalyzed synthesis of multi-substituted pyrrolo[1,2-a]pyrazines.*

Recently Li and Chen *et al.* developed a one-pot three-component reaction of 2-aminobenzonitriles, arylboronic acids, and ketones for the synthesis of poly-substituted quinolines *via* a Pd(II)-catalysis under an acidic condition (Scheme I.4.1.1.29).[102] The reaction proceeds through a palladium-catalyzed aryl addition to the cyano group, hydrolysis, and Friedländer-type cyclization to give quinolines.

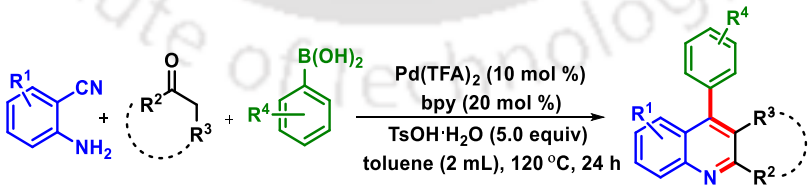

Scheme I.4.1.1.29. *Pd(II)-catalyzed three-component tandem reaction of nitriles.*

Chen and co-workers developed a Pd(II)-catalyzed synthesis of pyrazino-fused quinazolines *via* coupling of 2-(4-oxoquinazoline-3(4*H*)-yl)acetonitriles with arylboronic acids followed by an intramolecular cyclization in aqueous media (Scheme I.4.1.1.30).[103]

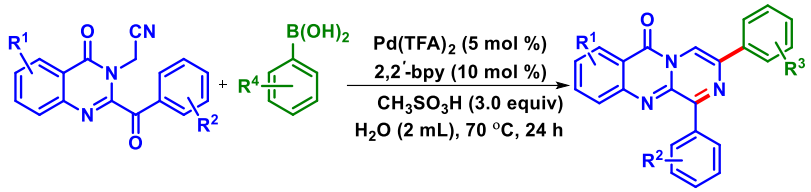

Scheme I.4.1.1.30. *Pd(II)-catalyzed synthesis of pyrazino-fused quinazolinones.*

Chen *et al.* further developed a Pd(II)-catalyzed decarboxylative addition/cyclization of aromatic carboxylic acids with functionalized aliphatic nitriles to synthesize imidazoles and oxazoles in a single step with good yields (Scheme I.4.1.1.31).[104]

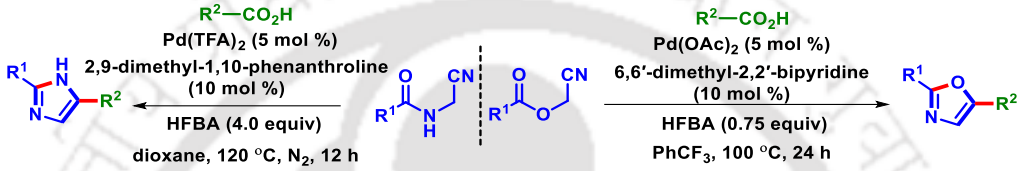

Scheme I.4.1.1.31. *Pd(II)-catalyzed addition of carboxylic acids to nitriles.*

I.4.1.2. Transition-Metal-Catalyzed Radical Cascades:

The transition-metal-catalyzed radical cascade process involving the nitrile functionality provides a convenient route for the construction of various important *N*-heterocycles. The application of the cyano group as a radical acceptor is shown below (Figure I.4.1.2.1). An iminyl radical is formed when an *in situ* generated radical adds to the nitrile group of a precursor (Path A). Alternatively, an iminyl radical can also be generated through the radical addition to the nitrile *via* an appropriately placed C=C bond or other unsaturated groups like isocyanides (N≡C) (Path B). Finally, nitrile insertion onto the aryl ring through the iminyl radical produces the corresponding *N*-heterocycle.

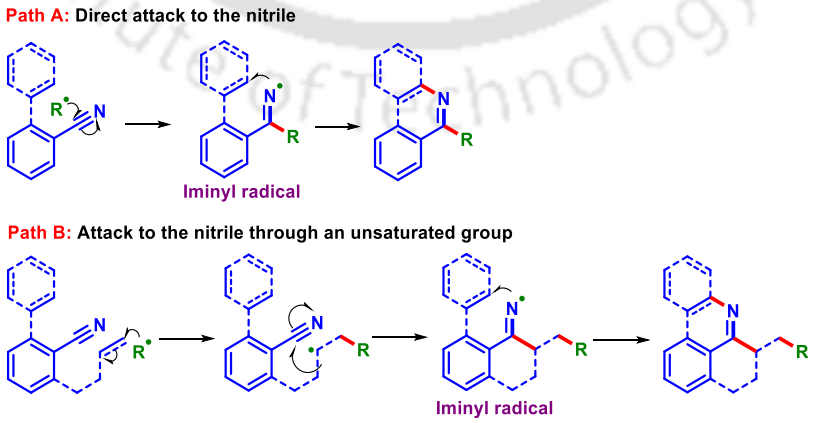

Figure I.4.1.2.1. *Nitrile as a radical acceptor for synthesis of N-heterocycles.*

In 2016, Cui *et al.* reported Ag(I)-mediated phosphorylation/cyclization of *N*-cyanamide alkenes to access quinazolinones. The addition of *in situ* generated phosphorus radical to *N*-cyanamide alkenes triggers the reaction followed by addition to the nitrile and finally, cyclization affords the quinazolinones (Scheme I.4.1.2.1).[105]

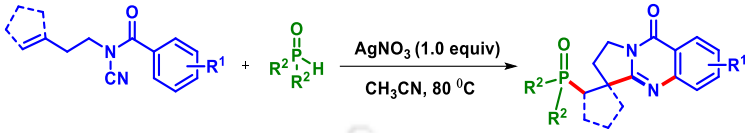

Scheme I.4.1.2.1. *Ag(I)-catalyzed radical cascade addition/cyclization of nitriles.*

In 2018, Ya-Min Li reported an atom economical strategy to access cyano substituted pyrido[4,3,2-*gh*]phenanthridines *via* an oxidative radical cascade cyclization of 2-cyano-3-arylanilines derived acrylamides with acetonitrile in the presence of $Cu(OAc)_2$ and *tert*-butyl peroxy benzoate (TBPB) (Scheme I.4.1.2.2).[106]

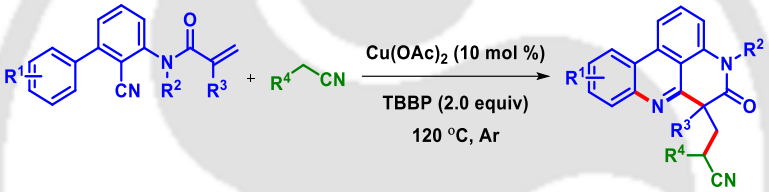

Scheme I.4.1.2.2. *Cu(II)-catalyzed radical cyclization of nitriles.*

A Mn(II)-catalyzed synthesis of silicon/nitrogen heterocycles is reported by He *et al. via* an intermolecular oxidative radical heteroannulation of *N*-(2-cyanoaryl)-acrylamides and tertiary silanes through a 1,6-hydrogen atom transfer (1,6-HAT) (Scheme I.4.1.2.3).[107] The reaction allows Si-incorporation using triisopropylsilane *via* C_{sp3}–H functionalization.

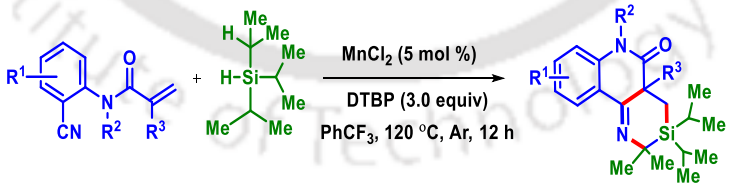

Scheme I.4.1.2.3. *Mn(II)-catalyzed radical cyclization of nitriles.*

In 2019, Kang *et al.* developed a Cu(II)-catalyzed addition of benzylic radical to the nitriles group followed by an intramolecular cyclization to access NH indoles (Scheme I.4.1.2.4).[108] The reaction proceeds through the *in situ* generations of an iminyl radical *via* an intermolecular carbanion-radical redox relay using a copper(II) catalyst.

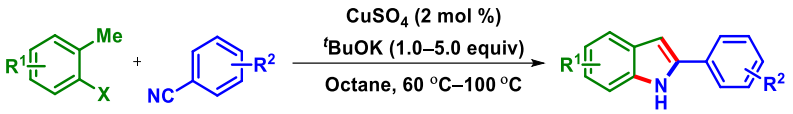

Scheme I.4.1.2.4. *Cu(II)-catalyzed radical cascades of nitriles.*

Ji and Wang's group proposed a Mn(III)-mediated reaction for the construction of pyrrolopyridines using multi-functionalized 3-isocyano-[1,1′-biphenyl]-2-carbonitriles with arylboronic acids (Scheme I.4.1.2.5).[109] The transformation occurred *via* a radical path with the formation of two new C–C bonds and one C–N bond.

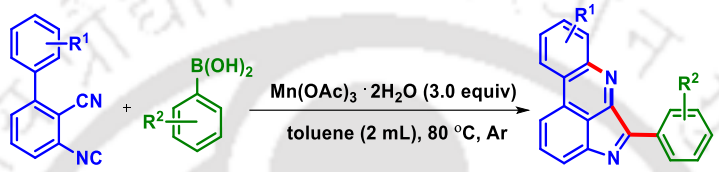

Scheme I.4.1.2.5. *Mn(III)-mediated radical cascade of nitriles.*

Ya-Min Li reported an efficient Ag(I)-catalyzed synthesis of pyrido[4,3,2-*gh*]phenanthridines using α-keto acids as acyl radical precursor with 2-cyano-3-arylaniline derived acrylamides in moderate to good yields (Scheme I.4.1.2.6).[110] The reaction proceeds through an oxidative decarboxylative cyclization leading to the formation of one C–N bond, two C–C bonds, and a quaternary carbon center in a single step.

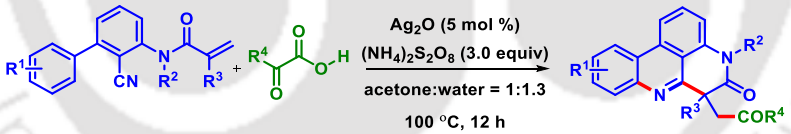

Scheme I.4.1.2.6. *Ag(I)-catalyzed radical cascade of nitriles.*

In 2020, the Wang group reported an efficient and atom-economic strategy for the synthesis of SCF_3-substituted tryptanthrin derivatives in the presence of $AgSCF_3$ as an SCF_3 radical source in moderate to good yields (Scheme I.4.1.2.7).[111]

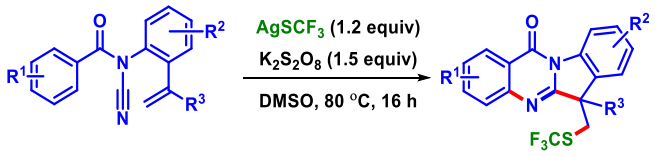

Scheme I.4.1.2.7. *Ag(I)-catalyzed SCF_3 radical addition.*

Recently in 2021, a Mn(III)-assisted radical reaction of multi-functionalized 2-isocyano-6-alkenyl(alkynyl) benzonitriles with arylboronic acids has been explored by Shun-Jun Ji (Scheme I.4.1.2.8).[112] This methodology provides an atom-economical synthesis of pyrroloisoquinolines through the formation of C–C and C–N bonds *via* a radical cyclization.

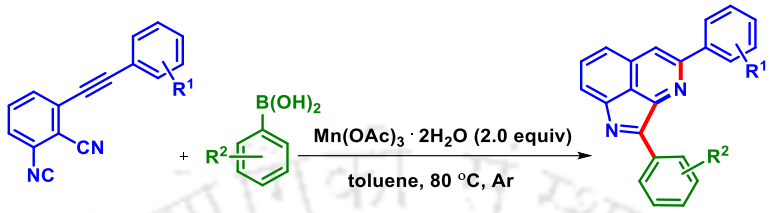

Scheme I.4.1.2.8. *Mn(III)-mediated radical cascade of nitriles.*

I.4.2. Visible-Light Mediated Radical Cascade Addition/Cyclizations:

The Visible-light-induced radical cascade addition/cyclization processes have been successfully used for the construction of *N*-heterocycles because of their simplicity, efficiency, and unique activation.[113] In this context construction of C–C and C–N bonds using photoredox catalysis has grabbed significant attention giving prominence to the nitrile functionality. In contrast to that of transition-metal-catalyzed radical reactions herein the radical is generated through the photocatalysts (PC) in its excited state (PC*) *via* single electron transfer (SET) by the influence of visible-light (Figure I.4.2.1). The generated radical adds to the cyano group to obtain an iminyl radical which subsequently underwent intramolecular cyclization to access *N*-heterocycles through a radical or a cationic species. The photocatalyst is regenerated to its ground state either *via* oxidative quenching or reductive quenching cycle.

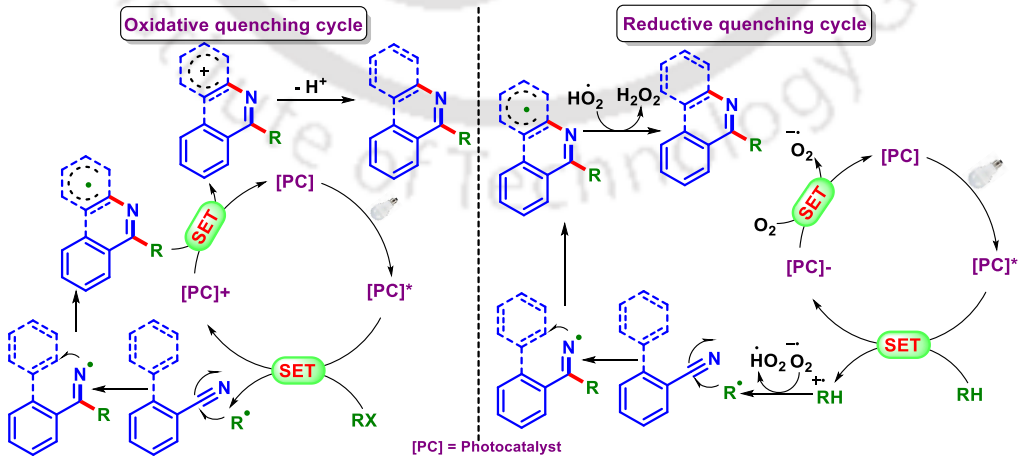

Figure I.4.2.1. *Visible-light mediated radical addition to nitrile.*

In 2014, Yu's group developed an Ir(III)-catalyzed visible-light promoted strategy for the synthesis of fused quinoxaline derivatives using diethyl 2-bromo-2-(2-cyanoethyl)malonate as the radical precursor with aryl isocyanides (Scheme I.4.2.1).[114] The reaction proceeds through the intermolecular radical addition to the isocyanide followed by an intramolecular radical addition to the nitrile.

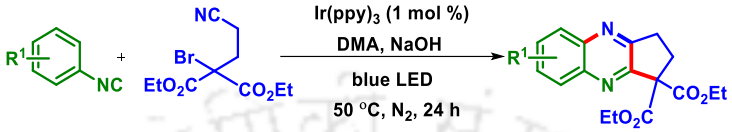

Scheme I.4.2.1. *Ir(III)-catalyzed inter- and intramolecular radical addition.*

In 2016, Yu and co-workers reported the synthesis of tetracyclic quinazolinones using a visible-light promoted intramolecular radical cascade approach using *fac*-Ir(ppy)$_3$ as photocatalyst (Scheme I.4.2.2).[115]

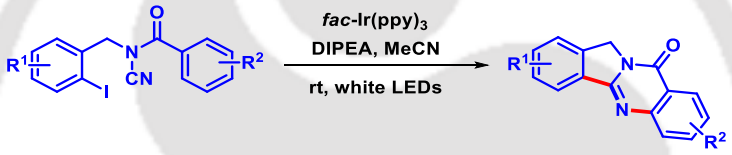

Scheme I.4.2.2. *Ir(III)-catalyzed radical addition to nitrile.*

In 2017, Sun *et al.* developed a visible-light-induced cascade addition cyclization sequence for the synthesis of ester-functionalized pyrido[4,3,2-*gh*]phenanthridind derivatives. The reaction proceeds via the addition of an ester radical from alkyl carbazate in the presence of eosin Y as the photoredox catalysts (Scheme I.4.2.3).[116]

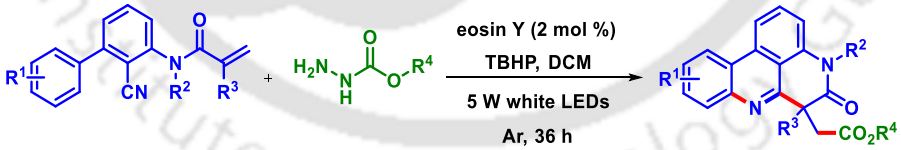

Scheme I.4.2.3. *Eosin Y catalyzed radical addition to nitrile.*

In the same year, they also developed a radical cascade addition/cyclization reaction to synthesize phenanthridines under an Ir-(III) photoredox catalysis (Scheme I.4.2.4).[117]

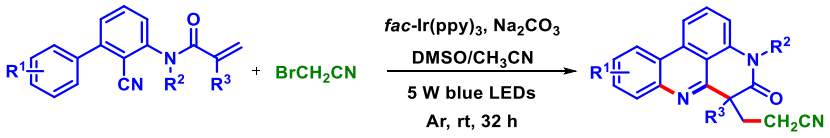

Scheme I.4.2.4. *Ir-(III)-catalyzed radical cyclization.*

In 2018, the Sun group published a visible-light-mediated decarboxylative alkylation *via* cascade addition/cyclization to *N*-arylacrylamides involving the combination of eosin Y and $(NH_4)_2S_2O_8$. Herein, decarboxylation of aliphatic carboxylic acids generates an alkyl radical which undergoes addition to the nitrile group followed by intramolecular cyclization to access alkylated phenanthridines (Scheme I.4.2.5).[118]

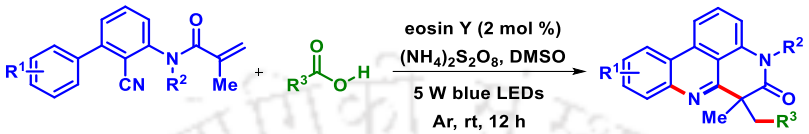

Scheme I.4.2.5. *Eosin Y catalyzed radical addition to nitrile.*

In 2018, Natarajan *et al*. demonstrated an efficient strategy for the construction of 2-substituted benzothiazoles *via* the radical coupling between nitriles and thiophenols in good to excellent yields through a sequential C–S and C–N bond formation under photoredox catalysis (Scheme I.4.2.6).[119] The reaction involves the direct oxidative radical coupling of thiophenols with nitriles to afford iminyl radical followed by intramolecular cyclization.

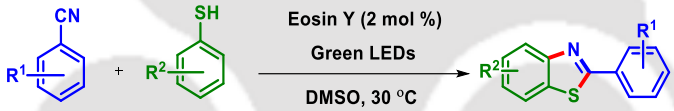

Scheme I.4.2.6. *Eosin Y catalyzed thiol radical addition to nitrile.*

Owing to the importance of fluorine-containing compounds Sun *et al.* reported a visible-light-induced radical cyclization of 2-cyano-3-arylaniline derived acrylamides in the presence of $Ru(phen)_3Cl_2$ or *fac*-$Ir(ppy)_3$. Two different fluorine-containing radical sources are used to deliver trifluoroalkyl phenanthridines and difluoroalkyl phenanthridines respectively in moderate to good yields (Scheme I.4.2.7).[120] The protocol underwent smoothly *via* the addition of fluorinated radicals to the C=C bond followed by the addition to the nitrile and finally an intramolecular cyclization process.

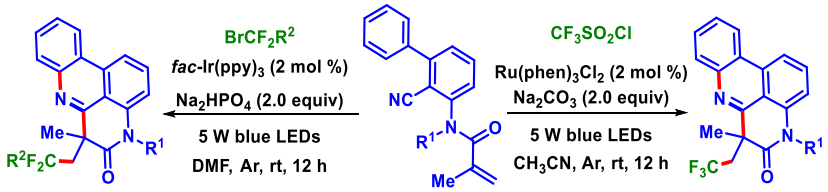

Scheme I.4.2.7. *Ru(II) and Ir(III)-catalyzed trifluoromethylation.*

In 2019, the Fu group demonstrated *N*-trifluoromethylthiosaccharin as an effective precursor of SCF_3 radical to access the SCF_3 containing phenanthridines under visible-light irradiation using Ir(III) photocatalyst (Scheme I.4.2.8).[121] A large variety of functional groups having electron-donating and electron-withdrawing substituents reacted smoothly to afford fused phenanthridines in moderate to good yields.

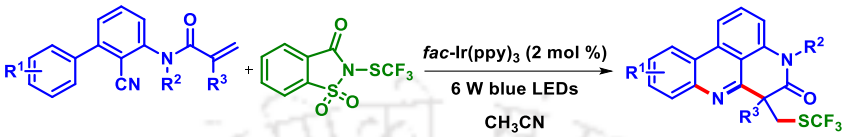

Scheme I.4.2.8. *Ir(III)-catalyzed thiotrifluoromethylation.*

I.5. Conclusion:

In conclusion, the C–H/N–H alkyne annulation and cascade addition/cyclization reactions remain a powerful and demanding synthetic methodology for the construction of nitrogen heterocycles through the formation of C–C and C–N bonds in a single step. The involvement of nitrile (C≡N) or cyano precursors utilizing these approaches has revolutionized the synthesis of several essential *N*-heterocycles from designer reactants. Synthetic precursors like β-ketodinitriles and γ-ketodinitriles having nitrile functionality can open up broad opportunities in this area. However, these precursors remain less explored either thermally or photochemically. Therefore in the subsequent chapters of this thesis, we report newer methodologies for a straightforward and efficient synthesis of various *N*-heterocycles such as isoquinolines, furopyridines, benz-imidazopyridines, cyanopyridines, and cyanopyrroles from these functionalized or activated nitrile precursors β-ketodinitriles and γ-ketodinitriles.

I.6. References:

[1] (a) Pyrroles, Part II; Jones, R. A., Ed.; Wiley: New York, **1992**. (b) Wilkerson, W. W.; Copeland, R. A.; Covington, M.; Trzaskos, J. M. *J. Med. Chem*. **1995**, *38*, 3895–3901. (c) Lee, H.; Lee, J.; Lee, S.; Shin, Y.; Jung, W.; Kim, J.-H.; Park, K.; Kim, K.; Cho, H. S.; Ro, S. *Bioorg. Med. Chem. Lett*. **2001**, *11*, 3069–3072. (d) Furstner, A. *Angew. Chem., Int. Ed*. **2003**, 42, 3582–3603. (e) Trofimov, B. A.; Sobenina, L. N.; Demenev, A. P.; Mikhaleva, A. I. *Chem. Rev*. **2004**, *104*, 2481–2506. (f) Wurz, R. P.; Charette, A. B. *Org. Lett*. **2005**, *7*, 2313–2316. (g) Walsh, C. T.; Garneau-Tsodikova, S.; Howard-Jones, A. R.

Nat. Prod. Rep. **2006**, 23, 517–531. (h) Santo, R. D.; Costi, R.; Artico, M.; Miele, G.; Lavecchia, A.; Novellino, E.; Bergamini, A.; Cancio, R.; Maga, G.; *ChemMedChem.* **2006**, *1*, 1367–1378. (i) Fan, H.; Peng, J.; Hamann, M. T.; Hu, J.-F. *Chem. Rev*. **2008**, *108*, 264–287. (j) Thirumalairajan, S.; Pearce, B. M.; Thompson, A. *Chem. Commun*. **2010**, *46*, 1797–1812. (k) Bhardwaj, V.; Gumber, D.; Abbot, V.; Dhiman, S.; Sharma, P. *RSC Advanced.* **2015**, *5*, 15233–15266.

[2] (a) Semple, G.; Ashworth, D. M.; Baker, G. R.; Batt, A. R.; Baxter, A. J.; Benzies, D. W. M.; Elliot, L. H.; Evans, D. M.; Franklin, R. J.; Hudson, P.; Jenkins, P. D.; Pitt, G. R.; Rooker, D. P.; Sheppard, A.; Szelke, M.; Yamamoto, S.; Isomura, Y. *Bioorg. Med. Chem. Lett.* **1997**, *7*, 1337–1342. (b) O′Hagan, D. *Nat. Prod. Rep*. **1997**, *14*, 637–651. (c) Silva, E. D.; Geiermann, de A.-S.; Mitova, M. I.; Kuegler, P.; Blunt, J. W.; Cole, A. L. J.; Munro, M. H. G. *J. Nat. Prod*. **2009**, *72*, 477–479. (d) Jessen, H. J.; Gademann, K. *Nat. Prod. Rep. **2010**, 27*, 1168–1185. (e) Kumarihamy, M.; Fronczek, F. R.; Ferreira, D.; Jacob, M.; Khan, S. I.; Nanayakkara, N. P. D. *J. Nat. Prod*. **2010**, *73*, 1250–1253. (f) Fischer, D. F.; Sarpong, R. *J. Am. Chem. Soc*. **2010**, *132*, 5926–5927. (g) C. Yuan, C.-T. Chang, A. Axelrod, D. Siegel, *J. Am. Chem. Soc.* **2010**, *132*, 5924–5925. (h) Kusakabe, K.; Tada, Y.; Iso, Y.; Sakagami, M.; Morioka, Y.; Chomei, N.; Shinonome, S.; Kawamoto, K.; Takenaka, H.; Yasui, K.; Hamana, H.; Hanasaki, K. *Bioorg. Med. Chem.* **2013**, *21*, 2045–2055. (i) Wang, P.; Verma, P.; Xia, G.; Shi, J.; Qiao, J. X.; Tao, S.; Cheng, P. T. W.; Poss, M. A.; Farmer, M. E.; Yeung, K.-S.; Yu, J. Q. *Nature.* **2017**, *551*, 489–494.

[3] (a) Saxton, J. E. *Nat. Prod. Rep*. **1996**, *13*, 327–363. . (b) Ihara, M.; Fukumoto, K. *Nat. Prod. Rep*. **1997**, *14*, 413–429. (c) Joule, J. A.; Mills, K. *Heterocyclic Chemistry*; *Blackwell Science Ltd.: Oxford*, **2000**. (d) Eicher, T.; Hauptmann, S. *The Chemistry of Heterocycles; Wiley-VCH: Weinheim,* **2003**. (e) Smart, B. P.; Oslund, R. C.; Walsh, L. A.; Gelb, M. H. *J. Med. Chem.* **2006**, *49*, 2858–2860. (f) Petit, S.; Duroc, Y.; Larue, V.; Giglione, C.; Léon, C.; Soulama, C.; Denis, A.; Dardel, F.; Meinnel, T.; Artaud, I. *ChemMedChem*. **2009**, *4*, 261–275. (g) Kochanowska-Karamyan, A. J.; Hamann, M. T. *Chem. Rev*. **2010**, *110*, 4489–4497. (h) Thanikachalam, P. V.; Maurya, R. K.; Garg, V.; Monga V. *Eur. J. Med. Chem*. **2019**, *180*, 562–612.

[4] (a) Phillipson, J. D., Roberts, M. F., Zenk, M. H., Eds. *The Chemistry and Biology of Isoquinoline Alkaloids; Springer Verlag: Berlin*, **1985**. (b) Bentley, K.W. *The Isoquinoline Alkaloids; Hardwood Academic: Amsterdam*, **1998**, Vol. *1*. (c) Kashiwada, Y.; Aoshima, A.; Ikeshiro, Y.; Chen, Y. P.; Furukawa, H.; Itoigawa, M.; Fujioka, T.; Mihashi, K.; Cosentino, L. M.; Morris-Natschke, S. L.; Lee, K. H. *Bioorg. Med. Chem*. **2005**, *13*, 443–448. (d) Bentley, K.W. *Nat. Prod. Rep*. **2006**, *23*, 444–463. (e) Bhadra, K.; Kumar, G. S. *Mini-Rev. Med. Chem*. **2010**, *10*, 1235–1247. (f) Giri, P.; Kumar, G. S. *Mini-Rev. Med. Chem*. **2010**, *10*, 568–577. (g) Gutteridge, C. E.; Hoffman, M. M.; Bhattacharjee, A. K.; Milhous, W. K.; Gerena, L. *Bioorg. Med. Chem. Lett.* **2011**, *21*, 786–789. (h) Liu, Y.; Li, W.; Morris-Natschke, S. L.; Qian, K.; Yang, L.; Zhu, G.; Wu, X.; Chen, A.; Zhang, S.; Nan, X.; Lee, K. *Med. Res. Rev*. **2015**, *35*, 753–789. (i) Zhou, S.-Q.; Tong, R.-B. *Chem. Eur. J*. **2016**, *22*, 7084–7089. (j) Li, K.; Ou, J.; Gao, S. *Angew. Chem., Int. Ed*. **2016**, *55*, 14778–14783.

[5] (a) Rupert, K. C.; Henry, J. R.; Dodd, J. H.; Wadsworth, S. A.; Cavender, D. E.; Olini, G. C.; Fahmy, B.; Siekierka, J. *Bioorg. Med. Chem. Lett*. **2003**, *13*, 347–350. (b) Enguehard-Gueiffier, C.; Gueiffier, A. *Mini-Rev. Med. Chem*. **2007**, *7*, 888–899. (c) Shukla, N. M.; Salunke, D. B.; Yoo, E.; Mutz, C. A.; Balakrishna, R.; David, S. A. *Bioorg. Med. Chem*. **2012**, *20*, 5850–5863. (d) Du, B.; Shan, A.; Zhang, Y.; Zhong, X.; Chen, D.; Cai, K. *Am. J. Med. Sci*. **2014**, *347*, 178–182.

[6] (a) Martin, M. W.; Newcomb, J.; Nunes, J. J.; Bemis, J. E.; McGowan, D. C.; White, R. D.; Buchanan, J. L.; DiMauro, E. F.; Boucher, C.; Faust, T.; Hsieh, F.; Huang, X.; Lee, J. H.; Schneider, S.; Turci, S. M.; Zhu, X. *Bioorg. Med. Chem. Lett*. **2007**, *17*, 2299–2304. (b) Wu, Z.; Robinson, R. G.; Fu, S.; Barnett, S. F.; Defeo-Jones, D.; Jones, R. E.; Kral, A. M.; Huber, H. E.; Kohl, N. E.; Hartman, G. D.; Bilodeau, M. T. *Bioorg. Med. Chem. Lett*. **2008**, *18*, 2211–2214. (c) Rodriguez, A. L.; Williams, R.; Zhou, Y.; Lindsley, S. R.; Le, U.; Grier, M. D.; Weaver, C. D.; Conn, P. J.; Lindsley, C. W. *Bioorg. Med. Chem. Lett.* **2009**, *19*, 3209–3213. (d) Debenham, J. S.; Madsen-Duggan, C. B.; Toupence, R. B.; Walsh, T. F.; Wang, J.; Tong, X.; Kumar, S.; Lao, J.; Fong, T. M.; Xiao, J. C.; Huang, C. R. R. C.; Shen, C.-P.; Feng, Y.; Marsh, D. J.; Stribling, D. S.; Shearman, L. P.; Strack, A. M.; Goulet, M. T. *Bioorg. Med. Chem. Lett*. **2010**, *20*, 1448–1452. (e) Sirakanyan, S. N.;

Hovakimyan, A. A.; Noravyan, A. S. *Russ. Chem. Rev*. **2015**, *84*, 441−454. (f) Parcella, K.; Eastman, K.; Yeung, K.-S.; Grant-Young, K. A.; Zhu, J.; Wang, T.; Zhang, Z.; Yin, Z.; Parker, D.; Mosure, K.; Fang, H.; Wang, Y.-K.; Lemm, J.; Zhuo, X.; Hanumegowda, U.; Liu, M.; Rigat, K.; Donoso, M.; Tuttle, M.; Zvyaga, T.; Haarhoff, Z.; Meanwell, N. A.; Soars, M. G.; Roberts, S. B.; Kadow, J. F. *ACS Med. Chem. Lett*. **2017**, *8*, 771−774.

[7] (a) Michael, J. P. *Nat. Prod. Rep.* **1995**, *12*, 465−475. (b) Chen, Z.; Hu, G.; Li, D.; Chen, J.; Li, Y.; Zhou, H.; Xie, Y. *Bioorg. Med. Chem.* **2009**, *17*, 2351−2359 (c) Vlahakis, J. Z.; Lazar, C.; Crandall, I. E.; Szarek, W. A. *Bioorg. Med. Chem.* **2010**, *18*, 6184–6196. (d) Kuarm, B. S.; Reddy, Y. T.; Madhav, J. V.; Crooks, P. A.; Rajitha, B. *Bioorg. Med. Chem. Lett.* **2011**, *21*, 524−527. (e) Gu, X.; Ren, Z.; Tang, X.; Peng, H.; Zhao, Q.; Lai, Y.; Peng, S.; Zhang, Y. *Eur. J. Med. Chem.* **2012**, *51*, 137−144. (f) Bright, S. A.; Brinkø, A.; Larsen, M. T.; Sinning, S.; Williams, D. C.; Jensen, H. H. *Bioorg. Med. Chem. Lett.* **2013**, *23*, 1220−1224. (g) Khan, I.; Ibrar, A.; Abbas, N.; Saeed, A. *Eur. J. Med. Chem.* **2014**, *76*, 193−244. (h) Zhang, L.; Peng, X. M.; Damu, G. L. V.; Geng, R.-X.; Zhou, C.-H. *Med. Res. Rev.* **2014**, *34*, 340−437. (i) Albrecht, B. K.; Gehling, V. S.; Hewitt, M. C.; Vaswani, R. G.; Cote, A.; Leblanc, Y.; Nasveschuk, C. G.; Bellon, S.; Bergeron, L.; Campbell, R.; Cantone, N.; Cooper, M. R.; Cummings, R. T.; Jayaram, H.; Joshi, S.; Mertz, J. A.; Neiss, A.; Normant, E.; O'Meara, M.; Pardo, E.; Poy, F.; Sandy, P.; Supko, J.; Sims, R. J.; Harmange, J.-C.; Taylor, A. M.; Audia, J. E. *J. Med. Chem.* **2016**, *59*, 1330−1339. (j) Becerra, A.; Quintero, C.; Morales, V.; Valderrama, M.; Aguirre, A.; Faúndez, M. A.; Rojas, R. S. *Bioorg. Med. Chem.* **2017**, *25*, 2681−2688. (k) Tariq, S.; Somakala, K.; Amir, M. *Eur .J. Med. Chem.* **2018**. *143*, 542−557. (l) Kim, J.; Park, M.; Choi, J.; Singh, D. K.; Kwon, H. J.; Kim, S. H.; Kim, I. *Bioorg. Med. Chem. Lett.* **2019**, *29*, 1350−1356. (m) Khandelia, T.; Ghosh, S.; Panigrahi, P.; Shome, R.; Ghosh, S. S. Patel, B. K. *J. Org. Chem*. **2021**, *86*, 16948−16964.

[8] (a) Curran, D.; Grimshaw, J.; Perera, S. D. *Chem. Soc. Rev*. **1991**, *20*, 391−404. (b) Novak, P.; Muller, K.; Santhanam, K. S. V.; Haas, O. *Chem. Rev*. **1997**, *97*, 207−282. (c) Higgins, S. J. *Chem. Soc. Rev*. **1997**, *26*, 247−257. (d) Wang, Y. Z.; Epstein, A. J. *Acc. Chem. Res*. **1999**, *32*, 217−224. (e) Tsuboyama, A.; Iwawaki, H.; Furugori, M.; Mukaide, T.; Kamatani, J.; Igawa, S.; Moriyama, T.; Miura, S.; Takiguchi, T.; Okada, S.; Hoshino,

M.; Ueno, K. *J. Am. Chem. Soc*. **2003**, *125*, 12971–12979. (f) Ulrich, G.; Ziessel, R.; Harriman, A. *Angew. Chem., Int. Ed*. **2007**, *47*, 1184–1201. (g) Pu, S. Z.; Liu, G.; Shen, L.; Xu, J. K. *Org. Lett*. **2007**, *9*, 2139–2142. (h) Su, S.-J.; Sasabe, H.; Takeda, T.; Kido, J. *Chem. Mater*. **2008**, *20*, 1691–1693. (i) Maeda, H.; Mihashi, Y.; Haketa, Y. *Org. Lett.* **2008**, *10*, 3179 –3182. (j) Barbafina, A.; Amelia, M.; Latterini, L.; Aloisi, G. G.; Elisei, F. *J. Phys. Chem. A.* **2009**, *113*, 14514–14520. (k) Li, C.-S.; Tsai, Y.-H.; Lee, W.-C.; Kuo, W.-J. *J. Org. Chem.* **2010**, *75*, 4004–4013. (l) Moni, L.; Gers-Panther, C. F.; Anselmo, M.; Müller, T. J. J.; Riva, R. *Chem. Eur. J*. **2016**, *22*, 2020–2031. (m) Ibrahim, M. M.; Al-Refai, M.; Al-Fawwaz, A.; Ali, B. F.; Geyer, A.; Harms, K.; Marsch, M.; Kruger, M.; Osman, H.; Azmi, M. N. *J. Fluoresc*. **2018**, *28*, 655–662. (n) Mestiri, T.; Ghomrasni, S.; Khlaifia, D.; Alimi, K. *Physica B Condens. Matter* **2018**, *544*, 1–9. (o) Ghosh, S.; Pal, S.; Rajamanickam, S.; Shome, R.; Mohanta, P. R.; Ghosh, S. S.; Patel, B. K. *ACS Omega*. **2019**, *4*, 5565–5577.

[9] (a) Friend, R. H.; Gymer, R. W.; Holmes, A. B.; Burroughes, J. H.; Marks, R. N.; Taliani, C.; Bradley, D. D. C.; Dos. Santos, D. A.; Bredas, J. L.; Logdlund, M.; Salaneck, W. R. *Nature* **1999**, *397*, 121–128. (b) Mitschke, U.; Bauerle, P. *J. Mater. Chem*. **2000**, *10*, 1471–1507. (c) Gondek, E.; Kityk, I. V.; Danel, A.; Wisla, A.; Sanetra, J. *Synth. Met*. **2006**, *156*, 1348–1354 (d) Abet, V.; Nun˜ez, A.; Mendicuti, F.; Burgos, C.; Alvarez-Builla, J. *J. Org. Chem*. **2008**, *73*, 8800–8807. (e) Ahmed, E.; Briseno, A. L.; Xia, Y.; Jenekhe, S. A. *J. Am. Chem. Soc*. **2008**, *130*, 1118–1119. (f) Mutai, T.; Tomoda, H.; Ohkawa, T.; Yabe, Y.; Araki, K. *Angew. Chem., Int. Ed*. **2008**, *47*, 9522–9524, *Angew. Chem.* **2008**, *120*, 9664–9666. (g) Manna, S. K.; Mandal, A.; Mondal, S. K.; Adak, A. K. Jana, A.; Das, S.; Chattopadhyay, S.; Roy, S.; Ghorai, S. K.; Samanta, S.; Hossain, M.; Baidya, M. *Org. Biomol. Chem*. **2015**, *13*, 8037–8047. (h) Paramasivam, M.; Chitumalla, R. K.; Singh, S. P.; Islam, A.; Han, L.; Rao, V. J.; Bhanuprakash, K. *J. Phys. Chem. C* **2015**, *119*, 17053–17064. (i) Qian, X.; Zhu, Y.-Z.; Chang, W.-Y.; Song, J.; Pan, B.; Lu, L.; Gao, H.-H.; Zheng, J.-Y. *ACS Appl. Mater. Interfaces.* **2015**, *7*, 9015–9022. (j) Lin, G.; Peng, H.; Chen, L.; Nie, H.; Luo, W.; Li, Y.; Chen, S.; Hu, R.; Qin, A.; Zhao, Z.; Tang, B. Z. *ACS Appl. Mater. Interfaces.* **2016**, *8*, 16799–16808. (k) Chen, C. H.; Wang,

Y.; Michinobu, T.; Chang, S.-W.; Chiu, Y. C.; Ke, C.-Y.; Liou, G.-S. *ACS Appl. Mater. Interfaces*. **2020**, *12*, 6144–6150.

[10] (a) Rappoport, Z. *The chemistry of the nitrile group, Interscience Publishers, London*, **1970**. (b) Larock, R. C. *Comprehensive Organic Transformations: A Guide to Functional Group Preparations, 2nd ed; John Wiley & Sons, Inc.: New York*, **1999**. (c) Kukushkin, V. Y.; Pombeiro, A. J. L. *Chem. Rev.* **2002**, *102*, 1771–1802. (d) Zhou, C.; Larock, R. C. *J. Am. Chem. Soc*. **2004**, *126*, 2302–2303. (e) Shimizu, H.; Murakami, M. *Chem. Commun*. **2007**, 2855–2857. (f) Rach, S. F.; Kühn, F. E. *Chem. Rev*. **2009**, *109*, 2061–2080. (g) Xin, X.; Xiang, D.; Yang, J.; Zhang, Q.; Zhou, F.; Dong, D. *J. Org. Chem*. **2013**, *78*, 11956–11961. (h) Ping, Y.; Wang, L.; Ding, Q.; Peng, Y. *Adv. Synth. Catal*. **2017**, *359*, 3274–3291. (i) Cheng, K.; Wang, G.; Meng, M.; Qi, C. *Org. Chem. Front.* **2017**, *4*, 398–403. (j) Kanda, T.; Naraoka, A.; Naka, H. *J. Am. Chem. Soc*. **2019**, *141*, 825–830. (k) Paul, B.; Maji, M.; Kundu, S. *ACS Catal.* **2019**, *9*, 10469–10476. (l) Sun, K.; Lv, Q.-Y.; Lin, Y.-W.; Yu, B.; He, W.-M. *Org. Chem. Front*. **2021**, *8*, 445–465.

[11] (a) Hsieh, J.-C.; Cheng, A.-Y.; Fu, J.-H.; Kang, T.-W. *Org. Biomol. Chem*. **2012**, *10*, 6404–6409. (b) Chen, Y.-F.; Wu, Y.-S.; Jhan, Y.-H.; Hsieh, J.-C. *Org. Chem. Front.* **2014**, *1*, 253–257.

[12] (a) Takahashi, T.; Tsai, F.-Y.; Li, Y.; Wang, H.; Kondo, Y.; Yamanaka, M.; Nakajima, K.; Kotora, M. *J. Am. Chem. Soc*. **2002**, *124*, 5059–5067. (b) Varela, J. A.; Saa, C. *Chem. Rev*. **2003**, *103*, 3787–3801. (c) Chopade, P. R.; Louie, J. *Adv. Synth. Catal*. **2006**, *348*, 2307–2327. (d) Heller, B.; Hapke, M. *Chem. Soc. Rev*. **2007**, *36*, 1085–1094. (e) Das, B.; Reddy, C. R.; Kumar, D. N.; Krishnaiah, M.; Narender, R. *Synlett*. **2010**, 391–394. (f) Domínguez, G.; Pérez-Castells, J. *Chem. Soc. Rev*. **2011**, *40*, 3430–3444. (g) Shaaban, M. R.; El-Sayed, R.; Elwahy, A. H. M. *Tetrahedron* **2011**, *67*, 6095–6130. (h) Cantillo, D.; Gutmann, B.; Kappe, C. O. *J. Am. Chem. Soc*. **2011**, *133*, 4465–4475.

[13] (a) Evdokimov, N. M.; Kireev, A. S.; Yakovenko, A. A.; Antipin, M. Y.; Magedov, I. V.; Kornienko, A. *J. Org. Chem.* **2007**, *72*, 3443–3453. (b) Yan, C. G.; Wang, Q. F.; Song, X. K.; Sun, J. *J. Org. Chem*. **2009**, *74*, 710–718. (c) Sun, J.; Xia, E.-Y. ; Wu, Q.; Yan, C.-G. *Org. Lett*. **2010**, *12*, 3678–3681. (d) Attanasi, O. A.; Favi, G.; Geronikaki, A.; Mantellini, F.; Moscatelli, G.; Paparisva, A. *Org. Lett*. **2013**, *15*, 2624–2627. (e) Liu, B.;

Wei, E.; Lin, S.; Zhaoa, B.; Liang, F. *Chem. Commun*. **2014**, *50*, 6995–6997. (f) Dandia, A.; Singh, R.; Maheshwari, S. *Current Organic Chemistry*. **2014**, *18*, 2513–2529. (g) Wen, L.-R.; Jin, X.-J.; Niu, X.-D.; Li, M. *J. Org. Chem*. **2015**, *80*, 90–98. (h) Lu, Y.-L.; Sun, J.; Xie, Y.-J.; Yan, C.-G. *RSC Adv*. **2016**, *6*, 23390–23395. (i) Thimmarayaperumal, S.; Shanmugam, S. *ACS Omega*. **2017**, *2*, 4900–4910. (j) Zhang, D.; Luo, N.; Gan, J.; Wan, X.; Wang, C. *J. Org. Chem*. **2021**, *86*, *13*, 9218–9224. (k) Chakraborty, N.; Dahiya, A.; Rakshit, A.; Modi, A.; Patel, B. K. *Org. Biomol. Chem*. **2021**, *19*, 6847–6857.

[14] (a) Lin, S.; Wei, Y.; Liang. F. *Chem. Commun.* **2012**, *48*, 9879–9881. (b) Abdelhamid, A. O.; Negm, A. M.; Abbas, I. M. *J. Prakt. Chem*. **1989**, *331*, 31–36. (c) Al-Mousawi, S. M.; Moustafa, M. S.; Meier, H.; Kolshorn, H.; Elnagdi, M. H. *Molecules* **2009**, *14*, 798–806.

[15] (a) Zheng, D.; Zhao, Q.; Hu, X.; Cheng, T.; Liu, G.; Wang, W. *Chem. Commun*. **2017**, *53*, 6113–6116. (b) Alishetty, S.; Shih, H.-P.; Han, C.-C. *Org. Lett*. **2018**, *20*, 2513–2516. (c) Li, Z.-H.; Jiang, Z.-J.; Shao, Q.-L.; Qin, J.-J.; Shu, Q.-F.; Lu, W.-H.; Su, W.-K. *J. Org. Chem*. **2018**, *83*, 6423–6431. (d) Chen, C.; Wei, R.; Yi, X.; Gao, L.; Zhang, M.; Liu, H.; Li, Q.; Song, H.; Ban, S. *J. Org. Chem*. **2019**, *84*, 15655–15661. (e) Chen, J.; Li, C.; Zhou, Y.; Sun, C.; Sun, T. *ChemCatChem*. **2019**, *11*, 1943–194. (f) Wang, Z.; Chen, W.; Luo, H.; He, C.; Zhang, G.; Yu, Y. *Synthesis*. **2020**, *52*, 1659–1665. (g) Vaishanv, N. K.; Chandrasekharan, S. P.; Zaheer, M. K.; Kant, R.; Mohanan, K. *Chem. Commun*. **2020**, *56*, 11054–11057. (h) Sahoo, A. K.; Rakshit, A.; Dahiya, A.; Pan, A.; Patel, B. K. *Org. Lett*. **2022**, *24*, 1918–1923.

[16] (a) Ackermann, L.; Vicente, R.; Kapdi, A. *Angew. Chem., Int. Ed*. **2009**, *48*, 9792–9826. (b) Bernini, R.; Fabrizi, G.; Sferrazza, A.; Cacchi, S. *Angew. Chem. Int. Ed*. **2009**, *48*, 8078–8081. (c) Sun, C.-L.; Li, B.-J.; Shi, Z.-J. *Chem. Commun*. **2010**, *46*, 677–685. (d) Yeung, C. S.; Dong, V. M. *Chem. Rev*. **2011**, *111*, 1215–1292. (e) Kuhl, N.; Hopkinson, M. N.; Wencel-Delord, J.; Glorius, F. *Angew. Chem., Int. Ed.* **2012**, *51*, 10236–10254. (f) Kuhl, N.; Schroeder, N.; Glorius, F. *Adv. Synth. Catal*. **2014**, *356*, 1443–1460. (g) Liu, B.; Hu, F.; Shi, B.-F. *ACS Catal*. **2015**, *5*, 1863–1881. (h) Zheng, Q.-Z.; Jiao, N. *Chem. Soc. Rev*. **2016**, *45*, 4590–4627. (i) He, J.; Wasa, M.; Chan, K. S. L.; Shao, Q.; Yu, J.-Q. *Chem. Rev*. **2017**, *117*, 8754–8786. (j) Ma, W.; Gandeepan, P.; Li, J.; Ackermann, L.

Org. Chem. Front. **2017**, *4*, 1435–1467. (k) Dong, Z.; Ren, Z.; Thompson, S. J.; Xu, Y.; Dong, G. *Chem. Rev*. **2017**, *117*, 9333–9403.

[17] (a) Ueura, K.; Satoh, T.; Miura, M. *J. Org. Chem*. **2007**, *72*, 5362–5367. (b) Ueura, K.; Satoh, T.; Miura, M. *Org. Lett*. **2007**, *9*, 1407–1409. (c) Shimizu, M.; Hirano, K.; Satoh, T.; Miura, M. *J. Org. Chem*. **2009**, *74*, 3478–3483. (d) Satoh, T.; Miura, M. *Chem. Eur. J*. **2010**, *16*, 11212–11222. (e) Patureau, F. W.; Glorius, F. *Angew. Chem., Int. Ed*. **2011**, *50*, 1977–1979. (f) Ackermann, L. *Chem. Rev*. **2011**, *111*, 1315–1345. (g) Colby, D. A.; Tsai, A. S.; Bergman, R. G.; Ellman, J. A. *Acc. Chem. Res*. **2012**, *45*, 814–825. (h) Engle, K. M.; Mei, T.-S.; Wasa, M.; Yu, J.-Q. *Acc. Chem. Res*. **2012**, *45*, 788–802. (i) Rouquet, G.; Chatani, N. *Angew. Chem., Int. Ed*. **2013**, *52*, 11726–11743. (j) Chen, Z.; Wang, B.; Zhang, J.; Yu, W.; Liu, Z.; Zhang, Y. *Org. Chem. Front.* **2015**, *2*, 1107–1295. (k) Hummel, J. R.; Boerth, J. A.; Ellman, J. A. *Chem. Rev*. **2017**, *117*, 9163–9227. (l) Tang, K.-X.; Wang, C.-M.; Gao, T.-H.; Chen, L.; Fan, L.; Sun, L.-P. *Adv. Synth. Catal*. **2019**, *361*, 26–38.

[18] (a) Ritleng, V.; Sirlin, C.; Pfeffer, M. *Chem. Rev*. **2002**, *102*, 1731–1769. (b) Ackermann, L.; Vicente, R.; Potukuchi, H. K.; Pirovano, V. *Org. Lett*. **2010**, *12*, 5032–5035. (c) Colby, D. A.; Bergman, R. G.; Ellman, J. A. *Chem. Rev*. **2010**, *110*, 624−655. (d) Liu, C.; Zhang, H.; Shi, W.; Lei, A. *Chem. Rev*. **2011**, *111*, 1780–1824. (e) Arockiam, P. B.; Bruneau, C.; Dixneuf, P. H. *Chem. Rev*. **2012**, *112*, 5879–5918.

[19] (a) Ackermann, L.; Pospech, J.; Graczyk, K.; Rauch, K. *Org. Lett*. **2012**, *14*, 930–933. (b) Ackermann, L. *Acc. Chem. Res*. **2014**, *47*, 281–295. (c) Baruah, S.; Kaishap, P. P.; Gogoi, S. *Chem. Commun.* **2016**, *52*, 13004–13007. (d) Yang, Y.; Li, K.; Cheng, Y.; Wan, D.; Li, M.; You, J. *Chem. Commun*. **2016**, *52*, 2872–2884. (e) Borthakur, S.; Sarma, B.; Gogoi, S. *Org. Lett*. **2019**, *21*, 7878–7882. (f) Duarah, G.; Kaishap, P.P.; Begum, T.; Gogoi, S. *Adv. Synth. Catal*. **2019**, *361*, 654–672. (g) Sun, P.; Yang, J.; Peng, J.; Mo, B.; Chen, X.; Li, X.; Chen, C. *J. Org. Chem*. **2020**, *85*, 6761–6769. (h) Wang, C.; Chen, F.; Qian, P.; Cheng, J. *Org. Biomol. Chem*. **2021**, *19*, 1705–1721. (i) Yang, Q.-L.; Jia, H.-W.; Liu, Y.; Xing, Y.-K.; Ma, R.-C.; Wang, M.-M.; Qu, G.-R.; Mei, T.-S.; Guo, H.-M. *Org. Lett*. **2021**, *23*, 1209–1215.

[20] Rakshit, S.; Patureau, F. W.; Glorius, F. *J. Am. Chem. Soc*. **2010**, *132*, 9585–9587.

[21] Wang, L.; Ackermann, L. *Org. Lett*. **2013**, *15*, 176–179.

[22] Li, B.; Wang, N.; Liang, Y.; Xu, S.; Wang, B. *Org. Lett*. **2013**, *15*, 136–139.

[23] Murugan, K.; Liu, S.-T. *Tetrahedron Lett*. **2013**, *54*, 2608–2611.

[24] Zhao, M.-N.; Ren, Z.-H.; Wang, Y.-Y.; Guan, Z.-H. *Org. Lett*. **2014**, *16*, 608–611.

[25] Xu, Y.-H.; He, T.; Zhang, Q.-C.; Loh, T.-P. *Chem. Commun*. **2014**, *50*, 2784–2786.

[26] Ladeab, D. M.; Pawar, A. B. *Org. Chem. Front*. **2016**, *3*, 836–840.

[27] Parthasarathy, K.; Jeganmohan, M.; Cheng, C.-H. *Org. Lett*. **2008**, *10*, 325–328.

[28] Su, Y.; Zhao, M.; Han, K.; Song, G.; Li, X. *Org. Lett*. **2010**, *12*, 5462–5465.

[29] Ackermann, L.; Lygin, A. V.; Hofmann, N. *Org. Lett*. **2011**, *13*, 3278–3281.

[30] Stuart, D. R.; Bertrand-Laperle, M.; Burgess, K. M. N.; Fagnou, K. *J. Am. Chem. Soc*. **2008**, *130*, 16474–16475.

[31] Ackermann, L.; Lygin, A. V. *Org. Lett*. **2012**, *14*, 764–767.

[32] Song, W.; Ackermann, L. *Chem. Commun*. **2013**, *49*, 6638–6640.

[33] Zhang, Z.; Jiang, H.; Huang, Y. *Org. Lett*. **2014**, *16*, 5976–5979.

[34] Xu, F.; Li, Y.-J.; Huang, C.; Xu, H.-C. *ACS Catal*. **2018**, *8*, 3820–3824.

[35] Fukutani, T.; Umeda, N.; Hirano, K.; Satoh, T.; Miura, M. *Chem. Commun*. **2009**, 5141–5143.

[36] Ackermann, L.; Lygin, A. V.; Hofmann, N. *Angew. Chem., Int. Ed*. **2011**, *50*, 6379–6382.

[37] Ackermann, L.; Fenner, S. *Org. Lett*. **2011**, *13*, 6548–6551.

[38] Zhong, H.; Yang, D.; Wang, S.; Huang, J. *Chem. Commun*. **2012**, *48*, 3236–3238.

[39] Chinnagolla, R. K.; Pimparkar, S.; Jeganmohan, M. *Org. Lett*. **2012**, *14*, 3032–3035.

[40] Kornhaaß, C.; Li, J.; Ackermann, L. *J. Org. Chem*. **2012**, *77*, 9190–9198.

[41] Villuendas, P.; Urriolabeitia, E. P. *J. Org. Chem*. **2013**, *78*, 5254–5263.

[42] Huang, X.-C.; Yang, X.-H.; Song, R.-J.; Li, J.-H. *J. Org. Chem*. **2014**, *79*, 1025−1031.

[43] Grigorjeva, L.; Daugulis, O. *Angew. Chem., Int. Ed*. **2014**, *53*, 10209–10212.

[44] Yang, F.; Ackermann, L. *J. Org. Chem*. **2014**, *79*, 12070–12082.

[45] Li, J.; John, M.; Ackermann, L. *Chem. Eur. J*. **2014**, *20*, 5403–5408.

[46] Allu, S.; Swamy, K. C. K. *J. Org. Chem*. **2014**, *79*, 3963–3972.

[47] Sen, M.; Kalsi, D.; Sundararaju, B. *Chem. Eur. J.* **2015**, *21*, 15529–15533.

[48] Kaishap, P. P.; Duarah, G.; Chetiab, D.; Gogoi, S. *Org. Biomol. Chem*. **2017**, *15*, 3491–3498.

[49] Ruiz, S.; Sayago, F. J.; Cativiela, C.; Urriolabeitia, E. P. *J. Mol. Catal. A Chem*. **2017**, *426*, 407–418.

[50] Song, G.; Chen, D.; Pan, C.-L.; Crabtree, R. H.; Li, X. *J. Org. Chem*. **2010**, *75*, 7487–7490.

[51] Ackermann, L.; Wang, L.; Lygin, A. V. *Chem. Sci*. **2012**, *3*, 177–180.

[52] Ma, W.; Graczyk, K.; Ackermann, L. *Org. Lett*. **2012**, *14*, 6318–6321.

[53] Wang, R.; Falck, J. R. *J. Organomet. Chem*. **2014**, *759*, 33–36.

[54] Jayakumar, J.; Parthasarathy, K.; Chen, Y.-H.; Lee, T.-H.; Chuang, S.-C.; Cheng, C.-H. *Angew. Chem., Int. Ed*. **2014**, *53*, 9889–9892.

[55] Lu, H.; Yang, Q.; Zhou, Y.; Guo, Y.; Deng, Z.; Ding, Q.; Peng, Y. *Org. Biomol. Chem*. **2014**, *12*, 758–764.

[56] Lingayya, R.; Vellakkaran, M.; Nagaiah, K.; Nanubolu, J. B. *Asian J. Org. Chem*. **2015**, *4*, 462–469.

[57] Tulichala, R. N. P.; Shankar, M.; Swamy, K. C. K. *J. Org. Chem*. **2017**, *82*, 5068–5079.

[58] Wang, Z.-Q.; Hou, C.; Zhong, Y.-F.; Lu, Y.-X.; Mo, Z.-Y.; Pan, Y.-M.; Tang, H.-T. *Org. Lett*. **2019**, *21*, 9841–9845.

[59] (a) Fleming, F. F.; Wang, Q. *Chem. Rev*. **2003**, *103*, 2035–2077. (b) Rach, S. F.; Kühn, F. E. *Chem. Rev*. **2009**, *109*, 2061–2080.

[60] Pletnev, A. A.; Tian, Q.; Larock, R. C. *J. Org. Chem*. **2002**, *67*, 9276–9287.

[61] Tian, Q.; Pletnev, A. A.; Larock, R. C. *J. Org. Chem*. **2003**, *68*, 339–347.

[62] Miura, T.; Murakami, M. *Org. Lett.* **2005**, *7*, 3339–3341.

[63] Tsukamoto, H.; Ikeda, T.; Doi, T. *J. Org. Chem*. **2016**, *81*, 1733–1745.

[64] (a) McCormick, M. M.; Duong, H. A.; Zuo, G.; Louie, J. *J. Am. Chem. Soc*. **2005**, *127*, 5030–5031. (b) Stolley, R. M.; Duong, H. A.; Louie, J. *Organometallics*. **2013**, *32*, 4952–4960.

[65] Onodera, G.; Shimizu, Y.; Kimura, J.; Kobayashi, J.; Ebihara, Y.; Kondo, K.; Sakata, K.; Takeuchi, R. *J. Am. Chem. Soc*. **2012**, *134*, 10515–10531.

[66] Xie, Y.; Wu, C.; Jia, C.; Tung, C.-H.; Wang, W. *Org. Chem. Front*. **2020**, *7*, 2196–2201.

[67] Wang, C.-S.; Sun, Q.; García, F.; Wang, C.; Yoshikai, N. *Angew. Chem., Int. Ed*. **2021**, *60*, 9627–9634.

[68] You, X.; Xie, X.; Wang, G.; Xiong, M.; Sun, R.; Chen, H.; Liu, Y. *Chem. Eur. J*. **2016**, *22*, 16765–16769.

[69] Reddy, M. C.; Manikandan, R.; Jeganmohan, M. *Chem. Commun*. **2013**, *49*, 6060–6062.

[70] (a) Li, J.; Chen, L.; Chin, E.; Lui, A. S.; Zecic, H. *Tetrahedron Lett*. **2010**, *51*, 6422–6425. (b) Shen, H.; Xie, Z. *J. Am. Chem. Soc*. **2010**, *132*, 11473–11480. (c) Kumar, R.; Asthana, M.; Singh, R. M. *J. Org. Chem*. **2017**, *82*, 11531–11542. (d) Liu, X.; Deng, G.; Liang, Y. *Tetrahedron Lett*. **2018**, *59*, 2844–2847. (e) Mishra, P. K.; Chatterjee, S.; Verma, A. K. *ACS Omega*. **2020**, *5*, 32133–32139.

[71] (a) Tietze, L. F.; Beifuss, U. *Angew. Chem., Int. Ed*. **1993**, *32*, 131–163. (b) Tietze, L. F. *Chem. Rev*. **1996**, *96*, 115–136. (c) Tietze, L. F. *Chem. Rev*. **1996**, *96*, 115–136. (d) Padwa, A.; Bur, S. K. *Tetrahedron*. **2007**, *63*, 5341–5378. (e) Li, Y.-M.; Wang, S.-S.; Yu, F.-C.; Shen, Y.-H.; Chang, K.-J. *Org. Biomol. Chem*. **2015**, *13*, 5376–5380. (f) Zhang, X.; Xie, X.; Liu, Y. *Chem. Sci*. **2016**, *7*, 5815–5820.

[72] (a) Nicolaou, K. C.; Edmonds, D. J.; Bulger, P. G. *Angew. Chem., Int. Ed*. **2006**, *45*, 7134–7186. (b) Grondal, C.; Jeanty, M.; Enders, D. *Nature Chem*. **2010**, *2*, 167–178.

[73] (a) Watanabe, T.; Ueda, S.; Inuki, S.; Oishi, S.; Fujii, N.; Ohno, H. *Chem. Commun*. **2007**, 4516–4518. (b) Yao, P.-Y.; Zhang, Y.; Hsung, R. P.; Zhao, K. *Org. Lett*. **2008**, *10*, 4275–4278. (c) Zhu, J.; Xie, H.; Chen, Z.; Li, S.; Wu, Y. *Chem. Commun*. **2009**, 2338–2340. (d) Verma, A. K.; Kesharwani, T.; Singh, J.; Tandon, V.; Larock, R. C. *Angew. Chem., Int. Ed*. **2009**, *48*, 1138–1143. (e) Lv, X.; Bao, W. *J. Org. Chem*. **2009**, *74*, 5618–5621. (f) Wang, F.; Cai, S.; Liao, Q.; Xi, C. *J. Org. Chem*. **2011**, *76*, 3174–3180. (g) Zhang, L.-L.; Chen, S.; Gao, Y.-Z.; Zhang, P.-B.; Wu, Y.-L.; Tang, G.; Zhao, Y.-F. *Org. Lett*. **2016**, *18*, 1286–1289. (h) Zhang, P.-B.; Zhang, L.-L.; Gao, Y.-Z.; Tang, G.; Zhao, Y.-F. *RSC Adv*. **2016**, *6*, 60922–60925. (i) Wang, S.-S. Fu, H.; Wang, G.; Sunb, M.; Li, Y.-M. *RSC Adv*. **2016**, *6*, 52391–52394. (j) Chen, W.; Zhang, Y.; Li, P.; Wang, L. *Org. Chem. Front*. **2018**, *5*, 855–859.

[74] Ueda, S.; Nagasawa, H. *J. Am. Chem. Soc*. **2009**, *131*, 15080–15081.

[75] Chen, Y.-F.; Hsieh, J.-C. *Org. Lett*. **2014**, *16*, 4642–4645.

[76] Li, C.; An, S.; Zhu, Y.; Zhang, J.; Kang, Y.; Liu, P.; Wang, Y.; Li, J. *RSC Adv*. **2014**, *4*, 49888–49891.

[77] Yu, S.; Qi, L.; Hu, K.; Gong, J.; Cheng, T.; Wang, Q.; Chen, J.; Wu, H. *J. Org. Chem*. **2017**, *82*, 3631–3638.

[78] Yousuf, M.; Adhikari, S. *Org. Lett*. **2017**, *19*, 2214–2217.

[79] Yu, H.; Xiao, L.; Yang, X.; Shao, L. *Chem. Commun*. **2017**, *53*, 9745–9748.

[80] Qi, L.; Hu, K.; Yu, S.; Zhu, J.; Cheng, T.; Wang, X.; Wu, H.; Chen, J. *Org. Lett*. **2017**, *19*, 218–221.

[81] Hu, K.; Qi, L.; Yu, S.; Cheng, T.; Wang, X.; Li, Z.; Xia, Y.; Wu, H.; Chen, J. *Green Chem*. **2017**, *19*, 1740–1750.

[82] Yu, X.; Gao, L.; Jia, L.; Yamamoto, Y.; Bao, M. *J. Org. Chem*. **2018**, *83*, 10352–10358.

[83] Jaiswal, Y.; Kumar, Y.; Pal, J.; Subramanian, R.; Kumar, A. *Chem. Commun*. **2018**, *54*, 7207–7210.

[84] Wang, T.-T.; Zhang, D.; Liao, W.-W. *Chem. Commun*. **2018**, *54*, 2048–2051.

[85] Zhu, J.; Shao, Y.; Hu, K.; Qi, L.; Cheng, T.; Chen, J. *Org. Biomol. Chem*., **2018**, *16*, 8596–8603.

[86] Zhang, Y.; Shao, Y.; Gong, J.; Hu, K.; Cheng, T.; Chen, J. *Adv. Synth. Catal*. **2018**, *360*, 3260–3265.

[87] Yang, X.; Yu, H.; Xu, Y.; Shao, L. *J. Org. Chem*. **2018**, *83*, 9682–9695.

[88] Yao, X.; Shao, Y.; Hu, M.; Xia, Y.; Cheng, T.; Chen, J. *Org. Lett*. **2019**, *21*, 7697–7701.

[89] Yao, X.; Shao, Y.; Hu, M.; Zhang, M.; Li, S.; Xia, Y.; Cheng, T.; Chen J. *Adv. Synth. Catal*. **2019**, *361*, 4707–4713.

[90] Fang, S.; Yu, H.; Yang, X.; Li, J.; Shao, L. *Adv. Synth. Catal*. **2019**, *361*, 3312-3317.

[91] Xu, T.; Shao, Y.; Dai, L.; Yu, S.; Cheng, T.; Chen, J. *J. Org. Chem*. **2019**, *84*, 13604–13614.

[92] Rodrigues, R.; Tran, L. Q.; Darses, B.; Dauban, P.; Neuville, L. *Adv. Synth. Catal*. **2019**, *361*, 4454–4460.

[93] Gong, J.; Hu, K.; Zhang, Y.; Shao, Y.; Cheng, T.; Chen, J.; Hu, M. *Molecules* **2019**, *24*, 463–476.

[94] Zhen, Q.; Chen, L.; Qi, L.; Hu, K.; Shao, Y.; Li, R.; Chen, J. *Chem. Asian J*. **2020**, *15*, 106–111.

[95] Xiong, W.; Hu, K.; Lei, Y.; Zhen, Q.; Zhao, Z.; Shao, Y.; Li, R.; Zhang, Y.; Chen, J. *Org. Lett*. **2020**, *22*, 1239–1243.

[96] Ye, X.; Xu, B.; Sun, J.; Dai, L.; Shao, Y.; Zhang, Y.; Chen, J. *J. Org. Chem*. **2020**, *85*, 13004–13014.

[97] Yao, X.; Qi, L.; Li, R.; Zhen, Q.; Liu, J.; Zhao, Z.; Shao, Y.; Hu, M.; Chen, J. *ACS Comb. Sci*. **2020**, *22*, 114–119.

[98] Xie, J.; Huang, H.; Xu, T.; Li, R.; Chen, J.; Ye, X. *RSC Adv.* **2020**, *10*, 8586–8593

[99] Chen, L.; Gong, J.; Zhang, Y.; Shao, Y.; Chen, Z.; Li, R.; Chen, J. *Org. Lett*. **2020**, *22*, 6943–6947.

[100] Zhen, Q.; Li, R.; Qi, L.; Hu, K.; Yao, X.; Shao, Y.; Chen, J. *Org. Chem. Front*. **2020**, *7*, 286–291.

[101] He, C.; Wang, Z.; Chen, Y.; Zhang, G.; Yu, Y. *Synthesis.* **2021**, *53*, 2051–2056.

[102] Zhang, Y.; Chen, L.; Shao, Y.; Zhang, F.; Chen, Z.; Lv, N.; Chen, J.; Li, R. *Org. Chem. Front*. **2021**, *8*, 254–259.

[103] Zhang, Y.; Xiong, W.; Chen, L.; Shao, Y.; Li, R.; Chen, Z.; Ge, J.; Lv, N.; Chen, J. *Org. Chem. Front*., **2021**, *8*, 304–309.

[104] Dai, L.; Yu, S.; Lv, N.; Ye, X.; Shao, Y.; Chen, Z.; Chen, J. *Org. Lett*. **2021**, *23*, 5664–5668.

[105] Zheng, J.; Zhang, Y.; Wang, D.; Cui, S. *Org. Lett*. **2016**, *18*, 1768–1771.

[106] Shang, J.-Q.; Wang, S.-S.; Fu, H.; Li, Y.; Yang, T.; Li, Y.-M. *Org. Chem. Front*. **2018**, *5*, 1945–1949.

[107] Wu, L.-J.; Yang, Y.; Song, R.-J.; Yu, J.-X.; Li, J.-H.; He, D.-L. *Chem. Commun*. **2018**, *54*, 1367–1370.

[108] Shan, X.-H.; Zheng, H.-X.; Yang, B.; Tie, L.; Fu, J.-L.; Qu, J.-P.; Kang, Y.-B. *Nat Commun.* **2019**, *10*, 908–916.

[109] Xu, P.; Zhu, Y.-M.; Wang, F.; Wang, S.-Y.; Ji, S.-J. *Org. Lett*. **2019**, *21*, 683–686.

[110] Shang, J.-Q.; Wang, X.-X.; Xin, Y.; Li, Y.; Zhou, B.; Li, Y.-M. *Org. Biomol. Chem.* **2019**, *17*, 9447–9455.

[111] Guo, J.; Hao, Y.; Li, G.; Wang, Z.; Liu, Y.; Li, Y.; Wang, Q. *Org. Biomol. Chem*. **2020**, *18*, 1994–2001.

[112] Xu, P.; Zhu, Y.-M.; Liu, X.-Y.; Zhou, X.-Z.; Wang, S.-Y.; Ji, S.-J. *Chin. Chem. Lett*. **2021**, *32*, 413–416.

[113] (a) Fu, W.; Xu, F.; Fu, Y.; Zhu, M.; Yu, J.; Xu, C.; Zou, D. *J. Org. Chem*. **2013**, *78*, 12202–12206. (b) Tang, S.; Deng, Y.-L.; Li, J.; Wang, W.-X.; Ding, G.-L.; Wang, M.-W.; Xiao, Z.-P.; Wang, Y.-C.; Sheng, R.-L. *J. Org. Chem*. **2015**, *80*, 12599–12605. (c) Bergonzini, G.; Cassani, C.; Wallentin, C.-J. *Angew. Chem., Int. Ed*. **2015**, *54*, 14066–14069. (d) Zhou, L.; Lokman Hossain, M.; Xiao, T. *Chem. Rec*. **2016**, *16*, 319–334. (e) Ji, W.; Tan, H.; Wang, M.; Li, P.; Wang, L. *Chem. Commun*. **2016**, *52*, 1462–1465. (f) Xia, D.; Li, Y.; Miao, T.; Li, P.; Wang, L. *Green Chem*. **2017**, *19*, 1732–1739. (g) Deng, Q.; Xu, Y.; Liu, P.; Tan, L.; Sun, P. *Org. Chem. Front*. **2018**, *5*, 19–23.

[114] Sun, X.; Li, J.; Ni, Y.; Ren, D.; Hu, Z.; Yu, S. *Asian J. Org. Chem*. **2014**, *3*, 1317–1325.

[115] Han, Y.-Y.; Jiang, H.; Wang, R.; Yu, S. *J. Org. Chem*. **2016**, *81*, 7276–7281.

[116] Li, X.; Fang, X.; Zhuang, S.; Liu, P.; Sun, P. *Org. Lett.* **2017**, *19*, 3580–3583.

[117] Yu, Y.; Cai, Z.; Yuan, W.; Liu, P.; Sun, P. *J. Org. Chem*. **2017**, *82*, 8148–8156.

[118] Yu, Y.; Yuan, W.; Huang, H.; Cai, Z.; Liu, P.; Sun, P. *J. Org. Chem*. **2018**, *83*, 1654–1660.

[119] Natarajan, P.; Muskan, M.; Brar, N. K.; Kaur, J. J. *Org. Chem. Front*. **2018**, *5*, 1527–1531.

[120] Liu, X.; Wu, Z.; Zhang, Z.; Liu, P.; Sun, P. *Org. Biomol. Chem*. **2018**, *16*, 414–423.

[121] Zhu, M.; Fu, W.; Guo, W.; Tian, Y.; Wang, Z.; Ji, B. *Org. Biomol. Chem*. **2019**, *17*, 3374–3380.

CHAPTER II

One-pot Sequential Synthesis of Fused Isoquinolines via Intramolecular-Cyclization/Annulation and their Photophysical Investigations

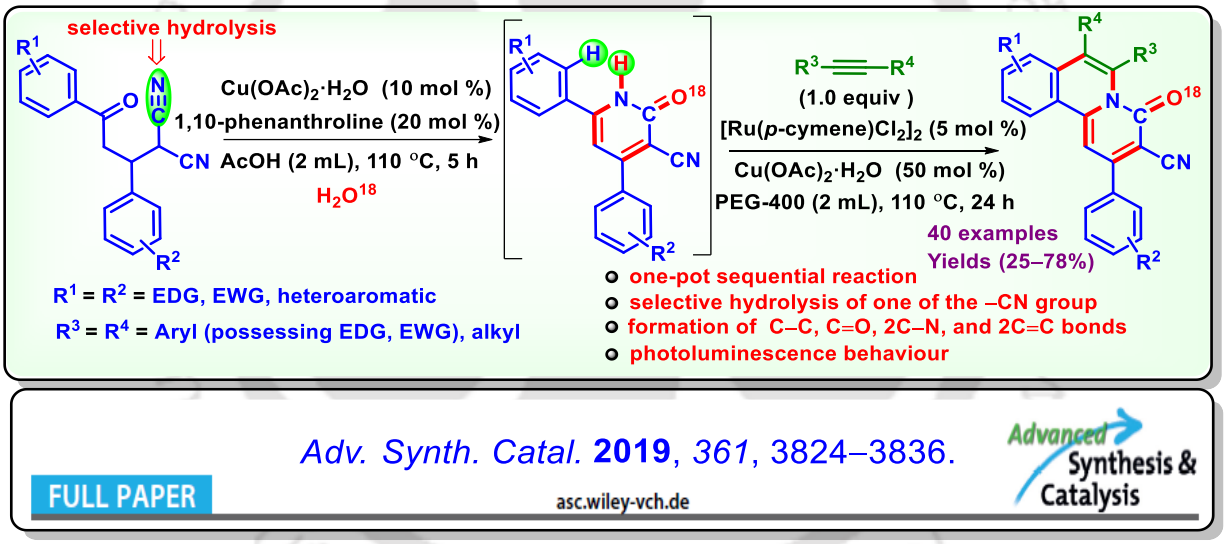

Adv. Synth. Catal. **2019**, *361*, 3824–3836.
FULL PAPER
asc.wiley-vch.de
Advanced Synthesis & Catalysis

ABSTRACT: A one-pot synthesis of fused conjugated isoquinolones was developed from γ-ketomalononitriles and internal alkynes in the presense of Cu(II) and Ru(II). This one-pot process consisting of a Cu(II)-catalyzed selective hydrolysis of a cyano group to an amide, dehydrative cyclization of the amide to a cyclic amide and finally the Ru(II)-catalyzed C–H/N–H annulation with an internal alkyne. The overall process is associated with the formation of one C–C, two C–N, two C=C and a C=O bonds leading to highly fluorescence active fused isoquinolone having emission in the green region (502–560) nm and absorption (λ_{max}) in the range of (454–490) nm. The $\Delta E_{(LUMO–HOMO)}$ of the synthesized compounds are in the range of 2.88 to 3.45 eV which is calculated on the basis of DFT.

CHAPTER II

One-pot Sequential Synthesis of Fused Isoquinolines *via* Intramolecular-Cyclization/Annulation and their Photophysical Investigations

II.1. Introduction:

Various heterocyclic compounds having potential biological activities have been synthesized *via* Michael adduct with numerous carbon nucleophiles.[1] Malononitrile is one of the useful and convenient precursors for the synthesis of a wide range of fused *N*- and *O*-heterocyclic skeletons.[2] Over the years, many publications have appeared for nitrogen-containing six-membered heterocyclic systems highlighting their biological importance as well as photophysical properties. Amid fused-ring nitrogen heterocycles, isoquinolines and isoquinolones are a special class possessing comprehensive biological activities (Figure II.1.1) and exist in many synthetic drugs and natural products.[3–5] Further, organic fluorescent molecules, used in organic light-emitting diodes (OLEDs),[6] liquid crystal displays (LCDs)[7] and fluorescent dyes[8] are important in bridging between the synthetic organic chemistry and material science.[9] Due to fascinating luminescent[10a,b,c] properties substituted fused isoquinolines[10d] play a significant role in material science (Figure II.1.1). Moreover, numerous organic transformations use isoquinolones as one of the key intermediate.[11] Therefore, it is desirable to develop synthetic protocols for these potentially active heterocycles as target structures for biological evaluation and application in material science.

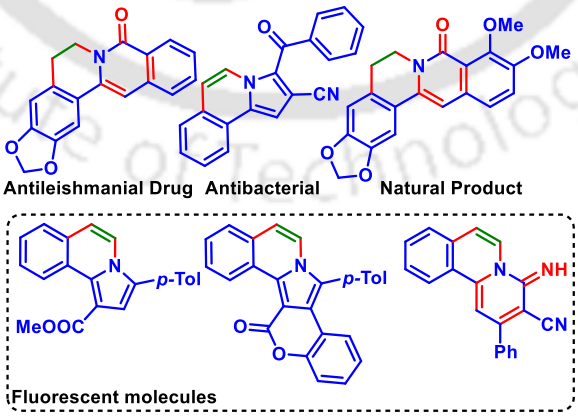

Figure II.1.1. *Representative biologically active natural product and highly fluorescent fused isoquinolines/isoquinolones.*

Of late, transition-metal-catalyzed C–H bond activation[12,13] has gained great attention for the synthesis of bioactive complex nitrogen-containing fused heterocycles, especially, isoquinolines and isoquinolones. In this context Rh(III), Pd(II), Ni(II), and Ru(II) catalysts are most common and have been used extensively to obtain isoquinolones[14] *via* the oxidative coupling between an internal alkyne and an amide. Further, in the recent past, a two-step protocol has been achieved utilizing two different catalytic systems for the synthesis of highly functionalized compounds.[15] The development of one-pot strategies is often ineffective because each step provides several byproducts along with unreacted starting materials. Inspired by transition-metal-catalyzed direct annulation of C–H bonds[16] and the advantage of two-step protocol we envisaged the synthesis of 4-oxo-2,6,7-triphenyl-4*H*-pyrido[2,1-*a*]isoquinoline-3-carbonitrile (**1a**) from a Michael-adduct,[17] 2-(3-oxo-1,3-diphenylpropyl)malononitrile (**1**) [Scheme II.1.1, (i)]. The selective hydrolysis of one of the cyano groups in γ-keto dicyano compound (**1**) would lead to an amide similar to hydrolysis of methylenemalononitriles [Scheme II.1.1, (ii)].[18] The *in situ* generated monoamide may undergo an intermolecular dehydrative cyclization followed by aromatization/oxidation to form a cyclic amide, 1,2-dihydropyridone (**1′**) which has potential C–H/N–H sites for annulation with an alkyne to afford 4-oxo-2,6,7-triphenyl-4*H*-pyrido[2,1-*a*]isoquinoline-3-carbonitrile (**1a**). This reaction involves an intramolecular dehydrative cyclization followed by an intermolecular annulation with an alkyne to obtain a fused isoquinolone framework. Our initial investigation started using 2-(3-oxo-1,3-diphenylpropyl)malononitrile (**1**) (0.20 mmol), diphenylacetylene (**a**) (1 equiv), $Cu(OAc)_2 \cdot H_2O$ (1 equiv), and $[Ru(p\text{-cymene})Cl_2]_2$ (2 mol %) in glacial AcOH at 110 ^oC. Interestingly, the reaction resulted in the formation of a new yellow fluorescent spot (viewed under 365 nm UV lamp) as observed by TLC. Unfortunately, the compound could not be separated for characterization as it was associated with several other side products. However, a decent amount (18%) of expected cyclic 1,2-dihydropyridone intermediate *viz.* 2-oxo-4,6-diphenyl-1,2-dihydropyridine-3-carbonitrile (**1′**) could be isolated [Scheme II.1.1, (iii)]. Encouraged by the success of our anticipated strategy we adopted a two-step protocol [Scheme II.1.1, (iv)]. In the first step the 2-(3-oxo-1,3-diphenylpropyl)malononitrile (0.2 mmol) (**1**) was treated with $Cu(OAc)_2 \cdot H_2O$ (1 equiv) in AcOH (2 mL) at 110 ^oC and the reaction was continued for 5 h, during this period all the starting materials got consumed giving 1,2-dihydropyridone intermediate (**1′**) as the major product along with significant amounts of other

uncharacterized by-products To this crude reaction mixture, diphenylacetylene (**a**) (1 equiv) and [Ru(*p*-cymene)Cl_2]$_2$ (5 mol %) were added and the reaction was allowed to proceed for 12 h. The reaction was found to be much cleaner and the product (**1a**) was isolated in 30% yield. The product was separated and characterized by spectroscopic analysis (IR, ^{1}H NMR, ^{13}C{^{1}H} NMR, and HRMS) and the structure was found to be 4-oxo-2,6,7-triphenyl-4*H*-pyrido[2,1-*a*]isoquinoline-3-carbonitrile (**1a**). Finally, the structure of the product (**1a**) was reconfirmed by a single-crystal X-ray diffraction study (Figure II.1.2, **CCDC–1885708**).

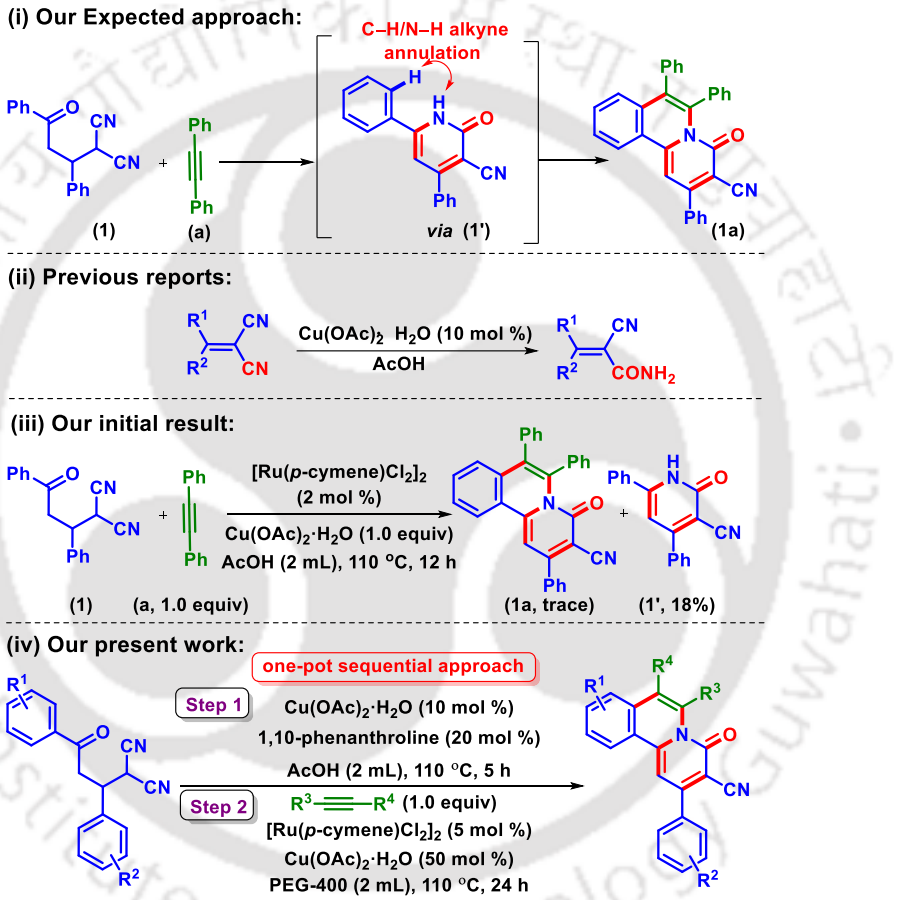

Scheme II.1.1. *Strategies for the synthesis of fused isoquinolones from γ-ketodinitriles.*

This one-pot transformation of 2-(3-oxo-1,3-diphenylpropyl)malononitrile (**1**) to a 4-oxo-2,6,7-triphenyl-4*H*-pyrido[2,1-*a*]isoquinoline-3-carbonitrile (**1a**) is accompanied by the formation of new C–C, C–N, C=C and C=O bonds. Observing the structure of the product it is evident that the amidic carbonyl group in the product (**1a**) is not the original carbonyl group of the starting material (**1**). Thus, the carbonyl group may be originating from the selective hydrolysis of one of the cyano groups. An O^{18} incorporated product was detected when the typical reaction was carried

out in the presence of H_2O^{18}, thereby confirming water to be the source of oxygen in the product (**1a**). Although, synthetic strategies of some of the isoquinolone involve C–H bond activation and annulation of various amides with internal alkynes employing transition metal catalysts we feel our report exploring the alternative pattern would be useful to the synthetic community.

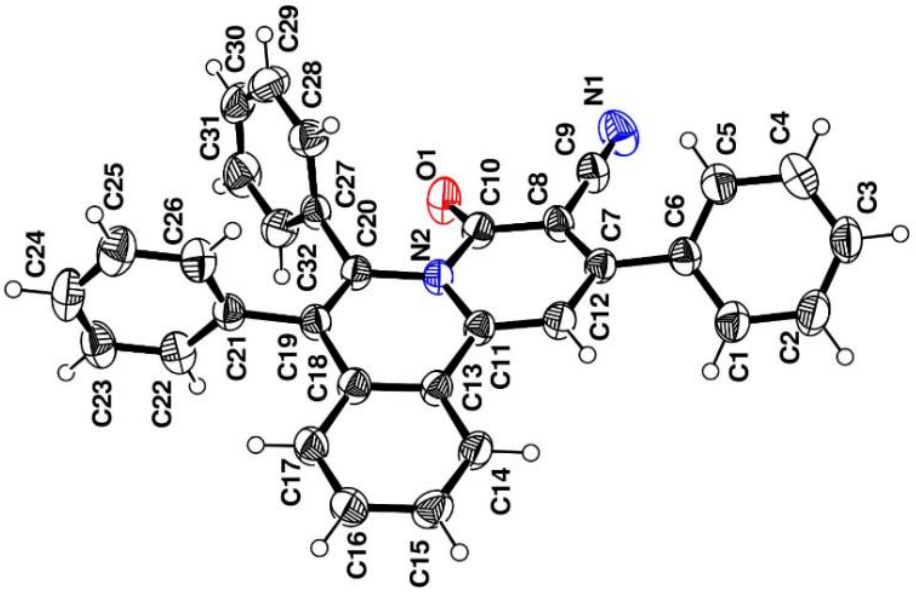

Figure II.1.2. *ORTEP diagram of (**1a**) with 40% ellipsoid probability (CCDC–1885708).*

II.2. Strategies for the Synthesis of Fused Isoquinolones:

Owing to the versatile utility of isoquinolones in both biological and synthetic fields, several methods have been implemented for their synthesis *via* transition-metal-catalyzed C–H/N–H oxidative alkyne annulation. A few of these strategies are enlisted below.

In 2010, the Li group reported a Rh(III)-catalyzed oxidative alkyne annulation using primary benzamides to access polycyclic fused isoquinolones through double C–H/N–H alkyne annulation (Scheme II.2.1).[19]

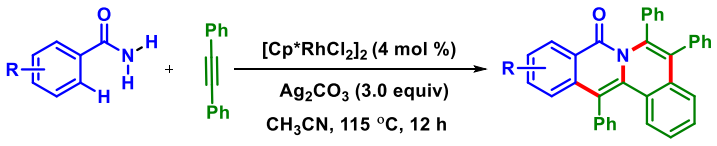

Scheme II.2.1. *Rh(III)-catalyzed synthesis of isoquinolones via double annulation.*

In 2011, Ackermann *et al*. reported a Ru(II)-catalyzed annulations between *N*-benzyl-substituted benzamides and internal alkynes for chemo- and site-selective synthesis of isoquinolones (Scheme II.2.2).[20] Mechanistic studies in deuterated ^{t}AmOH suggest an irreversible C–H bond ruthenation while the kinetic isotope effect (KIE) study provided strong evidence for a carboxylate assistance rate-limiting C–H bond ruthenation.

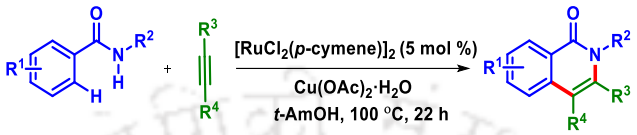

Scheme II.2.2. *Ru(II)-catalyzed synthesis of isoquinolones.*

In 2012, the Huang group reported a Pd(II)-catalyzed atom-economical synthesis of isoquinolinones *via* C–H and N–H bonds activation of benzamides with internal alkynes in excellent yields and good regioselectivity with unsymmetrical alkynes (Scheme II.2.3).[21]

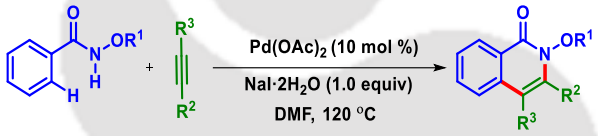

Scheme II.2.3. *Pd(II)-catalyzed synthesis of isoquinolones.*

In 2013, Jaganmohan *et al*. described a Ru(II)/Cu(II)-catalyzed cyclization of aromatic and heteroaromatic nitriles *via* oxidative annulation with alkynes in acetic acid under air to afford isoquinolones in good to excellent yields (Scheme II.2.4).[22] The reaction proceeds through the hydrolysis of the nitrile into an amide ($CONH_2$) in the presence of $Cu(OAc)_2{\cdot}H_2O$ in acetic acid. Further, an amide-directed C–H/N–H bond functionalization followed by annulation with internal alkyne provided substituted isoquinolones.

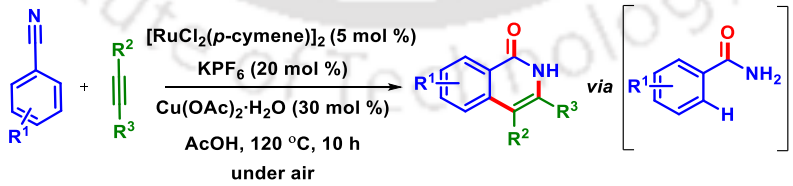

Scheme II.2.4. *Ru(II)/Cu(II)-catalyzed synthesis of isoquinolones from nitriles.*

In 2014, Daugulis *et al.* reported a Co(II)-catalyzed synthesis of isoquinolones *via* aminoquinoline-directed C(sp^2)–H bond activation. (Scheme II.2.5).[23] This method provides

excellent functional group tolerance and both internal and terminal alkynes are also well tolerated in this coupling process.

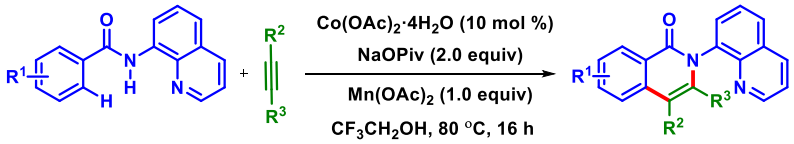

Scheme II.2.5. *Co(II)-catalyzed synthesis of isoquinolones.*

In 2018 Jaganmohan group further reported a Co(II)-catalyzed 8-aminoquinoline directed annulation of benzamides with alkynes to synthesize fused isoquinolines in good yields under an aerial atmosphere (Scheme II.2.6).[24]

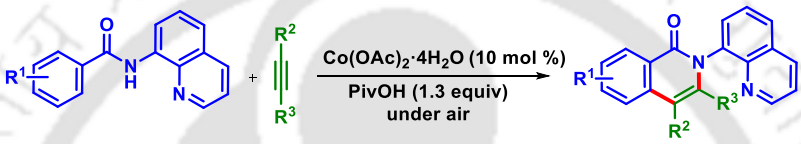

Scheme II.2.6. *Co(II)-catalyzed synthesis of fused isoquinolones.*

In the same year Van der Eycken, *et al.* described a microwave-assisted Ru(II)-catalyzed highly efficient intermolecular C–H functionalization sequence to access substituted isoquinolones using α-amino esters as the directing group (Scheme II.2.7).[25]

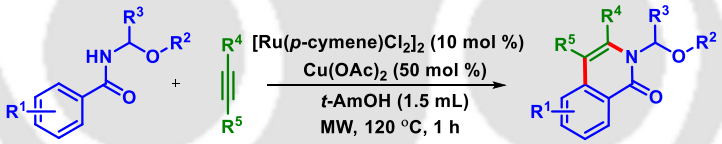

Scheme II.2.7. *Ru(II)-catalyzed synthesis of isoquinolones.*

In 2019, Tang and co-workers reported a Ru(II)-catalyzed electrochemically enabled dehydrogenative annulation reaction of amides and alkynes for the synthesis of polycyclic isoquinolinones through a double C−H activation route (Scheme II.2.8).[26]

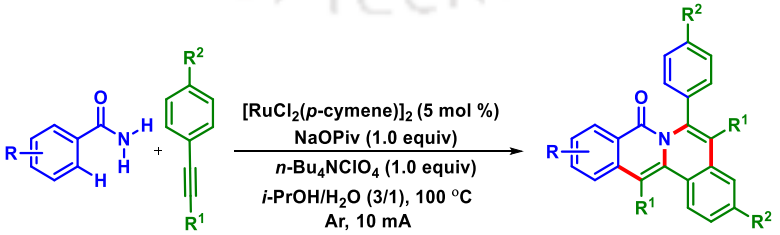

Scheme II.2.8. *Ru(II)-catalyzed synthesis of polycyclic isoquinolinones.*

II.3. Present Work:

II.3.1. Optimization of the Reaction Conditions:

Encouraged by the above one-pot two-fold sequential synthesis of fused isoquinoline, further optimizations were carried out by varying various reaction parameters using 2-(1-(4-chlorophenyl)-3-oxo-3-(*p*-tolyl)propyl)malononitrile (**18**) as the model substrate and diphenylacetylene (**a**) as the coupling partner in the presence of $Cu(OAc)_2 \cdot H_2O$ and [Ru(*p*-cymene)Cl_2]$_2$. Fixing the conditions [*i.e.* diphenyl acetylene (**a**) (1 equiv), $Cu(OAc)_2 \cdot H_2O$ (1 equiv) and [Ru(*p*-cymene)Cl_2]$_2$ (5 mol %)] of the second step (*i.e.* annulation step), reaction parameters for the first steps (*i.e.* hydrolytic-dehydrative cyclization) were varied. Various solvents such as *p*-xylene (00%), toluene (00%), DMF (00%), and DMSO (00%) were tested (Table II.3.1.1, entries 2–5) all were found to be ineffective compared to AcOH (45%) (Table II.3.1.1, entry 1). When the reaction was carried out in the absence of Cu(II)-catalyst very poor yield (<10%) of (**18a**) was detected (Table II.3.1.1, entry 6), suggesting the involvement of copper salt in facilitating the reaction, possibly *via* the coordination with the cyano (–CN) group. The selective hydrolysis of one of the cyano groups in the presence of Cu(II) catalyst is in agreement with the earlier report.[18] An improvement in the yield (55%) was observed when the ligand 1,10-phenanthroline (10 mol %) was used (Table II.3.1.1, entry 7). Keeping the catalyst loading constant (10 mol %), an increase in the ligand loading to 15 and 20 mol % improved the yield to 60 and 65% respectively (Table II.3.1.1, entries 8–9). Maintaining the ligand loading to 20 mol % and increasing the catalyst loading up to 20 mol % did not alter the product yield (65%) any further (Table II.3.1.1, entry 10). With $Cu(OAc)_2 \cdot H_2O$ (10 mol %) as the suitable catalyst and AcOH as the solvent the use of other ligands such as 2,2'-bipyridyl (52%), L-proline (48%), JhonPhos (28%), PPh_3 (27%) were screened (Table II.3.1.1, entries 11–14). All the ligands tested gave lower yields compared to 1,10-phenanthroline (65%) (Table II.3.1.1, entry 9). The reaction carried out both at higher 130 ^oC (42%) or lower 90 ^oC (26%) temperature was detrimental to the product formation (Table II.3.1.1, entries 15 and 16). No significant improvement in the overall yield (67%) was observed when the hydrolytic dehydrative-cyclization step of the reaction mixture was maintained up to 12 h (Table II.3.1.1, entry 17). After screening of various reaction parameters, the optimized condition for this transformation in the first step is found to be the use of 2-(1-(4-chlorophenyl)-3-oxo-3-(*p*-

tolyl)propyl)malononitrile (**18**) (0.20 mmol), $Cu(OAc)_2 \cdot H_2O$ (10 mol %), and 1,10-phenanthroline (20 mol %), at 110 °C in AcOH (2 mL) (Table II.3.1.1, entry 9).

Table II.3.1.1. *Optimization of the reaction conditions for the first step.*[a–e]

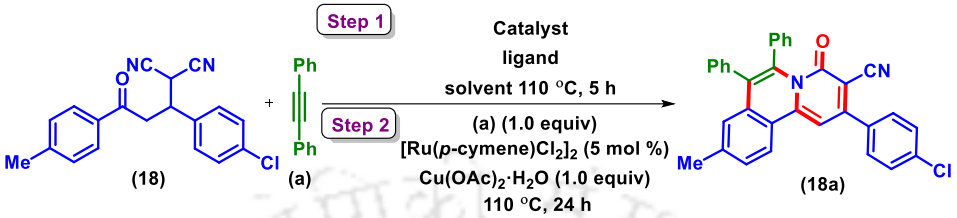

entry	catalyst (mol %)	ligand (mol %)	solvent	yield (%)[b]
1	$Cu(OAc)_2 \cdot H_2O$ (10)		AcOH	45
2	$Cu(OAc)_2 \cdot H_2O$ (10)		*p*-xylene	00
3	$Cu(OAc)_2 \cdot H_2O$ (10)		Toluene	00
4	$Cu(OAc)_2 \cdot H_2O$ (10)		DMF	00
5	$Cu(OAc)_2 \cdot H_2O$ (10)		DMSO	00
6			AcOH	<10
7	$Cu(OAc)_2 \cdot H_2O$ (10)	1,10-phenanthroline (10)	AcOH	55
8	$Cu(OAc)_2 \cdot H_2O$ (10)	1,10-phenanthroline (15)	AcOH	60
9	**$Cu(OAc)_2 \cdot H_2O$ (10)**	**1,10-phenanthroline (20)**	**AcOH**	**65**
10	$Cu(OAc)_2 \cdot H_2O$ (20)	1,10-phenanthroline (20)	AcOH	65
11	$Cu(OAc)_2 \cdot H_2O$ (10)	2,2'-bipyridyl (20)	AcOH	55
12	$Cu(OAc)_2 \cdot H_2O$ (10)	L-proline (20)	AcOH	48
13	$Cu(OAc)_2 \cdot H_2O$ (10)	Jhon Phos (20)	AcOH	28
14	$Cu(OAc)_2 \cdot H_2O$ (10)	PPh_3 (20)	AcOH	27
15	$Cu(OAc)_2 \cdot H_2O$ (10)	1,10-phenanthroline (20)	AcOH	26[c]
16	$Cu(OAc)_2 \cdot H_2O$ (10)	1,10-phenanthroline (20)	AcOH	42[d]
17	$Cu(OAc)_2 \cdot H_2O$ (10)	1,10-phenanthroline (20)	AcOH	67[e]

[a]Reaction condition: 2-(1-(4-chlorophenyl)-3-oxo-3-(*p*-tolyl)propyl)malononitrile (**18**) (0.20 mmol), catalyst (mol %), ligand (mol %) at 110 °C for 5 h. [b]Yields of the isolated product. [c]Temperature 90 °C. [d]Temperature 130 °C. [e]Yield after 12 h.

Maintaining the optimized condition for the hydrolytic-dehydrative cyclization step (Table II.3.1.1, entry 9), further optimization was carried out for the annulation step using [Ru(*p*-cymene)Cl_2]$_2$ as the catalyst in AcOH at 110 °C. Increasing the amount of catalyst loading (from 2 to 5 mol %) marginally enhanced the yield of the desired product (27 to 38%, Table II.3.1.2,

entries 1–2). No significant improvement in the product yield (40%) was observed even when the catalyst loading was increased to 10 mol % (Table II.3.1.2, entry 3). Among the additives such as $AgSbF_6$ (31%), AgOTf (33%), $Cu(OAc)_2$ (36%), and $Cu(OAc)_2·H_2O$ (38%) (Table II.3.1.2, entries 4–7), the later proved to be the best choice (Table II.3.1.2, entry 7).

Table II.3.1.2. *Optimization of the reaction conditions for the second step.*[a–h]

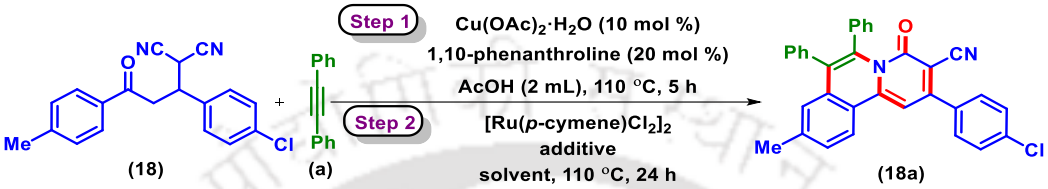

entry	catalyst (mol %)	additive (mol %)	solvent	yield (%)[b]
1	$[Ru(p\text{-cymene})Cl_2]_2$ (2)		AcOH	27
2	$[Ru(p\text{-cymene})Cl_2]_2$ (5)		AcOH	38
3	$[Ru(p\text{-cymene})Cl_2]_2$ (10)		AcOH	40
4	$[Ru(p\text{-cymene})Cl_2]_2$ (5)	$AgSbF_6$ (10)	AcOH	31
5	$[Ru(p\text{-cymene})Cl_2]_2$ (5)	AgOTf (10)	AcOH	33
6	$[Ru(p\text{-cymene})Cl_2]_2$ (5)	$Cu(OAc)_2$ (10)	AcOH	36
7	$[Ru(p\text{-cymene})Cl_2]_2$ (5)	$Cu(OAc)_2·H_2O$ (10)	AcOH	38
8	$[Ru(p\text{-cymene})Cl_2]_2$ (5)	$Cu(OAc)_2·H_2O$ (20)	AcOH	42
9	$[Ru(p\text{-cymene})Cl_2]_2$ (5)	$Cu(OAc)_2·H_2O$ (30)	AcOH	46
10	$[Ru(p\text{-cymene})Cl_2]_2$ (5)	$Cu(OAc)_2·H_2O$ (50)	AcOH	52
11	$[Ru(p\text{-cymene})Cl_2]_2$ (5)	$Cu(OAc)_2·H_2O$ (100)	AcOH	53[c]
12	$[Ru(p\text{-cymene})Cl_2]_2$ (5)	$Cu(OAc)_2·H_2O$ (50)	^{t}AmOH	18
13	$[Ru(p\text{-cymene})Cl_2]_2$ (5)	$Cu(OAc)_2·H_2O$ (50)	MeOH	12
14	$[Ru(p\text{-cymene})Cl_2]_2$ (5)	$Cu(OAc)_2·H_2O$ (50)	isopropanol	16
15	**$[Ru(p\text{-cymene})Cl_2]_2$ (5)**	$Cu(OAc)_2·H_2O$ (50)	**PEG-400**	**72**
16	$[Ru(p\text{-cymene})Cl_2]_2$ (5)	$Cu(OAc)_2·H_2O$ (50)	PEG-400	74[d]
17	$[Ru(p\text{-cymene})Cl_2]_2$ (5)	$Cu(OAc)_2·H_2O$ (50)	PEG-400	75[e]
18	$[Ru(p\text{-cymene})Cl_2]_2$ (5)	$Cu(OAc)_2·H_2O$ (50)	PEG-400	36[f]
19	$[Ru(p\text{-cymene})Cl_2]_2$ (5)	$Cu(OAc)_2·H_2O$ (50)	PEG-400	42[g]
20	$[Ru(p\text{-cymene})Cl_2]_2$ (5)	$Cu(OAc)_2·H_2O$ (50)	PEG-400	59[h]

[a]Reaction condition: 2-(1-(4-chlorophenyl)-3-oxo-3-(*p*-tolyl)propyl)malononitrile (**18**) (0.2 mmol), diphenylacetylene (**a**) (0.2 mmol), catalyst (mol %) additive (mol %.) at 110 °C for 24 h. [b]Yields of the isolated product. [c]1 equiv additive was used. [d]1.5 equiv of (**a**) was used. [e]2 equiv of (**a**) was used. [f]Temperature 80 °C. [g]Temperature 130 °C. [h]Yield after 12 h.

The yield progressively improved from 38 to 52% as the additive $Cu(OAc)_2 \cdot H_2O$ loading increased from 10 to 50 mol % (Table II.3.1.2, entries 7–10). No significant improvement in the product yield (53%) was observed even when the additive loading was increased up to 1 equiv (Table II.3.1.2, entry 11). Since the intermediate dihydropyridone (**18′**) form in the first step precipitated in the AcOH medium, thus, it was felt necessary to have additional co-solvent in the second step to make the medium homogeneous. Among few representative solvents tested such as ^{t}AmOH (18%), MeOH (12%), iso-propanol (16%) (Table II.3.1.2, entries 12–15), PEG-400 proved to be the best choice, affording the annulated product (**18a**) in 72% yield (Table II.3.1.2, entry 15). No major improvement in the yield was observed even when the quantity of diphenylacetylene (**a**) was increased to 1.5 equiv (74%) and 2 equiv (75%) (Table II.3.1.2, entries 16 and 17). Both decrease (80 ^{o}C) and increase (130 ^{o}C) in the reaction temperature resulted lowering in the product yields (36% and 42% respectively) (Table II.3.1.2, entries 18 and 19). When the reaction was stopped after 12 h the product (**18a**) was isolated in a lower yield (59%) as a substantial amount of intermediate 1,2-dihydropyridone remain unconsumed (Table II.3.1.2, entry 20). Hence the optimized condition for this annulation step is the use of diphenylacetylene (**a**) (0.2 mmol), [Ru(*p*-cymene)Cl_2]$_2$ (5 mol %). $Cu(OAc)_2 \cdot H_2O$ (50 mol %), at 110 ^{o}C in PEG-400 (2 mL) for 24 h (Table II.3.1.2, entry 15).

To see the efficacy in a step-wise process, the intermediate **1′** was isolated in 82% yield that was subsequently subjected to annulation step which provided 64% yield of the product (**1a**), thus giving an overall yield of 52%. Although this two-step yield (52%) is slightly better than the one-step process (45%) for convenience we preferred the latter.

II.3.2. Substrates Scopes for the Synthesis of Fused Isoquinolines:

This one-pot two-step synthesis of 4-oxo-2,6,7-triaryl-4*H*-pyrido[2,1-*a*]isoquinoline-3-carbonitrile was then explored with various other γ-ketomalononitriles with diphenylacetylene (**a**) under the optimized reaction condition (Scheme II.3.2.1). A substrate (**1**), having both unsubstituted phenyl rings coupled with diphenylacetylene (**a**), yielding its fused isoquinoline (**1a**, 45%) in moderate yield (Scheme II.3.2.1). Reactants having an electron-neutral substituent (–H) in the phenyl ring attached to the keto group and electron-donating substituents such as *p*-Me (**2**), *p*-OMe (**3**), *p*-SMe (**4**), and *p*-Ph (**5**) in the other phenyl ring reacted successfully with diphenylacetylene (**a**), yielding their fused isoquinolines (**2a**), (**3a**), (**4a**), and (**5a**) in 51%, 55%,

52%, and 48% yields respectively (Scheme II.3.2.1). When the phenyl ring α- to the malononitrile is substituted with electron-withdrawing substituents such as *p*-Cl (**6**), *o*-Br (**7**), and *m*-NO_2 (**8**) all provided their respective products (**6a**, 49%), (**7a**, 45%), and (**8a**, 35%) (Scheme II.3.2.1). This methodology was equally successful when the phenyl ring α- to the malononitrile is unsubstituted and the aroyl phenyl ring is substituted with either electron-donating *p*-Me (**9**), and *p*-OMe (**10**) or electron-withdrawing groups such as *p*-CF_3 (**11**), *p*-F (**12**), *p*-Cl (**13**), *p*-Br (**14**), and *p*-NO_2 (**15**) all yielded their respective fused isoquinolines (**9a**, 45%), (**10a**, 42%), (**11a,** 59%), (**12a**, 57%), (**13a**, 53%), (**14a**, 52%), and (**15a**, 30%). Although, the yields obtained here are not high but considering the number of steps involved in the process, such as selective hydrolysis of a cyano group to an amide, followed by a dehydrative cyclization of an unreactive amide, aromatization and finally, the C–H/N–H annulation with an alkyne, these yields are very well accepted. This protocol was explored to a substrate (**16**), having a naphthyl ring instead of a phenyl ring, and to another substrate (**17**) having a 1-naphthyl ring towards the malononitrile and a 2-naphthyl ring towards the keto side, both provided their respective products (**16a**) and (**17a**) in 44% and 43% yields (Scheme II.3.2.1). Similarly, the presence of various other substituents either electron-donating groups (EDGs) or electron-withdrawing groups (EWGs) in any or both the phenyl rings all provided their anticipated products. As demonstrated earlier, the substrate (**18**) having EDG *p*-Me and EWG *p*-Cl gave a good yield (72%) of the product (**18a**). Other Michael adducts bearing EWG *p*-Br/EWG *p*-Cl (**19**) and EDG *p*-OMe/EWG *p*-NO_2 (**20**) both provided their resultant products (**19a**, 58%) and (**20a**, 25%) respectively (Scheme II.3.2.1). Observing the trends in the yield obtained there is no correlation between the nature of the substituents present in either of the phenyl rings. Besides mono-substituted phenyl rings, di-substituted aryl rings α-to malononitrile sides such as 2,6-dichloro (**21**) and 3,4-di-OMe (**22**) reacted efficiently giving good yields of their products (**21a**, 57%) and (**22a**, 61%) respectively (Scheme II.3.2.1). Besides flexible keto substrates, a cyclic γ-keto substrate (**23**) underwent an efficient transformation to its fused isoquinoline product (**23a**) in 56% yield (Scheme II.3.2.1). Further, a furan (**24**) or thiophene (**25**) bearing substrates were quite compatible and yielded their resultant products (**24a**, 41%) and (**25a**, 43%) respectively (Scheme II.3.2.1).

To evaluate the potential of this two-step process and to expand the scope of this reaction, (**18**) and (**a**) were reacted on a 1 mmol scale which provided isoquinolone (**18a**) in 62% yield (Scheme II.3.2.1).

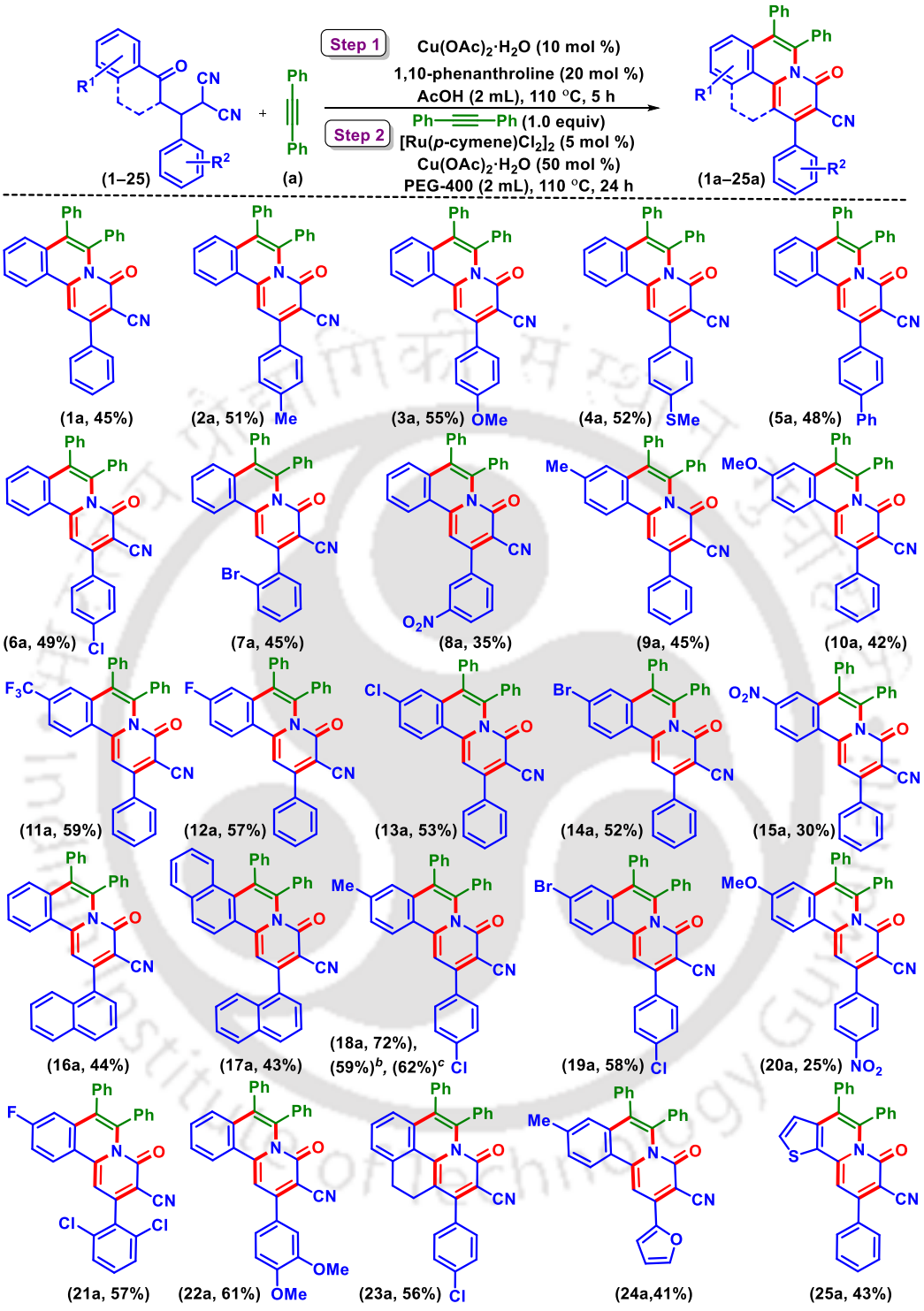

[a]Reaction conditions: (i) **1**–**25** (0.20 mmol), $Cu(OAc)_2·H_2O$ (0.02 mmol), 1,10-phenanthroline (0.04 mmol), and glacial AcOH (2 mL) at 120 °C for 5 h. (ii) diphenylacetelene (**a**) (0.20 mmol), $[Ru(p\text{-cymene})Cl_2]_2$ (0.01 mmol), $Cu(OAc)_2·H_2O$ (0.10 mmol) and PEG-400 (2 mL) at 120 °C for 24 h. [b]Yield after 12 h, [c]Yield reported for 1 mmol scale.

Scheme II.3.2.1. *Substrate scope for various γ-ketodinitriles.*[a,b,c]

To further expand the scope of this methodology, the compatibility of various alkynes was tested with two selected γ-ketomalononitriles namely, (**1**) and (**18**) (Scheme II.3.2.2). The reaction proceeded smoothly with different symmetrical 1,2-diarylacetylenes (**b**–**e**), possessing either electron-donating groups such as *p*-Me (**b**), *p*-OMe (**c**), or electron-withdrawing groups such as *p*-F (**d**) and *m*-Cl (**e**) irrespective of their position of attachments. All underwent efficient annulation when reacted with γ-ketomalononitrile (**1**) providing their expected fused isoquinolines (**1b**, 46%), (**1c**, 48%), (**1d**, 41%), and (**1e**, 42%) respectively. Besides symmetrical 1,2-diarylacetylenes (**b**–**e**), an aliphatic symmetrical alkyne, 4-octyne (**g**), upon reaction with (**1**) provided a 51% yield of the product (**1g**) (Scheme II.3.2.2). All these symmetrical internal alkynes (**b**–**g**) reacted competently with another γ-ketomalononitrile (**18**), providing their corresponding annulated products (**18b**, 75%), (**18c**, 78%), (**18d**, 61%), (**18e**, 55%), (**18f**, 58%), and (**18g**, 71%) respectively (Scheme II.3.2.2). Observing the trend in the yields for substrates (**1**) and (**18**) with various substituted aryl alkynes (**b**–**f**), it was found that aryl alkynes possessing electron-donating substituents (*p*-Me, *p*-OMe) provided better yields than the aryl alkynes having electron-withdrawing substituents (*p*-F, *m*-Cl, and *p*-Br) (Scheme II.3.2.2). To check the regioselectivity of this C–H/N–H annulation, an unsymmetrical alkyne, 1-phenyl-1-propyne (**h**), whether it is taking place towards the phenyl side or the alkyl side, was reacted with (**18**) under an identical condition. The reaction provided a regio-isomeric mixture of (**18h**) and (**18h′**) in a 2.4:1 ratio in a combined yield of 63%, suggesting the attachment of the benzylic carbon to the *N* atom of the *in situ* generated 2-pyridone intermediate. The structure of the major regioisomer (**18h**) was confirmed by X-ray crystallography analysis (Scheme II.3.2.2, **CCDC−1885709**). Further, another unsymmetrical alkyne, 1-phenyl-1-butyne (**i**) also afforded a regioisomeric mixture of products (**18i**) and (**18i′**) in the ratio of 2.3:1 in a combined yield of 66% which is almost identical to that of the product obtained from alkyne (**h**). This preferential reactivity of the *N* atom at the benzylic carbon of an unsymmetrical internal alkynes[14] (**h**) and (**i**) leading to regioselective C–H/N–H annulation is similar to other (C–H/O–H and C–H/S–H) hetero annulation reactions.[27] Highly electron-deficient symmetrical aliphatic alkynes, such as dimethylacetylenedicarboxylate (**j**) and diethylacetylenedicarboxylate (**k**) both failed to react with substrate (**18**) giving no traces of annulated products (**18j**) and (**18k**). It should be mentioned here that these electron-deficient alkynes (**j** and **k**) react efficiently during the C–H/S–H annulation process[27b] demonstrating the lower propensity for C–H/N–H annulation.

This method is however unsuccessful for terminal alkynes such as phenylacetylene (**l**) giving no annulated product (**18l**).

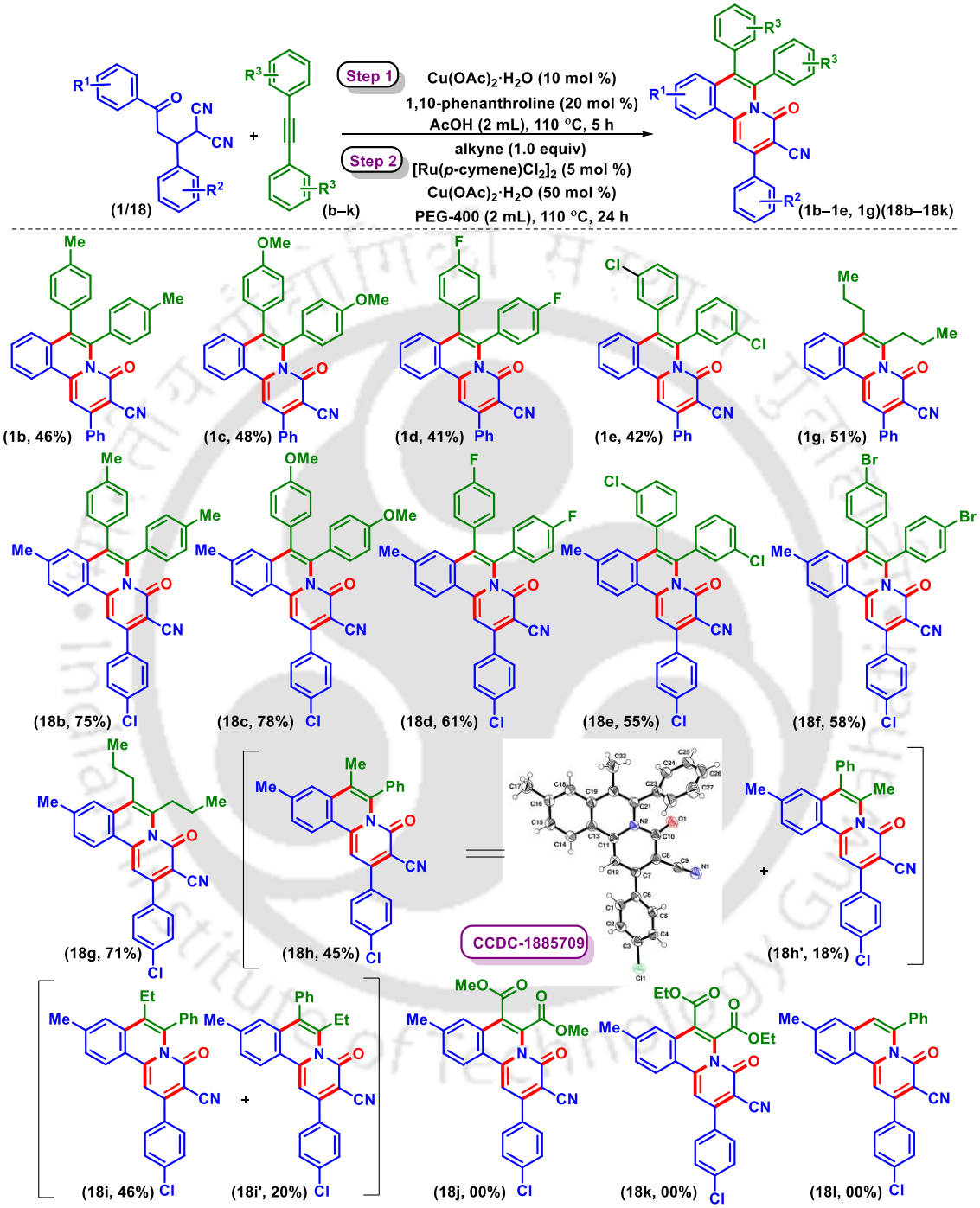

[a]Reaction conditions: (i) **1**/**18** (0.20 mmol), $Cu(OAc)_2·H_2O$ (0.02 mmol), 1,10-phenanthroline (0.04 mmol), and glacial AcOH (2 mL).at 110 °C for 5 h. (ii) **b**–**k** (0.20 mmol), $[Ru(p\text{-cymene})Cl_2]_2$ (0.01 mmol), $Cu(OAc)_2·H_2O$ (0.10 mmol) and PEG-400 (2 mL) at 110 °C for 24 h.

Scheme II.3.2.2. *Substrate scope for alkynes.*[a]

II.4. Mechanistic Investigations:

II.4.1. Intermolecular Competition Experiments:

Whether the electronic effect of the substituents (R^1) on the aroyl phenyl ring has any influence on the reaction, an equimolar mixture of substrates having an electron-donating *p*-OMe (**10**) and an electron-withdrawing *p*-F (**12**) were reacted with diphenylacetylene (**a**) (Scheme II.4.1.1). The ratio of the products **10a**:**12a** obtained was 1:2.53, suggesting higher reactivity of electron-withdrawing substrate *p*-F (**12**) compared to electron-donating substrate *p*-OMe (**10**).

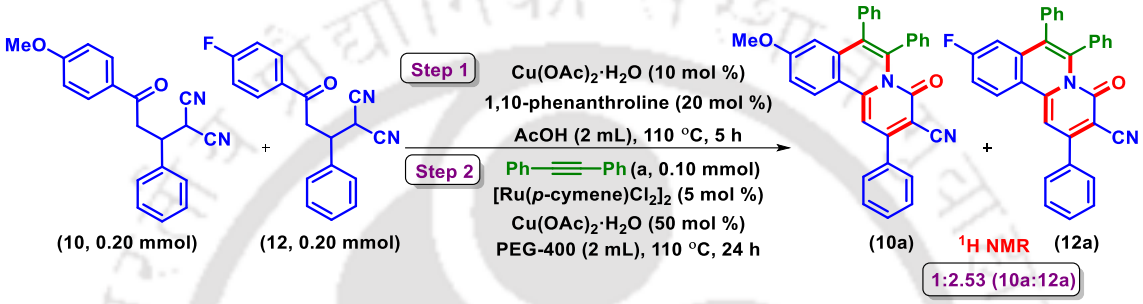

Scheme II.4.1.1. *Competition experiments between aroyl substituted γ-ketodinitriles.*

To see the effect of substituents, either an EDG *p*-Me (**2**) or an EWG *p*-Cl (**6**) present on the phenyl rings (R^2 *i.e.* α-to malononitrile) were reacted with diphenylacetylene (**a**). The ratio of the products **2a**:**6a** obtained was 1:0.80 (Scheme II.4.1.2) suggesting the preferential reactivity of electron-donating substituents (R^2) in this annulation reaction.

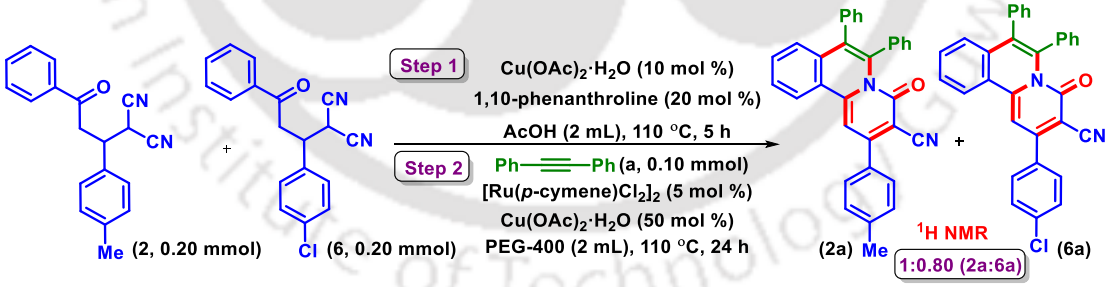

Scheme II.4.1.2. *Competition experiments between phenyl substituted γ-ketodinitriles.*

The nature of the substituents present on the phenyl rings of the alkynes was investigated. In an intermolecular competition reaction between an electron-rich alkyne *p*-OMe (**c**) and a relatively electron-deficient alkyne *p*-F (**d**), both yielded their annulated products (**1c**) and (**1d**) in the ratio of 1:0.80 suggesting a slight preferential reactivity of the electron-rich alkyne (**c**) over the electron-deficient alkyne *p*-F (**d**) (Scheme II.4.1.3).

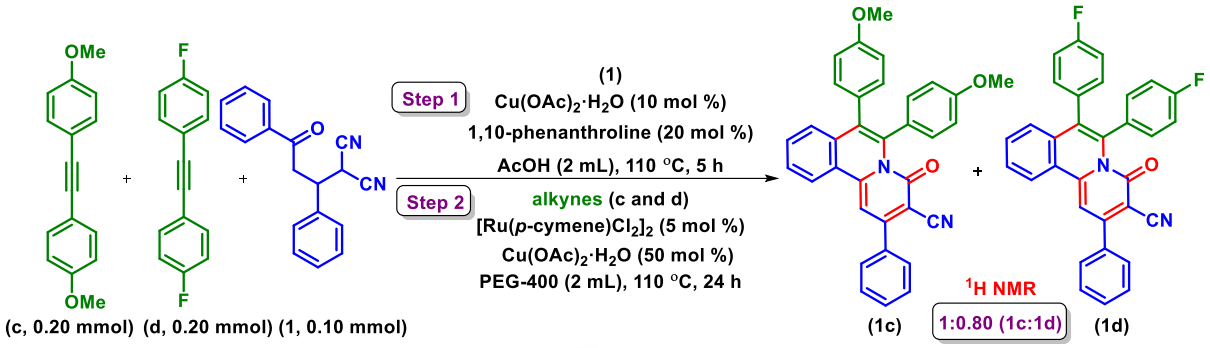

Scheme II.4.1.3. *Competition experiments between alkynes.*

II.4.2. Isotopic Labeling Experiments:

To ascertain the source of oxygen in the carbonyl group of the product a reaction of γ-ketodinitrile (**9**) was performed in the presence of H_2O^{18} under identical conditions (Scheme II.4.2.1). The formation of an O^{18} labeled product suggests that water might be the source of oxygen in the keto group. The formation of ^{18}O labeled intermediate (**9′**) and ^{18}O labeled product (**9a**) was detected by the HRMS analysis of the reaction mixture.

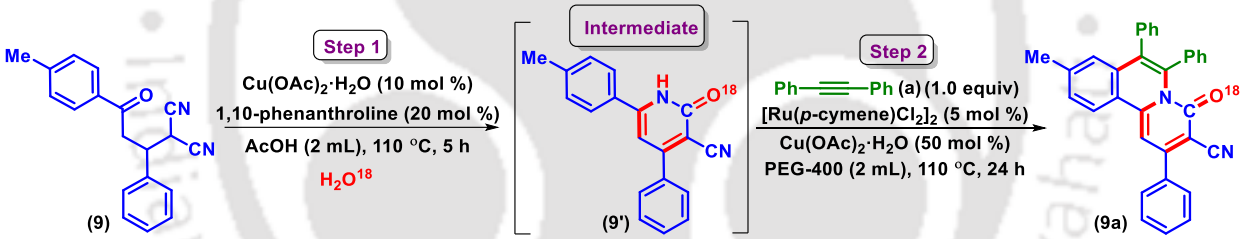

Scheme II.4.2.1. *H_2O^{18} labeling experiment.*

To understand the mechanism and nature of the C–H bond activation, and whether the C–H metalation step is reversible or irreversible a deuterium-scrambling experiment was performed. The deuterium exchange experiment on the isolated intermediate (**2′**) in the absence of an alkyne under the standard reaction condition in D_2O did not afford any deuterium exchange at the *ortho*-C–H of the annulating phenyl ring, suggesting an irreversible C–Ru bond formation (Scheme II.4.2.2).[28a]

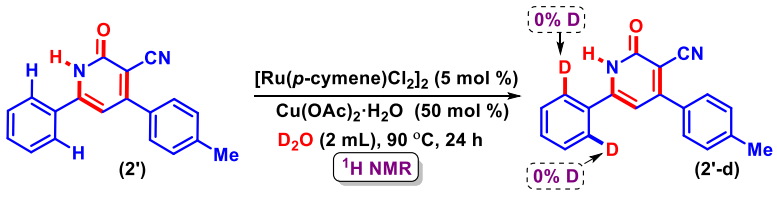

Scheme II.4.2.2. *Deuterium-exchange experiment.*

In an intermolecular competition experiment between (**6**) and its deuterated analog (**6-d$_5$**) with (**a**), an observed k_H/k_D = 3.00 signifies the irreversible C–H bond cleavage to be the rate-limiting step (Scheme II.4.2.3).[28b,c]

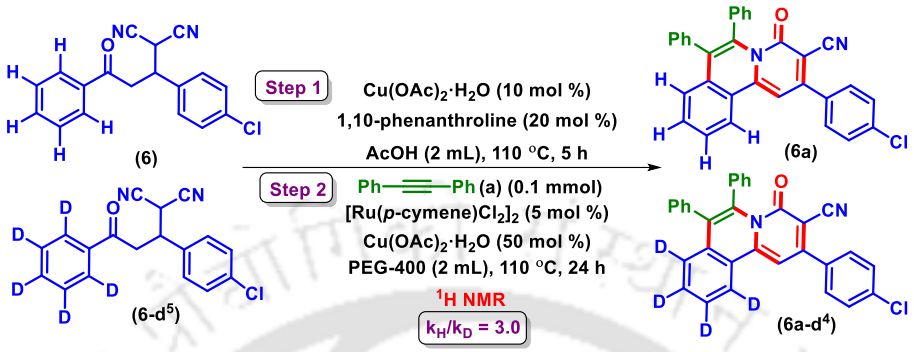

Scheme II.4.2.3. *Kinetic isotope effect experiment.*

II.4.3. Plausible Reaction Mechanism:

Based on the above isotopic experiments and from previous reports,[25,29,30] a plausible mechanism is depicted in Scheme II.4.3.1. In the first step, one of the nitrile (–CN) groups of the substrate (**1**) is hydrolyzed selectively to a mono amidic intermediate (**I**). The NH_2 of the amide then attacks the carbonyl group and undergoes a dehydrative cyclization to produce a six-membered cyclic intermediate (**II**). The intermediate (**II**) is oxidized/aromatized under the reaction conditions to an aromatic pyridone intermediate (**III**). The formation of intermediate (**I**), (**II**), and (**III**) has been detected by the HRMS analysis of the reaction aliquots at various time intervals (Figure II.4.3.1). In the second step, the catalyst $[RuCl_2(p\text{-cymene})]_2$ undergoes ligand exchange with $Cu(OAc)_2{\cdot}H_2O$ to generate the active catalytic species, which coordinates with the nitrogen atom of the intermediate (**III**) *via* NH deprotonation. This is then followed by *ortho* C–H bond activation through the elimination of AcOH, forming a five-membered ruthenacycle (**V**). Further coordination of the alkyne (**a**), followed by an alkyne insertion and reductive elimination afforded the final product (**1a**) *via* the intermediate (**VI**). The active catalyst species is then regenerated by the oxidant $Cu(OAc)_2{\cdot}H_2O$ and air for the next catalytic cycle.

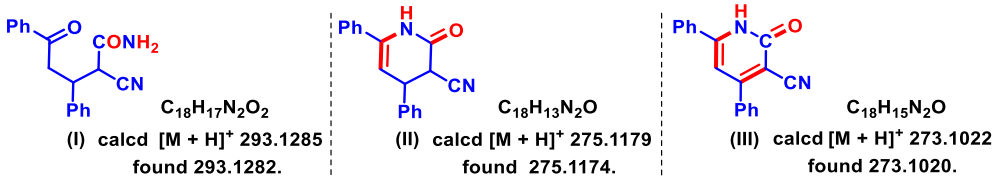

Figure II.4.3.1. *Intermediate detected from the HRMS analysis of the reaction aliquots.*

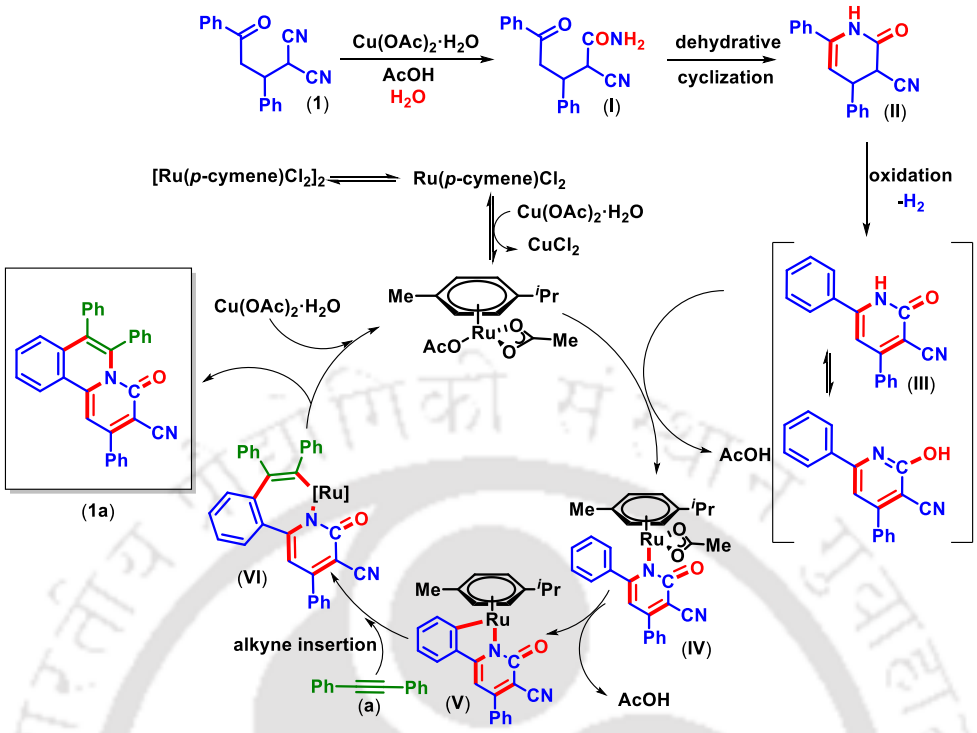

Scheme II.4.3.1. *Proposed mechanistic pathway.*

II.5. Theoretical Investigations:

The crystal structure of (**1a**) reveals the presence of a slightly twisted 4*H*-pyrido[2,1-*a*]isoquinoline-3-one core and the three phenyl rings are out of the molecular plane. While the aroyl ring is part of the 4*H*-pyrido[2,1-*a*]isoquinoline-3-one core, the phenyl ring α- to the malononitrile is twisted out of the planar core with a dihedral angle of 42.58°. The two phenyl rings originating from the diphenylacetylene moiety are also twisted out of the molecular plane with a dihedral angle of 78.16° and 85.24° respectively. To further ascertain the geometry and electronic structure of the annulated fused isoquinoline, density functional theory (DFT) calculations were performed with a B3LYP/6-31G (d, p) basis set level in acetonitrile solvent modeled by the PCM approach (the Gaussian 09 program).[31] The density functional theory (DFT) calculation of (**1a**) reveals that the electron density in the highest occupied molecular orbital (HOMO) is localized at the central core extending to the nitrile and minor contributions from the two phenyl rings originating from the diphenylacetylene. Whereas the lowest unoccupied molecular orbital (LUMO) is again localized at the central core and extended up to the phenyl ring attached to the α position of the malononitrile (Figure II.5.1).

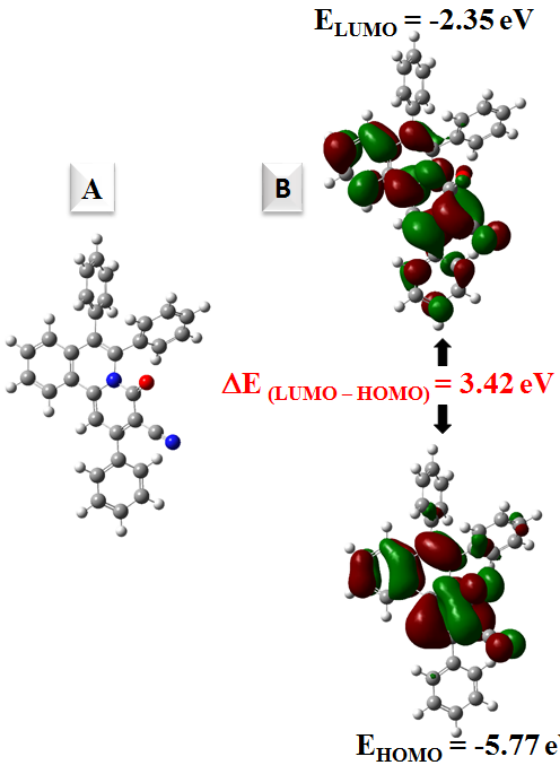

Figure II.5.1*. (A) Optimized structure of* ***1a****. (B) Molecular Orbitals amplitude plots of HOMO and LUMO of* ***1a*** *using density functional theory calculation at the B3LYP/6-31G (d, p) basis set level in acetonitrile solvent modeled by the PCM approach.*

In a donor-π-acceptor (D-π-A) type system the $\Delta E_{(LUMO-HOMO)}$ energy can be directly correlated with the presence of either electron-donating or electron-withdrawing groups on the donor (HOMO) or the acceptor (LUMO) part of the molecule.[32] Here, since both the HOMO and LUMO are localized on the central molecular core with very insignificant contributions from the three phenyl rings, no proper correlation between the HOMO-LUMO energy gap could be found due to the presence of electron-donating or electron-withdrawing groups. The calculated $\Delta E_{(LUMO-HOMO)}$ energy gap for unsubstituted (**1a**), *p*-Me substituted (**1b**), *p*-OMe substituted (**1c**), and *p*-F substituted (**1d**) isoquinolines respectively are 3.42, 3.41, 3.34 and 3.43 eV (Figure II.5.2). When a 1,2-dialkylacetylene, namely, 4-octyne (**g**) was replaced with the diphenylacetylene (**a**) in the fused isoquinolines moiety (**1g**), the energy gap was found to be 3.39 eV (Figure II.5.2). The calculated $\Delta E_{(LUMO-HOMO)}$ energy of various other substituents either in the acceptor (LUMO) or in the donor (HOMO) are summarized in Figure II.5.3, and Figure II.5.4.

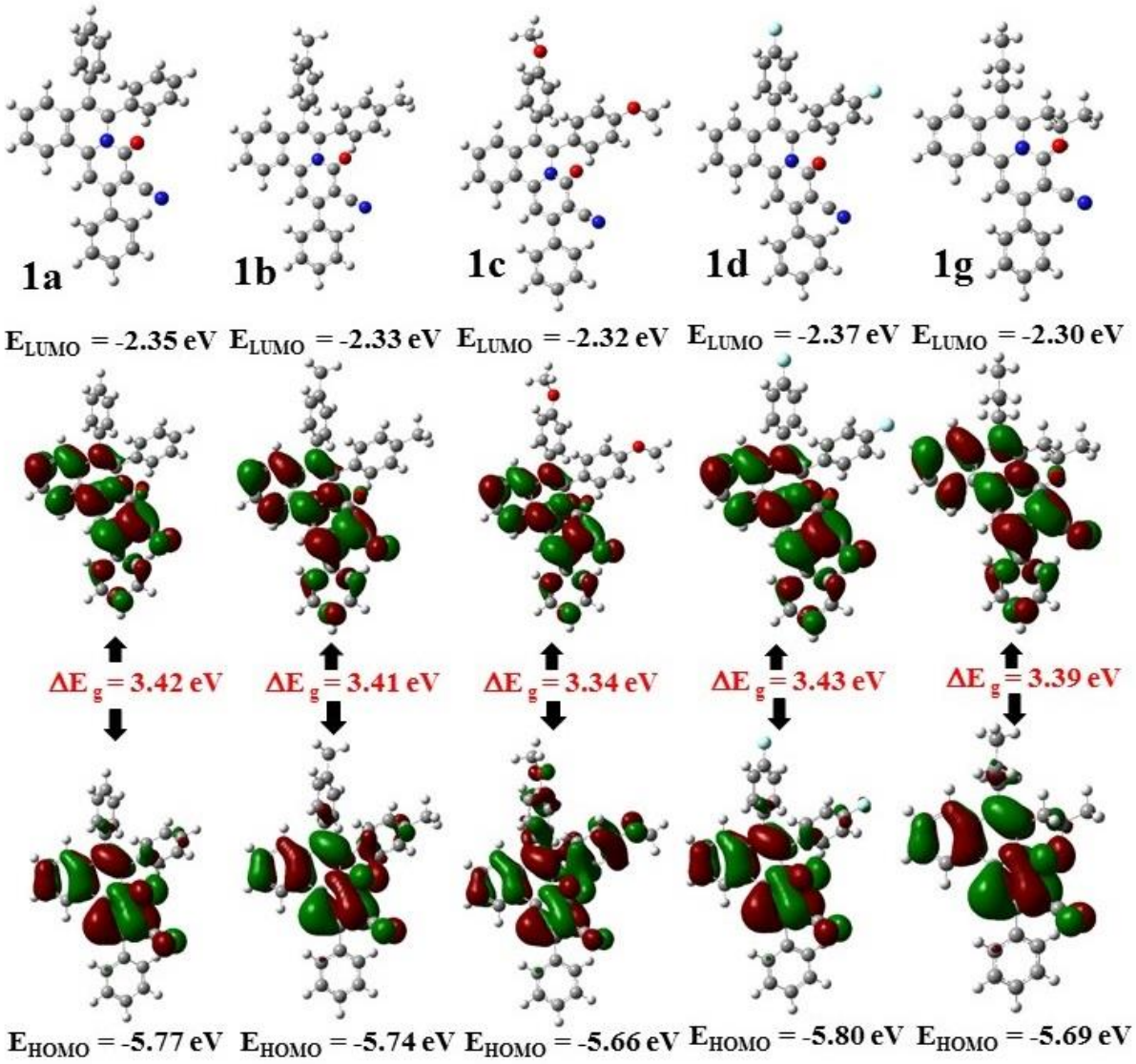

Figure II.5.2. *DFT optimized structures and HOMO-LUMO energy level diagrams of synthesized compounds* ***(1a)****,* ***(1b)****,* ***(1c)****,* ***(1d)****, and* ***(1g)*** *respectively using the B3LYP/6-31G (d, p) basis set level in acetonitrile solvent modeled by PCM approach.*

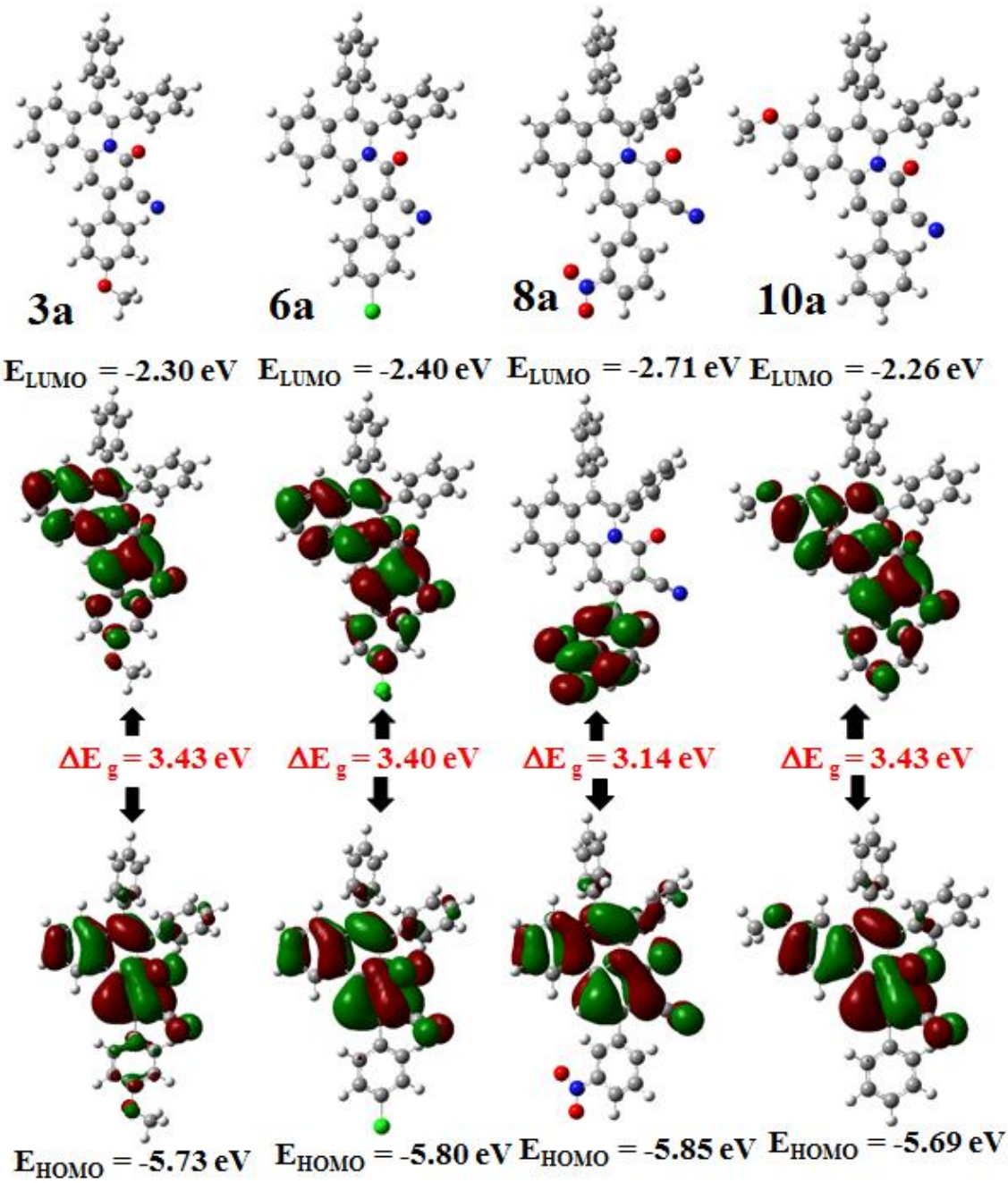

Figure II.5.3. *DFT optimized structures and HOMO-LUMO energy level diagrams of synthesized compounds (**3a**), (**6a**), (**8a**), and (**10a**) respectively using the B3LYP/6-31G (d, p) basis set level in acetonitrile solvent modeled by PCM approach.*

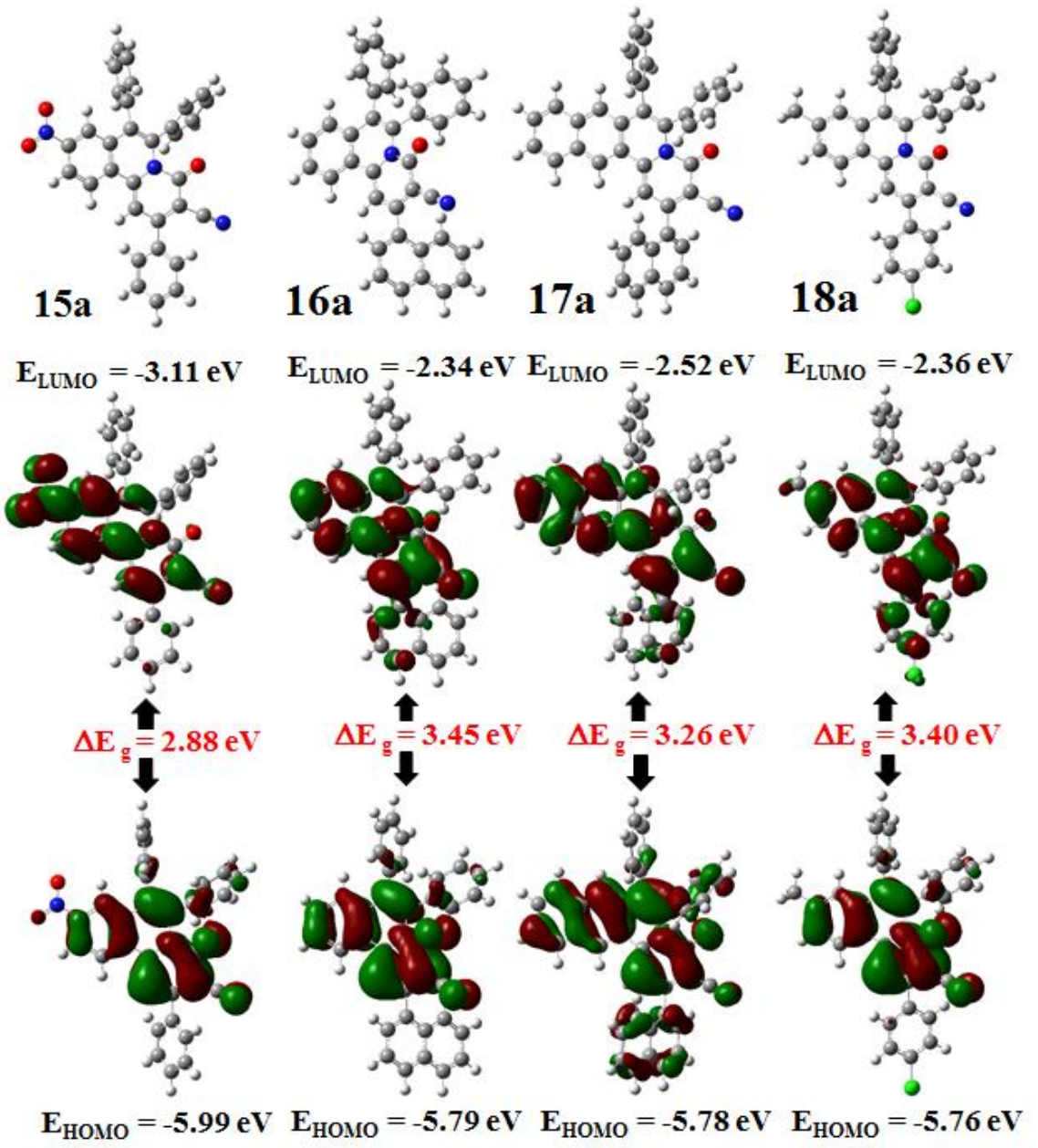

Figure II.5.4. *DFT optimized structures and HOMO-LUMO energy level diagrams of synthesized compounds (**15a**), (**16a**), (**17a**), and (**18a**) respectively using the B3LYP/6-31G (d, p) basis set level in acetonitrile solvent modeled by PCM approach.*

II.6. Photophysical Properties:

As stated earlier that the newly synthesized compounds having highly conjugated fused isoquinoline core display yellow fluorescent when viewed under a 365 nm UV lamp. In solution, this class of fused conjugated heterocycles exhibits an intense yellowish-green colour. Therefore, the absorption spectra (λ_{abs}) and emission spectra (λ_{em}) for a few selected compounds (**1a**, **2a**, **3a**, **6a**, **8a**, **10a**, **12a**, **13a**, **15a**, **18a**, **20a**, **1b**, **1c**, **1d**, and **1g**).were investigated in CH_2Cl_2 (10^{-5} M). The UV-visible spectra and photoluminescence spectra are shown in (Figure II.6.1). All these synthesized compounds showed strong absorptions, with the positions of maximum ranging from 454–490 nm. The compounds exhibit three distinct absorption maxima, a band in the region of 313–321 nm, a band in the region of 428–467 nm, and another in the region of 454–490 nm. In dichloromethane solution (10^{-5} M) one of the fused isoquinoline derivatives (**1a**) showed absorption peaks at 318, 431, and 458 nm with high extinction coefficients (ε) of 27000, 26000, and 35000 L mol^{-1} cm^{-1}, respectively (Table II.6, entry 1). All these compounds exhibit strong fluorescence emission in the range of 502–560 nm which belongs to the green region of the visible light spectrum.

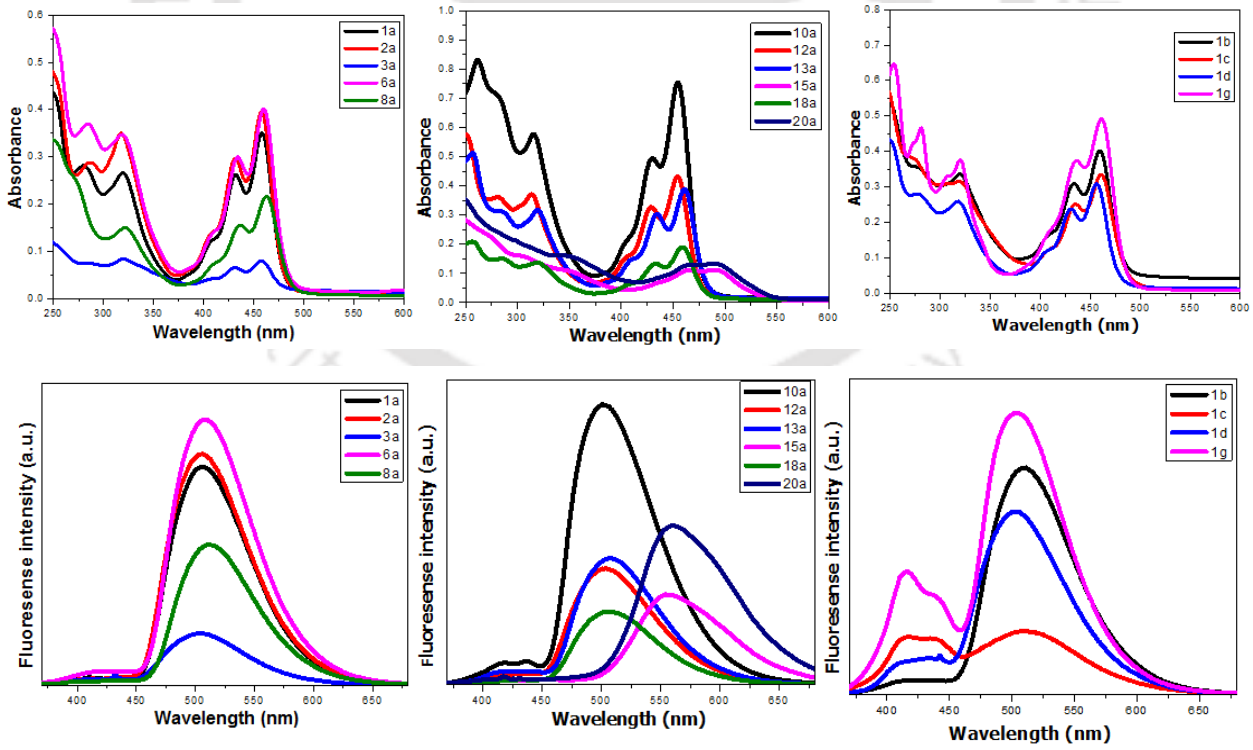

Figure II.6.1. *UV-visible and photoluminescence spectra in CH_2Cl_2 (1 x 10^{-5} M).*

Table II.6. *Photophysical studies.*

entry	compound	λ_{abs} (nm)	$\varepsilon \times 10^5$ (L mol^{-1} cm^{-1})	λ_{em} (nm)
1	**1a**	318, 431, 458	0.27, 0.26, 0.35	506
2	**2a**	317, 431, 457	0.35, 0.29, 0.39	506
3	**3a**	317, 436, 457	0.08, 0.07, 0.08	504
4	**6a**	318, 433, 459	0.34, 0.30, 0.40	507
5	**8a**	321, 436, 462	0.15, 0.16, 0.22	511
6	**10a**	315, 429, 454	0.58, 0.49, 0.75	502
7	**12a**	321, 436, 462	0.37, 0.33, 0.43	503
8	**13a**	319, 434, 460	0.32, 0.30, 0.39	507
9	**15a**	466, 490	0.11, 0.11	555
10	**18a**	319, 433, 458	0.14, 0.13, 0.19	505
11	**20a**	467, 489	0.13, 0.13	560
12	**1b**	319, 433, 459	0.34, 0.31, 0.40	510
13	**1c**	319, 434, 460	0.32, 0.25, 0.34	510
14	**1d**	318, 430, 456	0.26, 0.24, 0.31	502
15	**1g**	319, 436, 461	0.38, 0.37, 0.49	503

II.7. Conclusion:

In conclusion, we have utilized a Michael-adduct γ-ketomalononitrile, obtained from the reaction between α,β-unsaturated aromatic ketone and malononitrile as the substrate for the C–H/N–H annulation with an alkyne. In this one-pot sequential two-component synthesis of π-conjugated fused ring *N*-containing heterocycle 4-oxo-2,6,7-triaryl-4*H*-pyrido[2,1-*a*]isoquinoline-3-carbonitrile is accomplished *via* the formation of six new bonds namely a C–C, two C–N, two C=C, and a C=O bonds. The success of the strategies lies in the selective hydrolysis of one of the cyano groups of γ-ketomalononitrile to an aromatic cyclic amide and finally C–H/N–H annulation with disubstituted alkynes in the presence of Ru(II) catalyst. This process is compatible with a range

of substituents present in various coupling partners. Based on DFT calculation, the positions and electronic nature of MO levels were investigated but no significant correlation of the substituents effects with the HOMO-LUMO energy levels could be correlated since both the HOMO and LUMO are localized at the same central part of the molecule. These synthesized heterocyclic compounds having several phenyl rings are emissive under a 365 nm UV lamp, so beyond synthesis, the UV–vis and fluorescence spectra of some selected compounds were also examined. These molecules may therefore find application in fluorescent probes, optoelectronics applications in organic light-emitting diodes (OLEDs), and various other applications in material science.

II.8 Experimental Section:

II.8.1. General Information:

All the reagents and solvents used were purchased from commercially available sources and used without further purification. HPLC-grade solvents were purchased from commercial sources. Organic extracts were dried over anhydrous sodium sulfate. Solvents were removed in a rotary evaporator under reduced pressure. Silica gel (60–120 mesh size) was used for the column chromatography. Reactions were monitored by TLC on silica gel $60F_{254}$ (0.25 mm). All NMR spectra were recorded in $CDCl_3$ with tetramethylsilane (TMS) as the internal standard and a few were taken in DMSO-d_6 in 600 and 400 MHz NMR. The ^{1}H NMR spectra were referenced to the residual $CDCl_3$ (7.26 ppm) whereas for DMSO-d_6 it is 2.50 ppm. The ^{13}C NMR spectra were referenced to the residual $CDCl_3$ (77.230 ppm) and for DMSO-d_6 it is 39.50 ppm. All ^{19}F NMR spectra were recorded in 400 MHz, and hexafluorobenzene (C_6F_6) was taken as reference. Mass spectra were recorded using ESI mode (Q-TOF MS analyzer). IR spectra were recorded in KBr or neat in FT-IR spectrometer. All UV experiments were performed at a probe concentration of 10^{-5} M in 1 mL quartz cuvettes of path length 1 cm at 25 ^{o}C in a UV-visible spectrometer in HPLC grade dichloromethane solution. Photoluminescence was carried out at a concentration of 10^{-5} M in 1 mL quartz cuvettes at 25 ^{o}C in Spectrofluorometer in HPLC grade dichloromethane solution.

II.8.2. General Procedures:

II.8.2.1. General Procedure for the Synthesis of 2-(3-Oxo-1,3-diarylpropyl)malononitriles (1–25):

All the γ-ketodinitriles (**1**–**25)** were synthesized according to the literature procedure.[17]

II.8.2.2. General Procedure for the Synthesis of Internal Alkynes (b–f):

The internal alkynes (**b–f)** were synthesized according to the modified literature procedure.[33]

II.8.2.3. General Procedure for the Synthesis of 4-Oxo-2,6,7-triphenyl-4*H*-pyrido[2,1-*a*]isoquinoline-3-carbonitrile (1a) from 2-(3-Oxo-1,3-diphenylpropyl)malononitrile (1) and Diphenylacetylene (a):

To an oven-dried 10 mL round bottom flask was added 2-(3-oxo-1,3-diphenylpropyl)malononitrile (**1**) (55 mg, 0.20 mmol), $Cu(OAc)_2 \cdot H_2O$ (4 mg, 0.02 mmol), 1,10-phenanthroline (7 mg, 0.04 mmol), and glacial AcOH (2 mL). The reaction mixture was heated in an oil bath at 110 ^oC for 5 h. Then to this reaction mixture was added diphenylacetylene (**a**) (36 mg, 0.20 mmol), $[Ru(p\text{-cymene})Cl_2]_2$ (6 mg, 0.01 mmol), $Cu(OAc)_2 \cdot H_2O$ (20 mg, 0.10 mmol), and PEG-400 (2 mL). The reaction mixture was further heated for 24 h. Then the reaction mixture was cooled to room temperature, admixed with ethyl acetate (25 mL) and the organic layer was washed with saturated sodium bicarbonate solution (5 mL). The organic layer was dried over anhydrous sodium sulfate (Na_2SO_4) and the solvent was evaporated under reduced pressure. The crude product so obtained was purified over a column of silica gel (hexane/ethyl acetate, 9:1) to give pure 4-oxo-2,6,7-triphenyl-4*H*-pyrido[2,1-*a*]isoquinoline-3-carbonitrile (**1a**) (40 mg, yield 45%). The identity and purity of the product were confirmed by spectroscopic analysis.

II.8.3. Mechanistic Investigation:

II.8.3.1. ESI-MS Studies for the H_2O^{18} Labeled Experiment:

To an oven-dried 10 mL round bottom flask was added 2-(3-oxo-1-phenyl-3-(*p*-tolyl)propyl)malononitrile (**9**) (58 mg, 0.20 mmol), $Cu(OAc)_2 \cdot H_2O$ (4 mg, 0.02 mmol), 1,10-phenanthroline (7 mg, 0.04 mmol), H_2O^{18} (4 μL, 0.20 mmol), and glacial AcOH (2 mL). The reaction mixture was heated in an oil bath for 5 h at 110 ^oC. The formation of ^{18}O labeled intermediate (**9'**) was confirmed by HRMS analysis of the reaction mixture (Figure II.8.3.1.1). Then to this reaction mixture was added diphenylacetylene (**a**) (36 mg, 0.20 mmol), $[Ru(p\text{-cymene})Cl_2]_2$ (6 mg, 0.01 mmol), $Cu(OAc)_2 \cdot H_2O$ (20 mg, 0.10 mmol), and PEG-400 (2 mL). The reaction mixture was further heated in an oil bath for 24 h. Then the reaction mixture was cooled to room temperature, admixed with ethyl acetate (25 mL) and the organic layer was washed with saturated sodium bicarbonate solution (5 mL). The organic layer was dried over anhydrous sodium sulfate

(Na_2SO_4), and the solvent was evaporated under reduced pressure. The crude product so obtained was purified over a column of silica gel (hexane/ethyl acetate, 9:1) to give pure 9-methyl-4-oxo-2,6,7-triphenyl-4*H*-pyrido[2,1-*a*]isoquinoline-3-carbonitrile (**9a**) (42 mg, yield 45%). The identity and purity of the product were confirmed by spectroscopic analysis. The identity of the O^{18} labeled product was confirmed by HRMS analysis (Figure II.8.3.1.2).

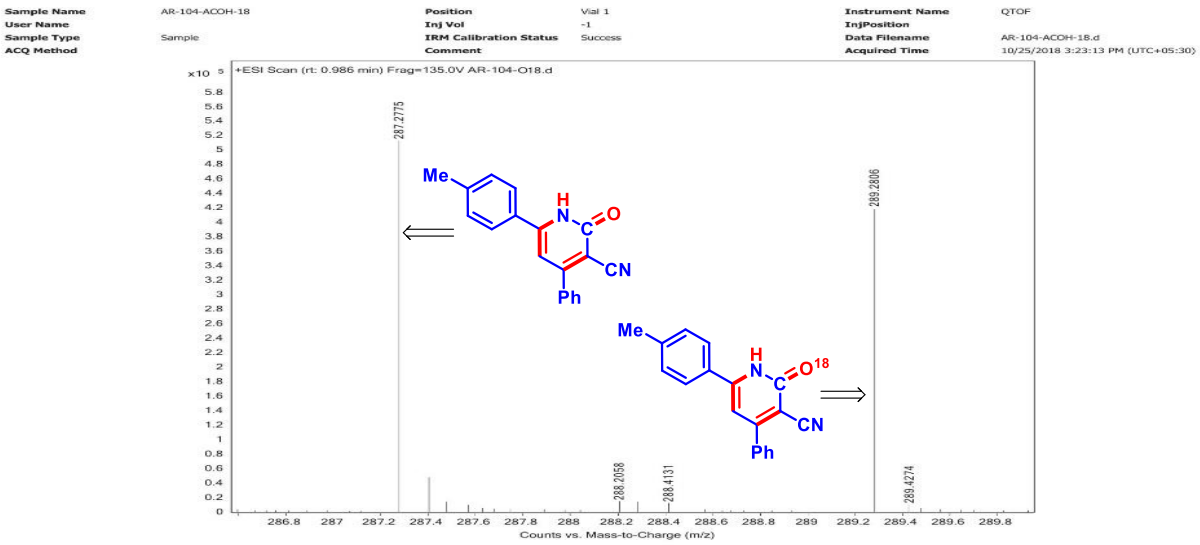

Figure II.8.3.1.1. *HRMS spectrum of ^{18}O labeled (**9'**).*

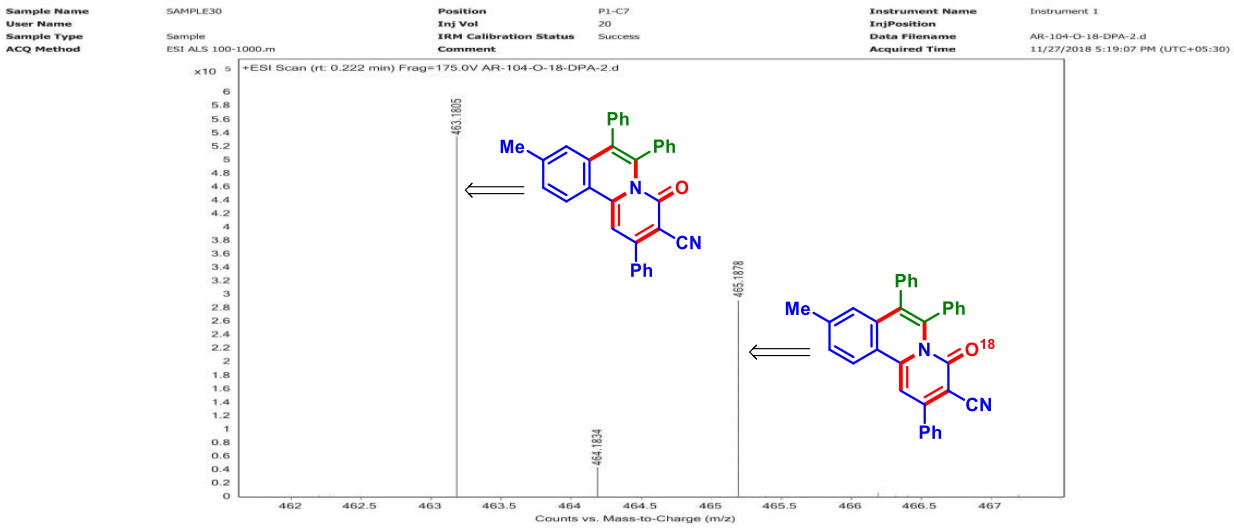

Figure II.8.3.1.2. *HRMS spectrum of ^{18}O labeled (**9a**).*

II.8.3.2. ESI-MS Studies for the Reaction Mixtures at Different Time Intervals:

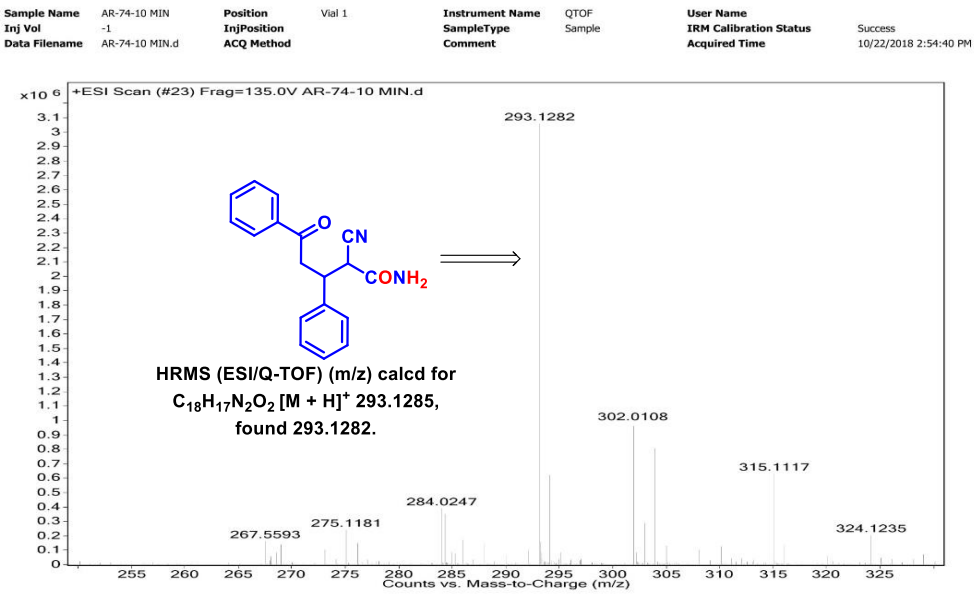

Figure II.8.3.2.1. *HRMS spectrum after 10 min.*

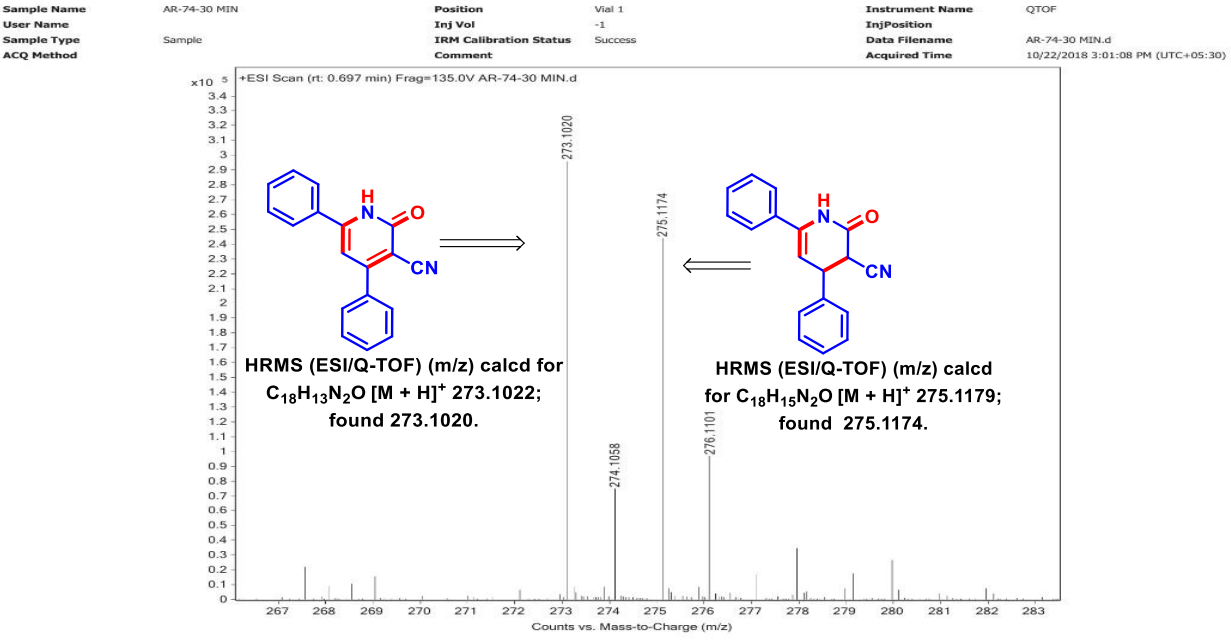

Figure II.8.3.2.2. *HRMS spectrum after 30 min.*

II.8.3.3. Intermolecular Competition Experiments:

II.8.3.3.1. Intermolecular Competitive Experiment Between 2-(3-(4-Methoxyphenyl)-3-oxo-1-phenylpropyl)malononitrile (10) and 2-(3-(4-Fluorophenyl)-3-oxo-1-phenylpropyl)malononitrile (12):

The intermolecular competition experiment was carried out according to the general procedure described in II.8.2.3 taking 2-(3-(4-methoxyphenyl)-3-oxo-1-phenylpropyl)malononitrile (**10**) (61 mg, 0.20 mmol), 2-(3-(4-fluorophenyl)-3-oxo-1-phenylpropyl)malononitrile (**12**) (58 mg, 0.20 mmol), and diphenylacetylene (**a**) (18 mg, 0.10 mmol) under standard reaction condition. The crude product so obtained was purified over a column of silica gel (hexane/ethyl acetate, 9:1) to give mixture of products 9-methoxy-4-oxo-2,6,7-triphenyl-4*H*-pyrido[2,1-*a*]isoquinoline-3-carbonitrile (**10a**), and 9-fluoro-4-oxo-2,6,7-triphenyl-4*H*-pyrido[2,1-*a*]isoquinoline-3-carbonitrile (**12a**). The ratio of the product obtained for **10a**:**12a** was (1:2.53), as determined from ^{1}H NMR spectra (Figure II.8.3.3.1.1).

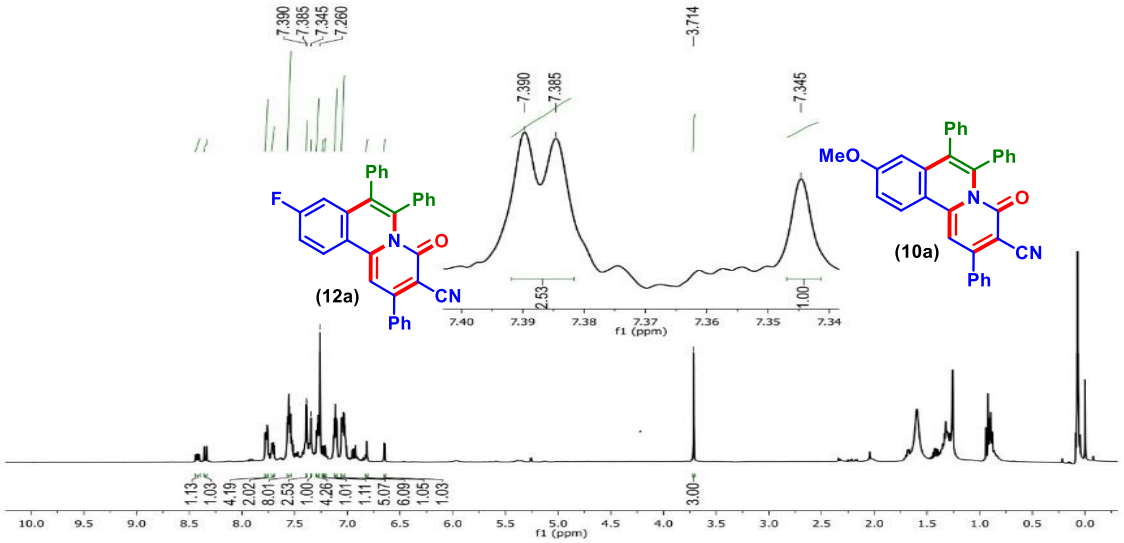

Figure II.8.3.3.1.1. *^{1}H NMR spectra of intermolecular competitive experiment between aroyl substituted γ–ketodinitriles.*

II.8.3.3.2. Intermolecular Competitive Experiment Between 2-(3-Oxo-3-phenyl-1-(*p*-tolyl)propyl)malononitrile (2) and 2-(1-(4-Chlorophenyl)-3-oxo-3-phenylpropyl)malononitrile (6):

The intermolecular competition experiment was carried out according to the general procedure described in II.8.2.3 taking 2-(3-oxo-3-phenyl-1-(*p*-tolyl)propyl)malononitrile (**2**) (58

mg, 0.20 mmol), 2-(1-(4-chlorophenyl)-3-oxo-3-phenylpropyl)malononitrile (**6**) (62 mg, 0.20 mmol), and diphenylacetylene (**a**) (18 mg, 0.10 mmol) under standard reaction condition. The crude product so obtained was purified over a column of silica gel (hexane/ethyl acetate, 9:1) to give mixture of products 4-oxo-6,7-diphenyl-2-(*p*-tolyl)-4*H*-pyrido[2,1-*a*]isoquinoline-3-carbonitrile (**2a**), and 2-(4-chlorophenyl)-4-oxo-6,7-diphenyl-4*H*-pyrido[2,1-*a*]isoquinoline-3-carbonitrile (**6a**). The products afforded yield **2a**:**6a** (1:0.80) as shown from ^{1}H NMR spectra (Figure II.8.3.3.2.1).

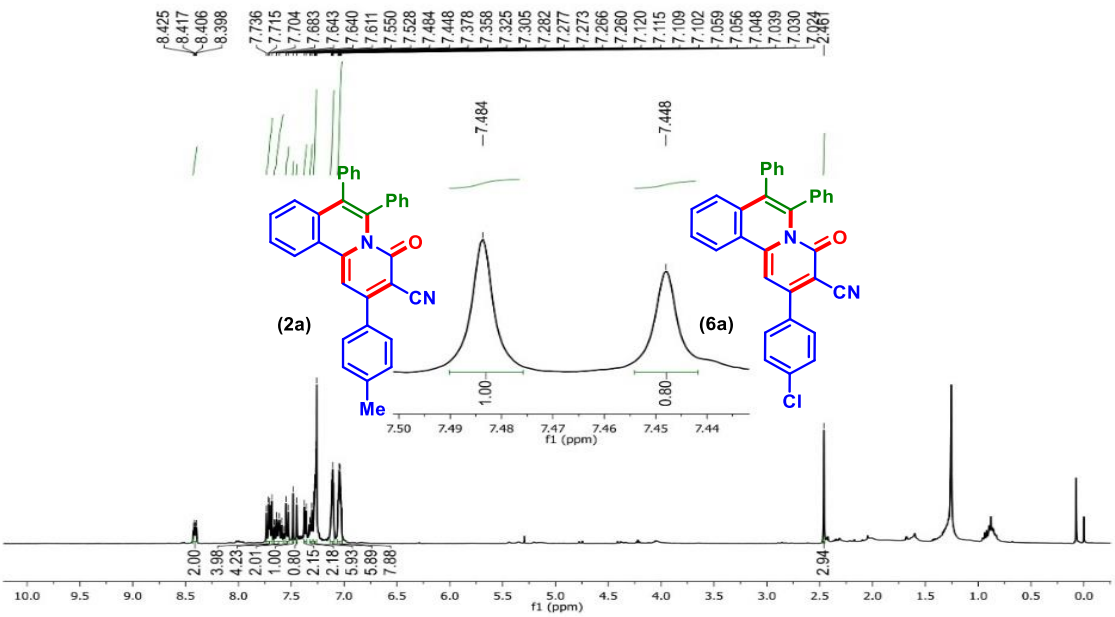

Figure II.8.3.3.2.1. *^{1}H NMR spectra of intermolecular competitive experiment between phenyl substituted γ–ketodinitriles.*

II.8.3.3.3. Intermolecular Competitive Experiment Between 1,2-Bis(4-methoxyphenyl)ethyne (c) and 1,2-Bis(4-fluorophenyl)ethyne (d):

The intermolecular competition experiment was carried out according to the general procedure described in II.8.2.3 taking 2-(3-oxo-1,3-diphenylpropyl)malononitrile (**1**) (27 mg, 0.10 mmol), 1,2-bis(4-methoxyphenyl)ethyne (**c**) (48 mg, 0.20 mmol), and 1,2-bis(4-fluorophenyl)ethyne (**d**) (43 mg, 0.20 mmol) under standard reaction condition. The crude product so obtained was purified over a column of silica gel (hexane/ethyl acetate, 9:1) to give mixture of products 6,7-bis(4-methoxyphenyl)-4-oxo-2-phenyl-4*H*-pyrido[2,1-*a*]isoquinoline-3-carbonitrile (**1c**), and 6,7-bis(4-fluorophenyl)-4-oxo-2-phenyl-4*H*-pyrido[2,1-*a*]isoquinoline-3-carbonitrile

(**1d**). The products afforded yield **1c**:**1d** (1:0.80), as estimated from ^{1}H NMR spectra (Figure II.8.3.3.3.1).

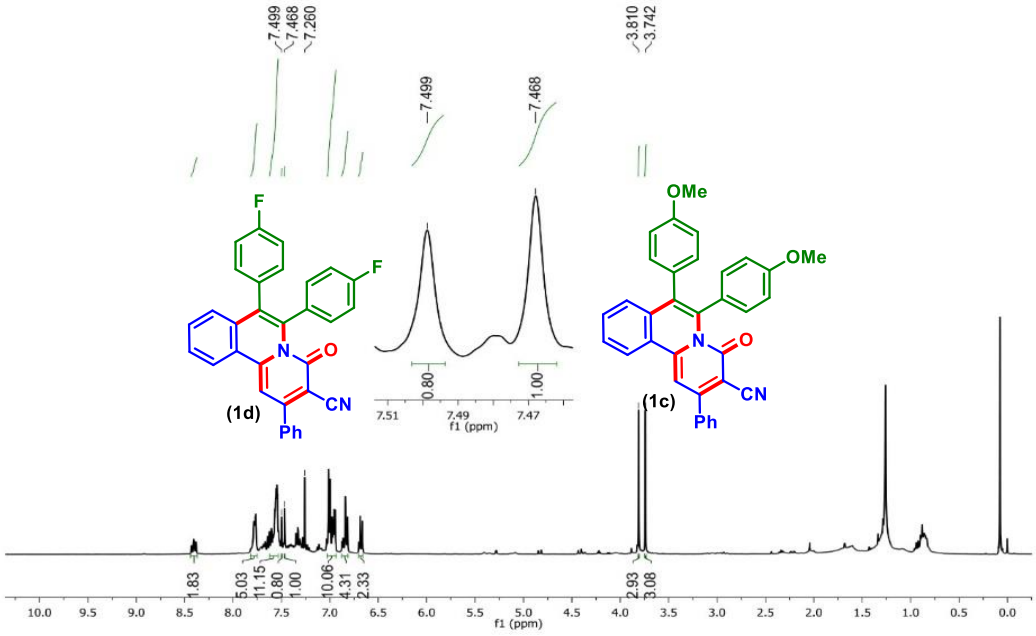

Figure II.8.3.3.3. *^{1}H NMR spectra of Intermolecular competitive experiment between internal alkynes.*

II.8.3.4. Isotopic Labeling Experiments:

II.8.3.4.1. Deuterium-Exchange Experiment:

To an oven-dried 10 mL round bottom flask a mixture of 2-oxo-6-phenyl-4-(*p*-tolyl)-1,2-dihydropyridine-3-carbonitrile (**2'**) (57 mg, 0.20 mmol,), $[RuCl_2(p\text{-cymene})]_2$ (6 mg, 0.01 mmol), and $Cu(OAc)_2{\cdot}H_2O$ (40 mg, 0.20 mmol) in D_2O (2 mL) was stirred on a preheated oil bath at 90 ^{o}C for 24 h. The reaction mixture was diluted with water (10 mL) and extracted with ethyl acetate (25 mL). The combined organic layer was dried over anhydrous sodium sulfate (Na_2SO_4) and the solvent was evaporated in a vacuum. The crude product so obtained was purified using column chromatography and eluted with ethyl acetate:hexane (1:1) to afford the expected product 2-oxo-6-phenyl-4-(*p*-tolyl)-1,2-dihydropyridine-3-carbonitrile (**2'-d**, 52 mg, 91%). The ^{1}H NMR analysis of the product reveals no deuterium incorporation (Figure II.8.3.4.1.1).

2'-d As a white solid (51 mg, 91% yield); ^{1}H NMR (DMSO-d_6, 400 MHz): δ 12.78 (s, 1H), 7.88 (d, 2H, J = 6.8 Hz), 7.65 (d, 2H, J = 8.0 Hz), 7.56–7.51 (m, 3H), 7.38 (d, 2H, J = 8.0 Hz), 6.79 (s, 1H), 2.39 (s, 3H).

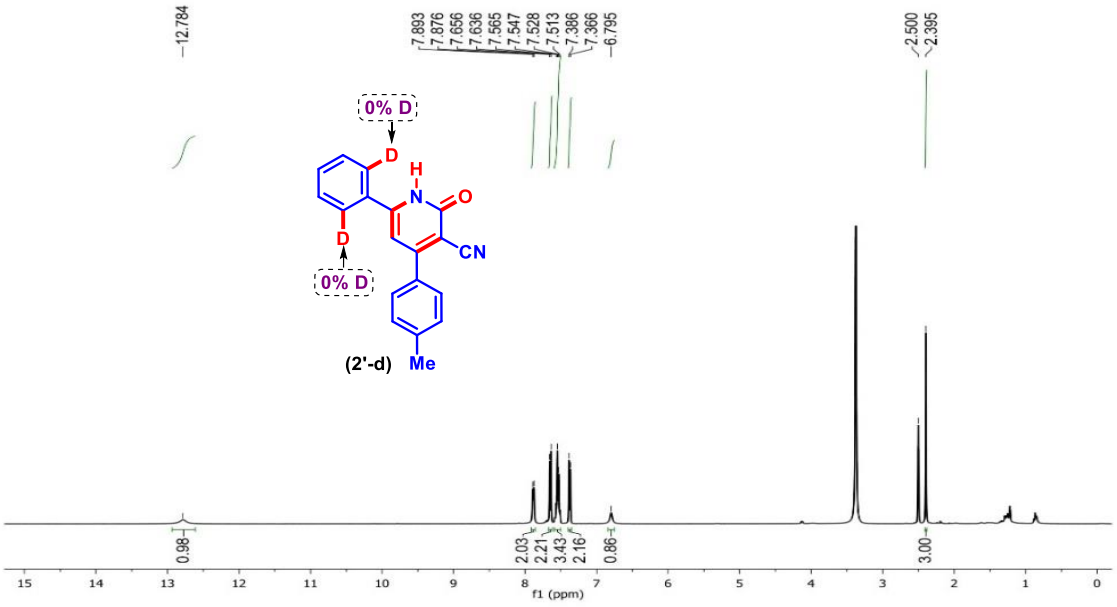

Figure II.8.3.4.1.1. *^1H NMR spectra of D_2O exchange experiment (**2'-d**).*

II.8.3.4.2. Kinetic Isotope Effect Studies:

To an oven-dried 10 mL round bottom flask was added 2-(1-(4-chlorophenyl)-3-oxo-3-phenylpropyl)malononitrile (**6**) (62 mg, 0.20 mmol), 2-(1-(4-chlorophenyl)-3-oxo-3-(phenyl-d_5)propyl)malononitrile (**6-d$_5$**) (63 mg, 0.20 mmol), $Cu(OAc)_2 \cdot H_2O$ (4 mg, 0.02 mmol), 1,10-phenanthroline (7 mg, 0.04 mmol), and glacial AcOH (2 mL). The reaction mixture was heated in an oil bath for 5 h at 110 ^oC. Then to these reaction mixture was added diphenylacetylene (**a**) (18 mg, 0.10 mmol), $[Ru(p\text{-cymene})Cl_2]_2$ (6 mg, 0.01 mmol), $Cu(OAc)_2 \cdot H_2O$ (20 mg, 0.10 mmol) and PEG-400 (2 mL). The reaction mixture was further heated for 24 h. Then the reaction mixture was cooled to room temperature, admixed with ethyl acetate (25 mL) and the organic layer was washed with saturated sodium bicarbonate solution (5 mL). The organic layer was dried over anhydrous sodium sulfate (Na_2SO_4), and the solvent was evaporated under reduced pressure. The crude product so obtained was purified over a column of silica gel (hexane/ethyl acetate, 9:1) to give mixture of expected products 2-(4-chlorophenyl)-4-oxo-6,7-diphenyl-4*H*-pyrido[2,1-*a*]isoquinoline-3-carbonitrile (**6a**), and 2-(4-chlorophenyl)-4-oxo-6,7-diphenyl-4*H*-pyrido[2,1-*a*]isoquinoline-3-carbonitrile-8,9,10,11-d_4 (**6a-d$_4$**) respectively. The ratio of the deuterated (**6a-d$_4$**) and non-deuterated (**6a**) product was calculated based on the integration ratio of the aromatic

proton peak at 7.59–7.52 (obtained as multiplet) and a singlet proton peak at 7.37 (Figure II.8.3.4.2.1).

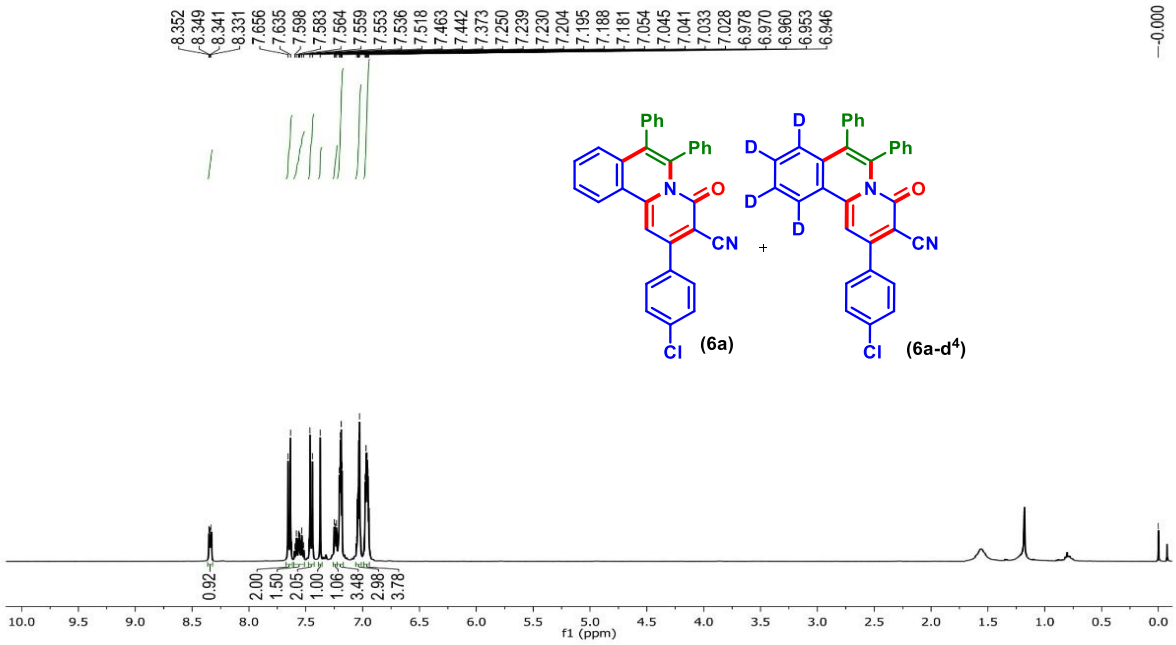

Figure II.8.3.4.2.1. *^{1}H NMR spectra of kinetic isotope effect studies.*

Calculation:

For one proton at 7.37, the integration value is 1.00

Thus for a single proton, the integration corresponds to 1.00/1 = 1.00

Now for the integration value of the protons originating from multiplet at 7.59–7.52 is 1.50

Thus the number of protons corresponding to this integration value is 1.50/1.00 = 1.50

Upon correlation with the original spectra of (**6a**), the number of protons at 7.59–7.52 should be 2

Hence the proton difference in this region is 2 - 1.50 = 0.50

Thus the K_H/K_D = 1.50/0.50 = 3.00

II.8.4. Crystallographic Information:

Diffraction data were collected at 298 K with MoKα radiation (λ = 0.71073 Å) using a Bruker Nonius SMART APEX CCD diffractometer equipped with a graphite monochromator and Apex CD camera. The SMART software was used for data collection and for indexing the reflections and determining the unit cell parameters. Data reduction and cell refinement were

performed using SAINT[1,2] software and the space groups of these crystals were determined from systematic absences by XPREP and further justified by the refinement results. The structures were solved by direct methods and refined by full-matrix least-squares calculations using SHELXL-2014[3] software. All the non-H atoms were refined in the anisotropic approximation against F^2 of all reflections.

1. G. M. Sheldrick, SADABS, 1996, based on the method described in: R. H. Blessing, *Acta Crystallogr.* 1995, **A51**, 33–38.
2. SMART and SAINT, Siemens Analytical X-ray Instruments Inc., Madison, WI, 1996.
3. G. M. Sheldrick, *Acta Crystallogr.* Struct. Chem. 2015, **71**, 3–8.

II.8.4.1. Crystallographic Description of 4-Oxo-2,6,7-triphenyl-4*H*-pyrido[2,1-*a*]isoquinoline-3-carbonitrile (1a):

$C_{32}H_{20}N_2O$, crystal dimensions 0.28 x 0.22 x 0.16 mm, M_r = 448.50, Monoclinic, space group P 21/n, a = 11.901(2) Å, b = 16.080(3) Å, c = 12.352(2) Å, α = 90 °, β = 97.524(2)°, γ = 90°, V = 2343.5(7) Å^3, Z = 4, ρ_{calcd} = 1.271 mg/m^3, μ = 0.077 mm^{-1}, F(000) = 936.0, reflection collected/unique = 2313/2053, refinement method = full-matrix least-squares on F^2, final R indices [I>2\s(I)]: R_1 = 0.0435, wR_2 = 0.1378, R indices (all data): R_1 = 0.0386, wR_2 = 0.1305, goodness of fit = 1.064. **CCDC–1885708** for 4-oxo-2,6,7-triphenyl-4*H*-pyrido[2,1-*a*]isoquinoline-3-carbonitrile (**1a**) contains the supplementary crystallographic data for this paper. These data can be obtained free of charge from The Cambridge Crystallographic Data Centre *via* www.ccdc.cam.ac.uk/data_request/cif.

II.8.4.2. Crystallographic Description of 2-(4-Chlorophenyl)-7,9-dimethyl-4-oxo-6-phenyl-4*H*-pyrido[2,1-*a*]isoquinoline-3-carbonitrile (18h):

$C_{28}H_{19}ClN_2O$, crystal dimensions 0.26 x 0.21 x 0.16 mm, M_r = 434.90, Monoclinic, space group P 21/c, a = 10.706(7) Å, b = 16.149(10) Å, c = 12.628(8) Å, α = 90 °, β = 92.33(2) °, γ = 90°, V = 2182(2) Å^3, Z = 4, ρ_{calcd} = 1.324 mg/m^3, μ = 0.199 mm^{-1}, F(000) = 904.0, reflection collected/unique = 5214/3389, refinement method = full-matrix least-squares on F^2, final R indices [I>2\s(I)]: R_1 = 0.0852, wR_2 = 0.1795, R indices (all data): R_1 = 0.0499, wR_2 = 0.1541, goodness of fit = 1.029. **CCDC–1885709** for 2-(4-chlorophenyl)-7,9-dimethyl-4-oxo-6-phenyl-4H-pyrido[2,1-*a*]isoquinoline-3-carbonitrile (**18h**) contains the supplementary crystallographic data for this paper. These data can be obtained free of charge from The Cambridge Crystallographic Data Centre *via* www.ccdc.cam.ac.uk/data_request/cif.

II.9. Spectral Data:

***2-Oxo-4,6-diphenyl-1,2-dihydropyridine-3-carbonitrile (1')*:**

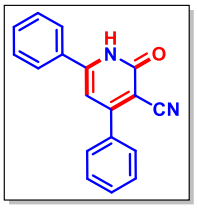

As a light yellow solid (18 mg, 15% yield, mp 305–307 °C); Purification over a column of silica gel (30% EtOAc in hexane); ^{1}H NMR (DMSO-d$_6$, 400 MHz): δ 12.79 (s, 1H), 7.89 (d, 2H, J = 6.8 Hz), 7.75–7.72 (m, 2H), 7.58–7.53 (m, 6H), 6.82 (s, 1H); ^{13}C{^{1}H} NMR (DMSO-d$_6$, 100 MHz): δ 167.1, 162.1, 159.9, 136.1, 131.8, 131.6, 131.3, 130.5, 129.0, 128.9, 128.3, 127.8, 116.6, 106.2; IR (KBr, cm^{-1}): 3425, 2958, 2925, 2855, 2218, 1647, 1607, 1574, 1531, 1497, 1471, 1399, 1352, 1262, 1224, 1175, 1122, 1075, 1001, 977, 962, 839, 802, 762, 699; HRMS (ESI/Q-TOF) (m/z) calcd for $C_{18}H_{13}N_2O$ $[M + H]^+$ 273.1022; found 273.1015.

***2-Oxo-6-phenyl-4-(p-tolyl)-1,2-dihydropyridine-3-carbonitrile (2')*:**

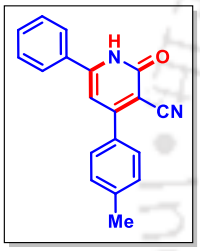

As a white solid (49 mg, 85% yield, mp 225–227 °C); Purification over a column of silica gel (30% EtOAc in hexane); ^{1}H NMR (DMSO-d$_6$, 600 MHz): δ 12.76 (s, 1H), 7.88 (d, 2H, J = 7.2 Hz), 7.64 (d, 2H, J = 7.8 Hz), 7.57–7.51 (m, 3H), 7.37 (d, 2H, J = 7.8 Hz), 6.79 (s, 1H), 2.39 (s, 3H); ^{13}C{^{1}H} NMR (DMSO-d$_6$, 150 MHz): δ 167.2, 162.2, 159.9, 151.4, 140.6, 133.2, 132.4, 131.3, 129.5, 129.1, 128.3, 127.8, 116.8, 106.2, 21.0; IR (KBr, cm^{-1}): 3435, 2956, 2923, 2854, 2218, 1646, 1609, 1573, 1534, 1471, 1450, 198, 1353, 1228, 1178, 1076, 1002, 964, 916, 842, 817, 770, 696; HRMS (ESI/Q-TOF) (m/z) calcd for $C_{19}H_{15}N_2O$ $[M + H]^+$ 287.1179; found 287.1187.

***4-Oxo-2,6,7-triphenyl-4H-pyrido[2,1-a]isoquinoline-3-carbonitrile (1a)*:**

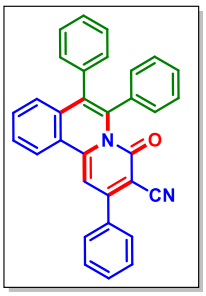

As a yellow solid (40 mg, 45% yield, mp 262–264 °C); Purification over a column of silica gel (10% EtOAc in hexane); ^{1}H NMR ($CDCl_3$, 600 MHz): δ 8.42 (d, 1H, J = 8.4 Hz), 7.78 (d, 2H, J = 6.0 Hz), 7.66–7.64 (m, 1H), 7.62–7.56 (m, 5H), 7.50 (s, 1H), 7.31–7.27 (m, 3H), 7.12–7.11 (m, 3H), 7.06–7.04 (m, 4H); ^{13}C{^{1}H} NMR ($CDCl_3$, 150 MHz): δ 160.9, 156.0, 145.1, 136.7, 136.51, 136.48, 135.1, 133.2, 132.4, 131.1, 130.9, 130.6, 129.24, 129.20, 128.6, 128.4, 128.3, 127.8, 127.5, 127.4, 127.3, 125.6, 124.7, 116.7, 100.9, 96.3; IR (KBr, cm^{-1}): 2961, 2925, 2854, 2214, 1643, 1608, 1573, 1495, 1472, 1384, 1262, 1224, 1178, 1156, 1077, 1022, 839, 801, 762, 701; HRMS (ESI/Q-TOF) (m/z) calcd for $C_{32}H_{21}N_2O$ $[M + H]^+$ 449.1648; found 449.1655.

***4-Oxo-6,7-diphenyl-2-(p-tolyl)-4H-pyrido[2,1-a]isoquinoline-3-carbonitrile (2a)*:**

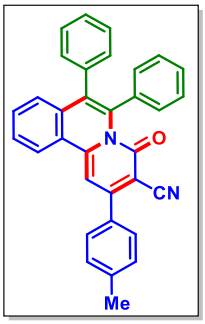

As a yellow solid (47 mg, 51% yield, mp 256–258 °C); Purification over a column of silica gel (10% EtOAc in hexane); ^{1}H NMR ($CDCl_3$, 600 MHz): δ 8.32 (d, 1H, J = 8.4 Hz), 7.61 (d, 2H, J = 7.8 Hz), 7.55 (t, 1H, J = 7.5 Hz), 7.50 (t, 1H, J = 7.2 Hz), 7.40 (s, 1H), 7.28 (d, 2H, J = 8.4 Hz), 7.22–7.17 (m, 4H), 7.03–7.01 (m, 3H), 6.97–6.94 (m, 4H), 2.37 (s, 3H); ^{13}C{^{1}H} NMR ($CDCl_3$, 150 MHz): δ 160.9, 155.9, 144.9, 140.9, 136.5, 136.4, 135.1, 133.7, 133.1, 132.3, 131.0, 130.8, 129.8, 129.2, 128.5, 128.4, 128.3, 127.7, 127.4, 127.3, 127.2, 125.6, 124.7, 116.9, 100.9, 95.9, 21.6; IR (KBr, cm^{-1}): 2955, 2924, 2854, 2215, 1670, 1610, 1566, 1506, 1491, 1471, 1366, 1261, 1224, 1165, 1082, 1044, 813, 762, 701; HRMS (ESI/Q-TOF) (m/z) calcd for $C_{33}H_{23}N_2O$ $[M + H]^+$ 463.1805; found 463.1807.

***2-(4-Methoxyphenyl)-4-oxo-6,7-diphenyl-4H-pyrido[2,1-a]isoquinoline-3-carbonitrile (3a)*:**

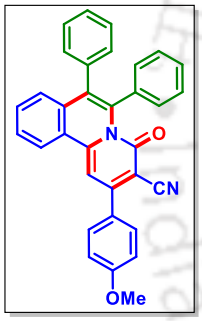

As a yellow solid (53 mg, 55% yield, mp 248–250 °C); Purification over a column of silica gel (15% EtOAc in hexane); ^{1}H NMR ($CDCl_3$, 400 MHz): δ 8.33 (d, 1H, J = 8.0 Hz), 7.70 (d, 2H, J = 8.8 Hz), 7.58–7.49 (m, 2H) 7.40 (s, 1H), 7.22–7.18 (m, 4H), 7.04–7.01 (m, 4H), 6.99–6.95 (m, 5H), 3.82 (s, 3H); ^{13}C{^{1}H} NMR ($CDCl_3$, 100 MHz): δ 161.7, 161.1, 155.5, 144.9, 136.6, 136.5, 135.2, 133.2, 132.2, 131.1, 130.7, 130.2, 129.2, 128.8, 128.4, 128.3, 127.7, 127.5, 127.4, 127.3, 125.7, 124.7, 117.1, 114.7, 100.7, 95.8, 55.7; IR (KBr, cm^{-1}): 2956, 2924, 2853, 2214, 1665, 1612, 1568, 1507, 1489, 1464, 1376, 1295, 1257, 1182, 1156, 1111, 1089, 1026, 885, 818, 762, 719, 707; HRMS (ESI/Q-TOF) (m/z) calcd for $C_{33}H_{23}N_2O_2$ $[M + H]^+$ 479.1754; found 479.1754.

***2-(4-(Methylthio)phenyl)-4-oxo-6,7-diphenyl-4H-pyrido[2,1-a]isoquinoline-3-carbonitrile (4a)*:**

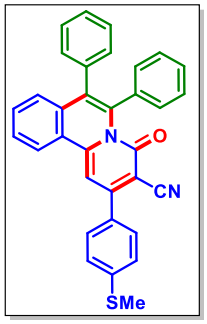

As a yellow solid (51 mg, 52% yield, mp 146–148 °C); Purification over a column of silica gel (10% EtOAc in hexane); ^{1}H NMR ($CDCl_3$, 400 MHz): δ 8.41 (d, 1H, J = 7.6 Hz), 7.72 (d, 2H, J = 8.4 Hz), 7.67–7.58 (m, 2H), 7.47 (s, 1H), 7.40 (d, 2H, J = 8.8 Hz), 7.31–7.27 (m, 4H), 7.12–7.10 (m, 3H), 7.06–7.02 (m, 4H), 2.56 (s, 3H); ^{13}C{^{1}H} NMR ($CDCl_3$, 100 MHz): δ 160.9, 155.3, 145.1, 142.6, 136.54, 136.51, 135.2, 133.2, 132.8, 132.4, 131.1, 130.9, 129.2, 128.9, 128.4, 128.3, 127.8, 127.5, 127.4, 127.3, 126.3, 125.6, 124.7, 116.9, 100.6, 95.8,

15.4; IR (KBr, cm^{-1}): 2955, 2923, 2853, 2212, 1666, 1595, 1567, 1550, 1466, 1490, 1377, 1261, 1155, 1094, 1022, 802, 762, 700; HRMS (ESI/Q-TOF) (m/z) calcd for $C_{33}H_{23}N_2OS$ $[M + H]^+$ 495.1526; found 495.1531.

***2-([1,1'-Biphenyl]-4-yl)-4-oxo-6,7-diphenyl-4H-pyrido[2,1-a]isoquinoline-3-carbonitrile (5a)*:**

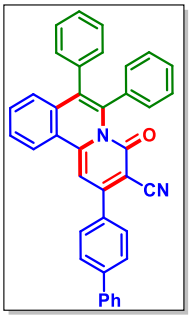

As a yellow solid (50 mg, 48% yield, mp 225–227 °C); Purification over a column of silica gel (10% EtOAc in hexane); ^1H NMR ($CDCl_3$, 400 MHz): δ 8.44 (d, 1H, J = 7.6 Hz), 7.88 (d, 2H, J = 8.4 Hz), 7.79 (d, 2H, J = 8.4 Hz), 7.68–7.66 (m, 2H), 7.64–7.58 (m, 2H), 7.54 (s, 1H), 7.50 (t, 2H, J = 7.4 Hz), 7.43–7.41 (m, 1H), 7.36–7.32 (m, 1H), 7.30–7.27 (m, 3H), 7.14–7.12 (m, 3H), 7.09–7.04 (m, 4H); $^{13}C\{^1H\}$ NMR ($CDCl_3$, 100 MHz): δ 160.9, 155.5, 145.1, 143.5, 140.3, 136.6, 136.5, 135.5, 135.2, 133.3, 133.4, 131.1, 130.9, 129.24, 129.18, 129.1, 128.5, 128.3, 128.2, 127.9, 127.8, 127.5, 127.45, 127.41, 127.3, 125.7, 124.7, 116.8, 100.8, 96.1; IR (KBr, cm^{-1}): 2955, 2924, 2854, 2214, 1669, 1603, 1565, 1467, 1375, 1305, 1262, 1223, 1080, 1042, 815, 761, 699; HRMS (ESI/Q-TOF) (m/z) calcd for $C_{38}H_{25}N_2O$ $[M + H]^+$ 525.1961; found 525.1961.

***2-(4-Chlorophenyl)-4-oxo-6,7-diphenyl-4H-pyrido[2,1-a]isoquinoline-3-carbonitrile (6a)*:**

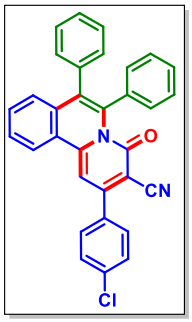

As a yellow solid (47 mg, 49% yield, mp 235–237 °C); Purification over a column of silica gel (10% EtOAc in hexane); ^1H NMR ($CDCl_3$, 400 MHz): δ 8.33 (d, 1H, J = 7.6 Hz), 7.64 (d, 2H, J = 8.4 Hz), 7.59–7.51 (m, 2H), 7.44 (d, 2H, J = 8.4 Hz), 7.37 (s, 1H), 7.24 (d, 1H, J = 8.0 Hz), 7.20–7.18 (m, 3H), 7.05–7.02 (m, 3H), 6.97–6.94 (m, 4H); $^{13}C\{^1H\}$ NMR ($CDCl_3$, 100 MHz): δ 160.7, 154.6, 145.3, 136.8, 136.5, 136.4, 135.0, 133.2, 132.5, 131.2, 131.0, 129.9, 129.4, 129.3, 128.4, 128.3, 127.8, 127.5, 127.38, 127.35, 125.5, 124.8, 116.6, 100.6, 95.9; IR (KBr, cm^{-1}): 2956, 2924, 2853, 2214, 1670, 1596, 1564, 1489, 1469, 1377, 1305, 1225, 1155, 1092, 1014, 814, 761, 725, 700; HRMS (ESI/Q-TOF) (m/z) calcd for $C_{32}H_{20}ClN_2O$ $[M + H]^+$ 483.1259; found 483.1257.

***2-(2-Bromophenyl)-4-oxo-6,7-diphenyl-4H-pyrido[2,1-a]isoquinoline-3-carbonitrile (7a)*:**

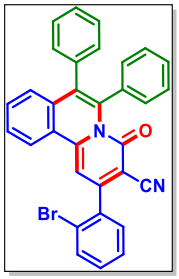

As a yellow solid (47 mg, 45% yield, mp 205–207 °C); Purification over a column of silica gel (10% EtOAc in hexane); ^{1}H NMR ($CDCl_3$, 400 MHz): δ 8.30 (d, 1H, J = 8.0 Hz), 7.69 (d, 1H, J = 8.0 Hz), 7.58–7.51 (m, 2H), 7.44–7.40 (m, 2H), 7.36 (s, 1H), 7.32–7.28 (m, 1H), 7.24–7.18 (m, 4H), 7.06–7.04 (m, 3H), 6.99–6.96 (m, 4H); ^{13}C{^{1}H} NMR ($CDCl_3$, 100 MHz): δ 160.4, 155.6, 145.0, 137.8, 136.6, 136.5, 135.1, 133.7, 133.2, 132.4, 131.29, 131.26, 131.0, 130.3, 129.3, 128.4, 128.3, 127.9, 127.8, 127.5, 127.4, 127.3, 125.7, 124.8, 121.6, 115.7, 102.0, 98.3; IR (KBr, cm^{-1}): 2956, 2924, 2853, 2218, 1674, 1566, 1507, 1464, 1377, 1261, 1094, 1023, 801, 701; HRMS (ESI/Q-TOF) (m/z) calcd for $C_{32}H_{20}BrN_2O$ $[M + H]^+$ 527.0754; found 527.0758.

***2-(3-Nitrophenyl)-4-oxo-6,7-diphenyl-4H-pyrido[2,1-a]isoquinoline-3-carbonitrile (8a)*:**

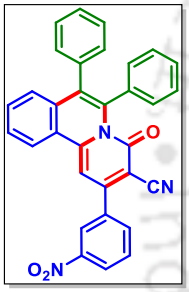

As a red solid (35 mg, 35% yield, mp 272–274 °C); Purification over a column of silica gel (15% EtOAc in hexane); ^{1}H NMR ($CDCl_3$, 400 MHz): δ 8.60–8.59 (m, 1H), 8.47 (d, 1H, J = 8.8 Hz), 8.41 (d, 1H, J = 8.0 Hz), 8.16 (d, 1H, J = 8.0 Hz), 7.77 (t, 1H, J = 8.0 Hz), 7.72–7.64 (m, 2H), 7.50 (s, 1H), 7.36 (d, 1H, J = 8.0 Hz), 7.29–7.28 (m, 3H), 7.14–7.12 (m, 3H), 7.07–7.04 (m, 4H); ^{13}C{^{1}H} NMR ($CDCl_3$, 100 MHz): δ 160.4, 153.2, 148.7, 145.8, 138.3, 136.6, 136.2, 134.9, 134.7, 133.4, 132.9, 131.7, 130.9, 130.4, 129.5, 128.45, 128.36, 127.9, 127.7, 127.51, 127.46, 125.4, 125.1, 124.9, 123.5, 116.2, 100.3, 95.9; IR (KBr, cm^{-1}): 2955, 2924, 2853, 2214, 1671, 1566, 1530, 1508, 1466, 1378, 1347, 1271, 1224, 1075, 1047, 889, 814, 763, 741, 704; HRMS (ESI/Q-TOF) (m/z) calcd for $C_{32}H_{20}N_3O_3$ $[M + H]^+$ 494.1499; found 494.1499.

***9-Methyl-4-oxo-2,6,7-triphenyl-4H-pyrido[2,1-a]isoquinoline-3-carbonitrile (9a)*:**

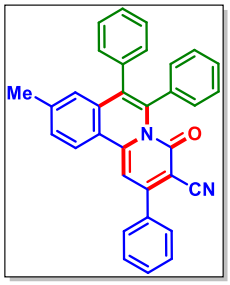

As a yellow solid (42 mg, 45% yield, mp 275–277 °C); Purification over a column of silica gel (10% EtOAc in hexane); ^{1}H NMR ($CDCl_3$, 400 MHz): δ 8.24 (d, 1H, J = 8.8 Hz), 7.72–7.69 (m, 2H), 7.49–7.47 (m, 2H), 7.39 (d, 2H, J = 8.0 Hz), 7.37 (s, 1H), 7.21–7.19 (m, 4H), 7.04–7.02 (m, 2H), 6.99–6.94 (m, 5H), 2.32 (s, 3H); ^{13}C{^{1}H} NMR ($CDCl_3$, 100 MHz): δ 161.0, 155.9, 145.3, 143.4, 136.9, 136.7, 135.3, 133.3, 131.1, 130.9, 130.8, 130.5, 129.2, 128.5, 128.4, 128.3, 127.7, 127.4, 127.24, 127.21, 124.8, 123.4, 116.9, 100.5, 95.5, 22.1; IR (KBr, cm^{-1}): 2955, 2924, 2854,

2214, 1671, 1563, 1493, 1464, 1378, 1264, 1073, 800, 701; HRMS (ESI/Q-TOF) (m/z) calcd for $C_{33}H_{23}N_2O$ $[M + H]^+$ 463.1805; found 463.1806.

***9-Methoxy-4-oxo-2,6,7-triphenyl-4H-pyrido[2,1-a]isoquinoline-3-carbonitrile (10a)*:**

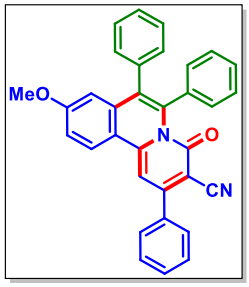

As a yellow solid (40 mg, 42% yield, mp 250–252 °C); Purification over a column of silica gel (15% EtOAc in hexane); ^{1}H NMR ($CDCl_3$, 400 MHz): δ 8.27 (d, 1H, J = 9.6 Hz), 7.70–7.68 (m, 2H), 7.48–7.46 (m, 3H), 7.27 (s, 1H), 7.19–7.18 (m, 4H), 7.15–7.13 (m, 1H), 7.04–7.02 (m, 3H), 6.98–6.94 (m, 4H), 3.64 (s, 3H); ^{13}C{^{1}H} NMR ($CDCl_3$, 100 MHz): δ 162.8, 161.1, 155.8, 145.3, 137.2, 136.9, 136.7, 135.5, 135.2, 130.9, 130.4, 129.1, 128.5, 128.38, 128.35, 127.8, 127.4, 127.3, 126.9, 119.4, 118.5, 117.0, 113.9, 109.0, 99.9, 94.3, 55.7; IR (KBr, cm^{-1}): 2955, 2924, 2853, 2213, 1666, 1610, 1560, 1510, 1491, 1464, 1401, 1377, 1264, 1222, 1125, 1086, 1030, 881, 802, 754, 727, 701; HRMS (ESI/Q-TOF) (m/z) calcd for $C_{33}H_{23}N_2O_2$ $[M + H]^+$ 479.1754; found 479.1754.

***4-Oxo-2,6,7-triphenyl-9-(trifluoromethyl)-4H-pyrido[2,1-a]isoquinoline-3-carbonitrile (11a)*:**

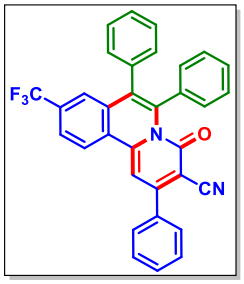

As a yellow solid (60 mg, 59% yield, mp 205–207 °C); Purification over a column of silica gel (10% EtOAc in hexane); ^{1}H NMR ($CDCl_3$, 400 MHz): δ 8.51 (d, 1H, J = 8.8 Hz), 7.83–7.77 (m, 3H), 7.59–7.57 (m, 3H), 7.53 (s, 1H), 7.51 (s, 1H), 7.31–7.29 (m, 3H), 7.14–7.12 (m, 3H), 7.06–7.02 (m, 4H); ^{13}C{^{1}H} NMR ($CDCl_3$, 100 MHz): δ 160.5, 156.4, 143.8, 137.9, 136.3, 135.9, 134.1, 133.4, 130.97, 130.88, 130.2, 129.3, 128.6, 128.5, 128.4, 128.3, 127.7, 127.6, 125.6, 125.2 (q, J = 3.3 Hz), 124.5, 124.4 (d, J = 4.0 Hz), 122.1, 116.2, 101.7, 98.2; ^{19}F NMR ($CDCl_3$ + hexafluorobenzene): δ –66.3 (s); IR (KBr, cm^{-1}): 2955, 2924, 2854, 2217, 1671, 1610, 1569, 1511, 1493, 1465, 1376, 1325, 1287, 1223, 1174, 1131, 1159, 1068, 1003, 943, 905, 879, 822, 759, 727, 704; HRMS (ESI/Q-TOF) (m/z) calcd for $C_{33}H_{20}F_3N_2O$ $[M + H]^+$ 517.1522; found 517.1522.

***9-Fluoro-4-oxo-2,6,7-triphenyl-4H-pyrido[2,1-a]isoquinoline-3-carbonitrile (12a)*:**

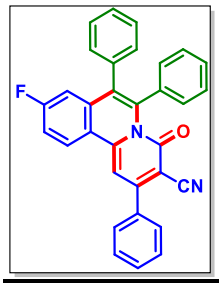

As a yellow solid (53 mg, 57% yield, mp 262–264 °C); Purification over a column of silica gel (10% EtOAc in hexane); ^{1}H NMR ($CDCl_3$, 600 MHz): δ 8.44–8.42 (m, 1H), 7.78–7.76 (m, 2H), 7.57–7.56 (m, 3H), 7.40 (s, 1H), 7.36 (t, 1H, J = 9.6 Hz), 7.29–7.28 (m, 3H), 7.13–7.12 (m, 3H), 7.05–7.01 (m, 4H),

6.94 (dd, 1H, J_1 = 6.6 Hz & J_2 = 3.0 Hz); $^{13}C\{^1H\}$ NMR ($CDCl_3$, 100 MHz): δ 166.2, 163.6, 160.8, 156.3, 144.6, 137.8, 136.6, 136.2, 134.6, 130.9, 130.7, 129.2, 128.54, 128.51, 128.3, 128.1, 127.54, 127.48, 122.2, 117.9 (d, J = 23.7 Hz), 116.5, 112.9 (d, J = 23.2 Hz), 100.7, 96.2; ^{19}F NMR ($CDCl_3$ + hexafluorobenzene): δ –107.4 (s); IR (KBr, cm^{-1}): 2955, 2924, 2853, 2212, 1658, 1568, 1507, 1493, 1464, 1377, 1261, 1092, 1018, 803, 721, 707; HRMS (ESI/Q-TOF) (m/z) calcd for $C_{32}H_{20}FN_2O$ $[M + H]^+$ 467.1554; found 467.1561.

***9-Chloro-4-oxo-2,6,7-triphenyl-4H-pyrido[2,1-a]isoquinoline-3-carbonitrile (13a)*:**

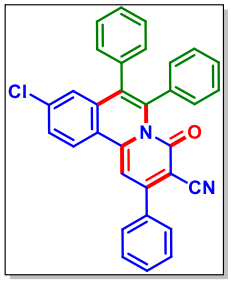

As a yellow solid (51 mg, 53% yield, mp 285–287 °C); Purification over a column of silica gel (10% EtOAc in hexane); ^1H NMR ($CDCl_3$, 600 MHz): δ 8.33 (d, 1H, J = 9.0 Hz), 7.78–7.76 (m, 2H), 7.59–7.55 (m, 4H), 7.42 (s, 1H), 7.29–7.28 (m, 3H), 7.25 (s, 1H), 7.13–7.12 (m, 3H), 7.04–7.01 (m, 4H); $^{13}C\{^1H\}$ NMR ($CDCl_3$, 100 MHz): δ 160.7, 156.2, 144.4, 139.0, 137.8, 136.5, 136.2, 134.5, 134.4, 130.9, 130.7, 129.8, 129.7, 129.2, 128.53, 128.51, 128.3, 128.1, 127.53, 127.46, 126.8, 126.3, 124.1, 116.5, 100.9, 96.8; IR (KBr, cm^{-1}): 2955, 2924, 2853, 2212, 1656, 1596, 1570, 1530, 1464, 1377, 1267, 1121, 1073, 1018, 877, 804, 758, 721; HRMS (ESI/Q-TOF) (m/z) calcd for $C_{32}H_{20}ClN_2O$ $[M + H]^+$ 483.1259; found 483.1259.

***9-Bromo-4-oxo-2,6,7-triphenyl-4H-pyrido[2,1-a]isoquinoline-3-carbonitrile (14a)*:**

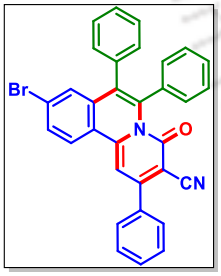

As a yellow solid (54 mg, 52% yield, mp 215–217 °C); Purification over a column of silica gel (10% EtOAc in hexane); ^1H NMR ($CDCl_3$, 600 MHz): δ 8.25 (d, 1H, J = 9.0 Hz), 7.77–7.76 (m, 2H), 7.73 (d, 1H, J = 9.0 Hz), 7.57–7.55 (m, 3H), 7.43–7.41 (m, 2H), 7.29–7.28 (m, 3H), 7.12–7.11 (m, 3H), 7.04–7.01 (m, 4H); $^{13}C\{^1H\}$ NMR ($CDCl_3$, 100 MHz): δ 160.7, 156.3, 144.5, 137.8, 136.5, 136.1, 134.7, 134.4, 132.5, 131.0, 130.7, 129.9, 129.7, 129.2, 128.6, 128.5, 128.3, 128.1, 127.6, 127.55, 127.48, 126.2, 124.5, 116.5, 100.9, 96.9; IR (KBr, cm^{-1}): 2955, 2924, 2853, 2217, 1650, 1560, 1507, 1463, 1377, 1264, 1121, 1073, 1024, 885, 802, 721, 701; HRMS (ESI/Q-TOF) (m/z) calcd for $C_{32}H_{20}BrN_2O$ $[M + H]^+$ 527.0754; found 527.0759.

***9-Nitro-4-oxo-2,6,7-triphenyl-4H-pyrido[2,1-a]isoquinoline-3-carbonitrile (15a)*:**

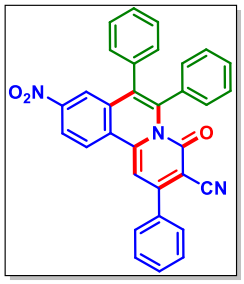

As a red solid (29 mg, 30% yield, mp 245–247 °C); Purification over a column of silica gel (15% EtOAc in hexane); ^{1}H NMR ($CDCl_3$, 400 MHz): δ 8.53 (d, 1H, J = 9.2 Hz), 8.38–8.36 (m, 2H), 8.11 (s, 1H), 7.79–7.77 (m, 2H), 7.74–7.69 (m, 1H), 7.59–7.58 (m, 3H), 7.53 (s, 1H), 7.33–7.32 (m, 3H), 7.07–7.06 (m, 2H), 7.05–7.03 (m, 3H); ^{13}C{^{1}H} NMR ($CDCl_3$, 100 MHz): δ 160.3, 156.5, 149.6, 143.1, 138.6, 135.9, 135.6, 134.1, 133.7, 131.0, 130.9, 129.9, 129.4, 128.9, 128.8, 128.5, 128.3, 127.9, 127.6, 126.4, 122.9, 122.5, 115.9, 102.9, 99.1; IR (KBr, cm^{-1}): 2955, 2924, 2854, 2220, 1646, 1462, 1378, 1262, 1099, 880, 803, 727; HRMS (ESI/Q-TOF) (m/z) calcd for $C_{32}H_{20}N_3O_3$ $[M + H]^+$ 494.1499; found 494.1492.

***2-(Naphthalen-1-yl)-4-oxo-6,7-diphenyl-4H-pyrido[2,1-a]isoquinoline-3-carbonitrile (16a)*:**

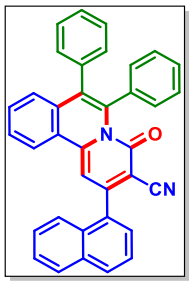

As a yellow solid (43 mg, 44% yield, mp 146–148 °C); Purification over a column of silica gel (10% EtOAc in hexane); ^{1}H NMR ($CDCl_3$, 400 MHz): δ 8.24–8.22 (m, 1H), 7.95–7.89 (m, 2H), 7.81 (d, 1H, J = 7.6 Hz), 7.59 (d, 1H, J = 7.2 Hz), 7.55 (d, 1H, J = 8.0 Hz), 7.53–7.48 (m, 4H), 7.46 (s, 1H), 7.25–7.18 (m, 5H), 7.01–7.00 (m, 5H), 6.98–6.96 (m, 1H); ^{13}C{^{1}H} NMR ($CDCl_3$, 100 MHz): δ 160.6, 155.9, 144.8, 136.7, 136.6, 135.2, 134.6, 134.0, 133.3, 132.4, 131.2, 131.12, 131.06, 130.5, 130.4, 129.3, 128.9, 128.5, 128.4, 128.3, 127.8, 127.5, 127.43, 127.36, 127.30, 127.1, 126.7, 125.6, 125.5, 125.2, 124.8, 116.0, 102.7, 99.0; IR (KBr, cm^{-1}): 2955, 2924, 2854, 2223, 1666, 1562, 1513, 1493, 1464, 1377, 1262, 1156, 1073, 1018, 803, 719, 703; HRMS (ESI/Q-TOF) (m/z) calcd for $C_{36}H_{23}N_2O$ $[M + H]^+$ 499.1805; found 499.1805.

***10-(Naphthalen-1-yl)-8-oxo-5,6-diphenyl-8H-benzo[f]pyrido[2,1-a]isoquinoline-9-carbonitrile (17a)*:**

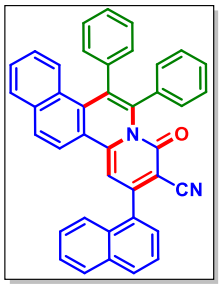

As a yellow solid (47 mg, 43% yield, mp 175–177 °C); Purification over a column of silica gel (10% EtOAc in hexane); ^{1}H NMR ($CDCl_3$, 600 MHz): δ 8.81 (s, 1H), 8.04 (d, 1H, J = 8.4 Hz), 8.01 (d, 1H, J = 7.2 Hz), 7.95–7.93 (m, 2H), 7.78–7.77 (m, 1H), 7.72–7.71 (m, 3H), 7.66–7.64 (m, 1H), 7.62–7.53 (m, 5H), 7.35–7.32 (m, 3H), 7.18–7.14 (m, 6H); ^{13}C{^{1}H} NMR ($CDCl_3$, 100 MHz):

δ 160.6, 156.5, 145.1, 136.6, 135.6, 135.3, 134.9, 134.4, 134.0, 132.7, 131.8, 131.2, 131.1, 130.9, 130.5, 128.85, 128.81, 128.4, 127.8, 127.5, 127.4, 127.3, 127.1, 126.8, 126.7, 125.54, 125.48, 125.2, 123.5, 115.8, 103.6, 100.6; IR (KBr, cm^{-1}): 2957, 2924, 2854, 2224, 1661, 1462, 1377, 1261, 1023, 803; HRMS (ESI/Q-TOF) (m/z) calcd for $C_{40}H_{25}N_2O$ $[M + H]^+$ 549.1961; found 549.1968.

***2-(4-Chlorophenyl)-9-methyl-4-oxo-6,7-diphenyl-4H-pyrido[2,1-a]isoquinoline-3-carbonitrile (18a)*:**

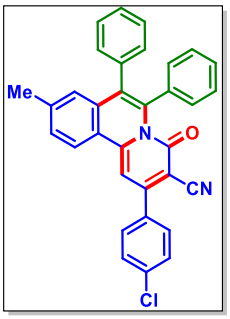

As a yellow solid (71 mg, 72% yield, mp 276–278 °C); Purification over a column of silica gel (10% EtOAc in hexane); ^{1}H NMR ($CDCl_3$, 600 MHz): δ 8.31 (d, 1H, *J* = 9.0 Hz), 7.72 (d, 2H, *J* = 8.4 Hz), 7.53 (d, 2H, *J* = 8.4 Hz), 7.48 (d, 1H, *J* = 8.4 Hz), 7.40 (s, 1H), 7.28–7.27 (m, 3H), 7.11–7.10 (m, 3H), 7.08 (s, 1H), 7.03–7.01 (m, 4H), 2.40 (s, 3H); ^{13}C{^{1}H} NMR ($CDCl_3$, 100 MHz): δ 160.8, 154.6, 145.5, 143.7, 136.8, 136.7, 136.6, 135.24, 135.17, 133.4, 131.0, 130.9, 129.9, 129.5, 128.4, 128.3, 127.8, 127.4, 127.31, 127.26, 124.8, 123.3, 116.7, 100.1, 95.2, 22.1; IR (KBr, cm^{-1}): 2955, 2924, 2853, 2210, 1639, 1465, 1261, 1090, 1020, 802; HRMS (ESI/Q-TOF) (m/z) calcd for $C_{33}H_{22}ClN_2O$ $[M + H]^+$ 497.1415; found 497.1419.

***9-Bromo-2-(4-chlorophenyl)-4-oxo-6,7-diphenyl-4H-pyrido[2,1-a]isoquinoline-3-carbonitrile (19a)*:**

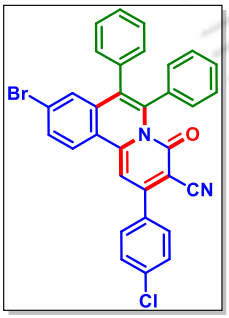

As a yellow solid (64 mg, 58% yield, mp 240–242 °C); Purification over a column of silica gel (10% EtOAc in hexane); ^{1}H NMR ($CDCl_3$, 400 MHz): δ 8.24 (d, 1H, *J* = 9.2 Hz), 7.75–7.72 (m, 2H), 7.69 (s, 1H), 7.54 (d, 2H, *J* = 8.4 Hz), 7.42 (s, 1H), 7.38 (s, 1H), 7.30–7.28 (m, 3H), 7.13–7.11 (m, 3H), 7.03–7.00 (m, 4H); ^{13}C{^{1}H} NMR ($CDCl_3$, 100 MHz): δ 160.5, 154.9, 144.7, 137.9, 137.1, 136.0, 134.9, 134.7, 134.3, 132.6, 130.9, 129.99, 129.93, 129.89, 129.6, 128.6, 128.4, 128.2, 127.8, 127.6, 127.5, 126.2, 124.4, 116.3, 100.6, 96.6; IR (KBr, cm^{-1}): 2956, 2923, 2854, 2216, 1668, 1595, 1566, 1492, 1463, 1388, 1309, 1263, 1220, 1091, 1018, 808, 702; HRMS (ESI/Q-TOF) (m/z) calcd for $C_{32}H_{19}BrClN_2O$ $[M + H]^+$ 561.0364; found 561.0364.

***2-(4-Methoxyphenyl)-9-nitro-4-oxo-6,7-diphenyl-4H-pyrido[2,1-a]isoquinoline-3-carbonitrile (20a)*:**

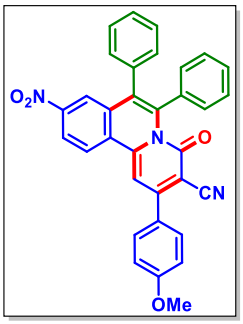

As a red solid (26 mg, 25% yield, mp 216–218 °C); Purification over a column of silica gel (15% EtOAc in hexane); ^{1}H NMR ($CDCl_3$, 400 MHz): δ 8.52 (d, 1H, J = 9.2 Hz), 8.36 (d, 1H, J = 9.0 Hz), 8.09 (s, 1H), 7.79–7.76 (m, 3H), 7.51 (s, 1H), 7.32–7.31 (m, 3H), 7.15–7.13 (m, 2H), 7.10–7.07 (m, 3H), 7.06–7.03 (m, 3H), 3.91 (s, 3H); ^{13}C{^{1}H} NMR ($CDCl_3$, 100 MHz): δ 162.1, 160.5, 155.9, 149.5, 142.8, 138.6, 135.6, 134.1, 133.8, 130.9, 130.6, 130.3, 129.9, 129.5, 128.9, 128.8, 128.5, 128.3, 128.0, 127.9, 127.7, 127.6, 126.2, 122.8, 122.4, 114.9, 102.7, 98.5, 55.8; IR (KBr, cm^{-1}): 2956, 2924, 2853, 2214, 1663, 1570, 1513, 1464, 1378, 1259, 1093, 1020, 883, 806, 717; HRMS (ESI/Q-TOF) (m/z) calcd for $C_{33}H_{22}N_3O_4$ $[M + H]^+$ 524.1605; found 524.1605.

***2-(2,6-Dichlorophenyl)-9-fluoro-4-oxo-6,7-diphenyl-4H-pyrido[2,1-a]isoquinoline-3-carbonitrile (21a)*:**

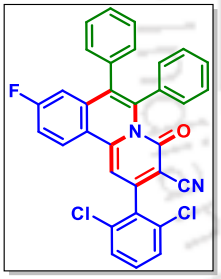

As a yellow solid (60 mg, 57% yield, mp 255–257 °C); Purification over a column of silica gel (10% EtOAc in hexane); ^{1}H NMR ($CDCl_3$, 600 MHz): δ 8.33–8.30 (m, 1H), 7.43 (d, 2H, J = 7.8 Hz), 7.33 (t, 1H, J = 8.1 Hz), 7.29 (t, 1H, J = 9.6 Hz), 7.23–7.22 (m, 3H), 7.19 (s, 1H), 7.08–7.06 (m, 3H), 6.99–6.95 (m, 4H), 6.88 (dd, 1H, J_1 = 7.2 Hz & J_2 = 2.4 Hz); ^{13}C{^{1}H} NMR ($CDCl_3$, 100 MHz): δ 166.3, 163.7, 160.1, 152.2, 145.4, 137.9, 136.2, 135.9, 135.8, 134.7, 134.6, 133.9, 131.4, 130.9, 128.7, 128.6, 128.3, 128.1, 127.98, 127.88, 127.6, 127.5, 122.27, 122.25, 118.1 (d, J = 23.7 Hz), 115.0, 112.9 (d, J = 23.2 Hz), 100.9, 98.9; ^{19}F NMR ($CDCl_3$ + hexafluorobenzene): δ –106.9 (s); IR (KBr, cm^{-1}): 2954, 2924, 2853, 2223, 1670, 1610, 1510, 1467, 1379, 1261, 1180, 1095, 1020, 873, 790, 758, 698; HRMS (ESI/Q-TOF) (m/z) calcd for $C_{32}H_{18}Cl_2FN_2O$ $[M + H]^+$ 535.0775; found 535.0775.

***2-(3,4-Dimethoxyphenyl)-4-oxo-6,7-diphenyl-4H-pyrido[2,1-a]isoquinoline-3-carbonitrile (22a)*:**

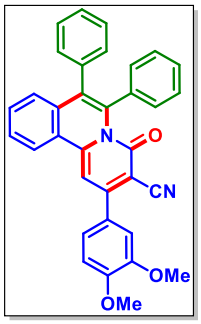

As a yellow solid (62 mg, 61% yield, mp 240–242 °C); Purification over a column of silica gel (15% EtOAc in hexane); ^{1}H NMR ($CDCl_3$, 600 MHz): δ 8.35 (d, 1H, J = 8.4 Hz), 7.58 (t, 1H, J = 7.2 Hz), 7.53 (t, 1H, J = 7.2 Hz), 7.43 (s, 1H), 7.33–7.31 (m, 2H), 7.23–7.19 (m, 4H), 7.05–7.04 (m, 3H), 6.98–6.96 (m, 5H), 3.94 (s, 3H), 3.91 (s, 3H); ^{13}C{^{1}H} NMR ($CDCl_3$, 100 MHz): δ 161.1, 155.5, 151.3, 149.4, 144.8, 136.54, 136.47, 135.2, 133.3, 133.2, 131.1, 130.7, 129.2, 129.0, 128.4, 128.3, 127.7, 127.5, 127.4, 127.3, 125.6, 124.7, 121.8, 117.1, 111.9, 111.6, 100.7, 95.7, 56.5, 56.3; IR (KBr, cm^{-1}): 2956, 2924, 2853, 2217, 1659, 1564, 1513, 1495, 1464, 1377, 1264, 1117, 1022, 885, 800, 762, 727, 699; HRMS (ESI/Q-TOF) (m/z) calcd for $C_{34}H_{25}N_2O_3$ [M + H]$^{+}$ 509.1860; found 509.1860.

***1-(4-Chlorophenyl)-3-oxo-5,6-diphenyl-10,11-dihydro-3H-benzo[de]pyrido[3,2,1-ij]quinoline-2-carbonitrile (23a)*:**

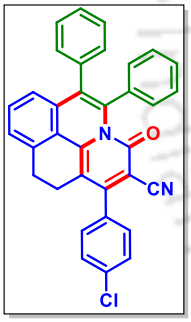

As a yellow solid (57 mg, 56% yield, mp 165–167 °C); Purification over a column of silica gel (10% EtOAc in hexane); ^{1}H NMR ($CDCl_3$, 400 MHz): δ 7.96 (d, 1H, J = 7.6 Hz), 7.88 (d, 1H, J = 7.6 Hz), 7.75 (t, 1H, J = 7.8 Hz), 7.66–7.59 (m, 2H), 7.56–7.49 (m, 3H), 7.47–7.44 (m, 2H), 7.39 (t, 1H, J = 7.2 Hz), 7.33–7.29 (m, 3H), 7.14–7.08 (m, 3H), 2.88 (t, 2H, J = 7.8 Hz), 2.53 (t, 2H, J = 7.8 Hz); ^{13}C{^{1}H} NMR ($CDCl_3$, 100 MHz): δ 164.9, 159.6, 158.3, 138.9, 137.2, 132.9, 131.6, 130.9, 130.85, 130.79, 129.8, 129.6, 129.2, 128.6, 128.5, 128.3, 127.9, 127.8, 127.5, 127.4, 127.1, 125.6, 125.3, 123.0, 121.9, 112.1, 98.2, 27.4, 23.2; IR (KBr, cm^{-1}): 2954, 2924, 2853, 2221, 1668, 1633, 1485, 1464, 1608, 1377, 1267, 1091, 1014, 836, 808, 766, 719; HRMS (ESI/Q-TOF) (m/z) calcd for $C_{34}H_{22}ClN2O$ [M + H]$^{+}$ 509.1415; found 509.1416.

***2-(Furan-2-yl)-9-methyl-4-oxo-6,7-diphenyl-4H-pyrido[2,1-a]isoquinoline-3-carbonitrile (24a)*:**

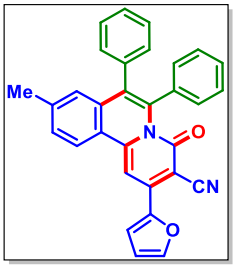

As a yellow solid (37 mg, 41% yield, mp 185–187 °C); Purification over a column of silica gel (10% EtOAc in hexane); ^{1}H NMR ($CDCl_3$, 400 MHz): δ 8.39 (d, 1H, J = 8.4 Hz), 7.89 (s, 1H), 7.79 (d, 1H, J = 3.6 Hz), 7.73 (s, 1H), 7.49 (d, 1H, J = 8.8 Hz), 7.27–7.26 (m, 3H), 7.10–7.08 (m, 3H), 7.04–6.99

(m, 5H), 6.68 (dd, 1H, J_1 = 3.6 Hz and J_2 = 1.6 Hz), 2.39 (s, 3H); $^{13}C\{^1H\}$ NMR ($CDCl_3$, 100 MHz): δ 161.2, 148.4, 145.5, 143.4, 141.9, 136.7, 135.3, 133.3, 131.1, 130.8, 130.6, 128.6, 128.4, 128.3, 127.7, 127.4, 127.22, 127.17, 124.9, 123.6, 116.2, 113.6, 95.8, 22.1; IR (KBr, cm^{-1}): 2954, 2924, 2853, 2214, 1641, 1510, 1465, 1378, 1265, 1029, 812, 756, 700; HRMS (ESI/Q-TOF) (m/z) calcd for $C_{31}H_{21}N_2O_2$ $[M + H]^+$ 453.1598; found 453.1595.

***7-Oxo-4,5,9-triphenyl-7H-thieno[2,3-a]quinolizine-8-carbonitrile (25a)*:**

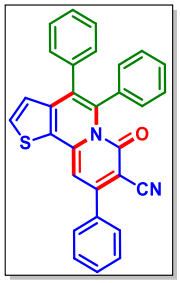

As a yellow solid (39 mg, 43% yield, mp 166–168 °C); Purification over a column of silica gel (10% EtOAc in hexane); ^1H NMR ($CDCl_3$, 400 MHz): δ 7.77–7.74 (m, 2H), 7.71 (d, 1H, J = 5.6 Hz), 7.57–7.53 (m, 3H), 7.26–7.24 (m, 3H), 7.16–7.15 (m, 3H), 7.08–7.05 (m, 2H), 7.04–7.02 (m, 2H), 6.96 (d, 1H, J = 5.2 Hz), 6.89 (s, 1H); $^{13}C\{^1H\}$ NMR ($CDCl_3$, 100 MHz): δ 160.8, 155.7, 142.3, 141.9, 138.0, 136.5, 135.9, 135.6, 132.9, 132.5, 130.5, 130.3, 129.1, 128.7, 128.5, 128.3, 127.9, 127.6, 127.4, 126.2, 117.2, 100.4, 93.2; IR (KBr, cm^{-1}): 2958, 2924, 2854, 2208, 1638, 1592, 1556, 1513, 1495, 1462, 1377, 1289, 1267, 1119, 1071, 1018, 885, 798, 748, 723, 699; HRMS (ESI/Q-TOF) (m/z) calcd for $C_{30}H_{19}N_2OS$ $[M + H]^+$ 455.1213; found 455.1213.

***4-Oxo-2-phenyl-6,7-di-p-tolyl-4H-pyrido[2,1-a]isoquinoline-3-carbonitrile (1b)*:**

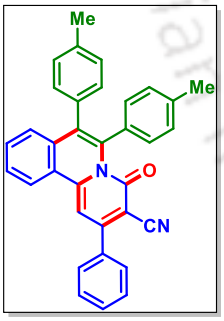

As a yellow solid (44 mg, 46% yield, mp 278–280 °C); Purification over a column of silica gel (10% EtOAc in hexane); ^1H NMR ($CDCl_3$, 400 MHz): δ 8.39 (d, 1H, J = 8.2 Hz), 7.79–7.77 (m, 2H), 7.64–7.53 (m, 5H), 7.46 (s, 1H), 7.31 (d, 1H, J = 8.0 Hz), 7.09 (d, 2H, J = 7.6 Hz), 6.94–6.92 (m, 6H), 2.35 (s, 3H), 2.26 (s, 3H); $^{13}C\{^1H\}$ NMR ($CDCl_3$, 100 MHz): δ 161.1, 155.8, 145.2, 137.4, 136.9, 136.8, 136.6, 133.6, 133.5, 132.22, 132.15, 130.9, 130.5, 129.1, 129.03, 129.01, 128.5, 128.25, 128.23, 127.5, 125.5, 124.6, 116.8, 100.8, 96.1, 21.53, 21.46; IR (KBr, cm^{-1}): 2959, 2924, 2855, 2217, 1659, 1577, 1500, 1463, 1405, 1381, 1312, 1261, 1221, 1153, 1091, 1023, 873, 807, 760, 728, 701; HRMS (ESI/Q-TOF) (m/z) calcd for $C_{34}H_{25}N_2O$ $[M + H]^+$ 477.1961; found 477.1961.

***6,7-Bis(4-methoxyphenyl)-4-oxo-2-phenyl-4H-pyrido[2,1-a]isoquinoline-3-carbonitrile (1c)*:**

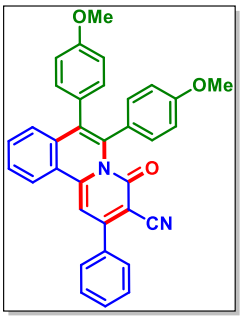

As a yellow solid (49 mg, 48% yield, mp 258–260 °C); Purification over a column of silica gel (15% EtOAc in hexane); ^{1}H NMR ($CDCl_3$, 400 MHz): δ 8.39 (d, 1H, J = 8.4 Hz), 7.79–7.77 (m, 2H), 7.63–7.55 (m, 6H), 7.47 (s, 1H), 6.98–6.94 (m, 4H), 6.83 (d, 2H, J = 8.8 Hz), 6.68 (d, 2H, J = 8.8 Hz), 3.81 (s, 3H), 3.75 (s, 3H); ^{13}C{^{1}H} NMR ($CDCl_3$, 100 MHz): δ 161.2, 158.9, 158.6, 155.8, 145.2, 136.8, 136.7, 133.7, 132.25, 132.16, 130.8, 130.5, 129.6, 129.2, 129.0, 128.6, 127.5, 127.3, 125.5, 124.7, 116.8, 113.9, 113.1, 100.8, 96.1, 55.4, 55.3; IR (KBr, cm^{-1}): 2955, 2925, 2854, 2221, 1654, 1560, 1546, 1507, 1463, 1377, 1264, 1180, 1117, 1077, 1026, 883, 812, 742, 705; HRMS (ESI/Q-TOF) (m/z) calcd for $C_{34}H_{25}N_2O_3$ $[M + H]^+$ 509.1860; found 509.1860.

***6,7-Bis(4-fluorophenyl)-4-oxo-2-phenyl-4H-pyrido[2,1-a]isoquinoline-3-carbonitrile (1d)*:**

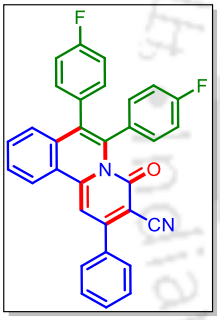

As a yellow solid (40 mg, 41% yield, mp 235–237 °C); Purification over a column of silica gel (10% EtOAc in hexane); ^{1}H NMR ($CDCl_3$, 400 MHz): δ 8.42 (d, 1H, J = 7.6 Hz), 7.79–7.77 (m, 2H), 7.69–7.56 (m, 6H), 7.50 (s, 1H), 7.06 (d, 6H, J = 6.8 Hz), 6.85 (t, 2H, J = 8.8 Hz); ^{13}C{^{1}H} NMR ($CDCl_3$, 100 MHz): δ 160.9, 160.6, 156.2, 144.9, 136.6, 135.9, 132.7 (d, J = 8.1 Hz), 132.5, 130.7, 130.3, 130.2 (d, J = 8.2 Hz), 130.1, 129.5, 129.3, 128.5, 127.3, 125.8, 124.8, 116.5, 115.7 (d, J = 21.5 Hz), 114.8 (d, J = 21.8 Hz), 101.1, 96.7; ^{19}F NMR ($CDCl_3$ + hexafluorobenzene): δ –116.5 (s), –116.9 (s); IR (KBr, cm^{-1}): 2956, 2924, 2855, 2213, 1661, 1609, 1562, 1495, 1461, 1376, 1263, 1226, 1092, 1016, 876, 807, 722; HRMS (ESI/Q-TOF) (m/z) calcd for $C_{32}H_{19}F_2N_2O$ $[M + H]^+$ 485.1460; found 485.1460.

***6,7-Bis(3-chlorophenyl)-4-oxo-2-phenyl-4H-pyrido[2,1-a]isoquinoline-3-carbonitrile (1e)*:**

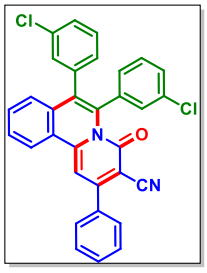

As a yellow solid (43 mg, 42% yield, mp 210–212 °C); Purification over a column of silica gel (10% EtOAc in hexane); ^{1}H NMR ($CDCl_3$, 400 MHz): δ 8.36 (d, 1H, J = 7.6 Hz), 7.73–7.71 (m, 2H), 7.62–7.58 (m, 2H), 7.52–7.49 (m, 3H), 7.44 (s, 1H), 7.23–7.19 (m, 3H), 7.04–6.98 (m, 4H), 6.89 (d, 2H, J = 6.4 Hz); ^{13}C{^{1}H} NMR ($CDCl_3$, 100 MHz): δ 160.7, 156.4, 144.8, 137.9, 136.6, 136.4, 135.2, 132.7, 132.4, 131.6, 130.8, 130.0, 129.8, 129.3, 128.5, 128.4,

127.7, 127.4, 126.7, 125.8, 124.9, 116.5, 101.3, 96.8; IR (KBr, cm^{-1}): 2955, 2924, 2853, 2208, 1649, 1544, 1505, 1463, 1377, 1289, 1265, 1121, 1071, 1020, 879, 802, 743, 722; HRMS (ESI/Q-TOF) (m/z) calcd for $C_{32}H_{19}Cl_2N_2O$ $[M + H]^+$ 517.0869; found 517.0869.

***4-Oxo-2-phenyl-6,7-dipropyl-4H-pyrido[2,1-a]isoquinoline-3-carbonitrile (1g)*:**

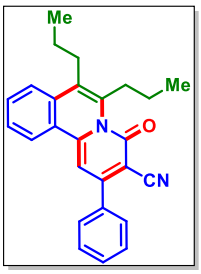

As a yellow solid (39 mg, 51% yield, mp 158–160 °C); Purification over a column of silica gel (10% EtOAc in hexane); ^1H NMR ($CDCl_3$, 400 MHz): δ 8.29 (d, 1H, J = 8.0 Hz), 7.84 (d, 1H, J = 8.4 Hz), 7.76–7.71 (m, 3H), 7.59–7.52 (m, 4H), 7.34 (s, 1H), 3.25 (t, 2H, J = 7.8 Hz), 2.93 (t, 2H, J = 8.2 Hz), 1.78–1.72 (m, 2H), 1.68–1.62 (m, 2H), 1.13 (t, 3H, J = 7.4 Hz), 0.98 (t, 3H, J = 7.2 Hz); $^{13}C\{^1H\}$ NMR ($CDCl_3$, 100 MHz): δ 162.3, 155.0, 145.1, 138.4, 136.6, 132.4, 130.4, 129.1, 128.5, 128.3, 127.4, 125.5, 125.2, 124.4, 117.3, 100.9, 95.4, 32.3, 30.3, 23.4, 23.0, 14.7, 14.5; IR (KBr, cm^{-1}): 2956, 2924, 2854, 2208, 1656, 1608, 1566, 1508, 1463, 1377, 1265, 1235, 1154, 1127, 1071, 1033, 881, 838, 778, 754, 723, 697; HRMS (ESI/Q-TOF) (m/z) calcd for $C_{26}H_{25}N_2O$ $[M + H]^+$ 381.1961; found 381.1961.

***2-(4-Chlorophenyl)-9-methyl-4-oxo-6,7-di-p-tolyl-4H-pyrido[2,1-a]isoquinoline-3-carbonitrile (18b)*:**

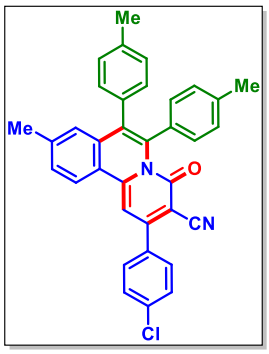

As a yellow solid (78 mg, 75% yield, mp 280–282 °C); Purification over a column of silica gel (10% EtOAc in hexane); ^1H NMR ($CDCl_3$, 400 MHz): δ 8.28 (d, 1H, J = 8.4 Hz), 7.71 (d, 2H, J = 8.4 Hz), 7.52 (d, 2H, J = 8.4 Hz), 7.45 (d, 1H, J = 8.4 Hz), 7.36 (s, 1H), 7.10–7.08 (m, 3H), 6.91–6.89 (m, 6H), 2.39 (s, 3H), 2.36 (s, 3H), 2.25 (s, 3H); $^{13}C\{^1H\}$ NMR ($CDCl_3$, 100 MHz): δ 161.0, 154.4, 145.6, 143.5, 137.3, 136.9, 136.8, 136.7, 135.3, 133.7, 133.6, 132.1, 131.0, 130.9, 130.7, 129.9, 129.4, 129.0, 128.2, 127.2, 124.7, 123.2, 116.8, 99.9, 94.9, 22.1, 21.54, 21.50; IR (KBr, cm^{-1}): 2955, 2924, 2854, 2214, 1660, 1563, 1493, 1463, 1376, 1262, 1223, 1179, 1090, 1018, 808, 727; HRMS (ESI/Q-TOF) (m/z) calcd for $C_{35}H_{26}ClN_2O$ $[M + H]^+$ 525.1728; found 525.1728.

***2-(4-Chlorophenyl)-6,7-bis(4-methoxyphenyl)-9-methyl-4-oxo-4H-pyrido[2,1-a]isoquinoline-3-carbonitrile (18c)*:**

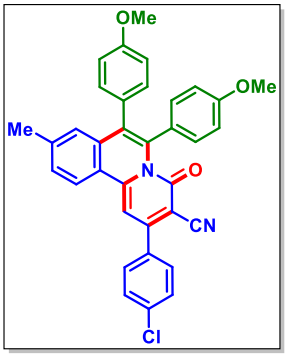

As a yellow solid (86 mg, 78% yield, mp 240–242 °C); Purification over a column of silica gel (15% EtOAc in hexane); ^{1}H NMR ($CDCl_3$, 400 MHz): δ 8.28 (d, 1H, J = 8.4 Hz), 7.71 (d, 2H, J = 8.8 Hz), 7.52 (d, 2H, J = 8.4 Hz), 7.45 (d, 1H, J = 8.4 Hz), 7.36 (s, 1H), 7.11 (s, 1H), 6.95–6.92 (m, 4H), 6.83 (d, 2H, J = 8.8 Hz), 6.67 (d, 2H, J = 8.8 Hz), 3.82 (s, 3H), 3.74 (s, 3H), 2.40 (s, 3H); ^{13}C{^{1}H} NMR ($CDCl_3$, 100 MHz): δ 161.0, 158.9, 158.6, 154.3, 145.6, 143.5, 136.8, 136.7, 135.3, 133.9, 132.2, 130.9, 130.7, 129.9, 129.6, 129.4, 129.0, 127.3, 127.2, 124.7, 123.2, 116.8, 113.9, 113.1, 99.9, 94.9, 55.4, 55.3, 22.1; IR (KBr, cm^{-1}): 2956, 2924, 2854, 2214, 1667, 1562, 1509, 1494, 1466, 1378, 1288, 1248, 1176, 1092, 1031, 805; HRMS (ESI/Q-TOF) (m/z) calcd for $C_{35}H_{26}ClN_2O_3$ [M + H]$^{+}$ 557.1626; found 557.1626.

***2-(4-Chlorophenyl)-6,7-bis(4-fluorophenyl)-9-methyl-4-oxo-4H-pyrido[2,1-a]isoquinoline-3-carbonitrile (18d)*:**

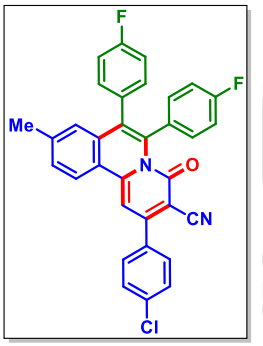

As a yellow solid (65 mg, 61% yield, mp 280–282 °C); Purification over a column of silica gel (10% EtOAc in hexane); ^{1}H NMR ($CDCl_3$, 400 MHz): δ 8.31 (d, 1H, J = 8.4 Hz), 7.71 (d, 2H, J = 8.4 Hz), 7.54–7.49 (m, 3H), 7.40 (s, 1H), 7.03–6.97 (m, 7H), 6.85–6.81 (m, 2H), 2.42 (s, 3H); ^{13}C{^{1}H} NMR ($CDCl_3$, 100 MHz): δ 163.5, 163.0, 161.1, 160.8, 160.5, 154.7, 145.4, 143.9, 136.9, 136.1, 135.0, 133.1, 132.7 (d, J = 8.0 Hz), 131.2, 130.1 (d, J = 8.1 Hz), 129.9, 129.5, 127.1, 124.9, 123.4, 116.6, 115.7 (d, J = 21.5 Hz), 114.7 (d, J = 21.8 Hz), 100.3, 95.5; ^{19}F NMR ($CDCl_3$ + hexafluorobenzene): δ –116.5 (s), –116.9 (s); IR (KBr, cm^{-1}): 2957, 2924, 2854, 2215, 1667, 1601, 1563, 1506, 1469, 1401, 1381, 1261, 1227, 1158, 1092, 1017, 843, 805, 762, 724; HRMS (ESI/Q-TOF) (m/z) calcd for $C_{33}H_{20}ClF_2N_2O$ [M + H]$^{+}$ 533.1227; found 533.1227.

***6,7-Bis(3-chlorophenyl)-2-(4-chlorophenyl)-9-methyl-4-oxo-4H-pyrido[2,1-a]isoquinoline-3-carbonitrile (18e)*:**

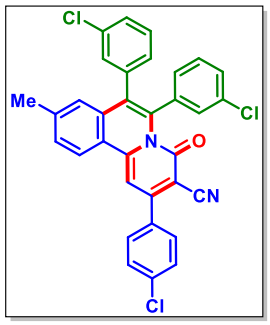

As a yellow solid (62 mg, 55% yield, mp 315–317 °C); Purification over a column of silica gel (10% EtOAc in hexane); ^{1}H NMR ($CDCl_3$, 400 MHz): δ 8.31 (d, 1H, J = 8.8 Hz), 7.72 (d, 2H, J = 8.4 Hz), 7.55–7.50 (m, 3H), 7.40 (s, 1H), 7.31–7.29 (m, 2H), 7.10–7.03 (m, 5H), 6.96–6.94 (m, 2H), 2.43 (s, 3H); ^{13}C{^{1}H} NMR ($CDCl_3$, 100 MHz): δ 160.6, 154.9, 145.2, 144.1, 137.9, 137.0, 136.6, 134.9, 132.6, 131.4, 130.3, 130.2, 129.9, 129.5, 129.3, 129.1, 129.0, 127.7, 127.1, 124.9, 124.8, 123.4, 116.5, 100.4, 95.7, 22.2; IR (KBr, cm^{-1}): 2955, 2924, 2855, 2213, 1668, 1614, 1596, 1566, 1505, 1470, 1403, 1314, 1261, 1227, 1185, 1091, 1019, 805, 712; HRMS (ESI/Q-TOF) (m/z) calcd for $C_{33}H_{20}Cl_3N_2O$ $[M + H]^+$ 565.0636; found 565.0636.

***6,7-Bis(4-bromophenyl)-2-(4-chlorophenyl)-9-methyl-4-oxo-4H-pyrido[2,1-a]isoquinoline-3-carbonitrile (18f)*:**

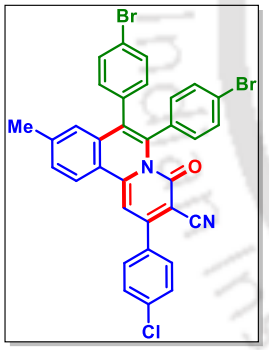

As a yellow solid (75 mg, 58% yield, mp 282–284 °C); Purification over a column of silica gel (10% EtOAc in hexane); ^{1}H NMR ($CDCl_3$, 400 MHz): δ 8.30 (d, 1H, J = 8.8 Hz), 7.71 (d, 2H, J = 8.4 Hz), 7.53 (d, 2H, J = 8.8 Hz), 7.46 (d, 2H, J = 8.0 Hz), 7.39 (s, 1H), 7.31–7.27 (m, 3H), 7.00 (s, 1H), 6.90 (d, 4H, J = 7.6 Hz), 2.42 (s, 3H); ^{13}C{^{1}H} NMR ($CDCl_3$, 100 MHz): δ 160.7, 154.9, 145.3, 144.0, 137.0, 135.6, 135.3, 134.9, 133.8, 132.8, 132.6, 131.9, 131.3, 130.9, 129.91, 129.88, 129.5, 127.0, 124.9, 123.4, 122.4, 121.7, 116.4, 100.4, 95.6, 22.1; IR (KBr, cm^{-1}): 2954, 2924, 2853, 2214, 1658, 1596, 1562, 1507, 1489, 1464, 1377, 1263, 1224, 1115, 1095, 1069, 1013, 877, 808, 741, 719; HRMS (ESI/Q-TOF) (m/z) calcd for $C_{33}H_{20}Br_2ClN_2O$ $[M + H]^+$ 652.9625; found 652.9623.

***2-(4-Chlorophenyl)-9-methyl-4-oxo-6,7-dipropyl-4H-pyrido[2,1-a]isoquinoline-3-carbonitrile (18g)*:**

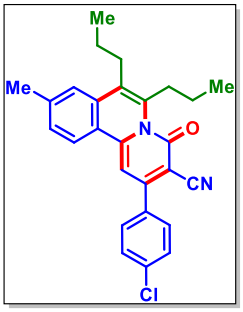

As a yellow solid (60 mg, 71% yield, mp 185–187 °C); Purification over a column of silica gel (10% EtOAc in hexane); ^{1}H NMR ($CDCl_3$, 400 MHz): δ 8.17 (d, 1H, J = 8.4 Hz), 7.68 (d, 2H, J = 8.4 Hz), 7.61 (s, 1H), 7.50 (d, 2H, J = 8.4 Hz), 7.41 (d, 1H, J = 8.4 Hz), 7.24 (s, 1H), 3.24 (t, 2H, J = 7.6 Hz), 2.91 (t, 2H, J = 8.2 Hz), 2.57 (s, 3H), 1.78–1.59 (m, 4H), 1.13 (t, 3H, J = 7.2 Hz), 0.97 (t, 3H, J = 7.4 Hz); ^{13}C{^{1}H} NMR ($CDCl_3$, 100 MHz): δ 162.2, 153.5, 145.4, 143.4, 138.6, 136.6, 135.1, 132.5, 129.9, 129.8, 129.4, 127.6, 125.2, 124.3, 123.2, 117.3, 100.2, 94.3, 32.3, 30.2, 23.4, 23.0, 22.4, 14.7, 14.5; IR (KBr, cm^{-1}): 2956, 2924, 2855, 2208, 1662, 1605, 1562, 1470, 1380, 1308, 1263, 1228, 1162, 1094, 1060, 814, 720; HRMS (ESI/Q-TOF) (m/z) calcd for $C_{27}H_{26}ClN_2O$ $[M + H]^+$ 429.1728; found 429.1728.

***2-(4-Chlorophenyl)-7,9-dimethyl-4-oxo-6-phenyl-4H-pyrido[2,1-a]isoquinoline-3-carbonitrile (18h)*:**

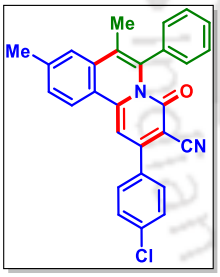

As a yellow solid (56 mg, 45% yield, mp 245–247 °C); Purification over a column of silica gel (10% EtOAc in hexane); ^{1}H NMR ($CDCl_3$, 400 MHz): δ 8.26 (d, 1H, J = 8.8 Hz), 7.71–7.68 (m, 2H), 7.66 (s, 1H), 7.51–7.49 (m, 3H), 7.45–7.36 (m, 3H), 7.30–7.27 (m, 3H), 2.59 (s, 3H), 2.26 (s, 3H); ^{13}C{^{1}H} NMR ($CDCl_3$, 100 MHz): δ 160.7, 154.2, 145.1, 143.8, 137.2, 136.6, 135.9, 135.2, 133.3, 130.7, 129.9, 129.4, 128.4, 128.1, 127.9, 125.0, 123.8, 123.3, 116.8, 99.9, 95.0, 22.2, 15.7; IR (KBr, cm^{-1}): 2956, 2924, 2854, 2213, 1664, 1561, 1463, 1378, 1261, 1168, 1093, 1014, 807, 700; HRMS (ESI/Q-TOF) (m/z) calcd for $C_{28}H_{20}ClN_2O$ $[M + H]^+$ 435.1259; found 435.1250.

***2-(4-Chlorophenyl)-6,9-dimethyl-4-oxo-7-phenyl-4H-pyrido[2,1-a]isoquinoline-3-carbonitrile (18h')*:**

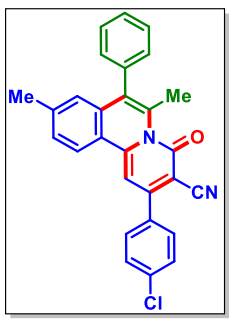

As a yellow solid (16 mg, 18% yield, mp 225–227 °C); Purification over a column of silica gel (10% EtOAc in hexane); ^{1}H NMR ($CDCl_3$, 400 MHz): δ 8.21 (d, 1H, J = 8.8 Hz), 7.71 (d, 2H, J = 8.4 Hz), 7.57–7.51 (m, 5H), 7.41 (d, 1H, J = 8.4 Hz), 7.32–7.28 (m, 3H), 6.95 (s, 1H), 2.55 (s, 3H), 2.39 (s, 3H); ^{13}C{^{1}H} NMR ($CDCl_3$, 100 MHz): δ 162.3, 154.2, 145.6, 143.4, 136.8, 136.7,

135.4, 135.2, 130.6, 130.2, 129.9, 129.5, 129.3, 128.6, 126.6, 124.7, 122.9, 117.0, 100.3, 95.0, 22.9, 14.3; IR (KBr, cm^{-1}): 2956, 2924, 2854, 2218, 1656, 1560, 1461, 1378, 1261, 1093, 1023, 874, 804, 704; HRMS (ESI/Q-TOF) (m/z) calcd for $C_{28}H_{20}ClN_2O$ $[M + H]^+$ 435.1259; found 435.1256.

***2-(4-Chlorophenyl)-7-ethyl-9-methyl-4-oxo-6-phenyl-4H-pyrido[2,1-a]isoquinoline-3-carbonitrile (18i)*:**

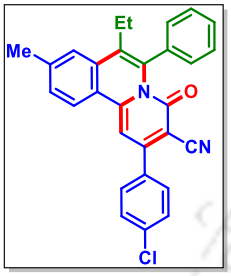

As a yellow solid (40 mg, 46% yield, mp 248–250 °C); Purification over a column of silica gel (10% EtOAc in hexane); ^1H NMR ($CDCl_3$, 400 MHz): δ 8.28 (d, 1H, J = 8.4 Hz), 7.73 (s, 1H), 7.67 (d, 2H, J = 8.4 Hz), 7.49 (d, 3H, J = 8.4 Hz), 7.43–7.38 (m, 3H), 7.32–7.30 (m, 3H), 2.69 (q, 2H, J = 7.6 Hz), 2.59 (s, 3H), 1.12 (t, 3H, J = 7.4 Hz); $^{13}C\{^1H\}$ NMR ($CDCl_3$, 100 MHz): δ 160.7, 154.2, 145.1, 143.7, 136.9, 136.6, 135.9, 135.2, 132.1, 130.7, 129.8, 129.6, 129.4, 128.2, 128.1, 127.9, 125.4, 124.9, 123.8, 116.9, 99.9, 94.9, 22.4, 21.7, 14.8; IR (KBr, cm^{-1}): 2961, 2924, 2854, 2211, 1665, 1614, 1561, 1493, 1474, 1398, 1310, 1264, 1221, 1178, 1090, 1014, 815, 761, 724, 698; HRMS (ESI/Q-TOF) (m/z) calcd for $C_{29}H_{22}ClN_2O$ $[M + H]^+$ 450.1493; found 450.1499.

***2-(4-Chlorophenyl)-6-ethyl-9-methyl-4-oxo-7-phenyl-4H-pyrido[2,1-a]isoquinoline-3-carbonitrile (18i')*:**

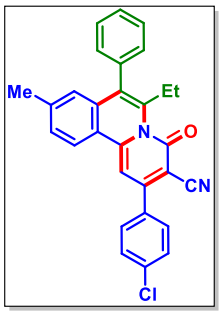

As a yellow solid (18 mg, 20% yield, mp 235–237 °C); Purification over a column of silica gel (10% EtOAc in hexane); ^1H NMR ($CDCl_3$, 400 MHz): δ 8.21 (d, 1H, J = 8.4 Hz), 7.73 (d, 2H, J = 8.4 Hz), 7.54 (d, 4H, J = 8.0 Hz), 7.40 (d, 1H, J = 8.4 Hz), 7.35 (s, 1H), 7.29–7.28 (m, 3H), 6.85 (s, 1H), 3.20 (q, 2H, J = 7.4 Hz), 2.37 (s, 3H), 1.02 (t, 3H, J = 7.2 Hz); $^{13}C\{^1H\}$ NMR ($CDCl_3$, 100 MHz): δ 162.2, 154.0, 143.8, 143.4, 140.9, 136.8, 136.5, 135.1, 133.7, 130.5, 130.3, 130.1, 129.9, 129.5, 129.2, 128.5, 126.9, 124.6, 122.9, 117.1, 100.6, 94.9, 25.4, 22.1, 13.9; IR (KBr, cm^{-1}): 2953, 2924, 2854, 2214, 1661, 1559, 1491, 1482, 1262, 1098, 1013, 807, 703; HRMS (ESI/Q-TOF) (m/z) calcd for $C_{29}H_{22}ClN_2O$ $[M + H]^+$ 450.1493; found 450.1498

II.10. Representative NMR Spectra:

4-Oxo-2,6,7-triphenyl-4H-pyrido[2,1-a]isoquinoline-3-carbonitrile (1a): ^{1}H NMR ($CDCl_3$, 600 MHz)

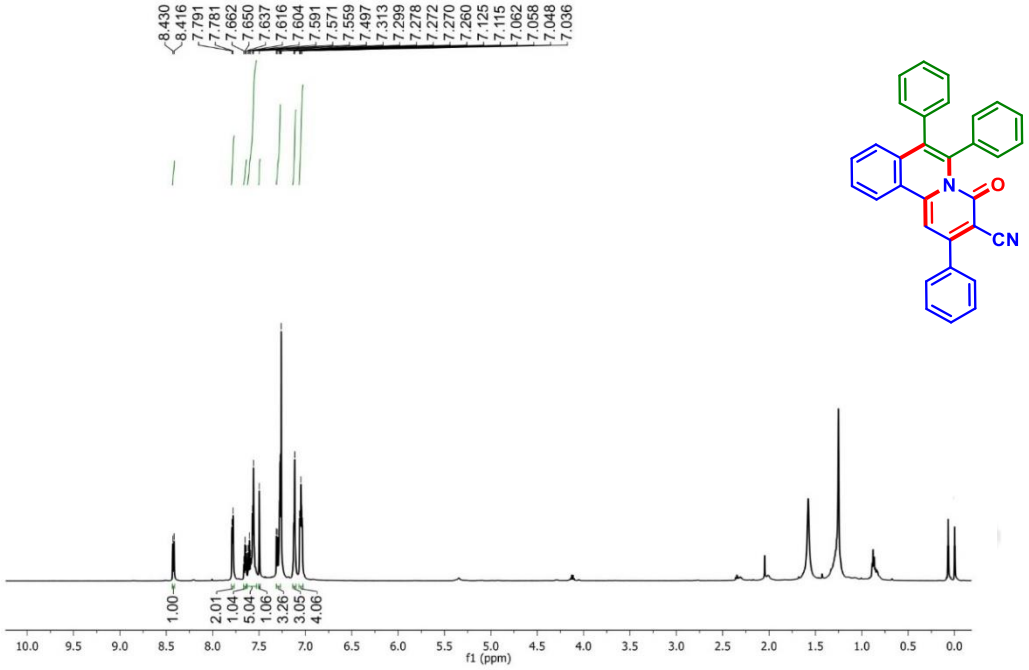

4-Oxo-2,6,7-triphenyl-4H-pyrido[2,1-a]isoquinoline-3-carbonitrile (1a): $^{13}C\{^{1}H\}$ NMR ($CDCl_3$, 150 MHz)

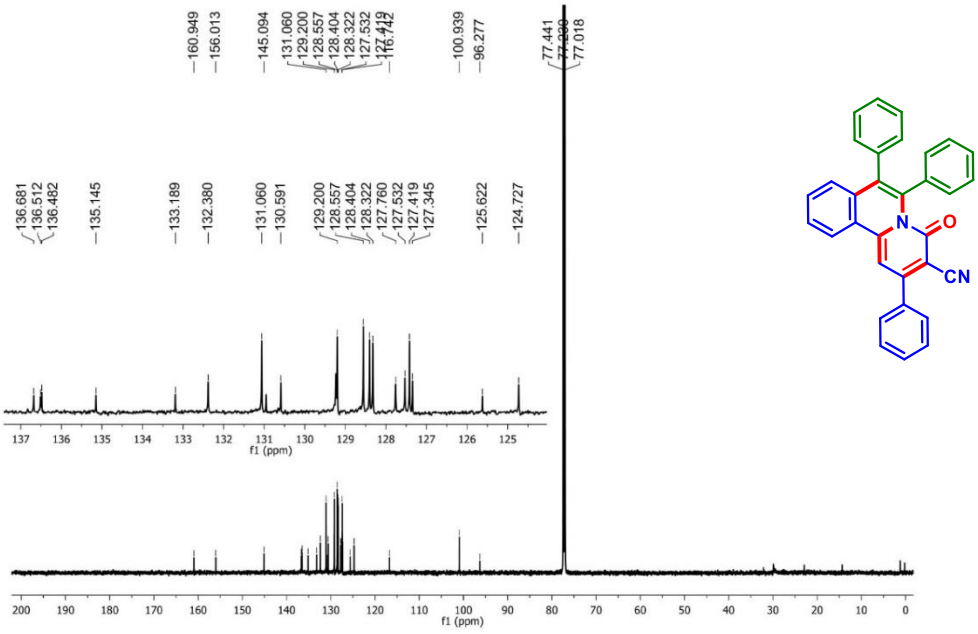

2-(4-Methoxyphenyl)-4-oxo-6,7-diphenyl-4H-pyrido[2,1-a]isoquinoline-3-carbonitrile (3a):

^{1}H NMR ($CDCl_3$, 400 MHz)

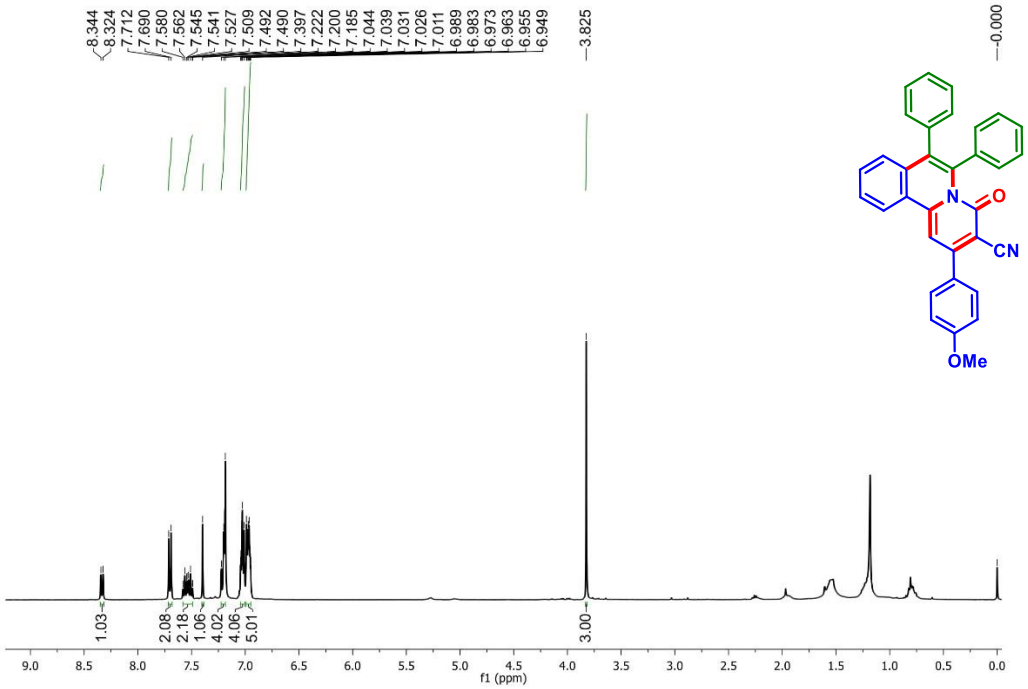

2-(4-Methoxyphenyl)-4-oxo-6,7-diphenyl-4H-pyrido[2,1-a]isoquinoline-3-carbonitrile (3a):

^{13}C{^{1}H} NMR ($CDCl_3$, 100 MHz)

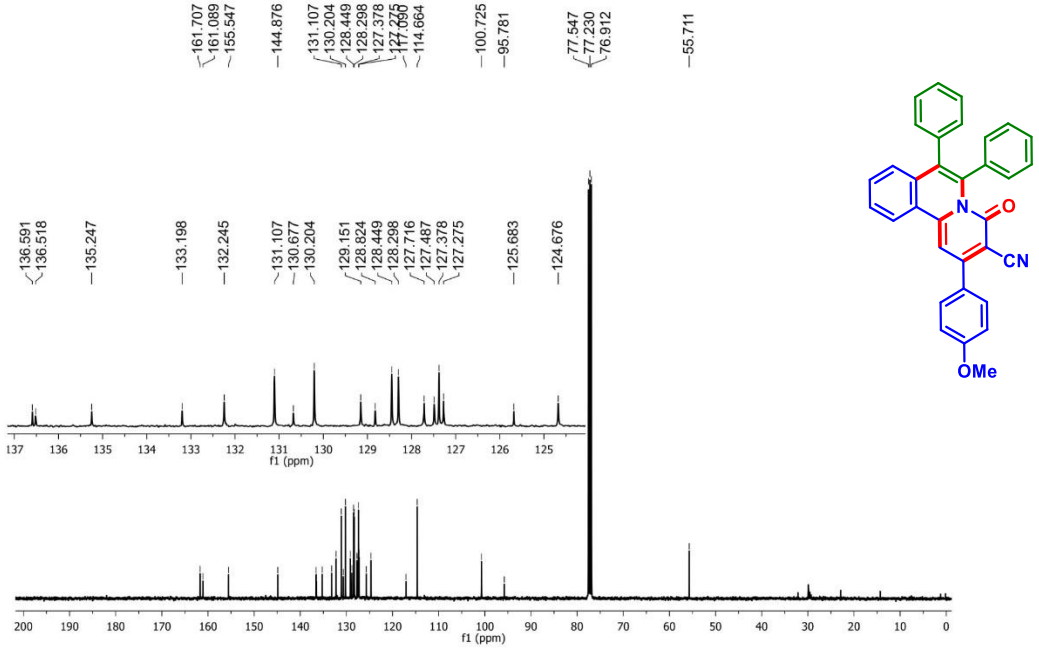

2-(4-Chlorophenyl)-4-oxo-6,7-diphenyl-4H-pyrido[2,1-a]isoquinoline-3-carbonitrile (6a):

^{1}H NMR ($CDCl_3$, 400 MHz)

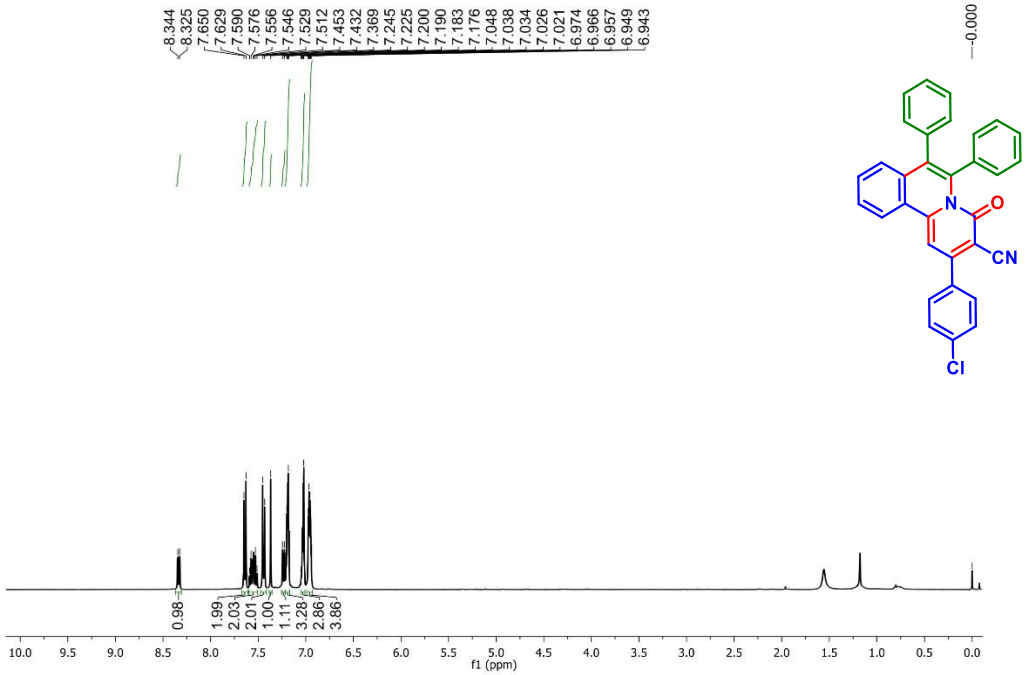

2-(4-Chlorophenyl)-4-oxo-6,7-diphenyl-4H-pyrido[2,1-a]isoquinoline-3-carbonitrile (6a):

^{13}C{^{1}H} NMR ($CDCl_3$, 100 MHz)

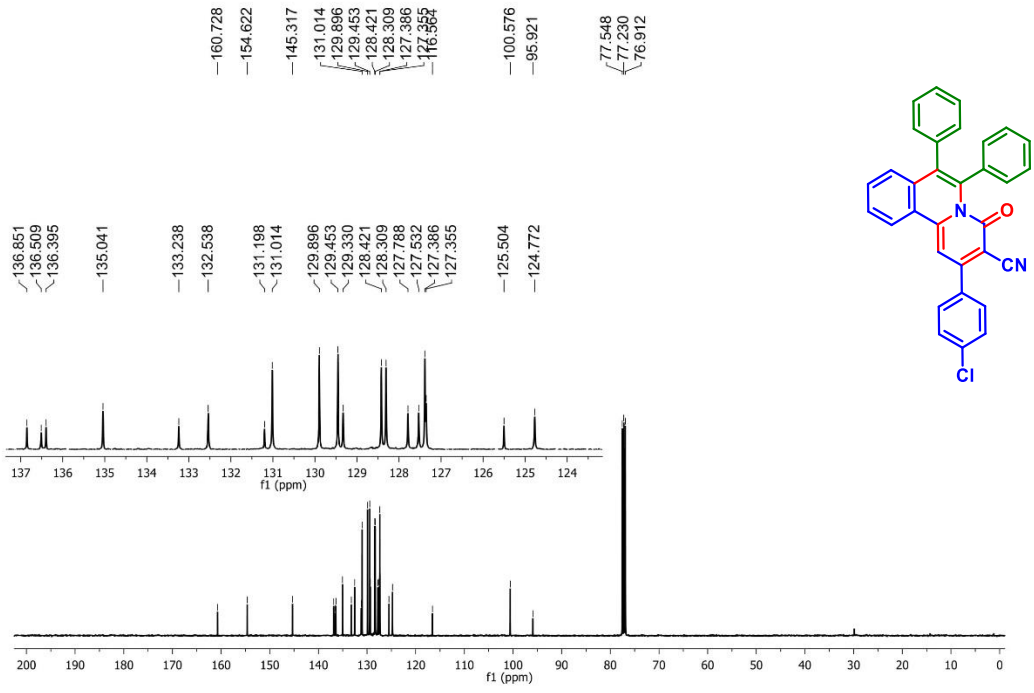

9-Methoxy-4-oxo-2,6,7-triphenyl-4H-pyrido[2,1-a]isoquinoline-3-carbonitrile (10a): ^{1}H NMR ($CDCl_3$, 400 MHz)

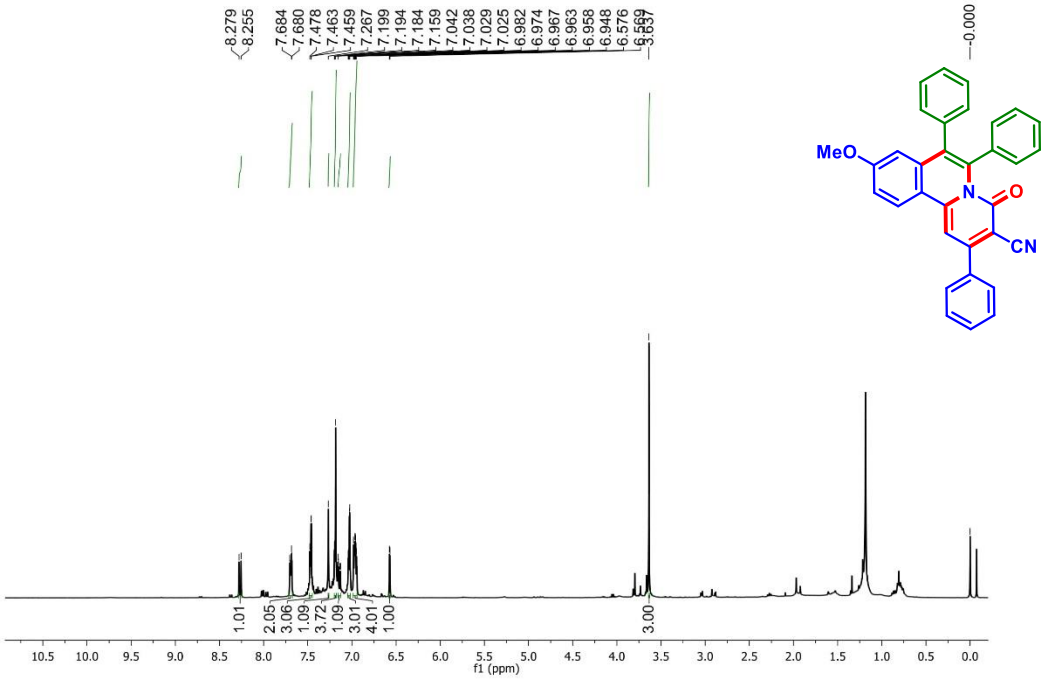

9-Methoxy-4-oxo-2,6,7-triphenyl-4H-pyrido[2,1-a]isoquinoline-3-carbonitrile (10a): $^{13}C\{^{1}H\}$ NMR ($CDCl_3$, 100 MHz)

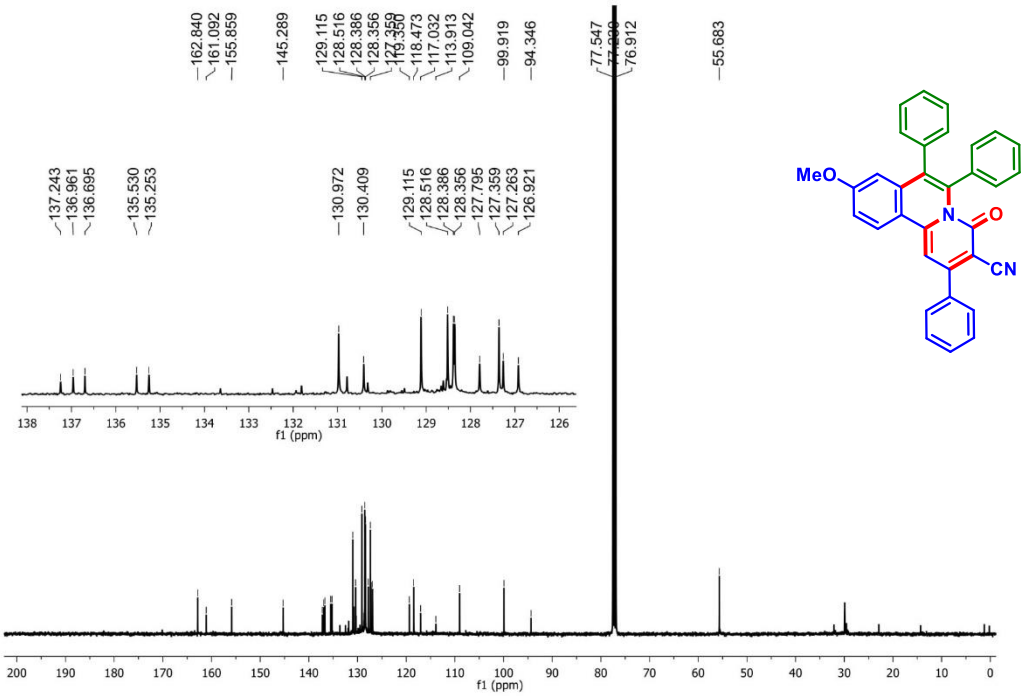

9-Chloro-4-oxo-2,6,7-triphenyl-4H-pyrido[2,1-a]isoquinoline-3-carbonitrile (13a): ^{1}H NMR ($CDCl_3$, 600 MHz)

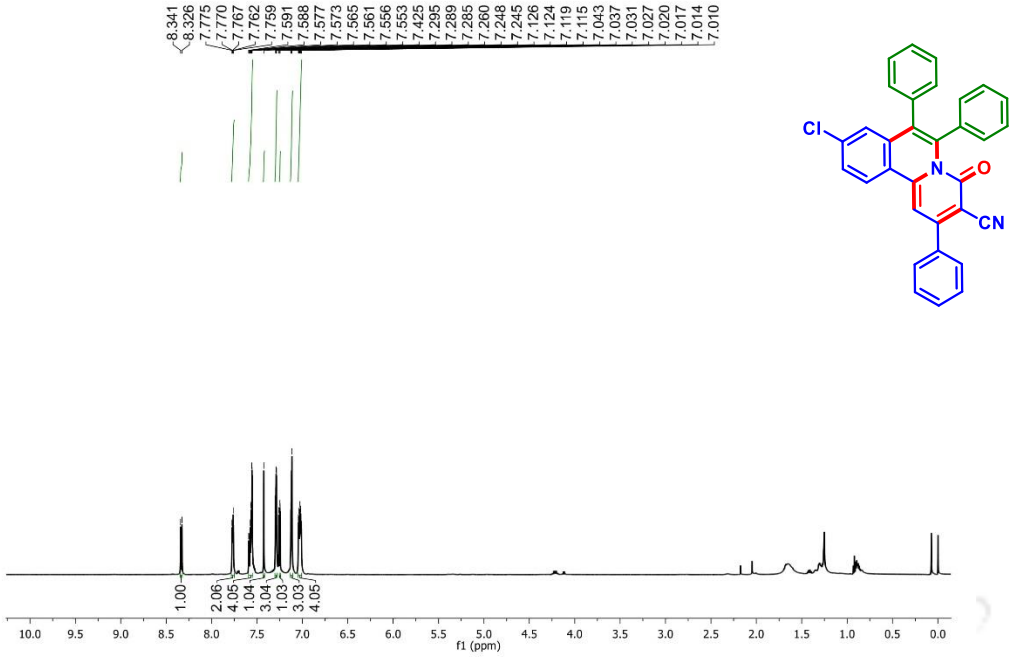

9-Chloro-4-oxo-2,6,7-triphenyl-4H-pyrido[2,1-a]isoquinoline-3-carbonitrile (13a): $^{13}C\{^{1}H\}$ NMR ($CDCl_3$, 100 MHz)

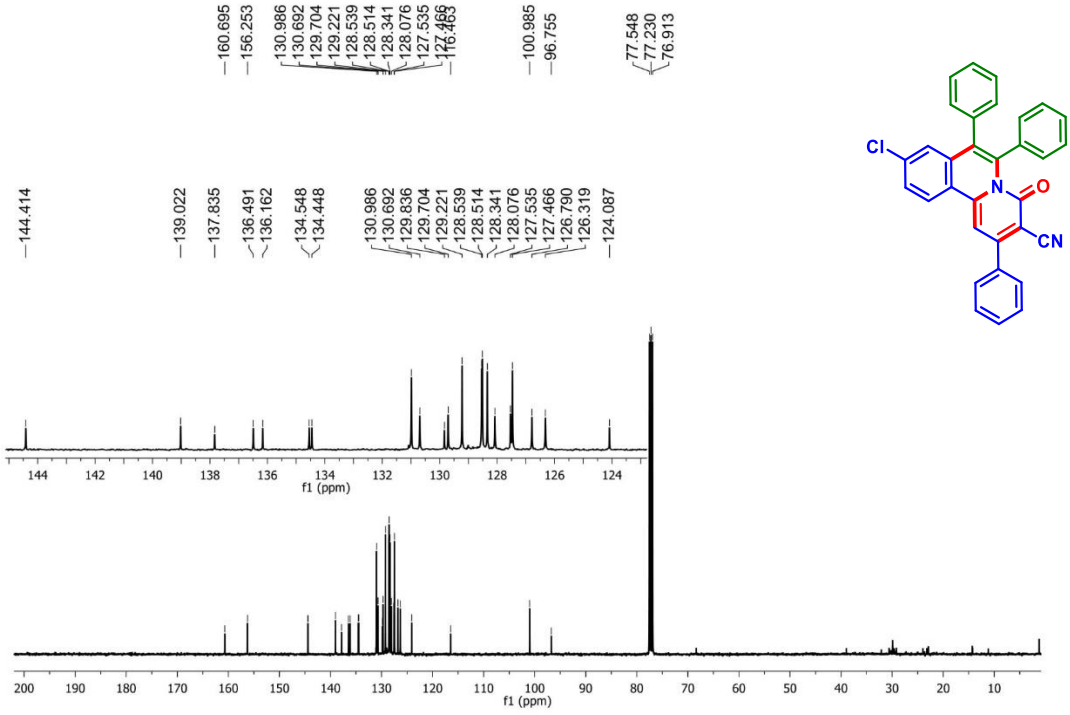

7-Oxo-4,5,9-triphenyl-7H-thieno[2,3-a]quinolizine-8-carbonitrile (25a): ^{1}H NMR ($CDCl_3$, 400 MHz)

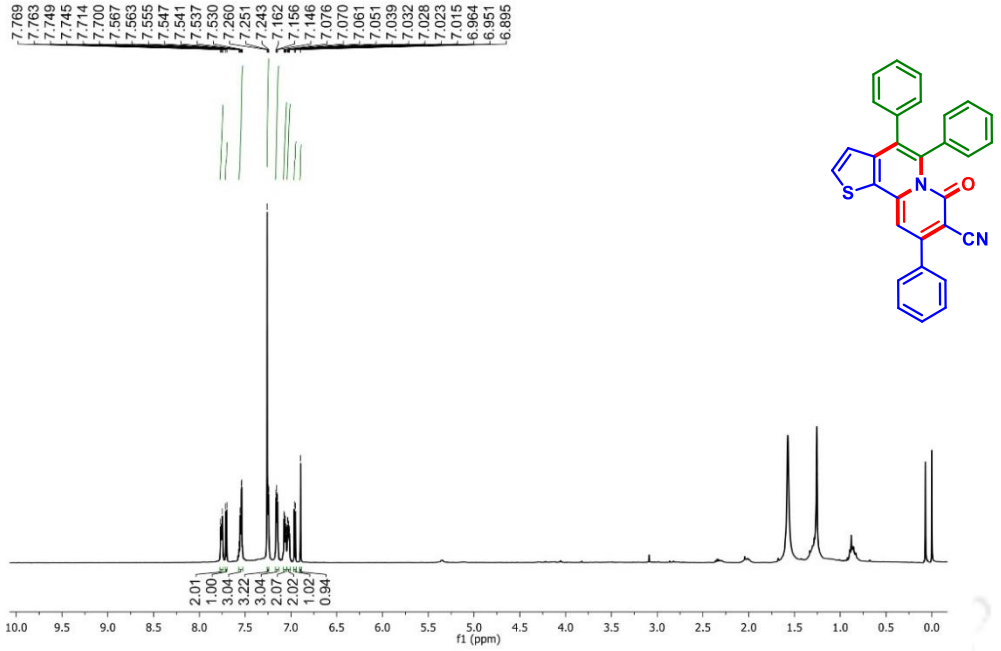

7-Oxo-4,5,9-triphenyl-7H-thieno[2,3-a]quinolizine-8-carbonitrile (25a): $^{13}C\{^{1}H\}$ NMR ($CDCl_3$, 100 MHz)

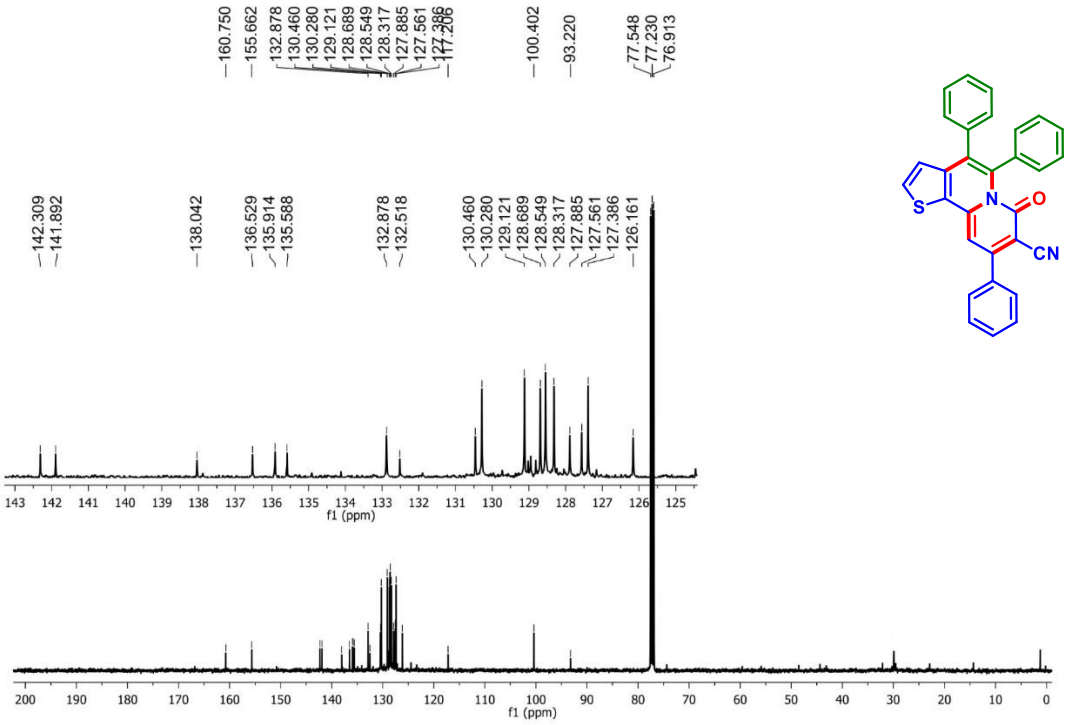

4-Oxo-2-phenyl-6,7-di-p-tolyl-4H-pyrido[2,1-a]isoquinoline-3-carbonitrile (1b): ^{1}H NMR ($CDCl_3$, 400 MHz)

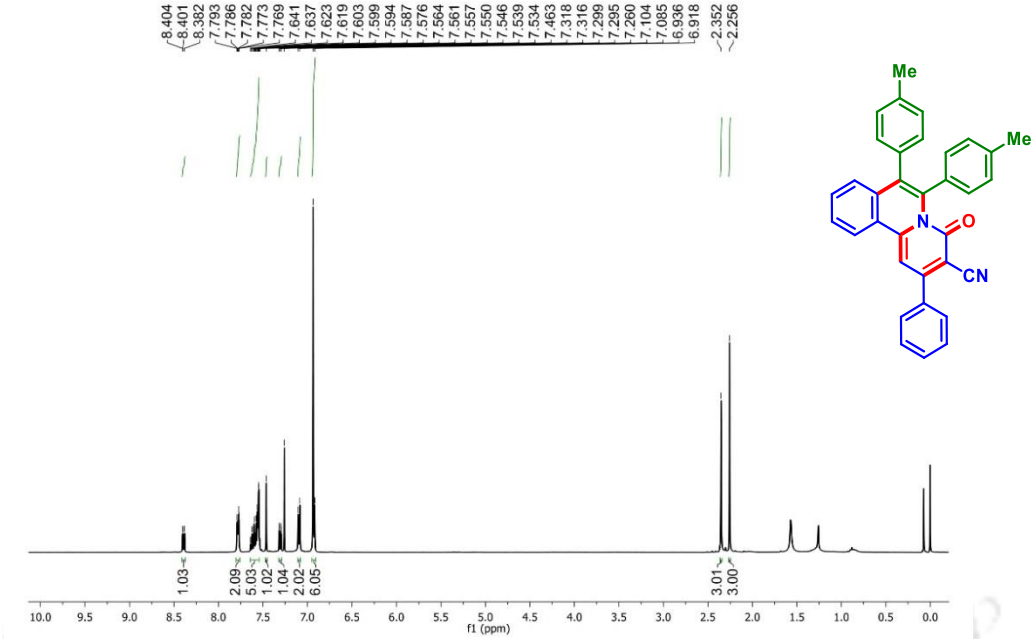

4-Oxo-2-phenyl-6,7-di-p-tolyl-4H-pyrido[2,1-a]isoquinoline-3-carbonitrile (1b): $^{13}C\{^{1}H\}$ NMR ($CDCl_3$, 100 MHz)

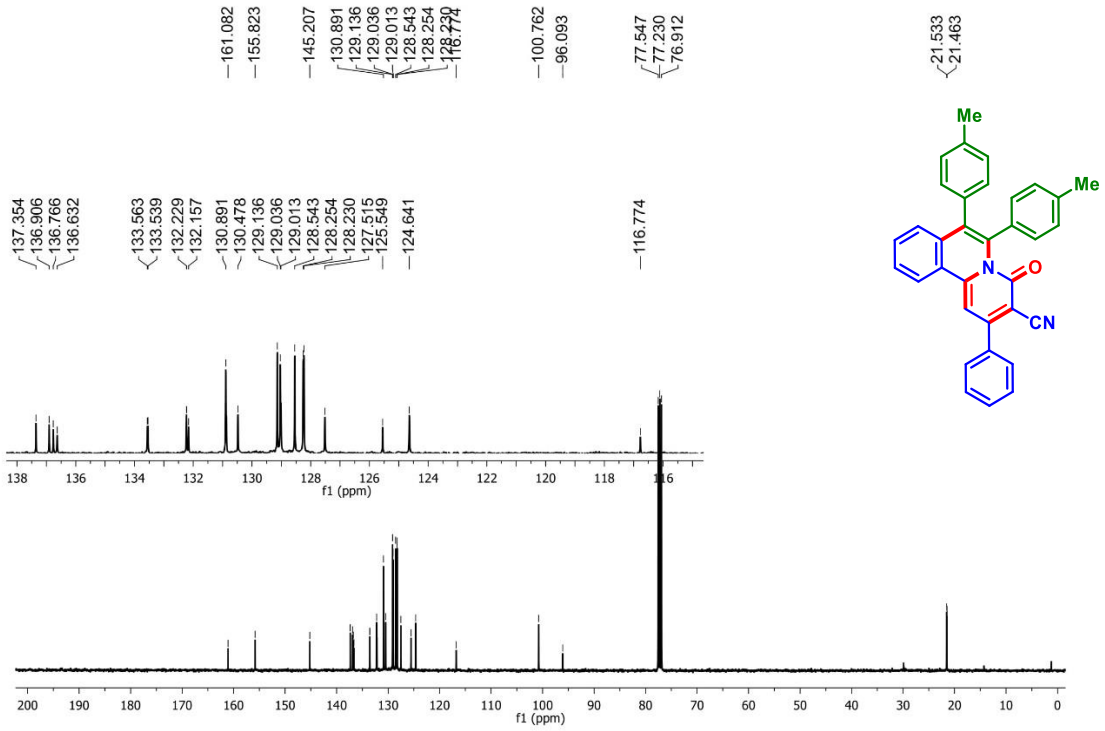

6,7-bis(3-Chlorophenyl)-4-oxo-2-phenyl-4H-pyrido[2,1-a]isoquinoline-3-carbonitrile (1e):

^{1}H NMR ($CDCl_3$, 400 MHz)

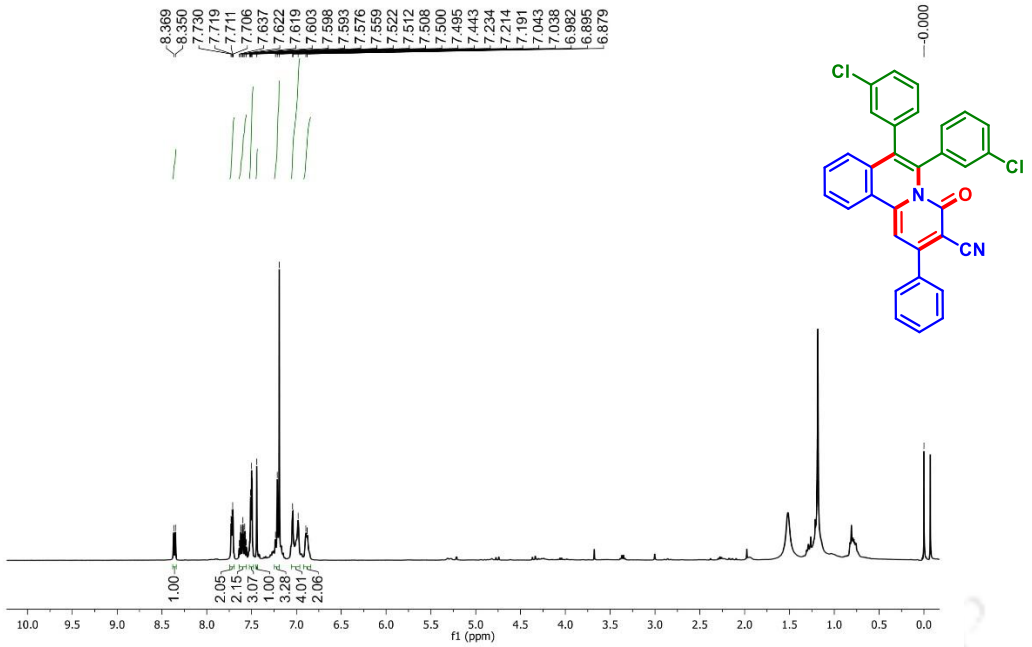

6,7-bis(3-Chlorophenyl)-4-oxo-2-phenyl-4H-pyrido[2,1-a]isoquinoline-3-carbonitrile (1e):

$^{13}C\{^{1}H\}$ NMR ($CDCl_3$, 100 MHz)

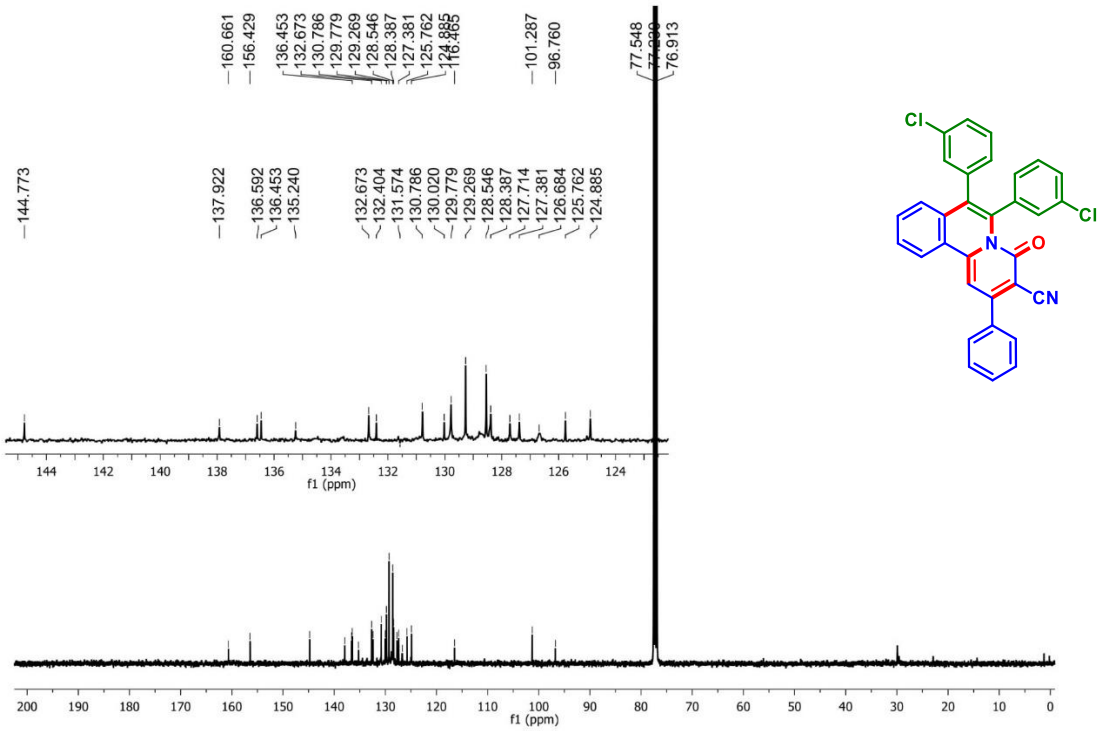

4-Oxo-2-phenyl-6,7-dipropyl-4H-pyrido[2,1-a]isoquinoline-3-carbonitrile (1g): ^{1}H NMR ($CDCl_3$, 400 MHz)

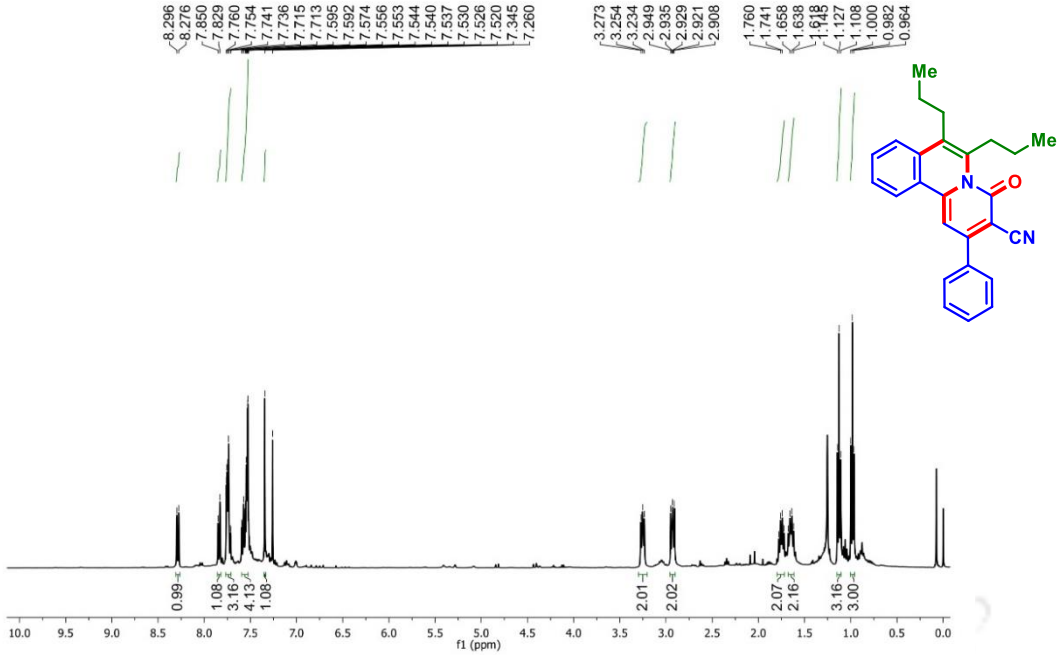

4-Oxo-2-phenyl-6,7-dipropyl-4H-pyrido[2,1-a]isoquinoline-3-carbonitrile (1g): $^{13}C\{^{1}H\}$ NMR ($CDCl_3$, 100 MHz)

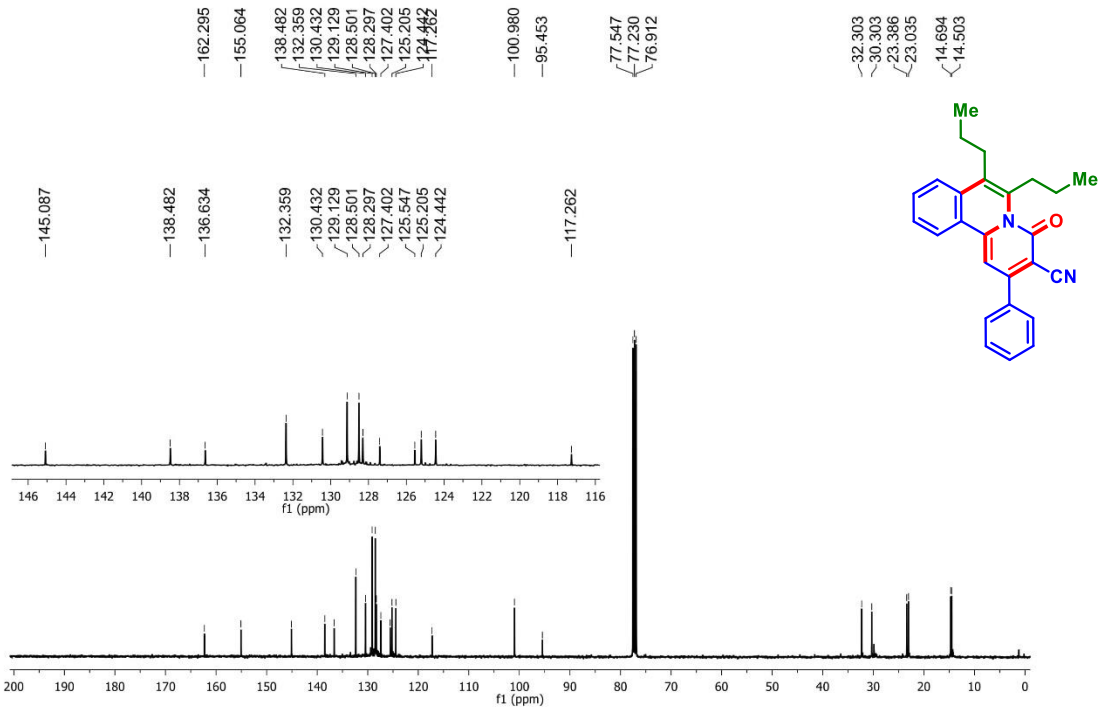

II.11. References:

[1] (a) Alberola, A.; Calvo, L. A.; Ortega, A. G.; Ruı´z, C. S.; Yustos, M. P. *J. Org. Chem.* **1999**, *64*, 9493–9498. (b) Wang, X.-S.; Wu, J.-R.; Zhou, J.; Tu, S.-J. *J. Comb. Chem.* **2009**, *11*, 1011–1022. (c) Li, X.-M.; Wang, B.; Zhang, J.-M.; Yan, M. *Org. Lett*. **2011**, *13*, 374–377. (d) Soylem, E. A.; Assy, M. G.; Morsi, G. M. *Croat. Chem. Acta*. **2017**, *90*, 461–469.

[2] (a) Freeman, F. *Chem. Rev.* **1969**, *69*, 591–624. (b) Evdokimov, N. M.; Kireev, A. S.; Yakovenko, A. A.; Antipin, M. Y; Magedov, I. V.; Kornienko, A. *J. Org. Chem*. **2007**,*72*, 3443–3453. (c) Costa, M.; Areias, F.; Abrunhosa, L.; Venâncio, A.; Proenca¸ F. *J. Org. Chem*. **2008**, *73*, 1954–1962. (d) Yan, C. G.; Wang, Q. F.; Song, X. K.; Sun, J. *J. Org. Chem*. **2009**, *74*, 710–718. (e) Sun, J.; Xia, E.-Y.; Wu, Q.; Yan, C.-G. *Org. Lett*. **2010**, *12*, 3678–3681. (f) Attanasi, O. A.; Favi, G.; Geronikaki, A.; Mantellini, F.; Moscatelli, G.; Paparisva, A. *Org. Lett*. **2013**, *15*, 2624–2627. (g) Liu, B.; Wei, E.; Lin, S.; Zhaoa, B.; Liang, F. *Chem. Commun*. **2014**, *50*, 6995–6997. (h) Dandia, A.; Singh, R.; Maheshwari, S. *Curr. Org. Chem.* **2014**, *18*, 2513–2529. (i) Wen, L.-R.; Jin, X.-J.; Niu, X.-D.; Li, M. *J. Org. Chem*. **2015**, *80*, 90–98. (j) Lu, Y.-L.; Sun, J.; Xie, Y.-J.; Yan, C.-G. *RSC Adv*. **2016**, *6*, 23390–23395. (k) Thimmarayaperumal, S.; Shanmugam, S. *ACS Omega*. **2017**, *2*, 4900–4910.

[3] (a) Handley, D. A.; Van Valen, R. G.; Melden, M. K.; Houlihan, W. J.; Saunders, R. N. *J. Pharmacol. Exp. Ther*. **1988**, *247*, 617–623. (b) Houlihan, W. J.; Cheon, S. H.; Parrino, V. A.; Handley, D. A.; Larson, D. A. *J. Med. Chem*. **1993**, *36*, 3098–3102. (c) Scholz, D.; Schmidt, H.; Prieschl, E. E.; Csonga, R.; Scheirer, W.; Weber, V.; Lembachner, A. ; Seidl, G.; Werner, G.; Mayer, P.; Baumruker, T. *J. Med. Chem*. **1998**, *41*, 1050–1059. (d) Griffin, R. J.; Fontana, G.; Golding, B. T.; Guiard, S.; Hardcastle, I. R.; Leahy, J. J. J.; Martin, N.; Richadson, C.; Rigoreau, L.; Stockley, M.; Smith, G. C. M. *J. Med. Chem.* **2005**, *48*, 569–585. (e) Paine, H. A.; Nathubhai, A.; Woon, E. C. Y.; Sunderland, P. T.; Wood, P. J.; Mahon, M. F.; Lloyd, M. D.; Thompson, A. S.; Haikarainen, T.; Narwal, M.; Lehtiö, L.; Threadgill, M. D. *Bioorg. Med. Chem*. **2015**, *23*, 5891–5908.

[4] (a) Coppola, G. M.; Schuster, H. F.; *The Chemistry of Heterocyclic Compounds: Isoquinolines*. Eds.: John Wiley & Sons: New York, **1981**, *38*, Part 3. (b) Krane, B. D.; Shamma, M. *J. Nat. Prod.* **1982**, *45*, 377–384. (c) Krane, B. D.; Fagbule, M. O.; Shamma, M.; Gözler, B. *J. Nat. Prod.* **1984**, *47*, 1–43. (d) Bentley, K. W. *Nat. Prod. Rep*. **1992**, *9*, 365–391. (e) Lewis, J. R. *Nat. Prod. Rep*. **1994**, *11*, 329–332. (f) Majumdar, K. C.; Chattopadhyay, S. K. *Heterocycles in Natural Product Synthesis.* Eds. Wiley-VCH: New York, **2011**. (g) Kiselev, E.; Sooryakumar, D.; Agama, K.; Cushman, M.; Pommier, Y. *J. Med. Chem.* **2014**, *57*, 1289–1298. (h) Brookings, D.; Davenport, R. J.; Davis, J.; Galvin, F. C. A.; Lloyd, S.; Mack, S. R.; Owens, R.; Sabin, V.; Wynn, J. *Bioorg. Med. Chem. Lett*. **2007**, *17*, 562–565.

[5] (a) Shamma, M. *In Isoquinoline Alkaloids. Chemistry and Pharmacology*, Academic Press, New York, **1972.** (b) Martin, S. F. *In the Alkaloids*. Brossi, A. Ed.; AC Press: San Diego. **1987**, *39*, 251–376. (c) Hoshino, O. *In the Alkaloids*. Cordell, G. A. Ed.; AC Press: San Diego. **1998**, *51*, 323–424. (d) Bentley, K. W. *Nat. Prod. Rep*. **2001**, *18*, 148–170.

[6] (a) Forrest, S. R.; Thompson, M. E. *Chem. Rev*. **2007**, *107*, 923–925. (b) Grimsdale, A. C.; Chan, K. L.; Martin, R. E.; Jokisz, P. G.; Holmes, A. B. *Chem. Rev.* **2009**, *109*, 897–1091. (c) Kanibolotsky, A. L.; Perepichka, I. F.; Skabara, P. J. *Chem. Soc. Rev*. **2010**, *39*, 2695–2728. (d) Figueira-Duarte, T. M.; Müllen, K. *Chem. Rev*. **2011**, *111*, 7260–7314. (e) Wang, X.; Zhang, F.; Liu, J.; Tang, R.; Fu, Y.; Wu, D.; Xu, Q.; Zhuang, X.; He, G.; Feng, X. *Org. Lett*. **2013**, *15*, 5714–5717.

[7] (a) Hassheider, T.; Benning, S. A.; Kitzerow, H.-S.; Achard, M.-F.; Bock, H. *Angew Chem., Int. Ed*. **2001**, *40*, 2060–2063. (b) Halleux, V. D.; Calbert, J.-P.; Brocorens, P.; Cornil, J.; Declercq, J.-P.; Bredas, J.-L.; Geerts, Y. *Adv. Funct. Mater*. **2004**, *14*, 649–659. (c) Kartha, K. K.; Babu, S. S.; Srinivasan, S.; Ajayaghosh, A. *J. Am. Chem. Soc*. **2012**, *134*, 4834–4841.

[8] (a) Lee, J. H.; So, J.-H.; Jeon, J. H.; Choi, E. B.; Lee, Y.-R.; Chang, Y.-T.; Kim, C.-H.; Bae, M. A.; Ahn, J. H. *Chem. Commun*. **2011**, *47*, 7500–7502. (b) Kim, E.; Lee, S.; Park, S. B. *Chem. Commun*. **2012**, *48*, 2331–2333.

[9] (a) Hoben, F. J. M.; Jonkheijm, P.; Meijer, E. W.; Schenning, A. P. H. *Chem. Rev*. **2005**, *105*, 1491–1546. (b) Anthony, J. E. *Chem. Rev*. **2006**, *106*, 5028–5048.

[10] (a) Henry, J. B.; MacDonald, R. J.; Gibbad, H. S.; McNab, H.; Mount, A. R. *Phys. Chem. Chem. Phys.* **2011**, *13*, 5235–5241. (b) Liu, B.; Wu, Z.; Wang, N.; Li, M.; You, J.; Lan, J. *Chem. Eur. J.* **2012**, *18*, 1599–1603. (c) Wan, J.; Zheng, C.-J.; Fung, M.-K.; Liu, X.-K.; Lee, C.-S.; Zhang, X.-H. *J. Mater. Chem.* **2012**, *22*, 4502–4510. (d) Kumar, N. S.; Rao, L. C.; Babu, N. J.; Meshram, H. M. *RSC Adv.* **2015**, *5*, 95539–95544.

[11] (a) Korivi, R. P.; Wu, Y.; Cheng, C.-H. *Chem. Eur. J.* **2009**, *15*, 10727–10731. (b) Liu, C.-C.; Parthasarathy, K.; Cheng, C.-H. *Org. Lett*. **2010**, *12*, 3518–3521. (c) Sugimoto, A.; Shinba-Tanaka, H.; Ishikawa, M.; *Synthesis*. **1995**, 431–434. (d) Taeko, I.; Yasuhiro, N.; Kunihiro, K.; Akira, K. *J. Heterocycl. Chem*. **1990**, *27*, 1419–1424. (e) Koltunov, K. Y.; Prakash, G. K. S.; Rasul, G.; Olah, G. A. *J. Org. Chem*. **2002**, *67*, 8943–8951. (f) Albini, A.; Bettinetti, G. F.; Minoli, G. *Tetrahedron Lett.* **1979**, *20*, 3761–3764. (g) Fisher, L. E.; Caroon, J. M.; Stabler, J. S. R.; Lundberg, S.; Muchowski, J. M. *J. Org. Chem*. **1993**, *58*, 3643–3647. (h) Varela-Fernández, A.; Varela, J. A.; Saá, C. *Adv. Synth. Catal*. **2011**, *353*, 1933–1937.

[12] (a) Ackermann, L. *J. Org. Chem*. **2014**, *79*, 8948–8954. (b) Alberico, D.; Scott, M. E.; Lautens, M. *Chem. Rev*. **2007**, *107*, 174–238. (c) Bergman, R. G. *Nature*. **2007**, *446*, 391–393. (d) Gensch, T.; Hopkinson, M. N.; Glorius, F.; Wencel-Delord, J. *Chem. Soc. Rev*. **2016**, *45*, 2900–2936. (e) Girard, S. A.; Knauber, T.; Li, C.-J. *Angew. Chem., Int. Ed*. **2014**, *53*, 74–100. (f) McMurray, L.; Hara, F. O.; Gaunt, M. J. *Chem. Soc. Rev*. **2011**, *40*, 1885–1898. (g) Rouquet, G.; Chatani, N. *Angew. Chem., Int. Ed*. **2013**, *52*, 11726–11743. (h) Satoh, T.; Miura, M. *Chem. Eur. J.* **2010**, *16*, 11212–11222. (i) Zhang, X.-S.; Chen, K.; Shi, Z.-J. *Chem. Sci*. **2014**, *5*, 2146–2159. (j) Zhu, R.-Y.; Farmer, M. E.; Chen, Y.-Q.; Yu, J.-Q. *Angew. Chem., Int. Ed*. **2016**, *55*, 10578–10599.

[13] (a) Wencel-Delord, J.; Dröge, T.; Liu, F.; Glorius, F. *Chem. Soc. Rev*. **2011**, *40*, 4740–4761. (b) Yeung, C. S.; Dong, V. M. *Chem. Rev*. **2011**, *111*, 1215–1292. (c) Cho, S. H.; Kim, J. Y.; Kwak, J.; Chang, S. *Chem. Soc. Rev*. **2011**, *40*, 5068–5083. (d) Li, B.-J.; Shi, Z.-J. *Chem. Soc. Rev*. **2012**, *41*, 5588–5598. (e) Arockiam, P. B.; Bruneau, C.;

Dixneuf, P. H. *Chem. Rev*. **2012**, *112*, 5879–5918. (f) Huang, H.; Ji, X.; Wu, W.; Jiang, H. *Chem. Soc. Rev*. **2015**, *44*, 1155–1171. (g) Moselage, M.; Li, J.; Ackermann, L. *ACS Catal*. **2016**, *6*, 498–525. (h) Yoshino, T.; Matsunaga, S. *Adv. Synth. Catal*. **2017**, *359*, 1245–1262. (i) He, J.; Wasa, M.; K. Chan, S. L.; Shao, Q.; Yu, J.-Q. *Chem. Rev*. **2017**, *117*, 8754–8786. (j) Yang, Y.; Lan, J.; You, J. *Chem. Rev*. **2017**, *117*, 8787–8863. (k) Wei, Y.; Hu, P.; Zhang, M.; Su, W. *Chem. Rev*. **2017**, *117*, 8864–8907. (l) Park, Y.; Kim, Y.; Chang, S. *Chem. Rev*. **2017**, *117*, 9247–9301.

[14] (a) Hyster, T. K.; Rovis, T. *J. Am. Chem. Soc*. **2010**, *132*, 10565–10569. (b) Guimond, N.; Gouliaras, C.; Fagnou, K. *J. Am. Chem. Soc*. **2010**, *132*, 6908–6909. (c) Guimond, N.; Gorelsky, I. S.; Fagnou, K. *J. Am. Chem. Soc*. **2011**, *133*, 6449–6457. (d) Mochida, S.; Umeda, N.; Hirano, K.; Satoh, T.; Miura, M. *Chem. Lett*. **2010**, *39*, 744–746. (e) Song, G.; Chen, D.; Pan, C.-L.; Crabtree, R. H.; Li, X. *J. Org. Chem*. **2010**, *75*, 7487–7490. (f) Upadhyay, N. S.; Thorat, V. H.; Sato, R.; Annamalai, P.; Chuang, S.-C.; Cheng, C.-H. *Green Chem*. **2017**, *19*, 3219–3224. (g) Xu, X.; Liu, Y.; Park, C.-M. *Angew. Chem., Int. Ed*. **2012**, *51*, 9372–9376. (h) Krieger, J.-P.; Ricci, G.; Lesuisse, D.; Meyer, C.; Cossy, J. *Chem. Eur. J*. **2016**, *22*, 13469–13473. (i) Shu, Z.; Li, W.; Wang, B. *ChemCatChem*. **2015**, *7*, 605–608. (j) Zhang, N.; Li, B.; Zhong, H.; Huang, J. *Org. Biomol. Chem*. **2012**, *10*, 9429–9439. (k) Zhong, H.; Yang, D.; Wang, S.; Huang, J. *Chem. Commun*. **2012**, *48*, 3236–3238. (l) Obata, A.; Ano, Y.; Chatani, N. *Chem. Sci*. **2017**, *8*, 6650–6655. (m) Ackermann, L.; Lygin, A. V.; Hofmann, N. *Angew. Chem., Int. Ed*. **2011**, *50*, 6379–6382. (n) Su, B.; Wei, J.-B.; Wu, W.-L.; Shi, Z. J. *ChemCatChem*. **2015**, *7*, 2986–2990. (o) Ackermann, L.; Fenner, S. *Org. Lett*. **2011**, *13*, 6548–6551. (p) Li, B.; Feng, H.; Xu, S.; Wang, B. *Chem. Eur. J*. **2011**, *17*, 12573–12577. (q) Allu, S.; Swamy, K. C. K. *J. Org. Chem*. **2014**, *79*, 3963–3972. (r) Huang, H.; Nakanowatari, S.; Ackermann, L. *Org. Lett.* **2017**, *19*, 4620–4623. (s) Deponti, M.; Kozhushkov, S. I.; Yufit, D. S.; Ackermann, L. *Org. Biomol. Chem*. **2013**, *11*, 142–148. (t) Swamy, T.; Rao, B. M.; Yadav, J. S.; Ravinder, V.; Sridhar, B.; Reddy, B. V. S. *RSC Adv*. **2015**, *5*, 68510–68514.

[15] (a) Ghosh, K.; Rit, R. K.; Ramesh, E.; Sahoo, A. K. *Angew. Chem., Int. Ed*. **2016**, *55*, 7821–7825. (b) Ghosh, K.; Shankar, M.; Rit, R. K.; Dubey, G.; Bharatam, P. V.; Sahoo, A. K. *J. Org. Chem*. **2018**, *83*, 9667–9681. (c) Shankar, M.; Guntreddi, T.; Ramesh, E.; Sahoo, A. K. *Org. Lett*. **2017**, *19*, 5665–5668.

[16] (a) Godula, K.; Sames, D. *Science*. **2006**, *312*, 67–72. (b) Davies, H. M. L.; Du Bois, J. D.; Yu, J. -Q. *Chem. Soc. Rev*. **2011**, *40*, 1855–1856 and references cited therein. (c) Chen, D. Y.-K.; Youn, S. W. *Chem. Eur. J*. **2012**, *18*, 9452–9474.

[17] Lin, S.; Wei, Y.; Liang, F. *Chem. Commun*. **2012**, *48*, 9879–9881.

[18] Xin, X.; Xiang, D.; Yang, J.; Zhang, Q.; Zhou, F.; Dong, D. *J. Org. Chem*. **2013**, *78*, 11956–11961.

[19] Song, G.; Chen, D.; Pan, C.-L.; Crabtree, R. H.; Li, X. *J. Org. Chem*. **2010**, *75*, 7487–7490.

[20] Ackermann, L.; Lygin, A. V.; Hofmann, N. *Angew. Chem., Int. Ed*. **2011**, *50*, 6379–6382.

[21] Zhong, H.; Yang, D.; Wang, S.; Huang, J. *Chem. Commun*. **2012**, *48*, 3236–3238.

[22] Reddy, M. C.; Manikandan, R.; Jeganmohan, M. *Chem. Commun*. **2013**, *49*, 6060–6062.

[23] Grigorjeva, L.; Daugulis, O. *Angew. Chem., Int. Ed*. **2014**, *53*, 10209–10212.

[24] Manoharan, R.; Jeganmohan, M. *Org. Biomol. Chem.* **2018**, *16*, 8384–8389.

[25] Sharma, N.; Bahadur, V.; Sharma, U. K.; Saha, D.; Li, Z.; Kumar, Y.; Colaers, J.; Singh, B. K.; Van der Eycken, E. V. *Adv. Synth. Catal*. **2018**, *360*, 3083–3089.

[26] Wang, Z.-Q.; Hou, C.; Zhong, Y.-F.; Lu, Y.-X.; Mo, Z.-Y.; Pan, Y.-M.; Tang, H.-T. *Org. Lett*. **2019**, *21*, 9841–9845.

[27] (a) Banerjee, A.; Santra, S. K.; Mohanta, P. R.; Patel, B. K. *Org. Lett*. **2015**, *17*, 5678–5681. (b) Modi, A.; Sau, P.; Chakraborty, N.; Patel, B. K. *Adv. Synth. Catal*. **2019**, *361*, 1368–1375.

[28] (a) Funes-Ardoiz, I.; Maseras, F. *Angew. Chem., Int. Ed.* **2016**, *55*, 2764–2767. (b) Roy, S.; Pradhan, S.; Punniyamurthy, T. *Chem. Commun.* **2018**, *54*, 3899–3902. (c) Sarkar, T.; Pradhan, S.; Punniyamurthy, T. *J. Org. Chem.* **2018**, *83*, 6444–6453.

[29] Rai, S. K.; Khanam, S.; Khanna, R. S.; Tewari, A. K. *RSC Adv*. **2014**, *4*, 44141–44145.

[30] (a) Kozhushkov, S. I.; Ackermann, L. *Chem. Sci*. **2013**, *4*, 886–896. (b) Ackermann, L. *Acc. Chem. Res*. **2014**, *47*, 281–295. (c) Thirunavukkarasu, V. S.; Donati, M.; Ackermann, L. *Org. Lett*. **2012**, *14*, 3416–3419. (d) Prakash, R.; Shekarrao, K.; Gogoi, S. *Org. Lett*. **2015**, *17*, 5264–5267.

[31] Frisch, M. J.; Trucks, G. W.; Schlegel, H. B.; Scuseria, G. E.; Robb, M. A.; Cheeseman, J. R.; Scalmani, G.; Barone, V.; Mennucci, B.; Petersson, G. A.; Nakatsuji, H.; Caricato, M.; Li, X.; Hratchian, H. P.; Izmaylov, A. F.; Bloino, J.; Zheng, G.; Sonnenberg, J. L.; Hada, M.; Ehara, M.; Toyota, K.; Fukuda, R.; Hasegawa, J.; Ishida, M.; Nakajima, T.; Honda, Y.; Kitao, O.; Nakai, H.; Vreven, T.; Montgomery, J. A.; Peralta, Jr., J. E.; Ogliaro, F.; Bearpark, M.; Heyd, J. J.; Brothers, E.; Kudin, K. N.; Staroverov, V. N.; Kobayashi, R.; Normand, J.; Raghavachari, K.; Rendell, A.; Burant, J. C.; Iyengar, S. S.; Tomasi, J.; Cossi, M.; Rega, N.; Millam, J. M.; Klene, M.; . Knox, J. E.; Cross, J. B.; Bakken, V.; Adamo, C.; Jaramillo, J.; Gomperts, R.; Stratmann, R. E.; Yazyev, O.; Austin, A. J.; Cammi, R.; Pomelli, C.; Ochterski, J. W.; Martin, R. L.; Morokuma, K.; Zakrzewski, V. G.; Voth, G. A.; Salvador, P.; Dannenberg, J. J.; Dapprich, S.; Daniels, A. D.; Farkas, Ö.; Foresman, J. B.; Ortiz, J. V.; Cioslowski, J.; Fox, D. J. *Gaussian 09*; Gaussian, Inc.: Wallingford CT, **2009**.

[32] Ghosh, S.; Pal, S.; Rajamanickam, S.; Shome, R.; Mohanta, P. R.; Ghosh, S. S.; Patel, B. K. *ACS Omega*. **2019**, *4*, 5565–5577.

[33] (a) Sonogashira, K.; Tohda, Y.; Hagihara, N. *Tetrahedron Lett*. **1975**, *16*, 4467–4470. (b) Sonogashira, K. *J. Organomet. Chem*. **2002**, *653*, 46–49.

CHAPTER III

Pd(II)-Catalyzed Synthesis of Furo[2,3-b]pyridine from β-Ketodinitriles and Alkynes via Cyclization and N–H/C Annulation

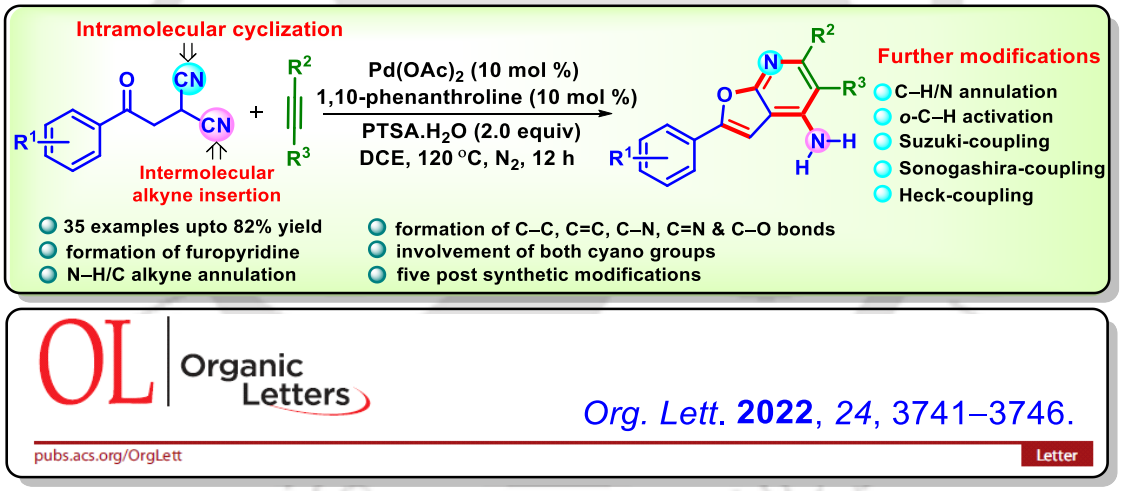

OL Organic Letters
Org. Lett. 2022, 24, 3741–3746.
pubs.acs.org/OrgLett
Letter

ABSTARCT: A Pd(II)-catalyzed synthesis of furopyridine has been developed from β–ketodinitriles and alkynes *via* an unusual N–H/C annulation. The participation of both the nitrile groups and the concurrent construction of furan and pyridine rings through the formation of C–C, C=C, C–O, C–N, and C=N bonds are the important features. The synthetic applicability is further demonstrated through a series of post-synthetic alterations.

भारतीय प्रौद्योगिकी संस्थान गुवाहाटी
Indian Institute of Technology Guwahati

CHAPTER III

Pd(II)-Catalyzed Synthesis of Furo[2,3-*b*]pyridine from β-Ketodinitriles and Alkynes *via* Cyclization and N–H/C Annulation

III.1. Introduction:

The fused ring *N*-heterocycles are common building blocks in pharmaceuticals and other analogues that are associated with remarkable biological activities. Amid fused ring nitrogenous heterocycles, furopyridine is found in alkaloids such as furomegistine I and II, phantasmidine, and dimethyl rhoifolinate, which are anticancer compounds, antiviral compounds, agonists/antagonists, etc (Figure III.1.1).[1] Further, the presence of π-excess furan ring and π-deficient pyridine ring systems makes them potential organic fluorophores.[2]

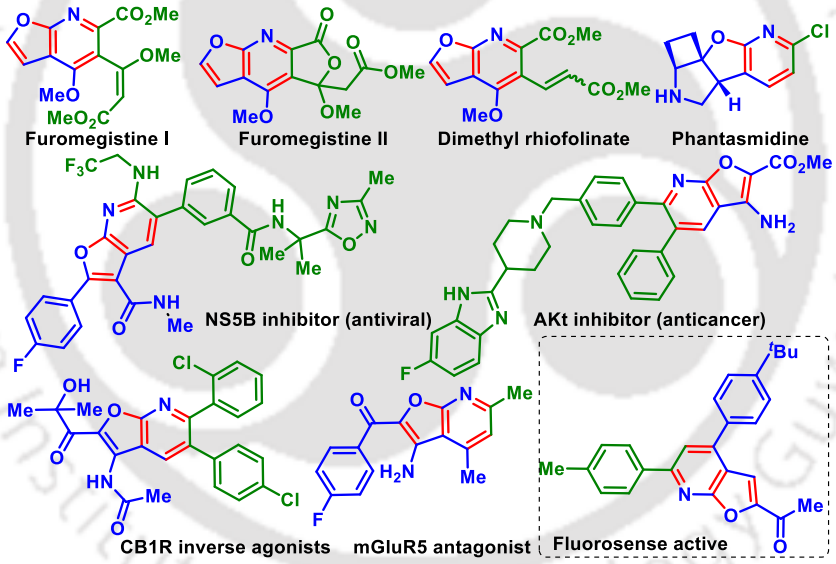

Figure III.1.1. *Representative bioactive furo[2,3-b]pyridines.*

The past decade has witnessed an upsurge in the transition-metal [Co(III), Rh(III), Ru(II), and Ni(II)/Ni(0)]-catalyzed insertion of an alkyne into C–H and N–H bonds for the synthesis of various fused heterocycles.[3–6] These strategies generally activate the *o*-C–H bonds of the precursors through a coordinating functional group. A subsequent cyclization with alkynes allows the synthesis of heterocycles in an atom economic manner. In this rapidly developing realm of oxidative annulation with alkynes, the Pd(II)-catalyzed annulation is gaining prominence to deliver diverse

carbocycles, heterocycles, and spirocycles.[7] Because of the inertness of the cyano group towards organopalladium reagents, this was an underdeveloped area of research. However, after the discovery of Pd-catalyzed annulation by the Larock group involving nitrile functionality, this area is becoming exciting and rapidly expanding.

Exactly two decades ago the Larock group developed an intramolecular carbopalladation of the nitrile group leading to the synthesis of 2,3-diarylindenone using 2-iodobenzonitrile and diphenylacetylene [Scheme III.1.1, (i)].[8] This was the first example of the addition of an organopalladium species across the C≡N bond known as Larock's annulation. Following the same strategy, they also develop a Pd(II)-catalyzed synthesis of 3,4-disubstituted 2-aminonaphthalene from 2-iodophenylacetonitrile and internal alkyne [Scheme III.1.1, (ii)].[9] These reactions proceed *via* the oxidative alkyne insertion between the *in situ* generated aryl–Pd bond followed by the nucleophilic addition of alkenyl Pd(II) to the proximal nitrile group. Finally, depending upon the conditions, hydrolysis or aromatization provided either 2,3-diarylindenones or 2-naphthalenamines. Later in 2016, Tsukamoto *et al.* extended this annulation to 2-(cyanomethyl)phenylboronates leading to the synthesis of 3,4-disubstituted 2-naphthalenamines [Scheme III.1.1, (iii)].[10] These reactions are triggered *via* the insertion of an *in situ* generated Pd(0) species into the C–I or C–B bonds. This is different from the standard C–H/N–H alkyne annulation, in which the active metal species is inserted through deprotonation of the acidic hydrogen attached with imine/amine nitrogen.

Following this, in 2019 our group reported a cascade [4 + 2] C–H/N–H annulation with internal alkyne to access highly fluorescent active fused isoquinolines from γ-ketodinitriles [Scheme III.1.1, (iv)].[11] In the recent past Pd(II)-catalyzed reactions have rapidly developed, extending the concept of catalytic carbopalladation of nitriles.[12] Taking advantage of this, subsequently, our group developed the synthesis of pyridines and pyrroles using γ-ketodinitriles and β-ketodinitriles respectively, in the presence of Pd(II) under visible-light excitation.[13] Subsequently we have also developed a visible-light mediated thio-functionalized pyrrole from β-ketodinitriles.[14] In the reactions mentioned above, one of the cyano groups remains silent while the other cyano group actively participates in the reaction. With our growing interest in the Pd-catalyzed insertion of an alkyne into the nitrile, herein we report the synthesis of furo[2,3-*b*]pyridine employing β-ketodinitrile and alkyne [Scheme III.1.1, (v)]. Gratifyingly, in this protocol

simultaneous participation of both the cyano groups leads to the construction of fused furopyridine rings through the formation of C–C, C=C, C–O, C–N, and C=N bonds in one pot.

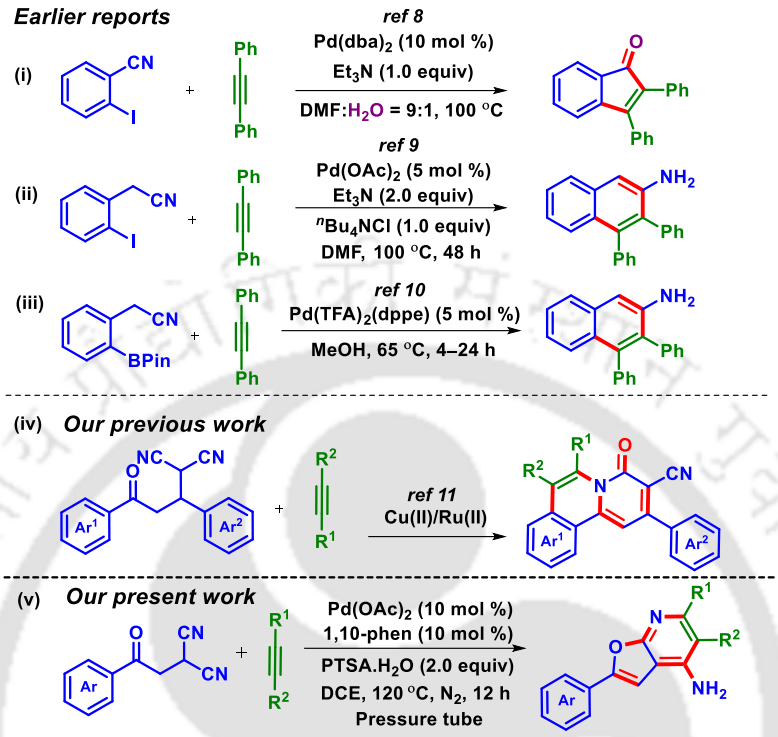

Scheme III.1.1. *Alkyne insertion into the nitrile.*

III.2. Strategies for the Synthesis of Furo[2,3-*b*]pyridine:

Owing to the importance of this furopyridine core, numerous efforts have been made for their construction.[15,16] Nevertheless, there have been few limitations because most of the existing strategies use functionalized pyridine or furan ring as the precursors, which is undesirable. Consequently, emerging an effective and mild process from easily available starting precursors to create furopyridine derivatives remains highly anticipated in modern organic chemistry.

III.2.1. Formation of the Furan Ring from Pyridine Derivatives:

In 2002, a Pd(II)-catalyzed electrophilic cyclization of *o*-acetoxyalkynylpyridines at room temperature was reported to access 2,3-disubstituted furo[2,3-*b*]pyridines (Scheme III.2.1.1).[15a]

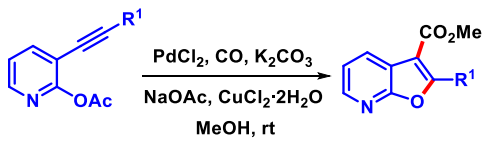

Scheme III.2.1.1. *Pd(II)-catalyzed synthesis of furo[2,3-b]pyridines.*

In 2003, a Pd(II)-mediated three-component synthesis of furo[2,3-*b*]pyridones was described by Balme and co-workers (Scheme III.2.1.2).[15b] The one-pot assembly of 4-alkoxy-3-iodo-2-pyridones, terminal alkynes, and organic halides has been accomplished *via* sequential Sonogashira-coupling and Wacker-type heteroannulation processes to afford furo[2,3-*b*]pyridones.

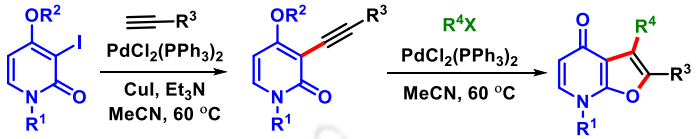

Scheme III.2.1.2. *One-pot sequential synthesis of furo[2,3-b]pyridines.*

A straightforward base-promoted synthesis of ethyl-3-aminofuropyridine-2-carboxylates was established from 1-halo-2-cyano or 1-hydroxy-2-cyano pyridines (Scheme III.2.1.3).[15c]

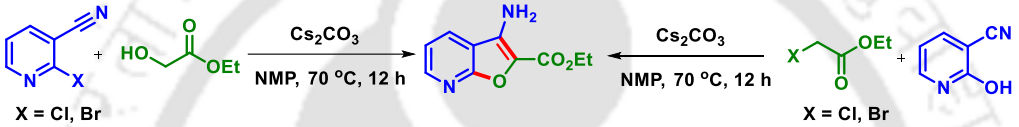

Scheme III.2.1.3. *Base-promoted synthesis of furo[2,3-b]pyridines.*

Further, furopyridine was synthesized by the reaction of tetrafluoro-4-cyanopyridine and 1,3-dicarbonyl derivatives by Sanford *et al*. in 2010 (Scheme III.2.1.4).[15d] Subsequently this fluorinated furopyridine scaffold can undergo reaction with other nucleophiles to provide highly functionalized heteroaromatic systems.

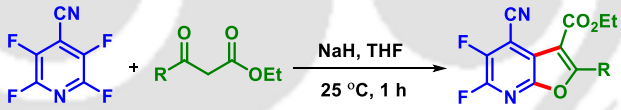

Scheme III.2.1.4. *Synthesis of furo[2,3-b]pyridines from highly fluorinated pyridines.*

III.2.2. Formation of the Pyridine Ring from Furan Derivatives:

The pyridine ring was mostly synthesized from furan derivatives having an amino group at the 2-position of the furan ring. For example, a Lewis acid-mediated synthesis of furopyridine having an amino group in the 4-position of the pyridine ring was described by Villarroya *et al*. starting from readily available 2-amino-4,5-diaryl-3-cyano furan derivatives (Scheme III.2.2.1).[15e]

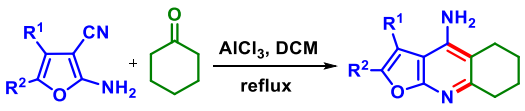

Scheme III.2.2.1. *Synthesis of 4-amino-substituted furo[2,3-b]pyridines.*

The condensation of 4,5-disubstituted 2-amino-3-furancarboxaldehyde with malononitrile in presence of catalytic NH_4Cl provided substituted 6-aminofuro[2,3-*b*]pyridine-5-carbonitriles in excellent yields (Scheme III.2.2.2).[15f]

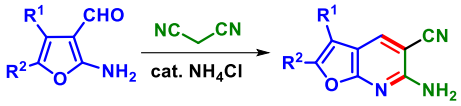

Scheme III.2.2.2. *Synthesis of furo[2,3-b]pyridines from 2-amino-3-furancarboxaldehyde.*

III.2.3. Other Miscellaneous Methods for the Synthesis of Furo[2,3-*b*]pyridines:

In 2014, Ma and co-workers developed a Pd(II)-catalyzed cyclizations of an enediyne-imides moiety in the presence of allyl bromide as an electrophile leading to furo[2,3-*b*]pyridines having allyl substituents at 3-position of both pyridine and furan rings (Scheme III.2.3.1).[16a]

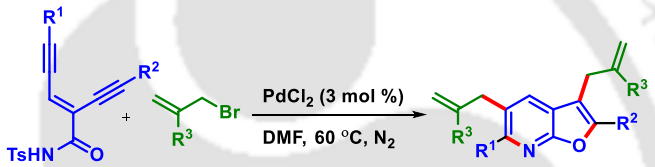

Scheme III.2.3.1. *Pd(II)-catalyzed synthesis of allyl-substituted furo[2,3-b]pyridines.*

In 2016, Emery *et al*. provided a concise strategy for the synthesis of 2,3-substituted furo[2,3-*b*]pyridines from pyridine-*N*-oxides and acyl chlorides or anhydrides under metal-free conditions in moderate to excellent yield (Scheme III.2.3.2).[16b]

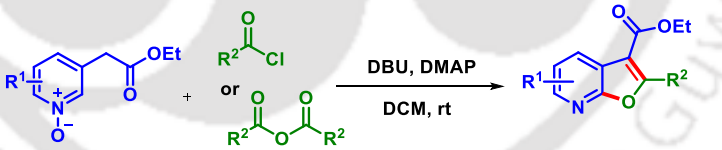

Scheme III.2.3.2. *Metal-free synthesis of furo[2,3-b]pyridines.*

In 2018, Ma *et al*. reported a Pd(II)-catalyzed cycloisomerization and cross-coupling reaction of readily accessible dienyne-imides with terminal olefins to access a series of highly substituted furo[2,3-*b*]dihydropyridine derivatives *via* 6π-electrocyclization (Scheme III.2.3.3).[16c]

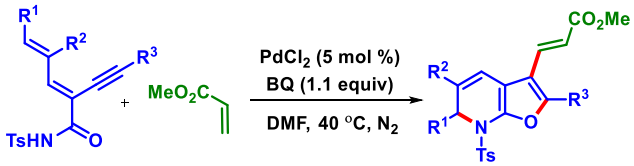

Scheme III.2.3.3. *Pd(II)-catalyzed synthesis of furo[2,3-b]pyridines via 6π-electrocyclization.*

III.3. Present Work:

III.3.1. Optimization of the Reaction Conditions:

We began this Pd(II)-catalyzed coupling of β-ketodinitrile (**1**) (0.25 mmol) and diphenylacetylene (**a**) (0.25 mmol, 1 equiv) in the presence of $Pd(OAc)_2$ (5 mol %), 2,2′-bipyridine (5 mol %) and *p*-toluenesulfonic acid ($PTSA{\cdot}H_2O$, 2 equiv) in 1,2-dichloroethane (DCE) (2 mL) at 120 °C in a pressure tube under N_2 atmosphere for 12 h. A new blue fluorescent spot was observed *via* TLC, and the product isolated after column chromatography was found to be furo[2,3-*b*]pyridine (**1a**) obtained in 37% yield (Table III.3.1, entry 1). From the spectroscopic evidence, the structure was assigned to be 2,5,6-triphenylfuro[2,3-*b*]pyridin-4-amine (**1a**) which was reconfirmed by a single-crystal X-ray study (**1a**) (Figure III.3.1.1, **CCDC–2164129**).

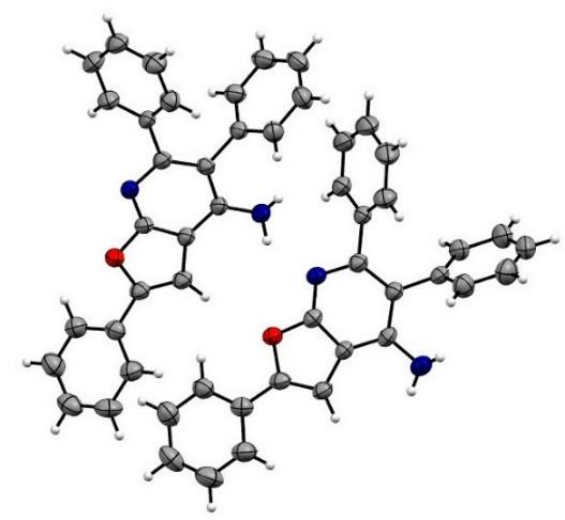

Figure III.3.1.1. *ORTEP diagram of* ***1a*** *with 40% ellipsoid probability (CCDC–2164129).*

To establish the optimal reaction conditions further screening process was carried out (Table III.3.1). Increasing the loading of $Pd(OAc)_2$ (10 mol %) and 2,2′-bipyridine (10 mol %) produces (**1a**) an improved yield of 54% (Table III.3.1, entry 2). Next, the amount of $PTSA{\cdot}H_2O$ was increased (4 equiv) but was not found beneficial, yielding the product with 56% yield (Table III.3.1, entry 3). Further experiments showed that only $Pd(TFA)_2$ was closer to $Pd(OAc)_2$ giving product in 48% yield (Table III.3.1, entry 4) while other palladium salts, such as $PdCl_2$, $Pd(PPh_3)_2Cl_2$, and $Pd(PPh_3)_4$ were far inferior (Table III.3.1, entries 5–7). The omission of 2,2'-bipyridine ligand gave a trace amount of the product, and no reaction occurred in the absence of $PTSA{\cdot}H_2O$ thereby proving their decisive role in this protocol (Table III.3.1, entries 8 and 9).

Table III.3.1. *Optimization of the reaction conditions.*[a–j]

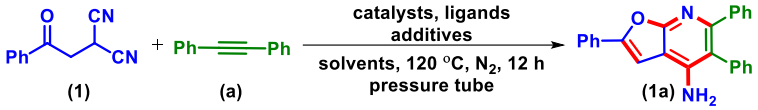

entry	catalyst (mol %)	ligand (mol %)	additive (equiv)	solvent	yield (%)[b]
1	$Pd(OAc)_2$ (5)	2,2'-bipyridyl (5)	PTSA·H_2O (2)	1,2-DCE	37
2	$Pd(OAc)_2$ (10)	2,2'-bipyridyl (10)	PTSA·H_2O (2)	1,2-DCE	54
3	$Pd(OAc)_2$ (10)	2,2'-bipyridyl (10)	PTSA·H_2O (4)	1,2-DCE	56
4	$Pd(TFA)_2$ (10)	2,2'-bipyridyl (10)	PTSA·H_2O (2)	1,2-DCE	48
5	$PdCl_2$ (10)	2,2'-bipyridyl (10)	PTSA·H_2O (2)	1,2-DCE	00
6	$PdCl_2(PPh_3)_2$ (10)	2,2'-bipyridyl (10)	PTSA·H_2O (2)	1,2-DCE	00
7	$Pd(PPh_3)_4$ (10)	2,2'-bipyridyl (10)	PTSA·H_2O (2)	1,2-DCE	00
8	$Pd(OAc)_2$ (10)		PTSA·H_2O (2)	1,2-DCE	trace
9	$Pd(OAc)_2$ (10)	2,2'-bipyridyl (10)		1,2-DCE	00
10	$Pd(OAc)_2$ (10)	2,2'-bipyridyl (10)	PTSA·H_2O (2)	CH_3CN	00
11	$Pd(OAc)_2$ (10)	2,2'-bipyridyl (10)	PTSA·H_2O (2)	Toluene	00
12	$Pd(OAc)_2$ (10)	2,2'-bipyridyl (10)	PTSA·H_2O (2)	DMF	00
13	$Pd(OAc)_2$ (10)	2,2'-bipyridyl (10)	PTSA·H_2O (2)	^{t}AmOH	00
14	$Pd(OAc)_2$ (10)	1,10-phen (10)	PTSA·H_2O (2)	1,2-DCE	62
15	$Pd(OAc)_2$ (10)	L-proline (10)	PTSA·H_2O (2)	1,2-DCE	00
16	$Pd(OAc)_2$ (10)	PPh_3 (10)	PTSA·H_2O (2)	1,2-DCE	00
17	$Pd(OAc)_2$ (10)	XPhos (10)	PTSA·H_2O (2)	1,2-DCE	00
18	$Pd(OAc)_2$ (10)	1,10-phen (10)	AcOH (2)	1,2-DCE	00
19	$Pd(OAc)_2$ (10)	1,10-phen (10)	CF_3SO_3H (2)	1,2-DCE	00
20	$Pd(OAc)_2$ (10)	1,10-phen (10)	$PhCO_2H$ (2)	1,2-DCE	00
21	**$Pd(OAc)_2$ (10)**	**1,10-phen (10)**	**PTSA·H_2O (2)**	**1,2-DCE**	**72**[c]
22	$Pd(OAc)_2$ (10)	1,10-phen (10)	PTSA·H_2O (2)	1,2-DCE	75[d]
23	$Pd(OAc)_2$ (10)	1,10-phen (10)	PTSA·H_2O (2)	1,2-DCE	74[e]
24	$Pd(OAc)_2$ (10)	1,10-phen (10)	PTSA·H_2O (2)	1,2-DCE	trace[f]
25	$Pd(OAc)_2$ (10)	1,10-phen (10)	PTSA·H_2O (2)	1,2-DCE	74[g]
26	$Pd(OAc)_2$ (10)	1,10-phen (10)	PTSA·H_2O (2)	1,2-DCE	54[h]
27	$Pd(OAc)_2$ (5)	1,10-phen (10)	PTSA·H_2O (2)	1,2-DCE	52[i]
28	$Pd(OAc)_2$ (2)	1,10-phen (10)	PTSA·H_2O (2)	1,2-DCE	28[j]

[a]Reaction condition: β-ketodinitrile (**1**) (0.25 mmol), diphenylacetylene (**a**) (0.25 mmol), catalyst (mol %), additives (equiv) at 120 °C in a pressure tube for 12 h. [b]Yields of the isolated product. [c]1.5 equiv of (**a**) was used. [d]2.0 equiv of (**a**) was used. [e]Yield after 24 h. [f]Temperature 80 °C. [g]Temperature 140 °C. [h]Without N_2. [i,j]Low Pd-catalyst loading.

Screening of various solvents, such as CH_3CN, toluene, DMF, and *t*-AmOH was found to be ineffective (Table III.3.1, entries 10–13). Next switching the ligand system to 1,10-phenanthroline (62%) gave an improved yield while screening of other ligands such as L-proline (00%), PPh_3 (00%), and XPhos (00%) was found completely ineffective (Table III.3.1, entries 14–17). Instead of $PTSA{\cdot}H_2O$, the use of other acid additives such as AcOH, CF_3SO_3H, and $PhCO_2H$ was found completely unsuccessful (Table III.3.1, entries 18–20). Increasing the amount of diphenylacetylene (**a**) to 1.5 equiv improved the yield significantly (72%) (Table III.3.1, entry 21), while further increasing the amount to 2 equiv does not provide any improvement in the reaction yield (75%) (Table III.3.1, entry 22). On allowing the reaction to continue up to 24 h, a 74% yield of the product was observed (Table III.3.1, entry 23). From the variation of temperature, it was found that reaction at lower (80 ^oC) temperature produces a trace amount of the product while reaction at higher (140 ^oC) temperature provided an almost similar yield (74%) (Table III.3.1, entries 24 and 25). Further, the reaction carried out in the air atmosphere (without N_2) gave a 54% yield of the product (Table III.3.1, entry 26). This might be due to the formation of other by-products from diphenylacetylene (**a**) upon aerial oxidation and therefore access amount of diphenylacetylene (**a**) may be needed. Additionally, reduced Pd-loading of 5 mol % and 2 mol % produces lower yields of 52% and 28% respectively keeping all other parameters identical (Table III.3.1, entries 27 and 28). Hence the best optimized condition was found to be the use of β-ketodinitrile (**1**) (0.25 mmol), diphenylacetylene (**a**) (0.375 mmol, 1.5 equiv), $Pd(OAc)_2$ (10 mol %), 1,10-phenanthroline (10 mol %) and $PTSA{\cdot}H_2O$ (2 equiv) in 1,2-dichloroethane (DCE) (2 mL) at 120 ^oC in a pressure tube under N_2 atmosphere for 12 h (Table III.3.1, entry 21).

III.3.2. Substrates Scopes for the Synthesis of Furo[2,3-*b*]pyridines:

Having established the optimal conditions, we studied the effect of substituents on β-ketomalononitriles (**1**–**14**) with diphenylacetylene (**a**) (Scheme III.3.2.1). β-Ketodinitriles having electron-donating substituents in the phenyl ring, *viz*. *p*-Me (**2**), *p*-OMe (**3**), and *p*-^{i}Pr (**4**), underwent smooth reactions with diphenylacetylene (**a**), affording their corresponding furopyridine (**2a**), (**3a**), and (**4a**) in 69%, 65%, and 68% yields respectively (Scheme III.3.2.1). Similarly, substrates bearing electron-withdrawing groups such as *p*-F (**5**), *p*-Cl (**6**), *p*-Br (**7**), *p*-I (**8**), *p*-CF3 (**9**), and *p*-NO_2 (**10**) provided their corresponding fused products (**5a**, 74%), (**6a**, 76%), (**7a**, 78%), (**8a**, 71%), (**9a**, 78%), and (**10a**, 80%) (Scheme III.3.2.1). This protocol was also

successful when the phenyl ring of β-ketomalononitriles was replaced with a naphthyl ring (**11**) and benzo[*d*][1,3]dioxole aroyl ring (**12**), giving their furopyridines (**11a**) and (**12a**) in 72% and 61% yields respectively (Scheme III.3.2.1). The β-ketomalononitriles having a thiophene ring (**13**) reacted to provide product (**13a**) in a 55% yield. Interestingly, the β-ketomalononitriles having a tetralone (**14**) ring reacted with diphenylacetylene (**a**) to produce a naphthyl-fused furopyridines (**14a**) in 60% yield. Herein, the tetralone ring was aromatized to a naphthyl moiety (Scheme III.3.2.1). In addition, this protocol was scaled up to 5 mmol, giving the desired product **1a** in 56% yield.

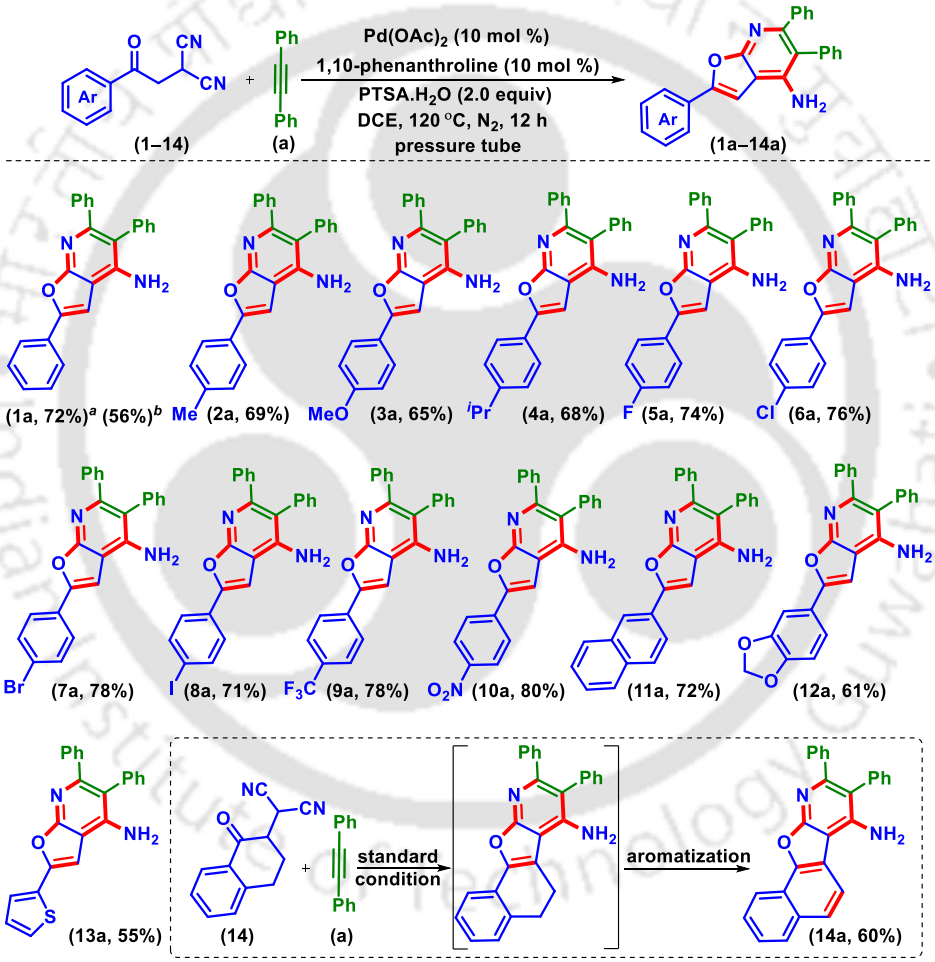

[a]Reaction conditions are as follows: (i) **1**–**14** (0.25 mmol), diphenylacetylene (**a**) (0.375 mmol), $Pd(OAc)_2$ (0.025 mmol), 1,10-phenanthroline (0.025 mmol), $PTSA{\cdot}H_2O$ (0.50 mmol) and 1,2-DCE (2 mL) at 120 °C in a pressure tube under N_2 atmosphere for 12 h. [b]5 mmol scale.

Scheme III.3.2.1. *Substrate scope for various β-ketodinitriles.*[a,b]

After successfully generating a library of furopyridines using various substituted β-keto malononitriles (**1−14**), we changed the scope of this methodology to substituted diphenylacetylenes (**b**–**n**) (Scheme III.3.2.2). Diphenylacetylenes possessing electron-rich groups such as *p*-Me (**b**), *m*-Me (**c**), *p*-OMe (**d**), and *p*-^{t}Bu (**e**) positively responded to this protocol, providing their annulated products (**1b**, 79%), (**1c**, 77%), (**1d**, 82%), and (**1e**, 80%) respectively (Scheme III.3.2.2). Diphenylacetylenes having electron-withdrawing groups *p*-F (**f**), *m*-F (**g**), *p*-Cl (**h**), 3-Cl (**i**), *p*-Br (**j**), and *p*-CF_3 (**k**) underwent annulations when reacted with β-ketomalononitrile (**1**), providing their anticipated products (**1f**, 73%), (**1g**, 71%), (**1h**, 70%), (**1i**, 68%), (**1j**, 65%), and (**1k**, 61%) respectively (Scheme III.3.2.2). As one can see from the yields pattern, diphenylacetylenes possessing electron-donating groups (**b**–**e**) gave higher yields than those of diphenylacetylenes bearing electron-withdrawing (**f**–**k**) substituents. An unsymmetrical diphenylacetylene having electron-donating *p*-Me and *p*-OMe (**l**) substituents provided exclusive annulated furopyridine (**1l**) in 78% yield, where the phenyl ring bearing *p*-OMe is towards the pyridyl nitrogen and the *p*-Me near the amino group. In addition, an unsymmetrical diphenylacetylene having *p*-Me and *p*-F (**m**) substituents provided an inseparable mixture of furopyridines (**1m** and **1m′**) in a 1:3 ratio as determined by ^{1}H NMR. Here, in the major isomer (**1m′**), the electron-rich phenyl ring bearing the *p*-Me group is oriented toward pyridyl nitrogen. Another diphenylacetylene having electron-donating *p*-OMe and electron-withdrawing *p*-Br (**n**) resulted in a single isomeric furopyridine (**1n**) in 70% yield. The structures of isomer **1l** and **1n** were predicted based on the literature reports,[7] where the insertion of alkyne generally occurs towards the benzylic carbon attached to the more electron-donating group. Two other unsymmetrical alkynes, *viz.* 1-phenyl-1-propyne (**o**), and 1-phenyl-1-butyne (**p**) delivered a regio-isomeric mixture of (**1o′**:**1o**) and (**1p′**:**1p**) in the ratio of 1:2.5. In the major isomer (**1o** and **1p**) the pyridyl nitrogen is on the electron-rich phenyl side and the amino group is on the methyl/ethyl side (Scheme III.3.2.2). In addition to internal alkynes, this protocol is also successful for terminal alkynes. Phenyl acetylenes having electron neutral –H (**q**), electron-donating (**r**), and electron-withdrawing (**s**) substituents all afforded the corresponding furopyridines (**1q**, 52%), (**1r**, 54%), and (**1s**, 43%) in moderate yields. In all these products, the phenyl ring is orienting towards pyridine *N* and the hydrogen near the amino side. The electron-deficient symmetrical aromatic alkynes, *viz.* *p*-NO_2 substituted diphenylacetylene (**t**), a heteroarylacetylene (**u**), and dialkylacetylenedicarboxylates (**v** and **v'**), all failed to react.

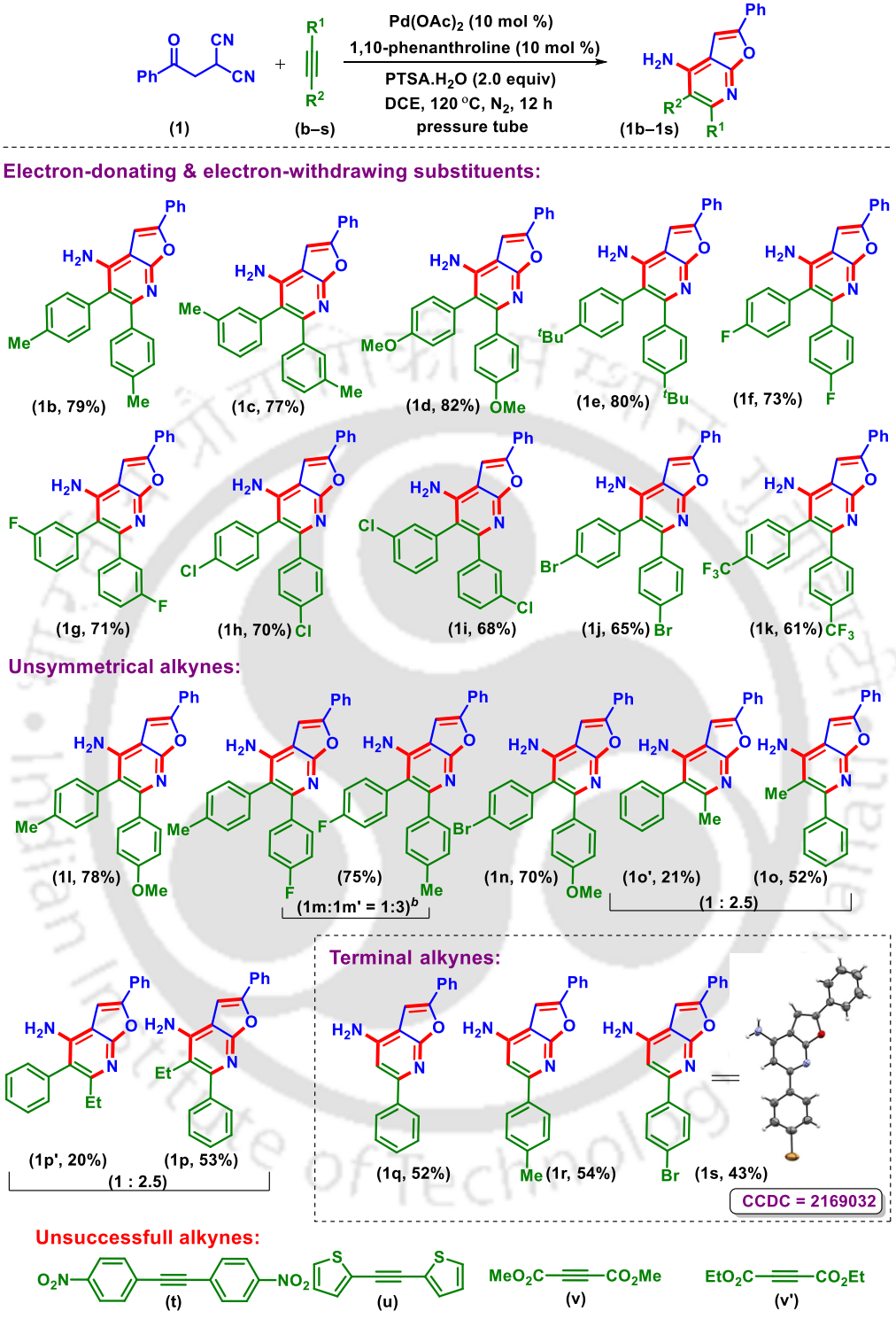

[a]Reaction conditions are as follows: (i) **1** (0.25 mmol), alkynes (**b–s**) (0.375 mmol), $Pd(OAc)_2$ (0.025 mmol), 1,10-phenanthroline (0.025 mmol), $PTSA{\cdot}H_2O$ (0.50 mmol) and 1,2-DCE (2 mL) at 120 °C in a pressure tube under N_2 atmosphere for 12 h. [b]Ratio determined by ^1H NMR analysis.

Scheme III.3.2.2. *Substrate scope for alkynes.*[a,b]

III.4. Mechanistic Investigations:

III.4.1. Control Experiments:

Next, to illuminate a plausible reaction mechanism, a few control experiments were performed. When β-ketodinitrile (**1**) was reacted in the absence of alkyne (**a**), it produced 2-amino-5-phenylfuran-3-carbonitrile (**1′**) in 90% yield after 6 h (Scheme III.4.1.1).

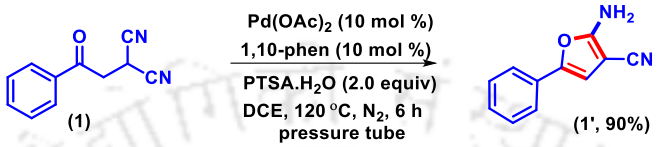

Scheme III.4.1.1. *Reaction in the absence of alkyne.*

A similar product (**1′**) was obtained in 82% yield when the reaction was carried out even in the absence of $Pd(OAc)_2$ and ligand (Scheme III.4.1.2). This confirms the involvement of PTSA in the construction of the furan ring.

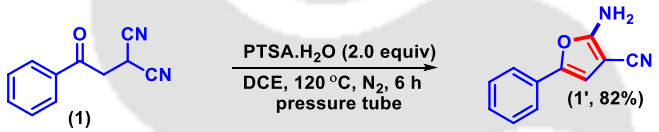

Scheme III.4.1.2. *Reaction in the absence of alkyne and Pd(II).*

To confirm the intermediacy of 2-amino-5-phenylfuran-3-carbonitrile (**1′**), its reaction with diphenylacetylene (**a**) under the standard condition afforded the furopyridine (**1a**) in 82% yield after 6 h (Scheme III.4.1.3).

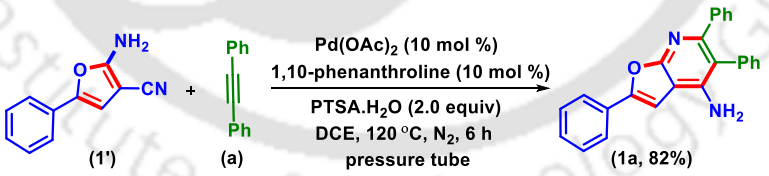

Scheme III.4.1.3. *Reaction with intermediate* (**1′**).

To ascertain whether the second annulation step is Pd-catalyzed or a Lewis acid-mediated process, an experiment with the intermediate (**1'**) and diphenylacetylene (**a**) without $Pd(OAc)_2$ was performed (Scheme III.4.1.4). The reaction was unproductive giving no trace of the product (**1a**), confirming the necessity of $Pd(OAc)_2$ for the second annulation step.

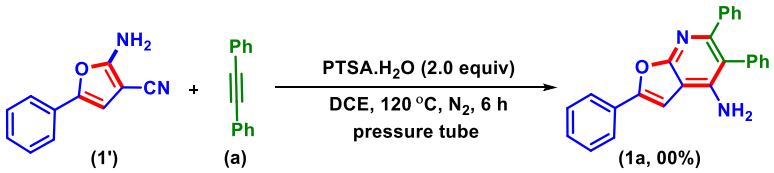

Scheme III.4.1.4. *Reaction with intermediate in the absence of Pd(II).*

Thus, amines and nitrile are the two possible sites for this N–H/C annulation, which is unprecedented. To establish the exact involvement of two proximal amines and nitrile the Pd(II)-catalyzed alkyne insertion between 2-aminobenzonitrile (**15**) and diphenylacetylene (**a**) was carried out. To our delight, an annulated product 2,3-diphenylquinolin-4-amine (**15a**) was obtained in 85% yield (Scheme III.4.1.5).

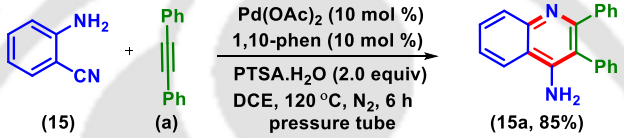

Scheme III.4.1.5. *Reaction with 2-aminobenzonitrile.*

III.4.2. Plausible Reaction Mechanism:

Based on control experiments and literature reports,[7–10] a tentative reaction mechanism is demonstrated (Scheme III.4.2.1). Initially, the β-ketodinitrile (**1**) undergoes an acid-catalyzed enolization in the presence of PTSA·H_2O to afford an intermediate (**I**). The intermediate (**I**) then undergoes another acid-catalyzed intramolecular cyclization to afford a five-membered cyclic intermediate (**1′**). In the presence of 1,10-phenanthroline (L) a ligand-coordinated Pd(II) complex (**A**) is generated *in situ*, which undergoes a deprotonative coordination with the amino group of intermediate (**1′**) to form another intermediate (**II**), eliminating AcOH. Next, diphenylacytelelene (**a**) is inserted intermolecularly into the *N* atom giving an alkynyl Pd(II) species (**III**). This intermediate (**III**) undergoes intramolecular insertion of the alkyne to another nitrile through a carbopalladation, giving a six-membered pyridine ring (**IV**), and the Pd(II) is coordinated with the other nitrile *N*-atom. Protonolysis of (**IV**) with PTSA·H_2O gives imine intermediate (**V**) and the OTs-ligated Pd(II) complex (**B**), which upon acetate ligand exchange regenerates the initial Pd(II) complex (**A**). Finally, the aromatization of intermediate **V** produces the corresponding furopyridine (**1a**).

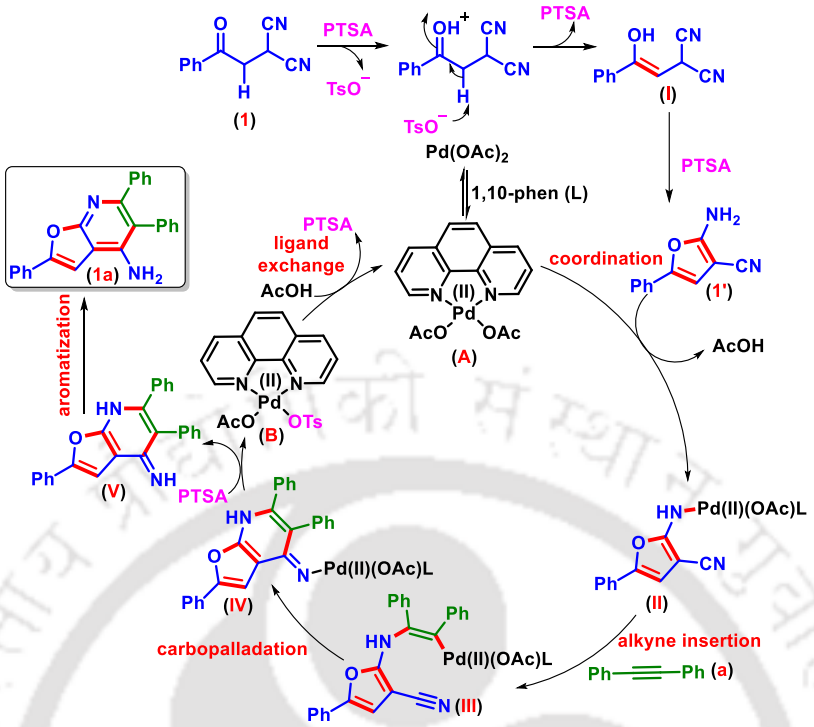

Scheme III.4.2.1. *Proposed reaction path.*

III.5. Post-Synthetic Applications:

To explore the synthetic utility and to expand the substrate scope, a few post-synthetic modifications such as Ru(II)-catalyzed C–H activation, oxidative alkyne annulation, and Pd(II)-catalyzed cross-coupling reactions were successfully carried out. The 2-phenyl pyridine ring of (**1a**) participates *via* a Ru(II)-catalyzed annulation reaction with diphenylacetylene (**a**) and *o*-C–H activation with *n*-propylmalimide (**w**) giving the corresponding functionalized product (**1aa**, 80%), and (**1aw**, 72%) respectively (Scheme III.5.1).[17,18]

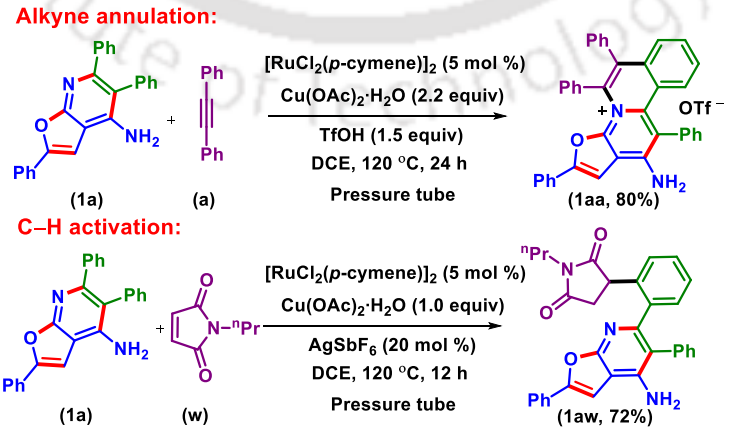

Scheme III.5.1. *Ru(II)-catalyzed oxidative annulation and o-C–H activation.*

Further, the *p*-Br substituted furopyridine (**7a**) undergoes a Pd(II)-catalyzed Suzuki coupling with phenylboronic acid (**x**), Sonogashira coupling with 4-ethynyltoluene (**y**), and Heck coupling with *p*-tolylstyrene (**z**) giving cross-coupled products (**7ax**, 68%), (**7ay**, 75%), and (**7az**, 70%) respectively (Scheme III.5.2).[19,20]

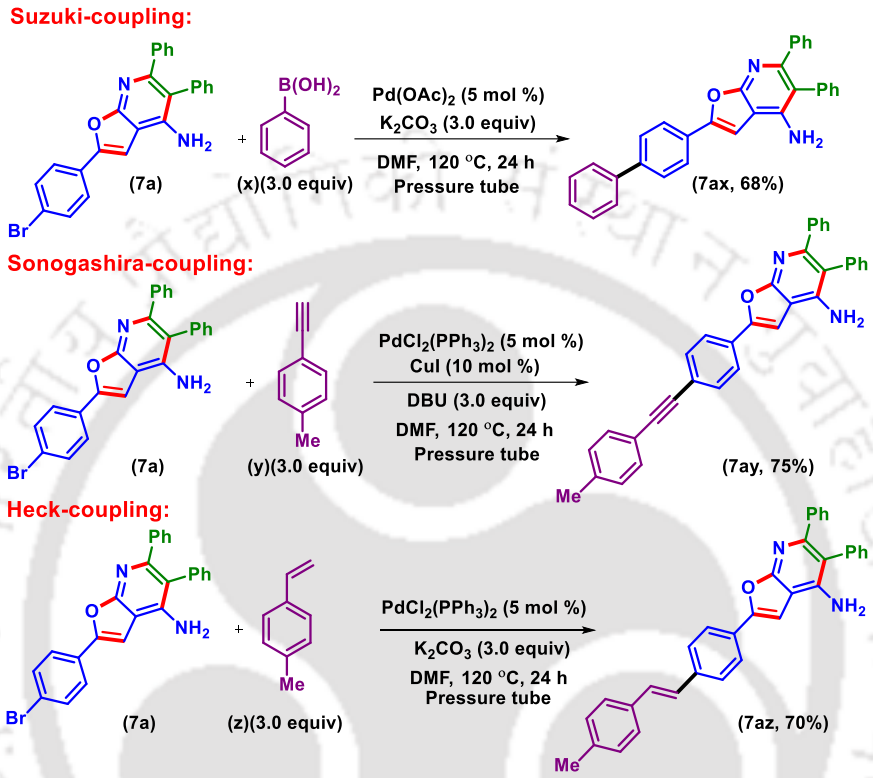

Scheme III.5.2. *Pd(II)-catalyzed cross-coupling reactions.*

III.6. Conclusion:

In summary, an elegant synthesis of furo[2,3-*b*]pyridine is established *via* Pd(II)-catalyzed N–H/C annulation between β-ketodinitriles and alkynes. In this protocol, both cyano groups of β-ketodinitriles actively participate in the simultaneous construction of furan and pyridine rings. The control experiment reveals the formation of a 2-amino-3-cyano intermediate in the absence of alkyne and therefore this protocol could be further employed for the synthesis of 2,3-substituted quinoline-4-amine from 2-aminobenzonitriles. Terminal alkynes afforded one of the regioselective isomers, whereas unsymmetrical internal alkyne provided either a single regioisomer or a mixture of regioisomers depending on the nature of the substituents attached to the phenyl rings. Finally, large-scale synthesis and a few post-synthetic functionalizations such as annulation, *o*-C–H activation, and cross-coupling reactions were also demonstrated.

III.7. Experimental Section:

III.7.1. General Information:

All the reagents were commercial grade and purified according to the established procedures. All the reagents were commercial grade and used without further purification unless otherwise stated. All the reactions were carried out in an oven-dried pressure tube (20.3 cm x 19 mm, 21 mL). Preparation of the starting materials was carried out in an oven-dried 100 mL or 50 mL round bottom flask. Reactions were monitored by thin-layer chromatography (TLC) on 0.25 mm silica gel plates ($60F_{254}$) and visualized under UV illumination at 254 nm. Organic extracts were dried over anhydrous sodium sulfate (Na_2SO_4). Column chromatography was performed to purify the crude product on silica gel 60−120 mesh using a mixture of hexane and ethyl acetate as eluent. The isolated compounds were characterized by spectroscopic [^1H, $^{13}C\{^1H\}$ NMR, and IR] techniques and HRMS analysis. NMR spectra were recorded in deuterochloroform ($CDCl_3$) or deuterated dimethyl sulfoxide (DMSO-d_6). ^1H, $^{13}C\{^1H\}$ were recorded in 500 (125) or 400 (100) MHz spectrometer and were calibrated using tetramethylsilane or residual undeuterated solvent for ^1H NMR, deuterochloroform for ^{13}C NMR as an internal reference {$Si(CH_3)_4$: 0.00 ppm or $CHCl_3$: 7.260 ppm for ^1H NMR, 77.230 ppm for ^{13}C NMR or $(CH_3)_2SO$: 2.50 ppm for ^1H NMR, 39.50 ppm for ^{13}C NMR}. ^{19}F NMR was calibrated without any internal standard in $CDCl_3$ in a 500 MHz spectrometer. The chemical shifts are quoted in δ units, parts per million (ppm). ^1H NMR data is represented as follows: Chemical shift, multiplicity (s = singlet, d = doublet, t = triplet, q = quartet, m = multiplet), integration and coupling constant(s) *J* in hertz (Hz). High-resolution mass spectra (HRMS) were recorded on a mass spectrometer using electrospray ionization-time of flight (ESI-TOF) reflection experiments. FT-IR spectra were recorded in KBr or neat and reported in the frequency of absorption (cm^{-1}).

III.7.2. General Procedures:

III.7.2.1. General Procedure for the Synthesis of 2-(2-Oxo-2-arylylethyl)malononitriles (1–14):

Compounds **1**–**14** were synthesized in slightly modified literature procedures.[21]

III.7.2.2. General Procedure for the Synthesis of Internal Alkynes (b–n):

The internal alkynes (**b–n)** were synthesized according to the modified literature procedure.[22]

III.7.2.3. General Procedure for the Synthesis of 2,5,6-Triphenylfuro[2,3-*b*]pyridin-4-amine (1a) from 2-(2-Oxo-2-phenylethyl)malononitriles (1) and Diphenylacetylene (a):

To an oven-dried pressure tube (20.3 cm x 19 mm, 21 mL) containing a magnetic bar was added 2-(2-oxo-2-phenylethyl)malononitriles (**1**) (46 mg, 0.25 mmol), diphenylacetylene (**a**) (67 mg, 0.375 mmol), $Pd(OAc)_2$ (5.6 mg, 0.025 mmol), 1,10-phenanthroline (4.5 mg, 0.025 mmol), $PTSA{\cdot}H_2O$ (95 mg, 0.50 mmol), and 1,2-DCE (2 mL). After that, the reaction mixture was purged with N_2 through a balloon and closed with the PTFE stopper. The reaction mixture was stirred at 120 ^oC in a preheated oil bath for 12 h. After completion of the reaction (monitored by TLC analysis), the reaction mixture was admixed with ethyl acetate (25 mL) and the organic layer was washed with saturated sodium bicarbonate solution (5 mL). The organic layer was dried over anhydrous Na_2SO_4, and the solvent was evaporated under reduced pressure. The crude product so obtained was purified over a column of silica gel using 10% ethyl acetate in hexane to give pure 2,5,6-triphenylfuro[2,3-*b*]pyridin-4-amine (**1a**) with 72% yield (65 mg). The identity and purity of the product were confirmed by spectroscopic analysis.

III.7.3. Mechanistic Investigation:

III.7.3.1. Control Experiments:

III.7.3.1.1. In the Absence of Alkyne:

The experiment was carried out according to the general procedure III.7.2.3 taking 2-(2-oxo-2-phenylethyl)malononitriles (**1**) (46 mg, 0.25 mmol) without diphenylacetylene (**a**). The crude product so obtained was purified over a column of silica gel using 15% ethyl acetate in hexane to give pure 2-amino-5-phenylfuran-3-carbonitrile (**1′**) with 90% yield (41 mg). The identity and purity of the product were confirmed by spectroscopic analysis.

III.7.3.1.2. In the Absence of Alkyne and $Pd(OAc)_2$:

The experiment was carried out according to the general procedure III.7.2.3 taking 2-(2-oxo-2-phenylethyl)malononitriles (**1**) (46 mg, 0.25 mmol), and $PTSA{\cdot}H_2O$ (95 mg, 0.50 mmol) without without diphenylacetylene (**a**) and the $Pd(OAc)_2$. The crude product so obtained was purified over a column of silica gel using 15% ethyl acetate in hexane to give pure 2-amino-5-phenylfuran-3-carbonitrile (**1′**) with 82% yield (37 mg). The identity and purity of the product were confirmed by spectroscopic analysis.

III.7.3.1.3. Reaction Between Intermediate (1') and Diphenylacetylene (a):

(i) The experiment was carried out according to the general procedure III.7.2.3 taking 2-amino-5-phenylfuran-3-carbonitrile (**1′**) (46 mg, 0.25 mmol), and diphenylacetylene (**a**) (67 mg, 0.375 mmol) under standard reaction condition. The crude product so obtained was purified over a column of silica gel using 10% ethyl acetate in hexane to give pure 2,5,6-triphenylfuro[2,3-*b*]pyridin-4-amine (**1a**) with 82% yield (74 mg). The identity and purity of the product were confirmed by spectroscopic analysis.

(ii) To an oven-dried pressure tube (20.3 cm x 19 mm, 21 mL) containing a magnetic bar was added 2-amino-5-phenylfuran-3-carbonitrile (**1′**) (46 mg, 0.25 mmol), diphenylacetylene (**a**) (67 mg, 0.375 mmol), PTSA·H_2O (95 mg, 0.50 mmol), and 1,2-DCE (2 mL). After that, the reaction mixture was purged with N_2 through a balloon and closed with the PTFE stopper. The reaction mixture was stirred at 120 ^oC in a preheated oil bath for 6 h. The reaction remains silent giving no trace of the product (**1a**) and the starting material was recovered.

III.7.3.1.4. Reaction Between 2-Amino-benzonitrile (15) and Diphenylacetylene (a):

The experiment was carried out according to the general procedure III.7.2.3 taking 2-amino-benzonitrile (**15**) (29 mg, 0.25 mmol), and diphenylacetylene (**a**) (67 mg, 0.375 mmol) under standard reaction conditions. The crude product so obtained was purified over a column of silica gel using 30% ethyl acetate in hexane to give pure 2,5,6- 2,3-diphenylquinolin-4-amine (**15a**) with 85% yield (63 mg). The identity and purity of the product were confirmed by spectroscopic analysis.

III.7.4. Post Synthetic Applications:

III.7.4.1. General procedure for the Synthesis of 12-Amino-2,5,6,11-tetraphenylfuro[3',2':5,6]pyrido[2,1-*a*]isoquinolin-4-ium (1aa) from 2,5,6-Triphenylfuro[2,3-*b*]pyridin-4-amine (1a) and Diphenylacetylene (a):

To an oven-dried pressure tube (20.3 cm x 19 mm, 21 mL) containing a magnetic bar was added triphenylfuro[2,3-*b*]pyridin-4-amine (**1a**) (72 mg, 0.20 mmol), diphenylacetylene (**a**) (43 mg, 0.24 mmol), [Ru(*p*-cymene)Cl_2]$_2$ (6.1 mg, 0.01 mmol), Cu(OAc)$_2$·H_2O (84 mg, 0.44 mmol), TfOH (45 mg, 0.30 mmol) and 1,2-DCE (2 mL). The reaction mixture was stirred in an oil bath preheated at 120 ^oC for 24 h. After completion of the reaction (monitored by TLC analysis), the reaction mixture was admixed with ethyl acetate (25 mL) and the organic layer was washed with saturated sodium bicarbonate solution (5 mL). The organic layer was dried over anhydrous sodium

sulfate (Na_2SO_4), and the solvent was evaporated under reduced pressure. The crude product so obtained was purified over a column of silica gel using 5% methanol in dichloromethane to give pure 12-amino-2,5,6,11-tetraphenylfuro[3',2':5,6]pyrido[2,1-*a*]isoquinolin-4-ium (**1aa**) in 80% yield. The identity and purity of the product were confirmed by spectroscopic analysis.

III.7.4.2. General procedure for the Synthesis of (R)-3-(2-(4-Amino-2,5-diphenylfuro[2,3-*b*]pyridin-6-yl)phenyl)-1-propylpyrrolidine-2,5-dione (1aw) from 2,5,6-Triphenylfuro[2,3-*b*]pyridin-4-amine (1a) and 1-Propyl-1*H*-pyrrole-2,5-dione (w):

To an oven-dried pressure tube (20.3 cm x 19 mm, 21 mL) containing a magnetic bar was added triphenylfuro[2,3-*b*]pyridin-4-amine (**1a**) (72 mg, 0.20 mmol), 1-propyl-1*H*-pyrrole-2,5-dione (**w**) (56 mg, 0.40 mmol), $[Ru(p\text{-cymene})Cl_2]_2$ (6.1 mg, 0.01 mmol), $Cu(OAc)_2{\cdot}H_2O$ (38 mg, 0.20 mmol), $AgSbF_6$ (14 mg, 0.04 mmol), and 1,2-DCE (2 mL). The reaction mixture was stirred in an oil bath preheated at 120 ^oC for 12 h. After completion of the reaction (monitored by TLC analysis), the reaction mixture was admixed with ethyl acetate (25 mL) and the organic layer was washed with water (10 mL). The organic layer was dried over anhydrous sodium sulfate (Na_2SO_4), and the solvent was evaporated under reduced pressure. The crude product so obtained was purified over a column of silica gel using 15% ethyl acetate in hexane to give pure (R)-3-(2-(4-amino-2,5-diphenylfuro[2,3-*b*]pyridin-6-yl)phenyl)-1-propylpyrrolidine-2,5-dione (**1aw**) in 72% yield. The identity and purity of the product were confirmed by spectroscopic analysis.

III.7.4.3. General procedure for the Synthesis of 2-([1,1'-Biphenyl]-4-yl)-5,6-diphenylfuro[2,3-*b*]pyridin-4-amine (7ax) from 2-(4-Bromophenyl)-5,6-diphenylfuro[2,3-*b*]pyridin-4-amine (7a) and Phenylboronic Acid (x):

To an oven-dried pressure tube (20.3 cm x 19 mm, 21 mL) containing a magnetic bar was added 2-(4-bromophenyl)-5,6-diphenylfuro[2,3-*b*]pyridin-4-amine (**7a**) (88 mg, 0.20 mmol), phenylboronic acid (**x**) (72 mg, 0.60 mmol), $Pd(OAc)_2$ (2.2 mg, 0.01 mmol), K_2CO_3 (83 mg, 0.60 mmol), and DMF (2 mL). The reaction mixture was stirred in an oil bath preheated at 120 ^oC for 24 h. After completion of the reaction (monitored by TLC analysis), the reaction mixture was admixed with ethyl acetate (25 mL) and the organic layer was washed with ice-cold water (5 mL). The organic layer was dried over anhydrous sodium sulfate (Na_2SO_4), and the solvent was evaporated under reduced pressure. The crude product so obtained was purified over a column of silica gel using 10% ethyl acetate in hexane to give pure 2-([1,1'-biphenyl]-4-yl)-5,6-

diphenylfuro[2,3-*b*]pyridin-4-amine (**7ax**) in 68% yield. The identity and purity of the product were confirmed by spectroscopic analysis.

III.7.4.4. General procedure for the Synthesis of 5,6-Diphenyl-2-(4-(*p*-tolylethynyl)phenyl)furo[2,3-*b*]pyridin-4-amine (7ay) from 2-(4-Bromophenyl)-5,6-diphenylfuro[2,3-*b*]pyridin-4-amine (7a) and 4-Methylphenylacetylene (y):

To an oven-dried pressure tube (20.3 cm x 19 mm, 21 mL) containing a magnetic bar was added 2-(4-bromophenyl)-5,6-diphenylfuro[2,3-*b*]pyridin-4-amine (**7a**) (88 mg, 0.20 mmol), 1-ethynyl-4-methylbenzene (**y**) (70 mg, 0.60 mmol), $PdCl_2(PPh_3)_2$ (7 mg, 0.01 mmol), CuI (3.8 mg, 0.02 mmol), DBU (91 mg, 0.60 mmol), and DMF (2 mL). The reaction mixture was stirred in an oil bath preheated at 120 ^oC for 24 h. After completion of the reaction (monitored by TLC analysis), the reaction mixture was admixed with ethyl acetate (25 mL) and the organic layer was washed with ice-cooled water (5 mL). The organic layer was dried over anhydrous sodium sulfate (Na_2SO_4), and the solvent was evaporated under reduced pressure. The crude product so obtained was purified over a column of silica gel using 10% ethyl acetate in hexane to give pure 5,6-diphenyl-2-(4-(*p*-tolylethynyl)phenyl)furo[2,3-*b*]pyridin-4-amine (**7ay**) in 75% yield. The identity and purity of the product were confirmed by spectroscopic analysis.

III.7.4.5. General procedure for the Synthesis of (E)-2-(4-(4-Methylstyryl)phenyl)-5,6-diphenylfuro[2,3-*b*]pyridin-4-amine (7az) from 2-(4-Bromophenyl)-5,6-diphenylfuro[2,3-*b*]pyridin-4-amine (7a) and 4-methylstyrene (z):

To an oven-dried pressure tube (20.3 cm x 19 mm, 21 mL) containing a magnetic bar was added 2-(4-bromophenyl)-5,6-diphenylfuro[2,3-*b*]pyridin-4-amine (**7a**) (88 mg, 0.20 mmol), 1-methyl-4-vinylbenzene (**z**) (71 mg, 0.60 mmol), $PdCl_2(PPh_3)_2$ (7 mg, 0.01 mmol), K_2CO_3 (83 mg, 0.60 mmol), and DMF (2 mL). The reaction mixture was stirred in an oil bath preheated at 120 ^oC for 24 h. After completion of the reaction (monitored by TLC analysis), the reaction mixture was admixed with ethyl acetate (25 mL) and the organic layer was washed with ice-cooled water (5 mL). The organic layer was dried over anhydrous sodium sulfate (Na_2SO_4), and the solvent was evaporated under reduced pressure. The crude product so obtained was purified over a column of silica gel using 10% ethyl acetate in hexane to give pure (E)-2-(4-(4-methylstyryl)phenyl)-5,6-diphenylfuro[2,3-*b*]pyridin-4-amine (**7az**) in 70% yield. The identity and purity of the product were confirmed by spectroscopic analysis.

III.7.5. Crystallographic Information:

III.7.5.1. Crystallographic Information of 2,5,6-Triphenylfuro[2,3-*b*]pyridin-4-amine (1a):

III.7.5.1.1 Sample Preparation:

The single crystal of compound **1a** was prepared by the slow evaporation method for which 5 mg of the compound (**1a**) was dissolved in 1 mL of ethyl acetate in a clean and dry 10 mL glass vial. Petroleum ether (1 mL) was added to this solution slowly with a dropper until faint turbidity appeared on the top. The mouth of the glass vial was covered with a cap having a small hole and kept for slow evaporation at room temperature. A single crystal of **1a** was obtained as a transparent white needle-like crystal after 2–3 days.

III.7.5.1.2. Crystallographic Description of 2,5,6-Triphenylfuro[2,3-*b*]pyridin-4-amine (1a):

A suitable crystal was selected on a SuperNova, Single source at offset/far, HyPix3000 diffractometer. The crystal was kept at 293(2) K during data collection. Using Olex2[1], the structure was solved with the ShelXT[2] structure solution program using Intrinsic Phasing and refined with the ShelXL[3] refinement package using Least Squares minimization.

1. Dolomanov, O.V., Bourhis, L.J., Gildea, R.J, Howard, J.A.K. & Puschmann, H. (2009), J. Appl. Cryst. 42, 339–341.
2. Sheldrick, G.M. (2015). Acta Cryst. A71, 3–8.
3. Sheldrick, G.M. (2015). Acta Cryst. C71, 3–8.

$C_{25}H_{18}N_2O$, crystal dimensions 0.06 x 0.03 x 0.02 mm, M_r = 362.41, Monoclinic, space group P 21/c, a = 13.1258(12) Å, b = 25.0415(18) Å, c = 12.2078(12) Å, α = 90 °, β = 109.049(10)°, γ = 90°, V = 3792.8(6) Å^3, Z = 8, ρ_{calcd} = 1.269 g/cm^3, μ = 0.078 mm^{-1}, F(000) = 1520.0, reflection collected/unique = 19042/5752, refinement method = full-matrix least-squares on F^2, final R indices [I>2\s(I)]: R_1 = 0.0690, wR_2 = 0.1543, R indices (all data): R_1 = 0.1491, wR_2 = 0.1925, goodness of fit = 0.992. CCDC-2164129 for 2,5,6-Triphenylfuro[2,3-*b*]pyridin-4-amine (**1a**) contains the supplementary crystallographic data for this paper. These data can be obtained free of charge from The Cambridge Crystallographic Data Centre *via* www.ccdc.cam.ac.uk/data_request/cif.

III.7.5.2. Crystallographic Information of 6-(4-Bromophenyl)-2-phenylfuro[2,3-*b*]pyridin-4-amine (1s):

III.7.5.2.1. Sample Preparation:

The single crystal of compound **1s** was prepared by the slow evaporation method for which 10 mg of the compound (**1s**) was dissolved in 1 mL of ethyl acetate in a clean and dry 10 mL glass

vial. Petroleum ether (1 mL) was added to this solution slowly with a dropper until faint turbidity appeared on the top. The mouth of the glass vial was covered with a cap having a small hole and kept for slow evaporation at room temperature. A single crystal of **1s** was obtained as a transparent white needle-like crystal after 2 days.

III.7.5.2.2. Crystallographic Description of 6-(4-Bromophenyl)-2-phenylfuro[2,3-*b*]pyridin-4-amine (1s):

Diffraction data were collected at 292 K with MoKα radiation (λ = 0.71073 Å) using a Bruker Nonius SMART APEX CCD diffractometer equipped with a graphite monochromator and Apex CD camera. The SMART software was used for data collection and for indexing the reflections and determining the unit cell parameters. Data reduction and cell refinement were performed using SAINT[1,2] software and the space groups of these crystals were determined from systematic absences by XPREP and further justified by the refinement results. The structures were solved by direct methods and refined by full-matrix least-squares calculations using SHELXTL-97[3] software. All the non-H atoms were refined in the anisotropic approximation against F^2 of all reflections.

1. G. M. Sheldrick, SADABS, 1996, based on the method described in: R. H. Blessing, *Acta Crystallogr*. 1995, **A51**, 33–38.
2. SMART and SAINT, Siemens Analytical X-ray Instruments Inc., Madison, WI, 1996.
3. G. M. Sheldrick, *Acta Crystallogr*., 2008, **A64**, 112–122.

$C_{19}H_{13}BrN_2O$, crystal dimensions 0.16 x 0.13 x 0.12 mm, M_r = 365.22, Monoclinic, space group P 21/c, a = 16.9710(4) Å, b = 13.6260(3) Å, c = 6.9714(16) Å, α = 90 °, β = 101.020(7)°, γ = 90°, V = 1582.4(6) Å^3, Z = 4, ρ_{calcd} = 1.533 g/cm^3, μ = 2.603 mm^{-1}, F(000) = 736.0, reflection collected/unique = 44185/2784, refinement method = full-matrix least-squares on F^2, final R indices [I>2\s(I)]: R_1 = 0.0431, wR_2 = 0.1167, R indices (all data): R_1 = 0.0587, wR_2 = 0.1390, goodness of fit = 1.008. CCDC-2169032 for 6-(4-Bromophenyl)-2-phenylfuro[2,3-*b*]pyridin-4-amine (**1s**) contains the supplementary crystallographic data for this paper. These data can be obtained free of charge from The Cambridge Crystallographic Data Centre *via* www.ccdc.cam.ac.uk/data_request/cif.

III.8. Spectral Data:

***2,5,6-Triphenylfuro[2,3-b]pyridin-4-amine (1a)*:**

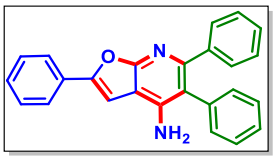

As a white solid (65 mg, 72% yield, mp 198–200 °C); Purification over a column of silica gel (10% EtOAc in hexane); ^{1}H NMR ($CDCl_3$, 500 MHz): δ 7.86 (d, 2H, J = 7.0 Hz), 7.42 (t, 2H, J = 7.5 Hz), 7.35–7.31 (m, 5H), 7.28 (d, 1H, J = 7.0 Hz), 7.19 (d, 2H, J = 6.5 Hz), 7.15–7.14 (m, 3H), 6.95 (s, 1H), 4.50 (s, 2H); ^{13}C{^{1}H} NMR ($CDCl_3$, 125 MHz): δ 162.1, 153.7, 153.4, 145.9, 140.8, 136.4, 131.5, 130.3, 130.2, 129.2, 129.0, 128.8, 127.62, 127.60, 127.3, 124.9, 116.9, 106.7, 97.4; IR (KBr, cm^{-1}): 3458, 3392, 2956, 2922, 2852, 1622, 1457, 1167, 1072, 880, 782; HRMS (ESI/Q-TOF) (m/z) calcd for $C_{25}H_{19}N_2O$ $[M + H]^+$ 363.1492; found 363.1493.

***5,6-Diphenyl-2-(p-tolyl)furo[2,3-b]pyridin-4-amine (2a)*:**

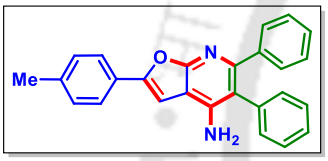

As a white solid (64 mg, 69% yield, mp 223–225 °C); Purification over a column of silica gel (10% EtOAc in hexane); ^{1}H NMR ($CDCl_3$, 500 MHz): δ 7.73 (d, 2H, J = 8.0 Hz), 7.32–7.29 (m, 4H), 7.24–7.23 (m, 1H), 7.20 (d, 2H, J = 7.5 Hz), 7.16 (d, 2H, J = 7.0 Hz), 7.12–7.11 (m, 3H), 6.86 (s, 1H), 4.47 (s, 2H), 2.36 (s, 3H); ^{13}C{^{1}H} NMR ($CDCl_3$, 125 MHz): δ 162.0, 153.7, 153.4, 145.7, 140.9, 138.9, 136.5, 131.5, 130.2, 129.7, 129.2, 127.6, 127.3, 124.9, 116.9, 106.8, 96.6, 21.6; IR (KBr, cm^{-1}): 3487, 3391, 2955, 2922, 2851, 1608, 1456, 1167, 1156, 1072, 822, 759; HRMS (ESI/Q-TOF) (m/z) calcd for $C_{26}H_{21}N_2O$ $[M + H]^+$ 377.1648; found 377.1649.

***2-(4-Methoxyphenyl)-5,6-diphenylfuro[2,3-b]pyridin-4-amine (3a)*:**

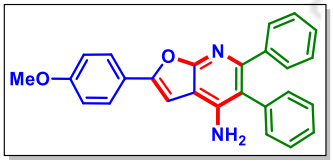

As a white solid (63 mg, 65% yield, mp 238–240 °C); Purification over a column of silica gel (10% EtOAc in hexane); ^{1}H NMR ($CDCl_3$, 400 MHz): δ 7.82 (d, 2H, J = 8.8 Hz), 7.36–7.28 (m, 5H), 7.22–7.19 (m, 2H), 7.15–7.14 (m, 3H), 6.98 (d, 2H, J = 9.2 Hz), 6.82 (s, 1H), 4.42 (s, 2H), 3.86 (s, 3H); ^{13}C{^{1}H} NMR ($CDCl_3$, 100 MHz): δ 161.9, 160.2, 153.5, 153.0, 145.5, 140.9, 136.5, 131.5, 130.2, 129.2, 127.6, 127.3, 126.4, 123.1, 116.9, 114.5, 106.9, 95.6, 55.6; IR (KBr, cm^{-1}): 3472, 3341, 2959, 2923, 2852, 1622, 1454, 1177, 1040, 1007, 879, 781; HRMS (ESI/Q-TOF) (m/z) calcd for $C_{26}H_{21}N_2O_2$ $[M + H]^+$ 393.1598; found 393.1590.

***2-(4-Isopropylphenyl)-5,6-diphenylfuro[2,3-b]pyridin-4-amine (4a)*:**

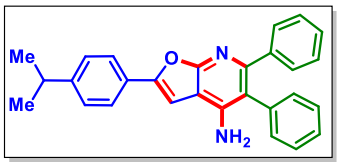

As a white solid (68 mg, 68% yield, mp 180–182 °C); Purification over a column of silica gel (10% EtOAc in hexane); ^{1}H NMR ($CDCl_3$, 500 MHz): δ 7.82 (d, 2H, J = 8.5 Hz), 7.35–7.29 (m, 6H), 7.28 (t, 1H, J = 7.5 Hz), 7.20 (d, 2H, J = 7.5 Hz), 7.15–7.14 (m, 3H), 6.91 (s, 1H), 4.45 (s, 2H), 2.98–2.91 (m, 1H), 1.30 (s, 3H), 1.29 (s, 3H); ^{13}C{^{1}H} NMR ($CDCl_3$, 125 MHz): δ 162.0, 153.7, 153.4, 149.9, 145.7, 140.9, 136.5, 131.5, 130.2, 129.2, 127.9, 127.6, 127.2, 125.0, 116.9, 106.9, 96.6, 34.2, 24.1; IR (KBr, cm^{-1}): 3466, 3391, 2956, 2923, 2853, 1624, 1433, 1167, 1055, 880, 836, 761; HRMS (ESI/Q-TOF) (m/z) calcd for $C_{28}H_{25}N_2O$ $[M + H]^+$ 405.1961; found 405.1984.

***2-(4-Fluorophenyl)-5,6-diphenylfuro[2,3-b]pyridin-4-amine (5a)*:**

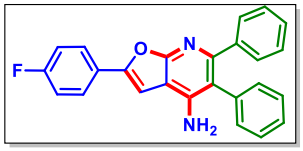

As a white solid (70 mg, 74% yield, mp 235–237 °C); Purification over a column of silica gel (10% EtOAc in hexane); ^{1}H NMR ($CDCl_3$, 500 MHz): δ 7.84–7.81 (m, 2H), 7.35–7.28 (m, 5H), 7.19 (d, 2H, J = 7.0 Hz), 7.15–7.09 (m, 5H), 6.88 (s, 1H), 4.48 (s, 2H); ^{13}C{^{1}H} NMR ($CDCl_3$, 125 MHz): δ 163.1 (d, J = 247.2 Hz), 153.7, 152.4, 145.9, 140.8, 136.3, 131.5, 130.1, 129.2, 127.7, 127.6, 127.4, 126.7 (d, J = 8.2 Hz), 126.65, 126.62, 117.0, 116.2 (d, J = 21.9 Hz), 106.7, 97.1; ^{19}F NMR ($CDCl_3$): δ –112.1 (s); IR (KBr, cm^{-1}): 3460, 3365, 2954, 2921, 2853, 1626, 1459, 1156, 1031, 880, 837, 785; HRMS (ESI/Q-TOF) (m/z) calcd for $C_{25}H_{18}FN_2O$ $[M + H]^+$ 381.1398; found 381.1405.

***2-(4-Chlorophenyl)-5,6-diphenylfuro[2,3-b]pyridin-4-amine (6a)*:**

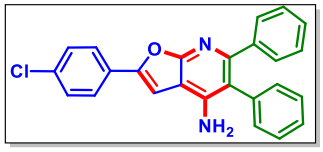

As a white solid (75 mg, 76% yield, mp 258–260 °C); Purification over a column of silica gel (10% EtOAc in hexane); ^{1}H NMR ($CDCl_3$, 500 MHz): δ 7.79 (d, 2H, J = 8.5 Hz), 7.40 (d, 2H, J = 8.5 Hz), 7.36–7.33 (m, 2H), 7.31–7.28 (m, 3H), 7.19 (d, 2H, J = 7.0 Hz), 7.15–7.14 (m, 3H), 6.94 (s, 1H), 4.48 (s, 2H); ^{13}C{^{1}H} NMR ($CDCl_3$, 125 MHz): δ 162.1, 153.9, 152.2, 145.9, 140.8, 136.3, 134.6, 131.5, 130.2, 129.32, 129.26, 128.8, 127.7, 127.6, 127.4, 126.1, 117.0, 106.6, 97.9; IR (KBr, cm^{-1}): 3461, 3384, 2960, 2922, 2851, 1620, 1489, 1116, 1012, 834, 780; HRMS (ESI/Q-TOF) (m/z) calcd for $C_{25}H_{18}ClN_2O$ $[M + H]^+$ 397.1102; found 397.1135.

***2-(4-Bromophenyl)-5,6-diphenylfuro[2,3-b]pyridin-4-amine (7a)*:**

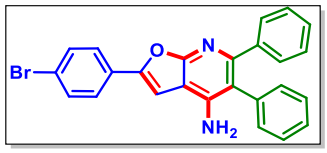

As a white solid (85 mg, 78% yield, mp 255–257 °C); Purification over a column of silica gel (10% EtOAc in hexane); ^{1}H NMR ($CDCl_3$, 500 MHz): δ 7.73 (d, 2H, J = 8.5 Hz), 7.56 (d, 2H, J = 8.5 Hz), 7.36–7.33 (m, 2H), 7.31–7.28 (m, 3H), 7.19 (d, 2H, J = 8.0 Hz), 7.15–7.14 (m, 3H), 6.96 (s, 1H), 4.48 (s, 2H); ^{13}C{^{1}H} NMR ($CDCl_3$, 125 MHz): δ 162.1, 154.0, 152.2, 146.0, 140.8, 136.3, 132.3, 131.5, 130.2, 129.3, 129.2, 127.7, 127.6, 127.4, 126.3, 122.8, 117.0, 106.6, 98.0; IR (KBr, cm^{-1}): 3455, 3388, 2956, 2922, 2851, 1620, 1433, 1072, 881, 731; HRMS (ESI/Q-TOF) (m/z) calcd for $C_{25}H_{18}BrN_2O$ $[M + H]^+$ 441.0597; found 441.0599.

***2-(4-Iodophenyl)-5,6-diphenylfuro[2,3-b]pyridin-4-amine (8a)*:**

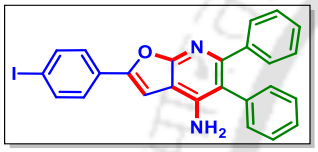

As a white solid (86 mg, 71% yield, mp 225–227 °C); Purification over a column of silica gel (10% EtOAc in hexane); ^{1}H NMR ($CDCl_3$, 500 MHz): δ 7.74 (d, 2H, J = 8.5 Hz), 7.56 (d, 2H, J = 8.5 Hz), 7.34–7.27 (m, 5H), 7.18 (d, 2H, J = 7.0 Hz), 7.14–7.13 (m, 3H), 6.96 (s, 1H), 4.51 (s, 2H); ^{13}C{^{1}H} NMR ($CDCl_3$, 125 MHz): δ 162.1, 153.9, 152.2, 146.1, 140.7, 138.1, 136.2, 131.4, 130.1, 129.7, 129.2, 127.7, 127.6, 127.4, 126.4, 116.9, 106.6, 98.2, 94.3; IR (KBr, cm^{-1}): 3462, 3386, 2955, 2922, 2852, 1624, 1457, 1155, 1003, 878, 781; HRMS (ESI/Q-TOF) (m/z) calcd for $C_{25}H_{18}IN_2O$ $[M + H]^+$ 489.0458; found 489.0472.

***5,6-Diphenyl-2-(4-(trifluoromethyl)phenyl)furo[2,3-b]pyridin-4-amine (9a)*:**

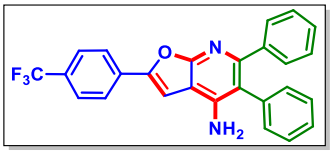

As a white solid (83 mg, 78% yield, mp 240–242 °C); Purification over a column of silica gel (10% EtOAc in hexane); ^{1}H NMR ($CDCl_3$, 500 MHz): δ 7.97 (d, 2H, J = 8.0 Hz), 7.69 (d, 2H, J = 8.0 Hz), 7.35 (t, 2H, J = 7.2 Hz), 7.32–7.28 (m, 3H), 7.20 (d, 2H, J = 7.0 Hz), 7.16–7.15 (m, 3H), 7.09 (s, 1H), 4.52 (s, 2H); ^{13}C{^{1}H} NMR ($CDCl_3$, 125 MHz): δ 162.3, 154.6, 151.6, 146.3, 140.7, 136.2, 133.5, 131.5, 130.2, 129.3, 127.8, 127.7, 127.5, 126.1 (q, J_1 = 3.8 Hz, J_2 = 7.7 Hz), 124.9, 117.1, 106.5, 99.5; ^{19}F NMR ($CDCl_3$): δ –62.7 (s); IR (KBr, cm^{-1}): 3461, 3396, 2956, 2922, 2851, 1619, 1458, 1166, 1068, 881, 782; HRMS (ESI/Q-TOF) (m/z) calcd for $C_{26}H_{18}F_3N_2O$ $[M + H]^+$ 431.1366; found 431.1388.

***2-(4-Nitrophenyl)-5,6-diphenylfuro[2,3-b]pyridin-4-amine (10a)*:**

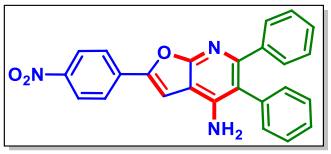

As a yellow solid (81 mg, 80% yield, mp 261–263 °C); Purification over a column of silica gel (15% EtOAc in hexane); ^{1}H NMR ($CDCl_3$, 500 MHz): δ 8.28 (d, 2H, J = 8.5 Hz), 7.97 (d, 2H, J = 8.5 Hz), 7.35 (t, 2H, J = 7.2 Hz), 7.32–7.28 (m, 3H), 7.20 (d, 2H, J = 7.0 Hz), 7.18 (s, 1H), 7.16–7.15 (m, 3H), 4.62 (s, 2H); ^{13}C{^{1}H} NMR ($CDCl_3$, 125 MHz): δ 162.5, 155.2, 150.6, 147.4, 146.6, 140.5, 136.1, 135.9, 131.4, 130.1, 129.4, 127.9, 127.73, 127.69, 125.1, 124.6, 117.2, 106.5, 101.5; IR (KBr, cm^{-1}): 3434, 3300, 2956, 2922, 2851, 1629, 1458, 1159, 1045, 802, 759; HRMS (ESI/Q-TOF) (m/z) calcd for $C_{25}H_{18}N_3O_3$ $[M + H]^+$ 408.1343; found 408.1346.

***2-(Naphthalen-2-yl)-5,6-diphenylfuro[2,3-b]pyridin-4-amine (11a)*:**

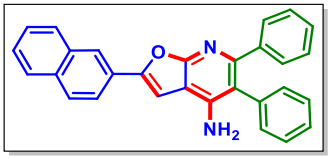

As a white solid (74 mg, 72% yield, mp 214–216 °C); Purification over a column of silica gel (10% EtOAc in hexane); ^{1}H NMR ($CDCl_3$, 500 MHz): δ 8.41 (s, 1H), 7.90–7.85 (m, 3H), 7.82 (d, 1H, J = 8.0 Hz), 7.52–7.46 (m, 2H), 7.36–7.33 (m, 4H), 7.28 (t, 1H, J = 7.2 Hz), 7.21 (d, 2H, J = 7.0 Hz), 7.16–7.15 (m, 3H), 7.05 (s, 1H), 4.49 (s, 2H); ^{13}C{^{1}H} NMR ($CDCl_3$, 125 MHz): δ 162.2, 153.7, 153.4, 145.9, 140.8, 136.4, 133.7, 133.5, 131.5, 130.2, 129.2, 128.71, 128.69, 127.9, 127.65, 127.61, 127.5, 127.4, 126.9, 126.7, 124.1, 122.5, 116.9, 106.8, 98.0; IR (KBr, cm^{-1}): 3462, 3394, 2956, 2922, 2851, 1626, 1458, 1159, 1037, 880, 781; HRMS (ESI/Q-TOF) (m/z) calcd for $C_{29}H_{21}N_2O$ $[M + H]^+$ 413.1648; found 413.1674.

***2-(Benzo[d][1,3]dioxol-5-yl)-5,6-diphenylfuro[2,3-b]pyridin-4-amine (12a)*:**

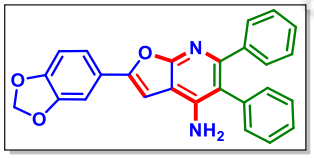

As a white solid (62 mg, 61% yield, mp 253–255 °C); Purification over a column of silica gel (10% EtOAc in hexane); ^{1}H NMR ($CDCl_3$, 500 MHz): δ 7.42 (d, 1H, J = 8.0 Hz), 7.36–7.28 (m, 6H), 7.20 (d, 2H, J = 7.0 Hz), 7.15–7.14 (m, 3H), 6.89 (d, 1H, J = 8.5 Hz), 6.79 (s, 1H), 6.02 (s, 2H), 4.42 (s, 2H); ^{13}C{^{1}H} NMR ($CDCl_3$, 125 MHz): δ 161.9, 153.32, 153.29, 148.4, 148.3, 145.6, 140.8, 136.4, 131.5, 130.2, 129.2, 127.65, 127.63, 127.3, 124.6, 119.2, 117.0, 109.0, 106.8, 105.4, 101.6, 96.1; IR (KBr, cm^{-1}): 3444, 3392, 2956, 2922, 2852, 1618, 1484, 1107, 1039, 874, 779; HRMS (ESI/Q-TOF) (m/z) calcd for $C_{26}H_{19}N_2O_3$ $[M + H]^+$ 407.1390; found 407.1390.

***5,6-Diphenyl-2-(thiophen-2-yl)furo[2,3-b]pyridin-4-amine (13a)*:**

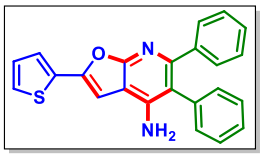

As a white solid (50 mg, 55% yield, mp 208–210 °C); Purification over a column of silica gel (10% EtOAc in hexane); ^{1}H NMR ($CDCl_3$, 400 MHz): δ 7.51 (s, 1H), 7.35–7.28 (m, 6H), 7.19 (d, 2H, J = 6.4 Hz), 7.15–7.13 (m, 3H), 7.10–7.08 (m, 1H), 6.78 (s, 1H), 4.46 (s, 2H); ^{13}C{^{1}H} NMR ($CDCl_3$, 100 MHz): δ 161.7, 153.5, 148.8, 145.7, 140.7, 136.3, 133.2, 131.4, 130.2, 129.2, 128.2, 127.65, 127.60, 127.4, 125.9, 124.9, 117.0, 106.6, 97.2; IR (KBr, cm^{-1}): 3456, 3387, 2956, 2922, 2851, 1617, 1261, 1156, 1047, 850, 780; HRMS (ESI/Q-TOF) (m/z) calcd for $C_{23}H_{17}N_2OS$ $[M + H]^+$ 369.1056; found 369.1059.

***8,9-Diphenylnaphtho[2',1':4,5]furo[2,3-b]pyridin-7-amine (14a)*:**

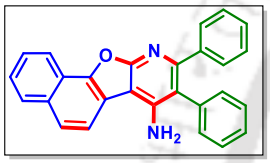

As a white solid (58 mg, 60% yield, mp 221–223 °C); Purification over a column of silica gel (10% EtOAc in hexane); ^{1}H NMR ($CDCl_3$, 400 MHz): δ 8.50 (d, 1H, J = 8.0 Hz), 7.99 (d, 1H, J = 8.4 Hz), 7.83 (q, 2H, J_1 = 8.4 Hz, J_2 = 12.4 Hz), 7.67 (t, 1H, J = 7.0 Hz), 7.58 (t, 1H, J = 7.0 Hz), 7.41–7.33 (m, 5H), 7.28–7.26 (m, 2H), 7.19–7.18 (m, 3H), 4.81 (s, 2H); ^{13}C{^{1}H} NMR ($CDCl_3$, 100 MHz): δ 163.2, 154.7, 149.5, 147.8, 140.6, 135.9, 132.4, 131.6, 130.3, 129.4, 128.5, 127.9, 127.7, 127.6, 127.0, 126.3, 123.9, 121.4, 121.3, 118.4, 117.9, 117.8, 101.7; IR (KBr, cm^{-1}): 3435, 3360, 2956, 2921, 2851, 1621, 1458, 880, 728; HRMS (ESI/Q-TOF) (m/z) calcd for $C_{27}H_{19}N_2O$ $[M + H]^+$ 387.1492; found 387.1514.

***2-Phenyl-5,6-di-p-tolylfuro[2,3-b]pyridin-4-amine (1b)*:**

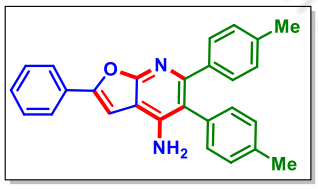

As a white solid (77 mg, 79% yield, mp 210–212 °C); Purification over a column of silica gel (10% EtOAc in hexane); ^{1}H NMR ($CDCl_3$, 500 MHz): δ 7.84 (d, 2H, J = 7.5 Hz), 7.40 (t, 2H, J = 7.8 Hz), 7.32 (t, 1H, J = 7.2 Hz), 7.23 (d, 2H, J = 8.0 Hz), 7.14 (d, 2H, J = 8.0 Hz), 7.07 (d, 2H, J = 8.0 Hz), 6.96 (d, 2H, J = 8.0 Hz), 6.91 (s, 1H), 4.48 (s, 2H), 2.35 (s, 3H), 2.26 (s, 3H); ^{13}C{^{1}H} NMR ($CDCl_3$, 125 MHz): δ 162.1, 153.5, 153.0, 146.1, 138.1, 137.1, 136.9, 133.4, 131.2, 130.3, 130.0, 129.9, 128.9, 128.6, 128.3, 124.8, 116.7, 106.5, 97.5, 21.4, 21.3; IR (KBr, cm^{-1}): 3465, 3388, 2956, 2921, 2852, 1624, 1451, 1166, 1019, 825, 784; HRMS (ESI/Q-TOF) (m/z) calcd for $C_{27}H_{23}N_2O$ $[M + H]^+$ 391.1805; found 391.1818.

***2-Phenyl-5,6-di-m-tolylfuro[2,3-b]pyridin-4-amine (1c)*:**

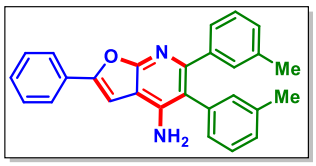

As a white solid (75 mg, 77% yield, mp 108–110 °C); Purification over a column of silica gel (10% EtOAc in hexane); ^{1}H NMR ($CDCl_3$, 500 MHz): δ 7.87 (d, 2H, J = 7.0 Hz), 7.43 (t, 2H, J = 7.8 Hz), 7.34 (t, 1H, J = 7.5 Hz), 7.27 (s, 1H), 7.22 (t, 1H, J = 7.5 Hz), 7.08 (d, 1H, J = 7.5 Hz), 7.04–6.99 (m, 2H), 6.98–6.96 (m, 3H), 6.94 (s, 1H), 4.47 (s, 2H), 2.29 (s, 3H), 2.23 (s, 3H); ^{13}C{^{1}H} NMR ($CDCl_3$, 125 MHz): δ 162.0, 153.7, 153.2, 145.9, 140.7, 138.7, 137.1, 136.4, 131.9, 130.9, 130.4, 129.04, 129.00, 128.7, 128.5, 128.3, 128.0, 127.3, 127.2, 124.9, 117.1, 106.6, 97.4, 21.6, 21.5; IR (KBr, cm^{-1}): 3465, 3394, 2955, 2921, 2851, 1626, 1455, 1156, 1039, 831, 794; HRMS (ESI/Q-TOF) (m/z) calcd for $C_{27}H_{23}N_2O$ $[M + H]^+$ 391.1805; found 391.1818.

***5,6-Bis(4-methoxyphenyl)-2-phenylfuro[2,3-b]pyridin-4-amine (1d)*:**

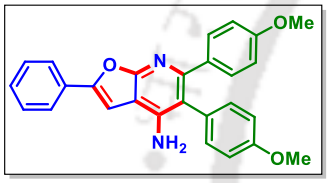

As a white solid (86 mg, 82% yield, mp 178–180 °C); Purification over a column of silica gel (10% EtOAc in hexane); ^{1}H NMR ($CDCl_3$, 500 MHz): δ 7.85 (d, 2H, J = 7.0 Hz), 7.41 (t, 2H, J = 7.8 Hz), 7.32 (t, 1H, J = 7.2 Hz), 7.26 (d, 2H, J = 9.0 Hz), 7.09 (d, 2H, J = 8.5 Hz), 6.91 (s, 1H), 6.88 (d, 2H, J = 8.5 Hz), 6.69 (d, 2H, J = 9.0 Hz), 4.45 (s, 2H), 3.79 (s, 3H), 3.73 (s, 3H); ^{13}C{^{1}H} NMR ($CDCl_3$, 125 MHz): δ 162.1, 159.0, 158.9, 153.4, 153.0, 146.2, 133.5, 132.5, 131.5, 130.4, 128.9, 128.63, 128.56, 124.8, 116.2, 114.8, 113.1, 106.4, 97.5, 55.4, 55.3; IR (KBr, cm^{-1}): 3465, 3381, 2956, 2922, 2852, 1623, 1488, 1173, 1021, 880, 760; HRMS (ESI/Q-TOF) (m/z) calcd for $C_{27}H_{23}N_2O_3$ $[M + H]^+$ 423.1703; found 423.1726.

***5,6-Bis(4-(tert-butyl)phenyl)-2-phenylfuro[2,3-b]pyridin-4-amine(1e)*:**

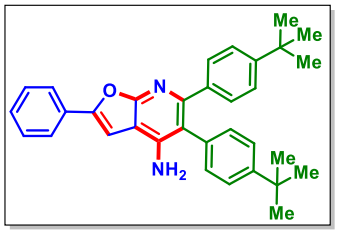

As a white solid (95 mg, 80% yield, mp 226–228 °C); Purification over a column of silica gel (10% EtOAc in hexane); ^{1}H NMR ($CDCl_3$, 500 MHz): δ 7.87 (d, 2H, J = 7.0 Hz), 7.43 (t, 2H, J = 7.8 Hz), 7.35–7.31 (m, 3H), 7.23 (d, 2H, J = 8.5 Hz), 7.13 (t, 4H, J = 9.2 Hz), 6.93 (s, 1H), 4.48 (s, 2H), 1.32 (s, 9H), 1.24 (s, 9H); ^{13}C{^{1}H} NMR ($CDCl_3$, 125 MHz): δ 162.1, 153.8, 153.1, 150.5, 150.1, 145.9, 137.9, 133.4, 131.1, 130.4, 129.8, 128.9, 128.6, 125.9, 124.9, 124.4, 116.8, 106.5, 97.5, 34.7, 34.6, 31.5, 31.4; IR (KBr, cm^{-1}): 3469, 3392, 2956, 2923, 2853, 1619, 1458, 1169, 1020, 839, 787; HRMS (ESI/Q-TOF) (m/z) calcd for $C_{33}H_{35}N_2O$ $[M + H]^+$ 475.2744; found 475.2766.

***5,6-Bis(4-fluorophenyl)-2-phenylfuro[2,3-b]pyridin-4-amine (1f)*:**

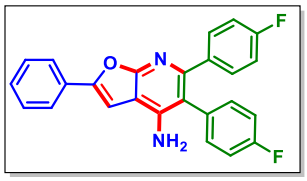

As a white solid (72 mg, 73% yield, mp 238–240 °C); Purification over a column of silica gel (10% EtOAc in hexane); ^{1}H NMR ($CDCl_3$, 500 MHz): δ 7.86 (d, 2H, J = 7.5 Hz), 7.42 (t, 2H, J = 7.8 Hz), 7.34 (t, 1H, J = 7.2 Hz), 7.26–7.23 (m, 2H), 7.15–7.12 (m, 2H), 7.04 (t, 2H, J = 8.5 Hz), 6.94 (s, 1H), 6.85 (t, 2H, J = 8.7 Hz), 4.46 (s, 2H); ^{13}C{^{1}H} NMR ($CDCl_3$, 125 MHz): δ 162.33 (d, J = 246.0 Hz), 162.27 (d, J = 245.0 Hz), 162.1, 153.6, 152.7, 146.0, 136.8, 136.7, 133.1 (d, J = 8.0 Hz), 132.1, 132.0, 131.8 (d, J = 8.0 Hz), 130.1, 129.1, 128.9, 124.9, 116.4 (d, J = 21.2 Hz), 115.7, 114.7 (d, J = 21.2 Hz), 106.8, 97.3; ^{19}F NMR ($CDCl_3$): δ –113.9 (s), –114.7 (s); IR (KBr, cm^{-1}): 3460, 3370, 2955, 2921, 2851, 1622, 1485, 1158, 1098, 838, 784; HRMS (ESI/Q-TOF) (m/z) calcd for $C_{25}H_{17}F_2N_2O$ $[M + H]^+$ 399.1303; found 399.1300.

***5,6-Bis(3-fluorophenyl)-2-phenylfuro[2,3-b]pyridin-4-amine (1g)*:**

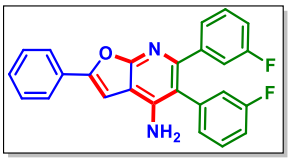

As a white solid (70 mg, 71% yield, mp 168–170 °C); Purification over a column of silica gel (10% EtOAc in hexane); ^{1}H NMR ($CDCl_3$, 500 MHz): δ 7.87 (d, 2H, J = 8.0 Hz), 7.44 (t, 2H, J = 7.5 Hz), 7.37–7.31 (m, 2H), 7.14–7.09 (m, 1H), 7.07–7.04 (m, 2H), 7.02–6.99 (m, 2H), 6.96 (s, 1H), 6.92 (d, 1H, J = 9.5 Hz), 6.88 (t, 1H, J = 9.0 Hz), 4.52 (s, 2H); ^{13}C{^{1}H} NMR ($CDCl_3$, 125 MHz): δ 163.4 (d, J = 246.0 Hz), 162.4 (d, J = 243.5 Hz), 162.1, 153.8, 152.11, 152.09, 145.8, 142.8 (d, J = 7.6 Hz), 138.3 (d, J = 7.6 Hz), 130.9 (d, J = 8.3 Hz), 130.0, 129.2 (d, J = 8.1 Hz), 129.1, 129.0, 127.24, 127.22, 125.83, 125.81, 124.9, 118.3 (d, J = 20.8 Hz), 117.5 (d, J = 22.4 Hz), 115.70, 115.69, 115.1, 114.9, 114.6, 114.5, 107.1; ^{19}F NMR ($CDCl_3$): δ –111.6 (s), –114.0 (s); IR (KBr, cm^{-1}): 3468, 3328, 2956, 2923, 2852, 1618, 1435, 1184, 1115, 1076, 877, 706; HRMS (ESI/Q-TOF) (m/z) calcd for $C_{25}H_{17}F_2N_2O$ $[M + H]^+$ 399.1303; found 399.1300.

***5,6-Bis(4-chlorophenyl)-2-phenylfuro[2,3-b]pyridin-4-amine (1h)*:**

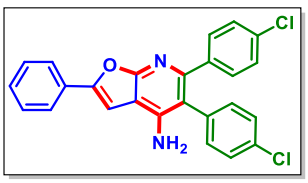

As a white solid (75 mg, 70% yield, mp 245–247 °C); Purification over a column of silica gel (10% EtOAc in hexane); ^{1}H NMR ($CDCl_3$, 500 MHz): δ 7.87 (d, 2H, J = 7.5 Hz), 7.44 (t, 2H, J = 7.8 Hz), 7.37–7.33 (m, 3H), 7.22 (d, 2H, J = 8.5 Hz), 7.16–7.12 (m, 4H), 6.95 (s, 1H), 4.46 (s, 2H); ^{13}C{^{1}H} NMR ($CDCl_3$, 125 MHz): δ 162.2, 153.8, 152.3,

145.8, 139.0, 134.6, 133.9, 133.6, 132.8, 131.5, 130.1, 129.7, 129.1, 129.0, 128.0, 124.9, 115.6, 106.9, 97.3; IR (KBr, cm^{-1}): 3442, 3368, 2955, 2920, 2852, 1628, 1450, 1167, 1089, 882, 757; HRMS (ESI/Q-TOF) (m/z) calcd for $C_{25}H_{17}Cl_2N_2O$ $[M + H]^+$ 431.0712; found 431.0716.

***5,6-Bis(3-chlorophenyl)-2-phenylfuro[2,3-b]pyridin-4-amine (1i)*:**

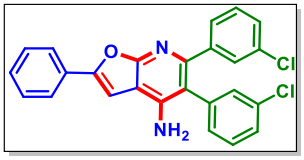

As a white solid (73 mg, 68% yield, mp 114–116 °C); Purification over a column of silica gel (10% EtOAc in hexane); ^1H NMR ($CDCl_3$, 500 MHz): δ 7.87 (d, 2H, J = 7.5 Hz), 7.44 (t, 2H, J = 7.5 Hz), 7.41 (s, 1H), 7.36 (t, 1H, J = 7.5 Hz), 7.29–7.28 (m, 2H), 7.24 (s, 1H), 7.17–7.15 (m, 1H), 7.08–7.05 (m, 3H), 6.96 (s, 1H), 4.50 (s, 2H); $^{13}C\{^1H\}$ NMR ($CDCl_3$, 125 MHz): δ 162.1, 153.9, 151.9, 145.8, 142.2, 137.9, 135.2, 133.8, 131.3, 130.7, 130.2, 130.0, 129.8, 129.1, 129.0, 128.9, 128.3, 128.2, 127.8, 124.9, 115.6, 107.1, 97.3; IR (KBr, cm^{-1}): 3466, 3397, 2956, 2922, 2852, 1624, 1451, 1171, 1078, 882, 793; HRMS (ESI/Q-TOF) (m/z) calcd for $C_{25}H_{17}Cl_2N_2O$ $[M + H]^+$ 431.0712; found 431.0715.

***5,6-Bis(4-bromophenyl)-2-phenylfuro[2,3-b]pyridin-4-amine (1j)*:**

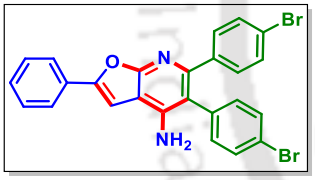

As a white solid (84 mg, 65% yield, mp 260–262 °C); Purification over a column of silica gel (10% EtOAc in hexane); ^1H NMR ($CDCl_3$, 500 MHz): δ 7.87 (d, 2H, J = 7.0 Hz), 7.50 (d, 2H, J = 8.5 Hz), 7.44 (t, 2H, J = 7.5 Hz), 7.36 (t, 1H, J = 7.2 Hz), 7.31 (d, 2H, J = 8.5 Hz), 7.17 (d, 2H, J = 8.5 Hz), 7.07 (d, 2H, J = 8.5 Hz), 6.95 (s, 1H), 4.45 (s, 2H); $^{13}C\{^1H\}$ NMR ($CDCl_3$, 125 MHz): δ 162.2, 153.8, 152.2, 145.8, 139.5, 135.1, 133.1, 132.7, 131.8, 131.0, 130.0, 129.1, 129.0, 124.9, 122.2, 122.0, 115.6, 107.0, 97.3; IR (KBr, cm^{-1}): 3444, 3310, 2956, 2922, 2852, 1633, 1456, 1121, 1071, 880, 771; HRMS (ESI/Q-TOF) (m/z) calcd for $C_{25}H_{17}Br_2N_2O$ $[M + H]^+$ 518.9702; found 518.9736.

***2-Phenyl-5,6-bis(4-(trifluoromethyl)phenyl)furo[2,3-b]pyridin-4-amine (1k)*:**

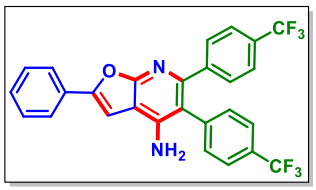

As a white solid (75 mg, 61% yield, mp 172–174 °C); Purification over a column of silica gel (10% EtOAc in hexane); ^1H NMR ($CDCl_3$, 500 MHz): δ 7.89 (d, 2H, J = 8.5 Hz), 7.64 (d, 2H, J = 8.0 Hz), 7.48–7.43 (m, 4H), 7.40–7.38 (m, 3H), 7.35 (d, 2H, J = 8.0 Hz), 6.99 (s, 1H), 4.48 (s, 2H); $^{13}C\{^1H\}$ NMR ($CDCl_3$, 125 MHz): δ 162.3, 154.2, 151.9,

145.8, 143.9, 140.0, 131.9, 130.4, 129.9, 129.22, 129.20, 129.15, 126.4 (q, J_1 = 3.8 Hz, J_2 = 7.6 Hz), 125.0, 124.8 (q, J_1 = 3.8 Hz, J_2 = 7.6 Hz), 115.7, 107.4, 97.2; ^{19}F NMR ($CDCl_3$): δ –62.56 (s), –62.63 (s); IR (KBr, cm^{-1}): 3472, 3399, 2956, 2922, 2851, 1619, 1457, 1166, 1069, 849, 785; HRMS (ESI/Q-TOF) (m/z) calcd for $C_{27}H_{17}F_6N_2O$ $[M + H]^+$ 499.1240; found 499.1241.

***6-(4-Methoxyphenyl)-2-phenyl-5-(p-tolyl)furo[2,3-b]pyridin-4-amine (1l)*:**

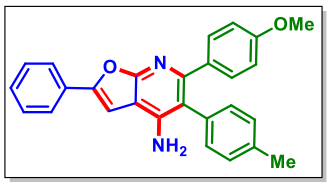

As a white solid (79 mg, 78% yield, mp 198–200 °C); Purification over a column of silica gel (10% EtOAc in hexane); ^{1}H NMR ($CDCl_3$, 500 MHz): δ 7.83 (d, 2H, J = 7.5 Hz), 7.39 (t, 2H, J = 7.8 Hz), 7.31 (t, 1H, J = 7.5 Hz), 7.26 (d, 2H, J = 8.5 Hz), 7.14 (d, 2H, J = 8.0 Hz), 7.06 (d, 2H, J = 8.0 Hz), 6.90 (s, 1H), 6.67 (d, 2H, J = 9.0 Hz), 4.47 (s, 2H), 3.72 (s, 3H), 2.33 (s, 3H); ^{13}C{^{1}H} NMR ($CDCl_3$, 125 MHz): δ 162.0, 158.9, 153.2, 152.9, 146.0, 137.1, 133.5, 133.4, 131.4, 131.2, 130.3, 130.0, 128.9, 128.6, 124.8, 116.5, 113.0, 106.4, 97.5, 55.3, 21.4; IR (KBr, cm^{-1}): 3443, 3392, 2957, 2923, 2853, 1620, 1451, 1167, 1036, 834, 759; HRMS (ESI/Q-TOF) (m/z) calcd for $C_{27}H_{23}N_2O_2$ $[M + H]^+$ 407.1754; found 407.1759.

***Mixture of 5-(4-fluorophenyl)-2-phenyl-6-(p-tolyl)furo[2,3-b]pyridin-4-amine (1m) and 6-(4-fluorophenyl)-2-phenyl-5-(p-tolyl)furo[2,3-b]pyridin-4-amine (1m')*:**

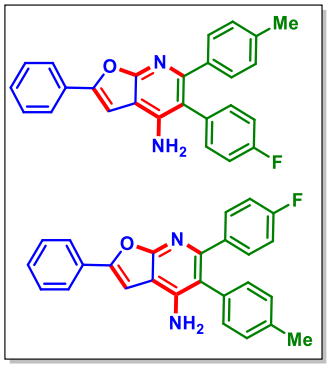

As a white solid (73 mg, 75% combined yield); Purification over a column of silica gel (10% EtOAc in hexane); ^{1}H NMR ($CDCl_3$, 500 MHz): δ 7.86 (d, 3H, J = 7.5 Hz), 7.42 (t, 3.40H, J = 7.5 Hz), 7.34 (t, 1.76H, J = 7.2 Hz), 7.31–7.28 (m, 1H), 7.18–7.15 (m, 5.72H), 7.06–7.02 (m, 3.46H), 6.97 (d, 2.40H, J = 8.0 Hz), 6.94 (s, 1.44H), 6.84 (t, 0.78H, J = 8.7 Hz), 4.49 (s, 0.66H), 4.44 (s, 2H), 2.36 (s, 1H), 2.27 (s, 3H); ^{13}C{^{1}H} NMR ($CDCl_3$, 125 MHz): δ 162.24 (d, J = 44.9 Hz), 162.17, 162.0, 153.8, 153.32, 153.30, 152.5, 146.1, 145.9, 137.8, 137.5, 137.2, 137.04, 137.01, 133.2 (d, J = 7.8 Hz), 133.0, 132.42, 132.39, 131.9 (d, J = 8.0 Hz), 131.2, 130.2, 130.10. 130.09, 130.0, 129.0, 128.8, 128.5, 124.9, 116.8, 116.3 (d, J = 21.2 Hz), 115.7, 114.5 (d, J = 21.4 Hz), 106.7, 106.6, 97.41, 97.38, 21.4, 21.3; ^{19}F NMR ($CDCl_3$, 500 MHz): δ –114.36 (s), –115.06 (s); IR (KBr, cm^{-1}): 3485, 3391, 2958, 2921, 2853, 1615, 1451, 1113, 1040, 880, 783; HRMS (ESI/Q-TOF) (m/z) calcd for $C_{26}H_{20}FN_2O$ $[M + H]^+$ 395.1554; found 395.1564.

***5-(4-Bromophenyl)-6-(4-methoxyphenyl)-2-phenylfuro[2,3-b]pyridin-4-amine (1n)*:**

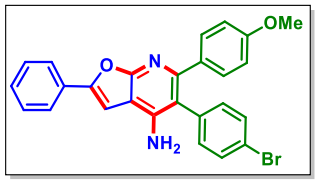

As a white solid (82 mg, 70% yield, mp 158–160 °C); Purification over a column of silica gel (10% EtOAc in hexane); ^{1}H NMR ($CDCl_3$, 400 MHz): δ 7.83 (d, 2H, J = 7.2 Hz), 7.46 (d, 2H, J = 8.4 Hz), 7.41 (t, 2H, J = 7.4 Hz), 7.32 (t, 1H, J = 7.2 Hz), 7.21 (d, 2H, J = 8.8 Hz), 7.05 (d, 2H, J = 8.4 Hz), 6.93 (s, 1H), 6.69 (d, 2H, J = 8.8 Hz), 4.48 (s, 2H), 3.74 (s, 3H); ^{13}C{^{1}H} NMR ($CDCl_3$, 100 MHz): δ 162.1, 159.0, 153.2, 153.1, 145.8, 135.6, 133.2, 132.9, 132.5, 131.4, 130.1, 129.0, 128.7, 124.8, 121.7, 115.2, 113.2, 106.5, 97.5, 55.3; IR (KBr, cm^{-1}): 3466, 3382, 2956, 2923, 2852, 1621, 1451, 1167, 1072, 879, 785; HRMS (ESI/Q-TOF) (m/z) calcd for $C_{26}H_{20}BrN_2O_2$ $[M + H]^+$ 471.0703; found 471.0713.

***5-Methyl-2,6-diphenylfuro[2,3-b]pyridin-4-amine (1o)*:**

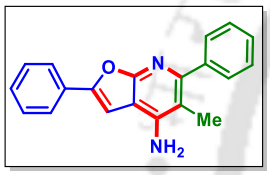

As a white solid (39 mg, 52% yield, mp 192–194 °C); Purification over a column of silica gel (10% EtOAc in hexane); ^{1}H NMR ($CDCl_3$, 500 MHz): δ 7.84 (d, 2H, J = 7.5 Hz), 7.51 (t, 2H, J = 7.8 Hz), 7.44–7.41 (m, 3H), 7.33 (t, 1H, J = 7.2 Hz), 7.29 (d, 2H, J = 7.5 Hz), 6.89 (s, 1H), 4.24 (s, 2H), 2.28 (s, 3H); ^{13}C{^{1}H} NMR ($CDCl_3$, 125 MHz): δ 161.9, 152.40, 152.35, 145.4, 136.6, 130.7, 130.4, 129.6, 129.0, 128.6, 128.1, 124.8, 117.5, 105.8, 97.3, 23.7; IR (KBr, cm^{-1}): 3453, 3397, 2956, 2923, 2852, 1628, 1463, 1122, 1043, 880, 783; HRMS (ESI/Q-TOF) (m/z) calcd for $C_{20}H_{17}N_2O$ $[M + H]^+$ 301.1335; found 301.1338.

***6-Methyl-2,5-diphenylfuro[2,3-b]pyridin-4-amine (1o')*:**

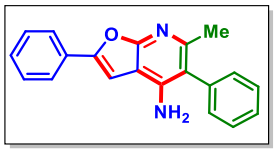

As a white solid (16 mg, 21% yield, mp 203–205 °C); Purification over a column of silica gel (10% EtOAc in hexane); ^{1}H NMR ($CDCl_3$, 500 MHz): δ 7.85 (d, 2H, J = 7.5 Hz), 7.53 (d, 2H, J = 7.0 Hz), 7.43 (q, 4H, J_1 = 7.5 Hz, J_2 = 15.5 Hz), 7.38 (t, 1H, J = 7.2 Hz), 7.33 (t, 1H, J = 7.5 Hz), 6.92 (s, 1H), 4.50 (s, 2H), 2.19 (s, 3H); ^{13}C{^{1}H} NMR ($CDCl_3$, 125 MHz): δ 161.3, 154.6, 153.1, 146.4, 141.4, 130.4, 129.7, 129.0, 128.7, 128.2, 127.8, 124.9, 109.4, 106.8, 96.9, 13.9; IR (KBr, cm^{-1}): 3463, 3365, 2955, 2923, 2853, 1632, 1457, 1119, 1071, 1041, 845, 756; HRMS (ESI/Q-TOF) (m/z) calcd for $C_{20}H_{17}N_2O$ $[M + H]^+$ 301.1335; found 301.1330.

***5-Ethyl-2,6-diphenylfuro[2,3-b]pyridin-4-amine (1p)*:**

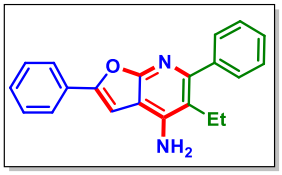

As a white solid (41 mg, 53% yield, mp 199–201 °C); Purification over a column of silica gel (10% EtOAc in hexane); ^{1}H NMR ($CDCl_3$, 500 MHz): δ 7.86 (d, 2H, J = 7.0 Hz), 7.50 (t, 2H, J = 7.8 Hz), 7.43 (t, 3H, J = 7.5 Hz), 7.34–7.29 (m, 3H), 6.89 (s, 1H), 4.21 (s, 2H), 2.54 (q, 2H, J_1 = 7.5 Hz, J_2 = 15.0 Hz), 1.17 (t, 3H, J = 7.5 Hz); ^{13}C{^{1}H} NMR ($CDCl_3$, 125 MHz): δ 162.3, 157.4, 152.4, 145.5, 136.4, 130.8, 130.4, 129.5, 128.9, 128.5, 128.0, 124.8, 117.1, 105.7, 97.3, 29.4, 14.2; IR (KBr, cm^{-1}): 3457, 3351, 2956, 2923, 2852, 1634, 1488, 1156, 1066, 813, 788; HRMS (ESI/Q-TOF) (m/z) calcd for $C_{21}H_{19}N_2O$ $[M + H]^+$ 315.1492; found 315.1491.

***6-Ethyl-2,5-diphenylfuro[2,3-b]pyridin-4-amine (1p')*:**

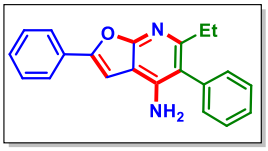

As a white solid (16 mg, 20% yield, mp 215–217 °C); Purification over a column of silica gel (10% EtOAc in hexane); ^{1}H NMR ($CDCl_3$, 500 MHz): δ 7.85 (d, 2H, J = 7.5 Hz), 7.49 (d, 2H, J = 7.0 Hz), 7.45–7.39 (m, 5H), 7.33 (t, 1H, J = 7.5 Hz), 6.93 (s, 1H), 4.54 (s, 2H), 2.59 (q, 2H, J_1 = 7.5 Hz, J_2 = 15.5 Hz), 1.16 (t, 3H, J = 7.5 Hz); ^{13}C{^{1}H} NMR ($CDCl_3$, 125 MHz): δ 161.0, 154.9, 153.1, 145.8, 141.7, 130.4, 129.1, 129.0, 128.7, 128.2, 127.8, 124.8, 115.8, 107.3, 96.9, 20.7, 13.6; IR (KBr, cm^{-1}): 3462, 3340, 2957, 2921, 2851, 1631, 1459, 1116, 1022, 880, 782; HRMS (ESI/Q-TOF) (m/z) calcd for $C_{21}H_{19}N_2O$ $[M + H]^+$ 315.1492; found 315.1509.

***2,6-Diphenylfuro[2,3-b]pyridin-4-amine (1q)*:**

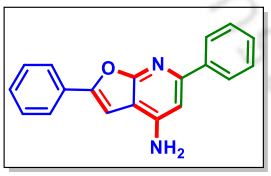

As a white solid (37 mg, 52% yield, mp 189–191 °C); Purification over a column of silica gel (15% EtOAc in hexane); ^{1}H NMR ($CDCl_3$, 400 MHz): δ 8.02 (d, 2H, J = 6.8 Hz), 7.88 (d, 2H, J = 7.2 Hz), 7.48–7.43 (m, 4H), 7.41–7.35 (m, 2H), 6.94 (s, 2H), 4.52 (s, 2H); ^{13}C{^{1}H} NMR ($CDCl_3$, 125 MHz): δ 163.8, 153.9, 153.1, 147.9, 139.7, 130.2, 129.0, 128.83, 128.78, 127.2, 124.9, 107.3, 102.1, 97.2; IR (KBr, cm^{-1}): 3393, 3339, 2960, 2922, 2892, 1626, 1481, 1113, 818, 749; HRMS (ESI/Q-TOF) (m/z) calcd for $C_{19}H_{15}N_2O$ $[M + H]^+$ 287.1179; found 287.1186.

***2-Phenyl-6-(p-tolyl)furo[2,3-b]pyridin-4-amine (1r)*:**

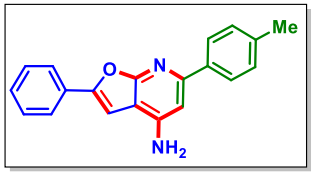

As a white solid (40 mg, 54% yield, mp 209–211 °C); Purification over a column of silica gel (15% EtOAc in hexane); ^{1}H NMR ($CDCl_3$,

500 MHz): δ 7.92 (d, 2H, J = 8.0 Hz), 7.87 (d, 2H, J = 7.5 Hz), 7.44 (t, 2H, J = 7.7 Hz), 7.34 (t, 1H, J = 7.2 Hz), 7.27 (s, 1H), 7.25 (s, 1H), 6.91 (d, 2H, J = 8.0 Hz), 4.49 (s, 2H), 2.40 (s, 3H); $^{13}C\{^{1}H\}$ NMR ($CDCl_3$, 125 MHz): δ 163.9, 154.0, 152.9, 147.9, 138.8, 136.9, 130.3, 129.5, 129.0, 128.7, 127.0, 124.9, 107.1, 101.7, 97.2, 21.5; IR (KBr, cm^{-1}): 3391, 3337, 2957, 2926, 2852, 1623, 1475, 1116, 1026, 858, 759; HRMS (ESI/Q-TOF) (m/z) calcd for $C_{20}H_{17}N_2O$ $[M + H]^+$ 301.1335; found 301.1336.

***6-(4-Bromophenyl)-2-phenylfuro[2,3-b]pyridin-4-amine (1s)*:**

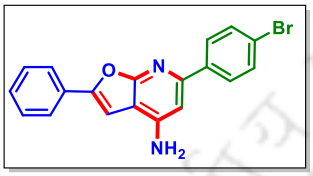

As a white solid (39 mg, 43% yield, mp 236–238 °C); Purification over a column of silica gel (15% EtOAc in hexane); ^{1}H NMR (DMSO-d_6, 400 MHz): δ 7.93 (d, 2H, J = 8.08 Hz), 7.80 (d, 2H, J = 7.2 Hz), 7.66 (d, 2H, J = 8.8 Hz), 7.53–7.49 (m, 2H), 7.41–7.37 (m, 2H), 6.98 (s, 1H), 6.77 (s, 2H); $^{13}C\{^{1}H\}$ NMR (DMSO-d_6, 100 MHz): δ 163.3, 150.9, 150.5, 150.2, 138.5, 131.6, 129.8, 129.2, 128.4, 128.3, 123.9, 121.9, 106.1, 100.2, 99.6; IR (KBr, cm^{-1}): 3381, 3327, 2955, 2923, 2852, 1628, 1407, 1113, 1026, 858, 759; HRMS (ESI/Q-TOF) (m/z) calcd for $C_{19}H_{14}BrN_2O$ $[M + H]^+$ 365.0824; found 365.0829.

***2-Amino-5-phenylfuran-3-carbonitrile (1')*:**

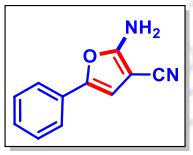

As a white solid (41 mg, 90% yield, mp 186–188 °C); Purification over a column of silica gel (15% EtOAc in hexane); ^{1}H NMR (DMSO-d_6, 400 MHz): δ 7.62 (s, 2H), 7.48 (d, 2H, J = 6.8 Hz), 7.36 (t, 2H, J = 7.8 Hz), 7.19 (t, 1H, J = 7.4 Hz), 6.98 (s, 1H); $^{13}C\{^{1}H\}$ NMR (DMSO-d_6, 100 MHz): δ 164.0, 141.8, 129.4, 128.8, 126.6, 122.1, 116.1, 106.7, 66.2; IR (KBr, cm^{-1}): 3412, 3324, 2956, 2921, 2851, 2205, 1646, 1490, 1173, 1066, 880, 759; HRMS (ESI/Q-TOF) (m/z) calcd for $C_{11}H_9N_2O$ $[M + H]^+$ 185.0709; found 185.0718.

***2,3-Diphenylquinolin-4-amine (15a)*:**

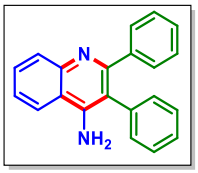

As a white solid (63 mg, 85% yield, mp 239–241 °C); Purification over a column of silica gel (30% EtOAc in hexane); ^{1}H NMR (DMSO-d_6, 500 MHz): δ 8.29 (d, 1H, J = 8.5 Hz), 7.86 (d, 1H, J = 8.0 Hz), 7.66 (t, 1H, J = 7.5 Hz), 5 Hz), 7.34 (t, 2H, J = 7.5 Hz), 7.28–7.23 (m, 3H), 7.18–7.14 (m, 5H), 6.05 (s, 2H); $^{13}C\{^{1}H\}$ NMR (DMSO-d_6, 125 MHz): δ 157.9, 148.6, 147.2, 141.7, 136.7, 131.2, 129.5, 129.2, 129.0, 128.8, 127.14, 127.08, 126.9, 124.2, 122.6, 117.3, 114.4; IR (KBr, cm^{-1}): 3431, 3301,

2956, 2922, 2852, 1615, 1493, 1113, 1073, 847, 760; HRMS (ESI/Q-TOF) (m/z) calcd for $C_{21}H_{17}N_2$ $[M + H]^+$ 297.1386; found 297.1391.

***12-Amino-2,5,6,11-tetraphenylfuro[3',2':5,6]pyrido[2,1-a]isoquinolin-4-ium (1aa)*:**

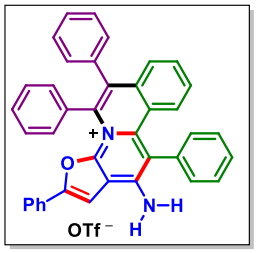

As a yellow solid (86 mg, 80% yield, mp 386–388 °C); Purification over a column of silica gel (2% MeOH in DCM); ^{1}H NMR (DMSO-d_6, 400 MHz): δ 8.95 (s, 1H), 7.78 (s, 1H), 7.75–7.67 (m, 3H), 7.58 (d, 2H, J = 8.0 Hz), 7.53 (t, 1H, J = 7.6 Hz), 7.45–7.41 (m, 3H), 7.34–7.28 (m, 9H), 7.19–7.13 (m, 4H), 6.85 (d, 2H, J = 8.0 Hz); ^{13}C{^{1}H} NMR (DMSO-d_6, 100 MHz): δ 152.7, 151.2, 148.8, 140.0, 135.1, 135.0, 134.5, 133.3, 132.3, 131.3, 131.0, 130.6, 130.5, 129.7, 129.6, 129.5, 128.9, 128.7, 128.1, 127.9, 127.7, 127.2, 126.9, 126.0, 124.3, 123.9, 122.3, 119.1, 114.9, 109.7, 99.7; IR (KBr, cm^{-1}): 3452, 3315, 3198, 2956, 2921, 2851, 1649, 1461, 1156, 1030, 879, 762; HRMS (ESI/Q-TOF) (m/z) calcd for $C_{39}H_{28}N_2O$ $[M + H]^+$ 540.2196; found 540.2195.

***(R)-3-(2-(4-Amino-2,5-diphenylfuro[2,3-b]pyridin-6-yl)phenyl)-1-propylpyrrolidine-2,5-dione (1aw)*:**

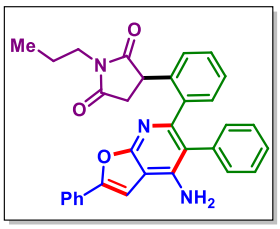

As a white solid (72 mg, 72% yield, mp 254–256 °C); Purification over a column of silica gel (15% EtOAc in hexane); ^{1}H NMR ($CDCl_3$, 400 MHz): δ 7.86 (d, 2H, J = 7.2 Hz), 7.45 (t, 2H, J = 7.4 Hz), 7.38–7.28 (m, 4H), 7.23–7.19 (m, 2H), 7.16–7.12 (m, 1H), 7.01 (d, 1H, J = 7.2 Hz), 6.98 (s, 1H), 6.96–6.88 (m, 2H), 4.56 (s, 2H), 4.27–4.24 (m, 1H), 3.44–3.38 (m, 2H), 3.30–3.23 (m, 1H), 2.99–2.93 (m, 1H), 1.56–1.53 (m, 2H), 0.87 (t, 3H, J = 7.6 Hz); ^{13}C{^{1}H} NMR ($CDCl_3$, 100 MHz): δ 175.8, 177.1, 161.4, 153.5, 152.9, 146.2, 140.5, 137.2, 135.4, 131.9, 131.6, 130.8, 130.1, 129.4, 129.1, 128.9, 128.8, 128.4, 127.6, 126.6, 124.9, 118.0, 106.9, 97.4, 44.4, 40.6, 39.2, 21.2, 11.5; IR (KBr, cm^{-1}): 3442, 3396, 2956, 2922, 2852, 1697, 1629, 1456, 1114, 1072, 728; HRMS (ESI/Q-TOF) (m/z) calcd for $C_{32}H_{28}N_3O_3$ $[M + H]^+$ 502.2125; found 502.2127.

***2-([1,1'-Biphenyl]-4-yl)-5,6-diphenylfuro[2,3-b]pyridin-4-amine (7ax)*:**

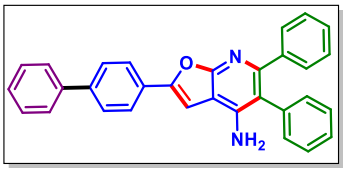

As a white solid (60 mg, 68% yield, mp 188–190 °C); Purification over a column of silica gel (10% EtOAc in hexane); ^{1}H NMR ($CDCl_3$, 400 MHz): δ 7.94 (d, 2H, J = 8.4 Hz), 7.68–7.62 (m, 4H),

7.46 (t, 2H, *J* = 7.4 Hz), 7.39–7.28 (m, 6H), 7.20 (d, 2H, *J* = 6.8 Hz), 7.16–7.14 (m, 3H), 6.99 (s, 1H), 4.49 (s, 2H); $^{13}C\{^{1}H\}$ NMR ($CDCl_3$, 100 MHz): δ 162.1, 153.6, 153.0, 145.9, 141.4, 140.8, 140.5, 136.3, 132.2, 131.5, 130.2, 129.2, 129.0, 127.7, 127.63, 127.61, 127.4, 127.1, 126.3, 125.3, 116.9, 106.8, 97.6; IR (KBr, cm^{-1}): 3466, 3393, 2955, 2922, 2852, 1620, 1456, 1168, 1072, 842, 781; HRMS (ESI/Q-TOF) (m/z) calcd for $C_{31}H_{23}N_2O$ $[M + H]^+$ 439.1805; found 439.1812.

***5,6-Diphenyl-2-(4-(p-tolylethynyl)phenyl)furo[2,3-b]pyridin-4-amine (7ay)*:**

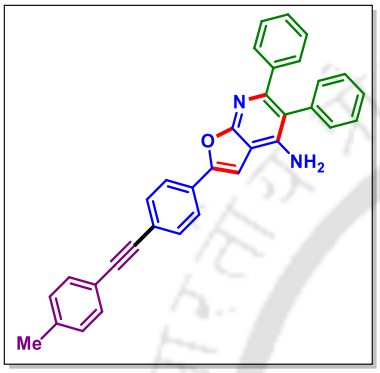

As a white solid (71 mg, 75% yield, mp 258–260 °C); Purification over a column of silica gel (10% EtOAc in hexane); ^{1}H NMR ($CDCl_3$, 400 MHz): δ 7.81 (d, 2H, *J* = 8.4 Hz), 7.56 (d, 2H, *J* = 8.4 Hz), 7.44 (d, 2H, *J* = 8.0 Hz), 7.35–7.28 (m, 5H), 7.21–7.14 (m, 7H), 6.95 (s, 1H), 4.51 (s, 2H), 2.38 (s, 3H); $^{13}C\{^{1}H\}$ NMR ($CDCl_3$, 100 MHz): δ 162.1, 153.8, 152.6, 145.9, 140.7, 138.8, 136.2, 132.1, 131.7, 131.4, 130.2, 129.6, 129.3, 129.2, 127.64, 127.61, 127.4, 124.6, 123.6, 120.2, 116.9, 106.7, 98.3, 91.4, 88.9, 21.7; IR (KBr, cm^{-1}): 3464, 3397, 2956, 2922, 2852, 2236, 1619, 1491, 1167, 880, 781; HRMS (ESI/Q-TOF) (m/z) calcd for $C_{34}H_{25}N_2O$ $[M + H]^+$ 477.1961; found 477.1961.

***(E)-2-(4-(4-Methylstyryl)phenyl)-5,6-diphenylfuro[2,3-b]pyridin-4-amine (7az)*:**

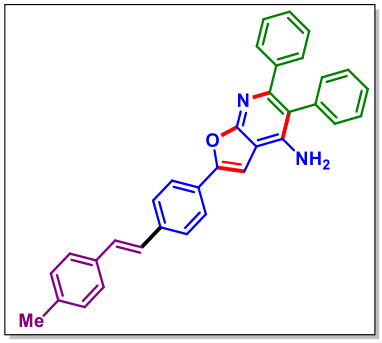

As a white solid (66 mg, 70% yield, mp 269–271 °C); Purification over a column of silica gel (10% EtOAc in hexane); ^{1}H NMR ($CDCl_3$, 400 MHz): δ 7.86 (d, 2H, *J* = 8.4 Hz), 7.57 (d, 2H, *J* = 8.4 Hz), 7.43 (d, 2H, *J* = 8.4 Hz), 7.34–7.28 (m, 6H), 7.20 (d, 3H, *J* = 8.0 Hz), 7.17–7.13 (m, 5H), 6.97 (s, 1H), 4.49 (s, 2H), 2.37 (s, 3H); $^{13}C\{^{1}H\}$ NMR ($CDCl_3$, 100 MHz): δ 162.1, 153.6, 153.2, 145.8, 140.8, 138.0, 137.9, 136.4, 134.6, 131.5, 130.2, 129.7, 129.4, 129.2, 129.1, 127.65, 127.63, 127.4, 127.0, 126.7, 125.1, 116.9, 106.8, 97.4, 21.5; IR (KBr, cm^{-1}): 3460, 3397, 2955, 2920, 2851, 1621, 1456, 1187, 1067, 881, 759; HRMS (ESI/Q-TOF) (m/z) calcd for $C_{34}H_{27}N_2O$ $[M + H]^+$ 479.2118; found 479.2129.

III.9. Representative NMR Spectra:

2,5,6-Triphenylfuro[2,3-b]pyridin-4-amine (1a): ^{1}H NMR ($CDCl_3$, 500 MHz)

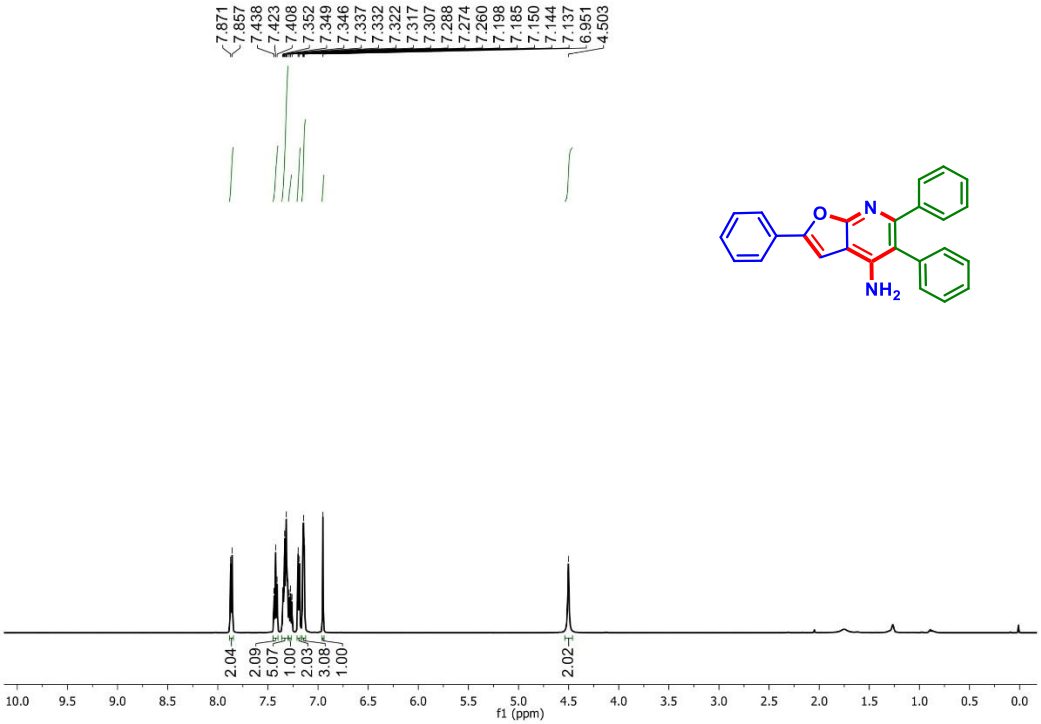

2,5,6-Triphenylfuro[2,3-b]pyridin-4-amine (1a):$^{13}C\{^{1}H\}$ NMR ($CDCl_3$, 125 MHz)

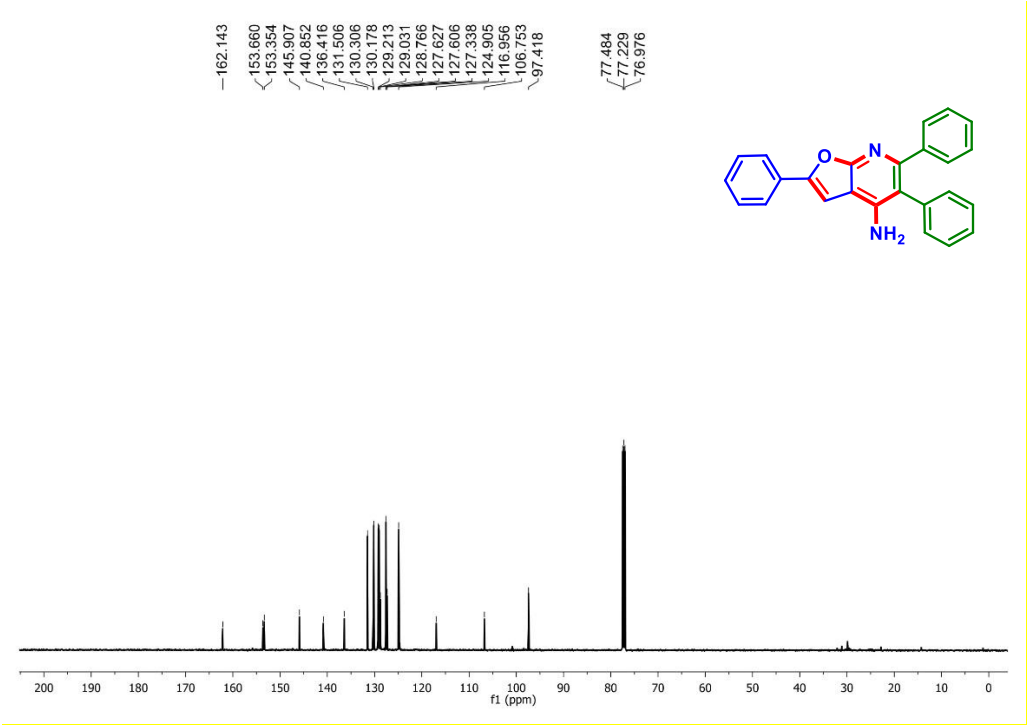

5,6-Diphenyl-2-(p-tolyl)furo[2,3-b]pyridin-4-amine (2a): ^{1}H NMR ($CDCl_3$, 500 MHz)

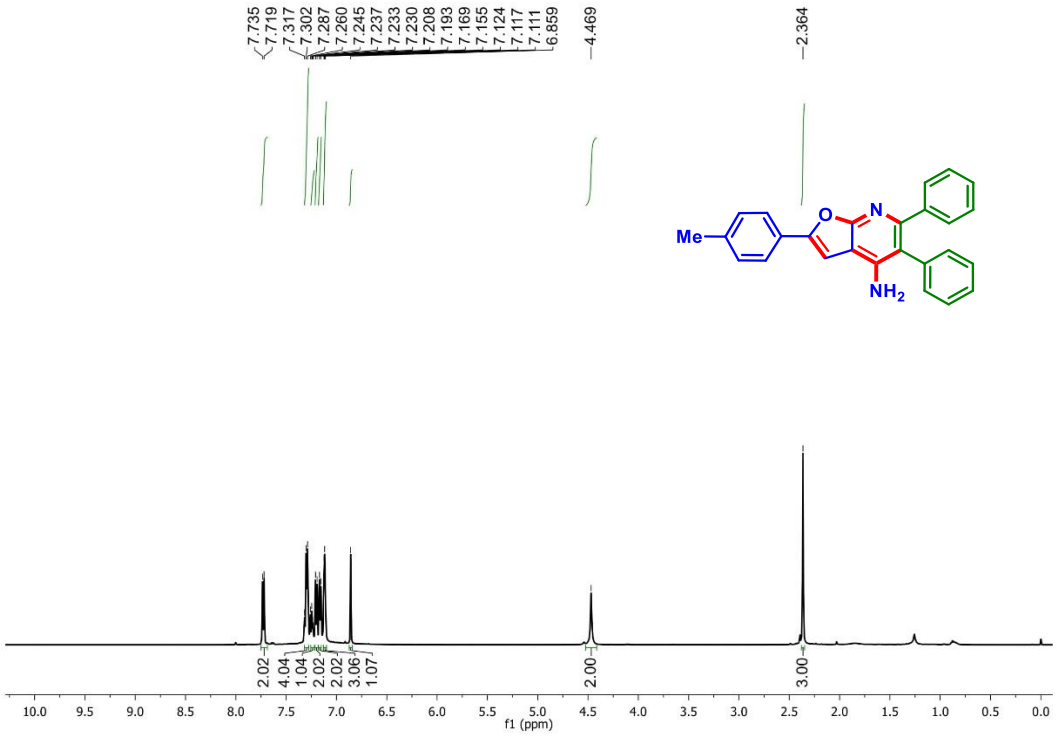

5,6-Diphenyl-2-(p-tolyl)furo[2,3-b]pyridin-4-amine (2a): $^{13}C\{^{1}H\}$ NMR ($CDCl_3$, 125 MHz)

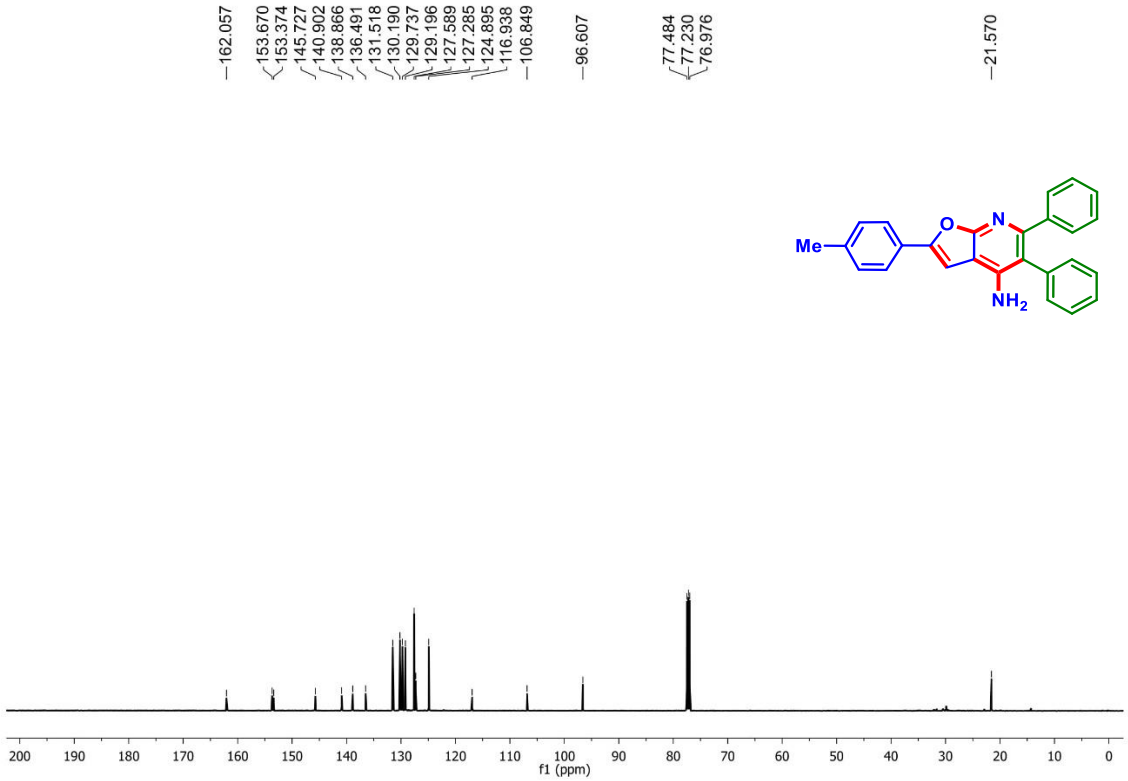

2-(4-Chlorophenyl)-5,6-diphenylfuro[2,3-b]pyridin-4-amine (6a): ^{1}H NMR ($CDCl_3$, 500 MHz)

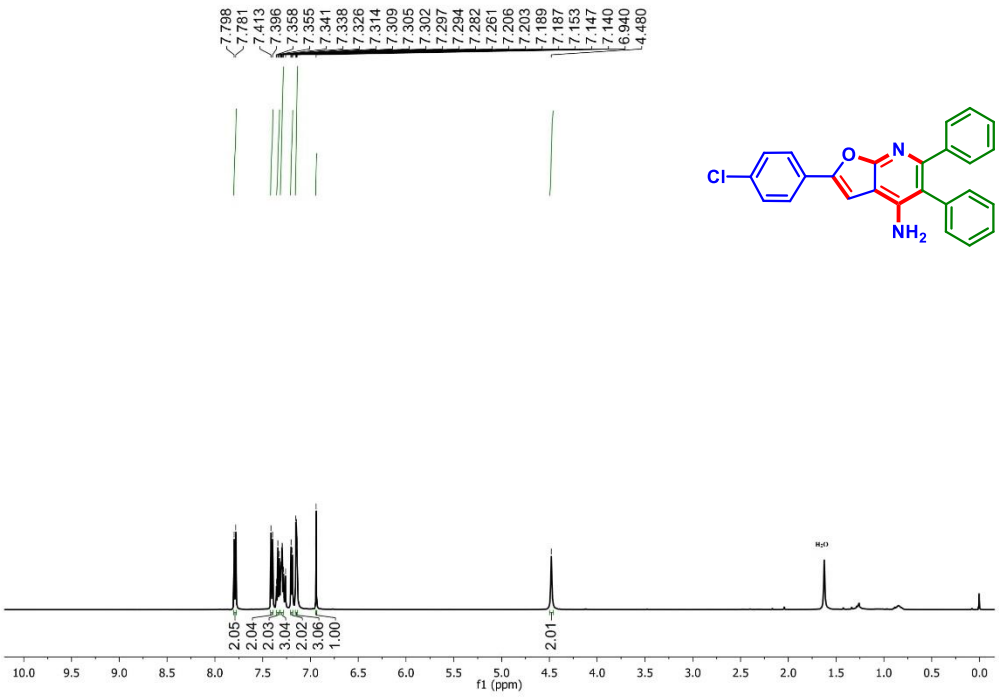

2-(4-Chlorophenyl)-5,6-diphenylfuro[2,3-b]pyridin-4-amine (6a): $^{13}C\{^{1}H\}$ NMR ($CDCl_3$, 125 MHz)

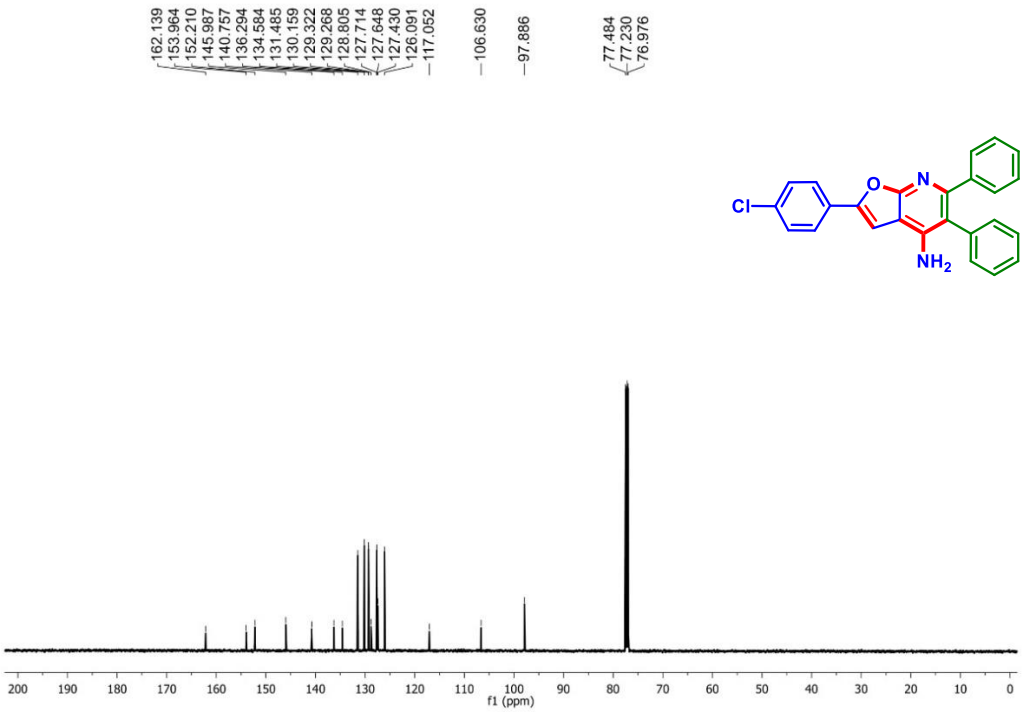

8,9-Diphenylnaphtho[2',1':4,5]furo[2,3-b]pyridin-7-amine (14a): ^{1}H NMR ($CDCl_3$, 400 MHz)

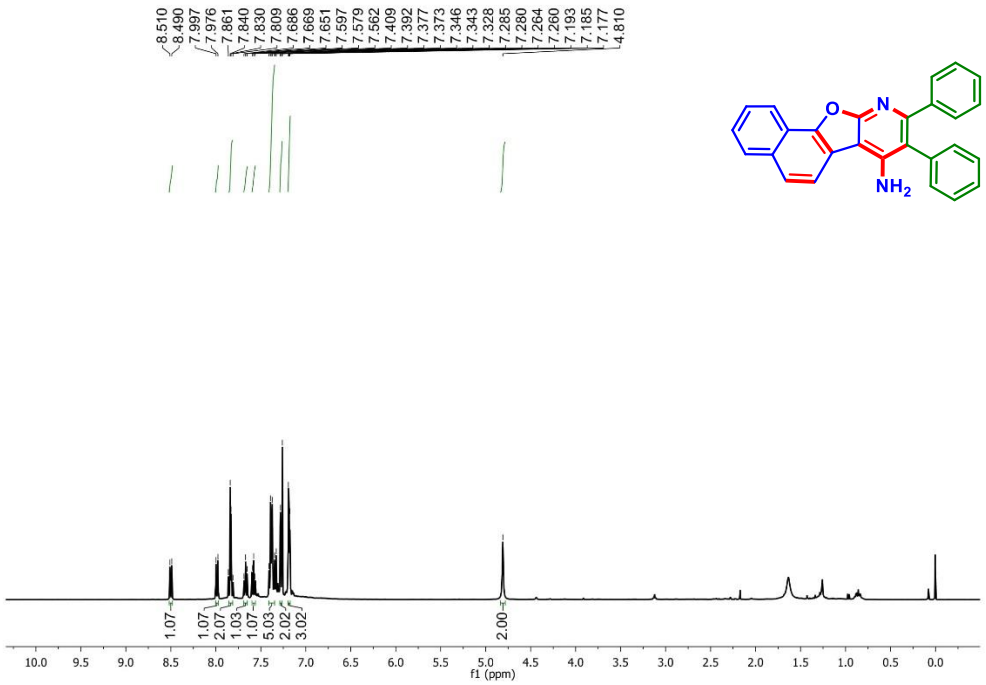

8,9-Diphenylnaphtho[2',1':4,5]furo[2,3-b]pyridin-7-amine (14a): $^{13}C\{^{1}H\}$ NMR ($CDCl_3$, 100 MHz)

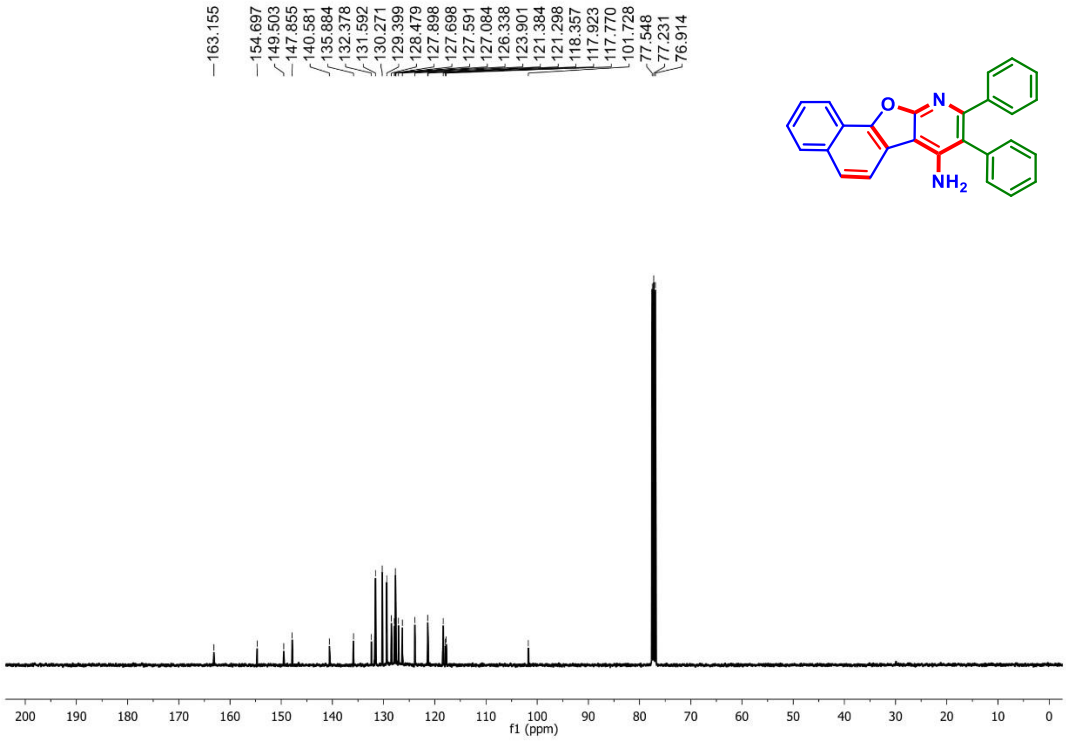

2-Phenyl-5,6-di-p-tolylfuro[2,3-b]pyridin-4-amine (1b): ^{1}H NMR ($CDCl_3$, 500 MHz)

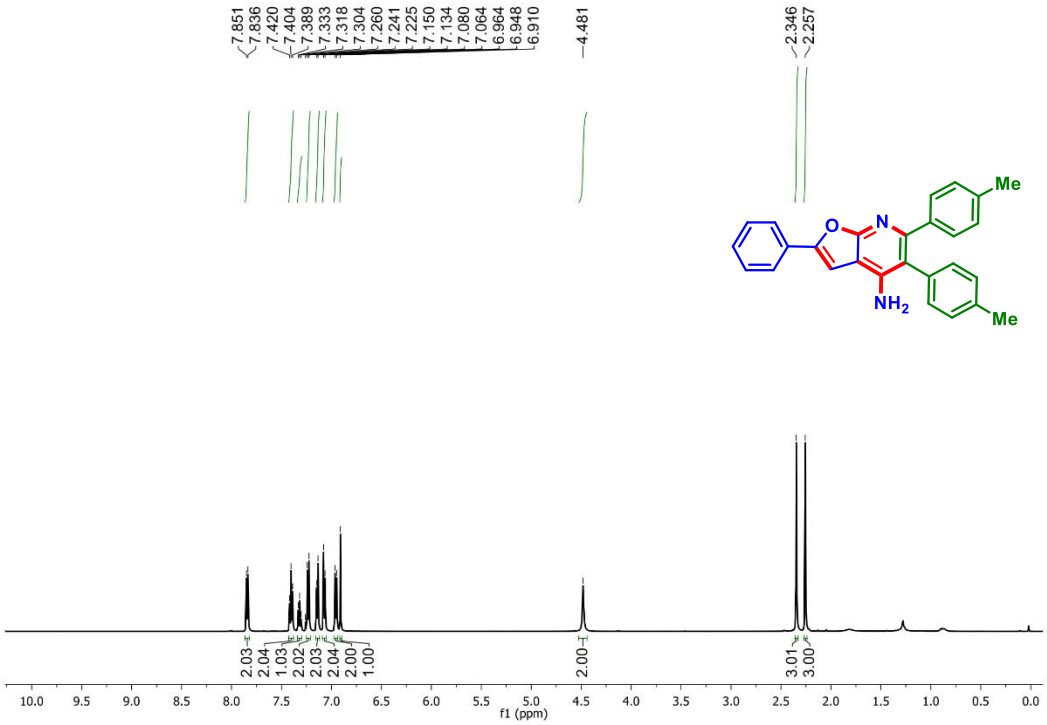

2-Phenyl-5,6-di-p-tolylfuro[2,3-b]pyridin-4-amine (1b): $^{13}C\{^{1}H\}$ NMR ($CDCl_3$, 125 MHz)

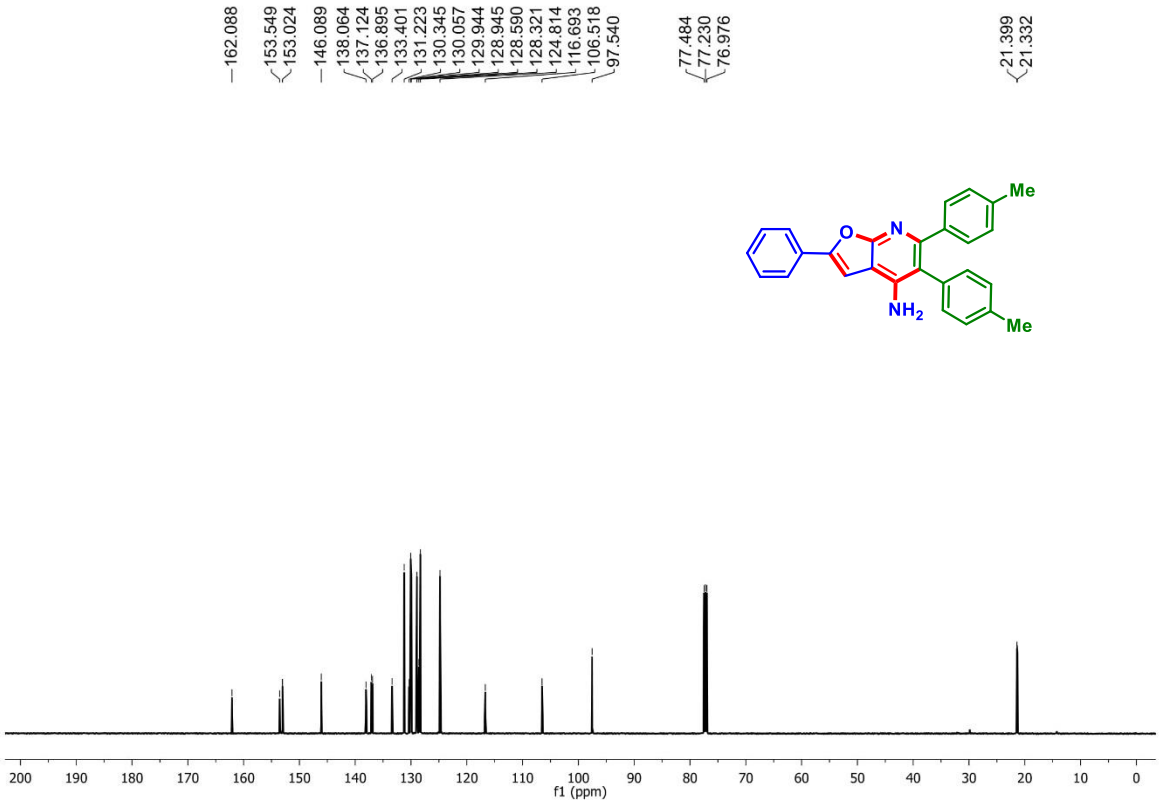

5,6-Bis(4-chlorophenyl)-2-phenylfuro[2,3-b]pyridin-4-amine (1h): ^{1}H NMR ($CDCl_3$, 500 MHz)

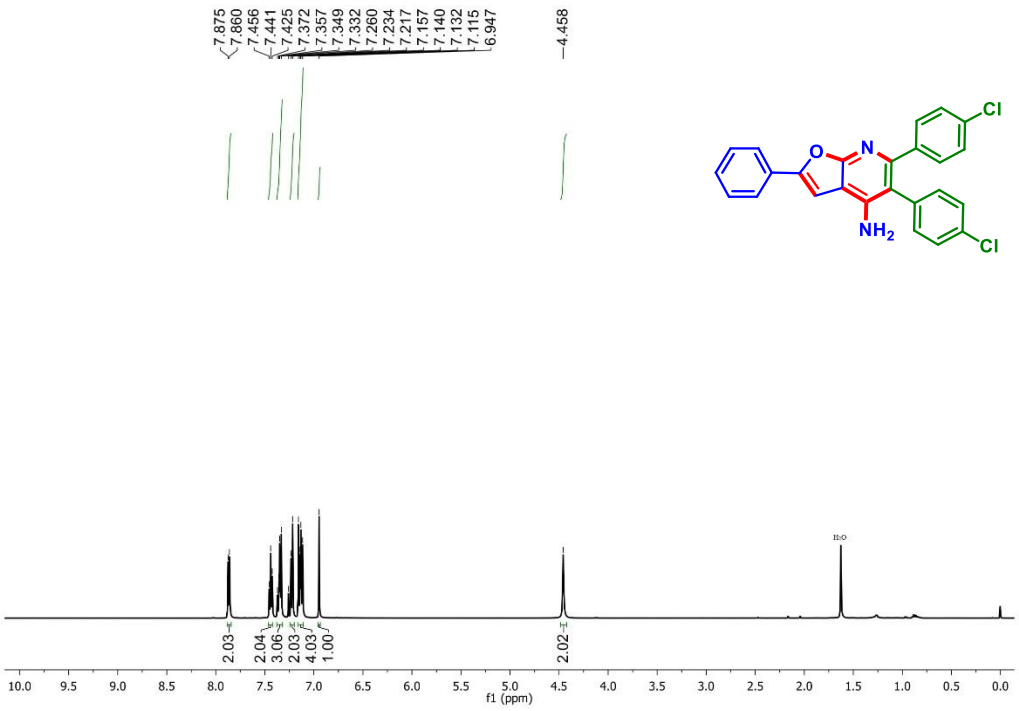

5,6-Bis(4-chlorophenyl)-2-phenylfuro[2,3-b]pyridin-4-amine (1h): $^{13}C\{^{1}H\}$ NMR ($CDCl_3$, 125 MHz)

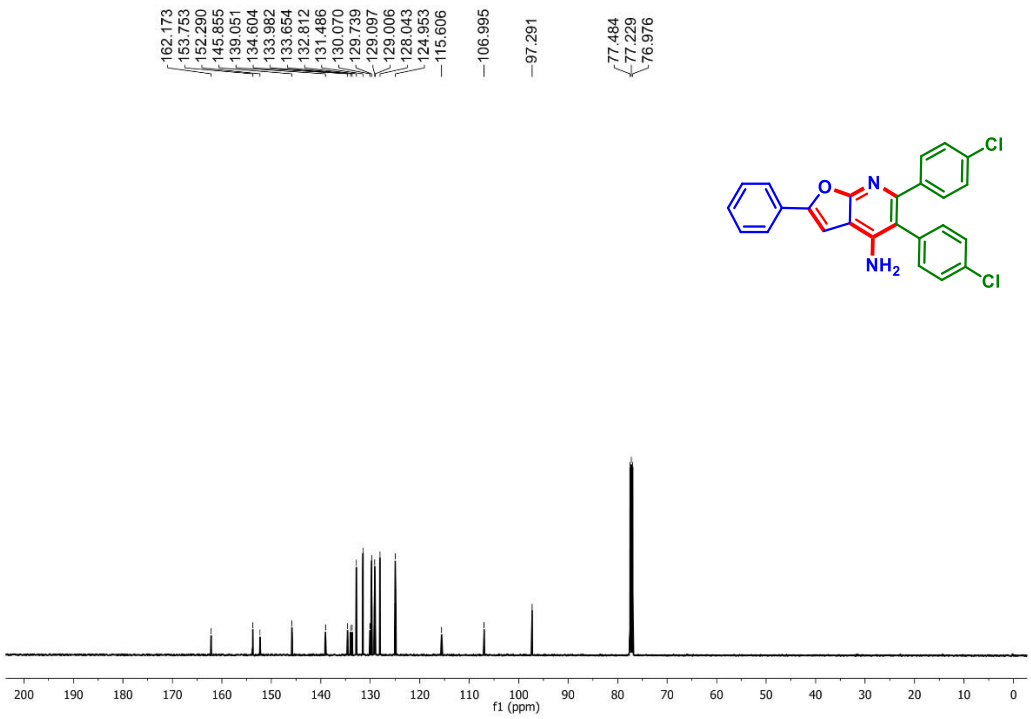

6-(4-Methoxyphenyl)-2-phenyl-5-(p-tolyl)furo[2,3-b]pyridin-4-amine (1l): ^{1}H NMR ($CDCl_3$, 500 MHz)

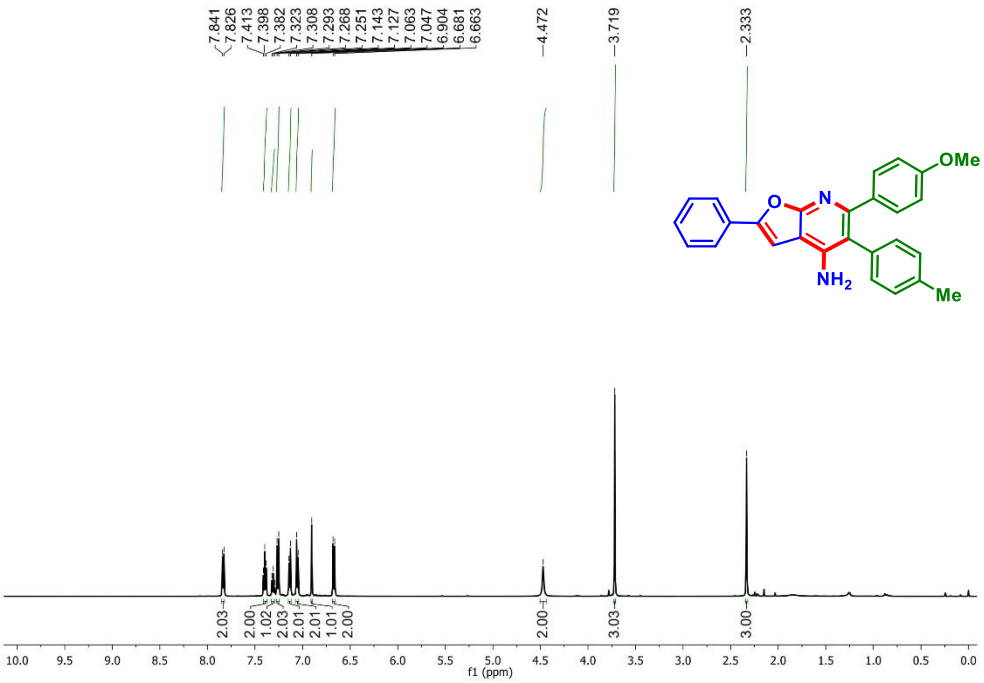

6-(4-Methoxyphenyl)-2-phenyl-5-(p-tolyl)furo[2,3-b]pyridin-4-amine (1l): $^{13}C\{^{1}H\}$ NMR ($CDCl_3$, 125 MHz)

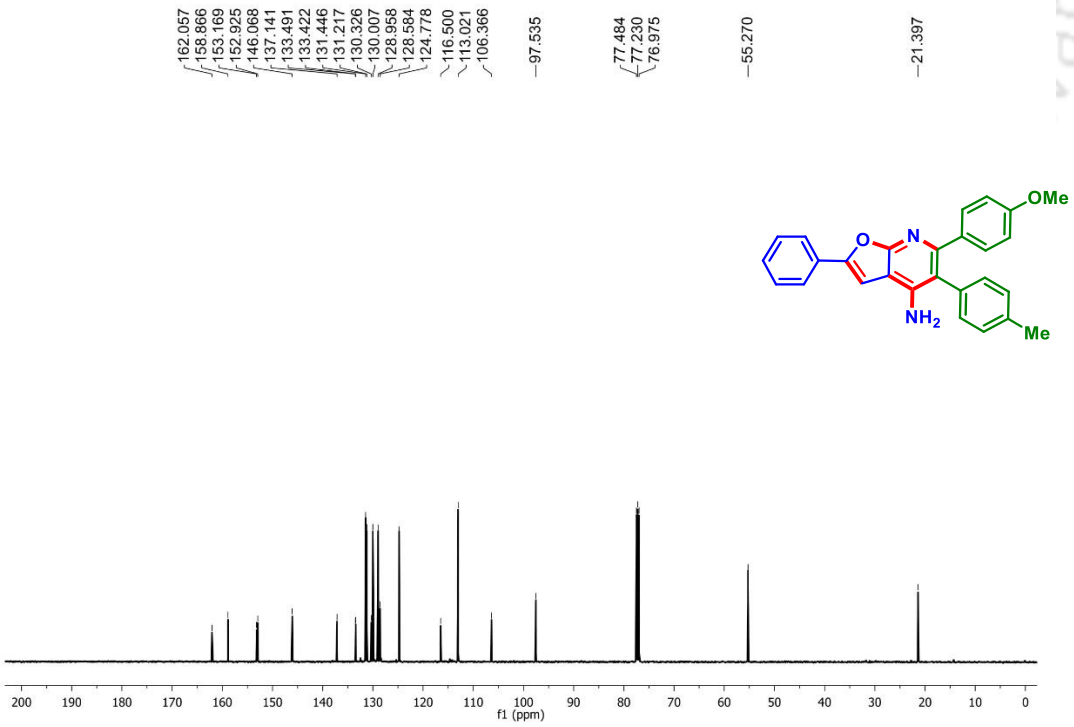

5-(4-Bromophenyl)-6-(4-methoxyphenyl)-2-phenylfuro[2,3-b]pyridin-4-amine (1n): ^{1}H NMR ($CDCl_3$, 400 MHz)

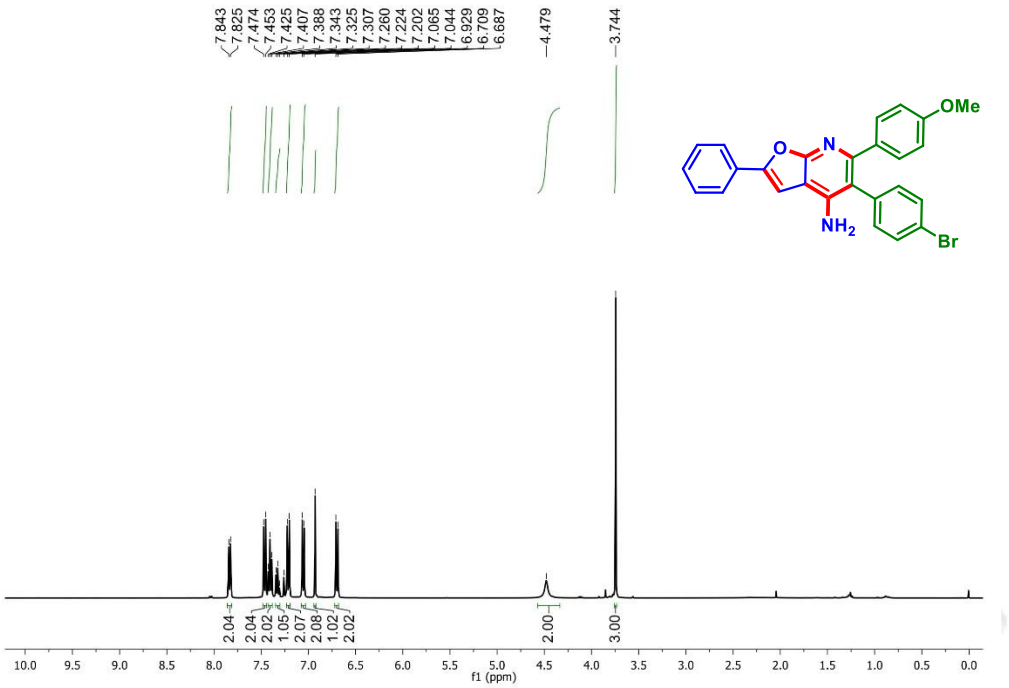

5-(4-Bromophenyl)-6-(4-methoxyphenyl)-2-phenylfuro[2,3-b]pyridin-4-amine (1n): $^{13}C\{^{1}H\}$ NMR ($CDCl_3$, 100 MHz)

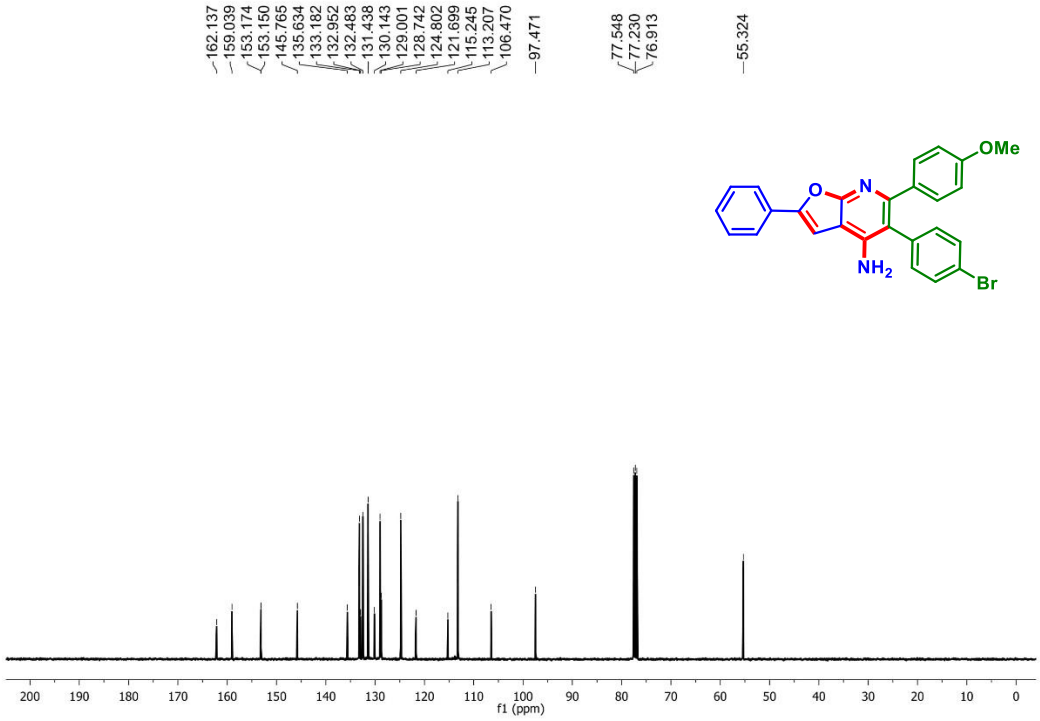

5-Methyl-2,6-diphenylfuro[2,3-b]pyridin-4-amine (1o): ^{1}H NMR (CDCl$_3$, 500 MHz)

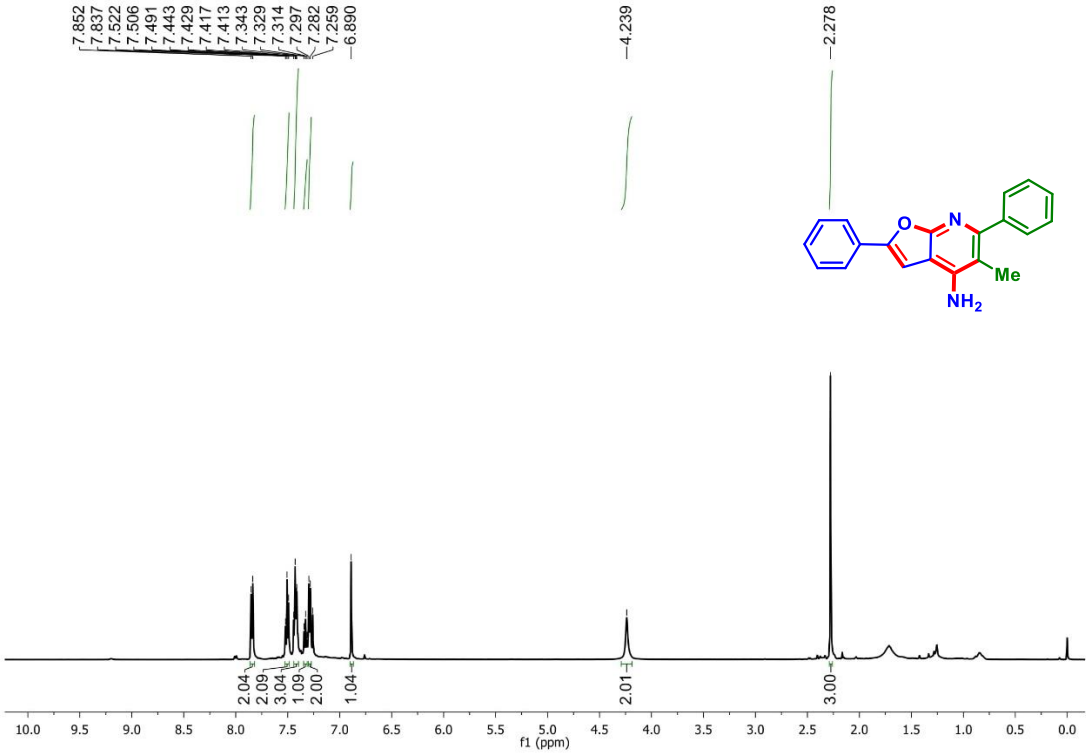

5-Methyl-2,6-diphenylfuro[2,3-b]pyridin-4-amine (1o): ^{13}C{^{1}H} NMR (CDCl$_3$, 125 MHz)

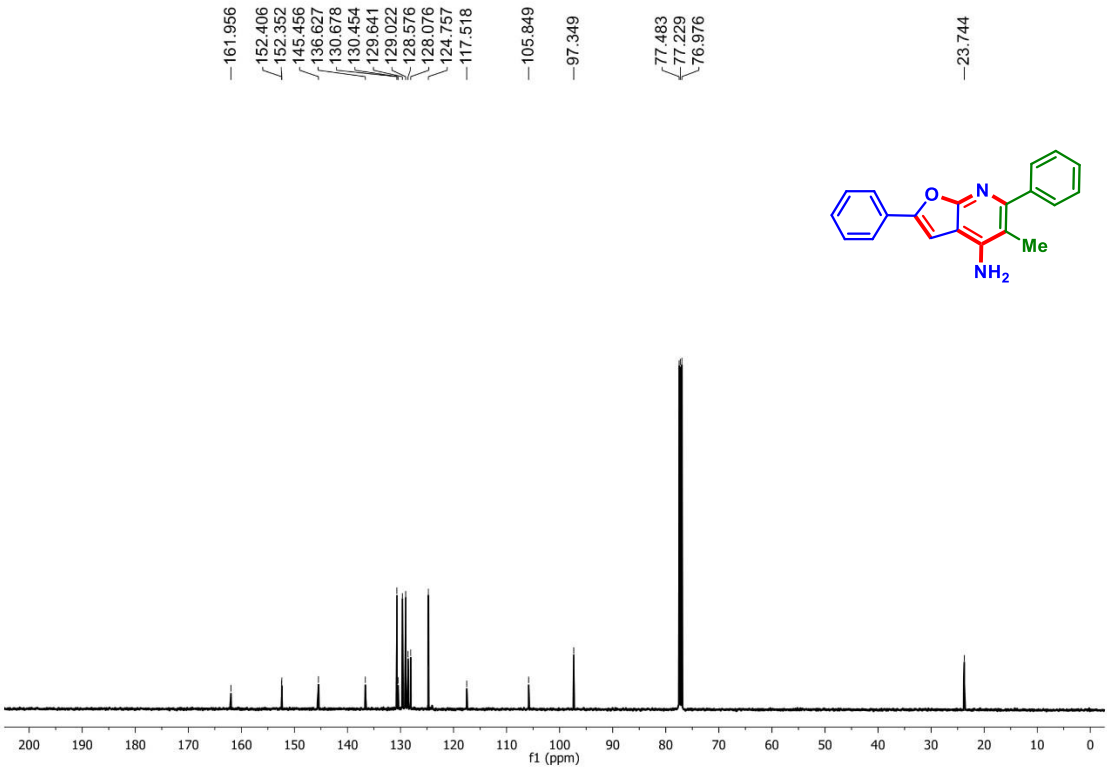

6-Methyl-2,5-diphenylfuro[2,3-b]pyridin-4-amine (1o'): ^{1}H NMR (CDCl3, 500 MHz)

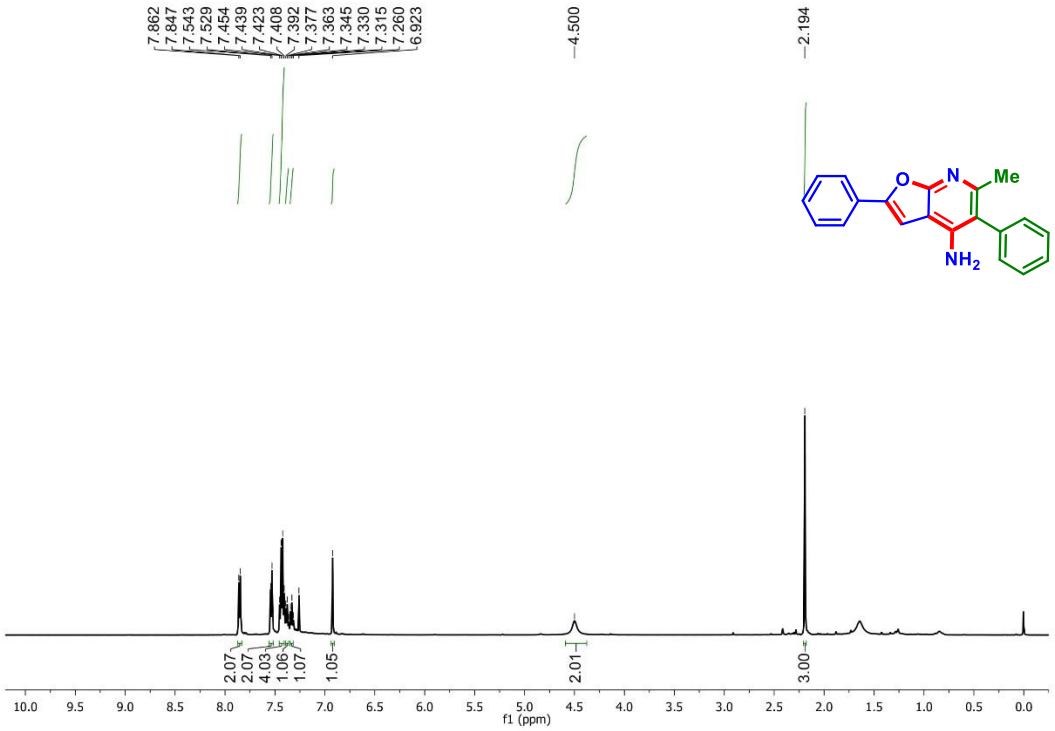

6-Methyl-2,5-diphenylfuro[2,3-b]pyridin-4-amine (1o'): ^{13}C{^{1}H} NMR (CDCl$_3$, 125 MHz)

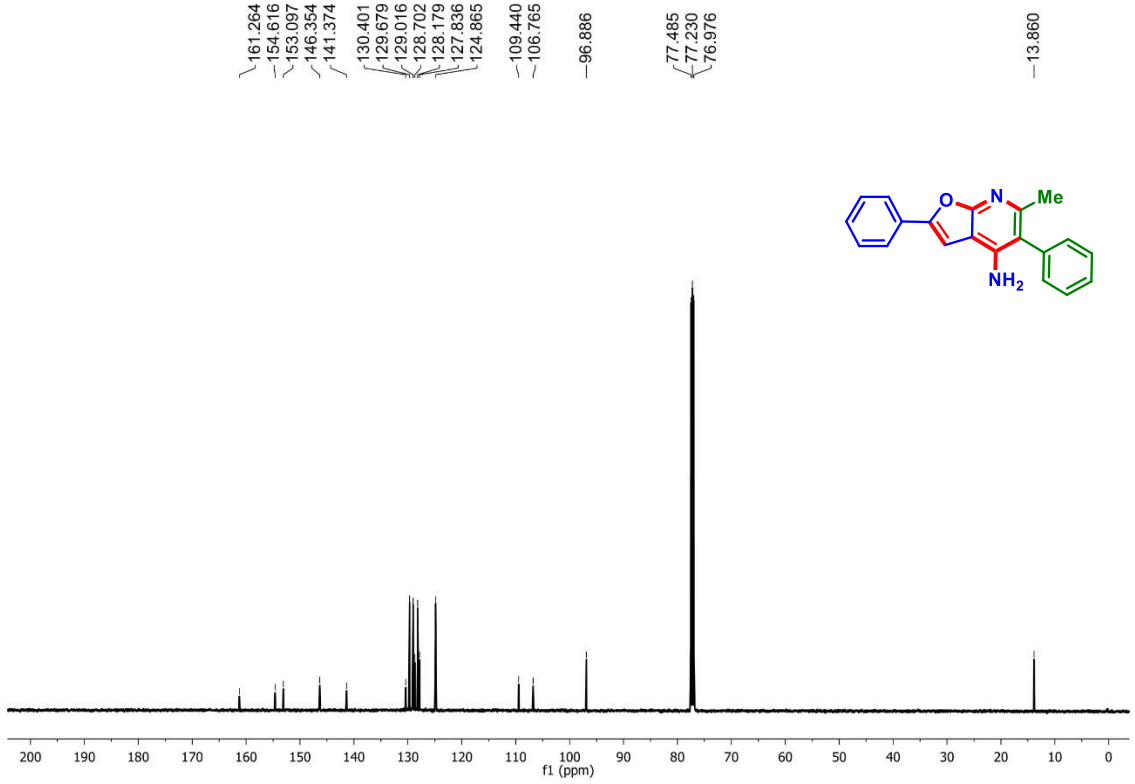

2,6-Diphenylfuro[2,3-b]pyridin-4-amine (1q): ^{1}H NMR (CDCl$_3$, 400 MHz)

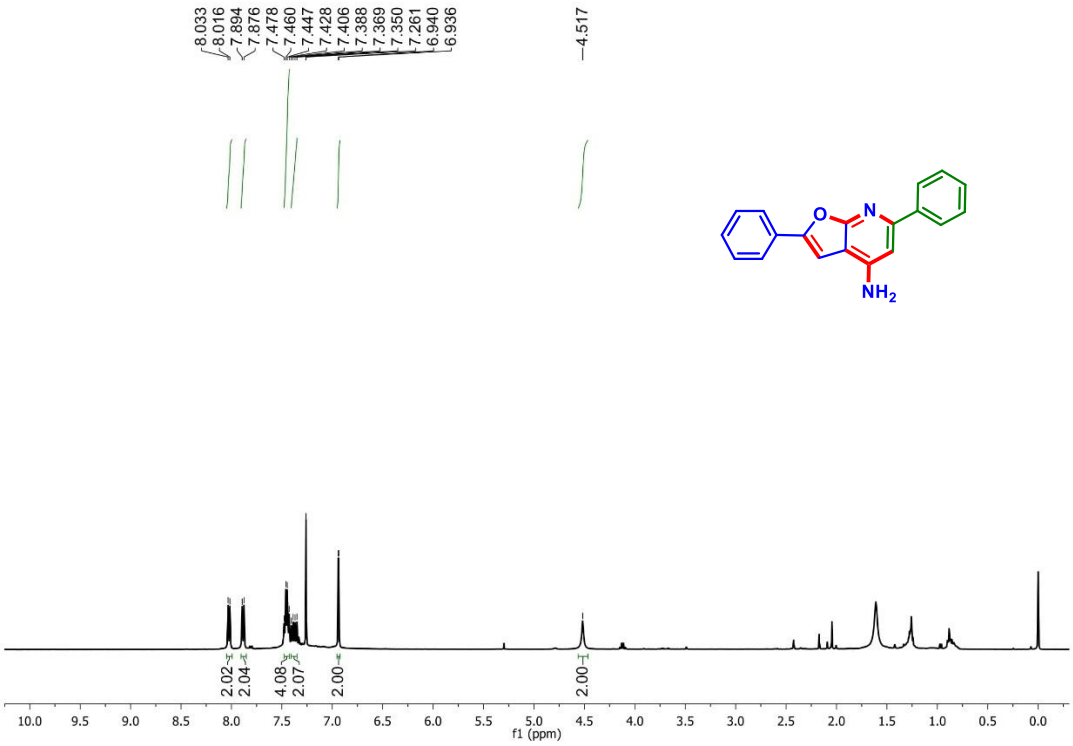

2,6-Diphenylfuro[2,3-b]pyridin-4-amine (1q): ^{13}C{^{1}H} NMR (CDCl$_3$, 125 MHz)

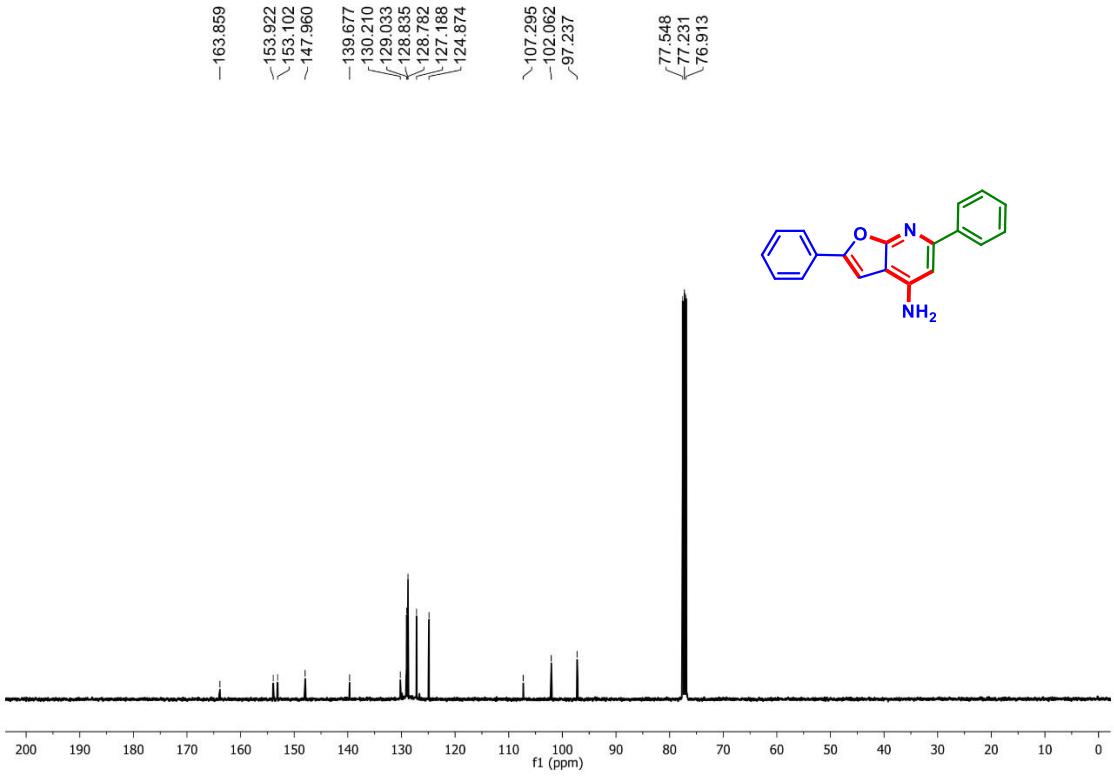

2-Amino-5-phenylfuran-3-carbonitrile (1'): ^{1}H NMR (DMSO-d_6, 400 MHz)

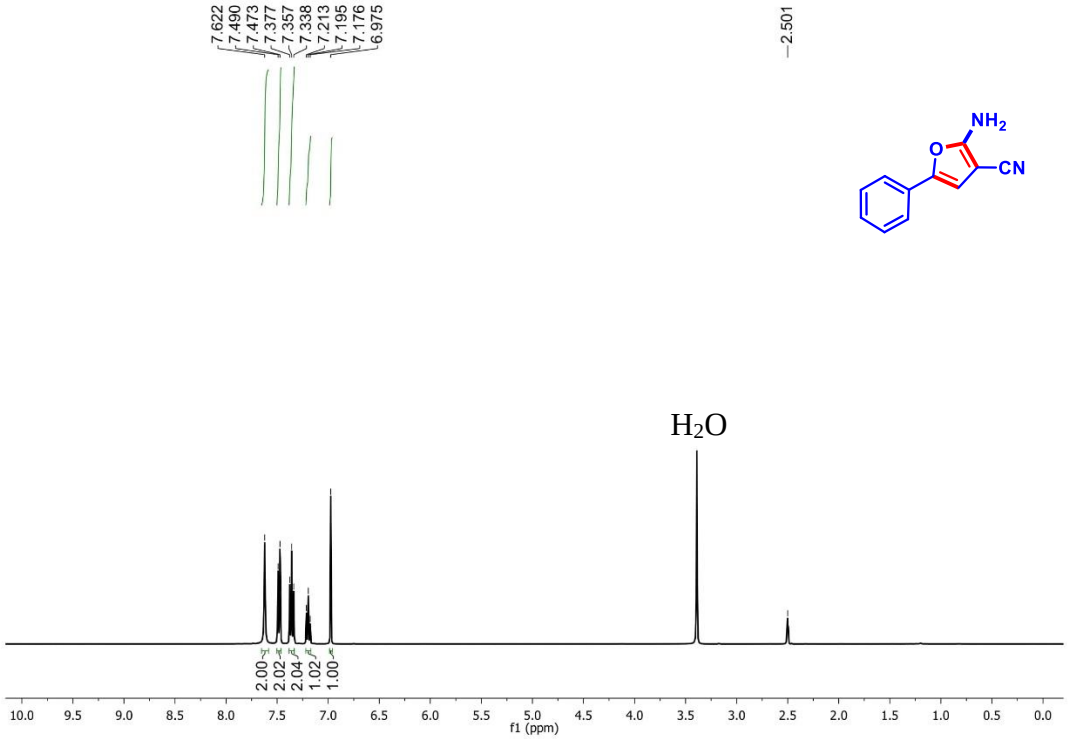

2-Amino-5-phenylfuran-3-carbonitrile (1'): ^{13}C{^{1}H} NMR (DMSO-d_6, 100 MHz)

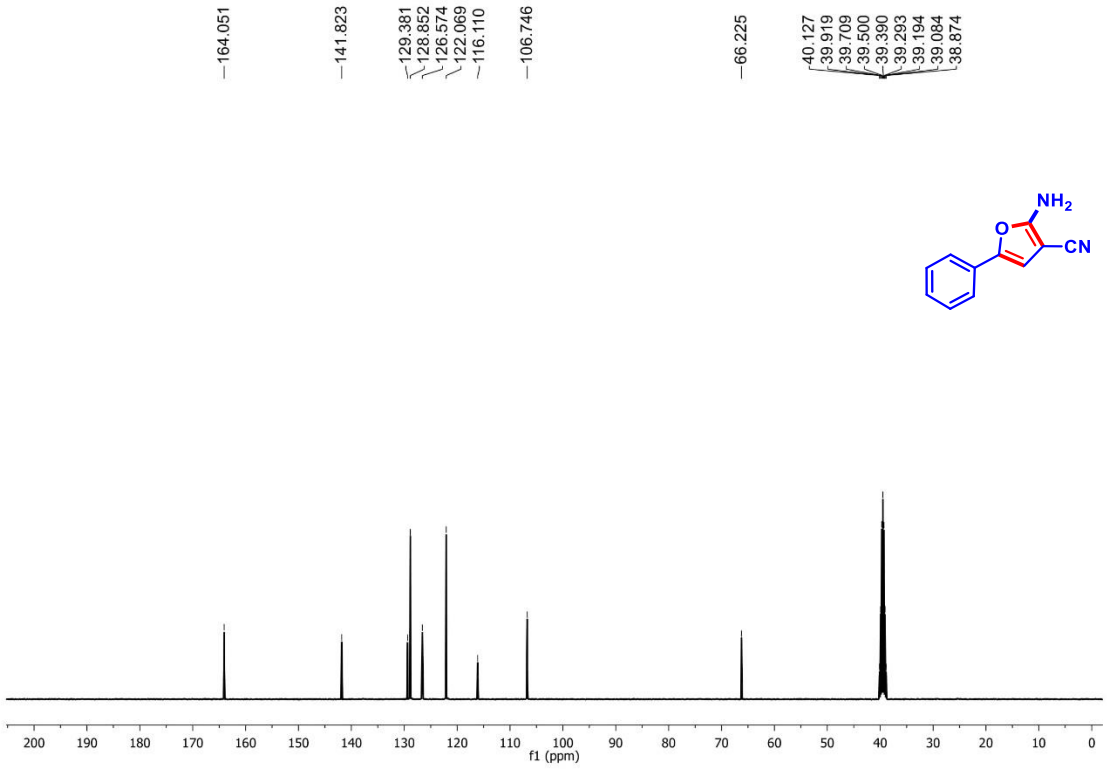

2,3-Diphenylquinolin-4-amine (15a): ^{1}H NMR (DMSO-d$_6$, 400 MHz)

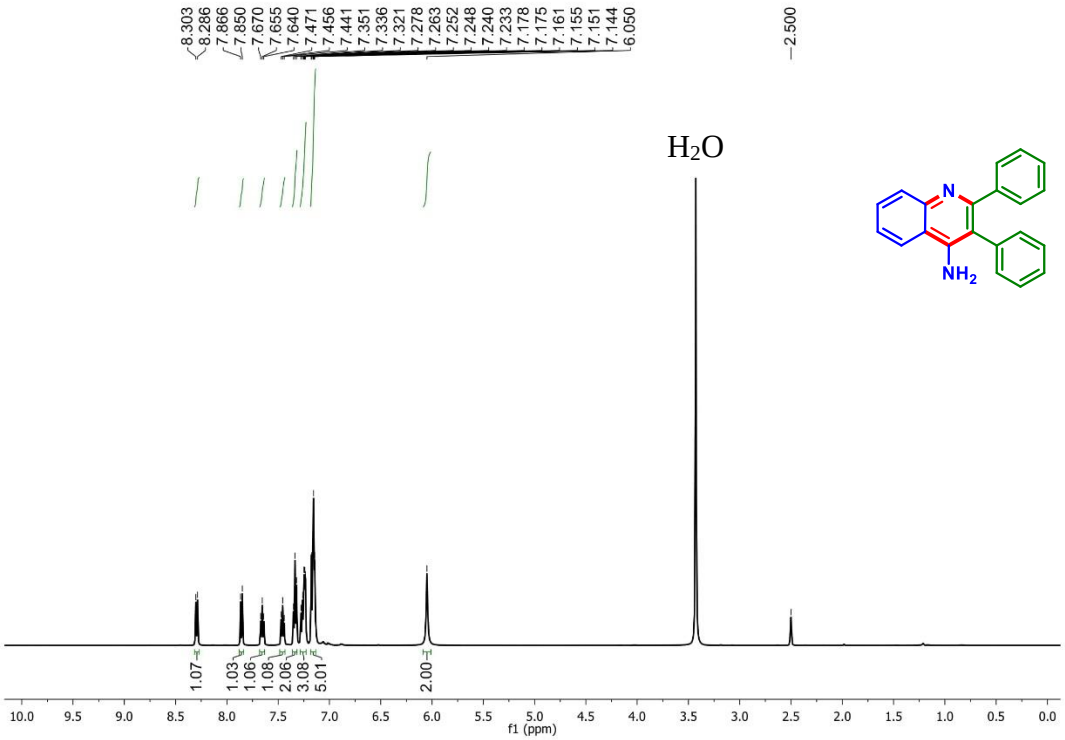

2,3-Diphenylquinolin-4-amine (15a): ^{13}C{^{1}H} NMR (DMSO-d$_6$, 100 MHz)

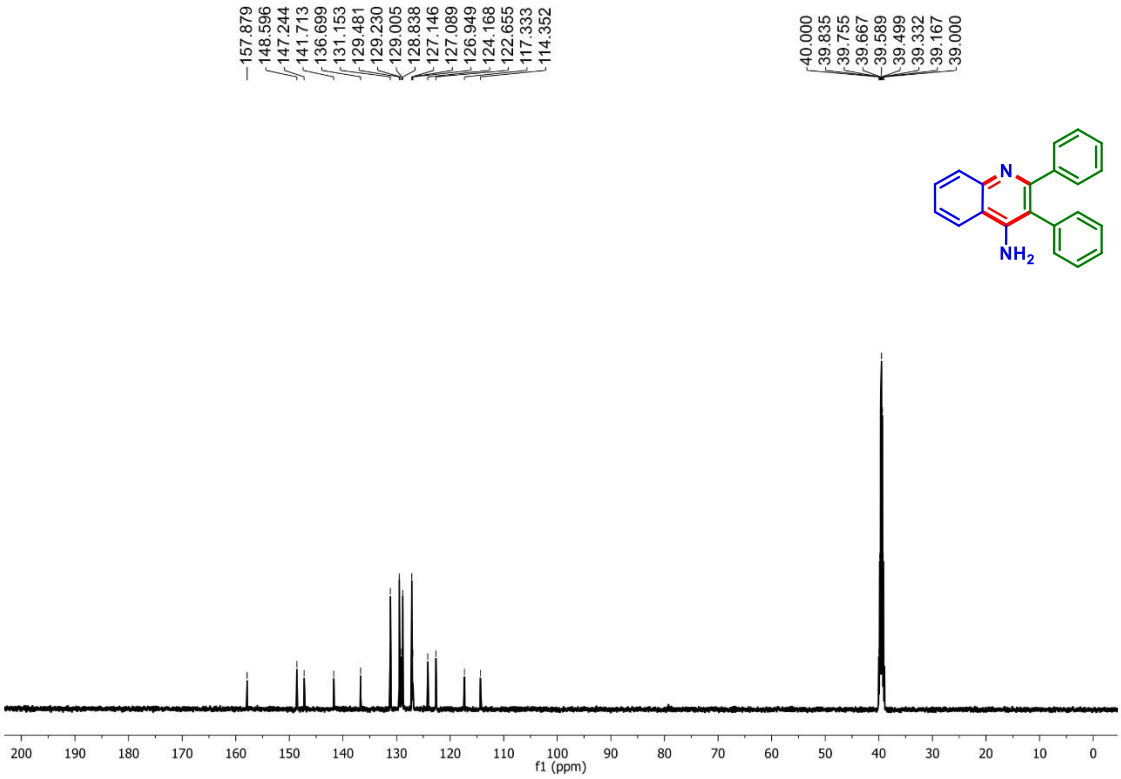

III.10. References:

[1] (a) Martin, M. W.; Newcomb, J.; Nunes, J. J.; Bemis, J. E.; McGowan, D. C.; White, R. D.; Buchanan, J. L.; DiMauro, E. F.; Boucher, C.; Faust, T.; Hsieh, F.; Huang, X.; Lee, J. H.; Schneider, S.; Turci, S. M.; Zhu, X. *Bioorg. Med. Chem. Lett*. **2007**, *17*, 2299–2304. (b) Wu, Z.; Robinson, R. G.; Fu, S.; Barnett, S. F.; Defeo-Jones, D.; Jones, R. E.; Kral, A. M.; Huber, H. E.; Kohl, N. E.; Hartman, G. D.; Bilodeau, M. T. *Bioorg. Med. Chem. Lett*. **2008**, *18*, 2211–2214. (c) Rodriguez, A. L.; Williams, R.; Zhou, Y.; Lindsley, S. R.; Le, U.; Grier, M. D.; Weaver, C. D.; Conn, P. J.; Lindsley, C. W. *Bioorg. Med. Chem. Lett.* **2009**, *19*, 3209–3213. (d) Debenham, J. S.; Madsen-Duggan, C. B.; Toupence, R. B.; Walsh, T. F.; Wang, J.; Tong, X.; Kumar, S.; Lao, J.; Fong, T. M.; Xiao, J. C.; Huang, C. R. R. C.; Shen, C.-P.; Feng, Y.; Marsh, D. J.; Stribling, D. S.; Shearman, L. P.; Strack, A. M.; Goulet, M. T. *Bioorg. Med. Chem. Lett*. **2010**, *20*, 1448–1452. (e) Parcella, K.; Eastman, K.; Yeung, K.-S.; Grant-Young, K. A.; Zhu, J.; Wang, T.; Zhang, Z.; Yin, Z.; Parker, D.; Mosure, K.; Fang, H.; Wang, Y.-K.; Lemm, J.; Zhuo, X.; Hanumegowda, U.; Liu, M.; Rigat, K.; Donoso, M.; Tuttle, M.; Zvyaga, T.; Haarhoff, Z.; Meanwell, N. A.; Soars, M. G.; Roberts, S. B.; Kadow, J. F. *ACS Med. Chem. Lett*. **2017**, *8*, 771–774.

[2] (a) Sirakanyan, S. N.; Hovakimyan, A. A.; Noravyan, A. S. *Russ. Chem. Rev*. **2015**, *84*, 441–454. (b) Ibrahim, M. M.; Al-Refai, M.; Al-Fawwaz, A.; Ali, B. F.; Geyer, A.; Harms, K.; Marsch, M.; Kruger, M.; Osman, H.; Azmi, M. N. *J. Fluoresc*. **2018**, *28*, 655–662.

[3] For Co(III)-catalyzed alkyne annulations: (a) Chakraborty, P.; Mandal, R.; Paira, S.; Sundararaju, B. *Chem. Commun*. **2021**, *57*, 13075–13083. (b) Mohanty, S. R.; Pati, B. V.; Banjare, S. K.; Adhikari, G. K. D.; Ravikumar, P. C. *J. Org. Chem*. **2021**, *86*, 1074–1083. (c) Ladeab, D. M.; Pawar, A. B. *Org. Chem. Front*. **2016**, *3*, 836–840. (d) Kalsi, D.; Sundararaju, B. *Org. Lett*. **2015**, *17*, 6118–6121.

[4] For Rh(III)-catalyzed alkyne annulations: (a) Dias, G. G.; Paz, E. R. S.; Kadooca, J.; Y. Sabino, A. A.; Cury, L. A.; Torikai, K.; Simone, C. A. de.; Fantuzzi, F.; Eufrânio Júnior, N. da S. *J. Org. Chem*. **2021**, *86*, 264–278. (b) Jayakumar, J.; Parthasarathy, K.; Chen, Y.-H.; Lee, T.-H.; Chuang, S.-C.; Cheng, C.-H. *Angew. Chem., Int. Ed*. **2014**, *53*,

9889–9892. (c) Rakshit, S.; Patureau, F. W.; Glorius, F. *J. Am. Chem. Soc*. **2010**, *132*, 9585–9587. (d) Su, Y.; Zhao, M.; Han, K.; Song, G.; Li, X. *Org. Lett*. **2010**, *12*, 5462–5465.

[5] For Ru(II)-catalyzed alkyne annulations: (a) Patel, B. K.; Rakshit, A. "Access to *N*-Heterocyclic Molecules *via* Ru(II)-Catalyzed Oxidative Alkyne Annulation Reactions". Ruthenium-An Element Loved by Researchers, edited by Hitoshi Ishida, *IntechOpen*, **2021**, 10.5772/intechopen.95987. (b) Song, L.; Ojeda-Carralero, G. M.; Parmar, D.; González-Martínez, D. A.; Meervelt, L. V.; Van der Eycken, J.; Goeman, J.; Rivera, D. G.; Van der Eycken, E. V. *Adv. Synth. Catal*. **2021**, *363*, 3297–3304. (c) Ackermann, L. *Acc. Chem. Res*. **2014**, *47*, 281–295.

[6] For Ni(II)/Ni(0)-catalyzed alkyne annulations: (a) Obata, A.; Sasagawa, A.; Yamazaki, K.; Ano, Y.; Chatani, N. *Chem. Sci*. **2019,** *10*, 3242–3248. (b) Song, W.; Ackermann, L. *Chem. Commun*. **2013**, *49*, 6638–6640.

[7] For Pd(II)-catalyzed alkyne annulations: (a) Sun, P.; Yang, J.; Peng, J.; Mo, B.; Chen, X.; Li, X.; Chen, C. *J. Org. Chem*. **2020**, *85*, 6761–6769. (b) Peng, S.; Sun, Z.; Zhu, H.; Chen, N.; Sun, X.; Gong, X.; Wang, J.; Wang, L. *Org. Lett*. **2020**, *22*, 3200–3204. (c) Borthakur, S.; Baruah, S.; Sarma, B.; Gogoi, S. *Org. Lett*. **2019**, *21*, 2768–2771. (d) Zhao, M.-N.; Ren, Z.-H.; Wang, Y.-Y.; Guan, Z.-H. *Org. Lett*. **2014**, *16*, 608–611. (e) Xu, Y.-H.; He, T.; Zhang, Q.-C.; Loh, T.-P. *Chem. Commun*. **2014**, *50*, 2784–2786.

[8] Pletnev, A. A.; Tian, Q.; Larock, R. C. *J. Org. Chem*. **2002**, *67*, 9276–9287.

[9] Tian, Q.; Pletnev, A. A.; Larock, R. C. *J. Org. Chem*. **2003**, *68*, 339–347.

[10] Tsukamoto, H.; Ikeda, T.; Doi, T. *J. Org. Chem*. **2016**, *81*, 1733–1745.

[11] Rakshit, A.; Sau, P.; Ghosh, S.; Patel, B. K. *Adv. Synth. Catal*. **2019**, *361*, 3824–3836.

[12] (a) Dai, L.; Yu, S.; Lv, N.; Ye, X.; Shao, Y.; Chen, Z.; Chen, J. *Org. Lett*. **2021**, *23*, 5664–5668. (b) Zhao, Z.; Zeng, G.; Chen, Y.; Zheng, J.; Chen, Z.; Shao, Y.; Zhang, F.; Chen, J.; Li, R. *Org. Lett*. **2021**, *23*, 7955–7960. (c) Xu, T.; Shao, Y.; Dai, L.; Yu, S.; Cheng, T.; Chen, J. *J. Org. Chem*. **2019**, *84*, 13604–13614. (d) Dhara, H. N.; Rakshit, A.; Alam, T.; Patel, B. K. *Org. Biomol. Chem.* **2022**, *20*, 4243–4277.

[13] Rakshit, A.; Kumar, P.; Alam, T.; Dhara, H.; Patel, B. K. *J. Org. Chem*. **2020**, *85*, 12482–12504.

[14] Sahoo, A. K.; Rakshit, A.; Dahiya, A.; Pan, A.; Patel, B. K. *Org. Lett*. **2022**, *24*, 1918–1923.

[15] (a) Arcadi, A.; Cacchi, S.; Di Giuseppe, S.; Fabrizi, G.; Marinelli, F. *Org. Lett*. **2002**, *4*, 2409–2412. (b) Bossharth, E.; Desbordes, P.; Monteiro, N.; Balme, G. *Org. Lett*. **2003**, *5*, 2441–2444. (c) Cailly, T.; Lemaître, S.; Fabis, F.; Rault, S. *Synthesis*. **2007**, *20*, 3247–3251. (d) Cartwright, M. W.; Parks, E. L.; Pattison, G.; Slater, R.; Sandford, G.; Wilson, I.; Yufit, D. S.; Howard, J. A. K.; Christopher, J. A.; Miller, D. D. *Tetrahedron*. **2010**, *66*, 3222–3227. (e) de los Ríos, C.; Marco, J. L.; Carreiras, M. D. C.; Chinchón, P. M.; García, A. G.; Villarroya, M. *Bioorg. Med. Chem*. **2002**, *10*, 2077–2088. (f) Denisenko, A. V.; Tverdokhlebov, A. V.; Tolmachev, A. A.; Volovenko, Y. M.; Shishkina, S. V.; Shishkin, O. V. *Synthesis.* **2010**, *6*, 1009–1013.

[16] (a) Li, Z.; Ling, F.; Cheng, D.; Ma, C. *Org. Lett*. **2014**, *16*, 1822–1825. (b) Fumagalli, F.; da Silva Emery, F. *J. Org. Chem*. **2016**, *81*, 10339–10347. (c) Wan, Y.; Zheng, X.; Ma, C. *Angew. Chem., Int. Ed*. **2018**, *57*, 5482–5486. (d) Agasti, S.; Pal, T.; Achar, T. K.; Maiti, S.; Pal, D.; Mandal, S.; Daud, K.; Lahiri, G. K.; Maiti, D. *Angew. Chem., Int. Ed*. **2019**, *58*, 11039–11043. (e) Liu, J.; Zhu, L.; Wan, W.; Huang, X. *Org. Lett*. **2020**, *22*, 3279–3285.

[17] Ghosh, S.; Pal, S.; Rajamanickam, S.; Shome, R.; Mohanta, P. R.; Ghosh, S. S.; Patel, B. K. *ACS Omega*. **2019**, *4*, 5565–5577.

[18] Laru, S.; Bhattacharjee, S.; Singsardar, M.; Samanta, S.; Hajra, A. *J. Org. Chem*. **2021**, *86*, 2784–2795.

[19] Chen, X.; Sun, P.; Mo, B.; Chen, C.; Peng, J. *J. Org. Chem*. **2021**, *86*, 352–366.

[20] Kumar, A.; Mishra, P. K.; Saini, K. M.; Verma, A. K. *Adv. Synth. Catal*. **2021**, *363*, 2546–2551.

[21] (a) Abdelhamid, A. O.; Negm, A. M.; Abbas, I. M. *J. Prakt. Chem*. **1989**, *331*, 31–36. (b) Al-Mousawi, S. M.; Moustafa, M. S.; Meier, H.; Kolshorn, H.; Elnagdi, M. H. *Molecules*. **2009**, *14*, 798–806.

[22] (a) Sonogashira, K.; Tohda, Y.; Hagihara, N. *Tetrahedron Lett*. **1975**, *16*, 4467–4470. (b) Sonogashira, K. *J. Organomet. Chem*. **2002**, *653*, 46–49.

CHAPTER IV

Cu(II)-Promoted Cascade Synthesis of Fused Imidazo-Pyridine-Carbonitriles

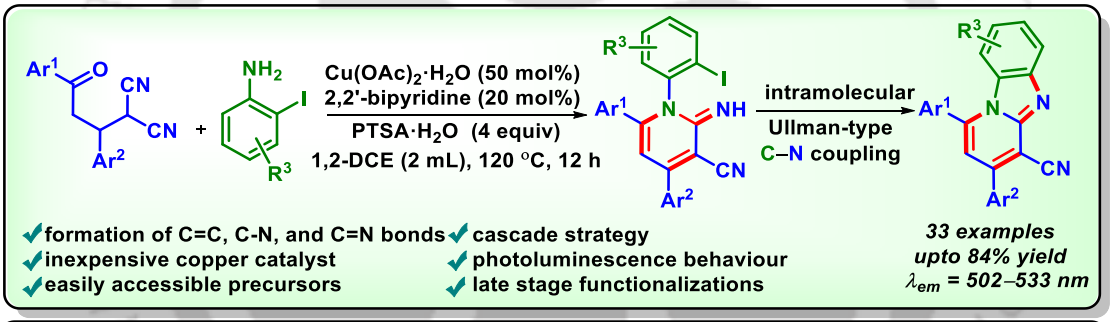

JOC The Journal of Organic Chemistry
J. Org. Chem. **2021**, *86*, 17504–17510.
pubs.acs.org/joc
Note

ABSTRACT: A Cu(II)-promoted synthesis of an aza-fused *N*-heterocycle having a benz-imidazopyridine scaffold is developed *via* an addition-cyclization followed by an Ullmann-type C–N coupling between *o*-iodoanilines and γ-ketodinitriles. This protocol features a broad substrate scope, giving products in the range of 32–84% yields. The compounds show excellent photoluminescence properties having two absorption maxima in the region between 270–280 and 338–350 nm and emission maxima in the range of 502–533 nm. The HOMO–LUMO energy gap of 3.49–3.57 eV was determined using Gaussian 09 program at the B3LYP/6-31G (d, p) basis set level. We also demonstrated a few post-synthetic modifications.

भारतीय प्रौद्योगिकी संस्थान गुवाहाटी
Indian Institute of Technology Guwahati

CHAPTER IV

Cu(II)-Promoted Cascade Synthesis of Fused Imidazo-Pyridine-Carbonitriles

IV.1. Introduction:

Constructing polyheterocyclic nitrogenous frameworks in a one-pot cascade process from readily accessible precursors is an attractive and demanding research area.[1] Nitrogen polyheterocycles are prevalent in several naturally occurring and synthetic compounds having biological activities and material applications.[2] The aza-fused scaffold, benzo[4,5]imidazo[1,2-*a*]pyridine possessing a cyano group at the 4-position is of interest in pharmaceuticals owing to its anticancer, antimalarial, antifungal, antibacterial, antiviral properties (Figure IV.1.1).[3] In addition, due to its π-extended features and remarkable photophysical properties, the aryl-fused (benz)-imidazole framework has also found its use in the field of electronics and optical materials.[4]

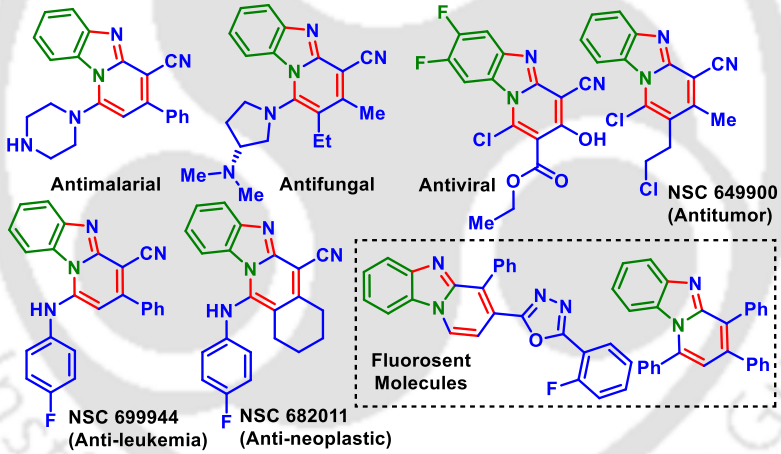

Figure IV.1.1. *Representative active benzo[4,5]imidazo[1,2-a] pyridines.*

The prevalent existence of this class of compounds leads to the development of several synthetic protocols. For example, In 2011, Wu *et al*. developed the synthesis of pyrido[1,2-*a*]benzimidazole *via* copper-catalyzed inter and intramolecular C–N couplings between 2-haloanilines and 2-halopyridines [Scheme IV.1.1, (i)].[5] In 2015, the Das group reported a similar Cu(II)-catalyzed, inter and intramolecular C–N bond formation for the synthesis of benzimidazole-fused heterocycles *via* a sequential Chan−Lam and Ullmann-type couplings [Scheme IV.1.1, (ii)].[6]

The transition-metal-catalyzed synthesis of nitrogen-heterocycles *via* C–N cross-coupling mainly involves Pd or Cu catalysts. However, the latter is preferred due to its low cost and high

environmental acceptability.[7] Further *o*-iodoanilines have been used as valuable precursors in transition-metal catalysis especially, copper-catalyzed couplings *via* the addition/cyclization cascade process.[8] The nucleophilic amino group promotes the intermolecular addition with the unsaturated electrophilic center, while the *o*-iodo group takes part in an intramolecular cyclization *via* a metal-mediated C–C or C–heteroatom bond formation. In 2018, Liang groups reported an efficient Cu(II)-catalyzed heteroannulation reaction for the synthesis of benzo[4,5]imidazo[2,1-*a*]isoquinoline derivatives captivating *o*-alkynylbenzonitriles and 2-iodoanilines [Scheme IV.1.1, (iii)].[9] The efficiency of this protocol relay on the nitrogen of the aniline moiety, as it undergoes both nucleophilic attacks on nitrile as well as on the alkyne in a cascade manner.

In addition, substrates bearing functionalized or activated cyano group has drawn substantial attention owing to their well-recognized potential to transform into a variety of nitrogen-containing heterocycles.[10] Previously, our group also successfully harnessed the cyano moiety of γ-ketodinitriles *via* Ru(II)- and Pd(II)-catalyzed cascade [4 + 2] and [5 + 1] annulation strategies with internal alkynes and arylboronic acids, respectively for accessing fused isoquinolines and pyridines.[11] Based on our interest in nitrile triggered process to access *N*-heterocycles and taking cues from the copper-catalyzed cascade addition/cyclization of *o*-iodoaniline herein, we report a Cu(II)-promoted strategy for the construction of benzo[4,5]imidazo[1,2-*a*] pyridine-4-carbonitriles [Scheme IV.1.1, (iv)].

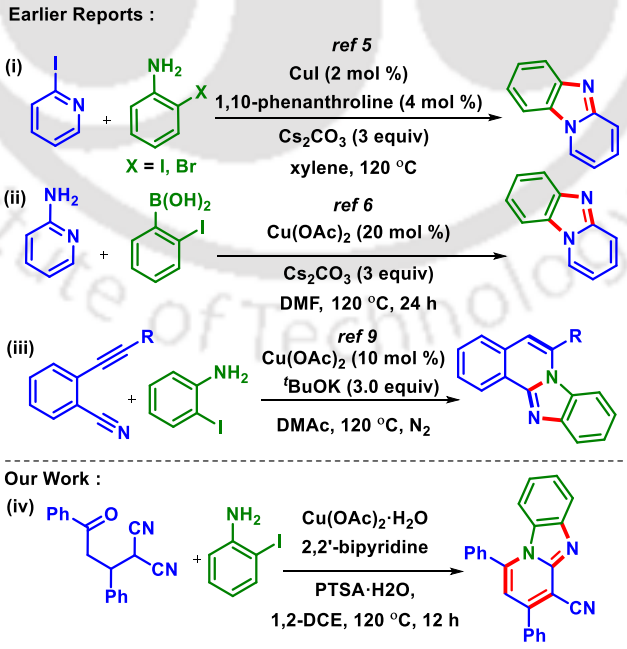

Scheme IV.1.1. *Synthetic approaches to fused benzimidazoles.*

IV.2. Strategies for the Synthesis of Aza-Fused Pyrido[1,2-*a*]benzimidazole:

Because of the significant pharmaceutical and photophysical properties of benzo[4,5]imidazo[1,2-*a*]pyridine, several elegant methods have been developed for their synthesis. In 2009, polysubstituted pyrido[1,2-*a*]benzimidazole derivatives are efficiently synthesized *via* a one-pot, four-component reaction using pyridine or 3-picoline, chloroacetonitrile, malononitrile, and aromatic aldehyde (Scheme IV.2.1).[12] The reaction was believed to proceed through the formation of polysubstituted benzenes followed by subsequent substitution and annulation reaction of pyridine.

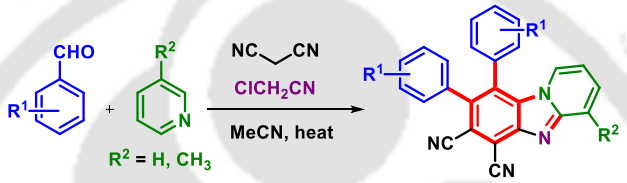

Scheme IV.2.1. *Multicomponent synthesis of fused pyrido-benzimidazoles.*

In 2010, Zhu *et al*. reported a Cu(II)-catalyzed intramolecular aromatic C–H amination of *N*-aryl-2-aminopyridines for the efficient synthesis of pyrido[1,2-*a*]benzimidazoles in moderate to excellent yields under oxygen atmosphere co-catalyzed by $Fe(NO_3)_3{\cdot}9H_2O$ (Scheme IV.2.2).[13] The reaction is believed to proceed *via* a Cu(II)-catalyzed electrophilic aromatic substitution pathway.

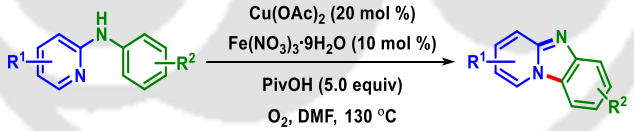

Scheme IV.2.2. *Cu(II)-catalyzed synthesis of pyrido-benzimidazoles.*

In 2013, a Rh(III)-catalyzed direct oxidative alkyne annulation without an extra directing group for the synthesis of pyrido[1,2-*a*]benzimidazoles *via* vinylic C–H activation is reported by the Peng group (Scheme IV.2.3).[14]

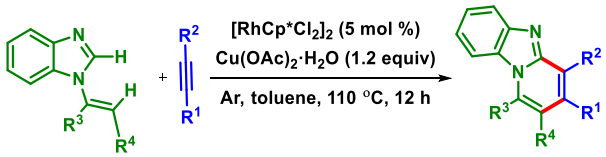

Scheme IV.2.3. *Rh(III)-catalyzed synthesis of pyrido-benzimidazoles.*

In 2014, Antonchick *et al.* reported a metal-free approach to access pyrido[1,2-*a*]benzimidazoles *via* annulation reaction between substituted 2-aminopyridines and arenes under mild reaction conditions (Scheme IV.2.4).[15]

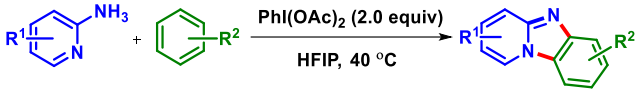

Scheme IV.2.4. *Metal-free synthesis of pyrido-benzimidazoles.*

In 2018, Pan *et al*. described a transition-metal free synthesis of benzo[4,5]imidazo[1,2-*a*]pyridines *via* reaction of ynones with 2-methyl benzimidazole (Scheme IV.2.5).[16] The reaction involved a Michael addition, intramolecular cycloaddition, and dehydration through a cascade manner to provide the desired product in moderate to good yield.

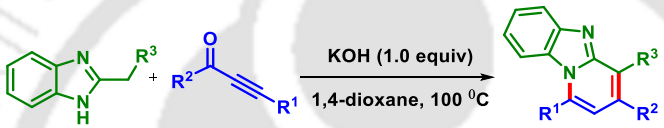

Scheme IV.2.5. *Transition-metal-free synthesis of pyrido-benzimidazoles.*

In 2020, Aiwen Lei and co-workers established the synthesis of pyrido[1,2-*a*]benzimidazoles *via* a Pd(II)-catalyzed electro-oxidative intramolecular C–H amination of *N*-aryl-2-aminopyridines reaction without an external oxidant or additive (Scheme IV.2.6).[17]

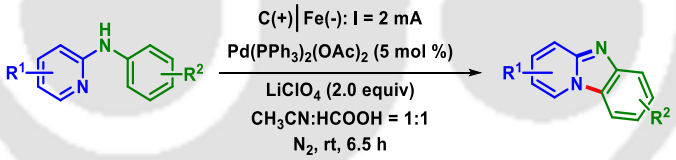

Scheme IV.2.6. *Electrochemical synthesis of pyrido-benzimidazoles.*

Very recently in 2021, the Jinsong Peng group developed a stereoselective nucleophilic addition of (benz)imidazoles to alkynyl bromides followed by a Pd(II)-catalyzed intermolecular C–H annulation with internal alkynes for the synthesis of fluorescence active Benzo[4,5]imidazo[1,2-*a*]pyridines in good to high yields (Scheme IV.2.7).[18]

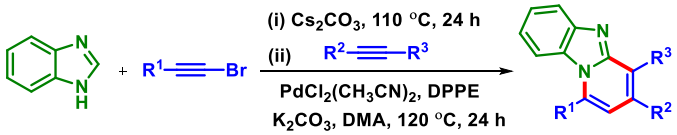

Scheme IV.2.7. *Pd(II)-catalyzed synthesis of pyrido-benzimidazoles.*

IV.3. Present Work:

IV.3.1. Optimization of the Reaction Conditions:

The initial assays were carried out by taking 2-(3-oxo-1,3-diphenylpropyl)malononitrile (**1**) (0.25 mmol) and 2-iodoaniline (**a**) (0.50 mmol, 2 equiv) as the reacting partners in the presence of $Cu(OAc)_2 \cdot H_2O$ (10 mol %) as the catalyst, 2,2′-bipyridine (20 mol %) as ligand and *p*-toluenesulfonic acid ($PTSA \cdot H_2O$, 2 equiv) as an additive in 1,2-dichloroethane (DCE) (2 mL) at 120 °C in a pressure tube for 12 h. The reaction furnished a yellow fluorescent spot (viewed under a 365 nm UV lamp) as observed by TLC, and the product (**1a**) was isolated in 15% yield (Table IV.3.1, entry 1). Further, increasing the loading of $Cu(OAc)_2 \cdot H_2O$ (50 mol %) produces (**1a**) an improved yield of 58% (Table IV.3.1, entries 2 and 3). From the spectroscopic analysis, the structure of the isolated product was found to be 1,3-diphenylbenzo[4,5]imidazo[1,2-*a*]pyridine-4-carbonitrile (**1a**) and was further confirmed by a single-crystal X-ray diffraction study of one of its derivative (**1h**) (Figure IV.3.1.1, **CCDC-2103595**).

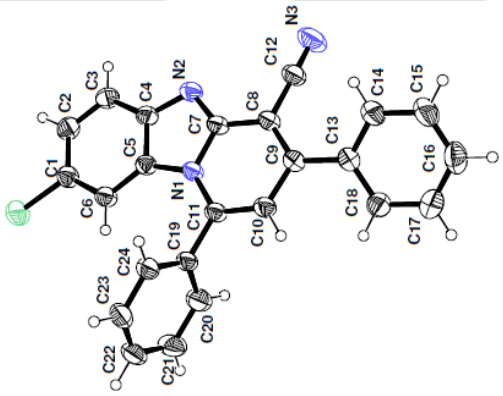

Figure IV.3.1.1. *ORTEP diagram of (**1h**) with 40% ellipsoid probability (CCDC-2103595).*

To find the optimal reaction conditions further screening process was initiated. Next, the amount of $PTSA \cdot H_2O$ was varied and four equivalence proved to be beneficial, yielding the product in 76% yield (Table IV.3.1, entries 4 and 5). The excess use of ligand 2,2′-bipyridine (50 mol %) was counterproductive, providing a trace amount of product (Table IV.3.1, entry 6). Additionally, switching the catalytic system to other copper salts did not improve the yield (Table IV.3.1, entries 7–11). Control experiments revealed that the omission of either 2,2'-bipyridine or $PTSA \cdot H_2O$ failed to give the desired product, thereby suggesting their crucial role in the present protocol (Table IV.3.1, entries 12 and 13). Among the solvent screened, both non-polar (toluene) and polar solvents (MeOH, acetonitrile, and DMSO) were found to be inferior to that of DCE (Table IV.3.1, entries

14–17). The use of other copper-binding ligands such as L-proline (00%), PPh_3 (00%), and XPhos (00%) was unproductive while 1,10-phenanthroline (72%) gave a comparable yield (Table IV.3.1, entries 18–21). Other acid additives such as AcOH, CF_3COOH, and $PhCO_2H$ instead of PTSA·H_2O were found completely ineffective (Table IV.3.1, entries 22–24). Further, increasing the amount of 2-iodoaniline (**a**) to 3 equiv did not improve the yield (76%) (Table IV.3.1, entry 25), while decreasing the amount to 1 equiv had a detrimental effect (48%) (Table IV.3.1, entry 26). When the reaction was continued for 24 h, a marginal increase in the yield was observed (Table IV.3.1, entry 27). The reaction at lower (80 °C) and higher (140 °C) temperatures failed to improve the product yield (Table IV.3.1, entries 28 and 29). The reaction was successful with 2-bromoanilne but the yield was only 52% after 24 h (Table IV.3.1, entry 30). After screening various reaction parameters, the optimized condition for this transformation was found to be the use of (**1**) (0.25 mmol), (**a**) (0.50 mmol, 2 equiv), $Cu(OAc)_2·H_2O$ (50 mol %), 2,2′-bipyridine (20 mol %), and PTSA·H_2O (4 equiv) in DCE (2 mL) at 120 °C in a pressure tube for 12 h (Table IV.3.1, entry 4).

Table IV.3.1. *Optimization of the reaction conditions.*[a–h]

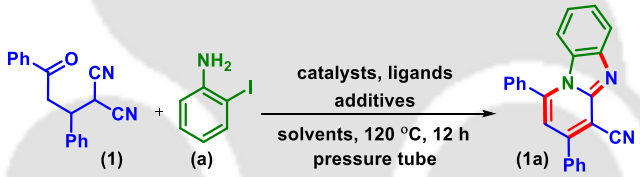

entry	catalyst (mol %)	ligand (mol %)	additive (equiv)	solvent	yield (%)[b]
1	$Cu(OAc)_2·H_2O$ (10)	2,2'-bipyridyl (20)	PTSA·H_2O (2)	1,2-DCE	15
2	$Cu(OAc)_2·H_2O$ (20)	2,2'-bipyridyl (20)	PTSA·H_2O (2)	1,2-DCE	31
3	$Cu(OAc)_2·H_2O$ (50)	2,2'-bipyridyl (20)	PTSA·H_2O (2)	1,2-DCE	58
4	**$Cu(OAc)_2·H_2O$ (50)**	**2,2'-bipyridyl (20)**	**PTSA·H_2O (4)**	**1,2-DCE**	**76**
5	$Cu(OAc)_2·H_2O$ (50)	2,2'-bipyridyl (20)	PTSA·H_2O (5)	1,2-DCE	78
6	$Cu(OAc)_2·H_2O$ (50)	2,2'-bipyridyl (50)	PTSA·H_2O (4)	1,2-DCE	trace
7	$Cu(OAc)_2$ (50)	2,2'-bipyridyl (20)	PTSA·H_2O (4)	1,2-DCE	72
8	$Cu(SO_4)_2·5H_2O$ (50)	2,2'-bipyridyl (20)	PTSA·H_2O (4)	1,2-DCE	<15
9	$Cu(OTf)_2$ (50)	2,2'-bipyridyl (20)	PTSA·H_2O (4)	1,2-DCE	nd
10	CuI (50)	2,2'-bipyridyl (20)	PTSA·H_2O (4)	1,2-DCE	00
11	Cu_2O (50)	2,2'-bipyridyl (20)	PTSA·H_2O (4)	1,2-DCE	00
12	$Cu(OAc)_2·H_2O$ (50)		PTSA·H_2O (4)	1,2-DCE	trace
13	$Cu(OAc)_2·H_2O$ (50)	2,2'-bipyridyl (20)		1,2-DCE	00
14	$Cu(OAc)·H_2O$ (50)	2,2'-bipyridyl (20)	PTSA·H_2O (4)	Toluene	00

15	$Cu(OAc)\cdot H_2O$ (50)	2,2'-bipyridyl (20)	$PTSA\cdot H_2O$ (4)	MeOH	00
16	$Cu(OAc)\cdot H_2O$ (50)	2,2'-bipyridyl (20)	$PTSA\cdot H_2O$ (4)	CH_3CN	00
17	$Cu(OAc)\cdot H_2O$ (50)	2,2'-bipyridyl (20)	$PTSA\cdot H_2O$ (4)	DMSO	00
18	$Cu(OAc)\cdot H_2O$ (50)	1,10-phen (20)	$PTSA\cdot H_2O$ (4)	1,2-DCE	72
19	$Cu(OAc)\cdot H_2O$ (50)	L-proline (20)	$PTSA\cdot H_2O$ (4)	1,2-DCE	00
20	$Cu(OAc)\cdot H_2O$ (50)	PPh_3 (20)	$PTSA\cdot H_2O$ (4)	1,2-DCE	00
21	$Cu(OAc)\cdot H_2O$ (50)	XPhos (20)	$PTSA\cdot H_2O$ (4)	1,2-DCE	00
22	$Cu(OAc)\cdot H_2O$ (50)	2,2'-bipyridyl (20)	AcOH (4)	1,2-DCE	00
23	$Cu(OAc)\cdot H_2O$ (50)	2,2'-bipyridyl (20)	CF_3SO_3H (4)	1,2-DCE	00
24	$Cu(OAc)\cdot H_2O$ (50)	2,2'-bipyridyl (20)	$PhCO_2H$ (4)	1,2-DCE	00
25	$Cu(OAc)\cdot H_2O$ (50)	2,2'-bipyridyl (20)	$PTSA\cdot H_2O$ (4)	1,2-DCE	76[c]
26	$Cu(OAc)\cdot H_2O$ (50)	2,2'-bipyridyl (20)	$PTSA\cdot H_2O$ (4)	1,2-DCE	48[d]
27	$Cu(OAc)\cdot H_2O$ (50)	2,2'-bipyridyl (20)	$PTSA\cdot H_2O$ (4)	1,2-DCE	73[e]
28	$Cu(OAc)\cdot H_2O$ (50)	2,2'-bipyridyl (20)	$PTSA\cdot H_2O$ (4)	1,2-DCE	trace[f]
29	$Cu(OAc)\cdot H_2O$ (50)	2,2'-bipyridyl (20)	$PTSA\cdot H_2O$ (4)	1,2-DCE	62[g]
30	$Cu(OAc)\cdot H_2O$ (50)	2,2'-bipyridyl (20)	$PTSA\cdot H_2O$ (4)	1,2-DCE	52[h]

[a]Reaction condition: 2-(3-oxo-1,3-diphenylpropyl)malononitrile (**1**) (0.25 mmol), 2-iodoaniline (**a**) (0.5 mmol), catalyst (mol %), additives (equiv) at 120 °C in a sealed tube for 12 h. [b]Yields of the isolated product. [c]3 equiv of (**a**) was used. [d]1 equiv of (**a**) was used. [e]Yield after 24 h. [f]Temperature 80 °C. [g]Temperature 140 °C. [h]Reaction carried out using 2-bromoaniline for 24 h.

IV.3.2. Substrates Scopes for the Synthesis of Fused Benz-Imidazopyridines:

With the best-optimized conditions in hand, the effect of R^1 and R^2 on γ-keto-malononitriles (**1**–**21**) was tested with 2-iodoaniline (**a**) (Scheme IV.3.2.1). Substrates having an unsubstituted aroyl ring (R^1 = H) and R^2 as electron-donating substituents *viz*. *p*-Me (**2**), *p*-OMe (**3**), and *p*-Ph (**4**) reacted successfully with (**a**), yielding their corresponding benz-imidazopyridines (**2a**), (**3a**), and (**4a**) in 75%, 80%, and 82% yield respectively. Similarly, substrates with R^2 as electron-withdrawing groups such as *p*-F (**5**), *p*-Cl (**6**), *o*-Br (**7**), and *m*-NO_2 (**8**) provided their respective products (**5a**, 79%), (**6a**, 72%), (**7a**, 61%), and (**8a**, 64%) (Scheme IV.3.2.1). Therefore, nearly identical yields were obtained regardless of the electronic effect suggesting the insignificant influence of R^2 on the reaction. Next, the effect of R^1 was screened, and both electron-donating groups *p*-Me (**9**), *p*-OMe (**10**) and electron-withdrawing groups *p*-F (**11**), *p*-Cl (**12**), *p*-Br (**13**), and *o*-NO_2 (**14**) were compatible giving the corresponding benz-imidazopyridines (**9a**, 82%), (**10a**, 84%), (**11a**, 66%), (**12a**, 63%), (**13a**, 62%), and (**14a**, 41%) (Scheme IV.3.2.1). The substrates

containing R^1 as EDG gave higher yields compared to the EWG which indicate EDGs in the aroyl moiety (R^1) show better reactivity. This might be due to the destabilization of the imine intermediate in substrates having EWG.

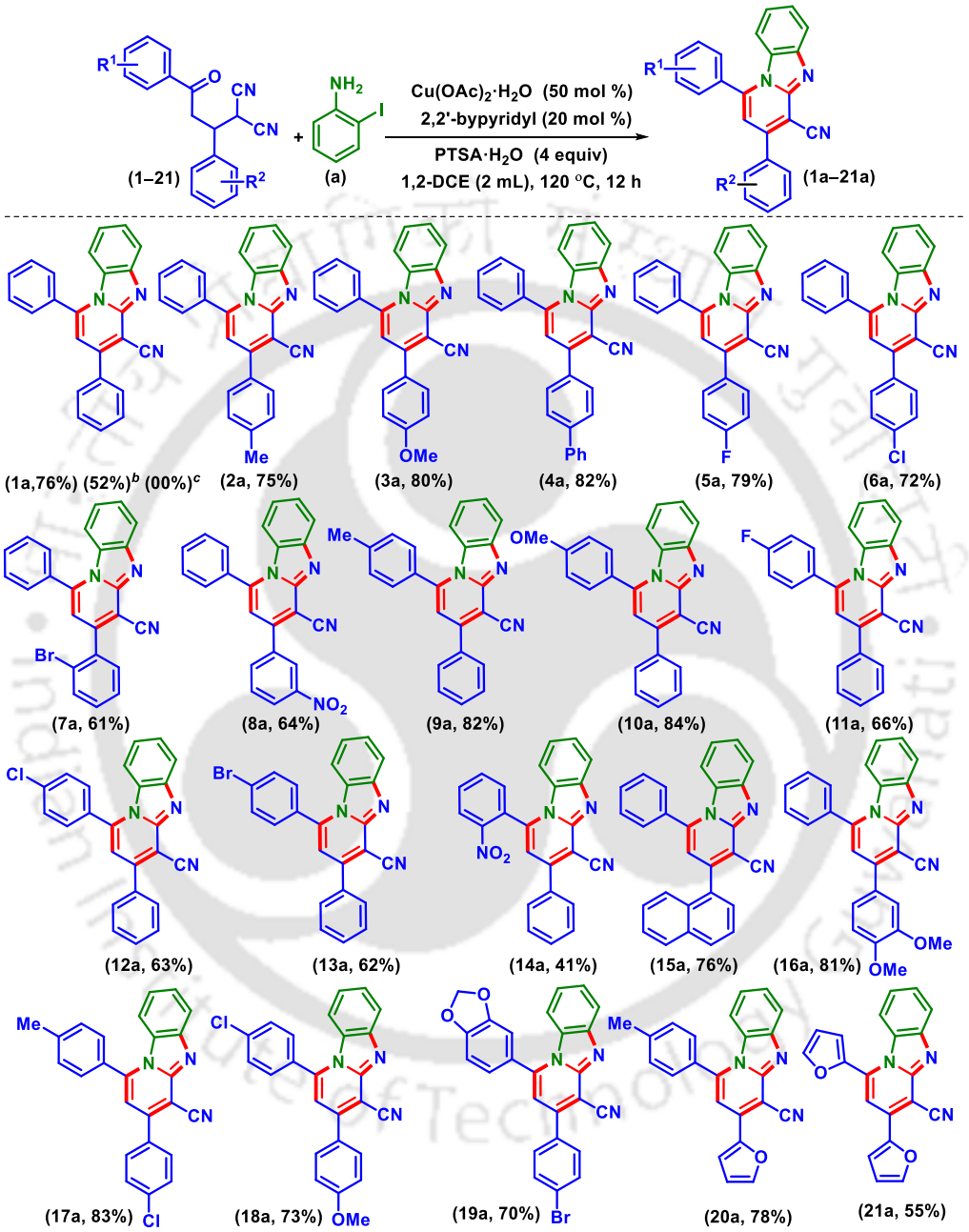

[a]Reaction conditions: (i) **1**–**21** (0.25 mmol), 2-iodoaniline (**a**) (0.50 mmol), $Cu(OAc)_2·H_2O$ (0.125 mmol), 2,2'-bipyridyl (0.050 mmol), $PTSA·H_2O$ (1 mmol) and 1,2-DCE (2 mL) at 120 °C in a pressure tube for 12 h. [b]Reaction carried out using 2-bromoaniline for 24 h. [c]Reaction carried out using 2-chloroaniline for 24 h.

Scheme IV.3.2.1. *Substrate scope for various γ-ketodinitriles.*[a,b,c]

This methodology was equally successful when the phenyl ring α to the malononitrile was replaced with a naphthyl ring (**15**), and a 3,4-disubstituted phenyl ring (**16**) giving their respective products (**15a**), and (**16a**) in 76% and 81% yields respectively (Scheme IV.3.2.1). Next, both R^1/R^2 of γ-keto-malononitriles were varied. The γ-keto-malononitriles having *p*-Me/*p*-Cl (**17**) and *p*-Cl/*p*-OMe (**18**) gave their expected products (**17a**, 83%), and (**18a**, 73%) in good yield respectively (Scheme IV.3.2.1). Similarly, γ-keto-malononitriles bearing benzo[*d*][1,3]dioxole aroyl ring and R^2 as *p*-Br (**19**) afforded the desired product (**19a**, 70%) in good yield respectively (Scheme IV.3.2.1). Furthermore, R^1 as *p*-Me in combination with furan (**20**) and substrate with two furan rings (**21**) gave their products (**20a**) and (**21a**) in 78% and 55% yields, respectively (Scheme IV.3.2.1).

After successfully synthesizing a library of fused benz-imidazopyridines using several γ-keto malononitriles (**1–21**), the scope of this methodology was then extended to substituted *o*-iodoanilines (**b**–**m**) (Scheme IV.3.2.2). *o*-Iodoanilines possessing electron-donating groups such as *p*-Me (**b**), 3,4-di-Me (**c**), *p*-^{i}Pr (**d**), and *p*-Bu (**e**) positively responded to this protocol providing their expected products (**1b**, 81%), (**1c**, 65%), (**1d**, 72%), and (**1e**, 76%) (Scheme IV.3.2.2).

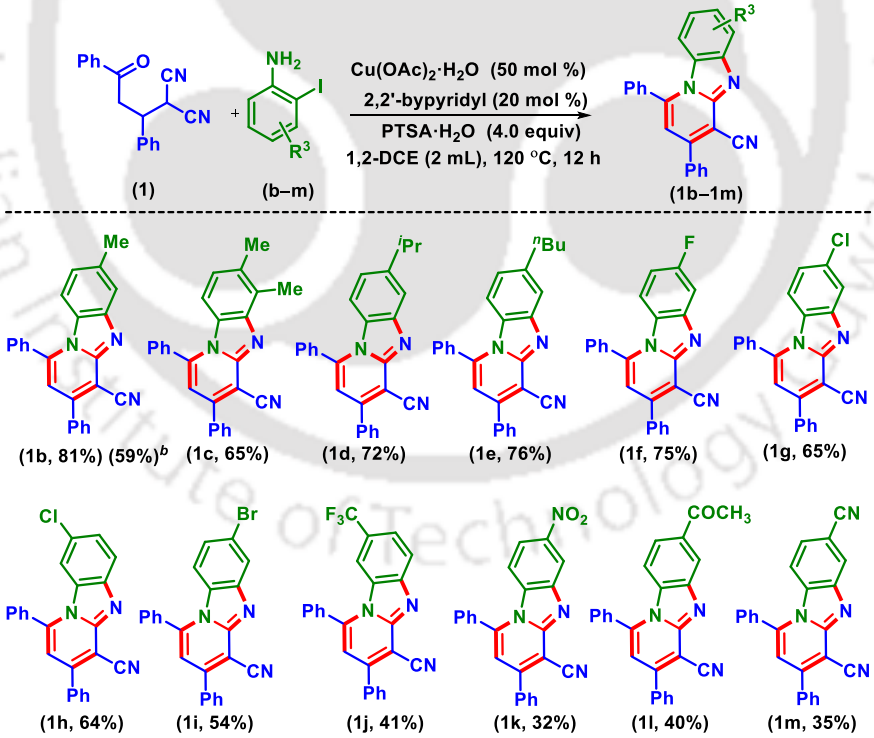

[a]Reaction conditions: (i) **1** (0.25 mmol), 2-iodoanilines (**b–m**) (0.50 mmol), $Cu(OAc)_2·H_2O$ (0.125 mmol), 2,2'-bipyridyl (0.050 mmol), $PTSA·H_2O$ (1 mmol) and 1,2-DCE (2 mL) at 120 °C in a pressure tube for 12 h. [b]5 mmol scale.

Scheme IV.3.2.2. *Substrate scope for o-iodoanilines.*[a,b]

o-Iodoanilines possessing electron-withdrawing groups *p*-F (**f**), *p*-Cl (**g**), 5-Cl (**h**), *p*-Br (**i**), 5-CF_3 (**j**), *p*-NO_2 (**k**), *p*-$COCH_3$ (**l**), and *p*-CN (**m**) underwent efficient cyclization when reacted with γ-keto malononitrile (**1**) providing their expected products (**1f**, 75%), (**1g**, 65%), (**1h**, 64%), (**1i**, 54%), (**1j**, 41%), (**1k**, 32%), (**1l**, 40%), and (**1m**, 35%) respectively (Scheme IV.3.2.2). As can be observed from the yields pattern, *o*-iodoanilines possessing electron-withdrawing groups (**b**–**e**) gave lower yields compared to substrates having electron-donating (**f**–**m**) substituents. This is because, the amino group in substrates possessing electron-donating groups are better nucleophiles during nucleophilic addition at the γ-keto group of the dinitrile precursors.

IV.4. Mechanistic Investigations:

IV.4.1. Control Experiments:

Several control experiments were carried out to elucidate a plausible reaction mechanism for this Cu(II)-promoted transformation. To ascertain the role of Cu(II), two independent reactions were performed. In the first reaction, (**9**) and (**a**) were reacted without $Cu(OAc)_2{\cdot}H_2O$ and 2,2′-bypyridine. The reaction failed to give the desired product (**9a**) instead, an imine intermediate (**9a′**) was obtained in 32% yield after 12 h (Scheme IV.4.1.1).

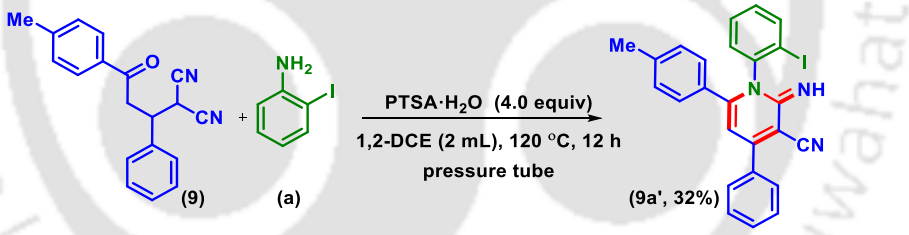

Scheme IV.4.1.1. *Reaction in the absence of catalyst and ligand.*

While in the second reaction, both (**9**) and (**a**) were reacted in the presence of $Cu(OAc)_2{\cdot}H_2O$ and 2,2′-bypyridine 20 mol % each. After 6 h, the formation of imine intermediate (**9a′**, 66%) and the desired product (**9a**, 24%) was observed (Scheme IV.4.1.2). These observations confirmed that the Cu(II) is assisting in the cyclic imine formation possibly *via* coordination with the cyano group and it can help the oxidation/aromatization process during the formation of the intermediate (**9a′**).

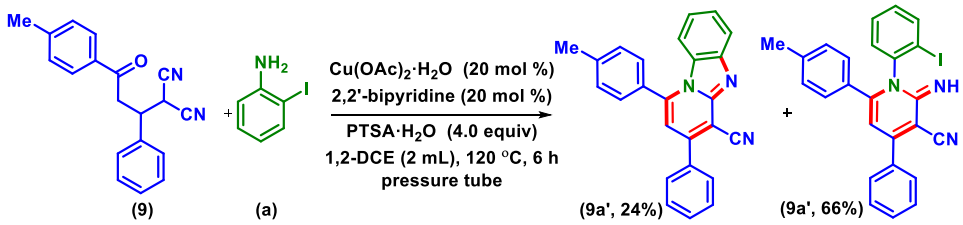

Scheme IV.4.1.2. *Reaction in the presence of lower catalyst loading.*

To check the exact role of the ligand, a pre-formed (**9a′**) and $Cu(OAc)_2{\cdot}H_2O$ (30 mol %) in the presence or absence of the ligand successfully produce the desired product (**9a**) almost in a similar yield of 92% and 88% respectively (Scheme IV.4.1.3). Thus, ruling out the involvement of ligand in Cu(II)-catalyzed intramolecular Ullmann-type cyclization. Also, the success of the reaction with 30 mol % catalyst loading hinted at the involvement of two different forms of Cu(II) catalyst, one in ligated and the other in non-ligated form.

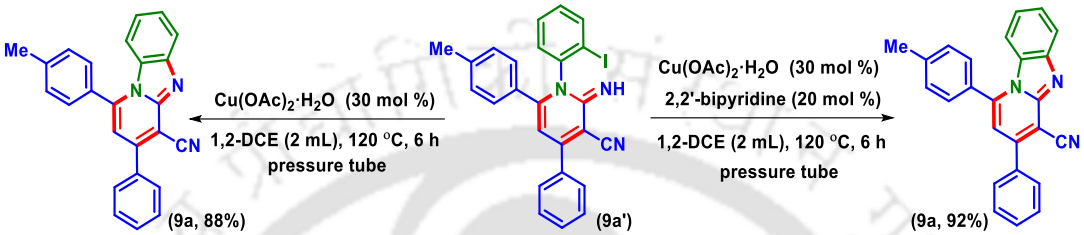

Scheme IV.4.1.3. *Reaction with and without ligand.*

To justify the role of the iodo group, a reaction was commenced between **1** and *p*-toluidine (**n**). The reaction delivers the hydrolyzed *N*-arylated-2-pyridone (**1n**, 62%) as a major product along with the minor formation of imine intermediate (**1n′**, 22%) (Scheme IV.4.1.4). This result recommends the presence of the iodo group in the ortho position for Cu(II)-catalyzed Ullmann cyclization.

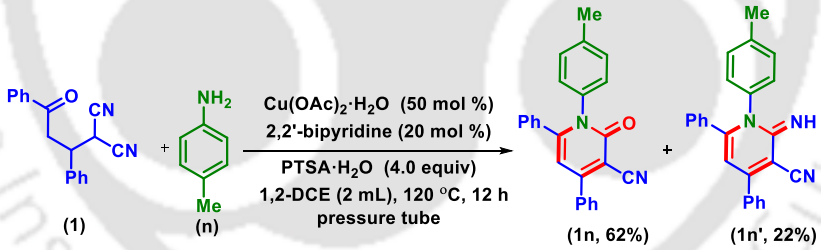

Scheme IV.4.1.4. *Reaction with p-toluidine.*

From the series of control experiments, it was found:

(i) Only the cyclic imine intermediate (**V**) (Scheme IV.4.2.1) was obtained in a lower yield (32%) in the absence of $Cu(OAc)_2{\cdot}H_2O$ and 2,2′-bipyridine.

(ii) Both catalyst and ligand help accelerate the formation of cyclic imine (**V**).

(iii) The Ullmann coupling step proceeds with equal efficiency either in the presence or absence of the ligand.

(iv) Distinct involvement of ligated Cu(II) and free Cu(II) in the reaction process.

(v) Requirement of the *ortho*-iodo group for cyclization.

IV.4.2. Plausible Reaction Mechanism:

Based on the control experiments, literature reports[19] and intermediate detected by HRMS analysis (Figure IV.4.2.1), a plausible reaction mechanism is proposed (Scheme IV.4.2.1). Initially, the γ-ketodinitrile (**1**) undergo an acid-catalyzed imine formation with 2-iodoaniline (**a**) to form an intermediate (**I**). In the presence of 2,2′-bipyridine (L) and PTSA, the *in situ* generated ligand-bound Cu(II) complex (**A**) undergo coordination with one of the nitrile groups of intermediate (**I**) to form intermediate (**II**). The intramolecular cyclization of (**II**) produces a six-membered cyclic intermediate (**III**) in which the Cu(II) is coordinated with the nitrile *N* atom with the elimination of PTSA. Protonolysis of (**III**) gives intermediate (**IV**) and regenerates the Cu(II) complex (**A**).

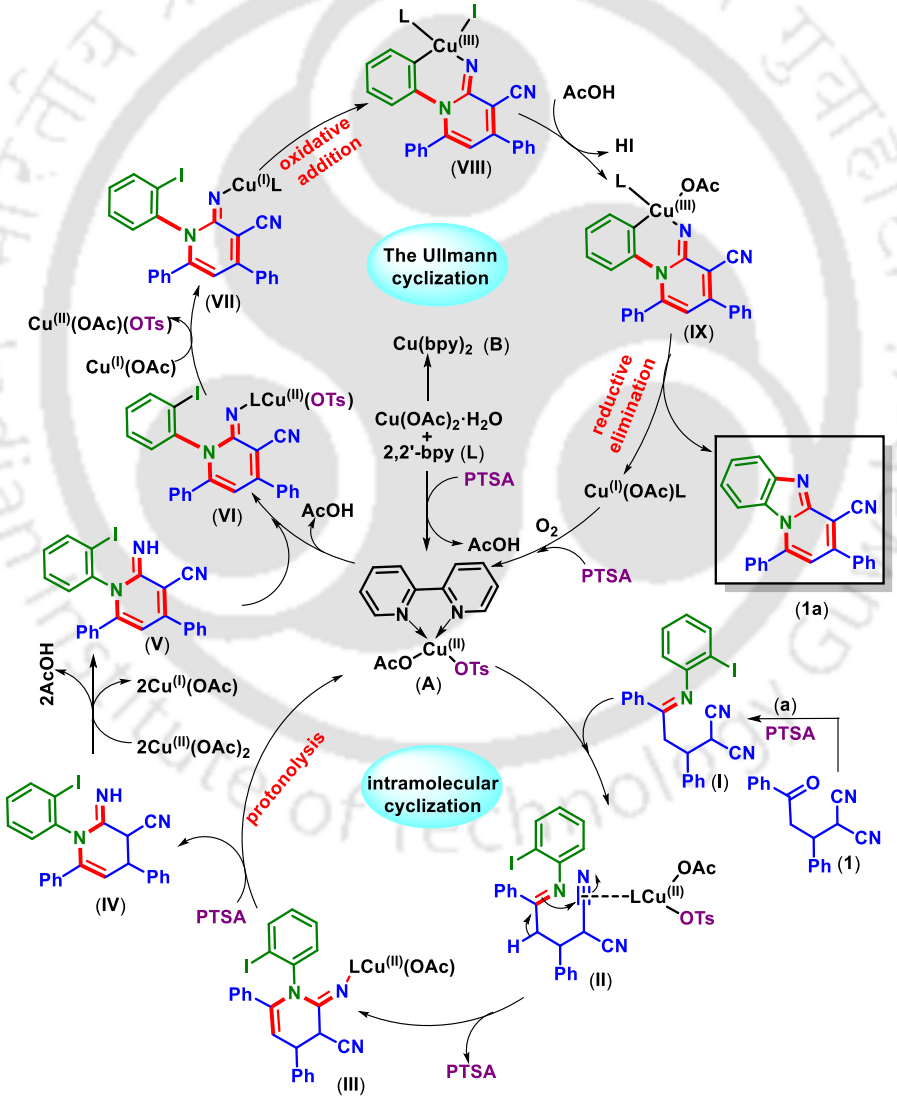

Scheme IV.4.2.1. *Proposed reaction path.*

In the presence of $Cu(OAc)_2 \cdot H_2O$/bpy, the intermediate (**IV**) aromatizes to a cyclic imine (**V**) (detected by HRMS analysis, Figure IV.4.2.1) which coordinates with complex (**A**) to give an intermediate (**VI**) (detected by HRMS analysis, Figure IV.4.2.1) *via* elimination of AcOH. The Cu(II) bound intermediate (**VI**) undergoes disproportionation in the presence of *in situ* generated Cu(I)OAc to generate a Cu(I) coordinated species (**VII**) (detected by HRMS analysis, IV.4.2.1). A subsequent intramolecular oxidative addition with the iodoaryl generates a Cu(III) intermediate (**VIII**). Next, the exchange of acetate ligand produces an intermediate (**IX**) with the elimination of HI. Finally, the reductive elimination gives the product (**1a**) with the formation of [Cu(I)(OAc)(bpy)] complex which coordinates with PTSA to regenerate the active catalyst (**A**).

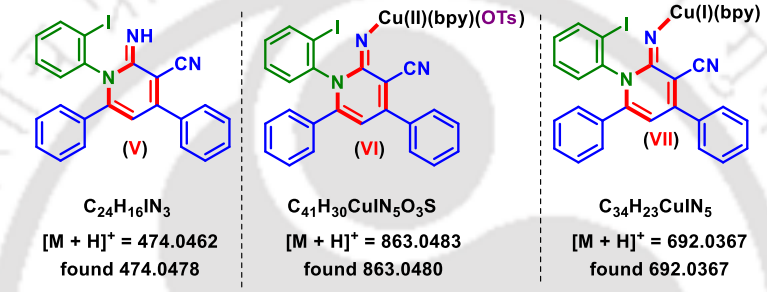

Figure IV.4.2.1. *Intermediate detected from the HRMS analysis of the reaction aliquots.*

IV.5. Post-Synthetic Applications:

To further explore the synthetic utility, a few late-stage functionalizations were successfully carried out. The nitrile moiety of 7-methyl-1,3-diphenylbenzo[4,5]imidazo[1,2-*a*]pyridine-4-carbonitrile (**1b**) was successfully converted to keto aryl group using a Pd(II)-catalyzed addition of phenylboronic acid (**o**), giving **1bo** in 72% yield (Scheme IV.5.1).[20]

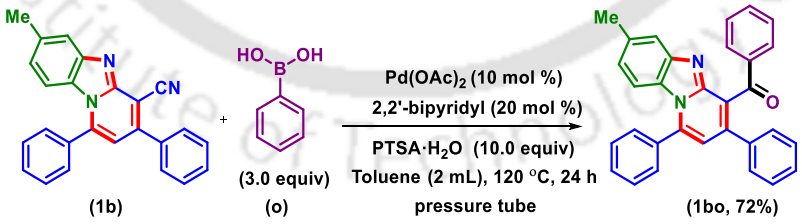

Scheme IV.5.1. *Pd(II)-catalyzed addition of phenylboronic acid.*

Further a Pd(II)-catalyzed Sonogashira coupling was performed between a bromo-substituted benz-imidazopyridine, 7-bromo-1,3-diphenylbenzo[4,5]imidazo[1,2-*a*]pyridine-4-carbonitrile (**1i**), and 4-ethynyltoluene (**p**) to produce an alkyne functionalized benz-imidazopyridine (**1ip**) in 52% yield (Scheme IV.5.2).[21]

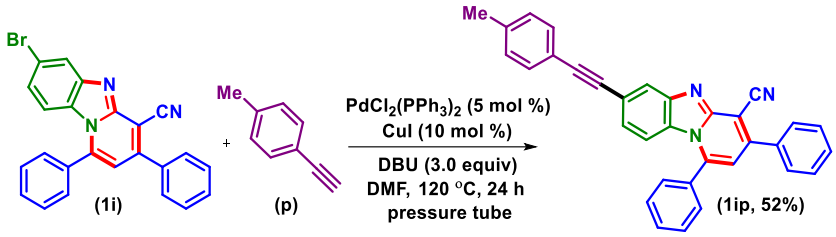

Scheme IV.5.2. *Pd(II)-catalyzed Sonogashira coupling.*

IV.6. Photophysical Properties:

Usually, π-conjugated nitrogen-containing flat, planner heterocycles display luminogenic[22] behavior under UV light. Thus, the photophysical behavior of some of the synthesized compounds was inspected. However, the introduction of electron-donating and electron-withdrawing groups to the phenyl rings of the diarylbenzo[4,5]imidazo[1,2-*a*]pyridine skeleton has a slight influence on their photophysical properties.

The UV-visible absorption spectra of **1a**, **3a**, **6a**, **7a**, **8a**, **10a**, **12a**, **13a**, **17a**, **18a, 1b**, **1d**, **1g**, **1i**, and **1m** (Figure IV.6.1) were recorded in dichloromethane having 1 x 10^{-5} M concentration. These (benzo)imidazopyridines derivatives exhibit two absorption maxima, one in the region of 270–280 nm and the other 338–350 nm.

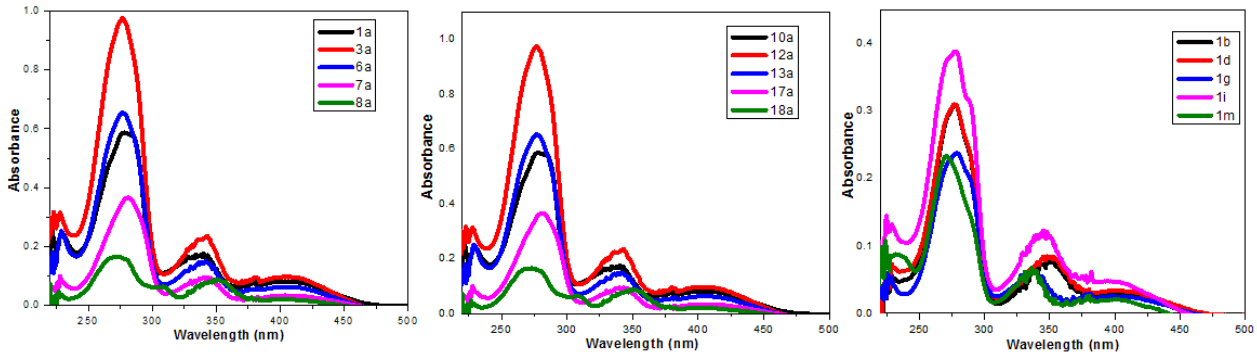

Figure IV.6.1. *UV-vis spectra in CH_2Cl_2 (concentrations: 1 x 10^{-5} M).*

The photoluminescence spectra of **1a**, **3a**, **6a**, **7a**, **8a**, **10a**, **12a**, **13a**, **17a**, **18a, 1b**, **1d**, **1g**, **1i**, and **1m** (Figure IV.6.2) were recorded in dichloromethane having 1 x 10^{-5} M concentration exciting at 380 nm. All these compounds emit green fluorescence with fluorescence emission between 502–533 nm (Table IV.6.1). Therefore, they could be developed as good organic fluorophores having important applications in materials sciences such as probes, bio-imaging, and optoelectronic devices.

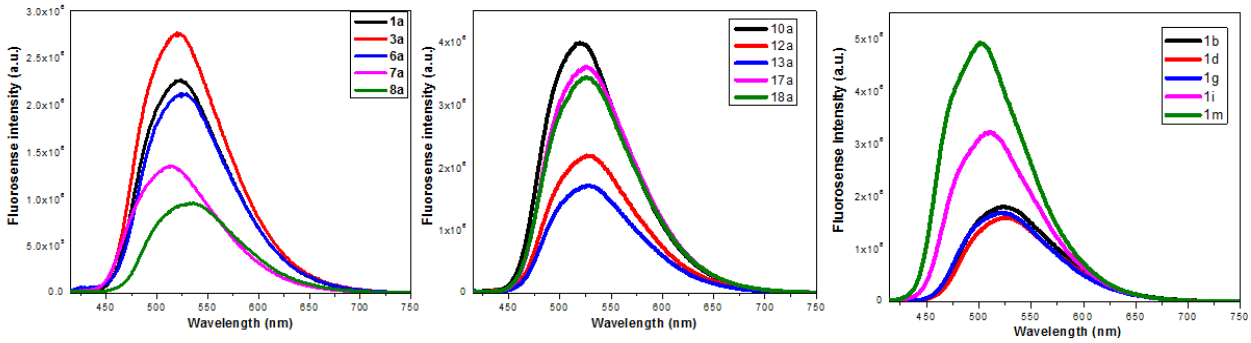

Figure IV.6.2. *Photoluminescence spectra in CH_2Cl_2 (concentrations: 1 x 10^{-5} M, excitation wavelength 380 nm).*

The effect of solvent polarity was also examined by measuring the fluorescence emissions of compounds **1a**, **3a**, **6a**, **10a**, and **12a** (Figure IV.6.3) in hexane, toluene, DCM, ethyl acetate, MeOH, acetonitrile, and DMSO. The emission wavelengths of the compounds with either electron-donating groups (**3a** and **10a**) or electron-withdrawing groups (**6a** and **12a**) in both polar and non-polar solvents were unaffected, suggesting a negligible solvent effect (Table IV.6.2).

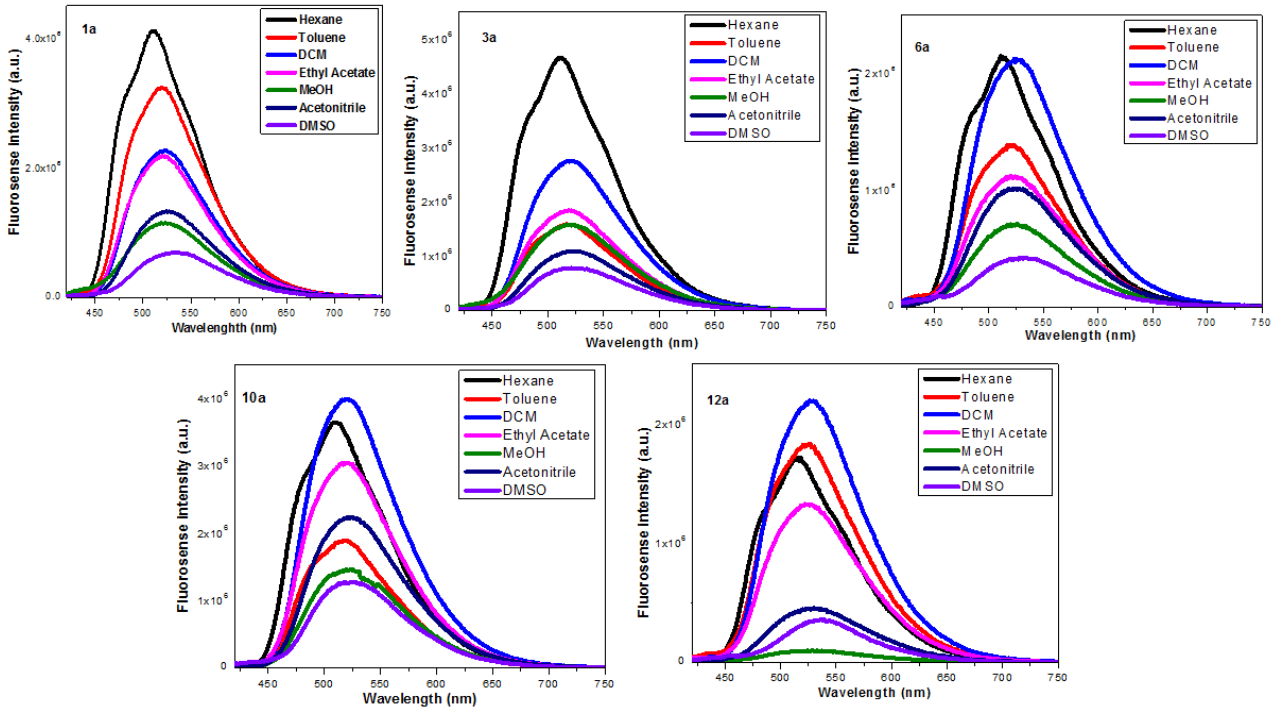

Figure IV.6.3. *Photoluminescence spectra in different solvents (concentrations: 1 x 10^{-5} M, excitation wavelength 380 nm).*

Table IV.6.1. *Absorbance and emission maxima of the selected compounds.*

Entry	Compound	λ_{abs} (nm)	λ_{em} (nm)
1	**1a**	280, 341	521
2	**3a**	276, 342	520
3	**6a**	277, 342	525
4	**7a**	281, 344	514
5	**8a**	273, 352	532
6	**10a**	280, 341	520
7	**12a**	277, 343	528
8	**13a**	277, 343	527
9	**17a**	281, 343	525
10	**18a**	271, 353	526
11	**1b**	277, 352	524
12	**1d**	277, 352	525
13	**1g**	279, 343	522
14	**1i**	278, 347	510
15	**1m**	270, 338	502

Table IV.6.2. *Emission maxima of the selected compounds in different solvents.*

Entry	Compound	λ_{em} (nm)						
		Hexane	Toluene	DCM	EtOAc	MeOH	CH_3CN	DMSO
1	**1a**	511	520	521	522	522	526	532
2	**3a**	511	518	520	520	520	522	527
3	**6a**	512	520	527	522	523	522	530
4	**10a**	511	520	520	520	518	523	525
5	**12a**	515	526	528	524	525	527	533

IV.7. Density Functional Theory (DFT) Calculations:

To determine more supplementary information concerning the properties of these molecules at their molecular level, density functional theory (DFT) calculations were performed using a suite of the Gaussian 09 program.[23] The highest occupied molecular orbital (HOMO) and lowest unoccupied molecular orbital (LUMO) energy levels of the derivatives were calculated using the B3LYP/6-31G (d, p) basis set level in the dichloromethane solvent modeled by the PCM approach. The LUMOs of each compound are distributed over the entire molecule, while the HOMOs were primarily distributed on the benzo[4,5]imidazo[1,2-*a*]pyridine skeleton excluding the two aryl ring at the 1 and 3 position positions having an energy gap in the range of 3.46–3.57 eV (Figure IV.7.1, and IV.7.2).

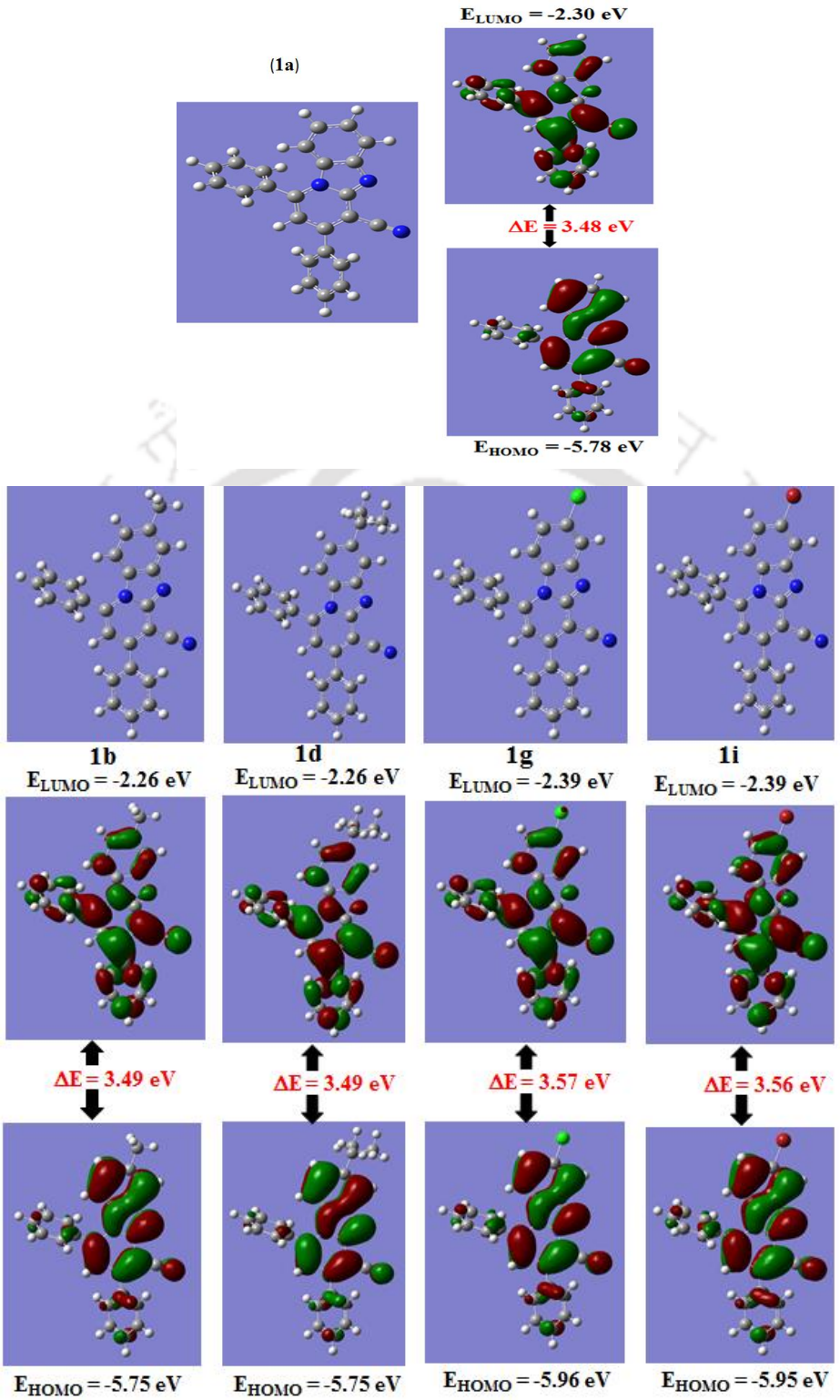

Figure IV.7.1. *DFT optimized structure and Molecular Orbitals amplitude plots of HOMO and LUMO of* ***1a***, ***3a***, ***6a***, ***10a***, *and* ***12a*** *using density functional theory calculation at the B3LYP/6-31G (d, p) basis set level in dichloromethane solvent modeled by the PCM approach.*

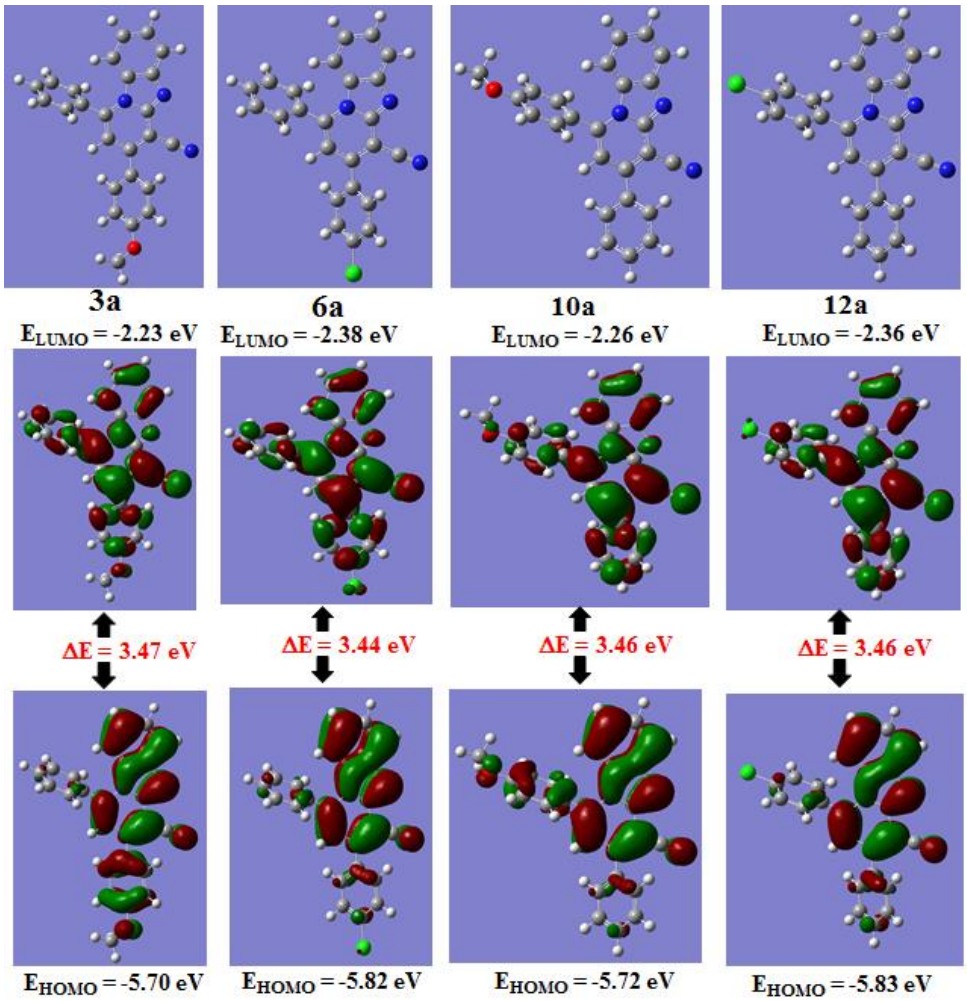

Figure IV.7.2. *DFT optimized structure and Molecular Orbitals amplitude plots of HOMO and LUMO of* ***3a***, ***6a***, ***10a***, *and* ***12a*** *using density functional theory calculation at the B3LYP/6-31G (d, p) basis set level in dichloromethane solvent modeled by the PCM approach.*

IV.8. Conclusion:

In conclusion, we have demonstrated an effective methodology for the synthesis of aza fused benz-imidazopyridine-carbonitriles *via* Cu(II)-promoted cascade C=C, C–N, and C=N bond formations. This protocol is scalable and features readily available starting materials having broad substrate scope. The prevalent existence of the core skeletons in medicinally pertinent compounds makes it synthetically useful. Beyond the synthesis, few post-synthetic functionalizations with the resulting molecules have been demonstrated. Further, these benz-imidazopyridines exhibit green emission (λ_{max} 502–533 nm) and HOMO-LUMO energy gap in the range of 3.44 to 3.57 eV making them potential candidates for material science applications.

IV.9 Experimental Section:

IV.9.1. General Information:

All the reagents were commercial grade and purified according to the established procedures. All the reagents were commercial grade and used without further purification unless otherwise stated. All the reactions were carried out in an oven-dried pressure tube (20.3 cm x 19 mm, 21 mL) under aerobic conditions. Reactions were monitored by thin-layer chromatography (TLC) on 0.25 mm silica gel plates ($60F_{254}$) and visualized under UV illumination at 254 nm. Organic extracts were dried over anhydrous sodium sulfate (Na_2SO_4). Column chromatography was performed to purify the crude product on silica gel 60–120 mesh using a mixture of hexane and ethyl acetate as eluent. The isolated compounds were characterized by spectroscopic [^1H, $^{13}C\{1H\}$ NMR, and IR] techniques and HRMS analysis. NMR spectra were recorded in deuterochloroform ($CDCl_3$). ^1H, $^{13}C\{1H\}$ were recorded in 600 (150) or 500 (125), or 400 (100) MHz spectrometer and were calibrated using tetramethylsilane or residual undeuterated solvent for ^1H NMR, deuterochloroform for ^{13}C NMR as an internal reference {$Si(CH_3)_4$: 0.00 ppm or $CHCl_3$: 7.260 ppm for ^1H NMR, 77.230 ppm for ^{13}C NMR}. ^{19}F NMR was calibrated without any internal standard in $CDCl_3$ in 400 MHz spectrometers. The chemical shifts are quoted in δ units, parts per million (ppm). ^1H NMR data is represented as follows: Chemical shift, multiplicity (s = singlet, d = doublet, t = triplet, q = quartet, m = multiplet, br = broad, dd = doublet of doublet, tt = triplet of triplet), integration and coupling constant(s) *J* in hertz (Hz). High-resolution mass spectra (HRMS) were recorded on a mass spectrometer using electrospray ionization-time of flight (ESI-TOF) reflection experiments. FT-IR spectra were recorded in KBr or neat and reported in the frequency of absorption (cm^{-1}). All UV experiments were performed at a probe concentration of 10^{-5} M in 1 mL quartz cuvettes of path length 1 cm at 25 ^oC in UV-Vis spectrometer. Photoluminescence was carried out at a concentration of 10^{-5} M in 1 mL quartz cuvettes at 25 ^oC in a spectrofluorometer in an HPLC grade dichloromethane solution.

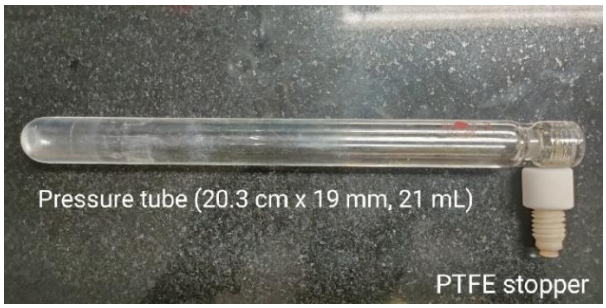

IV.9.2. General Procedures:

IV.9.2.1. General Procedure for the Synthesis of 2-(3-Oxo-1,3-diarylpropyl)malononitriles (1–21):

Compounds **1**–**21** are synthesized by slight modifying of the literature procedure.[24]

IV.9.2.2. General Procedure for the Synthesis of 2-Iodoaniline Derivatives:

2-Iodoaniline derivatives were synthesized by a slight modification of the literature procedure.[25]

IV.9.2.3. General Procedure for the Synthesis of 1,3-Diarylbenzo[4,5]imidazo[1,2-*a*]pyridine-4-carbonitriles (1a) from 2-(3-Oxo-1,3-diphenylpropyl)malononitriles (1) and 2-Iodoaniline (a):

To an oven-dried pressure tube (20.3 cm x 19 mm, 21 mL) containing a magnetic bar was added 2-(3-oxo-1,3-diphenylpropyl)malononitrile (**1**) (68 mg, 0.25 mmol), 2-iodoaniline (**a**) (109 mg, 0.50 mmol), $Cu(OAc)_2 \cdot H_2O$ (25 mg, 0.125 mmol), 2,2′-bipyridyl (7.8 mg, 0.05 mmol), $PTSA \cdot H_2O$ (190 mg, 1 mmol), and 1,2-DCE (2 mL). The reaction mixture was stirred at 120 ^oC for 12 h. After completion of the reaction (monitored by TLC analysis), the reaction mixture was admixed with ethyl acetate (25 mL) and the organic layer was washed with saturated sodium bicarbonate solution (5 mL). The organic layer was dried over anhydrous Na_2SO_4, and the solvent was evaporated under reduced pressure. The crude product so obtained was purified over a column of silica gel using 10% EtOAc in hexane to give pure 1,3-diphenylbenzo[4,5]imidazo[1,2-*a*]pyridine-4-carbonitriles (**1a**) in 76% yield (65 mg). The identity and purity of the product were confirmed by spectroscopic analysis.

IV.9.3. Mechanistic Investigation:

IV.9.3.1. Control Experiments:

IV.9.3.1.1. In the Absence of Ligand:

The experiment was carried out according to the general procedure IV.9.2.3 taking 2-(3-oxo-1-phenyl-3-(*p*-tolyl)propyl)malononitrile (**9**) (72 mg, 0.25 mmol), and 2-iodoaniline (**a**) (109 mg, 0.50 mmol) without the ligand. The crude product so obtained was purified over a column of silica gel using 30% ethyl acetate in hexane to give pure 2-imino-1-(2-iodophenyl)-4-phenyl-6-(*p*-

tolyl)-1,2-dihydropyridine-3-carbonitrile (**9a′**) with 32% yield. The identity and purity of the product were confirmed by spectroscopic analysis.

IV.9.3.1.2. In the Presence of Lower Catalyst Loading:

The experiment was carried out according to the general procedure IV.9.2.3 taking 2-(3-oxo-1-phenyl-3-(*p*-tolyl)propyl)malononitrile (**9**) (72 mg, 0.25 mmol), 2-iodoaniline (**a**) (109 mg, 0.50 mmol), and lower catalyst loading of $Cu(OAc)_2 \cdot H_2O$ (10 mg, 0.05 mmol). The crude product so obtained was purified over a column of silica gel using 10% ethyl acetate in hexane to give pure 3-phenyl-1-(*p*-tolyl)benzo[4,5]imidazo[1,2-*a*]pyridine-4-carbonitrile (**9a**) in 24% yield and using 30% ethyl acetate in hexane to give pure 2-imino-1-(2-iodophenyl)-4-phenyl-6-(*p*-tolyl)-1,2-dihydropyridine-3-carbonitrile (**9a′**) with 66% yield.

IV.9.3.1.3. Ullmann-type Cyclization Reaction with Pre-formed Cyclic Imine (9a′):

(i) The experiment was carried out according to the general procedure IV.9.2.3 taking 2-imino-1-(2-iodophenyl)-4-phenyl-6-(*p*-tolyl)-1,2-dihydropyridine-3-carbonitrile (**9a′**) (121 mg, 0.25 mmol), $Cu(OAc)_2 \cdot H_2O$ (14 mg, 0.075 mmol), 2,2′-bipyridyl (7.8 mg, 0.05 mmol), and 1,2-DCE (2 mL). The crude product so obtained was purified over a column of silica gel using 10% ethyl acetate in hexane to give pure 3-phenyl-1-(*p*-tolyl)benzo[4,5]imidazo[1,2-*a*]pyridine-4-carbonitrile (**9a**) in 92% yield.

(ii) The experiment was carried out according to the general procedure IV.9.2.3 taking 2-imino-1-(2-iodophenyl)-4-phenyl-6-(*p*-tolyl)-1,2-dihydropyridine-3-carbonitrile (**9a′**) (121 mg, 0.25 mmol), $Cu(OAc)_2 \cdot H_2O$ (14 mg, 0.075 mmol), and 1,2-DCE (2 mL). The crude product so obtained was purified over a column of silica gel using 10% ethyl acetate in hexane to give pure 3-phenyl-1-(*p*-tolyl)benzo[4,5]imidazo[1,2-*a*]pyridine-4-carbonitrile (**9a**) in 88% yield.

IV.9.3.1.4. Reaction in the Absence of *o*-Iodo Group:

The experiment was carried out according to the procedure IV.9.2.3 taking 2-(3-oxo-1,3-diphenylpropyl)malononitrile (**1**) (68 mg, 0.25 mmol), and *p*-toluidine (**a**) (54 mg, 0.50 mmol). The crude product so obtained was purified over a column of silica gel using 2% ethyl acetate in hexane to give pure 2-oxo-4,6-diphenyl-1-(*p*-tolyl)-1,2-dihydropyridine-3-carbonitrile (**1n**) in 62% yield and using 30% ethyl acetate in hexane to give pure 2-imino-4,6-diphenyl-1-(*p*-tolyl)-1,2-dihydropyridine-3-carbonitrile (**1n′**) with 22% yield.

IV.9.3.2. ESI-MS Studies for the Reaction Mixtures at Different Time Intervals:

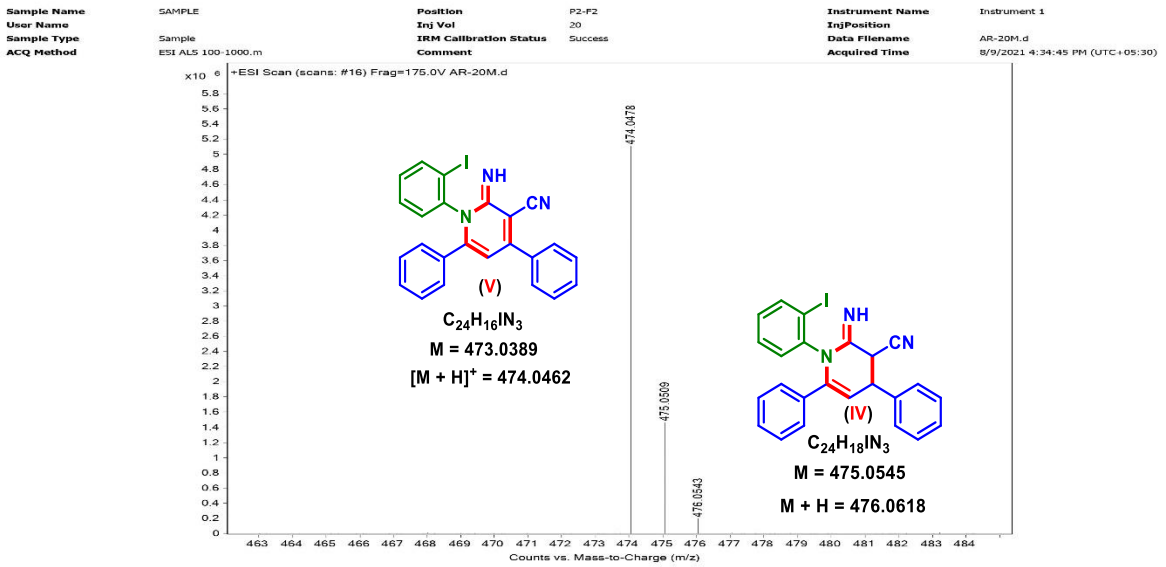

Figure IV.9.3.2.1. *HRMS spectrum after 20 min.*

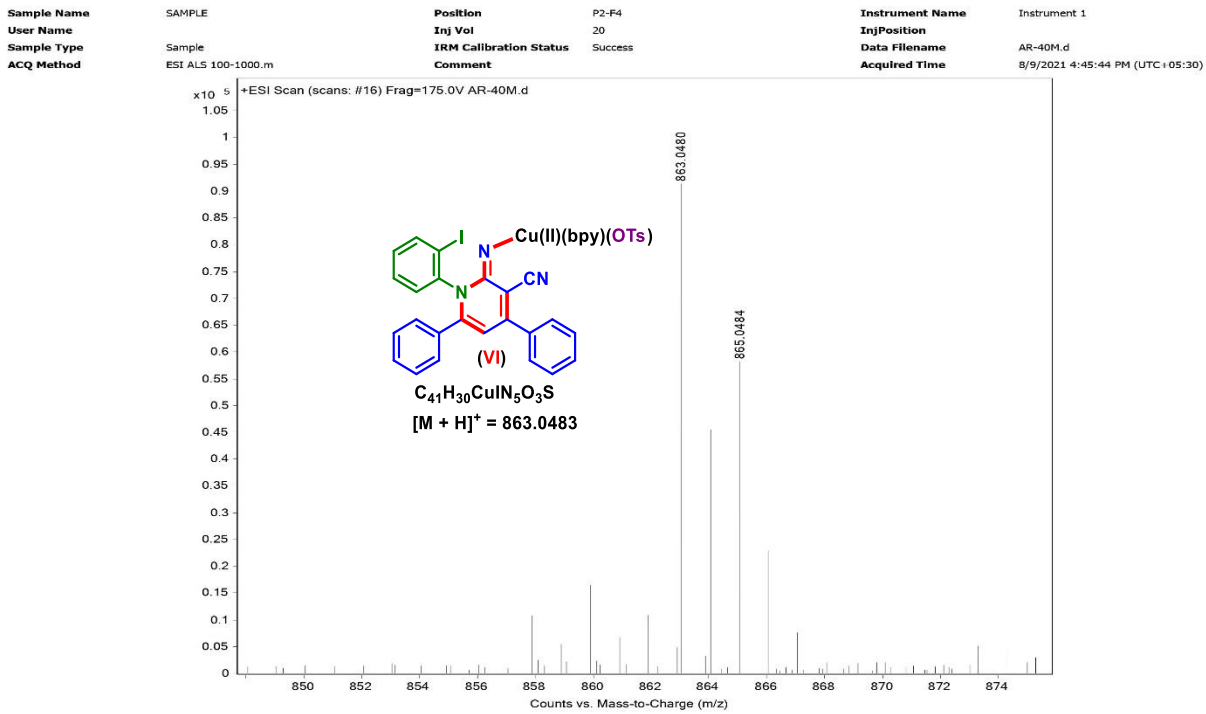

Figure IV.9.3.2.2. *HRMS spectrum after 40 min.*

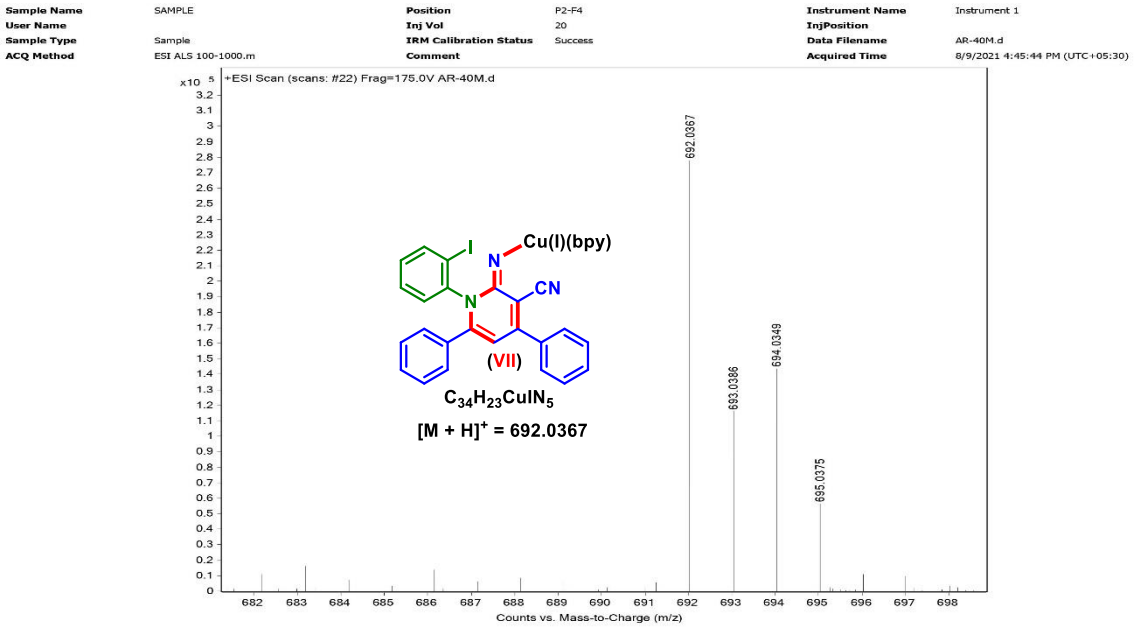

Figure IV.9.3.2.3. *HRMS spectrum after 40 min.*

IV.9.4. Post Synthetic Applications:

IV.9.4.1. General procedure for the Synthesis of (7-Methyl-1,3-diphenylbenzo[4,5]imidazo[1,2-*a*]pyridin-4-yl)(phenyl)methanone (1bo) from 7-Methyl-1,3-diphenylbenzo[4,5]imidazo[1,2-*a*]pyridine-4-carbonitrile (1b) and Phenylboronic Acid (o) :

To an oven-dried pressure tube (20.3 cm x 19 mm, 21 mL) containing a magnetic bar was added 7-methyl-1,3-diphenylbenzo[4,5]imidazo[1,2-*a*]pyridine-4-carbonitrile (**1b**) (89 mg, 0.25 mmol), phenylboronic acid (**o**) (91 mg, 0.75 mmol), $Pd(OAc)_2$ (5.6 mg, 0.025 mmol), 2,2´-bipyridyl (7.8 mg, 0.05 mmol), $PTSA{\cdot}H_2O$ (475 mg, 2.5 mmol), and toluene (2 mL). The reaction mixture was stirred in an oil bath preheated at 120 ^oC for 24 h. After completion of the reaction (monitored by TLC analysis), the reaction mixture was admixed with ethyl acetate (25 mL) and the organic layer was washed with saturated sodium bicarbonate solution (5 mL). The organic layer was dried over anhydrous sodium sulfate (Na_2SO_4), and the solvent was evaporated under reduced pressure. The crude product so obtained was purified over a column of silica gel using 5% ethyl acetate in hexane to give pure (7-methyl-1,3-diphenylbenzo[4,5]imidazo[1,2-*a*]pyridin-4-yl)(phenyl)methanone (**1bo**) in 72% yield. The identity and purity of the product were confirmed by spectroscopic analysis.

IV.9.4.2. General Procedure for the Synthesis of 1,3-Diphenyl-7-(*p*-tolylethynyl)benzo[4,5]imidazo[1,2-*a*]pyridine-4-carbonitrile (1ip) from 7-Bromo-1,3-diphenylbenzo[4,5]imidazo[1,2-*a*]pyridine-4-carbonitrile (1i):

To an oven-dried pressure tube (20.3 cm x 19 mm, 21 mL) containing a magnetic bar was added 7-bromo-1,3-diphenylbenzo[4,5]imidazo[1,2-*a*]pyridine-4-carbonitrile (**1i**) (105 mg, 0.25 mmol), 1-ethynyl-4-methylbenzene (**p**) (87 mg, 0.75 mmol), $PdCl_2(PPh_3)_2$ (8.7 mg, 0.0125 mmol), CuI (4.7 mg, 0.025 mmol), DBU (114 mg, 0.75 mmol), and DMF (2 mL). The reaction mixture was stirred in an oil bath preheated at 120 ^oC for 24 h. After completion of the reaction (monitored by TLC analysis), the reaction mixture was admixed with ethyl acetate (25 mL) and the organic layer was washed with ice-cooled water (10 mL) and saturated sodium chloride solution (5 mL). The organic layer was dried over anhydrous sodium sulfate (Na_2SO_4), and the solvent was evaporated under reduced pressure. The crude product so obtained was purified over a column of silica gel using 10% ethyl acetate in hexane to give pure 1,3-diphenyl-7-(*p*-tolylethynyl)benzo[4,5]imidazo[1,2-*a*]pyridine-4-carbonitrile (**1ip**) in 52% yield. The identity and purity of the product were confirmed by spectroscopic analysis.

IV.9.5. Crystallographic Information:

IV.9.5.1. Sample Preparation:

The single crystal of compound **1h** was prepared by the slow evaporation method for which 15 mg of the compound (**1h**) was dissolved in 1 mL of methanol in a clean and dry 10 mL glass vial. DCM (1 mL) was added to this solution slowly with a dropper. The mouth of the glass vial was covered with a cap having a small hole and kept for slow evaporation at room temperature. A single crystal of **1h** was obtained as a transparent yellow needle-like crystal after around 7 days.

IV.9.5.2. Crystallographic Information of 8-Chloro-1,3-diphenylbenzo[4,5]imidazo[1,2-*a*]pyridine-4-carbonitrile (1h):

Diffraction data were collected at 292 K with MoKα radiation (λ = 0.71073 Å) using a Bruker Nonius SMART APEX CCD diffractometer equipped with a graphite monochromator and Apex CD camera. The SMART software was used for data collection and for indexing the reflections and determining the unit cell parameters. Data reduction and cell refinement were performed using SAINT[1,2] software and the space groups of these crystals were determined from systematic absences by XPREP and further justified by the refinement results. The structures were

solved by direct methods and refined by full-matrix least-squares calculations using SHELXTL-97[3] software. All the non-H atoms were refined in the anisotropic approximation against F^2 of all reflections.

1. G. M. Sheldrick, SADABS, 1996, based on the method described in: R. H. Blessing, *Acta Crystallogr*. 1995, **A51**, 33–38.
2. SMART and SAINT, Siemens Analytical X-ray Instruments Inc., Madison, WI, 1996.
3. G. M. Sheldrick, *Acta Crystallogr.*, 2008, **A64**, 112–122.

IV.9.5.3. Crystallographic Description of 8-Chloro-1,3-diphenylbenzo[4,5]imidazo[1,2-*a*]pyridine-4-carbonitrile (1h):

$C_{24}H_{14}ClN_3$, crystal dimensions 0.25 x 0.22 x 0.16 mm, M_r = 379.83, Triclinic, space group P -1, a = 8.0354(10) Å, b = 10.0301(12) Å, c = 12.1559(13) Å, α = 88.390 (4)°, β = 73.215 (4)°, γ = 84.907 (4)°, V = 934.27 (19) Å^3, Z = 2, ρ_{calcd} = 1.350 mg/m^3, μ = 0.219 mm^{-1}, F(000) = 392.0, reflection collected/unique = 4642/3675, refinement method = full-matrix least-squares on F^2, final R indices [I>2\s(I)]: R_1 = 0.0562, wR_2 = 0.1372, R indices (all data): R_1 = 0.0425, wR_2 = 0.1220, goodness of fit = 0.726. CCDC-2103595 for 8-chloro-1,3-diphenylbenzo[4,5]imidazo[1,2-*a*]pyridine-4-carbonitrile (**1h**) contains the supplementary crystallographic data for this paper. These data can be obtained free of charge from The Cambridge Crystallographic Data Centre *via* www.ccdc.cam.ac.uk/data_request/cif.

IV.10. Spectral Data:

***1,3-Diphenylbenzo[4,5]imidazo[1,2-a]pyridine-4-carbonitrile (1a)*:**

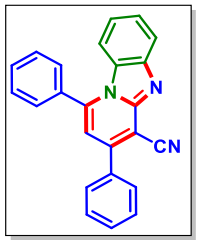

As a yellow solid (65 mg, 76% yield, mp 224–226 °C); Purification over a column of silica gel (10% EtOAc in hexane); ^{1}H NMR ($CDCl_3$, 500 MHz): δ 7.99 (d, 1H, J = 8.0 Hz), 7.78–7.77 (m, 2H), 7.70–7.62 (m, 5H), 7.55–7.51 (m, 3H), 7.44 (t, 1H, J = 7.5 Hz), 7.03 (t, 1H, J = 7.2 Hz), 6.86 (s, 1H), 6.62 (d, 1H, J = 8.5 Hz); ^{13}C{^{1}H} NMR ($CDCl_3$, 125 MHz): δ 149.3, 148.1, 145.6, 144.9, 136.1, 133.2, 131.1, 130.4, 129.6, 129.4, 129.2, 128.9, 128.8, 126.4, 121.9, 120.6, 115.6, 114.8, 113.4, 98.0; IR (KBr, cm^{-1}): 3061, 2956, 2924, 2854, 2223, 1627, 1594, 1524, 1489, 1448, 1308, 1291, 758, 698; HRMS (ESI/Q-TOF) m/z: $[M + H]^+$ calcd for $C_{24}H_{16}N_3$ 346.1339; found 346.1340.

***1-Phenyl-3-(p-tolyl)benzo[4,5]imidazo[1,2-a]pyridine-4-carbonitrile (2a)*:**

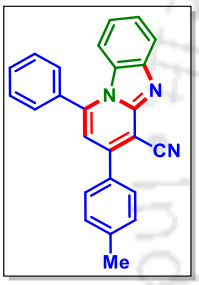

As a yellow solid (67 mg, 75% yield, mp 212–214 °C); Purification over a column of silica gel (10% EtOAc in hexane); ^{1}H NMR ($CDCl_3$, 500 MHz): δ 7.99 (d, 1H, J = 8.0 Hz), 7.69–7.61 (m, 7H), 7.44 (t, 1H, J = 7.8 Hz), 7.34 (d, 2H, J = 7.5 Hz), 7.02 (t, 1H, J = 7.8 Hz), 6.85 (s, 1H), 6.60 (d, 1H, J = 8.5 Hz), 2.43 (s, 3H); ^{13}C{^{1}H} NMR ($CDCl_3$, 125 MHz): δ 149.4, 148.2, 145.6, 144.8, 140.8, 133.3, 133.2, 131.1, 129.9, 129.6, 129.4, 128.78, 128.77, 126.4, 121.8, 120.5, 115.8, 114.7, 113.4, 97.6, 21.6; IR (KBr, cm^{-1}): 3054, 2995, 2923, 2849, 2226, 1625, 1598, 1520, 1490, 1446, 1418, 1305, 1264, 896, 826, 733, 703; HRMS (ESI/Q-TOF) m/z: $[M + H]^+$ calcd for $C_{25}H_{18}N_3$ 360.1495; found 360.1489.

***3-(4-Methoxyphenyl)-1-phenylbenzo[4,5]imidazo[1,2-a]pyridine-4-carbonitrile (3a)*:**

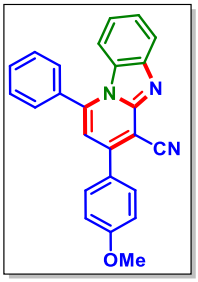

As a yellow solid (75 mg, 80% yield, mp 210–212 °C); Purification over a column of silica gel (15% EtOAc in hexane); ^{1}H NMR ($CDCl_3$, 400 MHz): δ 7.95 (d, 1H, J = 8.4 Hz), 7.74 (d, 2H, J = 8.8 Hz), 7.69–7.61 (m, 5H), 7.40 (t, 1H, J = 7.8 Hz), 7.04–6.98 (m, 3H), 6.83 (s, 1H), 6.58 (d, 1H, J = 8.8 Hz), 3.85 (s, 3H); ^{13}C{^{1}H} NMR ($CDCl_3$, 100 MHz): δ 161.5, 148.9, 148.3, 145.5, 144.7, 133.2, 131.0, 130.4, 129.5, 129.4, 128.8, 128.2, 126.2, 121.7, 120.3, 115.9, 114.7, 113.3, 96.9, 55.6; IR (KBr, cm^{-1}): 3056, 2954, 2925, 2854, 2221, 1604, 1522, 1489, 1446, 1308, 1258, 1180, 1028, 832, 762, 740, 706; HRMS (ESI/Q-TOF) m/z: $[M + H]^+$ calcd for $C_{25}H_{18}N_3O$ 376.1444; found 376.1448.

***3-([1,1'-Biphenyl]-4-yl)-1-phenylbenzo[4,5]imidazo[1,2-a]pyridine-4-carbonitrile (4a)*:**

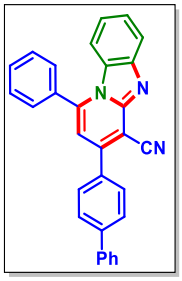

As a yellow solid (86 mg, 82% yield, mp 248–250 °C); Purification over a column of silica gel (10% EtOAc in hexane); ^{1}H NMR ($CDCl_3$, 500 MHz): δ 8.02 (d, 1H, J = 8.5 Hz), 7.87 (d, 2H, J = 8.5 Hz), 7.76 (d, 2H, J = 8.5 Hz), 7.72–7.62 (m, 7H), 7.47 (t, 3H, J = 7.5 Hz), 7.39 (t, 1H, J = 7.2 Hz), 7.05 (t, 1H, J = 7.8 Hz), 6.91 (s, 1H), 6.63 (d, 1H, J = 8.5 Hz); ^{13}C{^{1}H} NMR ($CDCl_3$, 125 MHz): δ 148.9, 148.2, 145.7, 144.9, 143.4, 140.1, 134.9, 133.3, 131.2, 129.6, 129.5, 129.4, 129.2, 128.8, 128.2, 127.9, 127.4, 126.5, 121.9, 120.7, 115.7, 114.8, 113.3, 97.9; IR (KBr, cm^{-1}): 3057, 2955, 2924, 2856, 2229, 1631, 1598, 1449, 1311, 1275, 1263, 765, 748, 704; HRMS (ESI/Q-TOF) m/z: $[M + H]^+$ calcd for $C_{30}H_{20}N_3$ 422.1652; found 422.1657.

***3-(4-Fluorophenyl)-1-phenylbenzo[4,5]imidazo[1,2-a]pyridine-4-carbonitrile (5a)*:**

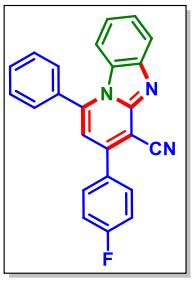

As a yellow solid (71 mg, 79% yield, mp 244–246 °C); Purification over a column of silica gel (10% EtOAc in hexane); ^{1}H NMR ($CDCl_3$, 400 MHz): δ 7.98 (d, 1H, J = 8.4 Hz), 7.79–7.75 (m, 2H), 7.72–7.61 (m, 5H), 7.45 (t, 1H, J = 7.6 Hz), 7.23 (t, 2H, J = 8.6 Hz), 7.04 (t, 1H, J = 7.6 Hz), 6.83 (s, 1H), 6.61 (d, 1H, J = 8.4 Hz); ^{13}C{^{1}H} NMR ($CDCl_3$, 100 MHz): δ 164.1 (d, J = 250.2 Hz), 148.2, 147.9, 145.6, 145.1, 133.1, 132.2 (d, J = 3.3 Hz), 131.2, 130.9 (d, J = 8.6 Hz), 129.6, 129.4, 128.8, 126.5, 122.0, 120.6, 116.5 (d, J = 21.8 Hz), 115.5, 114.8, 113.2, 97.9; ^{19}F NMR ($CDCl_3$): δ –109.8 (s); IR (KBr, cm^{-1}): 3058, 2967, 2925, 2852, 2223, 1626, 1602, 1520, 1489, 1446, 1310, 1263, 1235, 1160, 836, 763, 736, 703; HRMS (ESI/Q-TOF) m/z: $[M + H]^+$ calcd for $C_{24}H_{15}FN_3$ 364.1245; found 364.1252.

***3-(4-Chlorophenyl)-1-phenylbenzo[4,5]imidazo[1,2-a]pyridine-4-carbonitrile (6a)*:**

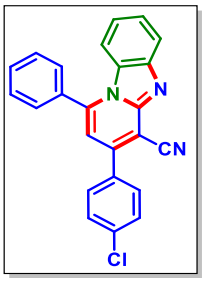

As a yellow solid (68 mg, 72% yield, mp 219–221 °C); Purification over a column of silica gel (10% EtOAc in hexane); ^{1}H NMR ($CDCl_3$, 500 MHz): δ 8.02 (d, 1H, J = 8.0 Hz), 7.73–7.69 (m, 3H), 7.66 (t, 2H, J = 7.5 Hz), 7.63–7.61 (m, 2H), 7.52 (d, 2H, J = 8.5 Hz), 7.47 (t, 1H, J = 7.0 Hz), 7.06 (t, 1H, J = 7.5 Hz), 6.82 (s, 1H), 6.62 (d, 1H, J = 8.5 Hz); ^{13}C{^{1}H} NMR ($CDCl_3$, 125 MHz): δ 147.98, 147.94, 145.7, 145.2, 136.9, 134.5, 133.2, 131.3, 130.2, 129.7, 129.6, 129.4, 128.8, 126.6,

122.1, 120.8, 115.4, 114.8, 113.0, 98.2; IR (KBr, cm^{-1}): 3064, 2954, 2924, 2854, 2223, 1625, 1596, 1523, 1489, 1446, 1310, 1264, 1091, 1013, 830, 762, 736, 703; HRMS (ESI/Q-TOF) m/z: $[M + H]^+$ calcd for $C_{24}H_{15}ClN_3$ 380.0949; found 380.0951.

***3-(2-Bromophenyl)-1-phenylbenzo[4,5]imidazo[1,2-a]pyridine-4-carbonitrile (7a)*:**

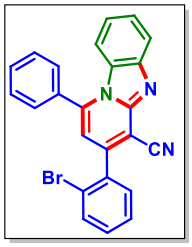

As a yellow solid (64 mg, 61% yield, mp 224–226 °C); Purification over a column of silica gel (10% EtOAc in hexane); ^1H NMR ($CDCl_3$, 400 MHz): δ 8.05 (d, 1H, J = 8.4 Hz), 7.75 (d, 1H, J = 8.0 Hz), 7.69–7.60 (m, 5H), 7.56–7.54 (m, 1H), 7.51–7.47 (m, 2H), 7.39–7.35 (m, 1H), 7.07 (t, 1H, J = 7.8 Hz), 6.79 (s, 1H), 6.68 (d, 1H, J = 8.4 Hz); $^{13}C\{^1H\}$ NMR ($CDCl_3$, 100 MHz): δ 149.1, 147.4, 145.6, 144.4, 137.2, 133.7, 133.1, 131.4, 131.2, 130.9, 129.6, 128.8, 128.0, 126.6, 122.12, 122.10, 120.8, 114.9, 114.6, 114.3, 100.8; IR (KBr, cm^{-1}): 3061, 2956, 2924, 2849, 2228, 1626, 1591, 1513, 1488, 1421, 1446, 1297, 1231, 1028, 961, 792, 756, 701; HRMS (ESI/Q-TOF) m/z: $[M + H]^+$ calcd for $C_{24}H_{15}BrN_3$ 424.0444; found 424.0450.

***3-(3-Nitrophenyl)-1-phenylbenzo[4,5]imidazo[1,2-a]pyridine-4-carbonitrile (8a)*:**

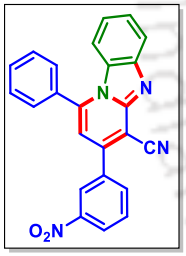

As a yellow solid (62 mg, 64% yield, mp 231–233 °C); Purification over a column of silica gel (10% EtOAc in hexane); ^1H NMR ($CDCl_3$, 400 MHz): δ 8.54 (s, 1H), 8.36 (d, 1H, J = 8.4 Hz), 8.18 (d, 1H, J = 8.0 Hz), 7.98 (d, 1H, J = 8.4 Hz), 7.78–7.66 (m, 6H), 7.47 (t, 1H, J = 7.8 Hz), 7.07 (t, 1H, J = 7.8 Hz), 6.88 (s, 1H), 6.65 (d, 1H, J = 8.4 Hz); $^{13}C\{^1H\}$ NMR ($CDCl_3$, 100 MHz): δ 148.8, 147.4, 146.3, 145.8, 145.7, 137.7, 134.9, 132.8, 131.4, 130.5, 129.7, 129.4, 128.7, 126.8, 124.9, 123.8, 122.4, 120.7, 114.95, 114.91, 112.6, 98.8; IR (KBr, cm^{-1}): 3058, 2954, 2923, 2860, 2224, 1626, 1595, 1531, 1490, 1446, 1349, 1310, 741, 693; HRMS (ESI/Q-TOF) m/z: $[M + H]^+$ calcd for $C_{24}H_{15}N_4O_2$ 391.1190; found 391.1198.

***3-Phenyl-1-(p-tolyl)benzo[4,5]imidazo[1,2-a]pyridine-4-carbonitrile (9a)*:**

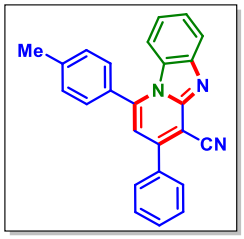

As a yellow solid (73 mg, 82% yield, mp 216–218 °C); Purification over a column of silica gel (10% EtOAc in hexane); ^1H NMR ($CDCl_3$, 400 MHz): δ 8.00 (d, 1H, J = 8.4 Hz), 7.78–7.76 (m, 2H), 7.55–7.50 (m, 5H), 7.48–7.44 (m, 3H), 7.06 (t, 1H, J = 7.8 Hz), 6.84 (s, 1H), 6.72 (d, 1H, J = 8.4 Hz), 2.55 (s, 3H); $^{13}C\{^1H\}$ NMR ($CDCl_3$, 100 MHz): δ 149.4, 148.2, 145.6, 145.2,

141.5, 136.1, 130.4, 130.3, 130.2, 129.4, 129.2, 128.8, 128.6, 126.4, 121.8, 120.5, 115.6, 114.9, 113.5, 97.8, 21.8; IR (KBr, cm^{-1}): 3042, 2956, 2923, 2860, 2223, 1628, 1597, 1531, 1503, 1448, 1309, 758, 698; HRMS (ESI/Q-TOF) m/z: $[M + H]^+$ calcd for $C_{25}H_{18}N_3$ 360.1495; found 360.1496.

***1-(4-Methoxyphenyl)-3-phenylbenzo[4,5]imidazo[1,2-a]pyridine-4-carbonitrile (10a)*:**

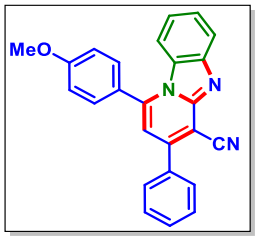

As a yellow solid (78 mg, 84% yield, mp 241–243 °C); Purification over a column of silica gel (15% EtOAc in hexane); ^1H NMR ($CDCl_3$, 500 MHz): δ 7.98 (d, 1H, J = 8.5 Hz), 7.77–7.75 (m, 2H), 7.56–7.49 (m, 5H), 7.44 (t, 1H, J = 7.2 Hz), 7.14 (d, 2H, J = 8.5 Hz), 7.06 (t, 1H, J = 7.5 Hz), 6.82 (s, 1H), 6.78 (d, 1H, J = 8.5 Hz), 3.95 (s, 3H); $^{13}C\{^1H\}$ NMR ($CDCl_3$, 125 MHz): δ 161.8, 149.4, 148.3, 145.6, 145.0, 136.2, 130.3, 130.2, 129.5, 129.2, 128.8, 126.4, 125.4, 121.8, 120.5, 115.6, 114.9, 113.6, 97.6, 55.7; IR (KBr, cm^{-1}): 3058, 2962, 2927, 2843, 2222, 1625, 1608, 1501, 1447, 1308, 1253, 1178, 1029, 836, 759, 740, 698; HRMS (ESI/Q-TOF) m/z: $[M + H]^+$ calcd for $C_{25}H_{18}N_3O$ 376.1444; found 376.1448.

***1-(4-Fluorophenyl)-3-phenylbenzo[4,5]imidazo[1,2-a]pyridine-4-carbonitrile (11a)*:**

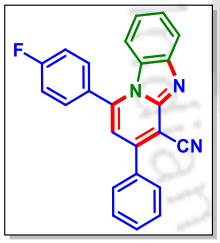

As a yellow solid (59 mg, 66% yield, mp 216–218 °C); Purification over a column of silica gel (10% EtOAc in hexane); ^1H NMR ($CDCl_3$, 500 MHz): δ 8.04 (d, 1H, J = 8.5 Hz), 7.79–7.77 (m, 2H), 7.65–7.62 (m, 2H), 7.57–7.53 (m, 3H), 7.49 (t, 1H, J = 7.5 Hz), 7.36 (t, 2H, J = 8.5 Hz), 7.09 (t, 1H, J = 7.8 Hz), 6.85 (s, 1H), 6.66 (d, 1H, J = 8.5 Hz); $^{13}C\{^1H\}$ NMR ($CDCl_3$, 125 MHz): δ 164.4 (d, J = 250.8 Hz), 149.3, 148.1, 145.8, 143.8, 136.0, 131.0 (d, J = 8.6 Hz), 130.5, 129.40, 129.35, 128.9, 126.6, 122.1, 120.9, 116.9 (d, J = 21.9 Hz), 115.5, 114.5, 113.7, 98.5; ^{19}F NMR ($CDCl_3$): δ –108.0 (s); IR (KBr, cm^{-1}): 3055, 2965, 2924, 2853, 2223, 1626, 1604, 1529, 1499, 1448, 1309, 1264, 1231, 1157, 1014, 758, 733, 698; HRMS (ESI/Q-TOF) m/z: $[M + H]^+$ calcd for $C_{24}H_{15}FN_3$ 364.1245; found 364.1249.

***1-(4-Chlorophenyl)-3-phenylbenzo[4,5]imidazo[1,2-a]pyridine-4-carbonitrile (12a)*:**

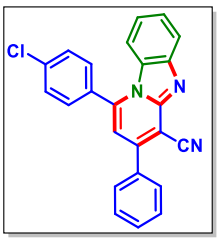

As a yellow solid (59 mg, 63% yield, mp 252–254 °C); Purification over a column of silica gel (10% EtOAc in hexane); ^1H NMR ($CDCl_3$, 500 MHz): δ 8.02 (d, 1H, J = 8.0 Hz), 7.78–7.76 (m, 2H), 7.66–7.64 (m, 2H), 7.60–7.59 (m, 2H), 7.57–7.53 (m, 3H), 7.49 (t, 1H, J = 8.0 Hz), 7.11 (t, 1H, J = 8.0 Hz),

6.84 (s, 1H), 6.71 (d, 1H, *J* = 8.5 Hz); $^{13}C\{^{1}H\}$ NMR ($CDCl_3$, 125 MHz): *δ* 149.2, 148.1, 145.7, 143.6, 137.6, 136.0, 131.6, 130.5, 130.3, 130.0, 129.4, 129.3, 128.9, 126.6, 122.2, 120.9, 115.4, 114.6, 113.7, 98.5; IR (KBr, cm^{-1}): 3053, 2962, 2932, 2857, 2226, 1626, 1601, 1522, 1484, 1448, 1309, 1090, 1016, 760, 740, 698; HRMS (ESI/Q-TOF) m/z: $[M + H]^+$ calcd for $C_{24}H_{15}ClN_3$ 380.0949; found 380.0955.

***1-(4-Bromophenyl)-3-phenylbenzo[4,5]imidazo[1,2-a]pyridine-4-carbonitrile (13a)*:**

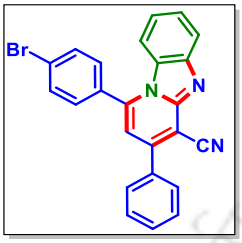

As a yellow solid (65 mg, 62% yield, mp 239–241 °C); Purification over a column of silica gel (10% EtOAc in hexane); ^{1}H NMR ($CDCl_3$, 400 MHz): *δ* 8.01 (d, 1H, *J* = 8.4 Hz), 7.81 (d, 2H, *J* = 8.4 Hz), 7.77–7.75 (m, 2H), 7.55–7.52 (m, 5H), 7.48 (t, 1H, *J* = 7.6 Hz), 7.11 (t, 1H, *J* = 7.8 Hz), 6.84 (s, 1H), 6.72 (d, 1H, *J* = 8.4 Hz); $^{13}C\{^{1}H\}$ NMR ($CDCl_3$, 100 MHz): *δ* 149.2, 148.0, 145.7, 143.6, 135.9, 132.9, 132.1, 130.5, 130.4, 129.33, 129.28, 128.9, 126.6, 125.8, 122.0, 120.8, 115.4, 114.6, 113.6, 98.5; IR (KBr, cm^{-1}): 3053, 2959, 2924, 2857, 2223, 1625, 1599, 1522, 1481, 1448, 1308, 1290, 1067, 1012, 829, 789, 759, 739, 697; HRMS (ESI/Q-TOF) m/z: $[M + H]^+$ calcd for $C_{24}H_{15}BrN_3$ 424.0444; found 424.0447.

***1-(2-Nitrophenyl)-3-phenylbenzo[4,5]imidazo[1,2-a]pyridine-4-carbonitrile (14a)*:**

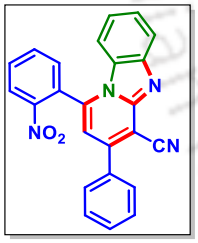

As a yellow solid (40 mg, 41% yield, mp 250–252 °C); Purification over a column of silica gel (10% EtOAc in hexane); ^{1}H NMR ($CDCl_3$, 500 MHz): *δ* 8.48 (d, 1H, *J* = 9.5 Hz), 8.06 (d, 1H, *J* = 8.5 Hz), 7.99–7.94 (m, 2H), 7.77–7.76 (m, 2H), 7.73–7.71 (m, 1H), 7.56–7.52 (m, 3H), 7.48 (t, 1H, *J* = 7.8 Hz), 7.05 (t, 1H, *J* = 8.2 Hz), 6.83 (s, 1H), 6.30 (d, 1H, *J* = 8.0 Hz); $^{13}C\{^{1}H\}$ NMR ($CDCl_3$, 100 MHz): *δ* 149.2, 147.8, 147.6, 145.7, 140.7, 135.9, 135.1, 132.6, 132.2, 130.6, 129.34, 129.29, 128.9, 128.4, 126.7, 125.9, 122.7, 121.1, 115.3, 112.7, 112.2, 99.0; IR (KBr, cm^{-1}): 3058, 2962, 2924, 2854, 2224, 1629, 1596, 1525, 1478, 1449, 1344, 1309, 1261, 853, 790, 752, 698; HRMS (ESI/Q-TOF) m/z: $[M + H]^+$ calcd for $C_{24}H_{15}N_4O_2$ 391.1190; found 391.1195.

***3-(Naphthalen-1-yl)-1-phenylbenzo[4,5]imidazo[1,2-a]pyridine-4-carbonitrile (15a)*:**

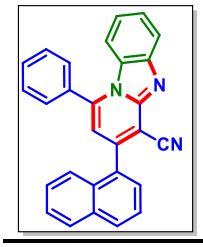

As a yellow solid (75 mg, 76% yield, mp 248–250 °C); Purification over a column of silica gel (10% EtOAc in hexane); ^{1}H NMR ($CDCl_3$, 400 MHz): *δ* 8.08 (d, 1H, *J* = 8.4 Hz), 7.99 (d, 1H, *J* = 8.4 Hz), 7.95 (d, 1H, *J* = 8.4 Hz), 7.79

(d, 1H, *J* = 8.0 Hz), 7.71–7.67 (m, 4H), 7.63–7.59 (m, 3H), 7.56–7.49 (m, 3H), 7.09 (t, 1H, *J* = 7.8 Hz), 6.89 (s, 1H), 6.71 (d, 1H, *J* = 8.4 Hz); $^{13}C\{^{1}H\}$ NMR ($CDCl_3$, 100 MHz): *δ* 149.4, 147.9, 145.6, 144.3, 134.0, 133.9, 133.1, 131.2, 130.7, 130.6, 129.62, 129.59, 129.55, 129.0, 128.78, 128.75, 127.9, 127.3, 126.7, 126.6, 125.5, 124.9, 122.0, 120.8, 114.97, 114.89, 101.1; IR (KBr, cm^{-1}): 3063, 2950, 2925, 2855, 2226, 1626, 1595, 1522, 1489, 1447, 1309, 1290, 1167, 804, 780, 739, 707; HRMS (ESI/Q-TOF) m/z: $[M + H]^+$ calcd for $C_{28}H_{18}N_3$ 396.1495; found 396.1499.

***3-(3,4-Dimethoxyphenyl)-1-phenylbenzo[4,5]imidazo[1,2-a]pyridine-4-carbonitrile (16a)*:**

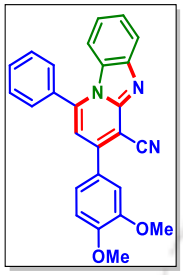

As a yellow solid (82 mg, 81% yield, mp 227–229 °C); Purification over a column of silica gel (15% EtOAc in hexane); ^{1}H NMR ($CDCl_3$, 400 MHz): *δ* 8.00 (d, 1H, *J* = 8.0 Hz), 7.71–7.61 (m, 5H), 7.45 (t, 1H, *J* = 7.6 Hz), 7.38–7.37 (m, 2H), 7.05–7.00 (m, 2H), 6.87 (s, 1H), 6.58 (d, 1H, *J* = 8.4 Hz), 3.99 (s, 3H), 3.96 (s, 3H); $^{13}C\{^{1}H\}$ NMR ($CDCl_3$, 100 MHz): *δ* 151.2, 149.5, 149.1, 148.4, 145.7, 144.7, 133.4, 131.1, 129.6, 129.5, 128.8, 128.5, 126.4, 122.2, 121.8, 120.6, 116.0, 114.7, 113.3, 112.0, 111.7, 97.2, 56.5, 56.3; IR (KBr, cm^{-1}): 3058, 2965, 2926, 2843, 2220, 1628, 1595, 1522, 1447, 1310, 1264, 1147, 1023, 733, 703; HRMS (ESI/Q-TOF) m/z: $[M + H]^+$ calcd for $C_{26}H_{20}N_3O_2$ 406.1550; found 406.1551.

***3-(4-Chlorophenyl)-1-(p-tolyl)benzo[4,5]imidazo[1,2-a]pyridine-4-carbonitrile (17a)*:**

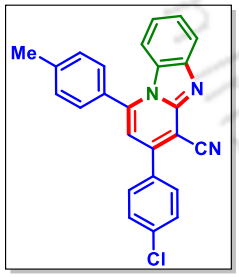

As a yellow solid (81 mg, 83% yield, mp 223–225 °C); Purification over a column of silica gel (10% EtOAc in hexane); ^{1}H NMR ($CDCl_3$, 400 MHz): δ 7.94 (d, 1H, *J* = 8.0 Hz), 7.69 (d, 2H, *J* = 8.4 Hz), 7.53–7.49 (m, 3H), 7.46–7.40 (m, 4H), 7.04 (t, 1H, *J* = 7.6 Hz), 6.78 (s, 1H), 6.70 (d, 1H, *J* = 8.8 Hz), 2.55 (s, 3H); $^{13}C\{^{1}H\}$ NMR ($CDCl_3$, 100 MHz): *δ* 147.89, 147.86, 145.53, 145.48, 141.6, 136.7, 134.5, 130.21, 130.16, 130.1, 129.5, 129.4, 128.6, 126.4, 121.9, 120.4, 115.4, 114.9, 113.0, 97.6, 21.8; IR (KBr, cm^{-1}): 3053, 2962, 2923, 2852, 2223, 1626, 1598, 1528, 1502, 1447, 1311, 1291, 1091, 1013, 820, 763, 741; HRMS (ESI/Q-TOF) m/z: $[M + H]^+$ calcd for $C_{25}H_{17}ClN_3$ 394.1106; found 394.1108.

***1-(4-Chlorophenyl)-3-(4-methoxyphenyl)benzo[4,5]imidazo[1,2-a]pyridine-4-carbonitrile (18a)*:**

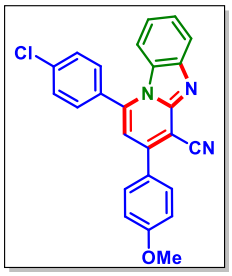

As a yellow solid (75 mg, 73% yield, mp 223–225 °C); Purification over a column of silica gel (15% EtOAc in hexane); ^{1}H NMR ($CDCl_3$, 400 MHz): δ 7.94 (d, 1H, J = 8.4 Hz), 7.73 (d, 2H, J = 8.8 Hz), 7.65–7.59 (m, 4H), 7.43 (t, 1H, J = 7.8 Hz), 7.08–7.02 (m, 3H), 6.81 (s, 1H), 6.66 (d, 1H, J = 8.4 Hz), 3.87 (s, 3H); ^{13}C{^{1}H} NMR ($CDCl_3$, 100 MHz): δ 161.6, 148.8, 148.3, 145.6, 143.4, 137.4, 131.7, 130.4, 130.3, 129.9, 129.3, 128.1, 126.4, 121.9, 120.6, 115.8, 114.8, 114.5, 113.6, 97.3, 55.7; IR (KBr, cm^{-1}): 3061, 2954, 2926, 2221, 1602, 1521, 1485, 1447, 1307, 1261, 1180, 1090, 1016, 899, 734, 700; HRMS (ESI/Q-TOF) m/z: $[M + H]^+$ calcd for $C_{25}H_{17}ClN_3O$ 410.1055; found 410.1045.

***1-(Benzo[d][1,3]dioxol-5-yl)-3-(4-bromophenyl)benzo[4,5]imidazo[1,2-a]pyridine-4-carbonitrile (19a)*:**

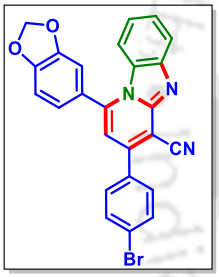

As a yellow solid (81 mg, 70% yield, mp 265–267 °C); Purification over a column of silica gel (10% EtOAc in hexane); ^{1}H NMR ($CDCl_3$, 500 MHz): δ 7.99 (d, 1H, J = 8.0 Hz), 7.68–7.62 (m, 4H), 7.47 (t, 1H, J = 7.8 Hz), 7.14–7.10 (m, 2H), 7.05 (d, 2H, J = 9.5 Hz), 6.86 (d, 1H, J = 8.5 Hz), 6.78 (s, 1H), 6.19 (s, 1H), 6.13 (s, 1H); ^{13}C{^{1}H} NMR ($CDCl_3$, 125 MHz): δ 150.1, 148.7, 147.96, 147.90, 145.7, 144.9, 134.9, 132.5, 130.4, 129.4, 126.6, 126.5, 125.1, 123.0, 122.1, 120.7, 115.4, 114.9, 113.1, 109.4, 109.1, 102.2, 97.9; IR (KBr, cm^{-1}): 3075, 2959, 2924, 2857, 2226, 1628, 1600, 1526, 1504, 1482, 1446, 1311, 1246, 1220, 1074, 1037, 1010, 933, 817, 765, 740; HRMS (ESI/Q-TOF) m/z: $[M + H]^+$ calcd for $C_{25}H_{15}BrN_3O_2$ 468.0342; found 468.0346.

***3-(Furan-2-yl)-1-(p-tolyl)benzo[4,5]imidazo[1,2-a]pyridine-4-carbonitrile (20a)*:**

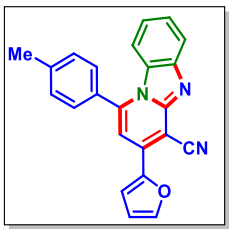

As a yellow solid (68 mg, 78% yield, mp 215–217 °C); Purification over a column of silica gel (10% EtOAc in hexane); ^{1}H NMR ($CDCl_3$, 500 MHz): δ 7.98 (d, 1H, J = 8.5 Hz), 7.69 (s, 1H), 7.65 (s, 1H), 7.49 (d, 2H, J = 8.5 Hz), 7.46–7.41 (m, 3H), 7.19 (s, 1H), 7.03 (t, 1H, J = 7.5 Hz), 6.67–6.64 (m, 2H), 2.56 (s, 3H); ^{13}C{^{1}H} NMR ($CDCl_3$, 125 MHz): δ 148.7, 148.3, 145.8, 145.4, 145.2, 141.5, 136.2, 130.5, 130.2, 129.8, 128.7, 126.7, 126.3, 121.8, 120.5, 116.1, 115.1, 114.8, 113.5, 108.9, 92.2, 21.8; IR (KBr, cm^{-1}): 3042, 2959, 2924, 2857, 2223, 1625, 1599, 1531, 1505,

1479, 1447, 1311, 1260, 1027,799, 759; HRMS (ESI/Q-TOF) m/z: $[M + H]^+$ calcd for $C_{23}H_{16}N_3O$ 350.1288; found 350.1290.

***1,3-Di(furan-2-yl)benzo[4,5]imidazo[1,2-a]pyridine-4-carbonitrile (21a)*:**

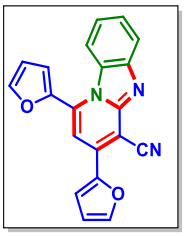

As a yellow solid (44 mg, 55% yield, mp 184–186 °C); Purification over a column of silica gel (10% EtOAc in hexane); ^{1}H NMR ($CDCl_3$, 400 MHz): δ 7.99 (d, 1H, *J* = 8.0 Hz), 7.78 (s, 1H), 7.69 (s, 1H), 7.66 (s, 1H), 7.48 (t, 1H, *J* = 7.8 Hz), 7.41 (s, 1H), 7.19 (t, 1H, *J* = 7.8 Hz), 7.00 (s, 1H), 6.81 (d, 1H, *J* = 8.4 Hz), 6.77–6.76 (m, 1H), 6.66–6.65 (m, 1H); ^{13}C{^{1}H} NMR ($CDCl_3$, 100 MHz): *δ* 148.3, 147.9, 145.6, 145.5, 145.4, 144.8, 135.5, 133.8, 129.5, 126.5, 122.5, 120.5, 115.8, 115.2, 114.0, 113.8, 113.6, 112.5, 110.2, 93.4; IR (KBr, cm^{-1}): 3125, 2954, 2857, 2924, 2226, 1629, 1586, 1518, 1479, 1446, 1311, 1017, 886, 845, 752; HRMS (ESI/Q-TOF) m/z: $[M + H]^+$ calcd for $C_{20}H_{12}N_3O_2$ 326.0924; found 326.0925.

***7-Methyl-1,3-diphenylbenzo[4,5]imidazo[1,2-a]pyridine-4-carbonitrile (1b)*:**

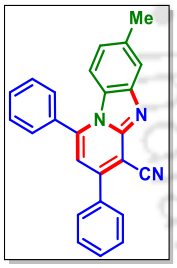

As a yellow solid (72 mg, 81% yield, mp 230–232 °C); Purification over a column of silica gel (10% EtOAc in hexane); ^{1}H NMR ($CDCl_3$, 500 MHz): *δ* 7.78–7.76 (m, 3H), 7.71–7.68 (m, 1H), 7.66–7.59 (m, 4H), 7.55–7.51 (m, 3H), 6.87 (d, 1H, *J* = 8.5 Hz), 6.84 (s, 1H), 6.49 (d, 1H, *J* = 8.5 Hz), 2.48 (s, 3H); ^{13}C{^{1}H} NMR ($CDCl_3$, 125 MHz): *δ* 149.0, 148.3, 146.1, 144.7, 136.7, 136.3, 133.4, 131.1, 130.3, 129.6, 129.2, 128.9, 128.8, 127.6, 123.7, 120.2, 115.6, 114.2, 113.2, 97.9, 21.9; IR (KBr, cm^{-1}): 3056, 2956, 2923, 2852, 2223, 1611, 1597, 1522, 1489, 1446, 1296, 1238, 1153, 792, 768, 752, 699; HRMS (ESI/Q-TOF) m/z: $[M + H]^+$ calcd for $C_{25}H_{18}N_3$ 360.1495; found 360.1499.

***6,7-Dimethyl-1,3-diphenylbenzo[4,5]imidazo[1,2-a]pyridine-4-carbonitrile (1c)*:**

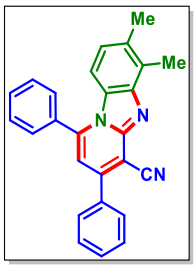

As a yellow solid (60 mg, 65% yield, mp 232–234 °C); Purification over a column of silica gel (10% EtOAc in hexane); ^{1}H NMR ($CDCl_3$, 500 MHz): *δ* 7.78–7.76 (m, 3H), 7.72–7.68 (m, 1H), 7.66–7.59 (m, 4H), 7.55–7.50 (m, 3H), 6.82 (s, 1H), 6.35 (s, 1H), 2.38 (s, 3H), 2.15 (s, 3H); ^{13}C{^{1}H} NMR ($CDCl_3$, 125 MHz): *δ* 148.5, 147.7, 144.57, 144.55, 136.4, 136.1, 133.6, 131.3, 130.9, 130.2, 129.4,

129.2, 128.90, 128.86, 127.9, 120.4, 115.7, 114.7, 112.9, 97.9, 20.9, 20.7; IR (KBr, cm^{-1}): 3061, 2965, 2923, 2852, 2229, 1611, 1598, 1523, 1461, 1488, 1306, 1278, 853, 766, 751, 700; HRMS (ESI/Q-TOF) m/z: $[M + H]^+$ calcd for $C_{26}H_{20}N_3$ 374.1652; found 374.1657.

***7-Isopropyl-1,3-diphenylbenzo[4,5]imidazo[1,2-a]pyridine-4-carbonitrile (1d)*:**

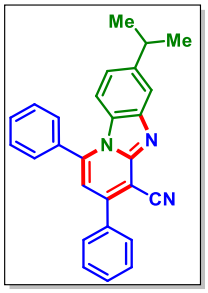

As a yellow solid (70 mg, 72% yield, mp 203–205 °C); Purification over a column of silica gel (10% EtOAc in hexane); ^1H NMR ($CDCl_3$, 500 MHz): δ 7.88 (s, 1H), 7.78 (d, 2H, J = 8.0 Hz), 7.71–7.68 (m, 1H), 7.64 (t, 2H, J = 7.5 Hz), 7.61–7.59 (m, 2H), 7.55–7.49 (m, 3H), 6.96 (d, 1H, J = 8.5 Hz), 6.85 (s, 1H), 6.53 (d, 1H, J = 8.5 Hz), 3.07–3.02 (m, 1H), 1.29 (s, 3H), 1.28 (s, 3H); $^{13}C\{^1H\}$ NMR ($CDCl_3$, 125 MHz): δ 148.9, 148.3, 147.9, 146.1, 144.7, 136.2, 133.3, 131.1, 130.3, 129.5, 129.2, 128.9, 128.8, 127.7, 121.5, 117.5, 115.6, 114.4, 113.1, 97.9, 34.5, 24.4; IR (KBr, cm^{-1}): 3064, 2959, 2923, 2871, 2223, 1611, 1596, 1524, 1489, 1434, 1296, 803, 768, 752, 699; HRMS (ESI/Q-TOF) m/z: $[M + H]^+$ calcd for $C_{27}H_{22}N_3$ 388.1808; found 388.1809.

***7-Butyl-1,3-diphenylbenzo[4,5]imidazo[1,2-a]pyridine-4-carbonitrile (1e)*:**

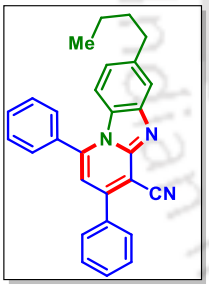

As a yellow solid (74 mg, 76% yield, mp 163–165 °C); Purification over a column of silica gel (10% EtOAc in hexane); ^1H NMR ($CDCl_3$, 600 MHz): δ 7.79 (s, 1H), 7.78–7.76 (m, 2H), 7.70–7.68 (m, 1H), 7.64 (t, 2H, J = 7.5 Hz), 7.61–7.59 (m, 2H), 7.54–7.49 (m, 3H), 6.88 (d, 1H, J = 8.7 Hz), 6.84 (s, 1H), 6.51 (d, 1H, J = 9.0 Hz), 2.72 (t, 2H, J = 7.5 Hz), 1.64–1.59 (m, 2H), 1.35–1.29 (m, 2H), 0.89 (t, 3H, J = 7.5 Hz); $^{13}C\{^1H\}$ NMR ($CDCl_3$, 150 MHz): δ 148.9, 148.2, 145.9, 144.6, 141.7, 136.1, 133.2, 131.0, 130.3, 129.5, 129.2, 128.8, 128.7, 127.5, 123.1, 119.4, 115.7, 114.3, 113.1, 97.6, 35.9, 33.8, 22.3, 14.1; IR (KBr, cm^{-1}): 3053, 2955, 2928, 2857, 2223, 1611, 1596, 1489, 1523, 1434, 1296, 1237, 1153, 1121, 851, 767, 752, 699; HRMS (ESI/Q-TOF) m/z: $[M + H]^+$ calcd for $C_{28}H_{24}N_3$ 402.1965; found 402.1968.

***7-Fluoro-1,3-diphenylbenzo[4,5]imidazo[1,2-a]pyridine-4-carbonitrile (1f)*:**

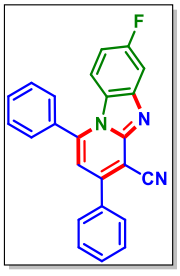

As a yellow solid (68 mg, 75% yield, mp 212–214 °C); Purification over a column of silica gel (10% EtOAc in hexane); ^1H NMR ($CDCl_3$, 400 MHz): δ 7.78–7.75 (m, 2H), 7.72–7.62 (m, 5H), 7.59–7.52 (m, 4H), 6.89 (s, 1H), 6.77 (t, 1H, J = 9.2 Hz), 6.55–6.51 (m, 1H); $^{13}C\{^1H\}$ NMR ($CDCl_3$, 100 MHz): δ 161.4 (d, J = 242.5 Hz),

149.6, 149.4, 146.7, 146.6, 144.7, 135.9, 132.9, 131.3, 130.5, 129.8, 129.3, 128.9, 128.7, 126.1, 115.6 (d, J = 10.3 Hz), 115.4, 113.7, 110.7 (d, J = 26.2 Hz), 105.7 (d, J = 23.8 Hz), 97.8; ^{19}F NMR ($CDCl_3$): δ –113.8 (s); IR (KBr, cm^{-1}): 3056, 2965, 2925, 2854, 2224, 1608, 1595, 1523, 1488, 1436, 1264, 1239, 1148, 1113, 971, 796, 767, 734, 700; HRMS (ESI/Q-TOF) m/z: $[M + H]^+$ calcd for $C_{24}H_{15}FN_3$ 364.1245; found 364.1251.

***7-Chloro-1,3-diphenylbenzo[4,5]imidazo[1,2-a]pyridine-4-carbonitrile (1g)*:**

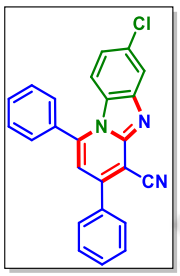

As a yellow solid (62 mg, 65% yield, mp 220–222 °C); Purification over a column of silica gel (10% EtOAc in hexane); ^{1}H NMR ($CDCl_3$, 400 MHz): δ 7.91 (s, 1H), 7.78–7.75 (m, 2H), 7.72–7.61 (m, 5H), 7.54–7.52 (m, 3H), 6.98 (d, 1H, J = 9.2 Hz), 6.90 (s, 1H), 6.49 (d, 1H, J = 9.2 Hz); ^{13}C{^{1}H} NMR ($CDCl_3$, 100 MHz): δ 149.9, 149.1, 146.4, 144.8, 135.9, 132.9, 132.3, 131.4, 130.6, 129.8, 129.3, 128.9, 128.7, 128.0, 122.5, 120.0, 115.5, 115.3, 113.9, 98.1; IR (KBr, cm^{-1}): 3061, 2954, 2929, 2852, 2229, 1629, 1522, 1489, 1458, 1301, 1169, 1093, 943, 813, 769, 752, 699; HRMS (ESI/Q-TOF) m/z: $[M + H]^+$ calcd for $C_{24}H_{15}ClN_3$ 380.0949; found 380.0952.

***8-Chloro-1,3-diphenylbenzo[4,5]imidazo[1,2-a]pyridine-4-carbonitrile (1h)*:**

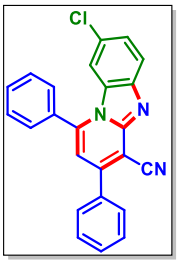

As a yellow solid (61 mg, 64% yield, mp 234–236 °C); Purification over a column of silica gel (10% EtOAc in hexane); ^{1}H NMR ($CDCl_3$, 500 MHz): δ 7.92 (d, 1H, J = 8.5 Hz), 7.79–7.77 (m, 2H), 7.73 (d, 1H, J = 7.5 Hz), 7.68 (t, 2H, J = 7.5 Hz), 7.61–7.59 (m, 2H), 7.56–7.53 (m, 3H), 7.43 (d, 1H, J = 8.8 Hz), 6.89 (s, 1H),), 6.56 (s, 1H); ^{13}C{^{1}H} NMR ($CDCl_3$, 125 MHz): δ 149.8, 148.7, 144.8, 144.2, 135.9, 132.7, 131.5, 130.6, 129.81, 129.75, 129.4, 128.9, 128.7, 127.4, 127.3, 121.4, 115.3, 114.8, 113.9, 98.4; IR (KBr, cm^{-1}): 2959, 2923, 2929, 2852, 2229, 1628, 1592, 1526, 1460, 1275, 1260, 765, 751, 702; HRMS (ESI/Q-TOF) m/z: $[M + H]^+$ calcd for $C_{24}H_{15}ClN_3$ 380.0949; found 380.0922.

***7-Bromo-1,3-diphenylbenzo[4,5]imidazo[1,2-a]pyridine-4-carbonitrile (1i)*:**

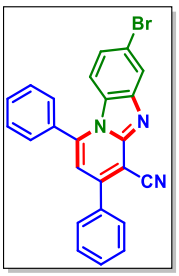

As a yellow solid (58 mg, 54% yield, mp 222–224 °C); Purification over a column of silica gel (10% EtOAc in hexane); ^{1}H NMR ($CDCl_3$, 400 MHz): δ 8.06 (s, 1H), 7.78–7.75 (m, 2H), 7.72–7.62 (m, 5H), 7.53–7.52 (m, 3H), 7.10 (d, 1H, J = 8.8 Hz), 6.90 (s, 1H), 6.44 (d, 1H, J = 8.8 Hz); ^{13}C{^{1}H} NMR ($CDCl_3$, 125 MHz): δ

149.9, 148.9, 146.7, 144.8, 135.8, 132.8, 131.4, 130.6, 129.8, 129.3, 128.9, 128.7, 128.3, 125.0, 123.1, 119.9, 115.8, 115.3, 113.9, 98.0; IR (KBr, cm^{-1}): 3058, 2962, 2924, 2852, 2224, 1628, 1591, 1511, 1488, 1426, 1295, 1231, 1051, 889, 792, 768, 722, 698; HRMS (ESI/Q-TOF) m/z: $[M + H]^+$ calcd for $C_{24}H_{15}BrN_3$ 424.0444; found 424.0444.

***1,3-Diphenyl-8-(trifluoromethyl)benzo[4,5]imidazo[1,2-a]pyridine-4-carbonitrile (1j)*:**

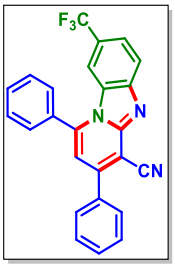

As a yellow solid (42 mg, 41% yield, mp 259–261 °C); Purification over a column of silica gel (10% EtOAc in hexane); ^{1}H NMR ($CDCl_3$, 600 MHz): δ 8.01 (d, 1H, J = 8.4 Hz), 7.79–7.77 (m, 2H), 7.75 (d, 1H, J = 7.2 Hz), 7.70 (t, 2H, J = 7.8 Hz), 7.67–7.64 (m, 3H), 7.55–7.54 (m, 3H), 6.99 (s, 1H), 6.82 (s, 1H); ^{13}C{^{1}H} NMR ($CDCl_3$, 150 MHz): δ 150.7, 149.9, 147.4, 145.1, 135.6, 132.3, 131.6, 130.8, 129.9, 129.4, 128.9, 128.64, 128.59, 125.2, 123.6 (d, J = 32.4 Hz), 123.4, 123.2 (q, J_1 = 3.48, J_2 = 6.4 Hz), 120.9, 115.2, 114.2, 112.6 (q, J_1 = 4.9 Hz, J_2 = 9.4 Hz), 98.1; ^{19}F NMR ($CDCl_3$): δ –61.0 (s); IR (KBr, cm^{-1}): 3061, 2959, 2925, 2852, 2217, 1611, 1523, 1489, 1445, 1325, 1300, 1263, 1165, 1114, 1054, 1230, 1078, 830, 755, 735, 700; HRMS (ESI/Q-TOF) m/z: $[M + H]^+$ calcd for $C_{25}H_{15}F_3N_3$ 414.1213; found 414.1218.

***7-Nitro-1,3-diphenylbenzo[4,5]imidazo[1,2-a]pyridine-4-carbonitrile (1k)*:**

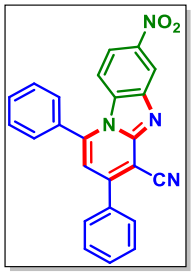

As a yellow solid (31 mg, 32% yield, mp 233–235 °C); Purification over a column of silica gel (10% EtOAc in hexane); ^{1}H NMR ($CDCl_3$, 500 MHz): δ 8.87 (s, 1H), 7.93 (d, 1H, J = 9.0 Hz), 7.81–7.79 (m, 2H), 7.76 (d, 1H, J = 7.5 Hz), 7.70 (t, 2H, J = 7.5 Hz), 7.63–7.61 (m, 2H), 7.59–7.57 (m, 3H), 7.00 (s, 1H), 6.68 (d, 1H, J = 9.5 Hz); ^{13}C{^{1}H} NMR ($CDCl_3$, 125 MHz): δ 151.1, 150.6, 146.3, 145.2, 145.0, 135.6, 133.0, 132.4, 131.8, 131.0, 130.0, 129.5, 128.9, 128.7, 116.79, 116.77, 115.1, 114.94, 114.90, 98.8; IR (KBr, cm^{-1}): 3056, 2967, 2924, 2854, 2226, 1633, 1595, 1525, 1438, 1345, 1300, 1264, 897, 734, 702; HRMS (ESI/Q-TOF) m/z: $[M + H]^+$ calcd for $C_{24}H_{15}N_4O_2$ 391.1190; found 391.1194.

***7-Acetyl-1,3-diphenylbenzo[4,5]imidazo[1,2-a]pyridine-4-carbonitrile (1l)*:**

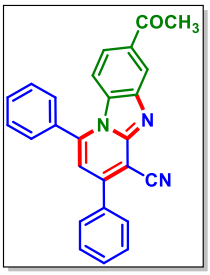

As a yellow solid (38 mg, 40% yield, mp 221–223 °C); Purification over a column of silica gel (10% EtOAc in hexane); ^{1}H NMR ($CDCl_3$, 600 MHz): δ 8.59 (s, 1H), 7.79–7.78 (m, 2H), 7.73 (t, 1H, J = 7.5 Hz), 7.71–7.66 (m, 3H), 7.63–7.62 (m, 2H), 7.57–7.54 (m, 3H), 6.94 (s, 1H), 6.65 (d, 1H, J = 9.0 Hz), 2.67 (s, 3H); ^{13}C{^{1}H} NMR ($CDCl_3$, 100 MHz): δ 197.8, 150.2, 149.4, 145.4, 145.0, 135.9, 135.4, 132.8, 132.3, 131.5, 130.8, 129.8, 129.4, 128.9, 128.8, 122.0, 121.4, 115.2, 114.9, 114.3, 98.5, 26.9; IR (KBr, cm^{-1}): 3061, 2959, 2924, 2852, 2223, 1681, 1628, 1524, 1488, 1429, 1358, 1300, 1208, 768, 752, 700; HRMS (ESI/Q-TOF) m/z: [M + H]$^{+}$ calcd for $C_{26}H_{18}N_3O$ 388.1444; found 388.1450.

***1,3-Diphenylbenzo[4,5]imidazo[1,2-a]pyridine-4,7-dicarbonitrile (1m)*:**

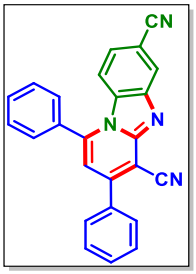

As a yellow solid (32 mg, 35% yield, mp 238–240 °C); Purification over a column of silica gel (15% EtOAc in hexane); ^{1}H NMR ($CDCl_3$, 600 MHz): δ 8.29 (s, 1H), 7.78–7.77 (m, 2H), 7.74 (t, 1H, J = 7.2 Hz), 7.68 (t, 2H, J = 7.5 Hz), 7.59 (d, 2H, J = 7.8 Hz), 7.56–7.55 (m, 3H), 7.25 (s, 1H), 6.97 (s, 1H), 6.65 (d, 1H, J = 8.4 Hz); ^{13}C{^{1}H} NMR ($CDCl_3$, 150 MHz): δ 150.9, 149.8, 145.02, 145.01, 135.5, 132.4, 131.9, 131.7, 130.9, 129.9, 129.5, 128.9, 128.7, 125.5, 124.5, 119.1, 115.9, 115.0, 114.8, 109.8, 98.6; IR (KBr, cm^{-1}): 3058, 2954, 2926, 2852, 2229, 1631, 1600, 1526, 1487, 1429, 1298, 804, 773, 757, 700; HRMS (ESI/Q-TOF) m/z: [M + H]$^{+}$ calcd for $C_{25}H_{15}N_4$ 371.1291; found 371.1291.

***2-Imino-1-(2-iodophenyl)-4-phenyl-6-(p-tolyl)-1,2-dihydropyridine-3-carbonitrile (9a')*:**

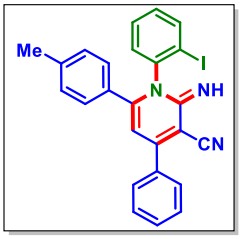

As a brown solid (38 mg, 32% yield, mp 108–110 °C); Purification over a column of silica gel (30% EtOAc in hexane); ^{1}H NMR ($CDCl_3$, 600 MHz): δ 7.79 (d, 1H, J = 7.8 Hz), 7.70–7.68 (m, 2H), 7.49–7.48 (m, 3H), 7.35 (t, 1H, J = 7.5 Hz), 7.26 (d, 1H, J = 6.0 Hz), 7.15 (d, 2H, J = 8.4 Hz), 6.99–6.97 (m, 3H), 6.01 (s, 1H), 4.74 (br s, 1H), 2.23 (s, 3H); ^{13}C{^{1}H} NMR ($CDCl_3$, 150 MHz): δ 156.7, 156.2, 153.0, 141.2, 140.4, 139.8, 136.2, 131.3, 131.2, 130.6, 130.4, 129.5, 128.9, 128.73, 128.68, 128.0, 116.8, 107.2, 100.0, 99.6, 21.4; IR (KBr, cm^{-1}): 3315, 3055, 2959, 2923, 2857, 2212, 1660, 1609, 1582, 1560, 1505, 1526, 1466, 1441, 1374, 1234, 1165, 1066, 1020,

815, 765, 731, 699; HRMS (ESI/Q-TOF) m/z: $[M + H]^+$calcd for $C_{25}H_{19}IN_3$ 488.0618; found 488.0619.

***2-Oxo-4,6-diphenyl-1-(p-tolyl)-1,2-dihydropyridine-3-carbonitrile (1n)*:**

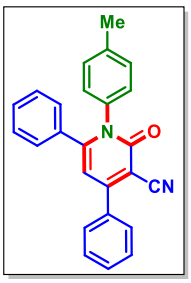

As a white solid (56 mg, 62% yield, mp 196–198 °C); Purification over a column of silica gel (5% EtOAc in hexane); ^{1}H NMR ($CDCl_3$, 500 MHz): δ 8.07 (d, 2H, J = 7.5 Hz), 7.68–7.63 (m, 4H), 7.56–7.53 (m, 3H), 7.50–7.46 (m, 2H), 7.31 (s, 1H), 7.23 (d, 3H, J = 8.0 Hz), 2.39 (s, 3H); ^{13}C{^{1}H} NMR ($CDCl_3$, 125 MHz): δ 159.1, 156.9, 155.6, 138.2, 137.3, 136.6, 133.4, 130.4, 130.0, 129.6, 129.2, 128.9, 128.4, 127.6, 121.1, 117.3, 111.4, 89.9, 21.1; IR (KBr, cm^{-1}): 3061, 2954, 2919, 2854, 2217, 1607, 1576, 1549, 1513, 1492, 1444, 1365, 1257, 815, 756, 700, 687; HRMS (ESI/Q-TOF) m/z: $[M + H]^+$ calcd for $C_{25}H_{19}N_2O$ 363.1492; found 363.1493.

***2-Imino-4,6-diphenyl-1-(p-tolyl)-1,2-dihydropyridine-3-carbonitrile (1n')*:**

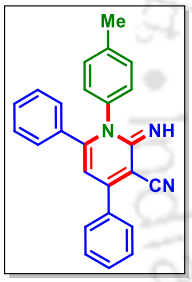

As a brown solid (19 mg, 22% yield, mp 220–222 °C); Purification over a column of silica gel (30% EtOAc in hexane); ^{1}H NMR ($CDCl_3$, 500 MHz): δ 7.69–7.67 (m, 2H), 7.50–7.49 (m, 3H), 7.22–7.16 (m, 3H), 7.14–7.10 (m, 4H), 7.01 (d, 2H, J = 8.0 Hz), 6.02 (s, 1H), 4.54 (br s, 1H), 2.28 (s, 3H); ^{13}C{^{1}H} NMR ($CDCl_3$, 125 MHz): δ 156.3, 153.4, 139.3, 136.4, 135.2, 135.1, 130.6, 129.3, 129.1, 129.0, 128.8, 128.2, 128.1, 124.6, 124.1, 119.3, 116.7, 107.3, 21.3; IR (KBr, cm^{-1}): 3315, 3058, 2955, 2923, 2854, 2216, 1622, 1562, 1523, 1509, 1489, 1376, 1264, 1165, 1078, 1018, 825, 764, 747, 699; HRMS (ESI/Q-TOF) m/z: $[M + H]^+$ calcd for $C_{25}H_{20}N_3$ 362.1652; found 362.1661.

***Phenyl(3-phenyl-1-(p-tolyl)benzo[4,5]imidazo[1,2-a]pyridin-4-yl)methanone (1bo)*:**

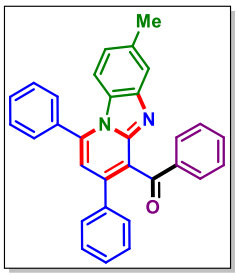

As a yellow solid (78 mg, 72% yield, mp 201–203 °C); Purification over a column of silica gel (5% EtOAc in hexane); ^{1}H NMR ($CDCl_3$, 500 MHz): δ 7.78 (d, 2H, J = 8.5 Hz), 7.59–7.54 (m, 6H), 7.38–7.33 (m, 3H), 7.22 (t, 2H, J = 7.8 Hz), 7.18–7.13 (m, 3H), 6.75–6.72 (m, 2H), 6.44 (d, 1H, J = 9.0 Hz), 2.34 (s, 3H); ^{13}C{^{1}H} NMR ($CDCl_3$, 125 MHz): δ 194.9, 147.8, 146.2, 141.5, 140.0, 137.8, 136.9, 135.5, 134.1, 133.6, 130.4, 130.0, 129.3, 129.0, 128.9, 128.7, 128.6, 128.5, 127.0, 125.2, 122.8, 119.9, 113.99, 113.93, 21.8; IR (KBr, cm^{-1}): 3061, 2956, 2923, 2857, 1673,

1596, 1526, 1510, 1485, 1448, 1303, 1256, 756, 700; HRMS (ESI/Q-TOF) m/z: $[M + H]^+$ calcd for $C_{31}H_{23}N_2O$ 439.1805; found 439.1805.

***1,3-Diphenyl-7-(p-tolylethynyl)benzo[4,5]imidazo[1,2-a]pyridine-4-carbonitrile (1ip)*:**

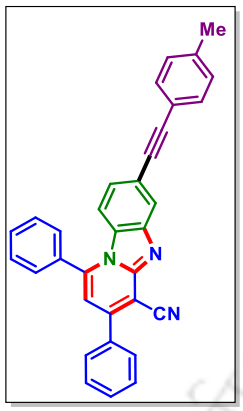

As a yellow solid (60 mg, 52% yield, mp 248–250 °C); Purification over a column of silica gel (10% EtOAc in hexane); ^{1}H NMR ($CDCl_3$, 500 MHz): δ 8.13 (s, 1H), 7.79–7.77 (m, 2H), 7.69–7.62 (m, 5H), 7.56–7.52 (m, 3H), 7.43 (d, 2H, J = 8.0 Hz), 7.18–7.13 (m, 3H), 6.88 (s, 1H), 6.56 (d, 1H, J = 9.0 Hz), 2.37 (s, 3H); ^{13}C{^{1}H} NMR ($CDCl_3$, 125 MHz): δ 149.6, 148.9, 145.6, 144.8, 136.8, 136.1, 133.1, 131.8, 131.6, 131.3, 130.5, 129.7, 129.33, 129.31, 128.9, 128.8, 125.5, 123.6, 121.8, 120.3, 118.0, 115.5, 114.7, 113.8, 98.2, 90.4, 89.0, 21.7; IR (KBr, cm^{-1}): 3067, 3036, 2989, 2923, 2857, 2226, 1631, 1595, 1522, 1488, 1292, 1264, 816, 767, 732, 700; HRMS (ESI/Q-TOF) m/z: $[M + H]^+$ calcd for $C_{33}H_{22}N_3$ 460.1808; found 460.1801.

IV.11. Representative NMR Spectra:

1,3-Diphenylbenzo[4,5]imidazo[1,2-a]pyridine-4-carbonitrile (1a): ^{1}H NMR ($CDCl_3$, 500 MHz)

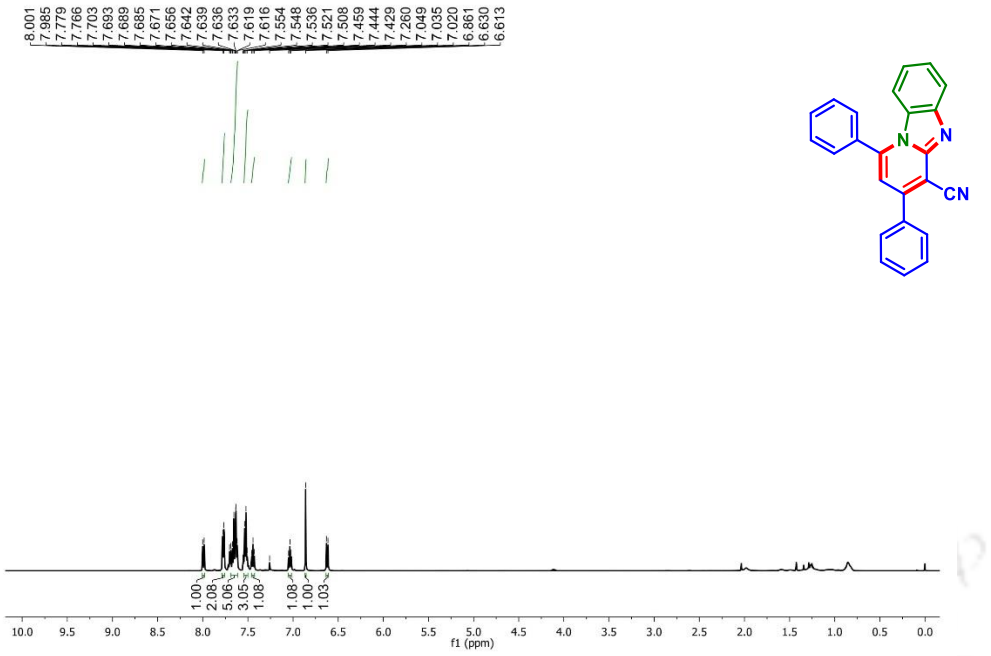

1,3-Diphenylbenzo[4,5]imidazo[1,2-a]pyridine-4-carbonitrile (1a): $^{13}C\{^{1}H\}$ NMR ($CDCl_3$, 125 MHz)

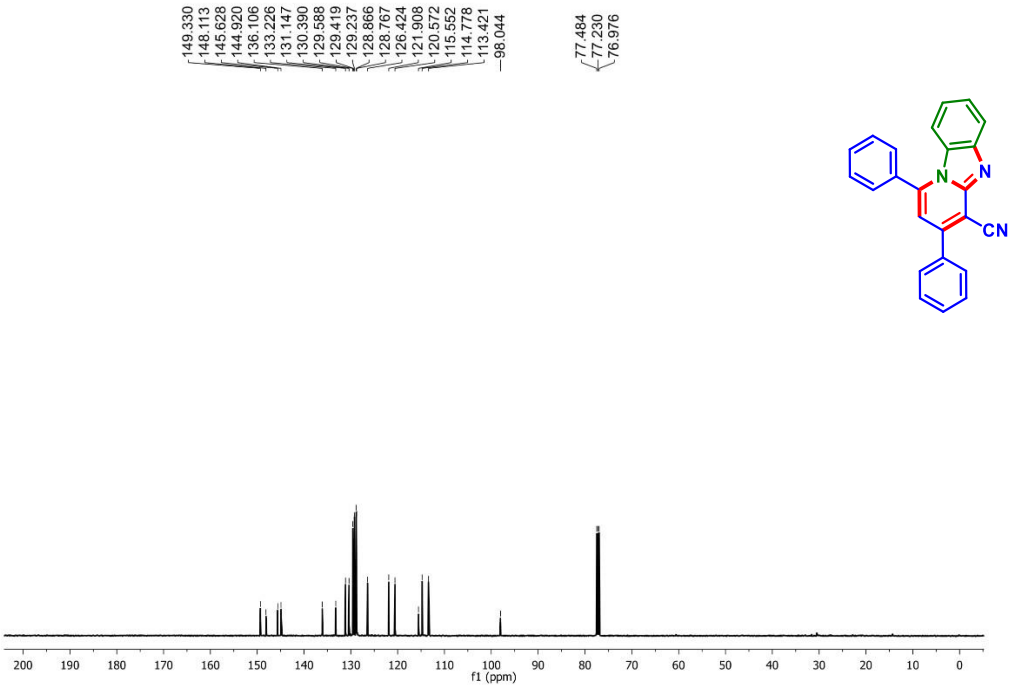

1-Phenyl-3-(p-tolyl)benzo[4,5]imidazo[1,2-a]pyridine-4-carbonitrile (2a): ^{1}H NMR ($CDCl_3$, 500 MHz)

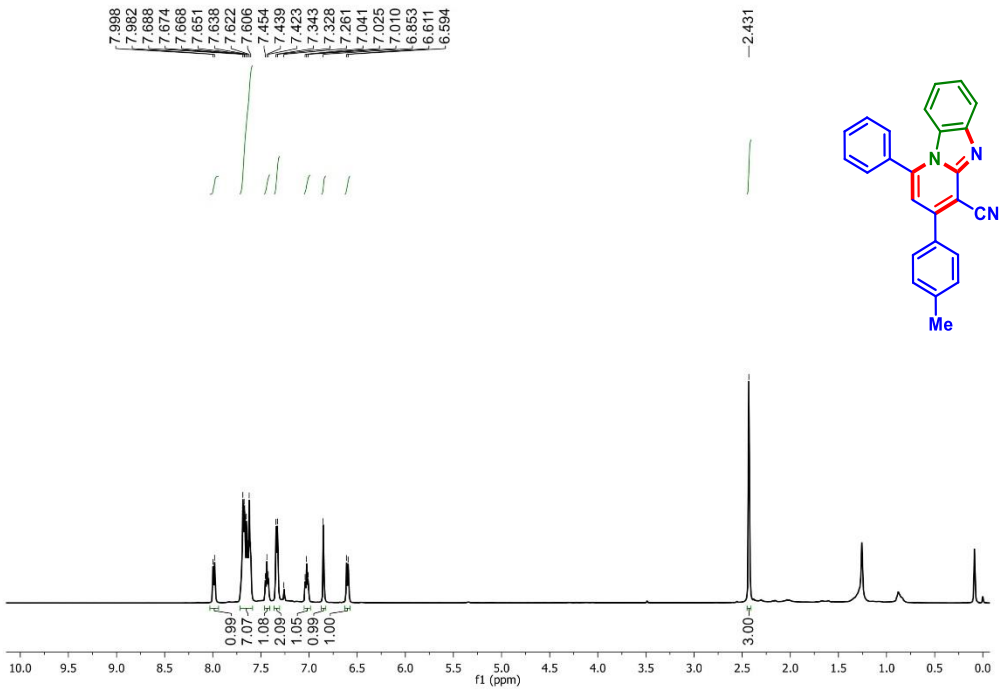

1-Phenyl-3-(p-tolyl)benzo[4,5]imidazo[1,2-a]pyridine-4-carbonitrile (2a): $^{13}C\{^{1}H\}$ NMR ($CDCl_3$, 125 MHz)

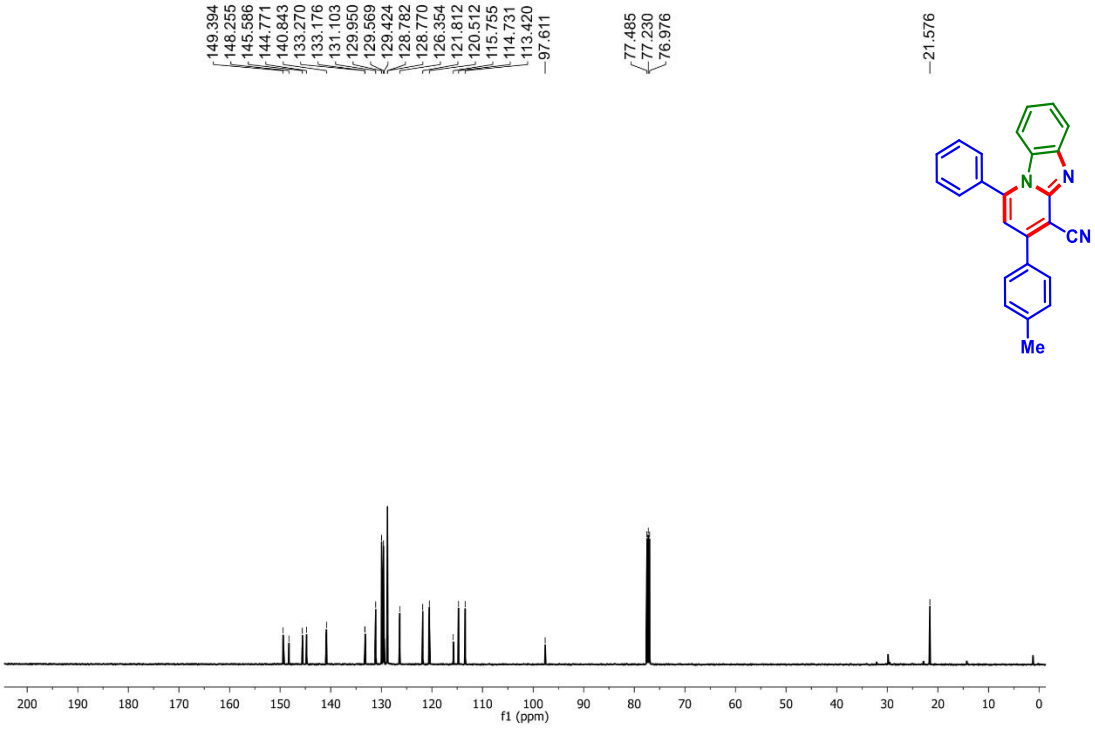

3-(4-Chlorophenyl)-1-phenylbenzo[4,5]imidazo[1,2-a]pyridine-4-carbonitrile (6a): ^{1}H NMR ($CDCl_3$, 500 MHz)

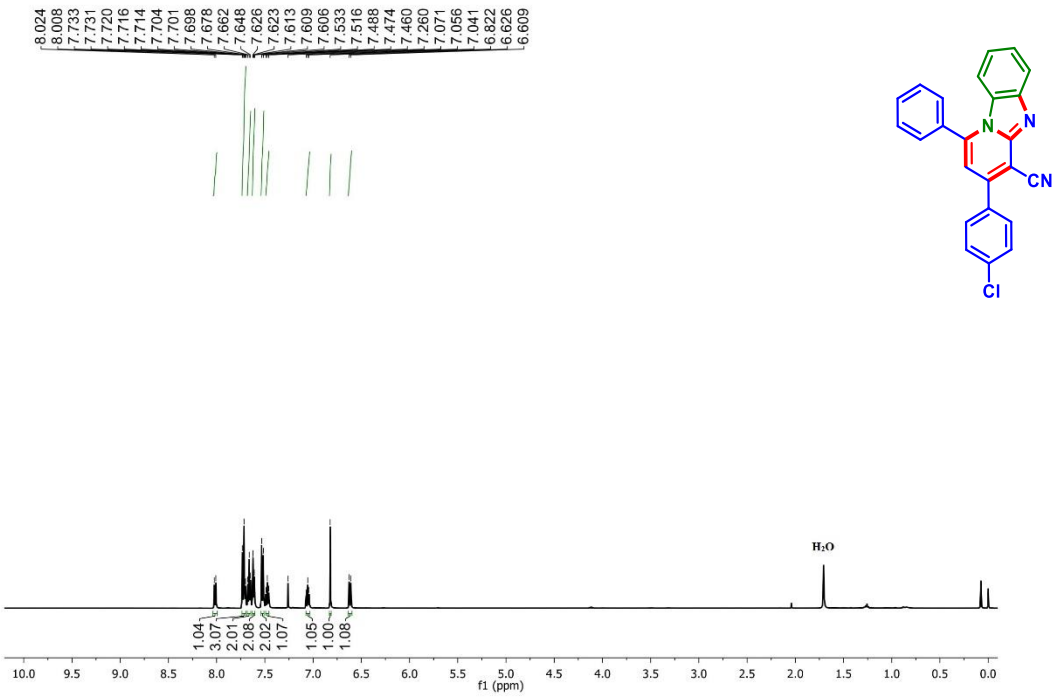

3-(4-Chlorophenyl)-1-phenylbenzo[4,5]imidazo[1,2-a]pyridine-4-carbonitrile (6a): $^{13}C\{^{1}H\}$ NMR ($CDCl_3$, 125 MHz)

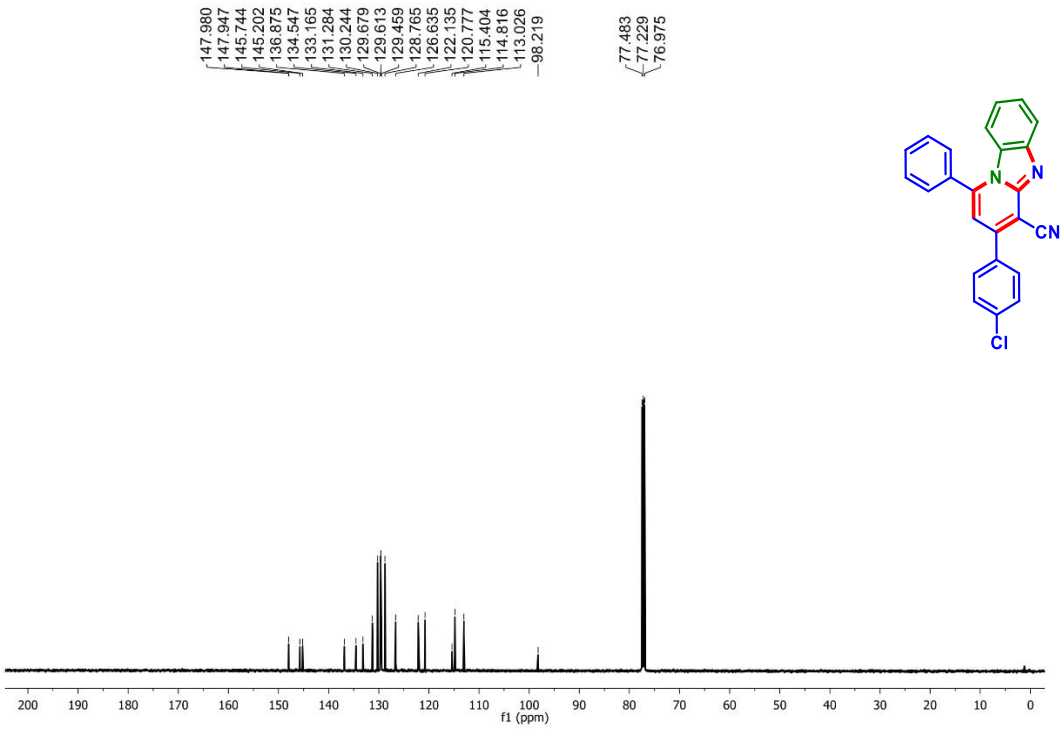

3-Phenyl-1-(p-tolyl)benzo[4,5]imidazo[1,2-a]pyridine-4-carbonitrile (9a): ^{1}H NMR ($CDCl_3$, 400 MHz)

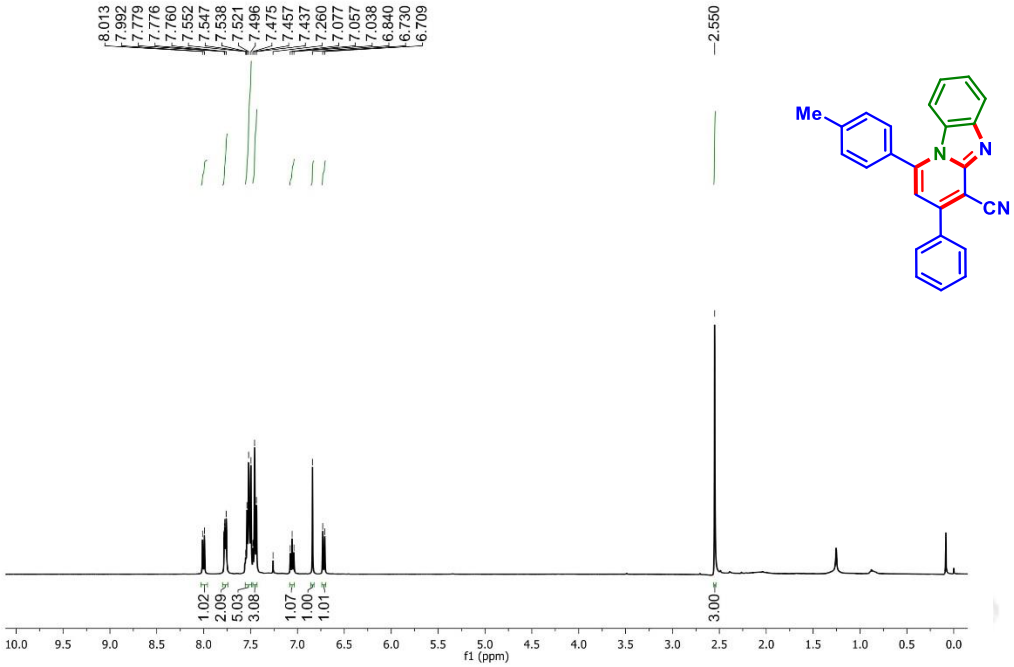

3-Phenyl-1-(p-tolyl)benzo[4,5]imidazo[1,2-a]pyridine-4-carbonitrile (9a): $^{13}C\{^{1}H\}$ NMR ($CDCl_3$, 100 MHz)

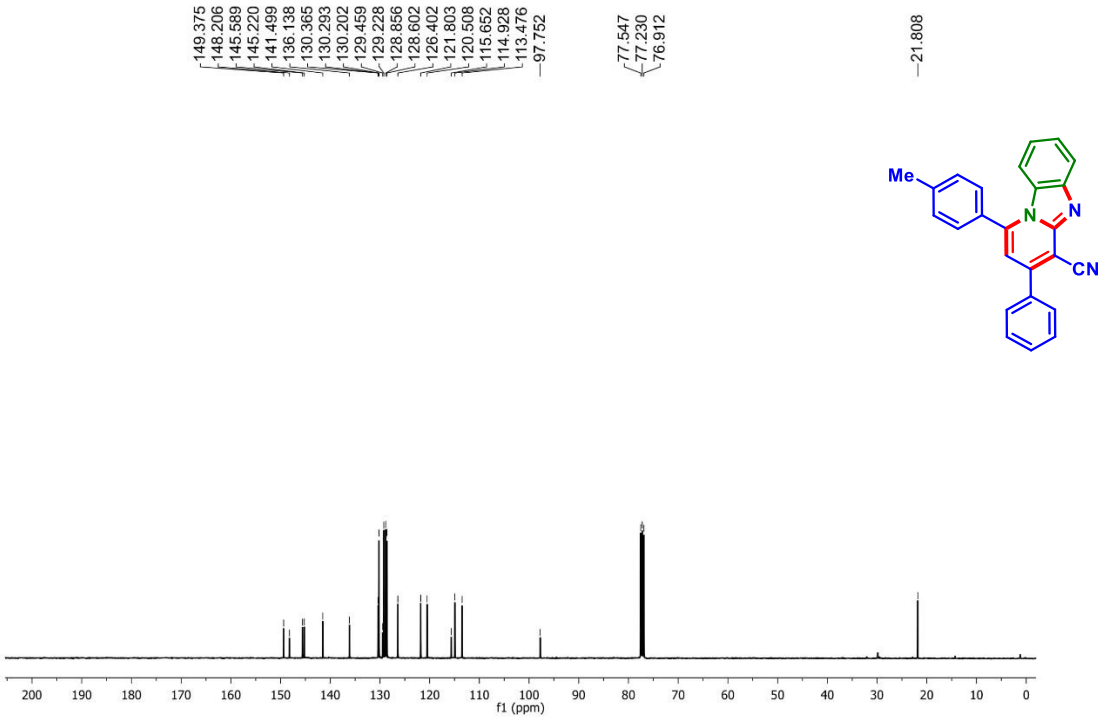

1-(4-Chlorophenyl)-3-phenylbenzo[4,5]imidazo[1,2-a]pyridine-4-carbonitrile (12a): ^{1}H NMR ($CDCl_3$, 500 MHz)

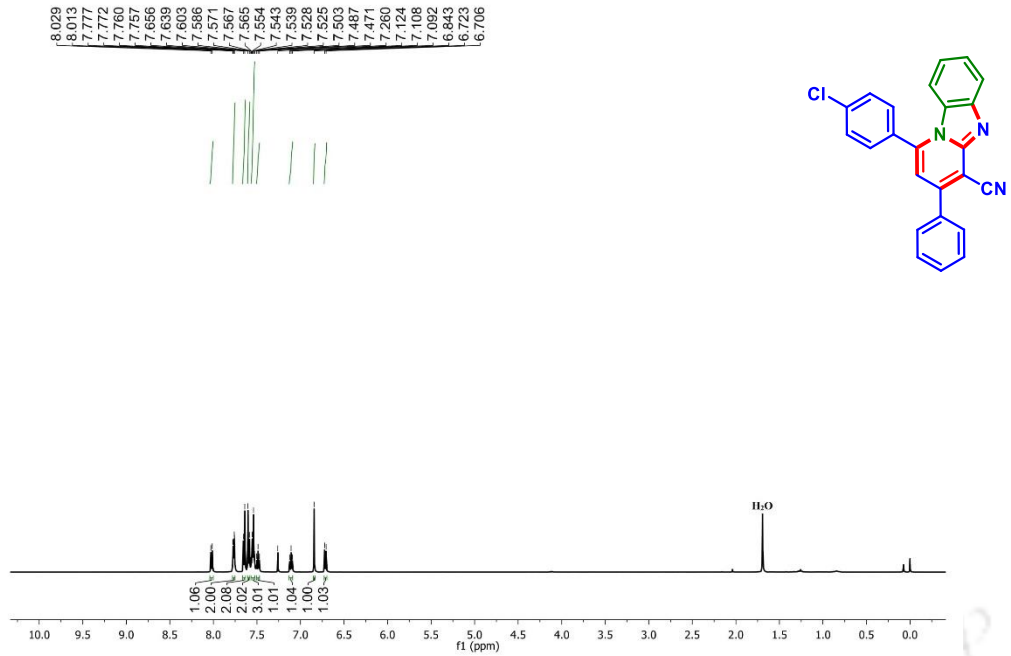

1-(4-Chlorophenyl)-3-phenylbenzo[4,5]imidazo[1,2-a]pyridine-4-carbonitrile (12a): $^{13}C\{^{1}H\}$ NMR ($CDCl_3$, 125 MHz)

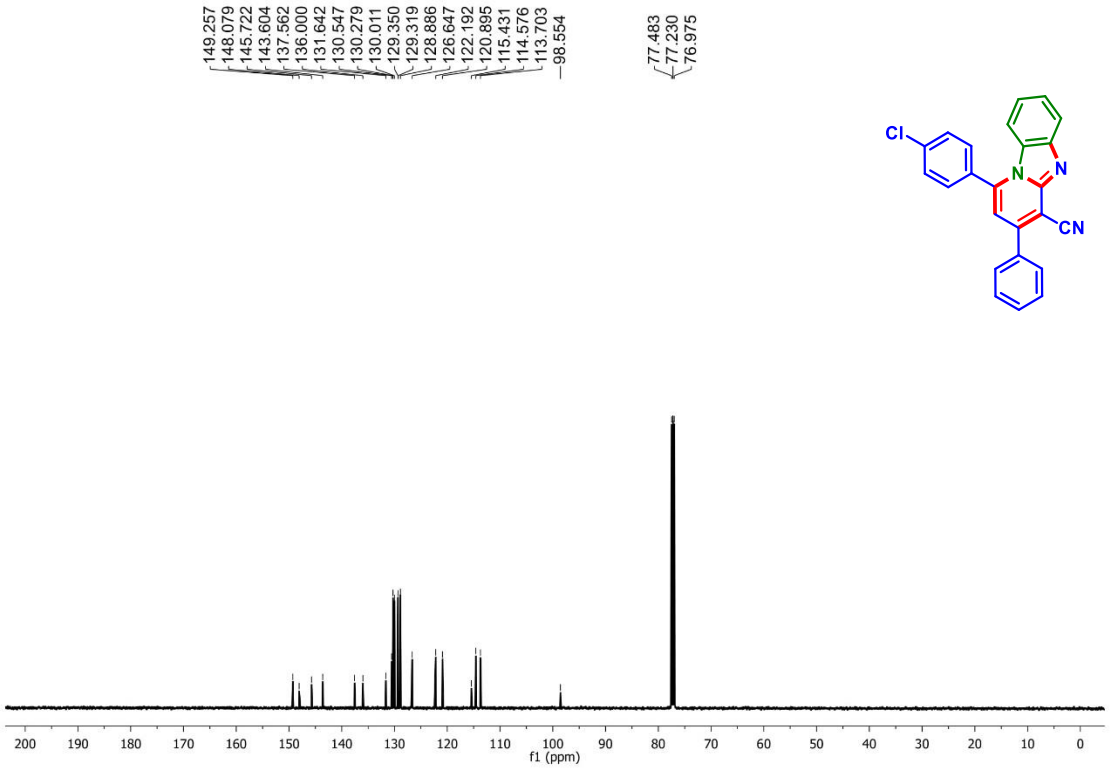

7-Methyl-1,3-diphenylbenzo[4,5]imidazo[1,2-a]pyridine-4-carbonitrile (1b): ^{1}H NMR ($CDCl_3$, 500 MHz)

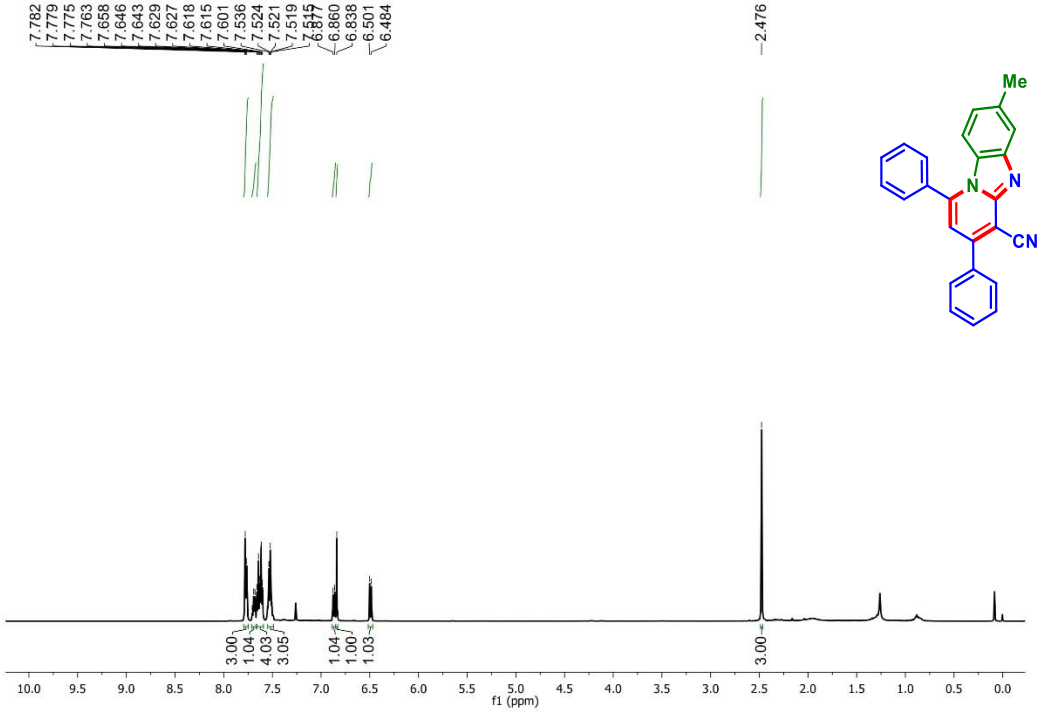

7-Methyl-1,3-diphenylbenzo[4,5]imidazo[1,2-a]pyridine-4-carbonitrile (1b): $^{13}C\{^{1}H\}$ NMR ($CDCl_3$, 125 MHz)

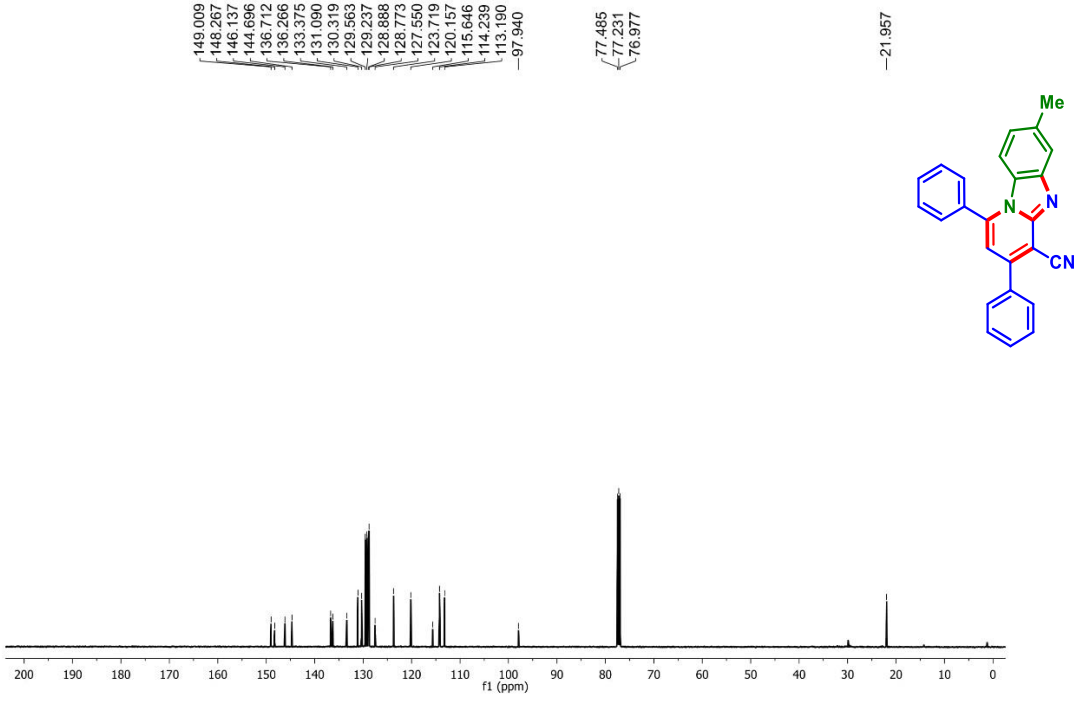

7-Chloro-1,3-diphenylbenzo[4,5]imidazo[1,2-a]pyridine-4-carbonitrile (1g): ^{1}H NMR ($CDCl_3$, 400 MHz)

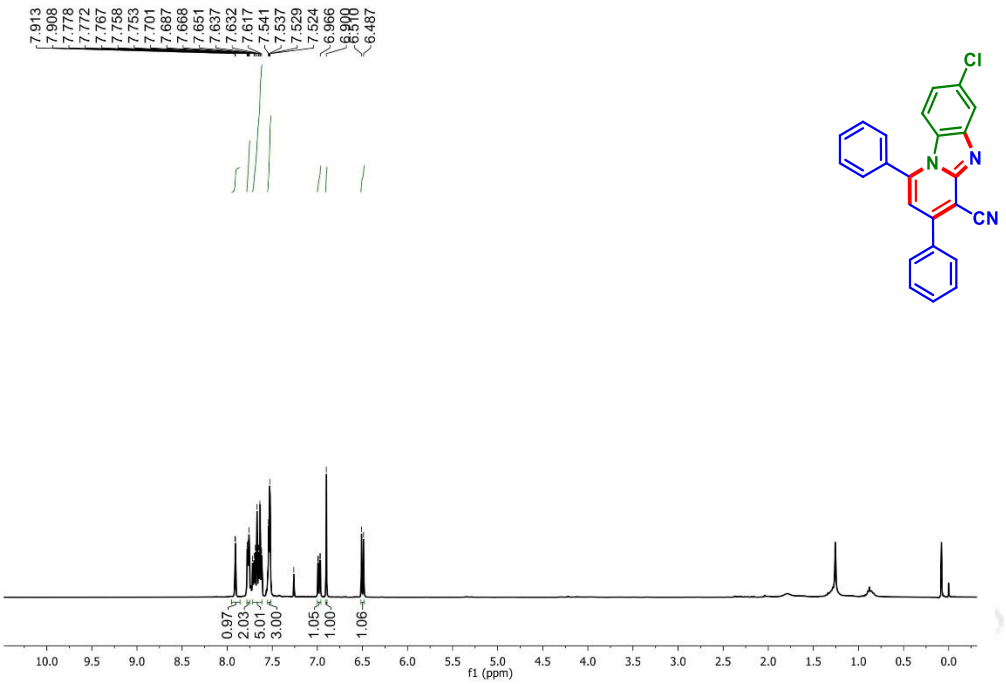

7-Chloro-1,3-diphenylbenzo[4,5]imidazo[1,2-a]pyridine-4-carbonitrile (1g): $^{13}C\{^{1}H\}$ NMR ($CDCl_3$, 100 MHz)

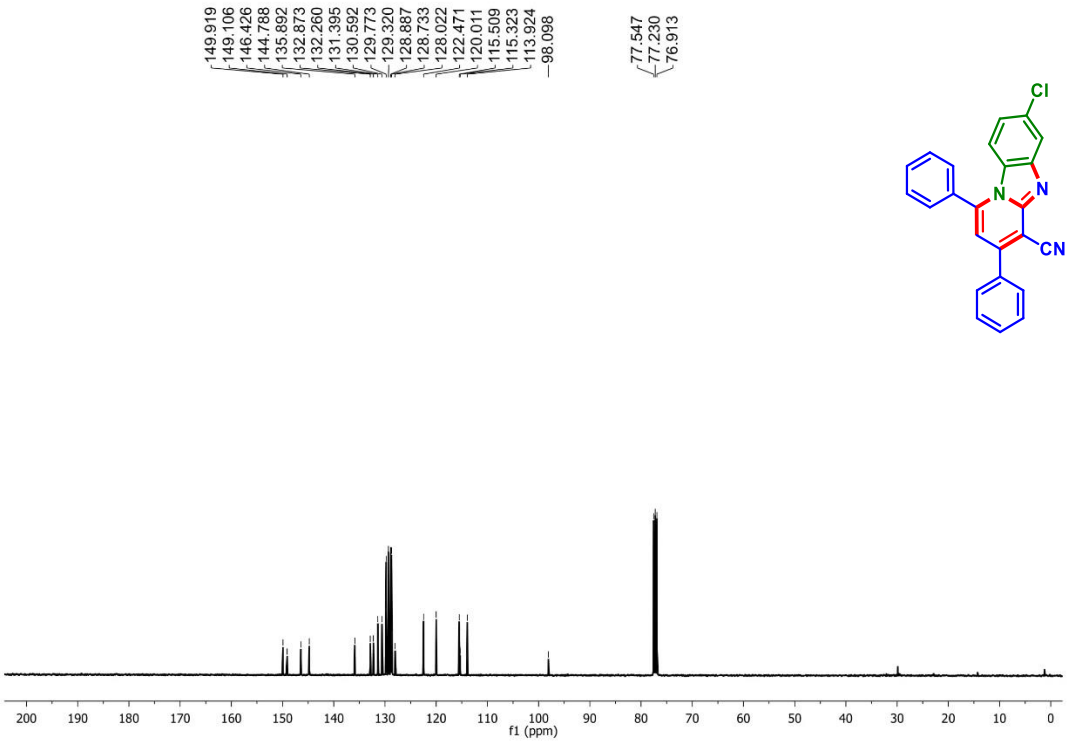

IV.12. References:

[1] (a) Adepu, R.; Sunke, R.; Meda, C. L. T.; Ramba, D.; Krishna, G. R.; Reddy, C. M.; Deora, G. S.; Parsa, K. V. L.; Pal, M. *Chem. Commun*. **2013**, *49*, 190–192. (b) Xu, C.; Jia, F.-C.; Zhou, Z.-W.; Zheng, S.-J.; Li, H.; Wu, A.-X. *J. Org. Chem*. **2016**, *81*, 3000–3006. (c) Ali, W.; Dahiya, A.; Pandey, R.; Alam, T.; Patel, B. K. *J. Org. Chem.* **2017**, *82*, 2089–2096. (d) Ye, X.; Xu, B.; Sun, J.; Dai, L.; Shao, Y.; Zhang, Y.; Chen, J. *J. Org. Chem*. **2020**, *85*, 13004–13014. (e) Baccalini, A.; Faita, G.; Zanoni, G.; Maiti, D. *Chem. Eur. J*. **2020**, 26, 9749–9783. (f) Zhang, Y.; Xiong, W.; Chen, L.; Shao, Y.; Li, R.; Chen, Z.; Ge, J.; Lv, N.; Chen, J. *Org. Chem. Front*. **2021**, *8*, 304–309.

[2] (a) Abet, V.; Nun˜ez, A.; Mendicuti, F.; Burgos, C.; Alvarez-Builla, J. *J. Org. Chem*. **2008**, *73*, 8800–8807. (b) Ahmed, E.; Briseno, A. L.; Xia, Y.; Jenekhe, S. A. *J. Am. Chem. Soc*. **2008**, *130*, 1118–1119. (c) Perin, N.; Uzelac, L.; Piantanida, I.; Karminski-Zamola, G.; Kralj, M.; Hranjec, M. *Bioorg. Med. Chem*. **2011**, *19*, 6329–6339. (d) Taylor, A. P.; Robinson, R. P.; Fobian, Y. M.; Blakemore, D. C.; Jonesb, L. H.; Fadeyi, O. *Org. Biomol. Chem*. **2016**, *14*, 6611–6637. (e) Janosik, T.; Rannug, A.; Rannug, U.; Wahlström, N.; Slätt, J.; Bergman, J. *Chem. Rev*. **2018**, *118*, 9058–9128. (f) Kerru, N.; Gummidi, L.; Maddila, S.; Gangu, K. K.; Jonnalagadda, S. B. *Molecules*. **2020**, *25*, 1909–1950.

[3] (a) Kotovskaya, S. K.; Baskakova, Z. M.; Charushin, V. N.; Chupakhin, O. N.; Belanov, E. F.; Bormotov, N. I.; Balakhnin, S. M.; Serova, O. A. *Pharm. Chem. J*. **2005**, *39*, 574–578. (b) Hranjec, M.; Kralj, M.; Piantanida, I.; Sedic´, M.; Šuman, L.; Pavelic´, K.; Karminski-Zamola, G. *J. Med. Chem*. **2007**, 50, 5696–5711. (c) Hranjec, M.; Piantanida, I.; Kralj, M.; Šuman, L.; Pavelic´, K.; Karminski-Zamola, G. *J. Med. Chem.* **2008**, *51*, 4899–4910. (d) Takeshita, H.; Watanabe, J.; Kimura, Y.; Kawakami, K.; Takahashi, H.; Takemura, M.; Kitamura, A.; Someya, K.; Nakajima, R. *Bioorg. Med. Chem. Lett*. **2010**, *20*, 3893–3896. (e) Ndakala, A. J.; Gessner, R. K.; Gitari, P. W.; October, N.; White, K. L.; Hudson, A.; Fakorede, F.; Shackleford, D. M.; Kaiser, M.; Yeates, C.; Charman, S. A.; Chibale, K. *J. Med. Chem*. **2011**, 54, 4581–4589. (f) Refaat, H. M. *Med. Chem. Res*. **2012**, *21*, 1253–1260.

[4] (a) Hirano, K.; Oderaotoshi, Y.; Minakata, S.; Komatsu, M. *Chem. Lett*. **2010**, *30*, 1262–1263. (b) Yang, H.; Ge, Y.Q.; Jia, J.; Wang, J. W. *J. Luminescence*. **2011**, *131*, 749–755. (c) Zhao, D.; Hu, J.; Wu, N.; Huang, X.; Qin, X.; Lan, J.; You, J. *Org. Lett*. **2011**, *13*, 6516–6519.

[5] Wu, Z.; Huang, Q.; Zhou, X.; Yu, L.; Li, Z.; Wu, D. *Eur. J. Org. Chem*. **2011**, 5242–5245.

[6] Rasheed, Sk.; D. Rao, N.; Das, P. *J. Org. Chem*. **2015**, *80*, 9321–9327.

[7] (a) Verma, A. K.; Kesharwani, T.; Singh, J.; Tandon, V.; Larock, R. C. *Angew. Chem., Int. Ed*. **2009**, *48*, 1138–1143. (b) Cai, Q.; Li, Z.; Wei, J.; Fu, L.; Ha, C.; Pei, D.; Ding, K. *Org. Lett*. **2010**, *12*, 1500–1503. (c) Qian, W.; Wang, H.; Allen, J. *Angew. Chem., Int. Ed*. **2013**, *52*, 10992–10996. (d) Dai, H.; Li, C.-X.; Yu, C.; Wang, Z.; Yan, H.; Lu, C. *Org. Chem. Front*. **2017**, *4*, 2008–2011. (e) Panday, A. K.; Mishra, R.; Jana, A.; Parvin, T.; Choudhury, L. H. *J. Org. Chem*. **2018**, *83*, 3624–3632. (f) Fairoosa, J.; Neethaa, M.; Anilkumar, G. *RSC Adv*. **2021**, *11*, 3452–3469.

[8] (a) Ding, Q.; Cao, B.; Liu, X.; Zonga, Z.; Peng, Y.-Y. *Green Chem*. **2010**, *12*, 1607–1610. (b) Wang, F.; Cai, S.; Liao, Q.; Xi, C. *J. Org. Chem*. **2011**, 76, 3174–3180. (c) Khatun, N.; Jamir, L.; Ganesha, M.; Patel, B. K. *RSC Adv*. **2012**, *2*, 11557–11565. (d) Ahmed, A.; Dhara, S.; Singha, R.; Nuree, Y.; Sarkar, P.; Ray, J. K. *RSC Adv*. **2014**, *4*, 53137–53141. (e) An, J.; Alper, H.; Beauchemin, A. *Org. Lett*. **2016**, *18*, 3482–3485.

[9] Liu, X.; Deng, G.; Liang, Y. *Tetrahedron Lett*. **2018**, *59*, 2844–2847.

[10] (a) Chen, Y.-F.; Hsieh, J.-C.. *Org. Lett*. **2014**, 16, 4642–4645. (b) Qi, L.; Hu, K.; Yu, S.; Zhu, J.; Cheng, T.; Wang, X.; Chen, J.; Wu, H. *Org. Lett*. **2017**, *19*, 218–221. (c) Yu, Y.; Cai, Z.; Yuan, W.; Liu, P.; Sun, P. *J. Org. Chem*. **2017**, *82*, 8148–8156. (d) Xu, T.; Shao, Y.; Dai, L.; Yu, S.; Cheng, T.; Chen, J. *J. Org. Chem*. **2019**, *84*, 13604–13614. (e) Mishra, P. K.; Chatterjee, S.; Verma, A. K. *ACS Omega*. **2020**, *5*, 32133–32139. (f) Dai, L.; Yu, S.; Lv, N.; Ye, X.; Shao, Y.; Chen, Z.; Chen, J. *Org. Lett*. **2021**, *23*, 5664–5668.

[11] (a) Rakshit, A.; Sau, P.; Ghosh, S.; Patel, B. K. *Adv. Synth. Catal*. **2019**, *361*, 3824–3836. (b) Rakshit, A.; Kumar, P.; Alam, T.; Dhara, H.; Patel, B. K. *J. Org. Chem*. **2020**, *85*, 12482–12504.

[12] Yan, C. G.; Wang, Q. F.; Song, X. K.; Sun, J. *J. Org. Chem*. **2009**, *74*, 710–718.

[13] Wang, H.; Wang, Y.; Peng, C.; Zhang, J.; Zhu, Q. *J. Am. Chem. Soc*. **2010**, *132*, 13217–13219.

[14] Dong, L.; Huang, J.-R.; Qu, C.-H.; Zhang, Q.-R.; Zhang, W.; Hanb, B.; Peng, C. *Org. Biomol. Chem*. **2013**, *11*, 6142–6149.

[15] Manna, S.; Matcha, K.; Antonchick, A. P. *Angew. Chem., Int. Ed*. **2014**, *53*, 8163–8166.

[16] Teng, Q.-H.; Peng, X.-J.; Mo, Z.-Y.; Xu, Y.-L.; Tang, H.-T.; Wang, H.-S.; Suna, H.-B.; Pan, Y.-M. *Green Chem*. **2018**, *20*, 2007–2012.

[17] Duan, Z.; Zhang, L.; Zhang, W.; Lu, L.; Zeng, L.; Shi, R.; Lei, A. *ACS Catal*. **2020**, *10*, 3828–3831.

[18] Chen, X.; Sun, P.; Mo, B.; Chen, C.; Peng, J. *J. Org. Chem*. **2021**, *86*, 352–366.

[19] (a) Sambiagio, C.; Marsden, S. P. A.; Blacker, J.; McGowan, P. C. *Chem. Soc. Rev*. **2014**, *43*, 3525–3550. (b) Jie, X.; Shang, Y.; Zhang, X.; Su, W. *J. Am. Chem. Soc*. **2016**, *138*, 5623–5633. (c) Li, Y.; Peng, J.; Chen, X.; Mo, B.; Li, X.; Sun, P.; Chen, C. *J. Org. Chem*. **2018**, *83*, 5288–5294.

[20] Qi, L.; Hu, K.; Yu, S.; Zhu, J.; Cheng, T.; Wang, X.; Chen, J.; Wu, H. *Org. Lett*. **2017**, *19*, 218–222.

[21] Chen, X.; Sun, P.; Mo, B.; Chen, C.; Peng, J. *J. Org. Chem*. **2021**, *86*, 352–366.

[22] (a) Abet, V.; Nun˜ez, A.; Mendicuti, F.; Burgos, C.; Alvarez-Builla, J. *J. Org. Chem*. **2008**, *73*, 8800–8807. (b) Xiong, W.; Hu, K.; Lei, Y.; Zhen, Q.; Zhao, Z.; Shao, Y.; Li, R.; Zhang, Y.; Chen, J. *Org. Lett*. **2020**, *22*, 1239–1243. (c) Dong, Y.; Yang, J.; Zhang, H.; Zhan, X.-Y.; He, S.; Shi, Z.-C.; Zhang, X.-M.; Wang, J.-Y. *Org. Lett*. **2020**, *22*, 5151–5156. (d) Sahoo, S.; Pal, S. *J. Org. Chem*. **2021**, *86*, 4081–4097.

[23] Frisch, M. J.; Trucks, G. W.; Schlegel, H. B.; Scuseria, G. E.; Robb, M. A.; Cheeseman, J. R.; Scalmani, G.; Barone, V.; Mennucci, B.; Petersson, G. A.; Nakatsuji, H.; Caricato, M.; Li, X.; Hratchian, H. P.; Izmaylov, A. F.; Bloino, J.; Zheng, G.; Sonnenberg, J. L.; Hada, M.; Ehara, M.; Toyota, K.; Fukuda, R.; Hasegawa, J.; Ishida, M.; Nakajima, T.; Honda, Y.; Kitao, O.; Nakai, H.; Vreven, T.; Mont-gomery, J. A. Jr.; Peralta, J. E.; Ogliaro, F.; Bearpark, M.; Heyd, J. J.; Brothers, E.; Kudin, K. N.; Staroverov, V. N.; Kobayashi, R.; Normand, J.; Raghavachari, K.; Rendell, A.; Burant, J. C.; Iyengar, S.

S.; Tomasi, J.; Cossi, M.; Rega, N.; Millam, J. M.; Klene, M.; Knox, J. E.; Cross, J. B.; Bakken, V.; Adamo, C.; Jaramillo, J.; Gomperts, R.; Stratmann, R. E.; Yazyev, O.; Austin, A. J.; Cammi, R.; Pomelli, C.; Ochterski, J. W.; Martin, R. L.; Morokuma, K.; Zakrzewski, V. G.; Voth, G. A.; Salvador, P.; Dannenberg, J. J.; Dapprich, S.; Daniels, A. D.; Farkas, Ö.; Foresman, J. B.; Ortiz, J. V.; Cioslowski, J.; Fox, D. J. Gaussian 09; Gaussian, Inc.: Walling-ford CT, **2009.**

[24] Lin, S.; Wei, Y.; Liang, F. *Chem. Commun*. **2012**, *48*, 9879–9881.

[25] (a) Choi, Y. R.; Chae, M. L.; Kim, D.; Lah, M. S.; Jeong, K.-S. *Chem. Commun*. **2012**, *48*, 10346–10348. (b) Jash, M.; Das, B.; Chowdhury, C. *J. Org. Chem*. **2016**, *81*, 10987–10999.

CHAPTER V

Visible-Light-Accelerated Pd-Catalyzed Cascade Addition/Cyclization of Arylboronic Acids to γ- and β-Ketodinitriles for the Construction of 3-Cyanopyridines and 3-Cyanopyrrole Analogues

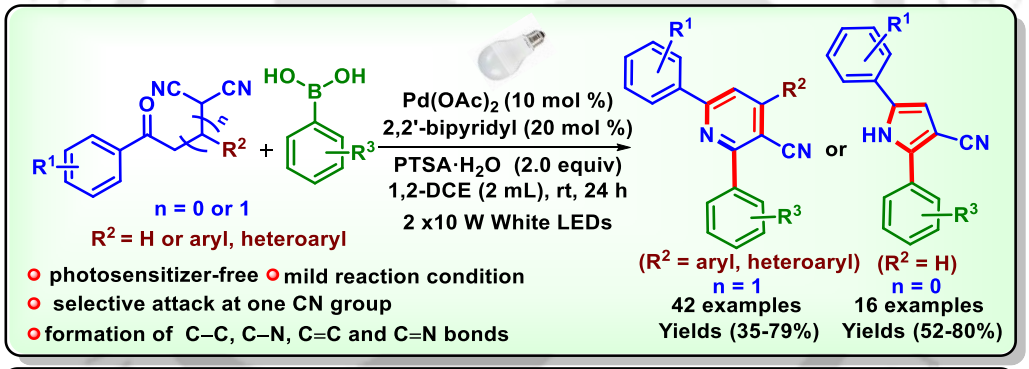

JOC The Journal of Organic Chemistry
J. Org. Chem. **2020**, *85*, 12482–12504.
pubs.acs.org/joc Article

***ABSTRACT*:** The one-pot synthetic strategies for 2,4,6-triarylnicotinonitriles and 2,5-diaryl-1*H*-pyrrole-3-carbonitriles have been accomplished *via* a Pd-catalyzed coupling of arylboronic acids with γ-ketomalononitriles and β-ketomalononitriles respectively under mild reaction conditions. The cascade reactions proceed in 1,2-dichloroethane solvent under visible-light irradiation, and the active catalyst is generated *in situ* in the presence of catalytic amounts of $Pd(OAc)_2$ and 2,2′-bipyridine. The active Pd-catalyst undergoes photoexcitation by the virtue of MLCT, and subsequent redox trans-metalation occurs with arylboronic acid, thus obviating the necessity of any exogenous photosensitizer.

भारतीय प्रौद्योगिकी संस्थान गुवाहाटी
Indian Institute of Technology Guwahati

CHAPTER V

Visible-Light-Accelerated Pd-Catalyzed Cascade Addition/Cyclization of Arylboronic Acids to γ- and β-Ketodinitriles for the Construction of 3-Cyanopyridines and 3-Cyanopyrrole Analogues

V.1. Introduction:

Heteroaromatics are an essential class of molecules in the realm of organic chemistry, among which the nitrogen-heterocycles comprised of pyridine and pyrrole frameworks have garnered the attention of chemists for several years. The widespread attention stems from the fact that substituted pyridine scaffolds constitute an essential structural feature in several natural products and other multipurpose molecules which find their applications in different fields of science ranging from biology to medicine to advanced materials.[1] Besides, pyridine-based structures also find utility in several other fields such as asymmetric catalysis,[2] supramolecular chemistry,[3] and cancer therapy.[4] Likewise, the pyrrole moiety has been identified in the structural frameworks of a wide array of natural products, unnatural products, and drug molecules.[5] The importance of pyrrole-based compounds can be substantiated by their diverse applications in the field of materials chemistry pertaining to the development of batteries, solar cells, and the exploration of diverse optoelectronic applications.[6] Interestingly, pyrrole and pyridine nuclei occur ubiquitously in a plethora of structurally diverse FDA-approved pharmaceutical drugs (Figure V.1.1 and Figure V.1.2).[7]

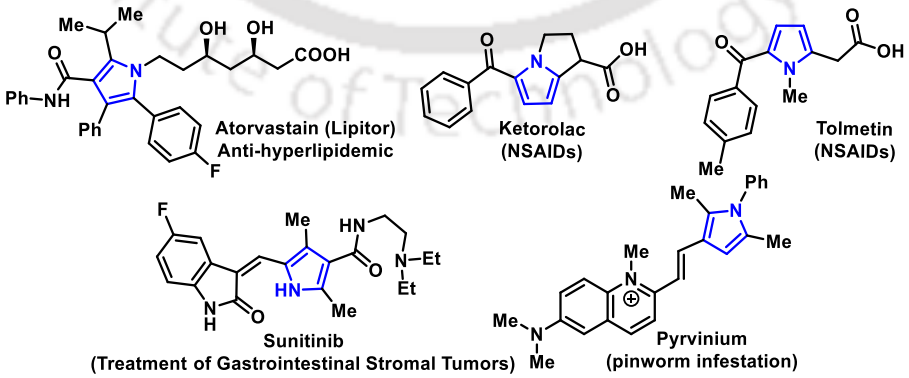

Figure V.1.1. *A few drugs bearing pyrrole nucleus.*

Some renowned drugs bearing the pyridine moiety include nexium (esomeprazole) and aciphex (rabeprazole) for the treatment of acid reflux and duodenal ulcers,[7a,b] avandia (rosiglitazone A) and Actos (pioglitazone B) as antidiabetic drugs,[7c,d] amrinone D (inocor) and etoricoxib E (arcoxia) for treating patients with acute heart failure and arthritis.[7e,f] Moreover, some potent anticancer drugs such as gleevec,[7g] sorafenib (nexovar),[7h] crizotinib (xalkori),[7i] nilotnib,[7j] and the anti-HIV drug altrazanavir (reyataz)[7k] also contain the pyridine moiety. Similarly, a few renowned drugs bearing the pyrrole moiety are atrovastatin, the best-selling cholesterol-lowering drug which functions by inhibiting the HMG-CoA reductase enzyme,[8a] ketorolac and tolmetin are nonsteroidal anti-inflammatory drugs (NSAIDs) used for treating acute pain and inflammation,[8b-c] sunitinib is a multi-targeted tyrosine kinase inhibitor possessing antitumor and antiangiogenic activities, and pyrvinium is used for treating pinworm infestation.[8d–e]

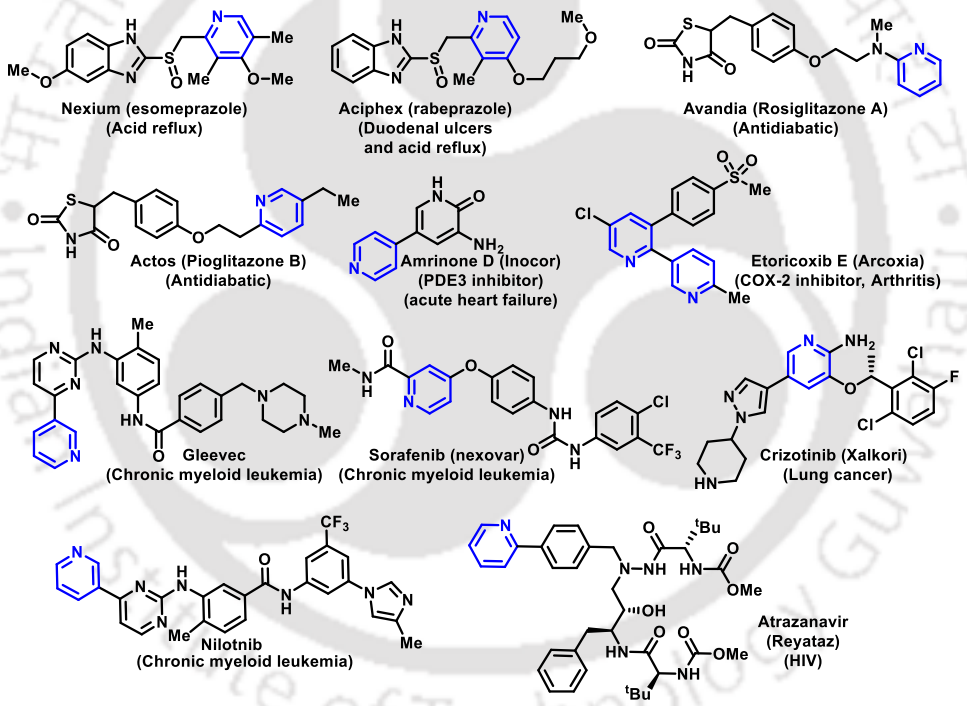

Figure V.1.2. *A few drugs bearing pyridine nucleus.*

In the last couple of decades, visible-light-mediated organic syntheses have gained immense popularity in the wake of several advantages associated with this regime. Several organic, as well as transition metal-based photocatalysts, have been developed to harness the energy of abundant visible-light and transform it into chemical energy, thereby enabling the generation of carbon-centered radicals under mild catalytic conditions, and hence tap the novel reactivity of these intermediates.[9] Unprecedented Pd-catalyzed transformations have been achieved under visible-

light irradiation, although an exogenous photo-catalyst may or may not be required.[10] In the case of the latter, the Pd-catalyst plays a dual role[11a] in several elegant reactions, for instance, the C_{sp3}–C_{sp2} Heck coupling reaction,[11b-e] carbonylative cross-coupling reactions,[11f-g] and others.[11h-j] The successful underpinnings of these strategies can be attributed to the fact that irradiation of Pd(0) catalyst induces a facile single electron transfer (SET) oxidative addition of unactivated alkyl halide, and the subsequent photoexcitation of Pd(II)-alkyl complex restrains the undesired β-hydride elimination process, which otherwise plagues the traditional reactions.[11b]

Recently, our group developed a cascade [4 + 2] Ru(II)-catalyzed annulation strategy for accessing fused isoquinolines, wherein, we noticed that one of the cyano groups, associated with malononitrile moiety, was selectively hydrolyzed.[12] We envisioned that the five-carbon core of the γ-ketomalononitrile may act as a harbinger of pyridine nucleus if cross-coupled with a suitable partner *via* a cascade [5 + 1] annulation strategy. A thorough literature survey revealed that recently several protocols have been developed for the synthesis of 5- and 6-membered nitrogen heterocycles. These studies are an extension of the catalytic carbopalladation/carbonickelation of eclectic nitrile substrates with suitable coupling partners such as arylboronic acids and arylhydrazines to obtain ketones and imines,[13] followed by intramolecular cyclization to afford diverse *N*-heterocycles.[14] Few of these recent works are highlighted in Scheme V.1.1. For instance, in 2017 Wu's group for the first time utilized the nitrile *N* atom *via* Pd-catalyzed nucleophilic addition of arylboronic acids with functionalized nitriles followed by an intramolecular cyclization to access biologically active isoquinolines and isoquinolones [Scheme V.1.1, (i)].[14a] Chen *et al.* reported a Ni(II)-catalyzed cascade coupling of arylboronic acids to ketonitriles into substituted pyrroles and pyridines [Scheme V.1.1, (ii)].[14e] A commonality that can be discerned from the mechanisms is that the initial step engages arylboronic acids in a traditional two-electron trans-metalation with electron-deficient Pd(II)-catalysts. The high activation energy barrier associated with this step predisposes the necessity of elevated temperatures.[15] Recently, Xu *et al.* discovered a Mn(III)-triggered radical pathway involving the cyclization of 3-isocyano-[1,1′-biphenyl]-2-carbonitriles with arylboronic acids to access pyrrolopyridine derivatives [Scheme V.1.1, (iii)].[16] Keeping in mind the natural propensity of Pd-catalyzed reactions to follow a facile SET mechanistic pathway under visible-light irradiation, and arylboronic acids as readily available radical progenitors,[17] we envisaged the synthesis of 2,4,6-triaryl-3-cyanopyridines and 2,5-diaryl-3-cyanopyrrole derivatives [Scheme V.1.1, (iv)].

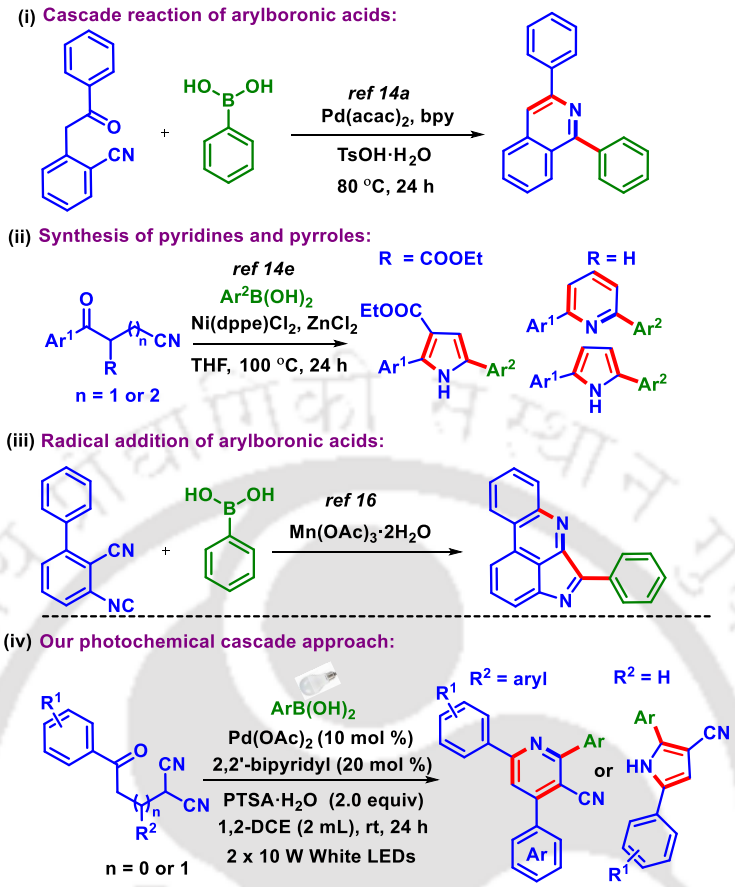

Scheme V.1.1. *Strategies for the synthesis of fused and isolated N-heterocycles from substrates containing functionalized or activated cyano groups.*

We embarked on our experimentation by selecting 2-(3-oxo-1,3-diphenylpropyl)malononitrile (**1**) (0.25 mmol) and phenylboronic acid (**a**) (1 equiv) as the rudimentary substrates; $Pd(OAc)_2$ (5 mol %) as the precatalyst, 2,2′-bipyridine (10 mol %) as the ligand, and PTSA·H_2O (1 equiv) as the additive. Toluene (2 mL) was employed as the solvent, and the reaction mixture was irradiated by 20 W (2 x 10 W) white LEDs at room temperature. The progress of the reaction was monitored *via* thin-layer chromatography, which indicated the formation of some new species in the mixture, in the form of a new fluorescent blue spot in a 365 nm UV chamber. The new compound was isolated, and characterized by standard spectroscopic techniques (IR, ^{1}H NMR, ^{13}C NMR, and HRMS). Delightfully, the analysis confirmed that the isolated compound was 2,4,6-triphenylnicotinonitrile (**1a**), and the yield was estimated to be 33%. Subsequently, single-crystal X-ray diffraction studies were performed on one of the derivatives (**1f**), which further validated the structure of the product (Figure V.1.3, ***CCDC-1999314***). It is

imperative to mention that the formation of 2,4,6-triphenylnicotinonitrile (**1a**) is associated with the genesis of a new C–C, C–N, C=N, and two C=C bonds.

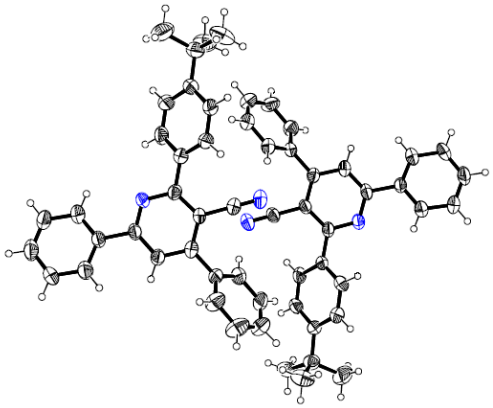

Figure V.1.3. *ORTEP diagram of (**1f**) with 40% ellipsoid probability (CCDC-1999314).*

In our strategy, the starting materials γ-ketomalononitriles and β-ketomalononitriles were readily prepared *via* the addition of malononitrile to various chalcones and α-bromoacetophenones.[18] Further, most arylboronic acids are commercially available. This developed photocatalytic reaction proceeds at room temperature without the usage of the exogenous photosensitizer. The constructed pyridine and pyrrole moiety having an inbuilt nitrile functionality can be further manipulated for various applications. Therefore, our protocol bypasses the toxic chemical maneuvers and harsh reaction conditions generally associated with the introduction of nitrile functionality into aromatic rings, consequently endowing synthetic benefits in the form of functional group transformations and derivatizations.

V.2. Strategies for the Synthesis of Pyridines:

On account of several multifaceted applications of substituted pyridines, synthetic chemists have long endeavored the discovery of various pathways to achieve these important structural motifs. Several classical methods for the synthesis of pyridine are based upon the condensation of ammonia or ammonia sources with a host of different carbonyl compounds (Scheme V.2.1).[19] Few of these are the [5 + 1] condensation of 1,5-diketones with ammonia,[19b] the [2 + 2 + 1 + 1] Hantzsch pyridine synthesis,[19c] and the Kröhnke synthesis.[19d]

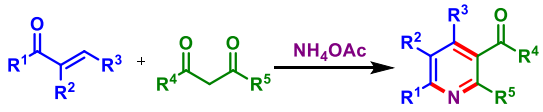

Scheme V.2.1. *Multi-component synthesis of pyridines.*

Later on, several transition metal-mediated annulation protocols were explored which have been highlighted by Gulevich *et al.* in their review article.[20a] Few of these cascade catalytic strategies involve oxidative Michael condensation of oximes with α,β-unsaturated carbonyl compounds (Scheme V.2.2).[20b–c]

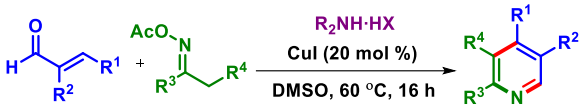

Scheme V.2.2. *Synthesis of multi-substituted pyridines via iminium catalysis.*

The transition metal-assisted coupling/condensation of diverse substrates to form the azatriene intermediates,[20d–f] which eventually follow the 6π-electrocyclization route affording pyridines (Scheme V.2.3).[20f] These methods possess several advantages over the conventional condensation-based strategies, as highly substituted unsymmetrical pyridines can be prepared from eclectic starting materials with high regioselectivity. Nevertheless, many of these protocols suffer from disadvantages such as the requirement of elevated temperatures and employing expensive metal catalysts.

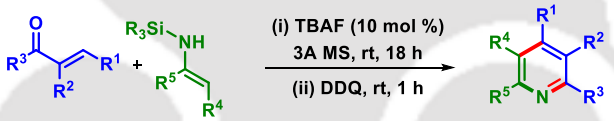

Scheme V.2.3. *Synthesis of pyridines via 6π-electrocyclization.*

The past couple of decades have witnessed a surge in the thermal and transition metal-assisted [4 + 2] hetero Diels-Alder reaction involving 1-azadienes and alkynes (Scheme V.2.4),[21] though inverse electron demand Diels-Alder strategies have also been explored.

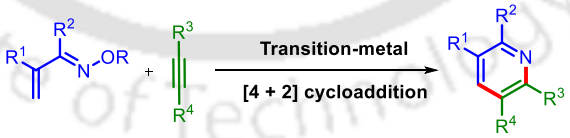

Scheme V.2.4. *Synthesis of pyridines via [4 + 2] cycloaddition.*

Earlier, researchers utilized the transition metals to catalyze the [2 +2 + 2] cycloadditions of alkynes and nitriles (Scheme V.2.5),[22a–d] however, later on, they discovered that the annulation can also be achieved under metal-free condtions.[22e]

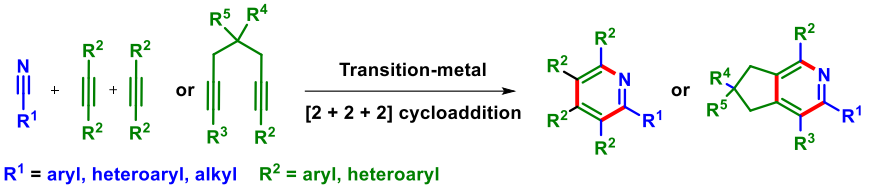

Scheme V.2.5. *Synthesis of pyridines via [2 + 2 + 2] cycloaddition.*

In the recent past, a Pd(II)-catalyzed cascades reaction of nitrile precursors with arylboronic acids is tremendously progressing to afford pyridine scaffold. In this regard, Chen, Hu, and Li group represented the construction of 2,6-disubstituted pyridines *via* a Pd(II)-catalyzed C–C, C–N cascade coupling using δ-ketonitriles and arylboronic acids (Scheme V.2.6).[23]

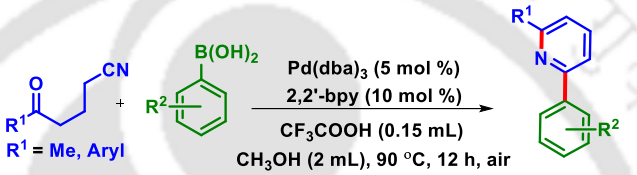

Scheme V.2.6. *Pd(II)-catalyzed cascade synthesis of pyridines.*

Similarly, many other strategies follow greener protocols by employing other readily available catalytic systems in place of metal-based catalysts or requiring solvent-free conditions.[24] Researchers have also managed to reap additional benefits by incorporating photoredox catalysis into multi-component strategies for the synthesis of pyridines (Scheme V.2.7).[25]

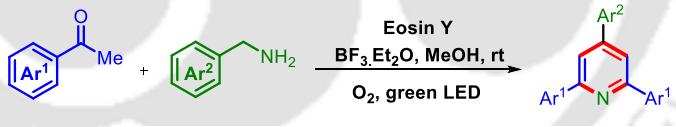

Scheme V.2.7. *Synthesis of pyridines via photoredox catalysis.*

Substituted pyridines synthesis has also been achieved under high stereo- and regioselectivity *via* direct C–H functionalization of the pyridine nucleus (Scheme V.2.8).[26]

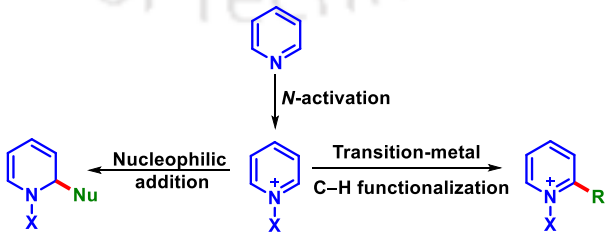

Scheme V.2.8. *Functionalization of N-activated pyridines.*

V.3. Strategies for the Synthesis of Pyrroles:

Advancements in synthetic strategies for achieving pyrrole motifs follow similar trends akin to the case of pyridines. Primeval strategies for the synthesis of pyrroles represent condensation-based protocols such as the Knorr, Paal–Knorr, and Hantzsch reactions that gained immense popularity.[27] Subsequently, the late 20th century marked an escalation in the transition metal-catalyzed cyclizations, annulations, and multicomponent tandem coupling reactions.[28]

In 2009, the synthesis of 3,5-disubstituted pyrroles is reported from the reaction between α,β-unsaturated carbonyl compounds and aminoacetonitrile in a one-pot reaction sequence under microwave irradiation (Scheme V.3.1).[28a]

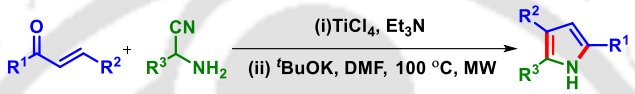

Scheme V.3.1. *Synthesis of multi-substituted pyrrole.*

In 2010, a cationic *N*-heterocyclic carbene-Au(I) complex catalyzed formation of tetra-substituted pyrroles is reported from *N*-propargyl β-enaminone derivatives *via* the cyclization of α-allenyl β-enaminone intermediates (Scheme V.3.2).[28b]

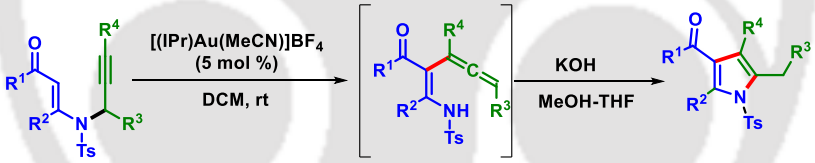

Scheme V.3.2. *Au(I)-catalyzed synthesis of pyrroles.*

In 2013, the Ackermann group reported a Ru(II)-catalyzed synthesis of pyrroles through C–H/N–H oxidative alkyne annulation strategy using electron-rich enamines accomplished aerobically with air as the ideal oxidant (Scheme V.3.3).[28e]

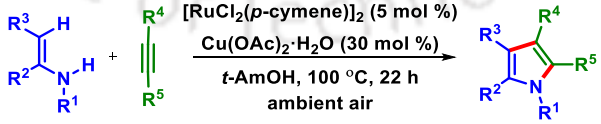

Scheme V.3.3. *Ru(II)-catalyzed pyrrole synthesis by C–H/N–H alkyne annulation.*

In 2014, Guan *et al.* established an efficient Pd(II)-catalyzed alkenyl C–H activation and oxidative alkyne annulation of enamides for the synthesis of substituted *N*-acetylpyrroles with a wide range of functional groups tolerance (Scheme V.3.4).[28f]

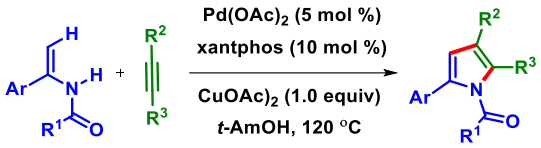

Scheme V.3.4. *Pd(II)-catalyzed synthesis of multi-substituted pyrrole.*

In 2017, Adhikari *et al*. reported a Pd(II)-catalyzed addition of arylboronic acids to substituted aliphatic nitriles in an aqueous acetic acid medium to achieve 3-carbethoxy-nitrile 2-aryl pyrroles with excellent functional group tolerance (Scheme V.3.5).[28i]

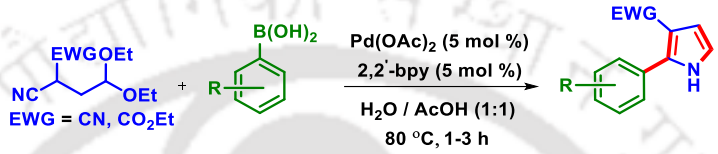

Scheme V.3.5. *Pd(II)-catalyzed synthesis of pyrroles from aliphatic nitriles.*

In 2020, Chen and Li *et al.* developed an effective Ni(II)-catalyzed C–C and C–N cascade coupling of ketonitriles with arylboronic acids to access 3-carboxylate-2,5-diaryl-pyrroles and 2,6-diarylpyridines (Scheme V.3.6).[28j] This transformation is highly versatile, atom-economical having broad substrate scope and excellent functional group tolerance.

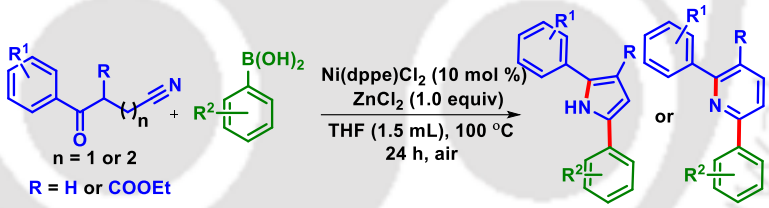

Scheme V.3.6. *Ni(II)-catalyzed synthesis of substituted pyrroles and pyridines.*

In 2022, our group reported the synthesis of the-functionalized pyrroles using β-ketodinitriles and thiophenols in the presence of eosin Y as the photocatalyst under green light irradiation (Scheme V.3.7).[28k]

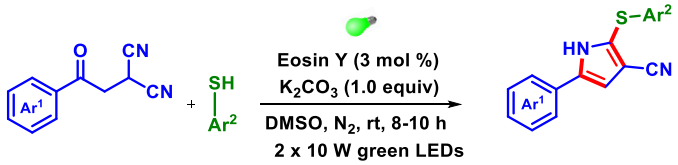

Scheme V.3.7. *Photochemical synthesis of thio-functionalized pyrroles.*

V.4. Present Work:

V.4.1. Optimization of the Reaction Conditions:

After successfully characterizing the desired product, a further screening process was carried out to find the optimal reaction condition, for which 2-(3-oxo-1,3-diphenylpropyl)malononitrile (**1**) (0.25 mmol) was chosen as the model substrate and phenylboronic acid (**a**) (1 equiv) as the coupling partner. Firstly, different solvents were screened by replacing toluene (33%) with *p*-xylene (35%), *m*-xylene (32%), cyclohexane (00%), 1,2-DCE (42%), MeOH (00%), CH_3CN (00%), DMF (00%) DMSO (00%), and H_2O (00%) (Table V.4.1, entries 1–10). In conclusion, 1,2-DCE (42%), was found to be the most effective out of the lot (Table V.4.1, entry 5). Next, the catalyst and ligands were screened by selecting alternatives to $Pd(OAc)_2$ and 2,2′-bipyridine. Although the replacement of $Pd(OAc)_2$ with $Pd(TFA)_2$ resulted in a relatively lower yield (38%; Table V.4.1, entry 11), no product was isolated when the former was replaced with $PdCl_2$ as the catalyst (Table V.4.1, entry 12). Moreover, the reaction completely failed in the absence of either $Pd(OAc)_2$, 2,2'-bipyridine, or PTSA·H_2O (Table V.4.1, entries 13–15). On the contrary, the yield of the isolated product was enhanced to 56% when the loadings of $Pd(OAc)_2$, 2,2'-bipyridine, and PTSA·H_2O were increased from that of the model reaction (Table V.4.1, entry 16). Further increasing the amount of PTSA·H_2O (from 2 to 5 equiv) did not significantly improve the isolated yield of the product (58%; Table V.4.1, entries 16 and 17). After identifying $Pd(OAc)_2$ (10 mol %) and 1,2-DCE as the suitable catalyst and solvent, respectively, few ligands such as 1,10-phenanthroline (52%), L-proline (00%), PPh_3 (trace), XPhos (00%), 1,1'-bis-2-naphthol (00%) were also screened in lieu of 2,2′-bipyridine (Table V.4.1, entries 18–22). Although the use of 1,10-phenanthroline as a ligand was able to produce the desired product in an appreciable yield (Table V.4.1, entry 18), nevertheless it was unable to dethrone 2,2′-bipyridine as the favorable ligand, due to the higher yield of product in case of latter. Further, experiments were carried out by replacing the additive, PTSA·H_2O with other acids such as acetic acid and trifluoroacetic acid which produced (**1a**) lower yields (25% and 23%, respectively) (Table V.4.1, entries 23–24). In contrast, the replacement of PTSA with benzoic acid or sulfuric acid turned out to be futile as almost no significant amount of the product was obtained (Table V.4.1, entries 25–26). Further fine-tuning of the reaction was achieved by increasing the amount of phenylboronic acid progressively from 1 to 5 equivalents. Adding 2 and 3 equivalents of

phenylboronic acid resulted in escalated yields of (**1a**) to 66% and 72%, respectively. Whereas, no further improvement was observed when 5 equivalents of the same were used (Table V.4.1, entries 27–29). The reaction carried out in the presence of 2 x 5 W green LEDs light (42%) and 2 x 5 W blue LEDs light (51%) was also quite favorable to the product formation (Table V.4.1, entries 30 and 31). The overall yield (42%) was decreased when the reaction stops after 12 h (Table V.4.1, entry 32). The reaction carried out in absence of LEDs is detrimental to product formation and only 22% of the desired product was obtained (Table V.4.1, entry 33). When the reaction was performed at a higher temperature (80 ^{o}C) in the absence of light the yield did not improve significantly. Further, the thermal reaction gave several other side products causing difficulties during the separation. As a measure, the temperature in the vicinity of the reaction was near to the room temperature (27–30 ^{o}C) as it was performed in a well-ventilated room below a fan. Here, the white LEDs are accelerating the reaction by reducing Pd(II) to an active exited state Pd(0) in the presence of bipyridine ligand and enhancing the subsequent formation of aryl palladium species (**I**) *via* redox trans-metalation. On the other hand in the absence of LEDs, there might be competitive trans-metalation with Pd(II) species there by giving only 22% yield of the product at room temperature. After screening of various reaction parameters, the optimized standard conditions for this transformation were established to be the use of 2-(3-oxo-1,3-diphenylpropyl)malononitrile (**1**) (0.25 mmol), phenylboronic acid (**a**) (3 equiv), $Pd(OAc)_2$ (10 mol %), 2,2′-bipyridine (20 mol %) and PTSA·H_2O (2 equiv) in 1,2-DCE (2 mL) as the solvent under irradiation by 20 W (2 x 10 W) white LEDs at room temperature (Table V.4.1, entry 28).

Table V.4.1. *Optimization of the reaction conditions.*[a–h]

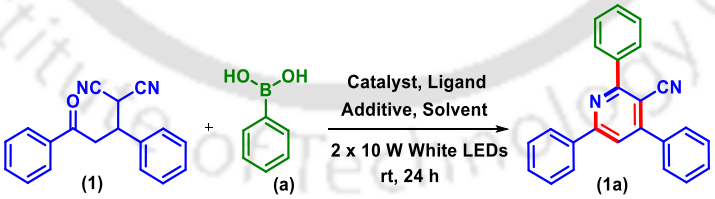

entry	catalyst (mol %)	ligand (mol %)	additive (equiv)	solvent	yield (%)[b]
1	$Pd(OAc)_2$ (5)	2,2'-bipyridyl (10)	PTSA·H_2O (1)	Toluene	33
2	$Pd(OAc)_2$ (5)	2,2'-bipyridyl (10)	PTSA·H_2O (1)	*p*-xylene	35
3	$Pd(OAc)_2$ (10)	2,2'-bipyridyl (10)	PTSA·H_2O (1)	*m*-xylene	32
4	$Pd(OAc)_2$ (5)	2,2'-bipyridyl (10)	PTSA·H_2O (1)	cyclohexane	00
5	$Pd(OAc)_2$ (5)	2,2'-bipyridyl (10)	PTSA·H_2O (1)	1,2-DCE	42
6	$Pd(OAc)_2$ (5)	2,2'-bipyridyl (10)	PTSA·H_2O (1)	MeOH	00

7	$Pd(OAc)_2$ (5)	2,2'-bipyridyl (10)	PTSA·H_2O (1)	CH_3CN	00
8	$Pd(OAc)_2$ (5)	2,2'-bipyridyl (10)	PTSA·H_2O (1)	DMF	00
9	$Pd(OAc)_2$ (5)	2,2'-bipyridyl (10)	PTSA·H_2O (1)	DMSO	00
10	$Pd(OAc)_2$ (5)	2,2'-bipyridyl (10)	PTSA·H_2O (1)	H_2O	00
11	$Pd(TFA)_2$ (5)	2,2'-bipyridyl (10)	PTSA·H_2O (1)	1,2-DCE	38
12	$PdCl_2$ (5)	2,2'-bipyridyl (10)	PTSA·H_2O (1)	1,2-DCE	00
13	---	2,2'-bipyridyl (10)	PTSA·H_2O (1)	1,2-DCE	00
14	$Pd(OAc)_2$ (5)	---	PTSA·H_2O (1)	1,2-DCE	00
15	$Pd(OAc)_2$ (5)	2,2'-bipyridyl (10)	---	1,2-DCE	00
16	$Pd(OAc)_2$ (10)	2,2'-bipyridyl (20)	PTSA·H_2O (2)	1,2-DCE	56
17	$Pd(OAc)_2$ (10)	2,2'-bipyridyl (20)	PTSA·H_2O (5)	1,2-DCE	58
18	$Pd(OAc)_2$ (10)	1,10-phen (20)	PTSA·H_2O (2)	1,2-DCE	52
19	$Pd(OAc)_2$ (10)	L-proline (20)	PTSA·H_2O (2)	1,2-DCE	00
20	$Pd(OAc)_2$ (10)	PPh_3 (20)	PTSA·H_2O (2)	1,2-DCE	trace
21	$Pd(OAc)_2$ (10)	XPhos (20)	PTSA·H_2O (2)	1,2-DCE	00
22	$Pd(OAc)_2$ (10)	1,1'-bi-2-naphthol (20)	PTSA·H_2O (2)	1,2-DCE	00
23	$Pd(OAc)_2$ (10)	2,2'-bipyridyl (20)	AcOH (2)	1,2-DCE	25
24	$Pd(OAc)_2$ (10)	2,2'-bipyridyl (20)	CF_3COOH (2)	1,2-DCE	23
25	$Pd(OAc)_2$ (10)	2,2'-bipyridyl (20)	$PhCO_2H$	1,2-DCE	trace
26	$Pd(OAc)_2$ (10)	2,2'-bipyridyl (20)	H_2SO_4	1,2-DCE	00
27	$Pd(OAc)_2$ (10)	2,2'-bipyridyl (20)	PTSA·H_2O (2)	1,2-DCE	66[c]
28	**$Pd(OAc)_2$ (10)**	**2,2'-bipyridyl (20)**	**PTSA·H_2O (2)**	**1,2-DCE**	**72[d]**
29	$Pd(OAc)_2$ (10)	2,2'-bipyridyl (20)	PTSA·H_2O (2)	1,2-DCE	73[e]
30	$Pd(OAc)_2$ (10)	2,2'-bipyridyl (20)	PTSA·H_2O (2)	1,2-DCE	42[f]
31	$Pd(OAc)_2$ (10)	2,2'-bipyridyl (20)	PTSA·H_2O (2)	1,2-DCE	51[g]
32	$Pd(OAc)_2$ (10)	2,2'-bipyridyl (20)	PTSA·H_2O (2)	1,2-DCE	42[h]
33	$Pd(OAc)_2$ (10)	2,2'-bipyridyl (20)	PTSA·H_2O (2)	1,2-DCE	22[i]

[a]Reaction condition: 2-(3-oxo-1,3-diphenylpropyl)malononitrile (**1**) (0.25 mmol), phenylboronic acid (**a**) (0.75 mmol), catalyst (mol %), ligand (mol %.), additive (equiv) at rt under 2 X 10 W white LEDs for 24 h. [b]Yields of the isolated product. [c]2equiv of (**a**) was used. [d]3 equiv of (**a**) was used. [e]5 equiv of (**a**) was used. [f]Reaction performed using 10 W green LEDs light. [g]Reaction performed using 10 W blue LEDs light. [h]Yield after 12 h. [i] in the absence of LEDs.

V.4.2. Substrates Scopes for the Synthesis of Pyridine-3-Carbonitriles:

With the optimized reaction conditions in hand, this photoreaction was subjected to further studies for the elucidation of substrate scope. Firstly, various γ-ketomalononitriles bearing electron-donating (EDGs) and electron-withdrawing groups (EWGs) were taken alongside phenylboronic acid (**a**) in a series of different reactions to generate the corresponding triaryl substituted cyanopyridines (Scheme V.4.2.1). The unsubstituted γ-ketomalononitrile (**1**) coupled with phenylboronic acid (**a**), to yield 3-cyano-2,4,6-triphenylpyridine in (**1a**) in 72% yield. Next, a series of γ-ketomalononitriles containing unsubstituted benzoyl ring alongside electron-rich phenyl ring bearing EDGs such as *p*-Me (**2**), *p*-OMe (**3**), *p*-OBu (**4**), *p*-SMe (**5**), *p*-NMe_2 (**6**), and *p*-Ph (**7**) were chosen to couple with the phenylboronic acid (**a**). The corresponding products (**2a**, 74%), (**3a**, 72%), (**4a**, 73%), (**5a**, 61%), (**6a**, 68%), and (**7a**, 70%) were obtained in good yields (Scheme V.4.2.1). Moreover, when the phenyl ring contains EWGs such as *p*-F (**8**), *p*-Cl (**9**), *o*-Br (**10**), and *m*-NO_2 (**11**), the corresponding products (**8a**, 70%), (**9a**, 68%), (**10a**, 65%), and (**11a**, 45%) were obtained in moderate to good yields (Scheme V.4.2.1). Next, the effect of substitution on benzoyl ring was studied by choosing suitable γ-ketomalononitrile substrates bearing an unsubstituted phenyl ring, and subjecting them to the optimized reaction condition. Both the scenarios wherein the benzoyl ring possessed EDGs such as *p*-Me (**12**) and *p*-OMe (**13**), and EWGs such as *p*-F (**14**), *p*-Cl (**15**), *p*-Br (**16**), *p*-NO_2 (**17**), and *o*-NO_2 (**18**), resulted in the desired products (**12a**, 72%), (**13a**, 71%), (**14a**, 69%), (**15a**, 66%), (**16a**, 64%), (**17a**, 45%), and (**18a**, 42%) respectively (Scheme V.4.2.1). It is interesting to note that akin to the previous set of experiments, the presence of an electron-deficient benzoyl ring abated the product formation. γ-Ketomalononitriles bearing the naphthyl moiety, (**19**) and (**20**), when chosen as substrates for the developed protocol, responded well to afford the respective (**19a**) and (**20a**) with 72% and 70% yields respectively (Scheme V.4.2.1). The protocol was also tested with γ-ketomalononitrile substrates bearing both substituted benzoyl/phenyl moieties simultaneously with groups such as EDG *p*-Me/EWG *p*-Cl (**21**), EWG *p*-Cl/EDG *p*-OMe (**22**), EWG *p*-Cl/EDG *p*-OH (**23**), and EWG *p*-NO_2/EDG *p*-OMe (**24**). All of these substrates coupled well with phenylboronic acid (**a**) to yield the substituted cyanopyridines (**21a**, 69%), (**22a**, 75%), (**23a**, 41%), and (**24a**, 46%), respectively (Scheme V.4.2.1). Further, substrates containing some di-substituted phenyl rings such as 2,6-dichlorophenyl (**25**), and the 3,4-dimethoxy phenyl (**26**), reacted efficiently to give the products (**25a**, 64%) and (**26a**, 68%), respectively, in good yields (Scheme V.4.2.1).

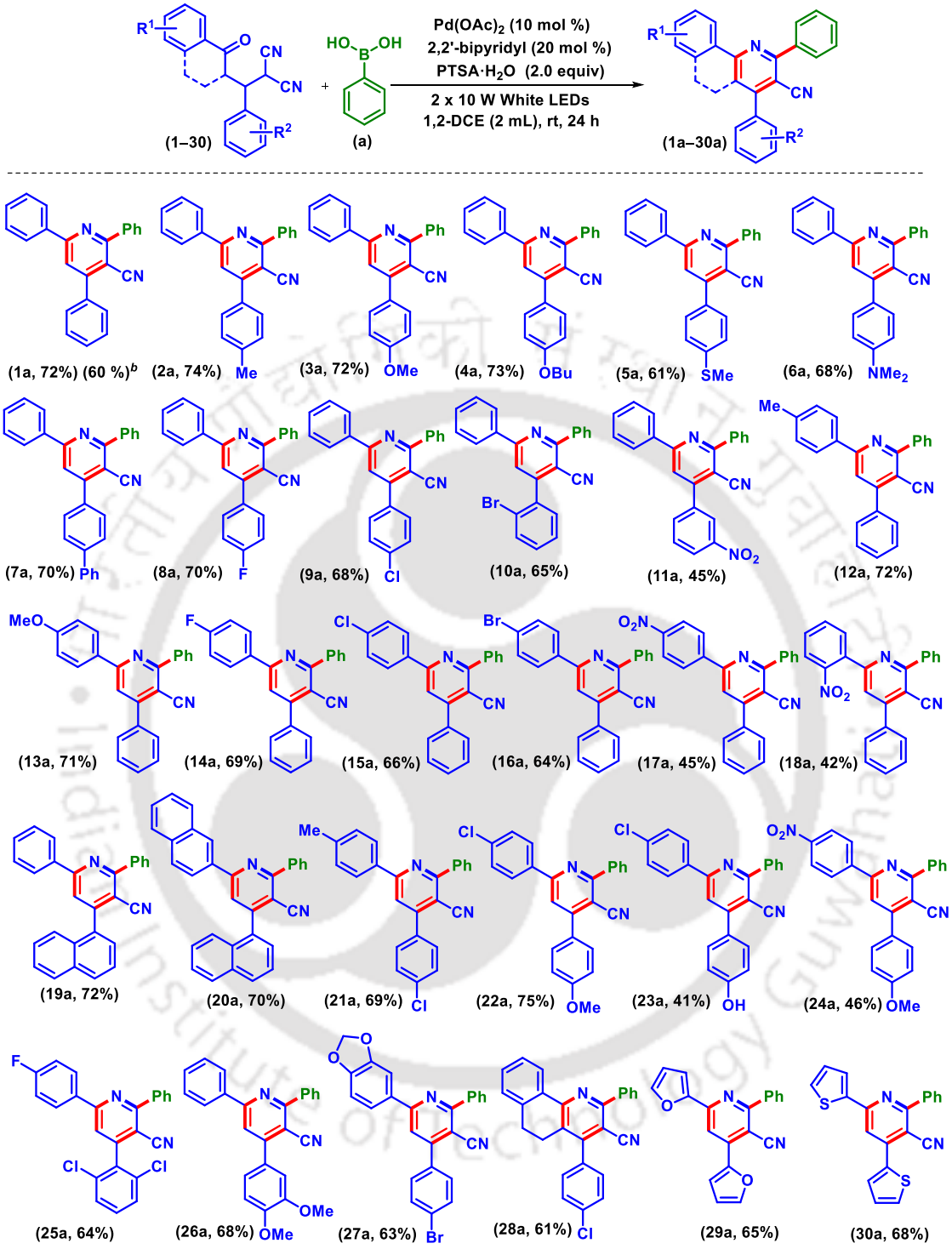

[a]Reaction conditions: (i) **1**–**30** (0.25 mmol), phenylboronic acid (**a**) (0.75 mmol), $Pd(OAc)_2$ (0.025 mmol), 2,2'-bipyridyl (0.05 mmol), PTSA·H_2O (0.5 mmol), and 1,2-DCE (2 mL) at rt for 24 h under 2 x 10 W white LEDs. [b]Yield reported for 1 gm scale.

Scheme V.4.2.1. *Substrate scope for various γ-ketodinitriles.*[a,b]

The Michael adduct bearing 3,4-methylene dioxo benzoyl ring and *p*-bromophenyl ring (**27**) reacted under standard conditions to afford the desired pyridine (**27a**, 63%). Besides, the cyclic γ-keto substrate (**28**) underwent an efficient transformation to the product (**28a**) in 61% yield (Scheme V.4.2.1). Furthermore, Michael adducts bearing hetero aryl rings such as, furan (**29**) or thiophene (**30**), were also compatible with the protocol and afforded the products (**29a**, 65%) and (**30a**, 68%), respectively, in good yields (Scheme V.4.2.1). To determine the efficiency of this photoinduced process and also to expand the scope of this method, 2-(3-oxo-1,3-diphenylpropyl)malononitrile (**1**) (1.37 gm, 5 mmol), and phenylboronic acid (**a**) were reacted on a gram scale which provided 2,4,6-triphenyl-substituted nicotinonitrile (**1a**) in 60% yield (Scheme V.4.2.1).

After successfully employing diverse γ-ketomalononitriles (**1**–**30**) to the developed strategy, the scope was further enhanced by reacting various arylboronic acids with 2-(3-oxo-1,3-diphenylpropyl)malononitrile (**1**) under standard conditions (Scheme V.4.2.2). The reaction was successful with 2-napthylboronic acid (**b**), which had produced 2-(naphthalen-2-yl)-4,6-diphenylnicotinonitrile (**1b**) in 66% yield. Arylboronic acids possessing electron-donating groups such as *p*-Me (**c**), *o*-Me (**d**), *p*-Et (**e**), *p*-^{t}Bu (**f**), *p*-OMe (**g**), and 3-Me-4-OMe (**h**) also responded positively towards the protocol, and afforded the desired cyanopyridines (**1c**, 73%), (**1d**, 43%), (**1e**, 75%), (**1f**, 77%), (**1g**, 79%), and (**1h**, 68%), respectively, in good yields. Arylboronic acids possessing electron-withdrawing groups such as *p*-F (**i**), *p*-Cl (**j**), *m*-Cl (**k**), *p*-Br (**l**), and *p*-CF_3 (**m**), also underwent efficient addition/cyclization with the γ-ketomalononitrile (**1**) to afford the desired cyanopyridines (**1i**, 62%), (**1j**, 55%), (**1k**, 51%), (**1l**, 52%), and (**1m**, 35%), respectively, albeit the yields were moderate to good in these cases. Unfortunately, the developed protocol turned out to be unsuccessful in the case of a few boronic acids such as *p*-CHO-phenylboronic acid (**n**), cyclohexylboronic acid (**o**), 2-thienylboronic acid (**p**), and allylboronic acid (**q**). We speculate that the electron-withdrawing substituents present in arylboronic acids may potentially impede the trans-metalation and the carbopalladation/migration of the aryl group to the electrophilic carbon center of the nitrile moiety. Perhaps, this might be the reason for the lower yields with electron-withdrawing substituents. For an electron-deficient aryl moiety, *p*-CHO-phenylboronic acid (**n**), the carbopalladation does not occur efficiently due to the poor migrating ability of such aryl moieties to electrophilic centres. The failure of boronic acids having a sp^3-C–B bond *viz.* cyclohexylboronic acid (**o**) and allylboronic acid (**q**) hints toward a putative two electron carbanion based-mechanism,

wherein β-hydride elimination reaction may be occurring.[11b] For thiophene-based boronic acid, the adjacent S atom may be depleting the electronic charge, built up at the C2-position by accepting electrons into its vacant d-orbitals, leading to an inefficient carbopalladation. Moreover, a strongly coordinating sulfur atom in the thiophene ring is known to poison Pd(II) catalysts.

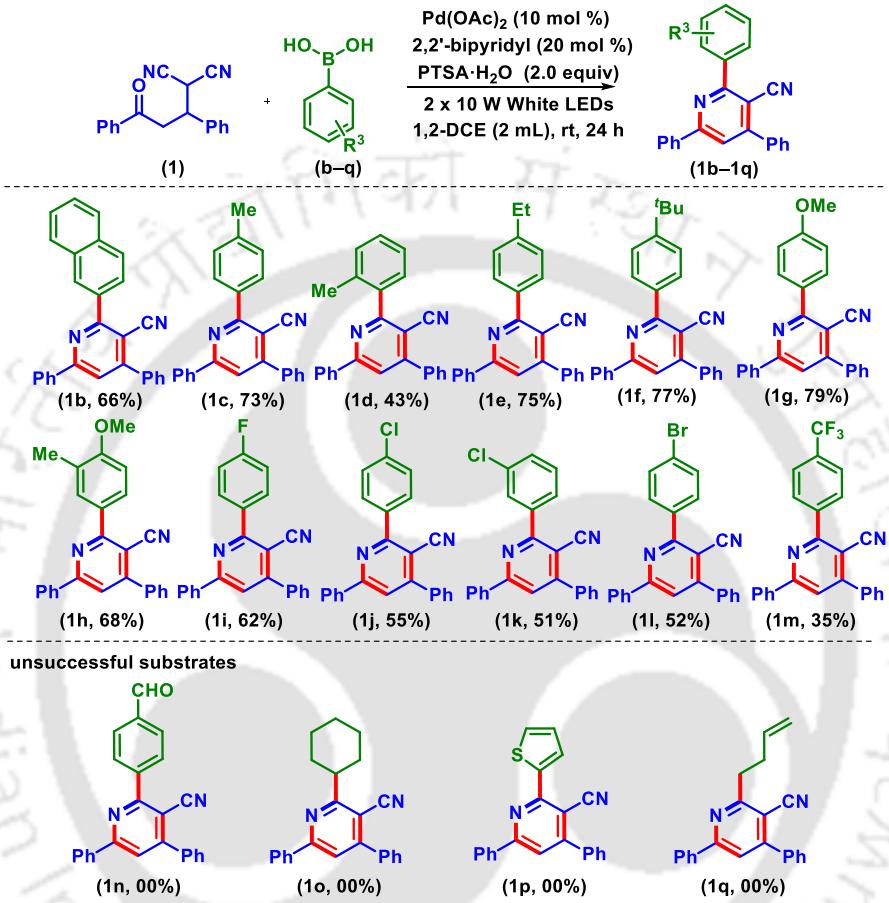

[a]Reaction conditions: (i) 2-(3-oxo-1,3-diphenylpropyl)malononitrile (**1**) (0.25 mmol), arylboronic acids (**b**–**q**) (0.75 mmol), $Pd(OAc)_2$ (0.025 mmol), 2,2'-bipyridyl (0.05 mmol), PTSA·H_2O (0.5 mmol), and 1,2-DCE (2 mL) at rt for 24 h under 2 x 10 W white LEDs.

Scheme V.4.2.2. *Substrate scope for arylboronic acids.*[a]

V.4.3. Substrates Scopes for the Synthesis of Pyrrole-3-Carbonitriles:

The synthetic utility of this photoreaction was further extended by investigating the addition/cyclization of phenylboronic acids to a few β-ketomalononitriles under the optimized reaction conditions to yield the substituted pyrroles (Scheme V.4.3.1). To our delight, the reaction of phenylboronic acid (**a**) with unsubstituted β-ketomalononitrile, 2-(2-oxo-2-phenylethyl)malononitrile (**31**) produced the five-membered *N*-heterocycle, 2,5-diphenyl-1*H*-

pyrrole-3-carbonitrile (**31a**) in 73% yield under the standard conditions. The formation of the pyrrole skeleton was confirmed by the ^{1}H NMR, ^{13}C NMR, and HRMS analysis. Later, β-ketomalononitriles bearing EDGs such as *p*-Me (**32**) and *p*-OMe (**33**), and EWGs such as, *p*-Cl (**34**), *p*-Br (**35**), and *p*-NO_2 (**36**) were selected alongside the phenylboronic acid (**a**) to participate in our reaction strategy. Fortunately, the desired 2,5-diaryl-3-cyanopyrrols (**32a**, 76%), (**33a**, 78%), (**34a**, 71%), (**35a**, 67%), and (**36a**, 55%) were obtained in good to moderate yields. A bicyclic substrate, 2-(1-oxo-1,2,3,4-tetrahydronaphthalen-2-yl)malononitrile (**37**) and a β-ketomalononitrile containing thiophene moiety (**38**), also coupled successfully with phenylboronic acid (**a**), and subsequently cyclized to afford the corresponding pyrrole derivatives (**37a**, 71%) and (**38a**, 69%) in good yields.

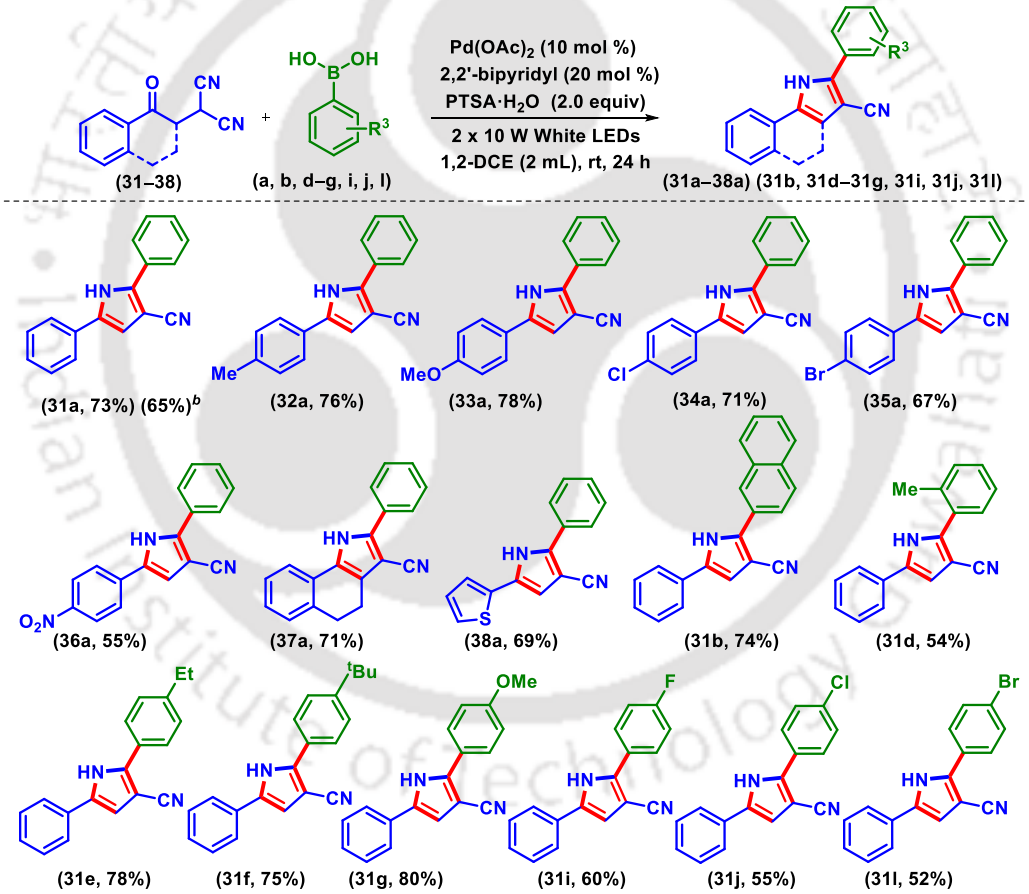

[a]Reaction conditions: (i) **31**–**38** (0.25 mmol), arylboronic acids (**a**, **b**, **d–g**, **i**, **j**, **l)** (0.75 mmol), $Pd(OAc)_2$ (0.025 mmol), 2,2'-bipyridyl (0.05 mmol),PTSA·H_2O (0.5 mmol), and 1,2-DCE (2 mL) at rt for 24 h. under 2 x 10 W white LEDs. . [b]Yield reported for mmol scale.

Scheme V.4.3.1. *Substrate scope for 2,5-diaryl-substituted-3-cyano pyrroles.*[a,b]

Naphthalen-2-ylboronic acid (**b**) reacted with 2-(2-oxo-2-phenylethyl)malononitrile (**31**) to yield 2-(β-naphthyl)-5-phenyl-1*H*-pyrrole-3-carbonitrile (**31b**) in 74% yield. Additionally, a host of phenylboronic acids possessing EDGs such as *o*-Me (**d**), *p*-Et (**e**), *p*-^{t}Bu (**f**), and *p*-OMe (**g**), and EWGs such as, *p*-F (**i**), *p*-Cl (**j**), and *p*-Br (**l**) were reacted with 2-(2-oxo-2-phenylethyl)malononitrile (**31**) under standard conditions to afford the corresponding pyrroles (**31d**, 54%), (**31e**, 78%), (**31f**, 75%), (**31g**, 80%), (**31i**, 60%), (**31j**, 55%), and (**31l**, 52%) in moderate to good yields.

V.5. Mechanistic Investigations:

V.5.1. Intermolecular Competition Experiments:

Intermolecular competition reactions were performed to study the electronic influence of the substituents present on the aroyl/aryl moieties of γ-ketomalononitriles and arylboronic acids. In an equimolar mixture of substrates (**13**) and (**14**), composed of aroyl groups possessing an EDG, *p*-OMe, and an EWG, *p*-F, respectively, were reacted with phenylboronic acid (**a**) (Scheme V.5.1.1). The yields of the corresponding products (**13a**, 25%) and (**14a**, 23%) were similar, which indicates that substrates possessing EDGs and EWGs in the aroyl moiety (R^1) show similar reactivity.

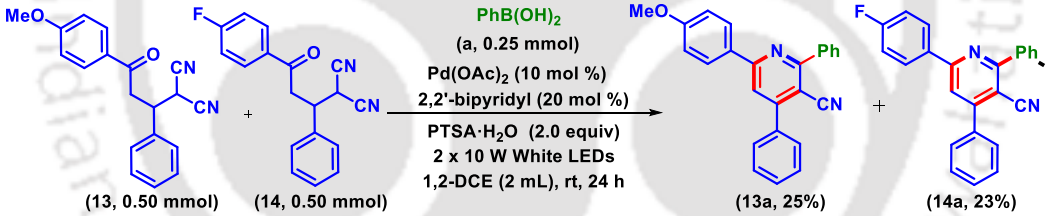

Scheme V.5.1.1. *Competition experiments between aroyl substituted γ-ketodinitriles.*

Next, two γ-ketomalononitrile substrates wherein the aryl moiety contains either an EDG *p*-OMe (**3**), or an EWG *p*-Cl (**9**) were chosen to react with the phenylboronic acid (**a**) under standard conditions (Scheme V.5.1.2). It was again observed that the electronic nature of the substituent R^2 present on the phenyl moiety had minimal effect on the outcome of the reaction, as evident from the almost equal yields of products (**3a**, 21%) and (**9a**, 20%), respectively.

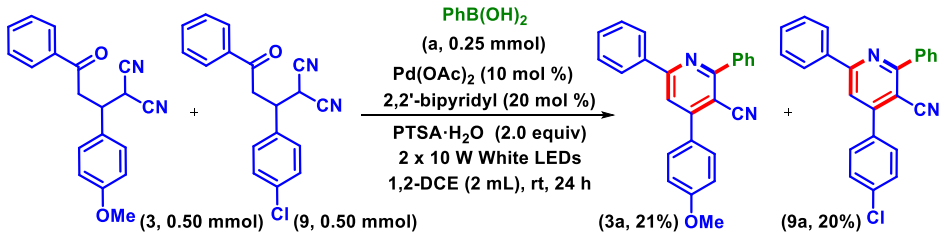

Scheme V.5.1.2. *Competition experiments between phenyl substituted γ-ketodinitriles.*

Finally, the effect of the electronic nature of substituents (R^3) present on the phenyl ring of the boronic acids was investigated (Scheme V.5.1.3). An equimolar mixture of electron-rich *p*-methoxyphenylboronic acid (**g**), and a relatively electron-deficient *p*-fluorophenylboronic acid (**i**) was reacted with (**1**) to afford the respective cyanopyridines (**1g**, 29%) and (**1i**, 20%). This suggests that the presence of an EDG on the phenyl ring of arylboronic acid renders higher compatibility.

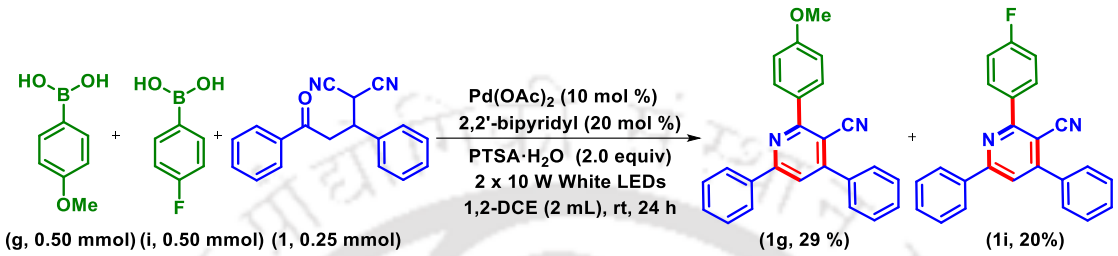

Scheme V.5.1.3. *Competition experiments between arylboronic acids.*

V.5.2. Control Experiments:

To understand the mechanistic underpinnings of the photoreaction, few control experiments were performed. Our initial experiment was performed under normal laboratory conditions at room temperature. It was observed that the reaction proceeded slowly, and only 22% yield of the desired product was obtained after 24 h (Scheme V.5.2.1).

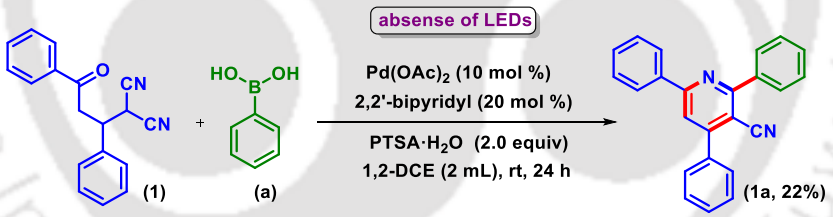

Scheme V.5.2.1. *Reaction in absence of LEDs..*

In the next experiment, the reaction flask was wrapped carefully with an aluminium foil, and the reaction was carried out in completely dark conditions. This time, even less than 16% of the product was isolated (Scheme V.5.2.2). Hence, it can be concluded that light does accelerate the desired reaction.

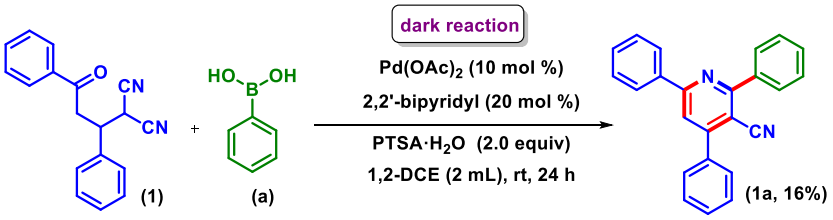

Scheme V.5.2.2. *Reaction in dark condition.*

Later, a radical scavenger 2,2,6,6-tetramethylpiperidine-1-oxyl (TEMPO) was added to the reaction mixture in varying quantities. Although the use of 2 equiv TEMPO resulted in poor yield (<20%), when 4 equiv TEMPO was added to the reaction mixture, no desired product was obtained (Scheme V.5.2.3). These results indicate that a radical pathway may be operative. However, no TEMPO adducts were detected while performing the HRMS analysis of the reaction mixture. Moreover, the alkylboronic acids such as cyclohexylboronic acid (**o**) and allylboronic acid (**q**) did not yield the desired products (**1o**) and (**1q**) when subjected to standard conditions (Scheme V.4.2.2).[11b] Surprisingly, these observations refute the existence of a radical pathway. According to the literature reports, there is a possibility that TEMPO may oxidize Pd(0) to Pd(II), thereby inhibiting the reaction in the forward direction.[29]

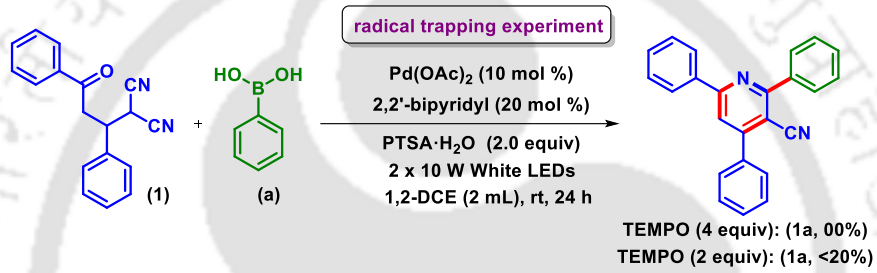

Scheme V.5.2.3. *Reaction in presence of TEMPO.*

V.5.3. Plausible Reaction Mechanism:

Based on these facts, the likelihood of a conventional SET mechanism involving organic radicals due to visible light irradiation is not obvious in our case, and a plausible reaction mechanism is outlined in Scheme V.5.3.1. Initially, $Pd(OAc)_2$ combines with 2,2′-bipyridyl ligand (**L**) to form a complex $Pd(II)(bpy)(OAc)_2$ (detected by HRMS analysis of reaction mixture). The protocol requires 3 equivalents of arylboronic acid with respect to the reacting substrate. The requirement of excess boronic acid can be rationalized by the *in situ* generations of Pd(0) by the reduction of $Pd(II)(bpy)(OAc)_2$, which is also accelerated under visible irradiation.[30] Another 2,2′-bipyridine ligand (**L**) combines with the *in situ* generated Pd(0) species, which subsequently undergoes photoexcitation *via* MLCT to form an excited palladium complex, $[L_2Pd(0)^*]$ (detected by HRMS analysis of reaction mixture). Although the next step, that is, transmetalation is not fully understood, we speculate that a redox reaction may be occurring, wherein the excited palladium complex, $[L_2Pd(0)^*]$ reduces the phenylboronic acid (**a**).[31] Concomitantly, transfer of aryl group (of boronic acid), and elimination of 2,2′-bipyridine ligand (**L**) occur to give the intermediate (**I**)

(detected by HRMS analysis of reaction mixture). The redox step may involve the M→Z σ-interaction between the palladium centre and the boron centre of boronic acid.[32] The Pd(II) centre of intermediate (**I**) then coordinates with the γ-ketomalononitrile substrate (**1**) to give the intermediate (**II**) (detected by HRMS analysis of reaction mixture). Next, intramolecular carbopalladation of nitrile occurs *via* the insertion of the phenyl group to the nitrile moiety followed by insertion of an acetate anion to the palladium centre which results in the corresponding ketimine complex (**III**) (detected by HRMS analysis of reaction mixture). Later, PTSA·H_2O protonates this intermediate to release 2-(imino(phenyl)methyl)-5-oxo-3,5-diphenylpentanenitrile (**IV**), and coordination of PTSA to the Pd(II) centre forms the intermediate (**VIII**) (detected by HRMS analysis of reaction mixture). The initial Pd(II) species is regenerated *via* the intermediacy of (**IX**) (detected by HRMS analysis of reaction mixture) and continues the catalytic cycle. Finally, PTSA·H_2O triggers the intramolecular cyclization of **IV**, which is followed by dehydration to form the intermediate **VII** (detected by HRMS analysis of reaction mixture). Finally, aromatization of intermediate **VII** affords the desired product, 3-cyano-2,4,6-triphenylpyridine (**1a**).

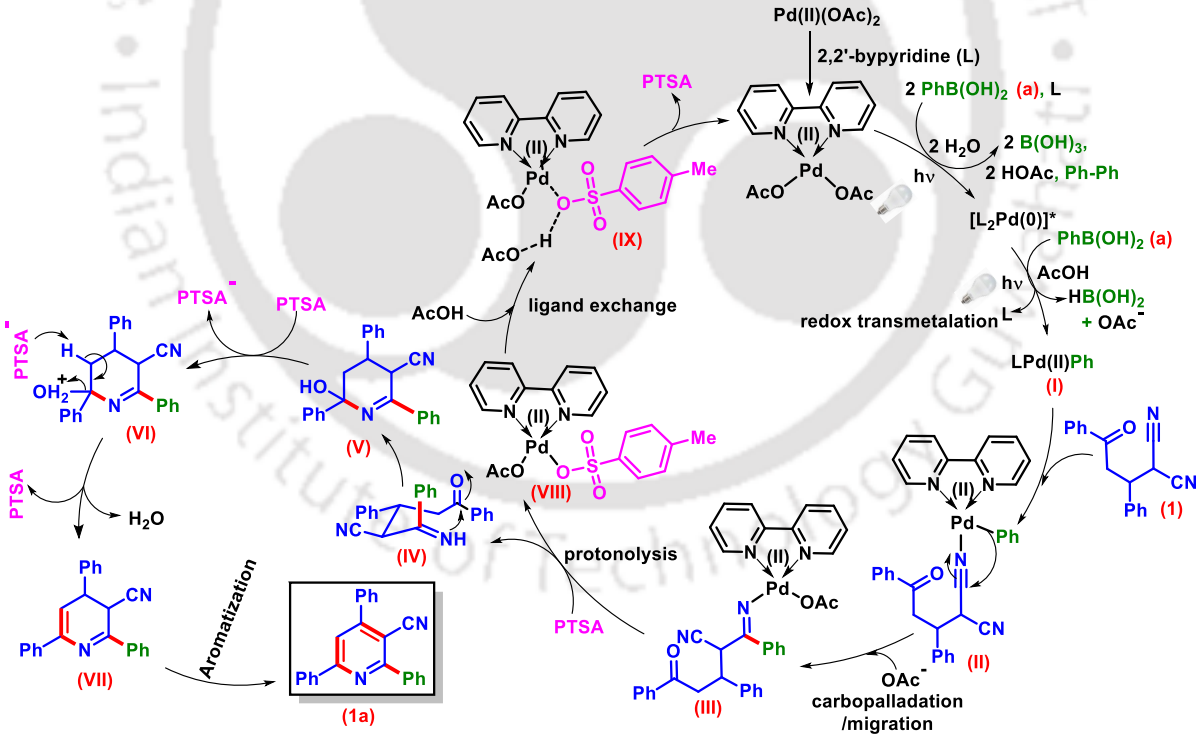

Scheme V.5.3.1. *Proposed mechanistic pathway.*

V.6. Conclusion:

In summary, we have devised an elegant strategy for the synthesis of 2,4,6-triarylnicotinonitriles and 2,5-diaryl-1*H*-pyrrole-3-carbonitriles at ambient temperature *via* a Pd-catalyzed reaction of arylboronic acid with γ- and β-ketodinitriles under visible-light irradiation. The present one-pot synthetic protocol obviates the necessity of an external photosensitizer and provides convenient access to the desired products in moderate to good yields under mild reaction conditions. The desired products possess nitrile moiety which can be later functionalized to generate useful molecules for diverse applications.

V.7. Experimental Section:

V.7.1. General Information:

All the reagents were commercial grade and purified according to the established procedures. All the reactions were carried out in oven-dried glassware under a degassed atmosphere. The highest commercial quality reagents were purchased and were used without further purification unless otherwise stated. Reactions were monitored by thin-layer chromatography (TLC) on 0.25 mm silica gel plates ($60F_{254}$) visualized under UV illumination at 254 nm. Organic extracts were dried over anhydrous sodium sulfate (Na_2SO_4). Solvents were removed using a rotary evaporator under reduced pressure. Column chromatography was performed to purify the crude product on silica gel 60–120 mesh using a mixture of hexane and ethyl acetate as eluent. All the isolated compounds were characterized by ^1H, $^{13}C\{^1H\}$ NMR and HRMS and IR spectroscopic techniques. NMR spectra for all the samples were recorded in deuterochloroform ($CDCl_3$) or deuterated dimethyl sulfoxide (DMSO-d_6). ^1H, $^{13}C\{^1H\}$ were recorded in 600 (150) or 400 (100) MHz spectrometer and were calibrated using tetramethylsilane or residual undeuterated solvent for ^1H NMR, deuterochloroform for ^{13}C NMR as an internal reference {$Si(CH_3)_4$: 0.00 ppm or $CHCl_3$: 7.260 ppm for ^1H NMR, 77.230 ppm for ^{13}C NMR or $(CH_3)_2SO$: 2.50 ppm for ^1H NMR, 39.50 ppm for ^{13}C NMR}. ^{19}F NMR was calibrated using hexafluorobenzene as an internal standard. The chemical shifts are quoted in δ units, parts per million (ppm). ^1H NMR data is represented as follows: Chemical shift, multiplicity (s = singlet, d = doublet, t = triplet, q = quartet, m = multiplet, br = broad, dd = doublet of doublet, tt = triplet of triplet), integration and coupling constant(s) *J* in hertz (Hz). High-resolution mass spectra (HRMS) were recorded on a mass spectrometer using electrospray ionization-time of flight (ESI-TOF) reflection experiments. FT-IR spectra were

recorded in KBr or neat and reported in the frequency of absorption (cm^{-1}). Philips 2 x 10 W white LED bulb was used as the light source for this light-promoted reaction and no filter was used. Borosilicate round bottom glass was used as the reaction vessel. The distance from the light source to the irradiation vessel was ~6–8 cm. Regular fan was used to ventilate the area to maintain the room temperature (27–30 ^oC).

V.7.2. General Procedures:

V.7.2.1. General Procedure for the Synthesis of 2-(3-Oxo-1,3-diarylpropyl)malononitriles (1–30):

All the γ-ketodinitriles (**1**–**30)** were synthesized according to the literature procedure.[18a]

V.7.2.2. General Procedure for the Synthesis of 2-(2-Oxo-2-arylylethyl)malononitriles (31–38):

Compounds (**31**–**38**) were synthesized by a slight modification of the literature procedures.[18b,c]

V.7.2.3. General Procedure for the Synthesis of 2,4,6-Triarylnicotinonitriles (1a) from 2-(3-Oxo-1,3-diarylpropyl)malononitriles (1) and Phenylboronic acid (a):

To an oven-dried 10 mL round bottom flask was added 2-(3-oxo-1,3-diphenylpropyl)malononitrile (**1**) (68 mg, 0.25 mmol), phenylboronic acid (**a**) (90.6 mg, 0.75 mmol), $Pd(OAc)_2$ (5.6 mg, 0.025 mmol), 2,2′-bipyridyl (7.8 mg, 0.05 mmol), $PTSA{\cdot}H_2O$ (95 mg, 0.5 mmol), and 1,2-DCE (2 mL). The reaction mixture was stirred at room temperature for 24 h, maintaining an approximate distance of ~6–8 cm from two 10 W white LED bulbs (Flux 46 mw/cm^2). After completion of the reaction (monitored by TLC analysis), the reaction mixture was admixed with ethyl acetate (25 mL) and the organic layer was washed with saturated sodium bicarbonate solution (5 mL). The organic layer was dried over anhydrous Na_2SO_4, and the solvent was evaporated under reduced pressure. The crude product so obtained was purified over a column of silica gel using 2% ethyl acetate in hexane to give pure 2,4,6-triphenylnicotinonitrile (**1a**) in 72% yield. The identity and purity of the product were confirmed by spectroscopic analysis.

V.7.2.4. General Procedure for the Synthesis of 2,5-Diaryl-1*H*-pyrrole-3-carbonitriles (31a) from 2-(2-Oxo-2-arylethyl)malononitriles (31) and Phenylboronic acid (a):

The experiment was carried out according to the general procedure V.7.2.3 taking 2-(2-oxo-2-phenylethyl)malononitrile (**31**) (46 mg, 0.25 mmol), and phenylboronic acid (**a**) (90.6 mg, 0.75 mmol) under standard reaction condition. The crude product so obtained was purified over a column of silica gel using 5% ethyl acetate in hexane to give pure 2,5-diphenyl-1*H*-pyrrole-3-carbonitriles (**31a**) in a 73% yield. The identity and purity of the product were confirmed by spectroscopic analysis.

V.7.3. Mechanistic Investigation:

V.7.3.1. ESI-MS Studies for the Reaction Mixtures at Different Time Intervals:

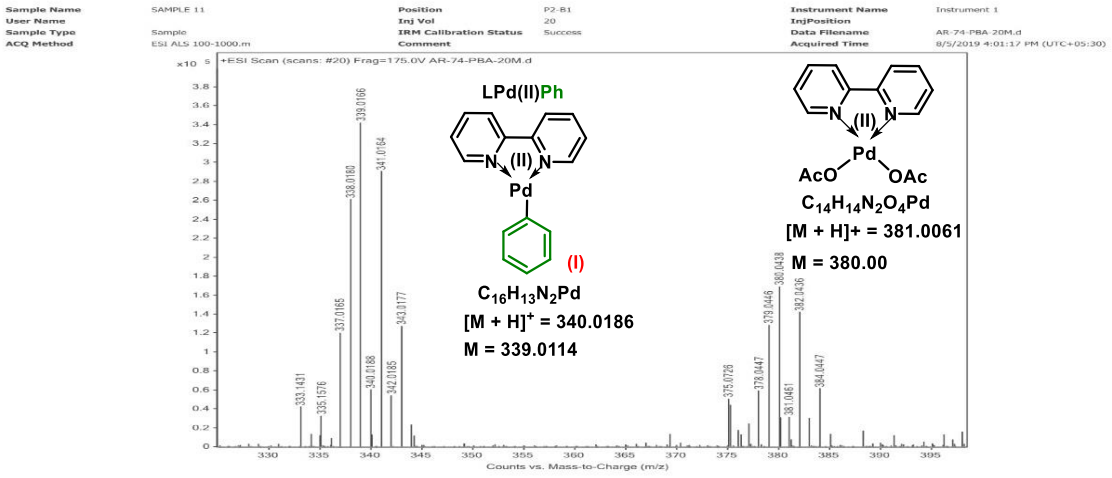

Figure V.7.3.1.1*. HRMS spectrum after 20 min.*

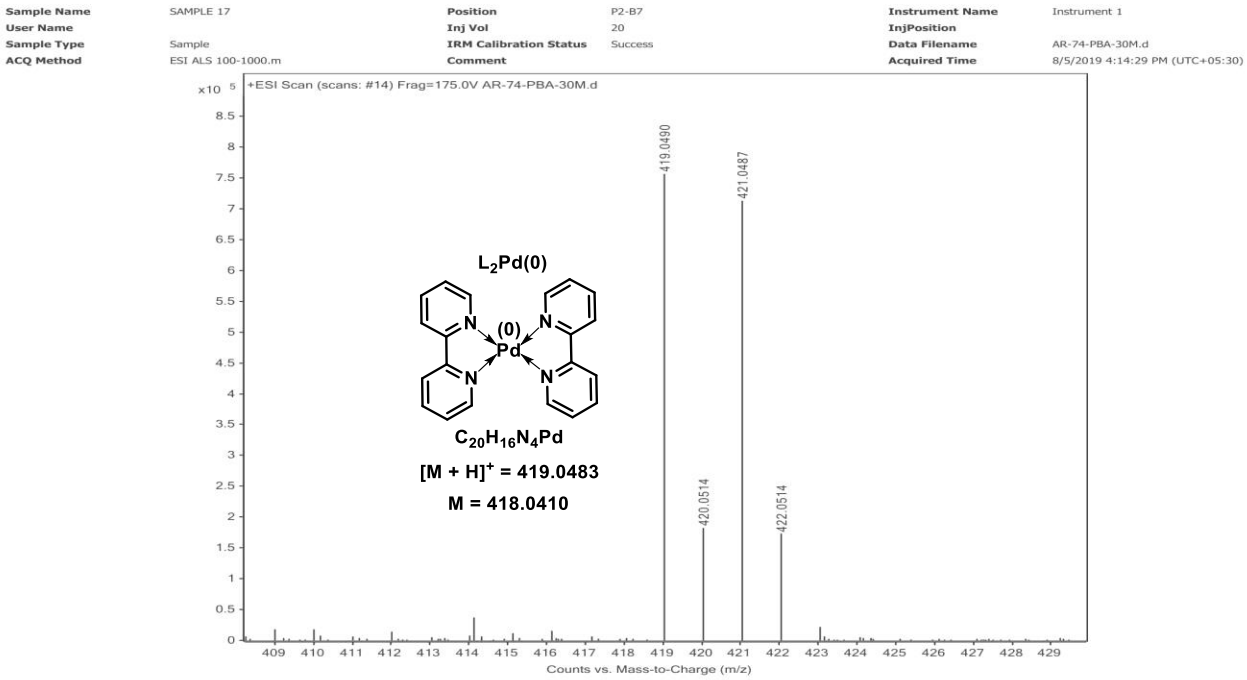

Figure V.7.3.1.2. *HRMS spectrum after 30 min.*

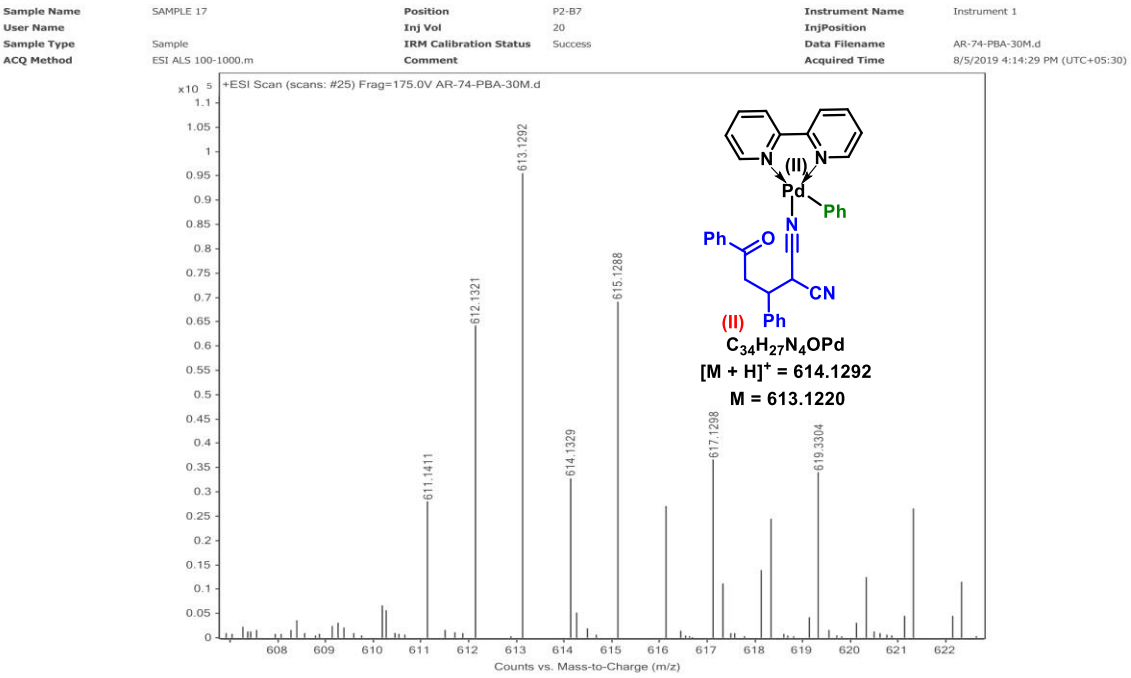

Figure V.7.3.1.3. *HRMS spectrum after 30 min.*

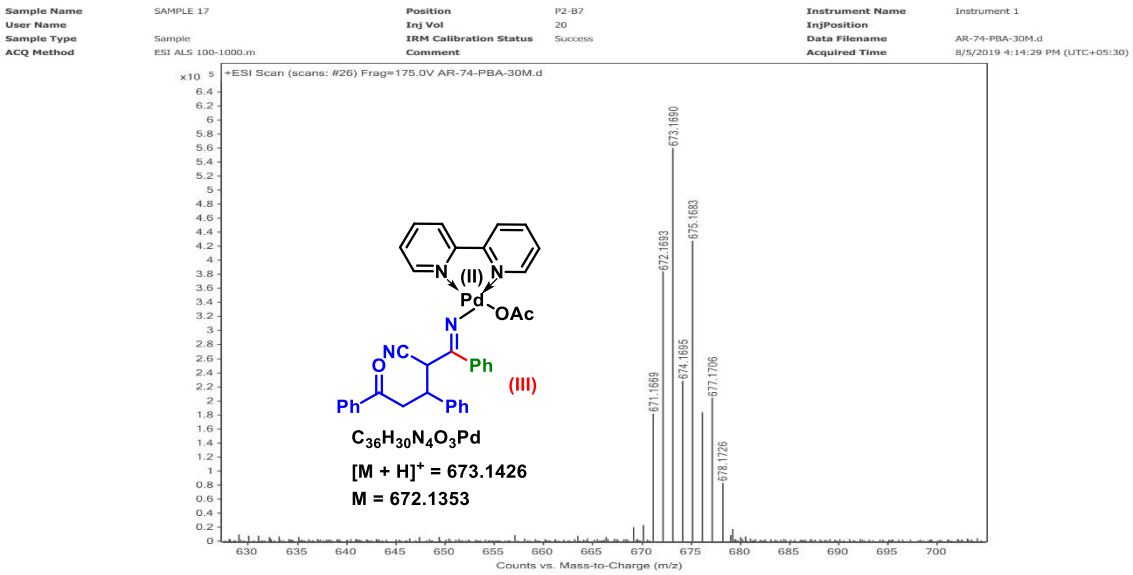

Figure V.7.3.1.4. *HRMS spectrum after 30 min.*

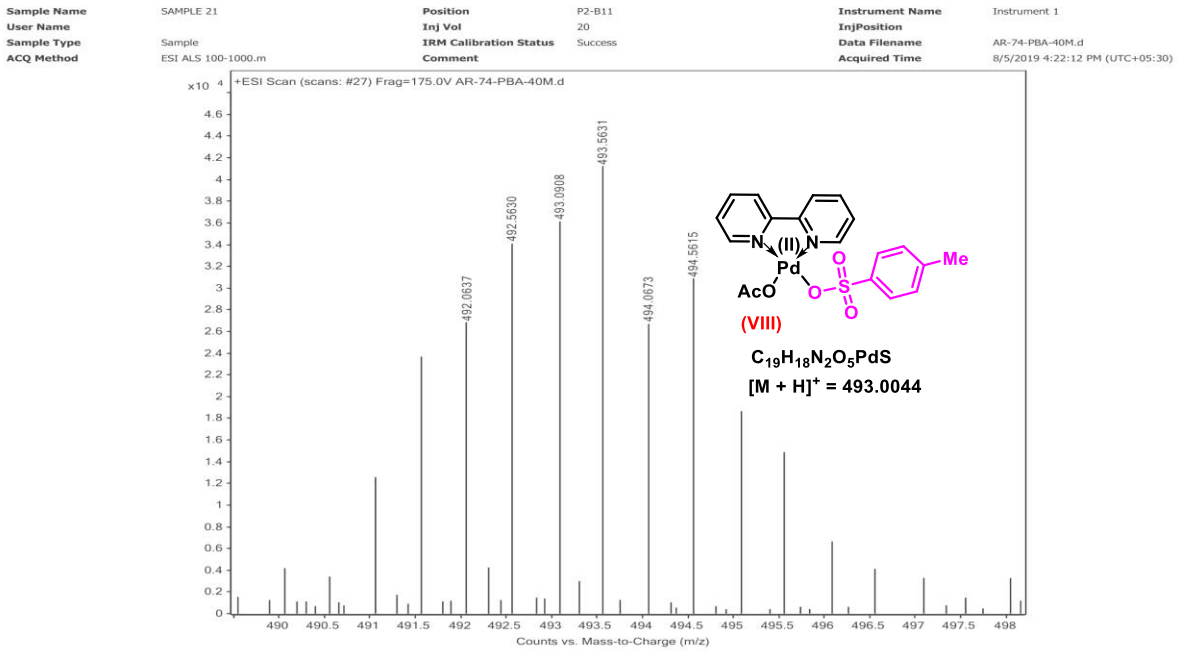

Figure V.7.3.1.5. *HRMS spectrum after 40 min.*

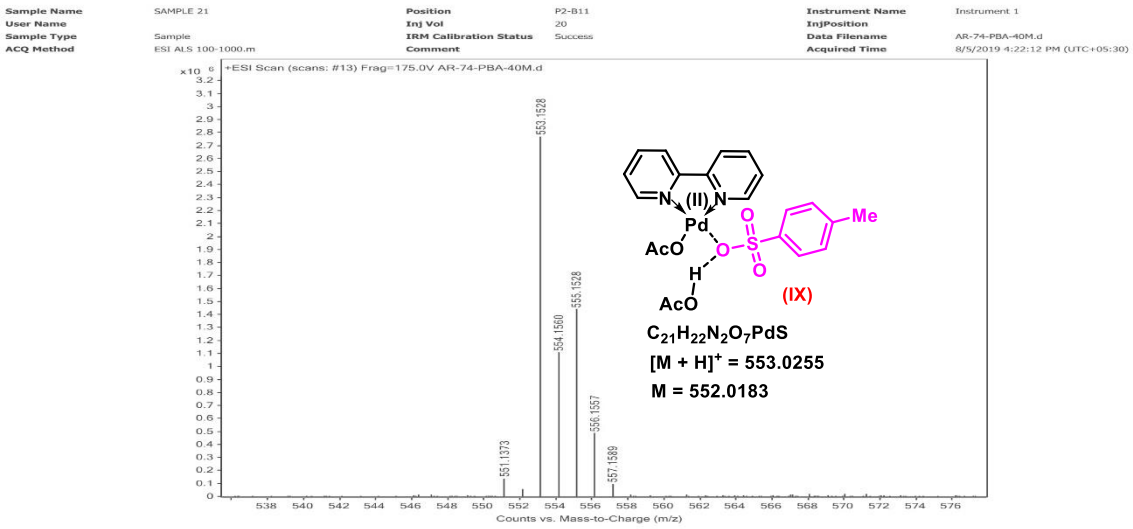

Figure V.7.3.1.6. *HRMS spectrum after 40 min.*

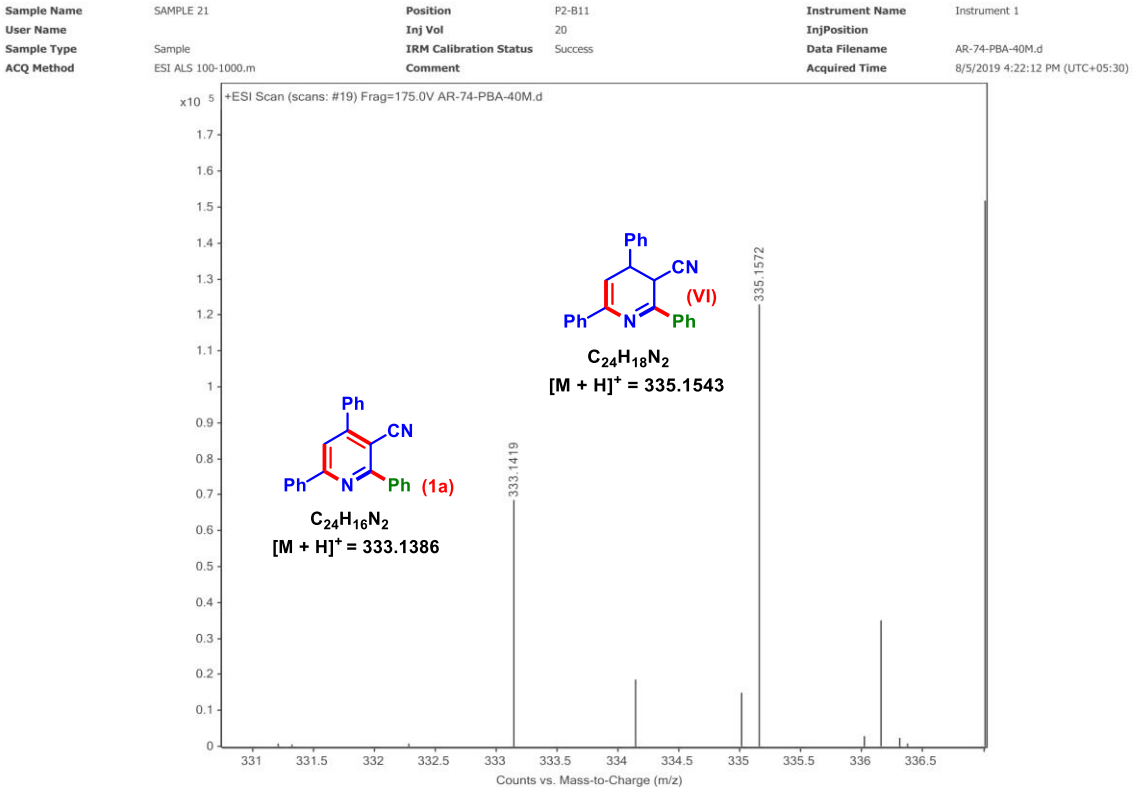

Figure V.7.3.1.7. *HRMS spectrum after 40 min.*

V.7.3.2. Intermolecular Competition Experiments:

V.7.3.2.1. Intermolecular Competitive Experiment Between 2-(3-(4-Methoxyphenyl)-3-oxo-1-phenylpropyl)malononitrile (13) and 2-(3-(4-Fluorophenyl)-3-oxo-1-phenylpropyl)malononitrile (14):

The experiment was carried out according to the general procedure V.7.2.3 taking 2-(3-(4-methoxyphenyl)-3-oxo-1-phenylpropyl)malononitrile (**13**) (152 mg, 0.5 mmol), 2-(3-(4-fluorophenyl)-3-oxo-1-phenylpropyl)malononitrile (**14**) (146 mg, 0.5 mmol), and phenylboronic acid (**a**) under the standard reaction condition. The crude product so obtained was purified over a column of silica gel using increasing 2% ethyl acetate in hexane to give pure 6-(4-methoxyphenyl)-2,4-diphenylnicotinonitrile (**13a**) (45 mg, 25% yield) and 6-(4-fluorophenyl)-2,4-diphenylnicotinonitrile (**14a**) (40 mg, 23% yield).

V.7.3.2.2. Intermolecular Competitive Experiment Between 2-(1-(4-Methoxyphenyl)-3-oxo-3-phenylpropyl)malononitrile (3) and 2-(1-(4-Chlorophenyl)-3-oxo-3-phenylpropyl)malononitrile (9):

The experiment was carried out according to the general procedure V.7.2.3 taking 2-(1-(4-methoxyphenyl)-3-oxo-3-phenylpropyl)malononitrile (**3**) (152 mg, 0.5 mmol), 2-(1-(4-chlorophenyl)-3-oxo-3-phenylpropyl)malononitrile (**9**) (154 mg, 0.5 mmol), and phenylboronic acid (**a**) under the standard reaction condition. The crude product so obtained was purified over a column of silica gel using 2% ethyl acetate in hexane to give pure 4-(4-methoxyphenyl)-2,6-diphenylnicotinonitrile (**3a**) (38 mg, 21% yield) and 4-(4-chlorophenyl)-2,6-diphenylnicotinonitrile (**9a**) (36 mg, 20% yield).

V.7.3.2.3. Intermolecular Competitive Experiment Between (4-Methoxyphenyl)boronic acid (g) and (4-Fluorophenyl)boronic acid (i):

The experiment was carried out according to the general procedure V.7.2.3 taking 2-(3-oxo-1,3-diphenylpropyl)malononitrile (**1**) (68.5 mg, 0.25 mmol), (4-methoxyphenyl)boronic acid (**g**) (75.5 mg, 0.5 mmol), and (4-fluorophenyl)boronic acid (**i**) (69.5 mg, 0.5 mmol) under standard reaction condition. The crude product so obtained was purified over a column of silica gel using 2% ethyl acetate in hexane to give pure 2-(4-methoxyphenyl)-4,6-diphenylnicotinonitrile (**1g**) (26 mg, 29% yield) and 2-(4-fluorophenyl)-4,6-diphenylnicotinonitrile (**1i**) (17 mg, 20% yield).

V.7.3.3. Control Experiments:

V.7.3.3.1. In the Absence of LEDs:

The experiment was carried out according to the general procedure V.7.2.3 in the absence of white LEDs. The crude product so obtained was purified over a column of silica gel using 2% ethyl acetate in hexane to give pure 2,4,6-triphenylnicotinonitriles (**1a**) (18 mg, 22% yield). The identity and purity of the product were confirmed by spectroscopic analysis.

V.7.3.3.2. Dark Reaction:

The experiment was carried out according to the general procedure V.7.2.3 in absence of white LEDs and the round bottom flask was covered with an aluminum foil so that light cannot interact with the reaction mixture. The crude product so obtained was purified over a column of silica gel using 2% ethyl acetate in hexane to give pure 2,4,6-triphenylnicotinonitriles (**1a**) (13 mg, 16% yield). The identity and purity of the product were confirmed by spectroscopic analysis.

V.7.3.3.3. Radical Trapping Experiment:

(i) The experiment was carried out according to the general procedure V.7.2.3 in presence of TEMPO (156 mg, 1 mmol). The reaction mixture was then stirred at room temperature for 24 h. The completion of the reaction was monitored by TLC analysis of the reaction mixture. But the reaction did not afford 2,4,6-triphenylnicotinonitriles (**1a**) rather an uncharacterized product was obtained.

(ii) The experiment was carried out according to the general procedure V.7.2.3. taking TEMPO (78 mg, 0.5 mmol). The crude product so obtained was purified over a column of silica gel using2% ethyl acetate in hexane to give pure 2,4,6-triphenylnicotinonitriles (**1a**) (15 mg, 18% yield). The identity and purity of the product were confirmed by spectroscopic analysis.

V.7.4. Crystallographic Information:

V.7.4.1. Sample Preparation:

The single crystal of compound **1f** was prepared by the slow evaporation method for which 5 mg of the compound (**1f**) was dissolved in 1 mL of ethyl acetate in a clean and dry 10 mL glass vial. Petroleum ether (2 mL) was added to this solution slowly with a dropper until faint turbidity appeared on the top. The mouth of the glass vial was covered with a cap having a small hole and

kept for slow evaporation at room temperature. A single crystal of **1f** was obtained as a transparent white needle-like crystal after 5 days.

V.7.4.2. Crystallographic Information of 2-(4-(*tert*-Butyl)phenyl)-4,6-diphenylnicotinonitrile (1f):

Diffraction data were collected at 292 K with MoKα radiation (λ = 0.71073 Å) using a Bruker Nonius SMART APEX CCD diffractometer equipped with a graphite monochromator and Apex CD camera. The SMART software was used for data collection and for indexing the reflections and determining the unit cell parameters. Data reduction and cell refinement were performed using SAINT[1,2] software and the space groups of these crystals were determined from systematic absences by XPREP and further justified by the refinement results. The structures were solved by direct methods and refined by full-matrix least-squares calculations using SHELXTL-97[3] software. All the non-H atoms were refined in the anisotropic approximation against F^2 of all reflections.

1. G. M. Sheldrick, SADABS, 1996, based on the method described in: R. H. Blessing, *Acta Crystallogr.* 1995, **A51**, 33–38.
2. SMART and SAINT, Siemens Analytical X-ray Instruments Inc., Madison, WI, 1996.
3. G. M. Sheldrick, *Acta Crystallogr.*, 2008, **A64**, 112–122.

V.7.4.3. Crystallographic Description of 2-(4-(*tert*-Butyl)phenyl)-4,6-diphenylnicotinonitrile (1f):

$C_{28}H_{24}N_2$, crystal dimensions 0.25 x 0.22 x 0.16 mm, M_r = 338.49, Monoclinic, space group P 21/n, a = 12.1240(11) Å, b = 21.9840(2) Å, c = 16.7347(15) Å, α = 90 °, β = 96.781(10)°, γ = 90°, V = 4429.2(7) Å^3, Z = 4, ρ_{calcd} = 1.165 mg/m^3, μ = 0.068 mm^{-1}, F(000) = 1648.0, reflection collected/unique = 7777/2307, refinement method = full-matrix least-squares on F^2, final R indices [I>2\s(I)]: R_1 = 0.2487, wR_2 = 0.2415, R indices (all data): R_1 = 0.0772, wR_2 = 0.1521, goodness of fit = 0.941. CCDC-1999314 for 2-(4-(*tert*-butyl)phenyl)-4,6-diphenylnicotinonitrile (**1f**) contains the supplementary crystallographic data for this paper. These data can be obtained free of charge from The Cambridge Crystallographic Data Centre *via* www.ccdc.cam.ac.uk/data_request/cif.

V.8. Spectral Data:

***2,4,6-Triphenylnicotinonitrile (1a)*:**

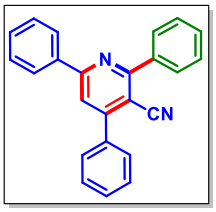

As a white solid (60 mg, 72% yield); Purification over a column of silica gel (2% EtOAc in hexane); ^{1}H NMR ($CDCl_3$, 400 MHz): δ 8.19 (d, 2H, J = 7.6 Hz), 8.06 (d, 2H, J = 7.8 Hz), 7.83 (s, 1H), 7.70 (d, 2H, J = 7.6 Hz), 7.60–7.55 (m, 6H), 7.53–7.48 (m, 3H); ^{13}C{^{1}H} NMR ($CDCl_3$, 100 MHz): δ 162.6, 159.3, 155.6, 138.2, 137.7, 136.9, 130.7, 130.2, 130.1, 129.6, 129.17, 129.16, 128.9, 128.7, 127.8, 118.8, 117.9, 104.5; IR (KBr, cm^{-1}): 2924, 2858, 2215, 1727, 1571, 1530, 1488, 1372, 1276, 1171, 1073, 1025, 873, 748, 688, 616, 568, 485; HRMS (ESI/Q-TOF) (m/z) calcd for $C_{24}H_{17}N_2$ $[M + H]^+$ 333.1386; found 333.1391.

***2,6-Diphenyl-4-(p-tolyl)nicotinonitrile (2a)*:**

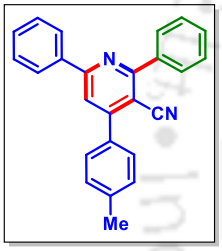

As a white solid (64 mg, 74% yield); Purification over a column of silica gel (2% EtOAc in hexane); ^{1}H NMR ($CDCl_3$, 400 MHz): δ 8.19 (d, 2H, J = 7.8 Hz), 8.07 (d, 2H, J = 7.8 Hz), 7.82 (s, 1H), 7.62–7.52 (m, 8H), 7.39 (d, 2H, J = 8.0 Hz), 2.48 (s, 3H); ^{13}C{^{1}H} NMR ($CDCl_3$, 100 MHz): δ 162.5, 159.2, 155.6, 140.3, 138.2, 137.8, 134.0, 130.6, 130.2, 129.9, 129.6, 129.1, 128.8, 128.6, 127.7, 118.7, 118.1, 104.4, 21.6; IR (KBr, cm^{-1}): 2925, 2862, 2214, 1578, 1511, 1377, 1290, 1247, 1170, 1072, 1024, 971, 875, 828, 762, 693, 609, 572, 520; HRMS (ESI/Q-TOF) (m/z) calcd for $C_{25}H_{19}N_2$ $[M + H]^+$ 347.1543; found 347.1558.

***4-(4-Methoxyphenyl)-2,6-diphenylnicotinonitrile (3a)*:**

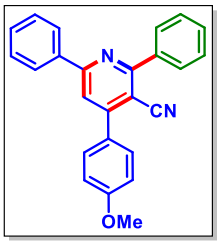

As a white solid (65 mg, 72% yield); Purification over a column of silica gel (2% EtOAc in hexane); ^{1}H NMR ($CDCl_3$, 400 MHz): δ 8.18 (d, 2H, J = 7.8 Hz), 8.05 (d, 2H, J = 6.6 Hz), 7.80 (s, 1H), 7.67 (d, 2H, J = 8.4 Hz), 7.59–7.49 (m, 6H), 7.09 (d, 2H, J = 8.8 Hz), 3.90 (s, 3H); ^{13}C{^{1}H} NMR ($CDCl_3$, 100 MHz): δ 162.7, 161.2, 159.2, 155.2, 138.3, 137.8, 130.6, 130.4, 130.2, 129.2, 129.1, 128.6, 127.7, 118.6, 118.3, 114.6, 114.3, 104.3, 55.6; IR (KBr, cm^{-1}): 2924, 2861, 2218, 1669, 1582, 1514, 1459, 1373, 1253, 1175, 1027, 819, 758, 690, 563; HRMS (ESI/Q-TOF) (m/z) calcd for $C_{25}H_{19}N_2O$ $[M + H]^+$ 363.1492; found 363.1497.

***4-(4-Butoxyphenyl)-2,6-diphenylnicotinonitrile (4a)*:**

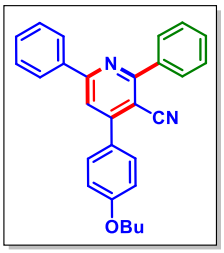

As a white solid (73 mg, 73% yield); Purification over a column of silica gel (2% EtOAc in hexane); ^{1}H NMR ($CDCl_3$, 400 MHz): δ 8.18 (d, 2H, J = 7.8 Hz), 8.05 (d, 2H, J = 7.6 Hz), 7.80 (s, 1H), 7.66 (d, 2H, J = 8.8 Hz), 7.59–7.49 (m, 6H), 7.08 (d, 2H, J = 8.4 Hz), 4.06 (t, 2H, J = 6.4 Hz), 1.87–1.80 (m, 2H), 1.59–1.50 (m, 2H), 1.02 (t, 3H, J = 7.4 Hz); ^{13}C{^{1}H} NMR ($CDCl_3$, 100 MHz): 162.7, 160.8, 159.2, 155.3, 138.3, 137.9, 130.6, 130.3, 130.2, 129.6, 129.1, 128.9, 128.6, 127.7, 118.5, 118.3, 115.1, 104.2, 68.1, 31.4, 19.4, 14.0; IR (KBr, cm^{-1}): 2919, 2857, 2213, 1660, 1574, 1529, 1455, 1373, 1237, 1179, 1074, 1024, 880, 816, 754, 684, 588, 546, 494; HRMS (ESI/Q-TOF) (m/z) calcd for $C_{28}H_{25}N_2O$ $[M + H]^+$ 405.1961; found 405.1976.

***4-(4-(Methylthio)phenyl)-2,6-diphenylnicotinonitrile (5a)*:**

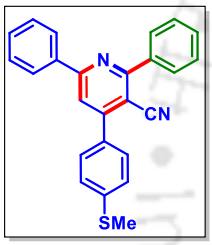

As a white solid (57 mg, 61% yield); Purification over a column of silica gel (2% EtOAc in hexane); ^{1}H NMR ($CDCl_3$, 400 MHz): δ 8.18 (d, 2H, J = 7.4 Hz), 8.04 (d, 2H, J = 7.6 Hz), 7.80 (s, 1H), 7.63 (d, 2H, J = 8.4 Hz), 7.58–7.50 (m, 6H), 7.42 (d, 2H, J = 8.4 Hz), 2.56 (s, 3H); ^{13}C{^{1}H} NMR ($CDCl_3$, 100 MHz): δ 162.7, 159.4, 154.9, 141.9, 138.2, 137.8, 133.2, 130.7, 130.3, 129.6, 129.23, 129.17, 128.7, 127.8, 126.4, 118.5, 118.0, 104.3, 15.4; IR (KBr, cm^{-1}): 2923, 2855, 2217, 1674, 1571, 1372, 1264, 1188, 1028, 812, 758, 690, 577, 497; HRMS (ESI/Q-TOF) (m/z) calcd for $C_{25}H_{19}N_2S$ $[M + H]^+$ 379.1263; found 379.1265.

***4-(4-(Dimethylamino)phenyl)-2,6-diphenylnicotinonitrile (6a)*:**

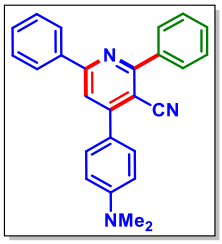

As a white solid (63 mg, 68% yield); Purification over a column of silica gel (2% EtOAc in hexane); ^{1}H NMR ($CDCl_3$, 400 MHz): δ 8.17 (d, 2H, J = 7.2 Hz), 8.03 (d, 2H, J = 7.4 Hz), 7.80 (s, 1H), 7.66 (d, 2H, J = 8.8 Hz), 7.58–7.48 (m, 6H), 6.85 (d, 2H, J = 8.8 Hz), 3.07 (s, 6H); ^{13}C{^{1}H} NMR ($CDCl_3$, 100 MHz): δ 162.9, 158.9, 155.6, 151.6, 138.6, 138.2, 130.4, 130.1, 130.0, 129.6, 129.1, 128.6, 127.7, 123.9, 118.8, 118.2, 103.8, 40.4; IR (KBr, cm^{-1}): 2922, 2854, 2216, 1677, 1615, 1573, 1453, 1369, 1523, 1200, 1026, 815, 757, 692; HRMS (ESI/Q-TOF) (m/z) calcd for $C_{26}H_{22}N_3$ $[M + H]^+$ 376.1808; found 376.1820.

***4-([1,1'-Biphenyl]-4-yl)-2,6-diphenylnicotinonitrile (7a)*:**

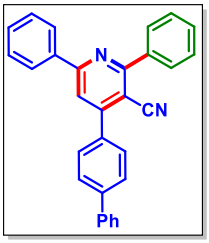

As a white solid (71 mg, 70% yield); Purification over a column of silica gel (2% EtOAc in hexane); ^{1}H NMR ($CDCl_3$, 400 MHz): δ 8.20 (d, 2H, J = 7.8 Hz), 8.06 (d, 2H, J = 7.8 Hz), 7.88 (s, 1H), 7.79 (s, 4H), 7.68 (d, 2H, J = 7.2 Hz), 7.58–7.48 (m, 8H), 7.41 (t, 1H, J = 7.2 Hz); ^{13}C{^{1}H} NMR ($CDCl_3$, 100 MHz): δ 162.7, 159.4, 155.2, 143.0, 140.3, 138.2, 137.8, 135.8, 130.8, 130.3, 129.6, 129.4, 129.20, 129.16, 128.7, 128.1, 127.9, 127.8, 127.4, 118.8, 118.1, 104.4,; IR (KBr, cm^{-1}): 2923, 2857, 2215, 1573, 1527, 1456, 1372, 1266, 1074, 1024, 838, 754, 689, 575; HRMS (ESI/Q-TOF) (m/z) calcd for $C_{30}H_{21}N_2$ $[M + H]^+$ 409.1699; found 409.1698.

***4-(4-Fluorophenyl)-2,6-diphenylnicotinonitrile (8a)*:**

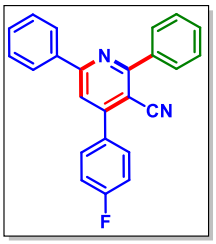

As a white solid (61 mg, 70% yield); Purification over a column of silica gel (2% EtOAc in hexane); ^{1}H NMR ($CDCl_3$, 400 MHz): δ 8.11–8.09 (m, 2H), 797–7.95 (m, 2H), 7.71 (s, 1H), 7.62–7.59 (m, 2H), 7.49–7.43 (m, 6H), 7.21–7.17 (m, 2H); ^{13}C{^{1}H} NMR ($CDCl_3$, 100 MHz): δ 163.9 (d, J = 249.1 Hz), 162.7, 159.5, 154.6, 138.1, 137.6, 133.0 (d, J = 3.4 Hz), 130.9, 130.8 (d, J = 3.7 Hz), 130.4, 129.6, 129.2, 128.7, 127.8, 118.7, 117.8, 116.4 (d, J = 21.8 Hz), 104.5; ^{19}F NMR ($CDCl_3$ + hexafluorobenzene): δ –113.8 (s); IR (KBr, cm^{-1}): 2923, 2855, 2212, 1644, 1576, 1504, 1454, 1377, 1226, 1164, 1097, 1022, 876, 836, 751, 688, 548; HRMS (ESI/Q-TOF) (m/z) calcd for $C_{24}H_{16}FN_2$ $[M + H]^+$ 351.1292; found 351.1304.

***4-(4-Chlorophenyl)-2,6-diphenylnicotinonitrile (9a)*:**

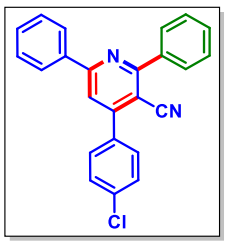

As a white solid (62 mg, 68% yield); Purification over a column of silica gel (2% EtOAc in hexane); ^{1}H NMR ($CDCl_3$, 400 MHz): δ 8.19–8.16 (m, 2H), 8.05–8.03 (m, 2H), 7.79 (s, 1H), 7.63 (d, 2H, J = 8.8 Hz), 7.56–7.51 (m, 8H); ^{13}C{^{1}H} NMR ($CDCl_3$, 100 MHz): δ 162.7, 159.6, 154.4, 138.0, 137.6, 136.6, 135.4, 130.9, 130.4, 130.2, 129.6, 129.5, 129.2, 128.8, 127.8, 118.6, 117.8, 104.3; IR (KBr, cm^{-1}): 2923, 2858, 2216, 1677, 1573, 1529, 1485, 1370, 1263, 1172, 1089, 1015, 822, 752, 688, 492; HRMS (ESI/Q-TOF) (m/z) calcd for $C_{24}H_{16}ClN2$ $[M + H]^+$ 367.0997; found 367.0999.

***4-(2-Bromophenyl)-2,6-diphenylnicotinonitrile (10a)*:**

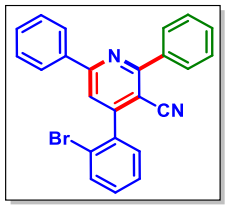

As a white solid (66 mg, 65% yield); Purification over a column of silica gel (2% EtOAc in hexane); ^{1}H NMR ($CDCl_3$, 400 MHz): δ 8.20 (d, 2H, J = 7.2 Hz), 8.10 (d, 2H, J = 7.6 Hz), 7.79 (s, 2H), 7.59–7.48 (m, 7H), 7.45–7.44 (m, 1H), 7.41–7.37 (m, 1H); ^{13}C{^{1}H} NMR ($CDCl_3$, 100 MHz): δ 161.7, 159.2, 154.9, 137.98, 137.92, 137.6, 133.6, 131.2, 130.8, 130.6, 130.4, 129.5, 129.2, 128.8, 127.9, 127.8, 122.3, 119.4, 117.0, 105.9; IR (KBr, cm^{-1}): 2923, 2855, 2219, 1572, 1532, 1470, 1404, 1262, 1078, 1374, 1024, 887, 755, 693; HRMS (ESI/Q-TOF) (m/z) calcd for $C_{24}H_{16}BrN_2$ $[M + H]^+$ 411.0491; found 411.0474.

***4-(3-Nitrophenyl)-2,6-diphenylnicotinonitrile (11a)*:**

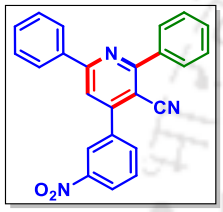

As a white solid (42 mg, 45% yield); Purification over a column of silica gel (2% EtOAc in hexane); ^{1}H NMR ($CDCl_3$, 400 MHz): δ 8.53 (s, 1H), 8.43–8.41 (m, 1H), 8.21–8.19 (m, 2H), 8.08–8.04 (m, 3H), 7.84 (s, 1H), 7.78 (t, 1H, J = 8.0 Hz), 7.58–7.53 (m, 6H); ^{13}C{^{1}H} NMR ($CDCl_3$, 100 MHz): δ 162.8, 159.9, 153.0, 148.8, 138.5, 137.8, 137.3, 134.9, 131.2, 130.6, 130.4, 129.6, 129.3, 128.8, 127.8, 124.8, 124.0, 118.5, 104.3; IR (KBr, cm^{-1}): 2924, 2857, 2218, 1713, 1576, 1528, 1460, 1350, 1263, 1178, 1082, 1031, 882, 805, 693, 521; HRMS (ESI/Q-TOF) (m/z) calcd for $C_{24}H_{16}N_3O_2$ $[M + H]^+$ 378.1237; found 378.1248.

***2,4-Diphenyl-6-(p-tolyl)nicotinonitriletrile (12a)*:**

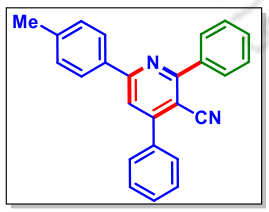

As a white solid (62 mg, 72% yield); Purification over a column of silica gel (2% EtOAc in hexane); ^{1}H NMR ($CDCl_3$, 400 MHz): δ 8.11–8.06 (m, 4H), 7.80 (s, 1H), 7.71–7.68 (m, 2H), 7.60–7.53 (m, 6H), 7.33 (d, 2H, J = 8.4 Hz), 2.44 (s, 3H); ^{13}C{^{1}H} NMR ($CDCl_3$, 100 MHz): δ 162.5, 159.3, 155.4, 141.1, 138.3, 137.1, 134.9, 130.2, 129.99, 129.87, 129.6, 129.1, 128.8, 128.6, 127.6, 118.4, 117.9, 104.1, 21.6; IR (KBr, cm^{-1}): 2923, 2856, 2215, 1575, 1532, 1494, 1451, 1404, 1373, 1261, 1157, 1079, 1026, 881, 818, 766, 701, 620, 530; HRMS (ESI/Q-TOF) (m/z) calcd for $C_{25}H_{19}N_2$ $[M + H]^+$ 347.1543; found 347.1560.

***6-(4-Methoxyphenyl)-2,4-diphenylnicotinonitrile (13a)*:**

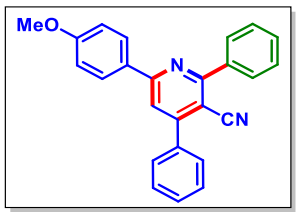

As a white solid (64 mg, 71% yield); Purification over a column of silica gel (2% EtOAc in hexane); ^{1}H NMR ($CDCl_3$, 400 MHz): δ 8.16 (d, 2H, J = 8.8 Hz), 8.04 (d, 2H, J = 7.6 Hz), 7.75 (s, 1H), 7.68 (d, 2H, J = 7.6 Hz), 7.58–7.53 (m, 6H), 7.02 (d, 2H, J = 8.8 Hz), 3.89 (s, 3H); ^{13}C{^{1}H} NMR ($CDCl_3$, 100 MHz): δ 162.5, 161.9, 158.9, 155.4, 138.4, 137.2, 130.3, 130.2, 130.0, 129.6, 129.3, 129.2, 128.9, 128.7, 118.1, 117.9, 114.6, 103.6, 55.6; IR (KBr, cm^{-1}): 2923, 2856, 2211, 1575, 522, 1457, 1372, 1251, 1167, 1025, 879, 829, 761, 696, 542; HRMS (ESI/Q-TOF) (m/z) calcd for $C_{25}H_{19}N_2O$ $[M + H]^+$ 363.1492; found 363.1500.

***6-(4-Fluorophenyl)-2,4-diphenylnicotinonitrile (14a)*:**

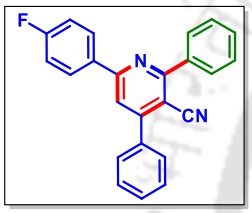

As a white solid (60 mg, 69% yield); Purification over a column of silica gel (2% EtOAc in hexane); ^{1}H NMR ($CDCl_3$, 400 MHz): δ 8.22–8.18 (m, 2H), 8.06–8.04 (m, 2H), 7.77 (s, 1H), 7.70–7.68 (m, 2H), 7.59–7.55 (m, 6H), 7.20 (t, 2H, J = 8.6 Hz); ^{13}C{^{1}H} NMR ($CDCl_3$, 100 MHz): δ 164.6 (d, J = 249.7 Hz), 162.6, 158.2, 155.7, 138.1, 136.9, 133.9 (d, J = 3.0 Hz), 130.3, 130.1, 129.8 (d, J = 8.6 Hz), 129.5, 129.2, 128.8, 128.7, 118.4, 117.8, 116.2 (d, J = 21.7 Hz), 104.5; ^{19}F NMR ($CDCl_3$ + hexafluorobenzene): δ –113.8 (s); IR (KBr, cm^{-1}): 2923, 2862, 2216, 1683, 1574, 1525, 1370, 1227, 1151, 1091, 1024, 830, 752, 690, 618, 527; HRMS (ESI/Q-TOF) (m/z) calcd for $C_{24}H_{16}FN_2$ $[M + H]^+$ 351.1292; found 351.1298.

***6-(4-Chlorophenyl)-2,4-diphenylnicotinonitrile (15a)*:**

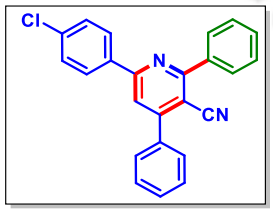

As a white solid (60 mg, 66% yield); Purification over a column of silica gel (2% EtOAc in hexane); ^{1}H NMR ($CDCl_3$, 400 MHz): δ 8.14 (d, 2H, J = 8.8 Hz), 8.04–8.02 (m, 2H), 7.79 (s, 1H), 7.69–7.67 (m, 2H), 7.59–7.55 (m, 6H), 7.49 (d, 2H, J = 8.4 Hz); ^{13}C{^{1}H} NMR ($CDCl_3$, 100 MHz): δ 162.7, 158.4, 155.8, 138.0, 137.0, 136.8, 136.1, 130.4, 130.2, 129.5, 129.4, 129.2, 129.0, 128.85, 128.75, 118.6, 117.8, 104.8; IR (KBr, cm^{-1}): 2923, 2862, 2217, 1652, 1573, 1528, 1489, 1369, 1260, 1172, 1091, 1018, 824, 753, 690, 492; HRMS (ESI/Q-TOF) (m/z) calcd for $C_{24}H_{16}ClN_2$ $[M + H]^+$ 367.0997; found 367.0998.

***6-(4-Bromophenyl)-2,4-diphenylnicotinonitrile (16a)*:**

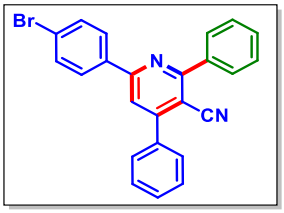

As a white solid (65 mg, 64% yield); Purification over a column of silica gel (2% EtOAc in hexane); ^{1}H NMR ($CDCl_3$, 400 MHz): δ 8.07–8.02 (m, 4H), 7.79 (s, 1H), 7.69–7.63 (m, 4H), 7.59–7.55 (m, 6H); $^{13}C\{^{1}H\}$ NMR ($CDCl_3$, 100 MHz): δ 162.7, 158.1, 155.9, 138.0, 136.8, 136.6, 132.4, 130.4, 130.2, 129.5, 129.24, 129.22, 128.8, 128.7, 125.5, 118.5, 117.7, 104.9; IR (KBr, cm^{-1}): 2922, 2862, 2218, 1681, 1573, 1528, 1486, 1367, 1272, 1169, 1071, 1004, 821, 753, 689, 622, 487; HRMS (ESI/Q-TOF) (m/z) calcd for $C_{24}H_{16}BrN_2$ $[M + H]^+$ 411.0491; found 411.0499.

***6-(4-Nitrophenyl)-2,4-diphenylnicotinonitrile (17a)*:**

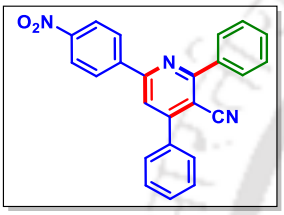

As a white solid (42 mg, 45% yield); Purification over a column of silica gel (2% EtOAc in hexane); ^{1}H NMR ($CDCl_3$, 400 MHz): δ 8.36 (s, 4H), 8.05–8.03 (m, 2H), 7.89 (s, 1H), 7.71–7.68 (m, 2H), 7.59–7.57 (m, 6H); $^{13}C\{^{1}H\}$ NMR ($CDCl_3$, 100 MHz): δ 162.9, 156.7, 156.4, 149.2, 143.5, 137.7, 136.5, 130.6, 130.5, 129.6, 129.4, 128.9, 128.6, 124.4, 119.6, 117.4, 106.1; IR (KBr, cm^{-1}): 2923, 2862, 2220, 1607, 1453, 1406, 1272, 1094, 1039, 807, 692; HRMS (ESI/Q-TOF) (m/z) calcd for $C_{24}H_{16}N_3O_2$ $[M + H]^+$ 378.1237; found 378.1245.

***6-(2-Nitrophenyl)-2,4-diphenylnicotinonitrile (18a)*:**

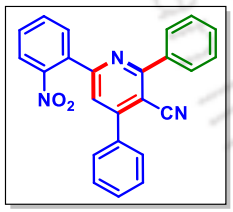

As a white solid (39 mg, 42% yield); Purification over a column of silica gel (2% EtOAc in hexane); ^{1}H NMR ($CDCl_3$, 600 MHz): δ 7.96 (d, 1H, J = 7.8 Hz), 7.93 (d, 2H, J = 7.5 Hz), 7.72–7.68 (m, 4H), 7.62–7.59 (m, 2H), 7.57–7.55 (m, 3H), 7.54–7.51 (m, 3H); $^{13}C\{^{1}H\}$ NMR ($CDCl_3$, 150 MHz): δ 162.4, 157.8, 155.9, 149.5, 137.4, 136.2, 134.0, 132.8, 131.2, 130.5, 130.44, 130.35, 129.5, 129.2, 128.9, 128.7, 124.9, 121.1, 117.4, 105.5; IR (KBr, cm^{-1}): 2922, 2856, 2216, 1694, 1567, 1522, 1453, 1340, 1235, 1159, 1076, 1028, 901, 850, 751, 695, 616, 483; HRMS (ESI/Q-TOF) (m/z) calcd for $C_{24}H_{16}N_3O_2$ $[M + H]^+$ 378.1237; found 378.1254.

***4-(Naphthalen-1-yl)-2,6-diphenylnicotinonitrile (19a)*:**

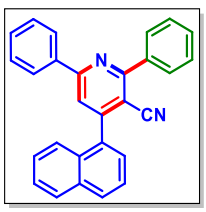

As a white solid (68 mg, 72% yield); Purification over a column of silica gel (2% EtOAc in hexane); ^{1}H NMR ($CDCl_3$, 400 MHz): δ 8.21–8.19 (m, 2H), 8.12 (d, 2H, J = 8.0 Hz), 8.03 (d, 1H, J = 8.0 Hz), 7.99 (d, 1H, J = 8.0 Hz),

7.89 (s, 1H), 7.68 (d, 1H, *J* = 8.4 Hz), 7.64 (d, 1H, *J* = 8.0 Hz), 7.61–7.56 (m, 5H), 7.54–7.51 (m, 4H); $^{13}C\{^{1}H\}$ NMR ($CDCl_3$, 100 MHz): *δ* 162.1, 158.9, 155.1, 138.0, 137.6, 134.6, 133.9, 130.9, 130.8, 130.4, 130.2, 129.6, 129.2, 128.9, 128.8, 127.8, 127.44, 127.35, 126.7, 125.5, 125.0, 120.3, 117.3, 106.6; IR (KBr, cm^{-1}): 2921, 2853, 2215, 1732, 1656, 1569, 1528, 1446, 1374, 1262, 1073, 1025, 906, 771, 692, 616, 533; HRMS (ESI/Q-TOF) (m/z) calcd for $C_{28}H_{19}N_2$ $[M + H]^+$ 383.1543; found 383.1548.

***4-(Naphthalen-1-yl)-6-(naphthalen-2-yl)-2-phenylnicotinonitrile (20a)*:**

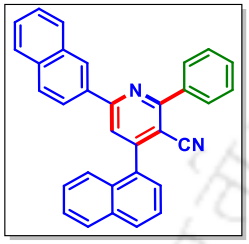

As a white solid (75 mg, 70% yield); Purification over a column of silica gel (2% EtOAc in hexane); ^{1}H NMR ($CDCl_3$, 400 MHz): *δ* 8.69 (s, 1H), 8.33 (d, 1H, *J* = 8.8 Hz), 8.16 (d, 2H, *J* = 7.8 Hz), 8.05–7.94 (m, 6H), 7.89 (d, 1H, *J* = 7.8 Hz), 7.72 (d, 1H, *J* = 8.0 Hz), 7.68–7.52 (m, 8H); $^{13}C\{^{1}H\}$ NMR ($CDCl_3$, 100 MHz): *δ* 162.1, 158.8, 155.0, 138.1, 134.9, 134.7, 134.6, 133.9, 133.5, 130.4, 130.2, 129.6, 129.2, 128.9, 128.8, 127.89, 127.92, 127.6, 127.4, 127.3, 126.8, 126.7, 125.4, 125.0, 124.6, 120.4, 117.3, 106.6; IR (KBr, cm^{-1}): 2921, 2850, 2218, 1679, 1564, 1529, 1385, 1336, 1233, 1168, 1026, 862, 763, 696, 628; HRMS (ESI/Q-TOF) (m/z) calcd for $C_{32}H_{21}N_2$ $[M + H]^+$ 433.1699; found 433.1730.

***4-(4-Chlorophenyl)-2-phenyl-6-(p-tolyl)nicotinonitrile (21a)*:**

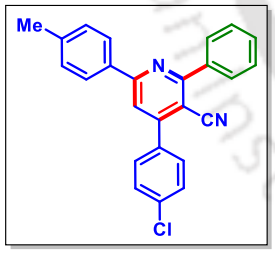

As a white solid (65 mg, 69% yield); Purification over a column of silica gel (2% EtOAc in hexane); ^{1}H NMR ($CDCl_3$, 400 MHz): δ 8.08 (d, 2H, *J* = 8.0 Hz), 8.04–8.02 (m, 2H), 7.75 (s, 1H), 7.62 (d, 2H, *J* = 8.4 Hz), 7.57–7.53 (m, 5H), 7.32 (d, 2H, *J* = 8.0 Hz), 2.44 (s, 3H); $^{13}C\{^{1}H\}$ NMR ($CDCl_3$, 100 MHz): *δ* 162.6, 159.5, 154.2, 141.3, 138.1, 136.5, 135.5, 134.8, 130.3, 130.2, 129.9, 129.6, 129.5, 128.7, 127.7, 118.2, 117.9, 103.9, 21.6; IR (KBr, cm^{-1}): 2923, 2860, 2212, 1658, 1575, 1531, 1486, 1455, 1370, 1266, 1174, 1089, 1016, 815, 753, 688, 628, 540, 495; HRMS (ESI/Q-TOF) (m/z) calcd for $C_{25}H_{18}ClN_2$ $[M + H]^+$ 381.1153; found 381.1170.

***6-(4-Chlorophenyl)-4-(4-methoxyphenyl)-2-phenylnicotinonitrile (22a)*:**

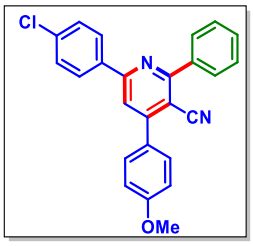

As a white solid (74 mg, 75% yield); Purification over a column of silica gel (2% EtOAc in hexane); ^{1}H NMR ($CDCl_3$, 400 MHz): δ 8.05 (d, 2H, J = 8.8 Hz), 7.96–7.93 (m, 2H), 7.68 (s, 1H), 7.58 (d, 2H, J = 8.8 Hz), 7.49–7.47 (m, 3H), 7.40 (d, 2H, J = 8.4 Hz), 7.01 (d, 2H, J = 8.8 Hz), 3.82 (s, 3H); ^{13}C{^{1}H} NMR ($CDCl_3$, 100 MHz): δ 162.7, 161.3, 157.9, 155.4, 138.1, 136.9, 136.2, 130.4, 130.3, 129.5, 129.3, 128.9, 128.7, 128.5, 118.3, 118.1, 114.7, 104.5, 55.6; IR (KBr, cm^{-1}): 2923, 2856, 2216, 1727, 1574, 1514, 1459, 1373, 1177, 1259, 1089, 1025, 820, 689, 568, 514; HRMS (ESI/Q-TOF) (m/z) calcd for $C_{25}H_{18}ClN_2O$ $[M + H]^+$ 397.1102; found 397.1106.

***6-(4-Chlorophenyl)-4-(4-hydroxyphenyl)-2-phenylnicotinonitrile (23a)*:**

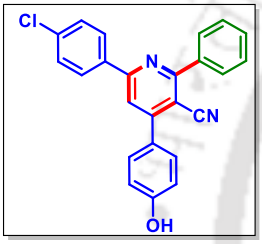

As a white solid (39 mg, 41% yield); Purification over a column of silica gel (5% EtOAc in hexane); ^{1}H NMR (DMSO-d_6 + $CDCl_3$, 400 MHz): δ 10.07 (s, 1H), 8.30 (d, 2H, J = 8.4 Hz), 8.07 (s, 1H), 7.96–7.94 (m, 2H), 7.67 (d, 2H, J = 8.4 Hz), 7.57–7.54 (m, 5H), 6.96 (d, 2H, J = 8.8 Hz); ^{13}C{^{1}H} NMR (DMSO-d_6 + $CDCl_3$, 100 MHz): δ 161.7, 159.3, 156.8, 154.9, 137.9, 135.8, 135.5, 130.6, 129.9, 129.3, 129.2, 128.9, 128.3, 126.7, 118.3, 117.9, 115.6, 103.9; IR (KBr, cm^{-1}): 3415, 2955, 2922, 2853, 2215, 1667, 1594, 1565, 1491, 1462, 1387, 1308, 1262, 1219, 1090, 1017, 807, 702; HRMS (ESI/Q-TOF) (m/z) calcd for $C_{24}H_{16}ClN_2O$ $[M + H]^+$ 383.0946; found 383.0949.

***4-(4-Methoxyphenyl)-6-(4-nitrophenyl)-2-phenylnicotinonitrile (24a)*:**

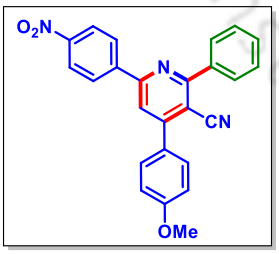

As a white solid (46 mg, 46% yield); Purification over a column of silica gel (2% EtOAc in hexane); ^{1}H NMR ($CDCl_3$, 400 MHz): δ 8.35 (s, 4H), 8.03–8.01 (m, 2H), 7.86 (s, 1H), 7.67 (d, 2H, J = 8.8 Hz), 7.58–7.56 (m, 3H), 7.10 (d, 2H, J = 8.8 Hz), 3.91 (s, 3H); ^{13}C{^{1}H} NMR ($CDCl_3$, 100 MHz): δ 163.1, 161.6, 156.6, 155.9, 149.4, 149.2, 143.6, 137.8, 130.6, 130.4, 129.6, 128.8, 128.6, 124.3, 119.4, 117.8, 114.8, 105.8, 55.7; IR (KBr, cm^{-1}): 2923, 2854, 2218, 1727, 1602, 1568, 1513, 1352, 1296, 1260, 1180, 1111, 1023, 825, 757, 691, 568, 511; HRMS (ESI/Q-TOF) (m/z) calcd for $C_{25}H_{18}N_3O_3$ $[M + H]^+$ 408.1343; found 408.1347.

***4-(2,6-Dichlorophenyl)-6-(4-fluorophenyl)-2-phenylnicotinonitrile (25a)*:**

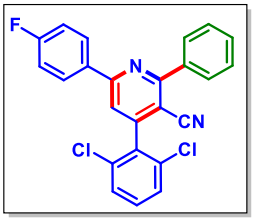

As a white solid (66 mg, 64% yield); Purification over a column of silica gel (2% EtOAc in hexane); ^{1}H NMR ($CDCl_3$, 400 MHz): δ 8.24–8.20 (m, 2H), 8.13–8.10 (m, 2H), 7.69 (s, 1H), 7.59–7.57 (m, 3H), 7.54–7.52 (m, 2H), 7.43–7.39 (m, 1H), 7.22 (t, 2H, J = 8.8 Hz); ^{13}C{^{1}H} NMR ($CDCl_3$, 100 MHz): δ 164.7 (d, J = 250.1 Hz), 161.8, 158.6, 151.4, 137.6, 134.8, 134.3, 133.6 (d, J = 3.1 Hz), 131.4, 130.5, 129.9 (d, J = 8.6 Hz), 129.4, 128.8 (d, J = 8.3 Hz), 118.9, 116.4, 116.2 (d, J = 21.6 Hz), 106.1; ^{19}F NMR ($CDCl_3$ + hexafluorobenzene): δ –112.9 (s); IR (KBr, cm^{-1}): 2922, 2855, 2217, 1660, 1589, 1535, 1406, 1369, 1230, 1151, 1094, 1013, 840, 778, 689, 512; HRMS (ESI/Q-TOF) (m/z) calcd for $C_{24}H_{14}Cl_2FN_2$ $[M + H]^+$ 419.0513; found 419.0514.

***4-(3,4-Dimethoxyphenyl)-2,6-diphenylnicotinonitrile (26a)*:**

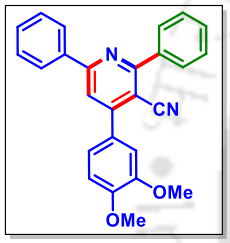

As a white solid (66 mg, 68% yield); Purification over a column of silica gel (2% EtOAc in hexane); ^{1}H NMR ($CDCl_3$, 400 MHz): δ 8.21 (d, 2H, J = 7.8 Hz), 8.06 (d, 2H, J = 7.4 Hz), 7.85 (s, 1H), 7.59–7.54 (m, 6H), 7.33–7.26 (m, 2H), 7.07 (d, 1H, J = 8.4 Hz), 4.02 (s, 3H), 3.99 (s, 3H); ^{13}C{^{1}H} NMR ($CDCl_3$, 100 MHz): δ 162.7, 159.2, 155.3, 150.8, 149.3, 138.3, 137.8, 130.6, 130.2, 129.6, 129.4, 129.2, 128.7, 127.7, 121.9, 118.6, 118.3, 112.0, 111.6, 104.3, 56.4, 56.2; IR (KBr, cm^{-1}): 2927, 2840, 2213, 1665, 1571, 1515, 1452, 1376, 1321, 1256, 1180, 1140, 1077, 1020, 920, 858, 803, 756, 691, 594; HRMS (ESI/Q-TOF) (m/z) calcd for $C_{26}H_{21}N_2O_2$ $[M + H]^+$ 393.1598; found 393.1598.

***6-(Benzo[d][1,3]dioxol-5-yl)-4-(4-bromophenyl)-2-phenylnicotinonitrile (27a)*:**

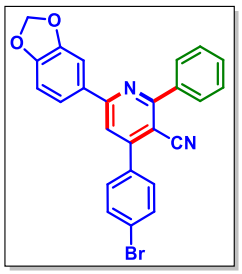

As a white solid (71 mg, 63% yield); Purification over a column of silica gel (2% EtOAc in hexane); ^{1}H NMR ($CDCl_3$, 400 MHz): δ 8.02–8.00 (m, 2H), 7.72–7.69 (m, 4H), 7.66 (s, 1H), 7.56–7.53 (m, 5H), 6.93 (d, 1H, J = 8.0 Hz), 6.05 (s, 2H); ^{13}C{^{1}H} NMR ($CDCl_3$, 100 MHz): δ 162.5, 158.8, 154.2, 150.2, 148.8, 138.0, 135.9, 132.4, 131.9, 130.42, 130.37, 129.5, 128.7, 124.8, 122.4, 117.84, 117.75, 108.8, 107.9, 103.6, 101.9; IR (KBr, cm^{-1}): 2923, 2859, 2214, 1650, 1591, 1484, 1446, 1319, 1255, 1106, 1039, 935, 810, 690, 488; HRMS (ESI/Q-TOF) (m/z) calcd for $C_{25}H_{16}BrN_2O_2$ $[M + H]^+$ 455.0390; found 455.0417.

***4-(4-Chlorophenyl)-2-phenyl-5,6-dihydrobenzo[h]quinoline-3-carbonitrile (28a)*:**

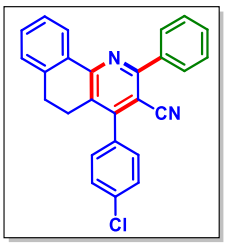

As a white solid (59 mg, 61% yield); Purification over a column of silica gel (2% EtOAc in hexane); ^{1}H NMR ($CDCl_3$, 400 MHz): δ 8.51–8.49 (m, 1H), 8.03 (d, 2H, J = 7.8 Hz), 7.57–7.51 (m, 5H), 7.42–7.38 (m, 2H), 7.33 (d, 2H, J = 8.4 Hz), 7.26 (s, 1H), 2.91–2.87 (m, 2H), 2.79–2.76 (m, 2H); ^{13}C{^{1}H} NMR ($CDCl_3$, 100 MHz): δ 159.6, 155.4, 152.3, 138.9, 138.1, 135.7, 134.2, 133.7, 131.1, 130.3, 130.1, 129.5, 129.4, 128.7, 128.4, 128.0, 127.6, 126.9, 117.7, 105.9, 27.7, 25.5; IR (KBr, cm^{-1}): 2924, 2854, 2221, 1598, 1544, 1489, 1391, 1240, 1177, 1086, 1018, 836, 757, 699, 589, 485; HRMS (ESI/Q-TOF) (m/z) calcd for $C_{26}H_{18}ClN_2$ $[M + H]^+$ 393.1153; found 393.1139.

***4,6-Di(furan-2-yl)-2-phenylnicotinonitrile (29a)*:**

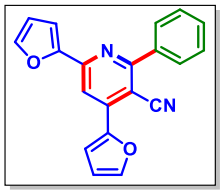

As a white solid (50 mg, 65% yield); Purification over a column of silica gel (2% EtOAc in hexane); ^{1}H NMR ($CDCl_3$, 400 MHz): δ 8.14 (s, 1H), 7.93–7.91 (m, 2H), 7.71 (d, 1H, J = 3.6 Hz), 7.68 (s, 1H), 7.63 (s, 1H), 7.54–7.53 (m, 3H), 7.31 (d, 1H, J = 3.6 Hz), 6.66–6.64 (m, 1H), 6.60–6.59 (m, 1H); ^{13}C{^{1}H} NMR ($CDCl_3$, 100 MHz): δ 163.5, 152.9, 151.2, 148.4, 145.13, 145.07, 141.9, 138.0, 130.3, 129.5, 128.6, 118.6, 114.7, 113.1, 112.9, 112.6, 111.7, 98.5; IR (KBr, cm^{-1}): 2923, 2853, 2214, 1639, 1510, 1465, 1372, 1261, 1028, 812, 756, 705; HRMS (ESI/Q-TOF) (m/z) calcd for $C_{20}H_{13}N_2O_2$ $[M + H]^+$ 313.0972; found 313.0991.

***2-Phenyl-4,6-di(thiophen-2-yl)nicotinonitrile (30a)*:**

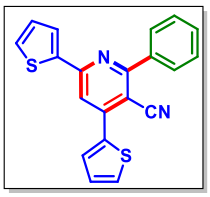

As a white solid (58 mg, 68% yield); Purification over a column of silica gel (2% EtOAc in hexane); ^{1}H NMR ($CDCl_3$, 400 MHz): δ 8.02–7.99 (m, 2H), 7.92 (d, 1H, J = 4.0 Hz), 7.78 (d, 1H, J = 3.6 Hz), 7.74 (s, 1H), 7.58–7.52 (m, 5H), 7.24 (t, 1H, J = 4.4 Hz), 7.16 (t, 1H, J = 4.4 Hz); ^{13}C{^{1}H} NMR ($CDCl_3$, 100 MHz): δ 163.3, 154.6, 146.9, 143.4, 137.69, 137.66, 130.6, 130.4, 129.9, 129.6, 129.3, 128.9, 128.65, 128.60, 127.4, 118.4, 115.9, 101.9; IR (KBr, cm^{-1}): 2921, 2852, 2215, 1639, 1591, 1552, 1513, 1495, 1462, 1377, 1289, 1266, 1111, 1069, 1012, 885, 798, 748, 723, 699; HRMS (ESI/Q-TOF) (m/z) calcd for $C_{20}H_{13}N_2S_2$ $[M + H]^+$ 345.0515; found 345.0522.

***2-(Naphthalen-2-yl)-4,6-diphenylnicotinonitrile (1b)*:**

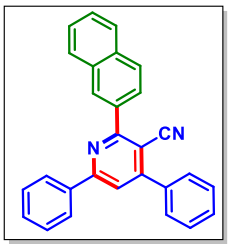

As a white solid (63 mg, 66% yield); Purification over a column of silica gel (2% EtOAc in hexane); ^{1}H NMR ($CDCl_3$, 400 MHz): δ 8.59 (s, 1H), 8.24–8.22 (m, 2H), 8.19–8.16 (m, 1H), 8.05–8.02 (m, 2H), 7.95–7.93 (m, 1H), 7.86 (s, 1H), 7.75–7.72 (m, 2H), 7.59–7.53 (m, 8H); ^{13}C{^{1}H} NMR ($CDCl_3$, 100 MHz): δ 162.5, 159.4, 155.7, 137.7, 136.9, 135.5, 134.1, 133.1, 130.7, 130.1, 129.7, 129.2, 129.1, 128.9, 128.5, 127.9, 127.8, 127.4, 126.7, 126.6, 118.8, 118.0, 104.7; IR (KBr, cm^{-1}): 2924, 2851, 2216, 1657, 1572, 1500, 1468, 1401, 1371, 1322, 1262, 1226, 1153, 1091, 1023, 873, 827, 761, 728, 701; HRMS (ESI/Q-TOF) (m/z) calcd for $C_{28}H_{19}N_2$ [M + H]$^{+}$ 383.1543; found 383.1548.

***4,6-Diphenyl-2-(p-tolyl)nicotinonitrile (1c)*:**

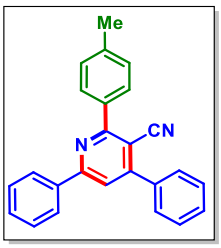

As a white solid (63 mg, 73% yield); Purification over a column of silica gel (2% EtOAc in hexane); ^{1}H NMR ($CDCl_3$, 400 MHz): δ 8.19 (d, 2H, J = 7.6 Hz), 7.97 (d, 2H, J = 8.0 Hz), 7.80 (s, 1H), 7.69 (d, 2H, J = 7.8 Hz), 7.58–7.51 (m, 6H), 7.37 (d, 2H, J = 8.0 Hz), 2.46 (s, 3H); ^{13}C{^{1}H} NMR ($CDCl_3$, 100 MHz): δ 162.6, 159.2, 155.6, 140.5, 137.8, 137.1, 135.4, 130.6, 130.0, 129.5, 129.4, 129.2, 129.1, 128.9, 127.7, 118.6, 118.1, 104.3, 21.6; IR (KBr, cm^{-1}): 2922, 2856, 2213, 1570, 1527, 1449, 1375, 1231, 1176, 1084, 1024, 874, 820, 755, 691, 490; HRMS (ESI/Q-TOF) (m/z) calcd for $C_{25}H_{19}N_2$ [M + H]$^{+}$ 347.1543; found 347.1545.

***4,6-Diphenyl-2-(o-tolyl)nicotinonitrile (1d)*:**

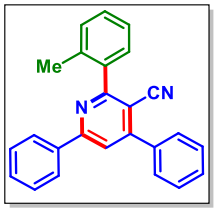

As a white solid (37 mg, 43% yield); Purification over a column of silica gel (2% EtOAc in hexane); ^{1}H NMR ($CDCl_3$, 400 MHz): δ 8.16–8.14 (m, 2H), 7.86 (s, 1H), 7.72 (d, 2H, J = 7.8 Hz), 7.59–7.55 (m, 3H), 7.52–7.49 (m, 4H), 7.44–7.34 (m, 3H), 2.41 (s, 3H); ^{13}C{^{1}H} NMR ($CDCl_3$, 100 MHz): δ 164.5, 159.2, 154.6, 138.2, 137.8, 136.8, 136.4, 130.9, 130.7, 130.2, 129.73, 129.70, 129.24, 129.16, 128.8, 127.8, 126.1, 118.8, 117.1, 106.6, 20.1; IR (KBr, cm^{-1}): 2922, 2856, 2215, 1570, 1529, 1488, 1455, 1372, 1260, 1166, 1072, 1029, 875, 747, 690, 620, 576, 453; HRMS (ESI/Q-TOF) (m/z) calcd for $C_{25}H_{19}N_2$ [M + H]$^{+}$ 347.1543; found 347.1528.

***2-(4-Ethylphenyl)-4,6-diphenylnicotinonitrile (1e)*:**

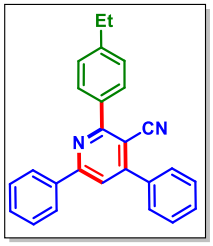

As a white solid (67 mg, 75% yield); Purification over a column of silica gel (2% EtOAc in hexane); ^{1}H NMR ($CDCl_3$, 400 MHz): δ 8.19 (d, 2H, J = 7.8 Hz), 8.00 (d, 2H, J = 8.0 Hz), 7.80 (s, 1H), 7.70 (d, 2H, J = 7.6 Hz), 7.59–7.51 (m, 6H), 7.40 (d, 2H, J = 8.0 Hz), 2.77 (q, 2H, J_1 = 7.6 Hz, J_2 = 15.2 Hz), 1.32 (t, 3H, J = 7.6 Hz); ^{13}C{^{1}H} NMR ($CDCl_3$, 100 MHz): δ 162.6, 159.2, 155.6, 146.7, 137.8, 137.1, 135.6, 130.6, 130.0, 129.6, 129.14, 129.12, 128.9, 128.2, 127.7, 118.5, 118.1, 104.3, 29.0, 15.6; IR (KBr, cm^{-1}): 2923, 2864, 2214, 1572, 1529, 1448, 1374, 1261, 1184, 1075, 1024, 874, 832, 754, 693, 564, 488; HRMS (ESI/Q-TOF) (m/z) calcd for $C_{26}H_{21}N_2$ $[M + H]^+$ 361.1699; found 361.1712.

***2-(4-(tert-Butyl)phenyl)-4,6-diphenylnicotinonitrile (1f)*:**

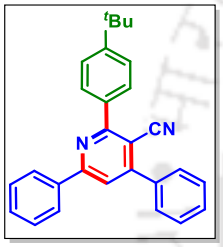

As a white solid (74 mg, 77% yield); Purification over a column of silica gel (2% EtOAc in hexane); ^{1}H NMR ($CDCl_3$, 400 MHz): δ 8.19 (d, 2H, J = 7.6 Hz), 8.03 (d, 2H, J = 8.4 Hz), 7.81 (s, 1H), 7.69 (d, 2H, J = 7.8 Hz), 7.60–7.56 (m, 5H), 7.53–7.51 (m, 3H), 1.41 (s, 9H); ^{13}C{^{1}H} NMR ($CDCl_3$, 100 MHz): δ 162.4, 159.2, 155.6, 153.6, 137.8, 137.1, 135.4, 130.6, 130.0, 129.3, 129.2, 129.1, 128.9, 127.7, 125.7, 118.6, 118.1, 104.2, 35.1, 31.5; IR (KBr, cm^{-1}): 2924, 2857, 2222, 1576, 1531, 1456, 1379, 1262, 1102, 1024, 804, 766, 696, 555; HRMS (ESI/Q-TOF) (m/z) calcd for $C_{28}H_{25}N_2$ $[M + H]^+$ 389.2012; found 389.2041.

***2-(4-Methoxyphenyl)-4,6-diphenylnicotinonitrile (1g)*:**

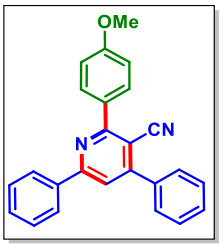

As a white solid (71 mg, 79% yield); Purification over a column of silica gel (2% EtOAc in hexane); ^{1}H NMR ($CDCl_3$, 600 MHz): δ 8.18 (d, 2H, J = 7.8 Hz), 8.06 (d, 2H, J = 8.4 Hz), 7.77 (s, 1H), 7.68 (d, 2H, J = 7.2 Hz), 7.58–7.51 (m, 6H), 7.08 (d, 2H, J = 8.4 Hz), 3.90 (s, 3H); ^{13}C{^{1}H} NMR ($CDCl_3$, 150 MHz): δ 162.0, 161.4, 159.2, 155.7, 137.8, 137.1, 131.2, 130.7, 130.6, 130.0, 129.2, 128.9, 127.7, 118.3, 114.1, 103.8, 55.6; IR (KBr, cm^{-1}): 2922, 2860, 2214, 1665, 1581, 1512, 1455, 1374, 1253, 1175, 1017, 819, 758, 691, 562; HRMS (ESI/Q-TOF) (m/z) calcd for $C_{25}H_{19}N_2O$ $[M + H]^+$ 363.1492; found 363.1514.

***2-(4-Methoxy-3-methylphenyl)-4,6-diphenylnicotinonitrile (1h)*:**

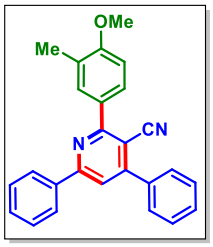

As a white solid (64 mg, 68% yield); Purification over a column of silica gel (2% EtOAc in hexane); ^{1}H NMR ($CDCl_3$, 600 MHz): δ 8.18 (d, 2H, J = 7.2 Hz), 7.92 (d, 1H, J = 8.4 Hz), 7.86 (s, 1H), 7.76 (s, 1H), 7.68 (d, 2H, J = 7.7 Hz), 7.57–7.51 (m, 6H), 6.98 (d, 1H, J = 8.4 Hz), 3.92 (s, 3H), 2.34 (s, 3H); ^{13}C{^{1}H} NMR ($CDCl_3$, 150 MHz): δ 162.4, 159.6, 159.2, 155.6, 137.9, 137.2, 131.9, 130.6, 130.2, 130.0, 129.1, 128.9, 128.6, 127.8, 127.1, 118.4, 118.2, 109.7, 103.9, 55.7, 16.6; IR (KBr, cm^{-1}): 2923, 2856, 2213, 1574, 1532, 1496, 1453, 1373, 1247, 1173, 1131, 1027, 879, 811, 759, 690, 578; HRMS (ESI/Q-TOF) (m/z) calcd for $C_{26}H_{21}N_2O$ $[M + H]^+$ 377.1648; found 377.1655.

***2-(4-Fluorophenyl)-4,6-diphenylnicotinonitrile (1i)*:**

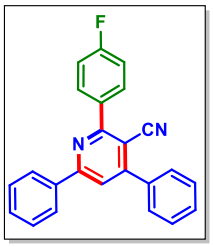

As a white solid (54 mg, 62% yield); Purification over a column of silica gel (2% EtOAc in hexane); ^{1}H NMR ($CDCl_3$, 400 MHz): δ 8.22–8.19 (m, 2H), 8.12–8.08 (m, 2H), 7.86 (s, 1H), 7.73–7.71 (m, 2H), 7.63–7.55 (m, 6H), 7.30–7.28 (m, 2H); ^{13}C{^{1}H} NMR ($CDCl_3$, 100 MHz): δ 164.2 (d, J = 249.0 Hz), 161.4, 159.4, 155.7, 137.6, 136.9, 134.3 (d, J = 3.2 Hz), 131.7 (d, J = 8.6 Hz), 130.8, 130.2, 129.2, 128.8, 127.7, 118.9, 117.9, 115.8 (d, J = 21.7 Hz), 104.4; ^{19}F NMR ($CDCl_3$ + hexafluorobenzene): δ –113.8 (s); IR (KBr, cm^{-1}): 2923, 2858, 2214, 1662, 1594, 1543, 1480, 1369, 1261, 1153, 1078, 1017, 879, 811, 748, 686, 587; HRMS (ESI/Q-TOF) (m/z) calcd for $C_{24}H_{16}FN_2$ $[M + H]^+$ 351.1292; found 351.1292.

***2-(4-Chlorophenyl)-4,6-diphenylnicotinonitrile (1j)*:**

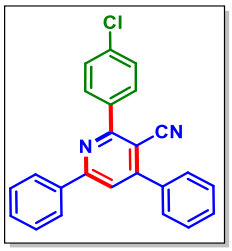

As a white solid (50 mg, 55% yield); Purification over a column of silica gel (2% EtOAc in hexane); ^{1}H NMR ($CDCl_3$, 400 MHz): δ 8.18–8.16 (m, 2H), 8.01 (d, 2H, J = 8.4 Hz), 7.84 (s, 1H), 7.69–7.67 (m, 2H), 7.58–7.52 (m, 8H); ^{13}C{^{1}H} NMR ($CDCl_3$, 100 MHz): δ 161.3, 159.5, 155.8, 137.6, 136.8, 136.62, 136.59, 135.4, 130.95, 130.87, 130.2, 129.2, 129.0, 128.9, 127.8, 119.0, 117.8, 104.4; IR (KBr, cm^{-1}): 2923, 2856, 2216, 1578, 1529, 1454, 1381, 1262, 1091, 1028, 804, 757, 693; HRMS (ESI/Q-TOF) (m/z) calcd for $C_{24}H_{16}ClN_2$ $[M + H]^+$ 367.0997; found 367.1006.

***2-(3-Chlorophenyl)-4,6-diphenylnicotinonitrile (1k)*:**

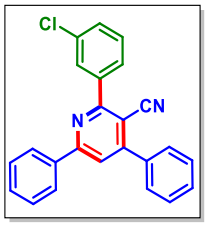

As a white solid (46 mg, 51% yield); Purification over a column of silica gel (2% EtOAc in hexane); ^{1}H NMR ($CDCl_3$, 400 MHz): δ 8.17 (d, 2H, J = 7.6 Hz), 8.02 (s, 1H), 7.94 (d, 1H, J = 6.8 Hz), 7.85 (s, 1H), 7.69–7.68 (m, 2H), 7.58–7.57 (m, 3H), 7.54–7.49 (m, 5H); ^{13}C{^{1}H} NMR ($CDCl_3$, 100 MHz): δ 161.1, 159.5, 155.7, 139.9, 137.5, 136.8, 134.8, 130.9, 130.3, 130.2, 129.9, 129.8, 129.2, 128.9, 127.8, 127.6, 119.3, 117.6, 104.6; IR (KBr, cm^{-1}): 2923, 2857, 2214, 1662, 1571, 1529, 1457, 1375, 1262, 1168, 1083, 1030, 876, 801, 755, 688, 579; HRMS (ESI/Q-TOF) (m/z) calcd for $C_{24}H_{16}ClN_2$ $[M + H]^+$ 367.0997; found 367.1003.

***2-(4-Bromophenyl)-4,6-diphenylnicotinonitrile (1l)*:**

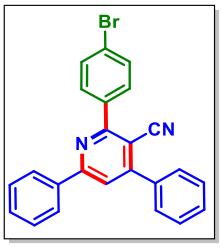

As a white solid (53 mg, 52% yield); Purification over a column of silica gel (2% EtOAc in hexane); ^{1}H NMR ($CDCl_3$, 400 MHz): δ 8.17 (d, 2H, J = 7.2 Hz), 7.94 (d, 2H, J = 8.4 Hz), 7.84 (s, 1H), 7.71–7.67 (m, 4H), 7.58–7.56 (m, 3H), 7.53–7.51 (m, 3H); ^{13}C{^{1}H} NMR ($CDCl_3$, 100 MHz): δ 161.4, 159.5, 155.8, 137.5, 137.0, 136.8, 131.9, 131.2, 130.9, 130.2, 129.2, 128.8, 127.8, 125.0, 119.1, 117.8, 104.4; IR (KBr, cm^{-1}): 2923, 2855, 2214, 1732, 1571, 1530, 1485, 1459, 1378, 1266, 1174, 1073, 1016, 825, 755, 692, 491; HRMS (ESI/Q-TOF) (m/z) calcd for $C_{24}H_{16}BrN_2$ $[M + H]^+$ 411.0491; found 411.0497.

***4,6-Diphenyl-2-(4-(trifluoromethyl)phenyl)nicotinonitrile (1m)*:**

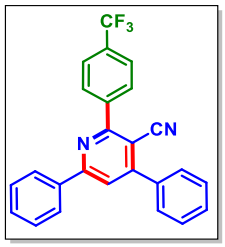

As a white solid (35 mg, 35% yield); Purification over a column of silica gel (2% EtOAc in hexane); ^{1}H NMR ($CDCl_3$, 400 MHz): δ 8.19–8.15 (m, 4H), 7.89 (s, 1H), 7.83 (d, 2H, J = 8.0 Hz), 7.71–7.68 (m, 2H), 7.59–7.57 (m, 3H), 7.55–7.52 (m, 3H); ^{13}C{^{1}H} NMR ($CDCl_3$, 100 MHz): δ 161.1, 159.6, 155.8, 137.4, 136.7, 130.9, 130.3, 130.0, 129.29, 129.27, 128.8, 128.4, 128.2, 128.0, 127.8, 125.7 (q, J_1 = 3.8 Hz, J_2 = 7.4 Hz), 119.5, 117.8, 104.8; ^{19}F NMR ($CDCl_3$ + hexafluorobenzene): δ –65.9 (s); IR (KBr, cm^{-1}): 2923, 2855, 2216, 1675, 1571, 1534, 1492, 1450, 1392, 1262, 1165, 1109, 1068, 1021, 807, 761, 692, 597, 495; HRMS (ESI/Q-TOF) (m/z) calcd for $C_{25}H_{16}F_3N_2$ $[M + H]^+$ 401.1260; found 401.1266.

***2,5-Diphenyl-1H-pyrrole-3-carbonitrile (31a)*:**

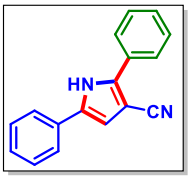

As a white solid (44 mg, 73% yield); Purification over a column of silica gel (5% EtOAc in hexane); ^{1}H NMR (DMSO-d$_6$, 600 MHz): δ 12.20 (s, 1H), 7.85 (d, 2H, J = 7.8 Hz), 7.81 (d, 2H, J = 7.8 Hz), 7.55 (t, 2H, J = 7.8 Hz), 7.45–7.42 (m, 3H), 7.30 (t, 1H, J = 7.2 Hz), 7.07 (s, 1H); ^{13}C{^{1}H} NMR (DMSO-d$_6$, 150 MHz): δ 139.6, 133.8, 130.7, 129.7, 128.9, 128.8, 128.6, 127.3, 126.5, 124.8, 117.6, 110.2, 90.2; IR (KBr, cm^{-1}): 3224, 3034, 2756, 2219, 1597, 1465, 1296, 1184, 1071, 1027, 908, 808, 760, 688, 595, 535, 490; HRMS (ESI/Q-TOF) (m/z) calcd for $C_{17}H_{13}N_2$ $[M + H]^+$ 245.1073; found 245.1077.

***2-Phenyl-5-(p-tolyl)-1H-pyrrole-3-carbonitrile (32a)*:**

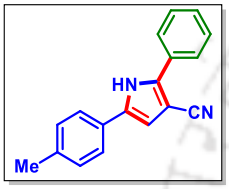

As a white solid (49 mg, 76% yield); Purification over a column of silica gel (5% EtOAc in hexane); ^{1}H NMR (DMSO-d$_6$, 600 MHz): δ 12.14 (s, 1H), 7.83 (d, 2H, J = 7.8 Hz), 7.69 (d, 2H, J = 8.4 Hz), 7.54 (t, 2H, J = 7.8 Hz), 7.43 (t, 1H, J = 7.5 Hz), 7.24 (d, 2H, J = 7.8 Hz), 7.00 (s, 1H), 2.31 (s, 3H); ^{13}C{^{1}H} NMR (DMSO-d$_6$, 150 MHz): δ 139.4, 136.8, 134.0, 129.8, 129.4, 129.0, 128.6, 128.0, 126.5, 124.8, 117.8, 109.6, 90.1, 20.8; IR (KBr, cm^{-1}): 3258, 2905, 2864, 2218, 1601, 1455, 1263, 1075, 1036, 803, 755, 692, 430; HRMS (ESI/Q-TOF) (m/z) calcd for $C_{18}H_{15}N_2$ $[M + H]^+$ 259.1230; found 259.1241.

***5-(4-Methoxyphenyl)-2-phenyl-1H-pyrrole-3-carbonitrile (33a)*:**

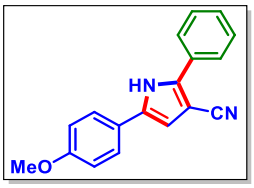

As a white solid (53 mg, 78% yield); Purification over a column of silica gel (5% EtOAc in hexane); ^{1}H NMR (DMSO-d$_6$, 400 MHz): δ 12.07 (s, 1H), 7.83 (d, 2H, J = 7.6 Hz), 7.73 (d, 2H, J = 8.8 Hz), 7.53 (t, 2H, J = 7.8 Hz), 7.42 (t, 1H, J = 7.4 Hz), 7.00 (d, 2H, J = 8.8 Hz), 6.92 (s, 1H), 3.78 (s, 3H); ^{13}C{^{1}H} NMR (DMSO-d$_6$, 100 MHz): δ 158.7, 139.0, 133.9, 129.8, 128.9, 128.4, 126.4, 126.3, 123.5, 117.8, 114.2, 108.9, 89.9, 55.2; IR (KBr, cm^{-1}): 3221, 2922, 2835, 2219, 1606, 1527, 1461, 1295, 1266, 1156, 1126, 1043, 939, 830, 805, 761, 692, 573, 515; HRMS (ESI/Q-TOF) (m/z) calcd for $C_{18}H_{15}N_2O$ $[M + H]^+$ 275.1179; found 275.1187.

***5-(4-Chlorophenyl)-2-phenyl-1H-pyrrole-3-carbonitrile (34a)*:**

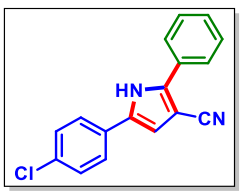

As a white solid (49 mg, 71% yield); Purification over a column of silica gel (5% EtOAc in hexane); ^{1}H NMR (DMSO-d$_6$, 400 MHz): δ 12.24 (s, 1H),

7.84–7.81 (m, 4H), 7.54 (t, 2H, *J* = 7.6 Hz), 7.48 (d, 2H, *J* = 8.4 Hz), 7.44 (t, 1H, *J* = 7.4 Hz), 7.09 (s, 1H); $^{13}C\{^{1}H\}$ NMR (DMSO-d_6, 100 MHz): δ 140.0, 132.6, 131.8, 129.7, 129.6, 129.0, 128.84, 128.78, 126.6, 126.5, 117.6, 110.8, 90.4; IR (KBr, cm^{-1}): 3226, 2928, 2853, 2221, 1599, 1473, 1299, 1263, 1171, 1092, 1024, 832, 805, 762, 687, 603, 495; HRMS (ESI/Q-TOF) (m/z) calcd for $C_{17}H_{12}ClN_2$ $[M + H]^+$ 279.0684; found 279.0697.

***5-(4-Bromophenyl)-2-phenyl-1H-pyrrole-3-carbonitrile (35a)*:**

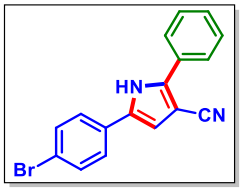

As a white solid (54 mg, 67% yield); Purification over a column of silica gel (5% EtOAc in hexane); ^{1}H NMR (DMSO-d_6, 400 MHz): δ 12.24 (s, 1H), 7.83 (d, 2H, *J* = 7.2 Hz), 7.76 (d, 2H, *J* = 8.8 Hz), 7.61 (d, 2H, *J* = 8.8 Hz), 7.54 (t, 2H, *J* = 7.6 Hz), 7.44 (t, 1H, *J* = 7.4 Hz), 7.10 (s, 1H); $^{13}C\{^{1}H\}$ NMR (DMSO-d_6, 100 MHz): δ 140.0, 132.6, 131.7, 129.9, 129.6, 128.9, 128.8, 126.7, 126.6, 120.3, 117.5, 110.8, 90.4; IR (KBr, cm^{-1}): 3225, 2921, 2856, 2223, 1600, 1471, 1384, 1303, 1264, 1174, 1076, 1022, 807, 751, 692, 491; HRMS (ESI/Q-TOF) (m/z) calcd for $C_{17}H_{12}BrN_2$ $[M + H]^+$ 323.0178; found 323.0181.

***5-(4-Nitrophenyl)-2-phenyl-1H-pyrrole-3-carbonitrile (36a)*:**

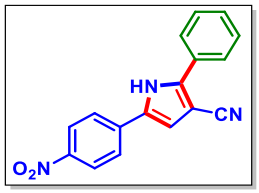

As a white solid (40 mg, 55% yield); Purification over a column of silica gel (5% EtOAc in hexane); ^{1}H NMR (DMSO-d_6, 400 MHz): δ 12.51 (s, 1H), 8.28 (d, 2H, *J* = 9.2 Hz), 8.07 (d, 2H, *J* = 8.8 Hz), 7.85 (d, 2H, *J* = 7.2 Hz), 7.57 (t, 2H, *J* = 7.6 Hz), 7.48 (t, 1H, *J* = 7.4 Hz), 7.41 (s, 1H); $^{13}C\{^{1}H\}$ NMR (DMSO-d_6, 100 MHz): δ 145.7, 141.5, 136.9, 131.5, 129.2, 129.0, 126.8, 125.1, 124.3, 117.1, 113.81, 113.78, 91.2; IR (KBr, cm^{-1}): 3224, 2926, 2746, 2219, 1595, 1464, 1298, 1183, 1072, 1027, 908, 805, 763, 687, 595, 535, 494; HRMS (ESI/Q-TOF) (m/z) calcd for $C_{17}H_{12}N_3O_2$ $[M + H]^+$ 290.0924; found 290.0947.

***2-Phenyl-4,5-dihydro-1H-benzo[g]indole-3-carbonitrile (37a)*:**

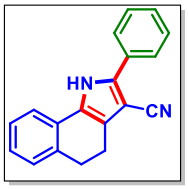

As a white solid (48 mg, 71% yield); Purification over a column of silica gel (5% EtOAc in hexane); ^{1}H NMR (DMSO-d_6, 400 MHz): δ 12.26 (s, 1H), 7.85 (d, 2H, *J* = 7.2 Hz), 7.75 (d, 1H, *J* = 7.6 Hz), 7.54 (t, 2H, *J* = 7.8 Hz), 7.42 (t, 1H, *J* = 7.4 Hz), 7.28–7.23 (m, 2H), 7.12 (t, 1H, *J* = 7.4 Hz), 2.93 (t, 2H, *J* = 7.6 Hz), 2.74 (t,

2H, *J* = 7.6 Hz); $^{13}C\{^{1}H\}$ NMR (DMSO-d_6, 100 MHz): *δ* 138.5, 134.4, 129.9, 129.3, 129.0, 128.4, 128.3, 127.7, 127.4, 126.7, 126.4, 126.0, 123.3, 120.6, 117.0, 88.7, 28.5, 19.9; IR (KBr, cm^{-1}): 3228, 3033, 2765, 2221, 1599, 1455, 1286, 1187, 1080, 1026, 918, 801, 765, 678, 585, 532, 498; HRMS (ESI/Q-TOF) (m/z) calcd for $C_{19}H_{15}N_2$ $[M + H]^+$ 271.1230; found 271.1238.

***2-Phenyl-5-(thiophen-2-yl)-1H-pyrrole-3-carbonitrile (38a)*:**

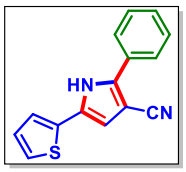

As a white solid (43 mg, 69% yield); Purification over a column of silica gel (5% EtOAc in hexane); ^{1}H NMR (DMSO-d_6, 400 MHz): *δ* 12.36 (s, 1H), 7.83 (d, 2H, *J* = 7.6 Hz), 7.56–7.49 (m, 4H), 7.44 (t, 1H, *J* = 7.4 Hz), 7.12 (t, 1H, *J* = 4.4 Hz), 7.12 (t, 1H, *J* = 7.4 Hz), 6.84 (s, 1H); $^{13}C\{^{1}H\}$ NMR (DMSO-d_6, 100 MHz): *δ* 139.3, 133.4, 129.5, 129.0, 128.7, 128.4, 127.9, 126.5, 125.0, 123.9, 117.4, 110.1, 90.0; IR (KBr, cm^{-1}): 3225, 2998, 2753, 2219, 1598, 1455, 1297, 1186, 1101, 1028, 918, 828, 762, 686, 594, 537, 490; HRMS (ESI/Q-TOF) (m/z) calcd for $C_{15}H_{11}N_2S$ $[M + H]^+$ 251.0637; found 251.0642.

***2-(Naphthalen-2-yl)-5-phenyl-1H-pyrrole-3-carbonitrile (31b)*:**

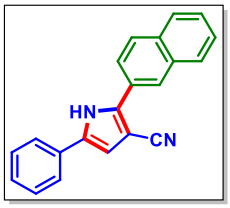

As a white solid (54 mg, 74% yield); Purification over a column of silica gel (5% EtOAc in hexane); ^{1}H NMR (DMSO-d_6, 600 MHz): *δ* 12.37 (s, 1H), 8.39 (s, 1H), 8.08 (d, 1H, *J* = 9.0 Hz), 7.98 (t, 3H, *J* = 8.4 Hz), 7.85 (d, 2H, *J* = 7.2 Hz), 7.61–7.56 (m, 2H), 7.45 (t, 2H, *J* = 7.8 Hz), 7.31 (t, 1H, *J* = 7.5 Hz), 7.13 (s, 1H); $^{13}C\{^{1}H\}$ NMR (DMSO-d_6, 150 MHz): *δ* 139.5, 134.1, 132.8, 132.6, 130.8, 128.9, 128.6, 128.2, 127.8, 127.4, 127.2, 127.0, 126.9, 125.5, 124.9, 124.3, 117.8, 110.5, 90.7; IR (KBr, cm^{-1}): 3225, 2924, 2855, 2224, 1582, 1459, 1377, 1263, 1178, 1100, 1026, 808, 753, 694; HRMS (ESI/Q-TOF) (m/z) calcd for $C_{21}H_{15}N_2$ $[M + H]^+$ 295.1230; found 295.1234.

***5-Phenyl-2-(o-tolyl)-1H-pyrrole-3-carbonitrile (31d)*:**

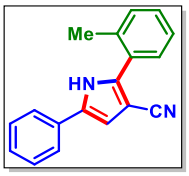

As a white solid (35 mg, 54% yield); Purification over a column of silica gel (5% EtOAc in hexane); ^{1}H NMR (DMSO-d_6, 600 MHz): *δ* 12.25 (s, 1H), 7.75 (d, 2H, *J* = 7.8 Hz), 7.42–7.39 (m, 5H), 7.35–7.34 (m, 1H), 7.27 (t, 1H, *J* = 7.2 Hz), 7.07 (s, 1H), 2.34 (s, 1H); $^{13}C\{^{1}H\}$ NMR (DMSO-d_6, 150 MHz): *δ* 140.3, 136.8, 132.9, 130.9, 130.6, 130.5, 129.8, 129.3, 127.1, 125.9, 124.3, 117.2, 108.6, 92.3, 19.8; IR (KBr, cm^{-1}): 3259, 2924, 2862, 2218, 1601, 1456, 1265, 1175, 1036, 806, 756, 692, 446; HRMS (ESI/Q-TOF) (m/z) calcd for $C_{18}H_{15}N_2$ $[M + H]^+$ 259.1230; found 259.1234.

***2-(4-Ethylphenyl)-5-phenyl-1H-pyrrole-3-carbonitrile (31e)*:**

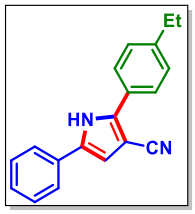

As a white solid (53 mg, 78% yield); Purification over a column of silica gel (5% EtOAc in hexane); ^{1}H NMR (DMSO-d$_6$, 600 MHz): δ 12.14 (s, 1H), 7.80 (d, 2H, J = 7.8 Hz), 7.76 (d, 2H, J = 8.4 Hz), 7.42 (t, 2H, J = 7.5 Hz), 7.38 (d, 2H, J = 8.4 Hz), 7.29 (t, 1H, J = 7.5 Hz), 7.05 (s, 1H), 2.66 (q, 2H, J_1 = 7.8 Hz, J_2 = 7.8 Hz), 1.21 (t, 3H, J = 7.8 Hz); ^{13}C{^{1}H} NMR (DMSO-d$_6$, 150 MHz): δ 144.6, 139.9, 133.5, 130.8, 128.8, 128.4, 127.3, 127.2, 126.6, 124.8, 117.8, 110.1, 89.8, 28.0, 15.6; IR (KBr, cm^{-1}): 3227, 2960, 2923, 2866, 2223, 1602, 1500, 1459, 1301, 1183, 1122, 1001, 833, 805, 759, 690, 512; HRMS (ESI/Q-TOF) (m/z) calcd for $C_{19}H_{17}N_2$ $[M + H]^+$ 273.1386; found 273.1387.

***2-(4-(tert-Butyl)phenyl)-5-phenyl-1H-pyrrole-3-carbonitrile (31f)*:**

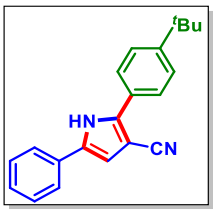

As a white solid (56 mg, 75% yield); Purification over a column of silica gel (5% EtOAc in hexane); ^{1}H NMR (DMSO-d$_6$, 600 MHz): δ 12.14 (s, 1H), 7.80 (d, 2H, J = 7.8 Hz), 7.77 (d, 2H, J = 8.4 Hz), 7.56 (d, 2H, J = 8.4 Hz), 7.43 (t, 2H, J = 7.5 Hz), 7.29 (t, 1H, J = 7.5 Hz), 7.05 (s, 1H), 1.32 (s, 9H); ^{13}C{^{1}H} NMR (DMSO-d$_6$, 150 MHz): δ 151.3, 139.9, 133.5, 130.8, 128.8, 127.2, 126.9, 126.4, 125.7, 124.7, 117.8, 110.0, 89.8, 34.5, 31.0; IR (KBr, cm^{-1}): 3247, 2924, 2860, 2219, 1602, 1537, 1383, 1264, 1457, 1183, 1104, 1022, 834, 807, 755, 690, 526; HRMS (ESI/Q-TOF) (m/z) calcd for $C_{21}H_{21}N_2$ $[M + H]^+$ 301.1699; found 301.1697.

***2-(4-Methoxyphenyl)-5-phenyl-1H-pyrrole-3-carbonitrile (31g)*:**

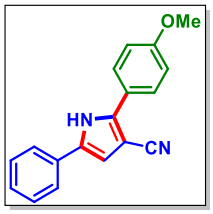

As a white solid (55 mg, 80% yield); Purification over a column of silica gel (5% EtOAc in hexane); ^{1}H NMR (DMSO-d$_6$, 400 MHz): δ 12.05 (s, 1H), 7.80 (d, 4H, J = 7.6 Hz), 7.42 (t, 2H, J = 7.6 Hz), 7.28 (t, 1H, J = 7.4 Hz), 7.11 (d, 2H, J = 8.8 Hz), 7.01 (s, 1H), 3.83 (s, 3H); ^{13}C{^{1}H} NMR (DMSO-d$_6$, 100 MHz): δ 159.5, 139.9, 133.1, 130.8, 128.7, 128.0, 127.1, 124.6, 122.3, 117.9, 114.4, 109.8, 89.2, 55.3; IR (KBr, cm^{-1}): 3217, 2921, 2839, 2223, 1606, 1528, 1463, 1291, 1246, 1176, 1116, 1033, 937, 830, 806, 760, 690, 574, 516; HRMS (ESI/Q-TOF) (m/z) calcd for $C_{18}H_{15}N_2O$ $[M + H]^+$ 275.1179; found 275.1179.

***2-(4-Fluorophenyl)-5-phenyl-1H-pyrrole-3-carbonitrile (31i)*:**

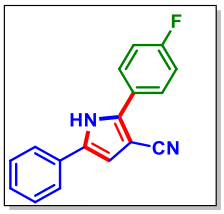

As a white solid (39 mg, 60% yield); Purification over a column of silica gel (5% EtOAc in hexane); ^{1}H NMR (DMSO-d$_6$, 400 MHz): δ 12.19 (s, 1H), 7.89–7.86 (m, 2H), 7.80 (d, 2H, J = 7.8 Hz), 7.45–7.38 (m, 4H), 7.30 (t, 1H, J = 7.4 Hz), 7.05 (s, 1H); ^{13}C{^{1}H} NMR (DMSO-d$_6$, 100 MHz): δ 162.1 (d, J = 245.0 Hz), 138.6, 133.7, 130.7, 128.8, 128.77, 128.74, 127.3, 126.2 (d, J = 3.2 Hz), 124.8, 117.5, 115.9 (d, J = 21.8 Hz), 90.2; IR (KBr, cm^{-1}): 3228, 2923, 2855, 2220, 1603, 1529, 1494, 1458, 1247, 1182, 1100, 1024, 835, 807, 756, 689, 511; HRMS (ESI/Q-TOF) (m/z) calcd for $C_{17}H_{12}FN_2$ [M + H]$^+$ 263.0979; found 263.0974.

***2-(4-Chlorophenyl)-5-phenyl-1H-pyrrole-3-carbonitrile (31j)*:**

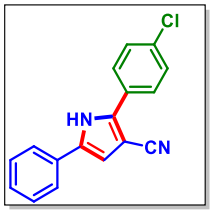

As a white solid (38 mg, 55% yield); Purification over a column of silica gel (5% EtOAc in hexane); ^{1}H NMR (DMSO-d$_6$, 600 MHz): δ 12.26 (s, 1H), 7.86 (d, 2H, J = 8.4 Hz), 7.80 (d, 2H, J = 7.8 Hz), 7.63 (d, 2H, J = 8.4 Hz), 7.44 (t, 2H, J = 7.5 Hz), 7.31 (t, 1H, J = 7.5 Hz), 7.09 (s, 1H); ^{13}C{^{1}H} NMR (DMSO-d$_6$, 150 MHz): δ 138.2, 134.2, 133.2, 130.6, 129.1, 128.8, 128.5, 128.2, 127.5, 124.9, 117.5, 110.4, 90.6; IR (KBr, cm^{-1}): 3226, 2923, 2854, 2223, 1597, 1463, 1299, 1268, 1181, 1092, 1014, 830, 809, 760, 689, 604, 495; HRMS (ESI/Q-TOF) (m/z) calcd for $C_{17}H_{12}ClN_2$ [M + H]$^+$ 279.0684; found 279.0692.

***2-(4-Bromophenyl)-5-phenyl-1H-pyrrole-3-carbonitrile (31l)*:**

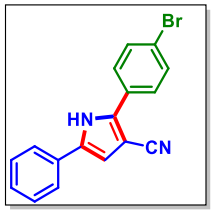

As a white solid (42 mg, 52% yield); Purification over a column of silica gel (5% EtOAc in hexane); ^{1}H NMR (DMSO-d$_6$, 600 MHz): δ 12.26 (s, 1H), 7.80 (d, 4H, J = 8.4 Hz), 7.76 (d, 2H, J = 9.0 Hz), 7.44 (t, 2H, J = 7.8 Hz), 7.31 (t, 1H, J = 7.5 Hz), 7.09 (s, 1H); ^{13}C{^{1}H} NMR (DMSO-d$_6$, 150 MHz): δ 138.2, 134.2, 131.9, 130.6, 128.8, 128.4, 127.5, 124.93, 124.87, 121.8, 117.5, 110.5, 90.6; IR (KBr, cm^{-1}): 3227, 2923, 2855, 2223, 1600, 1461, 1387, 1301, 1262, 1184, 1074, 1022, 807, 761, 690, 492; HRMS (ESI/Q-TOF) (m/z) calcd for $C_{17}H_{12}BrN_2$ [M + H]$^+$ 323.0178; found 323.0171.

V.9. Representative NMR Spectra:

***2,4,6-Triphenylnicotinonitrile (1a)*: ^{1}H NMR ($CDCl_3$, 400 MHz)**

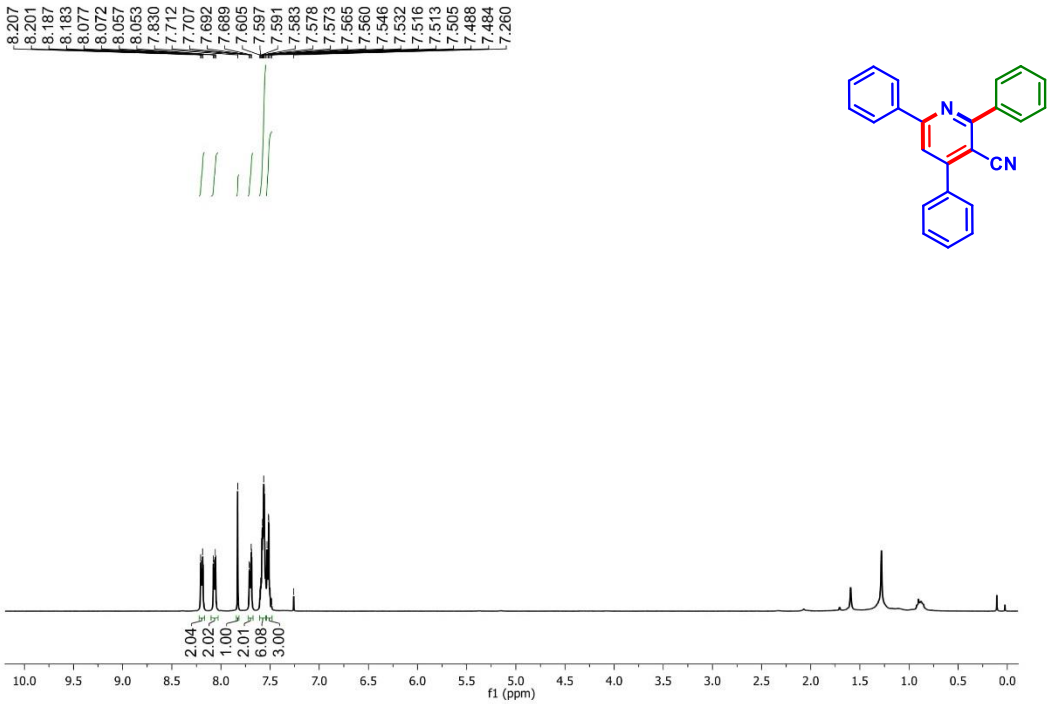

***2,4,6-Triphenylnicotinonitrile (1a)*: $^{13}C\{^{1}H\}$ NMR ($CDCl_3$, 100 MHz)**

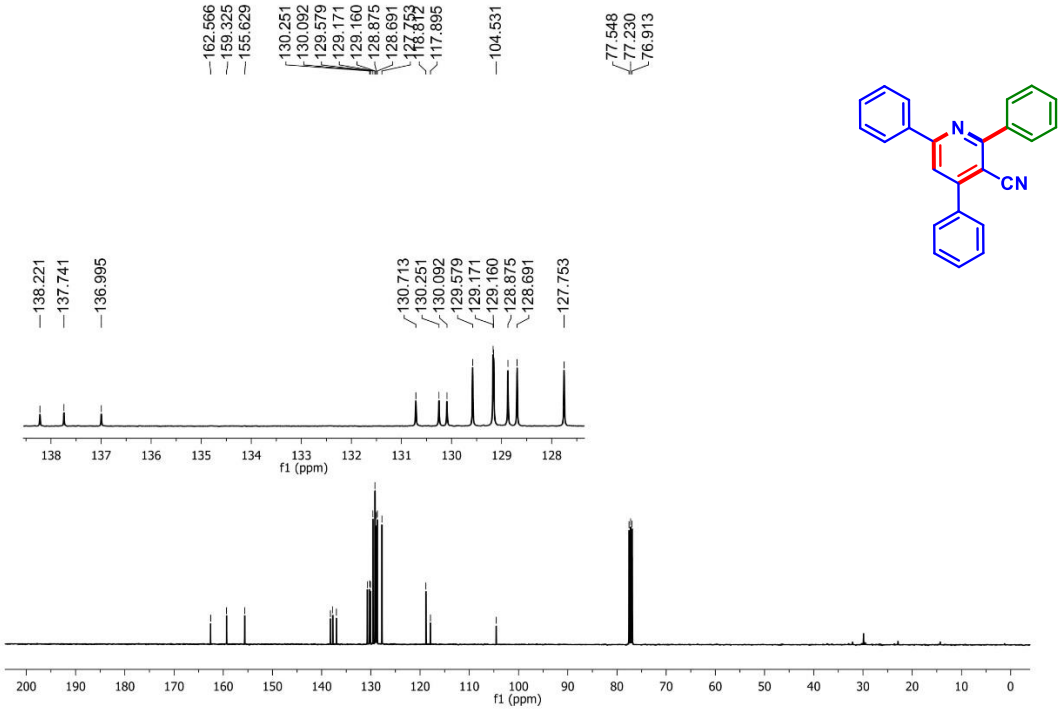

2,6-Diphenyl-4-(p-tolyl)nicotinonitrile (2a): ^{1}H NMR (CDCl$_3$, 400 MHz)

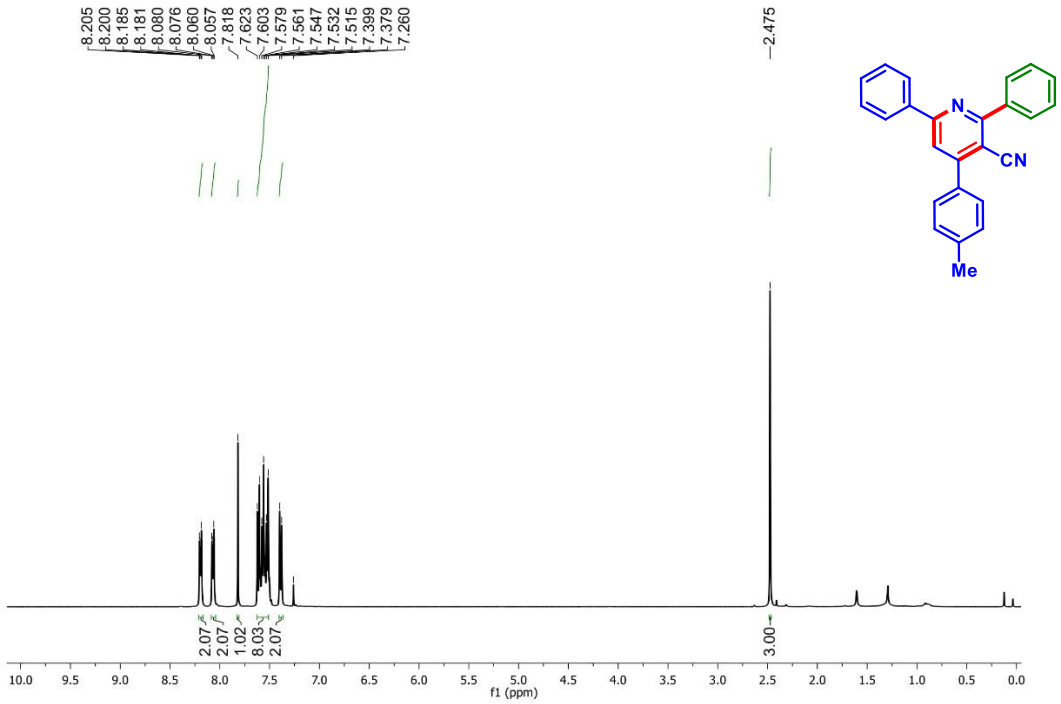

2,6-Diphenyl-4-(p-tolyl)nicotinonitrile (2a): ^{13}C{^{1}H} NMR (CDCl$_3$, 100 MHz)

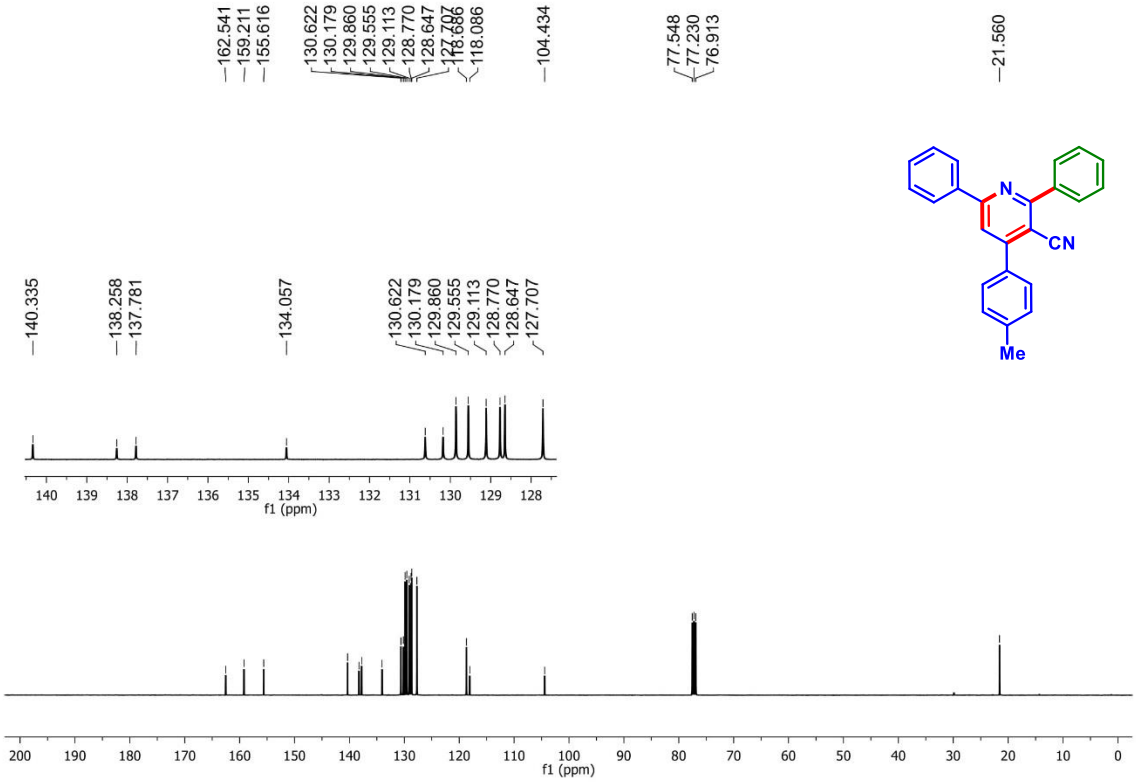

4-(4-Chlorophenyl)-2,6-diphenylnicotinonitrile (9a): ^{1}H NMR ($CDCl_3$, 400 MHz)

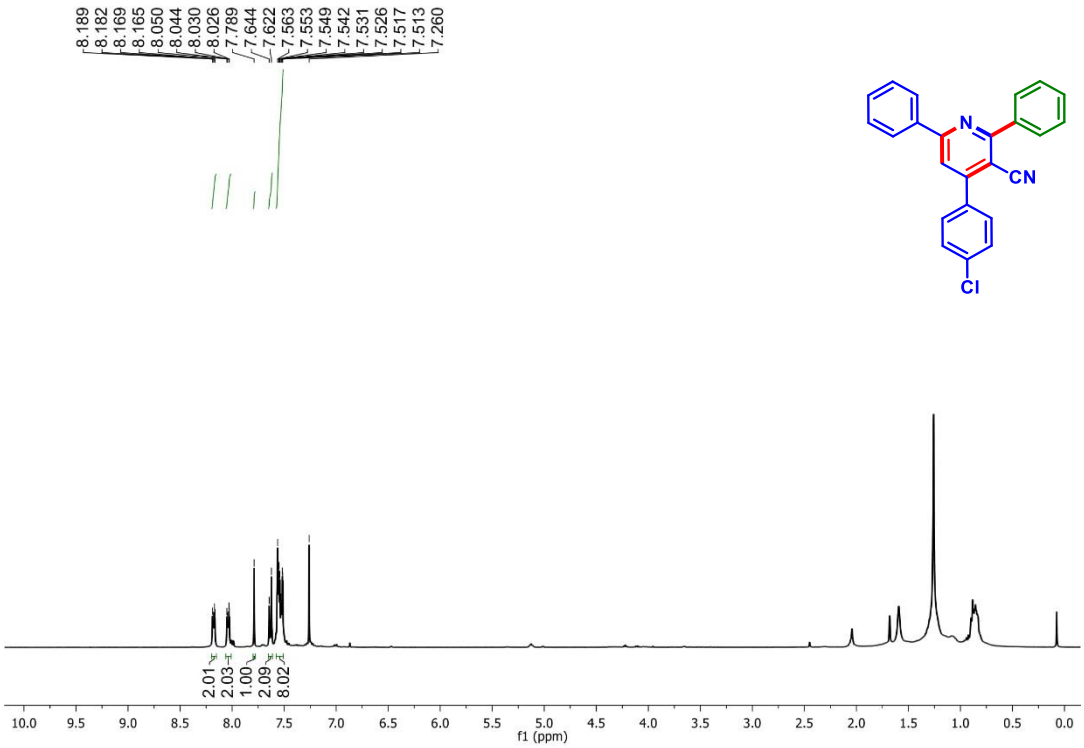

4-(4-Chlorophenyl)-2,6-diphenylnicotinonitrile (9a): $^{13}C\{^{1}H\}$ NMR ($CDCl_3$, 100 MHz)

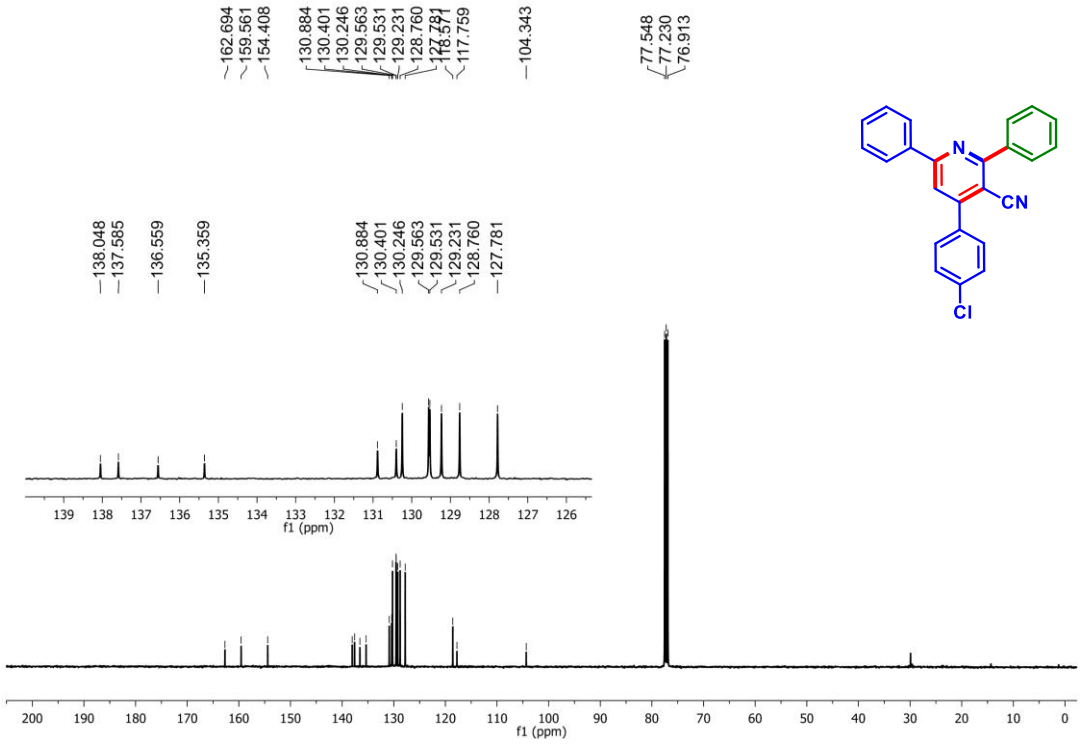

2,4-Diphenyl-6-(p-tolyl)nicotinonitriletrile (12a): ^{1}H NMR ($CDCl_3$, 400 MHz)

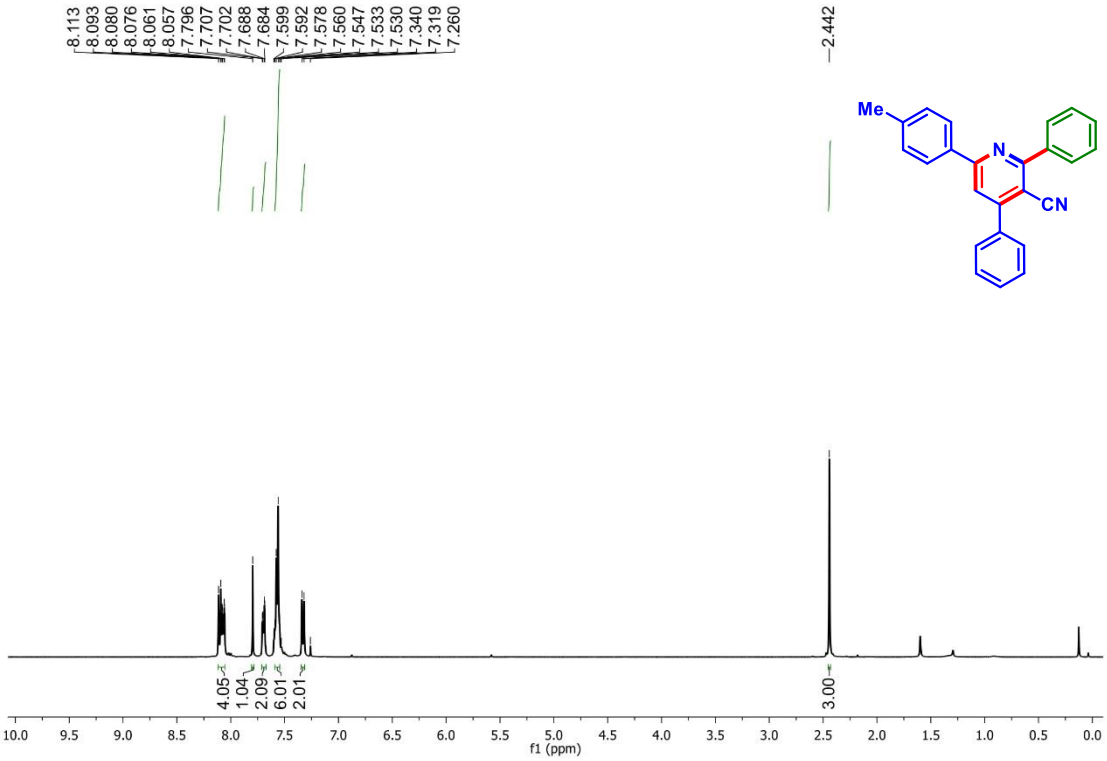

2,4-Diphenyl-6-(p-tolyl)nicotinonitriletrile (12a): $^{13}C\{^{1}H\}$ NMR ($CDCl_3$, 100 MHz)

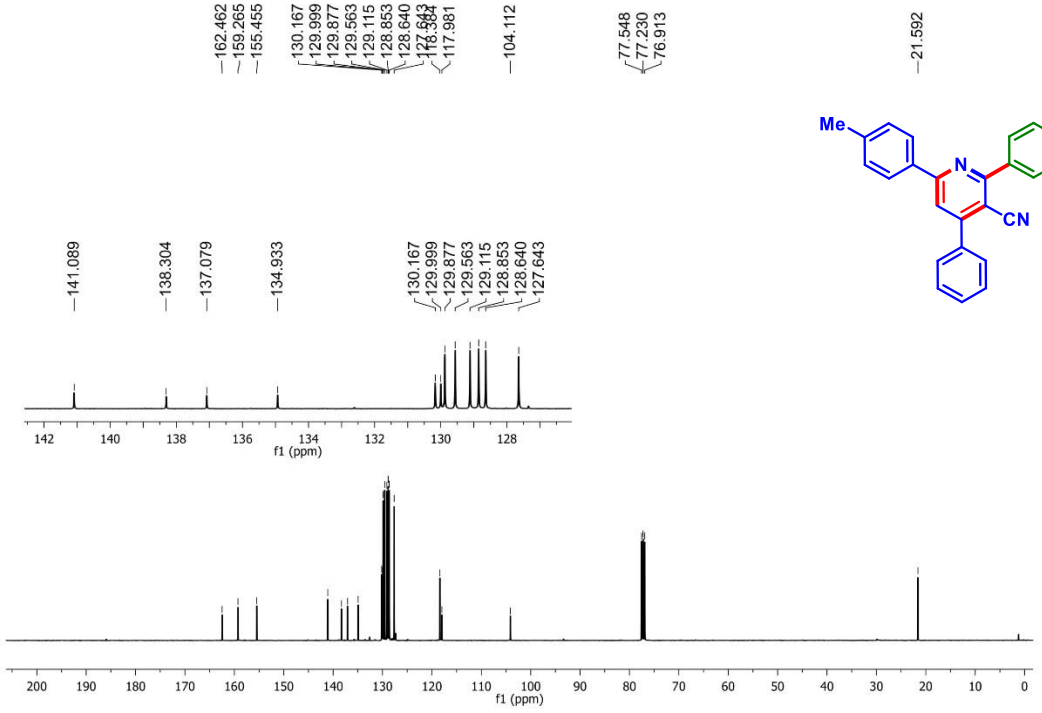

6-(4-Chlorophenyl)-2,4-diphenylnicotinonitrile (15a): ^{1}H NMR ($CDCl_3$, 400 MHz)

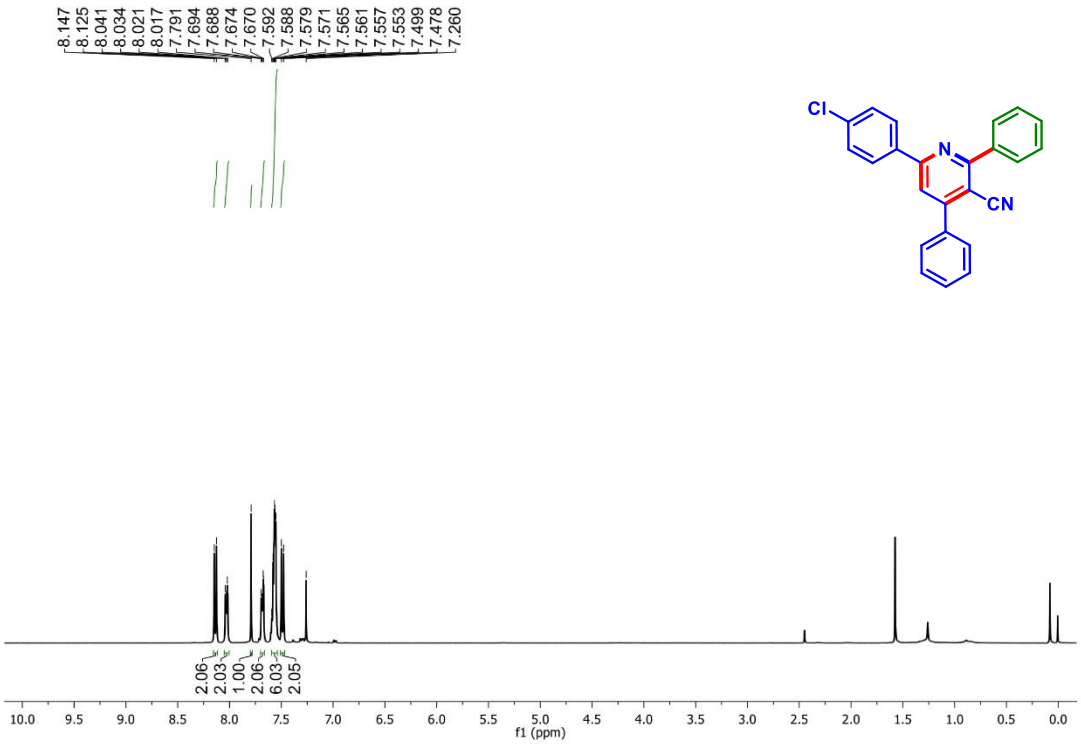

6-(4-Chlorophenyl)-2,4-diphenylnicotinonitrile (15a): $^{13}C\{^{1}H\}$ NMR ($CDCl_3$, 100 MHz)

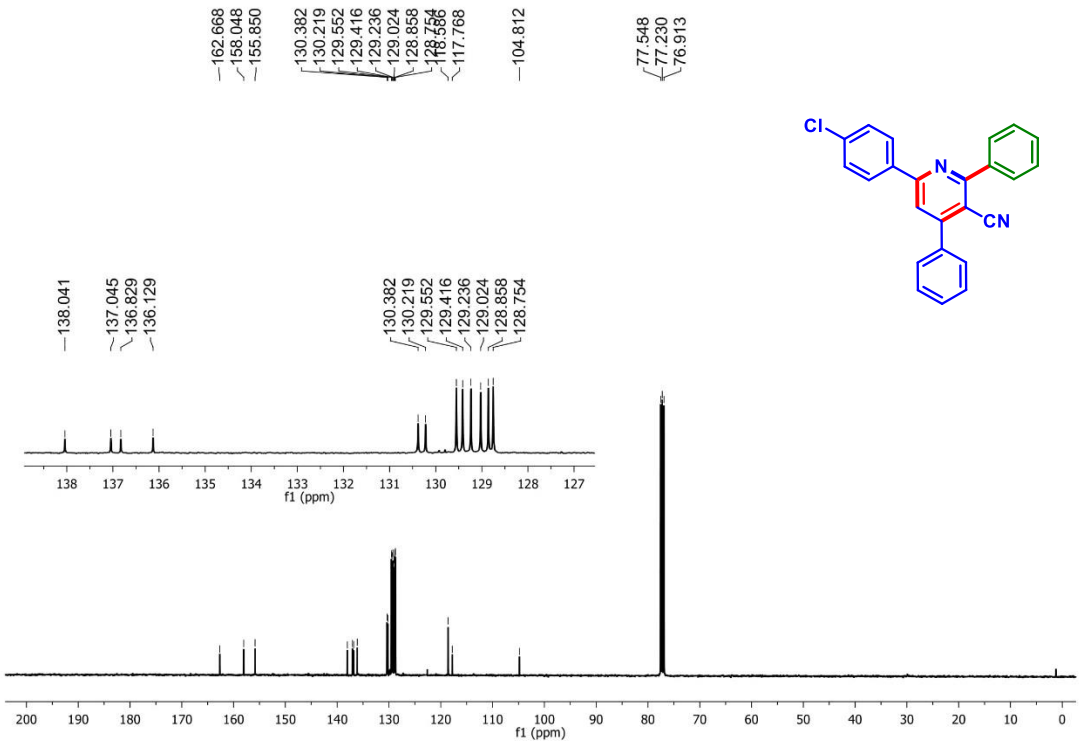

4,6-Diphenyl-2-(p-tolyl)nicotinonitrile (1c): ^{1}H NMR (CDCl$_3$, 400 MHz)

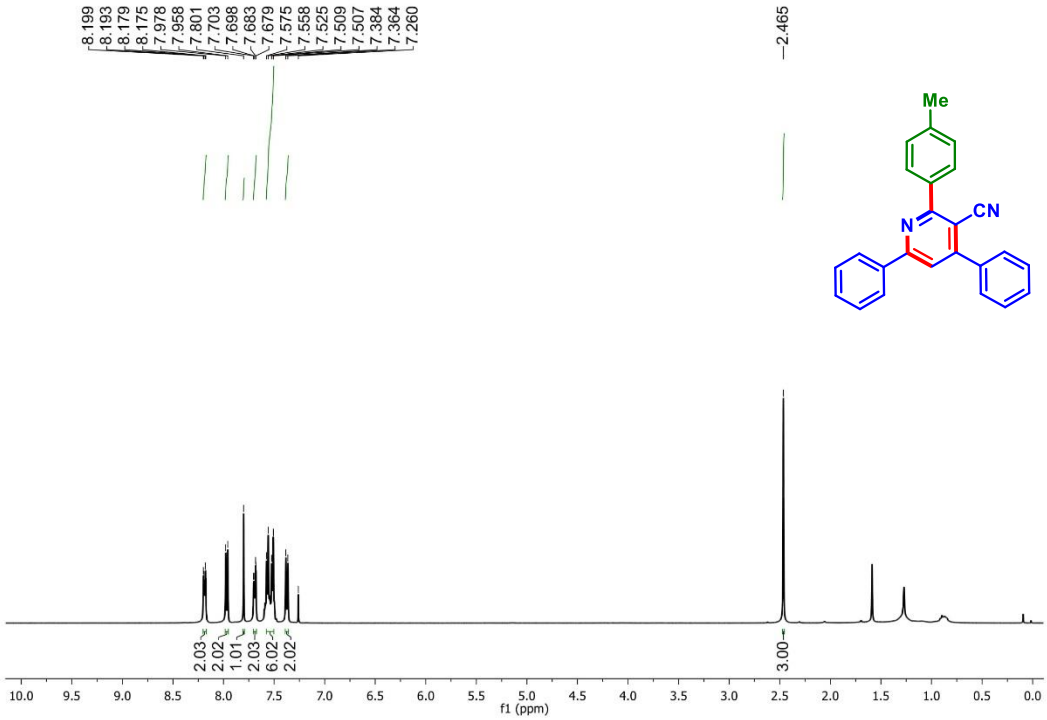

4,6-Diphenyl-2-(p-tolyl)nicotinonitrile (1c): ^{13}C{^{1}H} NMR (CDCl$_3$, 100 MHz)

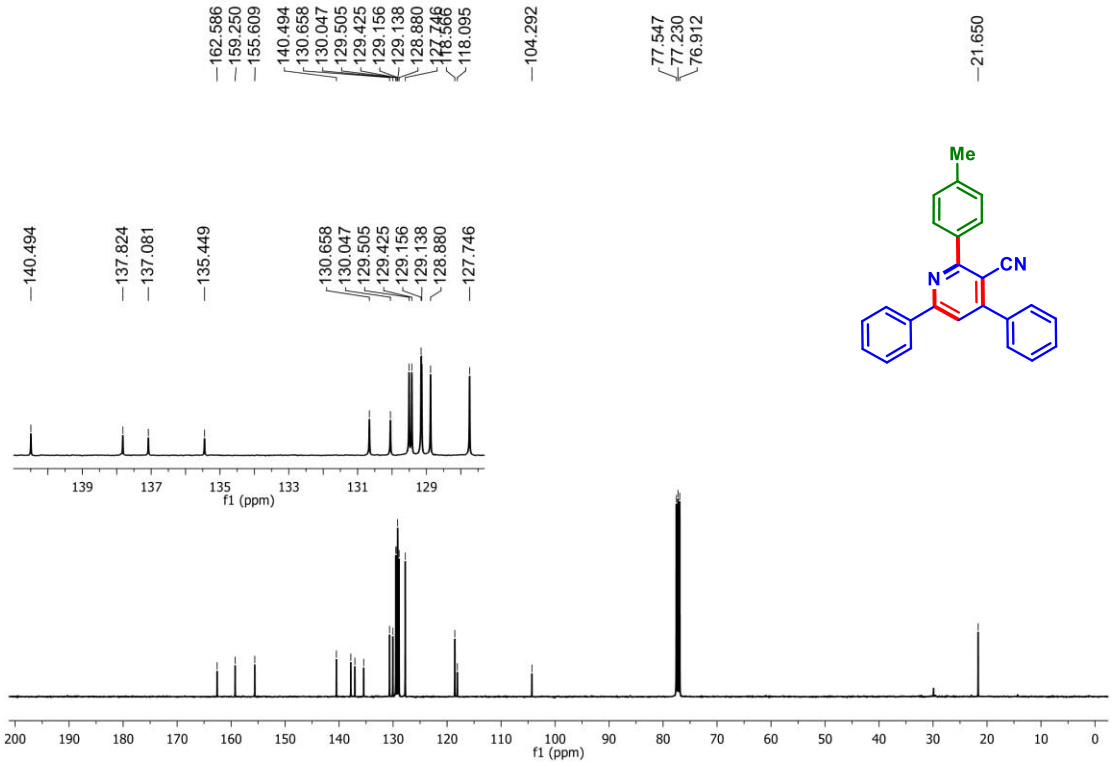

2-(4-Chlorophenyl)-4,6-diphenylnicotinonitrile (1j): ^{1}H NMR (CDCl$_3$, 400 MHz)

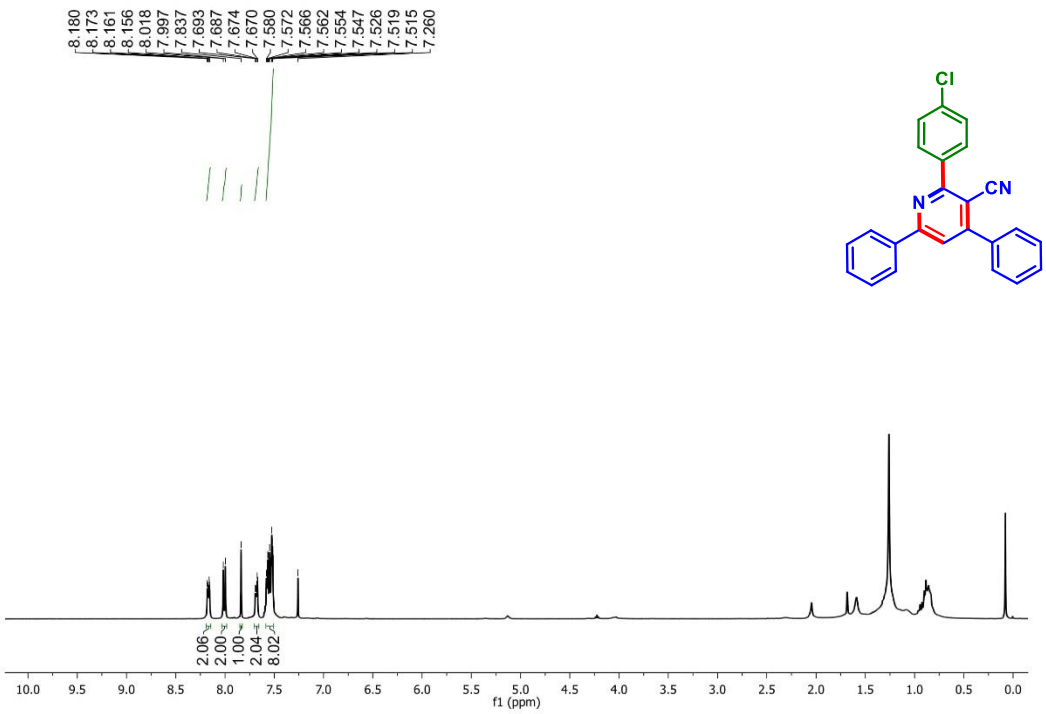

2-(4-Chlorophenyl)-4,6-diphenylnicotinonitrile (1j): ^{13}C{^{1}H} NMR (CDCl$_3$, 100 MHz)

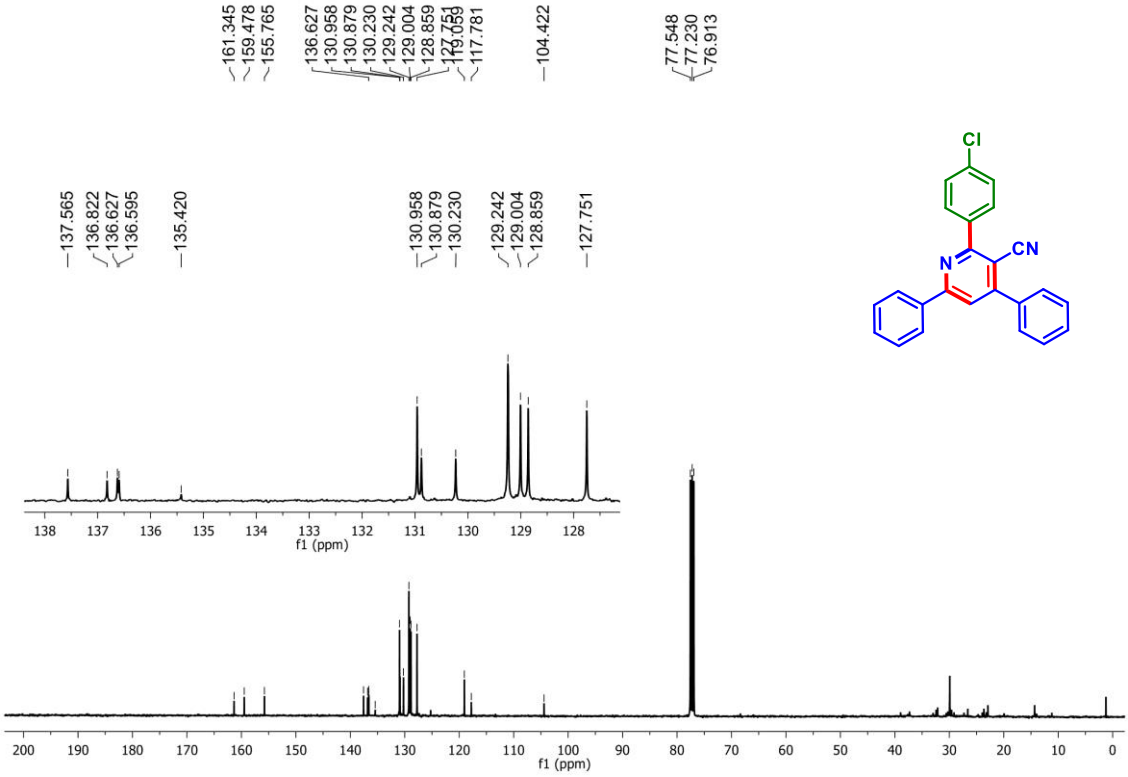

2,5-Diphenyl-1H-pyrrole-3-carbonitrile (31a): ^{1}H NMR (DMSO-d_6, 600 MHz)

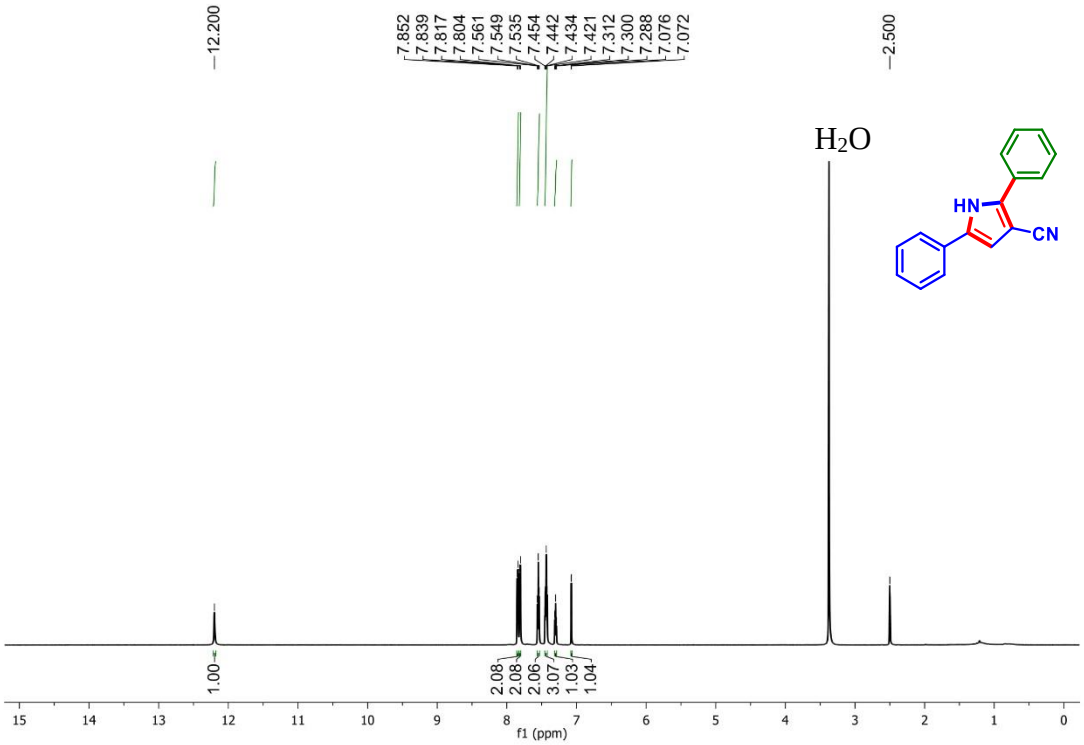

2,5-Diphenyl-1H-pyrrole-3-carbonitrile (31a): $^{13}C\{^{1}H\}$ NMR (DMSO-d_6, 150 MHz)

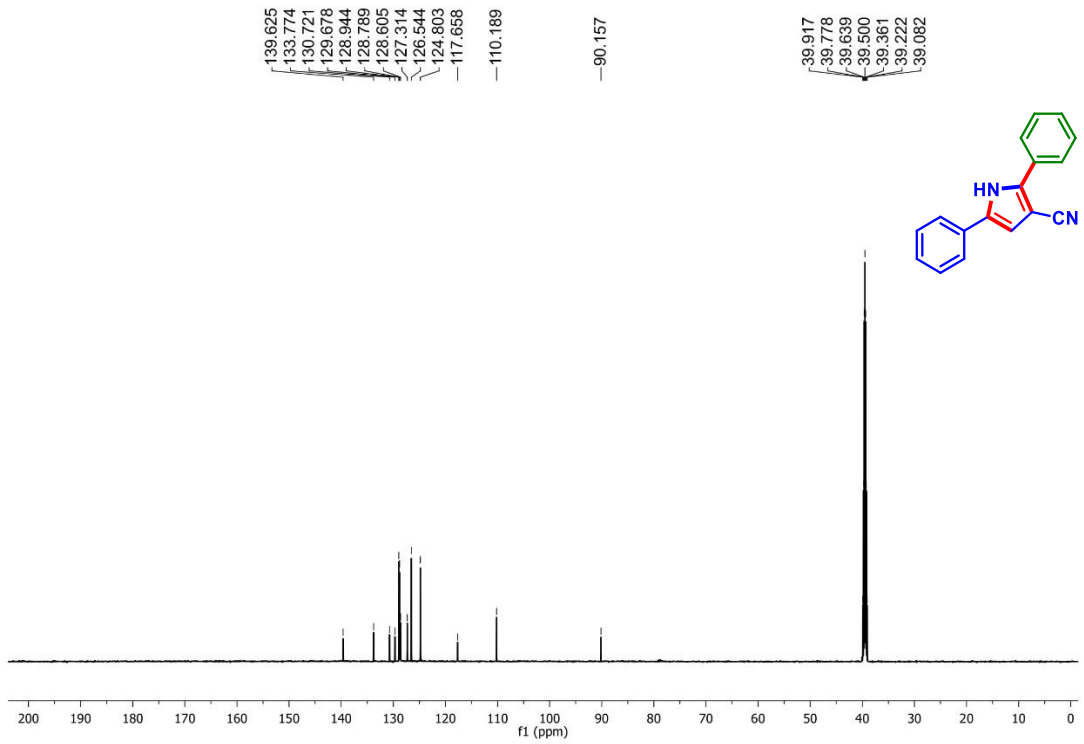

2-Phenyl-5-(p-tolyl)-1H-pyrrole-3-carbonitrile (32a): ^{1}H NMR (DMSO-d$_6$, 600 MHz)

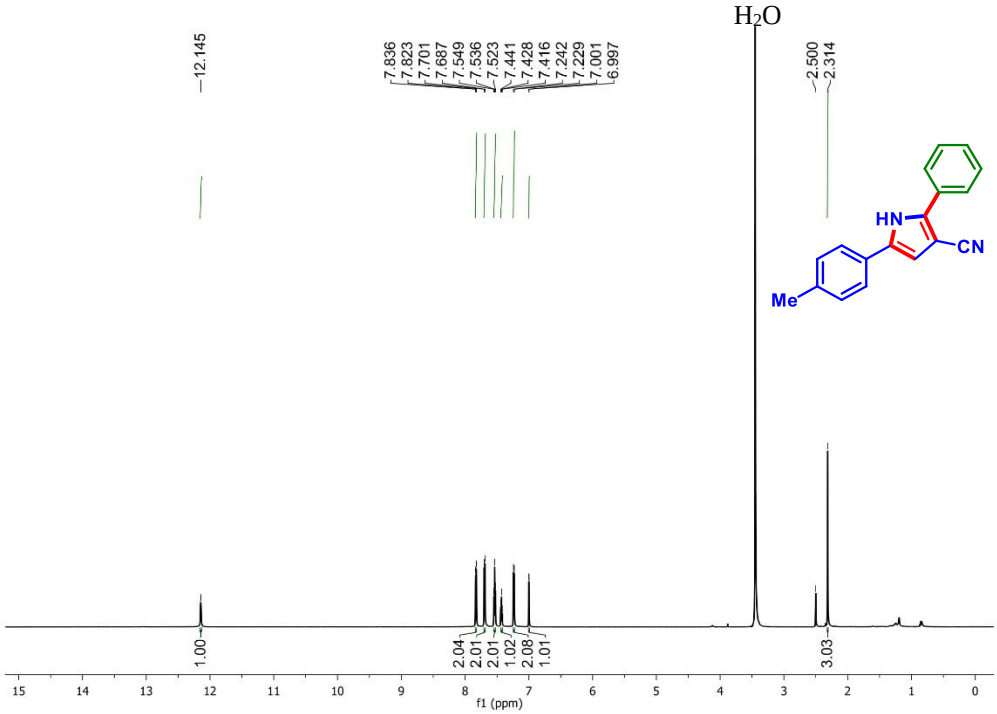

2-Phenyl-5-(p-tolyl)-1H-pyrrole-3-carbonitrile (32a): ^{13}C{^{1}H} NMR (DMSO-d$_6$, 150 MHz)

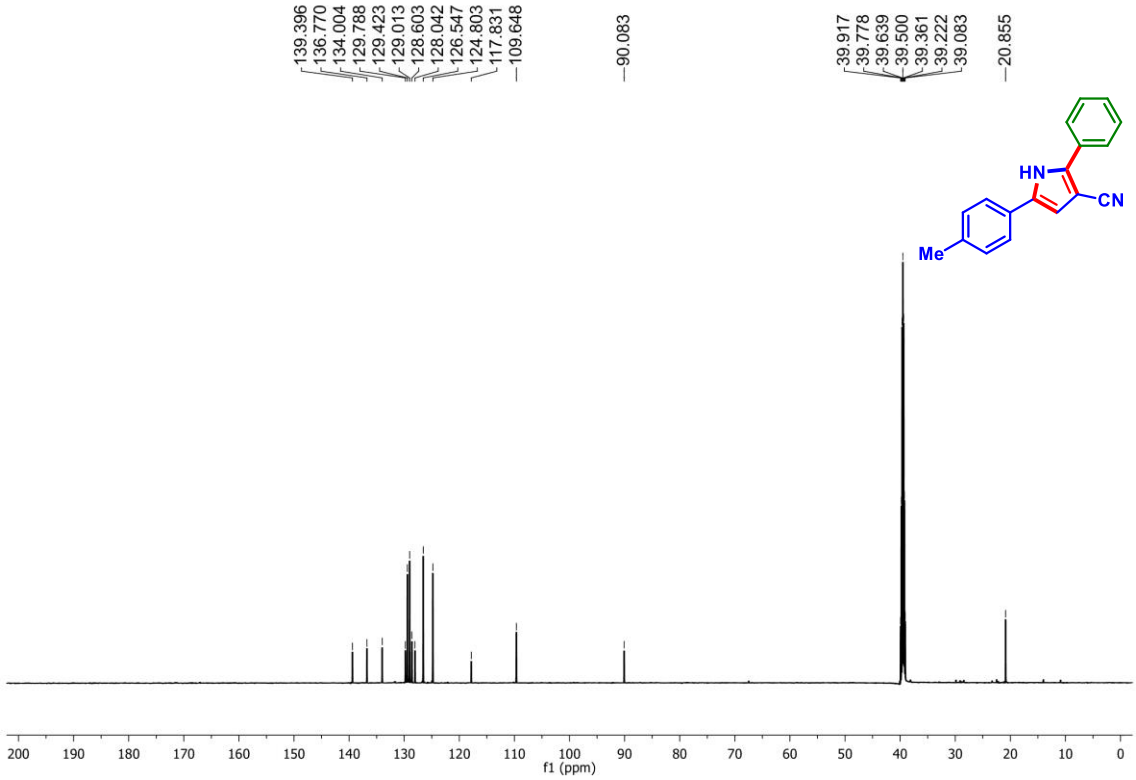

5-(4-Chlorophenyl)-2-phenyl-1H-pyrrole-3-carbonitrile (34a): ^{1}H NMR (DMSO-d_6, 400 MHz)

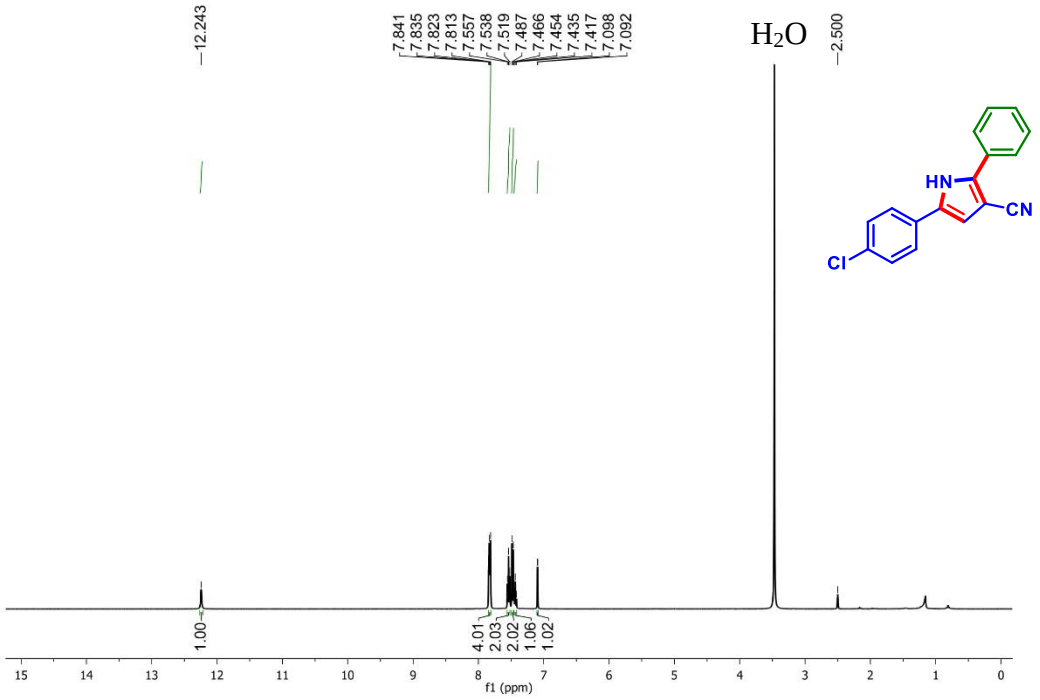

5-(4-Chlorophenyl)-2-phenyl-1H-pyrrole-3-carbonitrile (34a): $^{13}C\{^{1}H\}$ NMR (DMSO-d_6, 100 MHz)

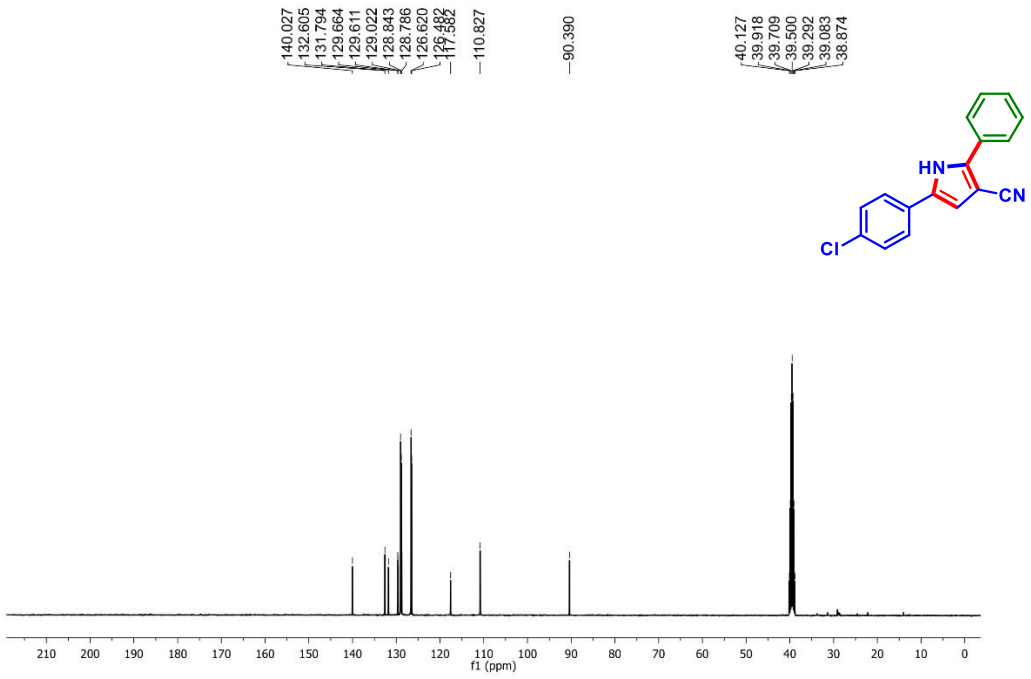

2-(4-Methoxyphenyl)-5-phenyl-1H-pyrrole-3-carbonitrile (31g): ^{1}H NMR (DMSO-d_6, 400 MHz)

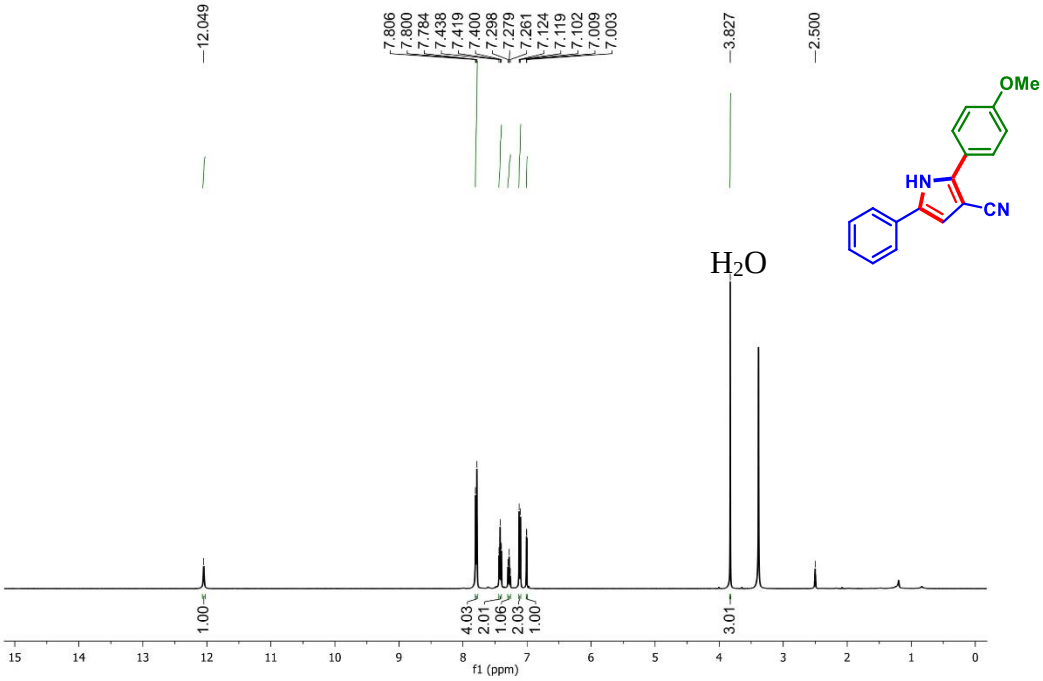

2-(4-Methoxyphenyl)-5-phenyl-1H-pyrrole-3-carbonitrile (31g): $^{13}C\{^{1}H\}$ NMR (DMSO-d_6, 100 MHz)

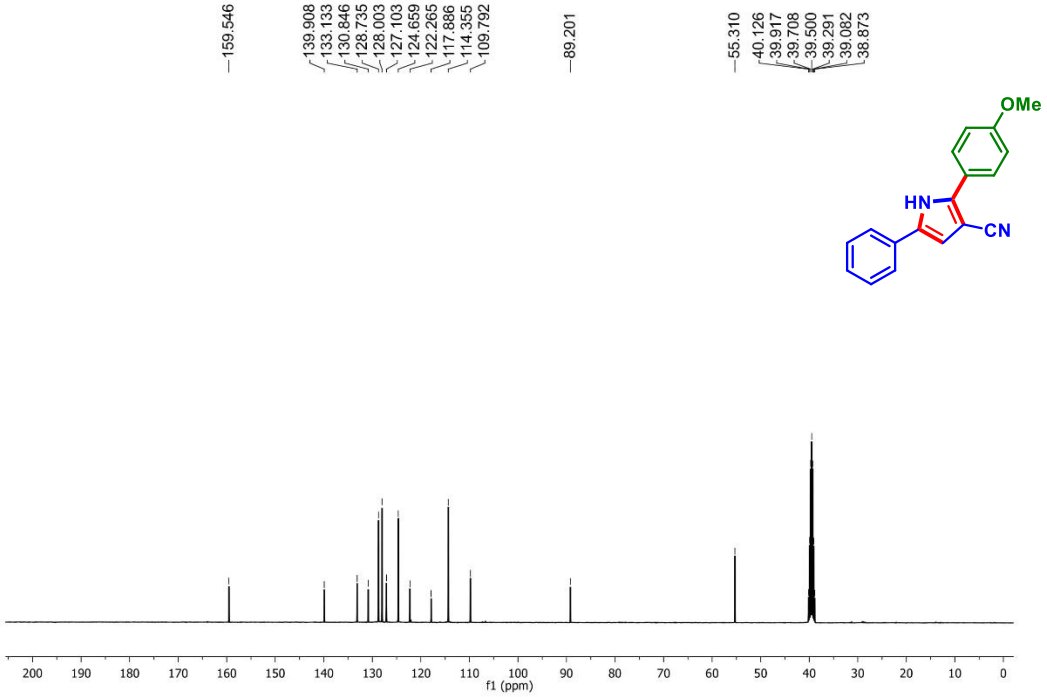

2-(4-Chlorophenyl)-5-phenyl-1H-pyrrole-3-carbonitrile (31j): ^{1}H NMR (DMSO-d_6, 600 MHz)

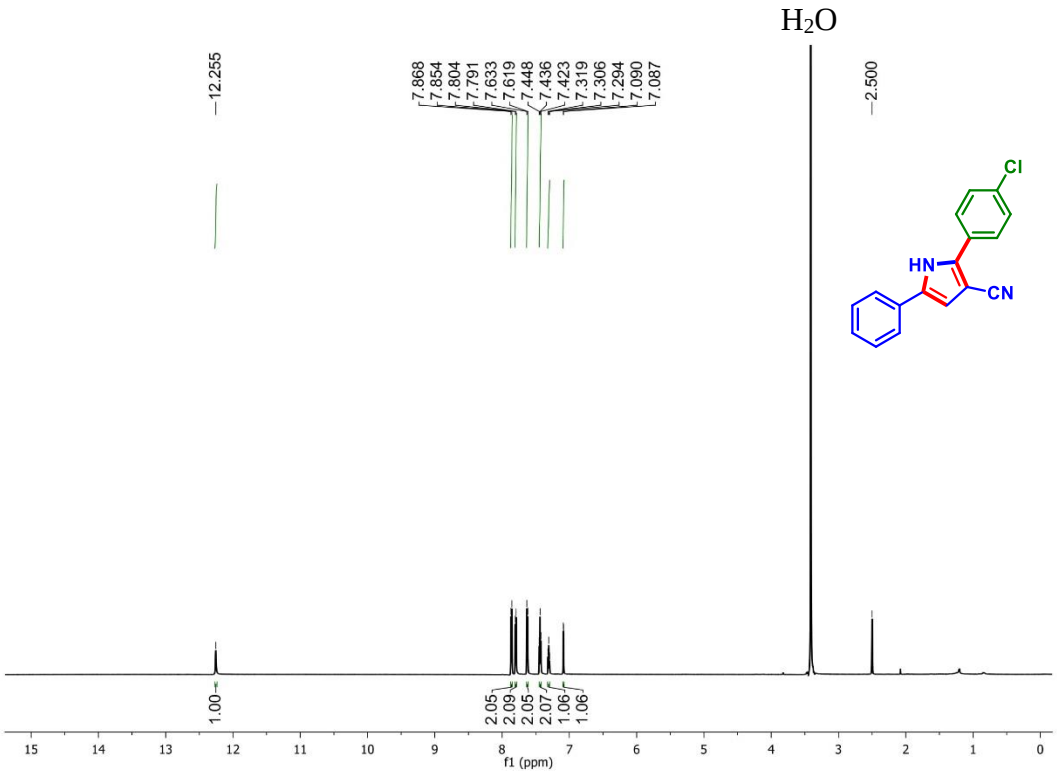

2-(4-Chlorophenyl)-5-phenyl-1H-pyrrole-3-carbonitrile (31j): $^{13}C\{^{1}H\}$ NMR (DMSO-d_6, 150 MHz)

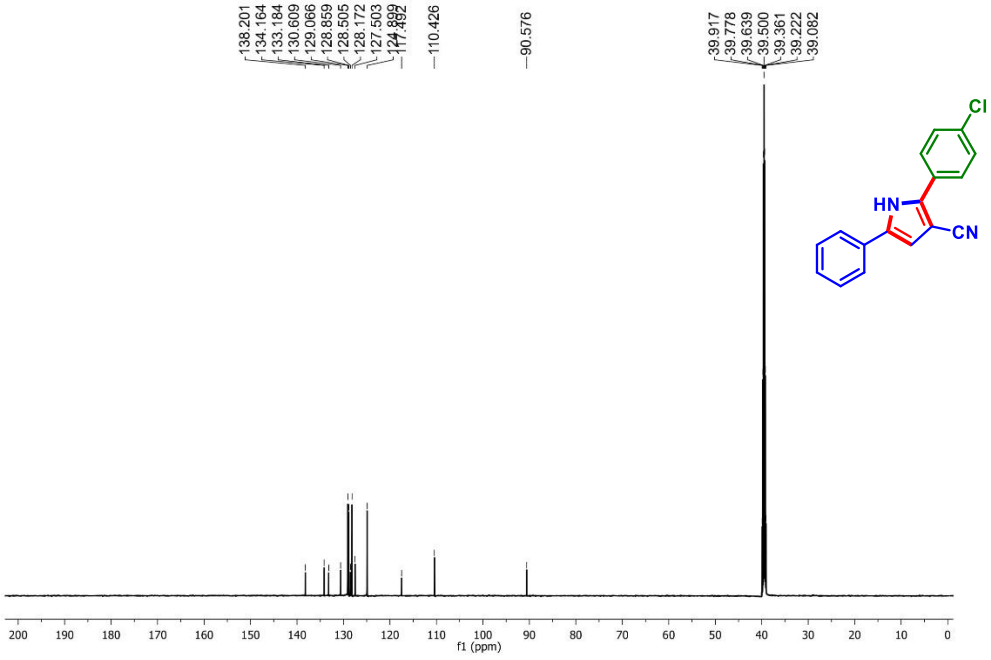

V.10. References:

[1] (a) Eicher, T.; Hauptmann, S.; Speicher, A. *The Chemistry of Heterocycles, Wiley-VCH Verlag GmbH & Co, Weinheim, 2nd edn.* **2003**. (b) Su, S.-J.; Sasabe, H.; Takeda, T.; Kido, J. *Chem. Mater*. **2008**, *20*, 1691–1693. (c) Hill, M. D. *Chem. Eur. J.* **2010**, *16*, 12052–12062. (d) Allais, C.; Grassot, J.-M.; Rodriguez, J.; Constantieux, T. *Chem. Rev.* **2014**, *114*, 10829–10868. (e) Yang, L.; Mihali, V.-A.; Brandell, D.; Strømme, M.; Sjödin, M. *J. Phys. Chem.* **2014**, *118*, 25956–25963. (f) Prachayasittikul, S.; Pingaew, R.; Worachartcheewan, A.; Sinthupoom, N.; Prachayasittikul, V.; Ruchirawat, S.; Prachayasittikul, V. *Mini-Rev. Med. Chem.* **2017**, *17*, 869–901 and references cited therein. (g) Stolar, M.; Baumgartner, T. *Chem. Commun.* **2018**, *54*, 3311–3322. (h) Panja, S.; Ghosh, S.; Ghosh, K. *New J. Chem*. **2018**, *42*, 6488–6497.

[2] Chelucci, G. *Chem. Soc. Rev.* **2006**, *35*, 1230–1243.

[3] (a) Constable, E. C.; Housecroft, C. E.; Neuburger, M.; Phillips, D.; Raithby, P. R.; Schofield, E.; Sparr, E.; Tocher, D. A.; Zehnder, M.; Zimmermann, Y. *J. Chem. Soc., Dalton Trans.* **2000**, *13*, 2219–2228. (b) Wang, P.; Moorefield, C. N.; Newkome, G. R. *Angew. Chem., Int. Ed.* **2005**, *44*, 1679–1683. (c) Constable, E. C.; Dunphy, E. L.; Housecroft, C. E.; Kylberg, W.; Neuberger, M.; Schaffner, S.; Schofield, E. R.; Smith, C. B. *Chem. Eur. J*. **2006**, *12*, 4600–4610.

[4] (a) Han, H.; Hurley, L. H. *Trends Pharmacol. Sci*. **2000**, *21*, 136–142. (b) Li, J. L.; Harrison, R. J.; Reszka, A. P.; Brosh, R. M.; Bohr, V. A.; Neidle, S.; Hickson, I. D. *Biochemistry*. **2001**, *40*, 15194–15202. (c) Dexheimer, T. S.; Sun, D.; Hurley, L. H. *J. Am. Chem. Soc*. **2006**, *128*, 5404–5415. (d) Waller, Z. A. E.; Shirude, P. S.; Rodriguez, R.; Balasubramanian, S. *Chem. Commun*. **2008**, 1467–1469. (e) Smith, N. M.; Labrunie, G.; Corry, B.; Tran, P. L. T.; Norret, M.; Djavaheri-Mergny, M.; Raston, C. L.; Mergny, J.-L. *Org. Biomol. Chem*. **2011**, *9*, 6154–6162.

[5] (a) Curran, D.; Grimshaw, J.; Perera, S. D. *Chem. Soc. Rev*. **1991**, *20*, 391–404. (b) Santo, R. D.; Costi, R.; Artico, M.; Miele, G.; Lavecchia, A.; Novellino, E.; Bergamini, A.; Cancio, R.; Maga, G. *ChemMedChem* **2006**, *1*, 1367–1378. (c) Fan, H.; Peng, J.; Hamann, M. T.; Hu, J.-F. *Chem. Rev*. **2008**, *108*, 264–287. (d) Morris, J. C.; Phillips, A.

J. *Nat. Prod. Rep*. **2008**, *25*, 95–117. (e) Thirumalairajan, S.; Pearce, B. M.; Thompson, A. *Chem. Commun*. **2010**, *46*, 1797–1812. (f) Li, C.-S.; Tsai, Y.-H.; Lee, W.-C.; Kuo, W.-J. *J. Org. Chem*. **2010**, *75*, 4004–4013. (g) Bhardwaj, V.; Gumber, D.; Abbot, V.; Dhiman, S.; Sharma, P. *RSC Adv*. **2015**, *5*, 15233–15266 and references cited therein.

[6] (a) Kros, A.; Nolte, R. J. M.; Sommerdijk, N. A. J. M. *Adv. Mater*. **2002**, *14*, 1779–1782. (b) Gabriel, S.; Cécius, M.; Fleury-Frenette, K.; Cossement, D.; Hecq, M.; Ruth, N.; Jérôme, R.; Jérôme, C. *Chem. Meter*. **2007**, *19*, 2364–2371. (c) Nishide, H.; Oyaizu, K. *Science*. **2008**, *319*, 737–738. (d) Hagfeldt, A.; Boschloo, G.; Sun, L.; Kloo, L.; Pettersson, H. *Chem. Rev*. **2010**, *110*, 6595–6663.

[7] (a) **Nexium**: Boushra A. F.; Elsayed, A. M.; Ibrahim, N. A.; Abdelwahed, M. K.; Ahmed. E. I. A. *Mol. Biol. Rep*. **2019**, *46*, 4843–4860. (b) **Aciphex:** Baldwin, C. M.; Keam, S. J. *Drugs*. **2009**, 69, 1373–1401. (c) **Avandia (Rosiglitazone A):** Liu, J.; Huang, Z.; Ma, W.; Peng, S.; Li, Y.; Miranda, K. M.; Zhang, Y. *Eur. J. Med. Chem*. **2019**, *162*, 650–665. (d) **Actos (Pioglitazone B):** Mosure, S. A.; Shang, J.; Eberhardt, J.; Brust, R.; Zheng. J.; Griffin, P. R.; Forli, S.; Kojetin, D. J. *J. Med. Chem*. **2019**, 62, 2008–2023. (e) **Amrinone D (Inocor):** Charrier, J.-D.; Miller, A.; Kay, D. P.; Brenchley, G.; Twin, H. C.; Collier, P. N.; Ramaya, S.; Keily, S. B.; Durrant, S. J.; Knegtel, R. M. A.; Tanner, A. J.; Brown, K.; Curnock, A. P.; Jimenez, J.-M. *J. Med. Chem*. **2011**, *54*, 2341–2350. (f) **Etoricoxib (Arcoxia):** Croom, K. F.; Siddiqui, M. A. A. *Drugs*. **2009**, *69*, 1513–1532. (g) **Gleevec:** Takami, A.; Ohtake, S.; Morishita, E.; Terasaki, Y.; Fukushima, T.; Kurokawa, T.; Sugimori, N.; Matono, S.; Ohata, K.; Saito, C.; Yamaguchi, M.; Hosokawa, K.; Yamazaki, H.; Kondo, Y.; Nakao, S. *Int. J. Hematol*. **2012**, *96*, 357–363. (h) **Sorafenib (nexovar):** Chen, F.; Fang, Y.; Zhao, R.; Le, J.; Zhang, B.; Huang, R.; Chen, Z.; Shao, J. *Eur. J. Med. Chem*. **2019**, *179*, 916–936. (i) **Crizotinib (Xalkori):** Frampton, J. E. *Drugs*. **2013**, *73*, 2031–2051. (j) **Nilotnib:** Garnock-Jones, K. P.. *Drugs*. **2011**, *71*, 1579–1590. (k) **Altrazanavir (Reyataz):** Croom, K. F.; Dhillon, S.; Keam, S. J. *Drugs*. **2012**, *69*, 1107–1140.

[8] (a) **Atrovastatin**: Thompson, R. B. *Foundations for Blockbuster Drugs in Federally Sponsored Research FASEB J*. **2001**, *66*, 405. (b) **Ketorolac**: Mallinson, T. E. A. *J. Paramed. Pract*. **2017**, *9*, 522–526. (c) **Tolmetin**: Brogden, R. N.; Heel, R. C.; Speight,

T. M.; Avery, G. S. *Drugs.* **2012**, *15*, 429–450. (d) **Sunitinib**: Tourneau, C. Le.; Raymond, E.; Faivre, S. *Ther. Clin. Risk Manag.* **2007**, *3*, 341–348. (e) **Pyrvinium**: Cui, L.; Zhao, J.; Liu, J. *Am. J. Med. Sci.* **201**, *355*, 274–280.

[9] (a) Romero, N. A.; Nicewicz, D. A. *Chem. Rev.* **2016**, *116*, 10075–10166 and references cited therein. (b) Shaw, M. H.; Twilton, J.; MacMillan, D. W. C. *J. Org. Chem.* **2016**, *81*, 6898–6926. (c) Marzo, L.; Pagire, S. K.; Reiser, O.; König, B. *Angew. Chem., Int. Ed.* **2018**, *57*, 10034–10072. (d) Milligan, J. A.; Phelan, J. P.; Badir, S. O.; Molander, G. A. *Angew. Chem., Int. Ed.* **2019**, *58*, 6152–6163. (e) Xu, R.; Cai, C. *Chem. Commun.* **2019**, *55*, 4383–4386. (f) Shukla, G.; Alam, T.; Srivastava, H. K.; Kumar, R.; Patel, B. K. *Org. Lett.* **2019**, *21*, 3543–3547. (g) Yadav, A. K.; Sharma, A. K.; Singh, K. N. *Org. Chem. Front.* **2019**, *6*, 989–993. (h) Alam, T.; Rakshit, A.; Begum, P.; Dahiya, A.; Patel, B. K. *Org. Lett.* **2020**, *22*, 3728–3733. (i) Gupta, P. K.; Yadav, A. K.; Singh, K. N. *Asian J. Org. Chem.* **2020**, *9*, 1213–1216.

[10] (a) Kalyani, D.; McMurtrey, K. B.; Neufeldt, S. R.; Sanford, M. S. *J. Am. Chem. Soc.* **2011**, *133*, 18566–18569. (b) Lang, S. B.; O'Nele, K. M.; Tunge, J. A. *J. Am. Chem. Soc.* **2014**, *136*, 13606–13609. (c) Xuan, J.; Zeng, T.-T.; Feng, Z.-J.; Deng, Q.-H.; Chen, J.-R.; Lu, L.-Q.; Xiao, W.-J.; Alper, H. *Angew. Chem., Int. Ed.* **2015**, *54*, 1625–1628. (d) Jian g, J.; Zhang, W.-M.; Dai, J.-J.; Xu, J.; Xu, H.-J. *J. Org. Chem.* **2017**, *82*, 3622–3630. (e) Kato, S.; Saga, Y.; Kojima, M.; Fuse, H.; Matsunaga, S.; Fukatsu, A.; Kondo, M.; Masaoka, S.; Kanai, M. *J. Am. Chem. Soc.* **2017**, *139*, 2204–2207. (f) Chuentragool, P.; Kurandina, D.; Gevorgyan, V. *Angew. Chem., Int. Ed.* **2019**, *58*, 11586–11598.

[11] (a) Parasram, M.; Gevorgyan, V. *Chem. Soc. Rev.* **2017**, *46*, 6227–6240. (b) Wang, G.-Z.; Shang, R.; Cheng, W.-M.; Fu, Y. *J. Am. Chem. Soc.* **2017**, *139*, 18307–18312. (c) Kurandina, D.; Rivas, M.; Radzhabov, M.; Gevorgyan, V. *Org. Lett.* **2018**, *20*, 357–360. (d) Wang, G.-Z.; Shang, R.; Fu, Y. *Org. Lett.* **2018**, *20*, 888–891. (e) Kurandina, D.; Parasram, M.; Gevorgyan, V. *Angew. Chem., Int. Ed.* **2017**, *56*, 14212–14216. (f) Roslin, S.; Odell, L. R. *Chem. Commun.* **2017**, *53*, 6895–6898. (g) Sumino, S.; Fusano, A.; Fukuyama, T.; Ryu, I. *Acc. Chem. Res.* **2014**, *47*, 1563–1574. (h) Liu, Q.; Dong, X.;

Li, J.; Xiao, J.; Dong, Y.; Liu, H. *ACS Catal.* **2015**, *5*, 6111–6137. (i) Parasram, M.; Chuentragool, P.; Sarkar, D.; Gevorgyan, V. *J. Am. Chem. Soc.* **2016**, *138*, 6340–6343. (j) Parasram, M.; Chuentragool, P.; Wang, Y.; Shi, Y.; Gevorgyan, V. *J. Am. Chem. Soc.* **2017**, *139*, 14857–14860.

[12] Rakshit, A.; Sau, P.; Ghosh, S.; Patel, B. K. *Adv. Synth. Catal.* **2019**, *361*, 3824–3836.

[13] (a) Zhou, C.; Larock, R. C. *J. Am. Chem. Soc.* **2004**, *126*, 2302–2303. (b) Zhou, C.; Larock, R. C. *J. Org. Chem.* **2006**, *71*, 3551–3558. (c) Zhao, B.; Lu, X. *Org. Lett.* **2006**, *8*, 5987–5990. (d) Wong, Y.-C.; Parthasarathy, K.; Cheng, C.-H. *Org. Lett.* **2010**, *12*, 1736–1739. (e) Tsui, G. C.; Glenadel, Q.; Lau, C.; Lautens, M. *Org. Lett.* **2011**, *13*, 208–211. (f) Chen, J.; Ye, L.; Su, W. *Org. Biomol. Chem.* **2014**, *12*, 8204–8211. (g) Wang, X.; Huang, Y.; Xu, Y.; Tang, X.; Wu, W.; Jiang, H. *J. Org. Chem.* **2017**, *82*, 2211–2218.

[14] (a) Qi, L.; Hu, K.; Yu, S.; Zhu, J.; Cheng, T.; Wang, X.; Chen, J.; Wu, H. *Org. Lett.* **2017**, *19*, 218–221. (b) Zhu, J.; Shao, Y.; Hu, K.; Qi, L.; Cheng, T.; Chen, J. *Org. Biomol. Chem.* **2018**, *16*, 8596–8603. (c) Xu, T.; Shao, Y.; Dai, L.; Yu, S.; Cheng, T.; Chen, J. *J. Org. Chem.* **2019**, *84*, 13604–13614. (d) Qi, L.; Li, R.; Yao, X.; Zhen, Q.; Ye, P.; Shao, Y.; Chen, J. *J. Org. Chem.* **2020**, *85*, 1097–1108 and references cited therein. (e) Zhen, Q.; Li, R.; Qi, L.; Hu, K.; Yao, X.; Shao, Y.; Chen, J. *Org. Chem. Front.* **2020**, *7*, 286–291 and references cited therein. (f) Xie, J.; Huang, H.; Xu, T.; Li, R.; Chen, J.; Ye, X. *RSC Adv.* **2020**, *10*, 8586–8593. (g) Xiong, W.; Hu, K.; Lei, Y.; Zhen, Q.; Zhao, Z.; Shao, Y.; Li, R.; Zhang, Y.; Chen, J. *Org. Lett.* **2020**, *22*, 1239–1243 and references cited therein. (h) Yao, X.; Qi, L.; Li, R.; Zhen, Q.; Liu, J.; Zhao, Z.; Shao, Y.; Hu, M.; Chen, J. *ACS Comb. Sci.* **2020**, *22*, 114–119. (i) Zhen, Q.; Chen, L.; Qi, L.; Hu, K.; Shao, Y.; Li, R.; Chen, J. *Chem. Asian J.* **2020**, *15*, 106–111.

[15] Tellis, J. C.; Primer, D. N.; Molander, G. A. *Science.* **2014**, *345*, 433–436.

[16] Xu, P.; Zhu, Y.-M.; Wang, F. Wang, S.-Y; Ji, S.-J. *Org. Lett.* **2019**, *21*, 683–686.

[17] (a) Seiple, I. B.; Su, S.; Rodriguez, R. A.; Gianatassio, R.; Fujiwara, Y.; Sobel, A. L.; Baran, P. S. *J. Am. Chem. Soc.* **2010**, *132*, 13194–13196. (b) Yan, G.; Yang, M.; Wu, X. *Org. Biomol. Chem.* **2013**, *11*, 7999–8008. (c) Iwata, Y.; Tanaka, Y.; Kubosaki, S.; Morita, T.; Yoshimi, Y. *Chem. Commun.* **2018**, *54*, 1257–1260.

[18] (a) Lin, S.; Wei, Y.; Liang. F. *Chem. Commun.* **2012**, *48*, 9879–9881. (b) Abdelhamid, A. O.; Negm, A. M.; Abbas, I. M. *J. Prakt. Chem*. **1989**, *331*, 31–36. (c) Al-Mousawi, S. M.; Moustafa, M. S.; Meier, H.; Kolshorn, H.; Elnagdi, M. H. *Molecules.* **2009**, *14*, 798–806.

[19] (a) Allais, C.; Liéby-Muller, F.; Rodriguez, J.; Constantieux, T. *Eur. J. Org. Chem.* **2013**, *19*, 4131–4145. (b) Kelly, T. R.; Lebedev, R. L. *J. Org. Chem*. **2002**, *67*, 2197–2205. (c) Hantzsch, A. *Chemische Berichte*. **1881**, *14*, 1637–1638. (d) Kröhnke, F. *Synthesis.* **1976**, 1–24.

[20] (a) Gulevich, A. V.; Dudnik, A. S.; Chernyak, N.; Gevorgyan, V. *Chem. Rev.* **2013**, *113*, 3084–3213. (b) Wei, Y.; Yoshikai, N. *J. Am. Chem. Soc*. **2013**, *135*, 3756–3759. (c) Tan, W. W.; Ong, Y. J.; Yoshikai, N. *Angew. Chem., Int. Ed.* **2017**, *56*, 8240–8244. (d) Jiang, Y.; Park, C.-M. *Chem. Sci.* **2014**, *5*, 2347–2351. (e) Scherbinina, S. I.; Fedorov, O. V.; Levin, V. V.; Kokorekin, V. A.; Struchkova, M. I.; Dilman, A. D. *J. Org. Chem.* **2017**, *82*, 12967–12974. (f) Lui, E. K. J.; Hergesell, D.; Schafer, L. L. *Org. Lett.* **2018**, *20*, 6663–6667.

[21] (a) Neely, J. M.; Rovis, T. *Org. Chem. Front.* **2014**, *1*, 1010–1015. (b) Boger, D. L. *Chem. Rev.* **1986**, *86*, 781–793. (c) Wu, J.; Xu, W.; Yu, Z.-X.; Wang, J. *J. Am. Chem. Soc.* **2015**, *137*, 9489–9496. (d) Monbaliu, J.-C. M.; Masschelein, K. G. R.; Stevens, C. V. *Chem. Soc. Rev.* **2011**, *40*, 4708–4739. (e) Foster, R. A. A.; Willis, M. C. *Chem. Soc. Rev.* **2012**, *42*, 63–76. (f) Parthasarathy, K.; Jeganmohan, M.; Cheng, C.-H. *Org. Lett*. **2008**, *10*, 325–328.

[22] (a) McCormick, M. M.; Duong, H. A.; Zuo, G.; Louie, J. *J. Am. Chem. Soc*. **2005**, *127*, 5030–5031. (b) Heller, B.; Hapke, M. *Chem. Soc. Rev*. **2007**, *36*, 1085–1094. (c) Kumar, P.; Prescher, S.; Louie, J. *Angew. Chem., Int. Ed.* **2011**, *50*, 10694–10698. (d) Onodera, G.; Shimizu, Y.; Kimura, J.; Kobayashi, J.; Ebihara, Y.; Kondo, K.; Sakata, K.; Takeuchi, R. *J. Am. Chem. Soc.* **2012**, *134*, 10515–10531. (e) Xie, L.-G.; Shaaban, S.; Chen, X.; Maulide, N. *Angew. Chem. Int., Ed.* **2016**, *55*, 12864–12867.

[23] Yao, X.; Qi, L.; Li, R.; Zhen, Q.; Liu, J.; Zhao, Z.; Shao, Y.; Hu, M.; Chen, J. *ACS Comb. Sci*. **2020**, *22*, 114–119.

[24] (a) Wei, H.; Li, Y.; Xiao, K.; Cheng, B.; Wang, H.; Hu, L.; Zha, H. *Org. Lett.* **2015**, *17*, 5974–5977. (b) Yin, G.; Liu, Q.; Ma, J.; She, N. *Green Chem.* **2012**, *14*, 1796–1798. (c) Nakamura, I.; Oyama, Y.; Zhang, D.; Terada, M. *Org. Chem. Front.* **2017**, *4*, 1034–1036. (d) Huang, H.; Cai, J.; Tang, L.; Wang, Z.; Li, F.; Deng, G.-J. *J. Org. Chem.* **2016**, *81*, 1499–1505. (e) Jiang, Y.; Park, C.-M.; Loh, T.-P. *Org. Lett*. **2014**, *16*, 3432–3435. (f) Song, Z.; Huang, X.; Yi, W.; Zhang, W. *Org. Lett*. **2016**, *18*, 5640–5643.

[25] Rohokale, R. S.; Koenig, B.; Dhavale, D. D. *J. Org. Chem*. **2016**, *81*, 7121–7126.

[26] (a) Bull, J. A.; Mousseau, J. J.; Pelletier, G.; Charette, A. B. *Chem. Rev.* **2012**, *112*, 2642–2713. (b) Larionov, O. V.; Stephens, D.; Mfuh, A.; Chavez, G. *Org. Lett.* **2014**, *16*, 864–867. (c) Colombe, J. R.; Bernhardt, S.; Stathakis, C.; Buchwald, S. L.; Knochel, P. *Org. Lett*. **2013**, *15*, 5754–5757. (d) Guan, B.-T.; Hou, Z. *J. Am. Chem. Soc*. **2011**, *133*, 18086–18089.

[27] (a) Knorr, L. *Ber. Dtsch. Chem. Ges*. **1884**, *17*, 1635–1642. (b) Paal, C. *Ber. Dtsch. Chem. Ges*. **1885**, *18*, 367–371. (c) Hantzsch, A. *Ber. Dtsch. Chem. Ges*. **1890**, *23*, 1474–1476.

[28] (a) Bergner, I.; Wiebe, C.; Meyer, N.; Opatz, T. *J. Org. Chem*. **2009**, *74*, 8243–8253. (b) Saito, A.; Konishi, T.; Hanzawa, Y. *Org. Lett.* **2010**, *12*, 372–374. (c) Lin, X.; Mao, Z.; Dai, X.; Lu, P.; Wang, Y. *Chem. Commun*. **2011**, *47*, 6620–6622. (d) Feng, X.; Wang, Q.; Lin, W.; Dou, G.-L.; Huang, Z. B.; Shi, D.-Q. *Org. Lett*. **2013**, *15*, 2542–2545. (e) Wang, L.; Ackermann, L. *Org. Lett*. **2013**, *15*, 176–179. (f) Zhao, M.-N.; Ren, Z.-H.; Wang, Y.-Y.; Guan, Z.-H. *Org. Lett*. **2014**, *16*, 608–611. (g) Xuan, J.; Xia, X.-D.; Zeng, T.-T. Feng, Z.-J.; Chen, J.-R.; Lu, L.-Q.; Xiao, W.-J. *Angew. Chem., Int. Ed*. **2014**, *53*, 5653–5656. (h) Kim, D.-S.; Seo, Y.-S.; Jun, C.-H. *Org. Lett*. **2015**, *17*, 3842–3845. (i) Zheng, Y.; Wang, Y.; Zhou, Z. *Chem. Commun*. **2015**, *51*, 16652–16655. (j) Reekie, T. A.; Donckele, E. J.; Manenti, G.; Püntener, S.; Trapp, N.; Diederich, F. *Org. Lett*. **2016**, *18*, 2252–2255. (k) Yousuf, M.; Adhikari, S. *Org. Lett*. **2017**, *19*, 2214–2217. (l) Zhen, Q.; Li, R.; Qi, L.; Hu, K.; Yao, X.; Shao, Y.; Chen, J. *Org. Chem. Front*. **2020**, *7*, 286–291. (m) Sahoo, A. K.; Rakshit, A.; Dahiya, A.; Pan, A.; Patel, B. K. *Org. Lett*. **2022**, *24*, 1918–1923.

[29] (a) Kirchberg, S.; Fröhlich, R.; Studer, A. *Angew. Chem., Int. Ed.* **2009**, *48*, 4235–4238. (b) Mitsudo, K.; Kaide, T.; Nakamoto, E.; Yoshida, K.; Tanaka, H. *J. Am. Chem. Soc.* **2007**, *129*, 2246–2247.

[30] (a) Li, Z.; García-Domínguez, A.; Nevado, C. *J. Am. Chem. Soc.* **2015**, *137*, 11610–11613. (b) Fredricks, M. A.; Drees, M.; Köhler, K. *ChemCatChem* **2010**, *2*, 1467–1476.

[31] Fuchigami, T.; Inagi, S. Electrochemistry of Organoboron Compounds. In *PATAI'S Chemistry of Functional Groups*; American Cancer Society, 2019; pp 1–26. (b) Morris, J. H.; Gysling, H. J.; Reed, D. *Chem. Rev.* **1985**, *85*, 51–76.

[32] Amgoune, A.; Bourissou, D. *Chem. Commun.* **2011**, *47*, 859–871.

List of Publications

1. Sau, P.; Santra, S. K.; **Rakshit**, **A**.; Patel, B. K. *tert*-Butyl Nitrite-Mediated Domino Synthesis of Isoxazolines and Isoxazoles from Terminal Aryl Alkenes and Alkynes. *J. Org. Chem*. **2017**, *82*, 6358–6365.
2. Sau, P.; **Rakshit**, **A**.; Modi, A.; Behera, A.; Patel, B. K. Three Sequential C–N Bond Formations: *tert*-Butyl Nitrite as a *N1* Synthon in a Three Component Reaction Leading to Imidazo[1,2-*a*]quinolines and Imidazo[2,1-*a*]isoquinolines. *J. Org. Chem*. **2018**, *83*, 1056–1064.
3. Behera, A.; **Rakshit**, **A**.; Sahoo, A. K.; Patel, B. K. One-pot Sequential Synthesis of *N*-(2-(phenylsulfinyl)phenyl)acetamides: A Ring Opening Rearrangement Functionalisation (RORF). *Eur. J. Org. Chem*. **2019**, 1154–1165.
4. Sau, P.; **Rakshit**, **A**.; Alam, T.; Srivastava, H.; Patel, B. K. *tert*-Butyl Nitrite-Mediated Greener Synthesis of 1,2,4-Oxadiazol-5(4*H*)-ones from Terminal Aryl Alkenes. *Org. Lett*. **2019**, *21*, 4966–4970.
5. **Rakshit**, **A**.; Sau, P.; Ghosh, S.; Patel, B. K. One-pot Sequential Synthesis of Fused Isoquinolines *via* Intramolecular-Cyclization/Annulation and their Photophysical Investigations. *Adv. Synth. Catal*. **2019**, *361*, 3824–3836.
6. Alam, T.; **Rakshit**, **A**.; Begum, P.; Dahiya, A.; Patel, B. K. Visible-Light-Induced Difunctionalization of Styrenes: Synthesis of *N*-Hydroxybenzimidoyl Cyanides. *Org. Lett.* **2020**, *22*, 3728–3733.
7. **Rakshit**, **A**.; Kumar, P.; Alam, T.; Dhara, H.; Patel, B. K. Visible-Light Accelerated Pd-Catalyzed Cascade Addition/Cyclization of Aryl Boronic Acids to γ- and β-Ketodinitriles for the Construction of 3-Cyanopyridines and 3-Cyanopyrrole Analogues *J. Org. Chem.* **2020**, *85*, 12482–12504.
8. Chakraborty, N.; Dahiya, A. **Rakshit**, **A**.; Modi, A. Patel, B. K. An Expedient Route to Tricyanovinylindoles and Indolylmaleimides from *o*-Alkynylanilines Utilising DMSO as a One-Carbon Synthon. *Org. Biomol. Chem*. **2021**, *19*, 6847–6857.
9. **Rakshit**, **A**.; Dhara, H. N.; Alam, T.; Dahiya, A.; Patel, B. K. Cu(II)-Promoted Cascade Synthesis of Fused Imidazo-Pyridine-Carbonitriles. *J. Org. Chem*. **2021**, *86*, 17504–17510.

10. Sahoo, A. K.; **Rakshit**, **A**.; Dahiya, A.; Pan, A.; Patel, B. K. Visible-Light-Mediated Synthesis of Thio-Functionalized Pyrroles. *Org. Lett*. **2022**, *24*, 1918–1923.
11. **Rakshit**, **A**.; Dhara, H. N.; Sahoo, A. K.; Alam, T.; Patel, B. K. Pd(II)-Catalyzed Synthesis of Furo[2,3-*b*]pyridine from β-Ketodinitriles and Alkynes *via* Cyclization and N–H/C Annulation. *Org. Lett*. **2022**, *24*, 3741–3746.
12. Alam, T.; **Rakshit**, **A**.; Dhara, H. N.; Palai, A.; Patel, B. K. Electrochemical Amidation: Benzoyl Hydrazine/Carbazate and Amine as Coupling Partners. *Org. Lett*. **2022**, *24*, 6619–6624.
13. Sahoo, A. K.; **Rakshit**, **A**.; Pan, A.; Dhara, H. N.; Patel, B. K. Visible/Solar-Light-Driven Thiyl-Radical-Triggered Synthesis of Multi-Substituted Pyridines. (***submitted***).
14. Dhara, H. N.; **Rakshit**, **A**.; Alam, T.; Sahoo, A. K.; Patel, B. K.Visible-light mediated solvent-switched photosensitizer-free synthesis of poly-functionalized quinolines and pyridines. (***submitted***).

Review Articles

1. Sahoo, A. K.; Dahiya, A.; **Rakshit**, **A**.; Patel, B. K. The Renaissance of Alkali Metabisulfites as SO_2 Surrogates. *Syn Open*. **2021**, *5*, 232–251.
2. Dhara, H. N.; **Rakshit**, **A**.; Alam, T.; Patel, B. K. Metal-Catalyzed Reactions of Organic Nitriles and Boronic Acids to Access Diverse Functionality. *Org. Biomol. Chem*. **2022**, *20*, 4243–4277.
3. **Rakshit**, **A**.; Dhara, H. N.; Sahoo, A. K. Patel, B. K. The Renaissance of Organo Nitriles in Organic Synthesis. *Chem. Asian J.* **2022**, e202200792, https://doi.org/10.1002/asia.202200792.

Book Chapters

1. Patel, B. K.; **Rakshit**, **A**. Access to *N*-Heterocyclic Molecules *via* Ru(II)-Catalyzed Oxidative Alkyne Annulation Reactions. Ruthenium-An Element Loved by Researchers, edited by Hitoshi Ishida, IntechOpen, **2021**, 10.5772/intechopen.95987.
2. Patel, B. K.; Alam, T.; **Rakshit**, **A**. Construction of C–N Bond *via* Visible-Light-Mediated Difunctionalization of Alkenes. Alkenes-Recent Advances, New Perspectives and Applications, edited by Reza Davarnejad, IntechOpen, **2021**, 10.5772/intechopen.98949.

PRESENT ADDRESS

C/O – Prof. Bhisma K. Patel
Department of Chemistry
IIT Guwahati
Guwahati–781039
Assam, India

PERMANENT ADDRESS

Vill.– Murgaboni
P.O.– Jhantipahari
P.S. – Chhatna
Dist. –Bankura
West Bengal, India – 722137

CONTACT

PHONE:
+918617551984
+919641293555

EMAIL:
amitavarakshit93@iitg.ac.in
amitavarakshit93@gmail.com

PERSONAL INFORMATION

Sex: Male
Date of Birth: 10th February'1993
Nationality: Indian
Languages: Bengali, English, Hindi

ORCID ID

0000-0002-2605-9401

TH-2725_166122029

AMITAVA RAKSHIT
Ph.D.

EDUCATION

2022
Doctor of Philosophy (Ph.D.) in organic chemistry (CPI: 9.75/10)
Indian Institute of Technology Guwahati
Thesis Title: ***Nitrile Triggered Access of N-Heterocycles under Thermal and Photochemical Processes***
Supervisor: Prof. Bhisma K. Patel

2016
Master of Science (M.Sc.) in Chemistry (CPI: 9.01/10)
Indian Institute of Technology Kharagpur

2014
Bachelor of Science (B.Sc.) in Chemistry (69.125%)
Bankura Christian College (The University of Burdwan)

WORK EXPERIENCE

Field: ***Total Synthesis of Natural Products*** **(M.Sc. project)**
Indian Institute of Technology Kharagpur, Kharagpur-721302, West Bengal, India under the supervision of Dr. Samik Nanda, Department of Chemistry, IIT Kharagpur.
Duration: July 2015 to April 2016

Field**:** ***HRMS instrumental duty as an operator***
Department of Chemistry**,** IIT Guwahati.
Duration: July 2018 to July 2021.

Learned and handled a wide range of analytical instruments such as NMR, HRMS, IR, UV–visible spectrophotometer, and Spectrofluorometer etc required during my research work

TEACHING/MENTORING EXPERIENCE

- ✓ Mentored two M.Sc. and one Ph.D. students during Ph.D.
- ✓ Teaching Assistantship (TA) at IIT Guwahati at the undergraduate lab in July–November 2017 and January–May 2018 semesters.

RESEARCH INTERST

- Synthetic organic chemistry.
- Newer methodology in organic synthesis.
- Photochemical organic synthesis.
- Electrochemical organic synthesis.

ACADEMIC ACHIEVEMENTS

- Qualified for the UGC-Junior Research Fellowship (All India Rank = 55) in the ***National Eligibility Test (NET)***, jointly organized by Council of Scientific and Industrial Research (CSIR) and University Grants Commission (UGC). **[2016]**

- Ranked AIR-933 in ***Graduate Aptitude Test in Engineering (GATE)*** organised by Department of Higher Education, Ministry of Human Resources Development (MHRD), Government of India. **[2016]**

- Ranked AIR-271 in ***Joint Admission Test for M.Sc. (JAM)***. **[2014]**

SCHOLARSHIPS AWARDED

- Awarded ***'INSPIRE SCHOLARSHIP'*** by ***Ministry of Science & Technology, Department Of Science & Technology (DST), Govt. Of India.*** **[2010]**

PUBLICATION DETAILS

Number of published scientific papers : 14

Number of published review articles: 3

Number of book chapters: 2

Research Articles:

1. Sau, P.; Santra, S. K.; **Rakshit**, **A**.; Patel, B. K. *tert*-Butyl Nitrite-Mediated Domino Synthesis of Isoxazolines and Isoxazoles from Terminal Aryl Alkenes and Alkynes. ***J. Org. Chem***. **2017**, *82*, 6358–6365. (**IF: 4.354**)

2. Sau, P.; **Rakshit**, **A**.; Modi, A.; Behera, A.; Patel, B. K. Three Sequential C–N Bond Formations: *tert*-Butyl Nitrite as a *N1* Synthon in a Three Component Reaction Leading to Imidazo[1,2-*a*]quinolines and Imidazo[2,1-*a*]isoquinolines. ***J. Org. Chem***. **2018**, *83*, 1056–1064. (**IF: 4.354**)

3. Behera, A.; **Rakshit**, **A**.; Sahoo, A. K.; Patel, B. K. One-pot Sequential Synthesis of *N*-(2-(phenylsulfinyl)phenyl)acetamides: A Ring Opening Rearrangement Functionalisation (RORF). ***Eur. J. Org. Chem*. 2019, 1154–1165**. (**IF: 3.021**)

4. Sau, P.; **Rakshit**, **A**.; Alam, T.; Srivastava, H.; Patel, B. K. *tert*-Butyl Nitrite-Mediated Greener Synthesis of 1,2,4-Oxadiazol-5(4*H*)-ones from Terminal Aryl Alkenes. ***Org. Lett.*** **2019**, *21*, 4966–4970. (**IF: 6.005**)

5. **Rakshit**, **A**.; Sau, P.; Ghosh, S.; Patel, B. K. One-pot Sequential Synthesis of Fused Isoquinolines *via* Intramolecular-Cyclization/Annulation and their Photophysical Investigations. ***Adv. Synth. Catal.*** **2019**, *361*, 3824–3836. (**IF: 5.837**)

6. Alam, T.; **Rakshit**, **A**.; Begum, P.; Dahiya, A.; Patel, B. K. Visible-Light-Induced Difunctionalization of Styrenes: Synthesis of *N*-Hydroxybenzimidoyl Cyanides. ***Org. Lett.*** **2020**, *22*, 3728–3733. (**IF: 6.005**)

7. **Rakshit**, **A**.; Kumar, P.; Alam, T.; Dhara, H.; Patel, B. K. Visible-Light Accelerated Pd-Catalyzed Cascade Addition/Cyclization of Aryl Boronic Acids to γ- and β-Ketodinitriles for the Construction of 3-Cyanopyridines and 3-Cyanopyrrole Analogues. ***J. Org. Chem.*** **2020**, *85*, 12482–12504. (**IF: 4.354**)

8. Chakraborty, N.; Dahiya, A. **Rakshit**, **A**.; Modi, A. Patel, B. K. An Expedient Route to Tricyanovinylindoles and Indolylmaleimides from *o*-Alkynylanilines Utilising DMSO as a One-Carbon Synthon. ***Org. Biomol. Chem.*** **2021**, *19*, 6847–6857. (**IF: 3.876**)

9. **Rakshit**, **A**.; Dhara, H. N.; Alam, T.; Dahiya, A.; Patel, B. K. Cu(II)-Promoted Cascade Synthesis of Fused Imidazo-Pyridine-Carbonitriles. ***J. Org. Chem.*** **2021**, *86*, 17504–17510. (**IF: 4.354**)

10. Sahoo, A. K.; **Rakshit**, **A**.; Dahiya, A.; Pan, A.; Patel, B. K. Visible-Light-Mediated Synthesis of Thio-Functionalized Pyrroles. ***Org. Lett.*** **2022**, *24*, 1918–1923. (**IF: 6.005**)

11. **Rakshit**, **A**.; Dhara, H. N.; Sahoo, A. K.; Alam, T.; Patel, B. K. Pd(II)-Catalyzed Synthesis of Furo[2,3-*b*]pyridine from β-Ketodinitriles and Alkynes *via* Cyclization and N–H/C Annulation. ***Org. Lett.*** **2022**, *24*, 3741–3746. (**IF: 6.005**)

12. Alam, T.; **Rakshit**, **A**.; Dhara, H. N.; Palai, A.; Patel, B. K. Electrochemical Amidation: Benzoyl Hydrazine/Carbazate and Amine as Coupling Partners. ***Org. Lett.*** **2022,** *24*, 6619–6624. (**IF: 6.005**)

13. Sahoo, A. K.; **Rakshit**, **A**.; Pan, A.; Dhara, H. N.; Patel, B. K. Visible/Solar-Light-Driven Thiyl-Radical-Triggered Synthesis of Multi-Substituted Pyridines. (***manuscript submitted).***

14. Dhara, H. N.; **Rakshit**, **A**.; Alam, T.; Sahoo, A. K.; Patel, B. K.Visible-light mediated solvent-switched photosensitizer-free synthesis of poly-functionalized quinolines and pyridines. (***manuscript submitted***).

Review Articles:

1 Sahoo, A. K.; Dahiya, A.; **Rakshit**, **A**.; Patel, B. K. The Renaissance of Alkali Metabisulfites as SO_2 Surrogates. ***Syn Open*. 2021**, *5*, 232–251.

2 Dhara, H. N.; **Rakshit**, **A**.; Alam, T.; Patel, B. K. Metal-Catalyzed Reactions of Organic Nitriles and Boronic Acids to Access Diverse Functionality. ***Org. Biomol. Chem***. **2022**, *20*, 4243–4277. (**IF: 3.876**)

3 **Rakshit**, **A**.; Dhara, H. N.; Sahoo, A. K.; Patel, B. K. The Renaissance of Organo Nitriles in Organic Synthesis. ***Chem. Asian J. 2022, e202200792,*** https://doi.org/10.1002/asia.202200792. (**IF: 4.839**)

Book Chapters:

1 Patel, B. K.; **Rakshit**, **A**. Access to *N*-Heterocyclic Molecules *via* Ru(II)-Catalyzed Oxidative Alkyne Annulation Reactions. Ruthenium-An Element Loved by Researchers, edited by Hitoshi Ishida, **IntechOpen**, **2021**, 10.5772/intechopen.95987.

2 Patel, B. K.; Alam, T.; **Rakshit**, **A**. Construction of C–N Bond *via* Visible-Light-Mediated Difunctionalization of Alkenes. Alkenes-Recent Advances, New Perspectives and Applications, edited by Reza Davarnejad, **IntechOpen**, **2021**, 10.5772/intechopen.98949.

CONFERENCE AND SEMINARS ATTENDED

- Participated in the poster presentation in **"Frontiers in Chemical Sciences (FICS)-2018"**, Organized by Department of Chemistry, Indian Institute of Technology Guwahati, Guwahati, Assam, India. **[Dec 2018]**
- Participated in the poster presentation in **"Research Conclave (RC)-2019"** Organized by Indian Institute of Technology Guwahati, Guwahati, Assam, India. **[March 2019]**
- Participated in the poster presentation in "**National Conference On Sustainable and Evolving Scienses (GSES-2019)",** Cotton University, Guwahati, Assam, India. **[June 2019]**
- Participated in the poster presentation in "**National Organic Symposium Trust XV J-NOST Conference for Research Scholars**", Organized by University of Delhi, Delhi, India. **[October 2019]**
- Participated in the online poster presentation in **"First Virtual JNOST Conference (JNOST 16)**", Organized by Indian Institute of Science, Bangalore, India. **[October 2020]**